Novel potent antiviral molecules targeting the nucleocapsid protein of the HIV-1 virus

Beata Szafarowicz Basta

UNIVERSITÉ DE STRASBOURG

ÉCOLE DOCTORALE __ED414__

Ecole Doctorale des Sciences de la Vie et de la Santé

Université de Strasbourg

THÈSE présentée par :

Beata BASTA

soutenue le : **26 Septembre 2012**

pour obtenir le grade de : **Docteur de l'université de Strasbourg**

Discipline/ Spécialité : Biophysique

Nouvelles molécules antivirales ciblant la protéine de la nucléocapside du virus VIH-1.

THÈSE dirigée par :

MELY Yves	prof. Université de Strasbourg

RAPPORTEURS :

Olivier MAUFRET	dr, ENS de Cachan
May MORRIS	dr, CNRS Montpelier

AUTRES MEMBRES DU JURY :

Jan MISIEWICZ	prof, Wroclaw University of Technology
Marc RUFF	dr, IGBMC, Strasbourg

UNIVERSITÉ DE STRASBOURG

Beata BASTA

Nouvelles molécules antivirales ciblant la protéine de la nucléocapside du virus VIH-1.

Résumé

Etant donnée la séquence hautement conservée de la NC et son rôle crucial dans le cycle viral de VIH-1, les molécules inhibant la NC sont susceptibles d'agir comme complément aux thérapies anti-rétrovirales à haute activité (HAART) basées sur des médicaments ciblant les enzymes virales. Des médicaments anti-NC sont ainsi susceptibles d'entraîner un maintien de l'inhibition de la réplication d'un large panel d'isolats VIH-1 incluant des lignées virales résistantes aux médicaments ciblant les enzymes virales. Récemment, dans le cadre du consortium Européen TRIoH, de nouvelles stratégies visant à cibler spécifiquement les propriétés chaperonnes de la NC sur les acides nucléiques ont été développées. Selon une stratégie protégée par un brevet soumis, une série de peptides a été conçue afin d'agir comme compétiteurs de la NC et pouvant ainsi inhiber la réplication du virus. Au sein de cette série, plusieurs peptides ont montré une inhibition efficace des propriétés de déstabilisation des acides nucléiques par la NC. Quatre de ces peptides ont été testés en milieu cellulaire et trois d'entre eux ont montré qu'ils pouvaient inhiber efficacement la réplication du HIV-1 dans les lymphocytes. Dans ce contexte, un premier objectif de cette thèse fût de caractériser avec précision les propriétés de ces peptides. En outre, un objectif supplémentaire fût de caractériser le mécanisme moléculaire vis-à-vis de la NC de petites molécules anti-virales développées par les groupes de D. Daelemans (Leuven) et M. Botta (Sienne).

Résumé en anglais

Due to the highly conserved sequence of NC and its crucial function during HIV-1 life cycle, molecules directed against NC are believed to be able to complement the highly active anti-retroviral therapies (HAART) based on drugs targeting the viral enzymes. Anti-NC drugs are thought to provide a sustained replication inhibition of a large panel of HIV-1 isolates including virus strains resistant to drugs targeting viral enzymes. Recently, within the

European consortium TRIoH, new strategies to specifically target the nucleic acid chaperone properties of NC were developed. According to a strategy protected by a submitted patent, a series of peptides have been designed to act as competitors for NC and thus, inhibit virus replication. Among this series, several peptides were found to efficiently inhibit the nucleic acid destabilization properties of NC. Four of them have been tested in the cellular context and three out of them were found to efficiently inhibit the replication of HIV-1 in lymphocytes. In this context, the objective of the thesis was to characterize in depth the properties of these peptides. Moreover, an additional objective was to characterize the molecular mechanism in respect to NC of small antiviral drugs developed by the group of D. Daelemans (Leuven) and M. Botta (Siena).

This work was conducted in cooperation between Wroclaw University of Technology (Wroclaw, Poland) and University of Strasbourg (Alsace, France). I also would like to express my gratitude to the French National Agency for Research on AIDS and Viral Hepatitis and the Regional Parliament of Lower Silesia Province for financial support.

I would like to express my heartfelt gratitude to Director of my thesis Prof. Yves MELY for his supervision, inspiration and encouragement during my research. He has been generous with his time and knowledge. It has been a privilege for me, to be a student of him.

I would like to express my deepest gratitude and sincere appreciation to my co-Director Prof. Jan Misiewicz for help and guidance for monitoring my research.

I would like to extend my gratitude to Prof. Jean-Luc Darlix for his discussion and fruitful comments.

I am greatly honored by the kind acceptance of Dr. May MORRIS, Dr. Marc RUFF and Dr. Olivier MAUFFRET as members of jury for my thesis and would like to thanks them for serving as my advisory committee.

Special thanks to Dr. Guy DUPORTAIL for his help and support, and Dr. Hughes de ROCQUIGNY for his help with the HPLC and peptide synthesis. I would like to extend my gratitude to Dr. Eleonore REAL for valuable discussion and help in antiviral activity assays, Dr. Andrey KLIMCHENKO for his discussion, Dr. Ludovic RICHERT and Dr. Pascal DIDIER for their help in fluorescence correlation spectroscopy experiments. I would like to thank group of Dr. Daelemans (Leuven, Belgium) and Prof. Botta (Siena, Italy) for fruitful collaboration.

I would like to give special thanks to my friend, Armelle JOUONANG for all the help and support. I would like to thank all my friends from the lab Victoria PUSTUPALENKO, Kamal kant SHARMA, Zeinab DARWICH, Hussein FTOUNI, Avisek GHOSH, Vanille GRENIER, Noemy KEMPF, Julien GODET and Frederic PRZYBILLA for their constant help and our great discussions.

On the personal note, I would like to thank my beloved husband, for all the support during my graduate studies.

Abbreviations

ORF	Open reading frame
MMTV	Mause Mammary Tumor Virus
ALV	Avian Leucosis Virus
RSV	Rous sarcoma virus
HERVs	Human endogenous retroviruses
HAART	Highly Acitve Antiviral Theraphy
CNS	Central nervous system
HIVD	HIV-1 dementia
SIV	Simian immunodeficiency virus
CRFs	Circulating recombinant forms
UTR	Non-translated region
RNA	Ribonucleic Acid
DNA	De-oxyribonucleic Acid
NLS	Nuclear Localization Signal
PIC	Preintegration complex
CRM1	Chromosomal Region maintenance 1
CDK9	Cyclin-dependent kinase 9
NES	Nuclear Export Signal
Cyp A	Cyclophylin A
MHR	Major Homology Region
CTD	C-terminal domain
NTD	N-terminal domain
Hrs	Hepatocyte growth factor-regulated kinase substrate
LEDGF	Lens epithelium derived factor
pTEFb	Transcriptional elongation factor
MHC	Major Histocompatibility Complex
β-COP	β-coatomer protein
CCR5/CXCR4	Chemokine receptors
HR	Heptad Repeat region
MLV	Murine Leukaemia Virus
RTC	Reverse transcription complex
LTR	Long terminal repeats
PPT	Polypurine track
cPPT	Central polypurine track
APOBEC3G	Apoliprotein B mRNA-editing-enzyme catalytic polypeptide-like 3G
A3	APOBEC3
A3G	APOBEC3G
NPC	Nuclear Pore Complex
RRE	Rev Responsive elements
IRES	Internal ribosome entry site
ITAF	IRES trans-acting factor
DLS	Dimer linkage signal
SL	Stem loop
DIS	Dimerization initiation site
PBS	Primer binding site
TAR	Trans-activation response element
cTAR	Complementary trans-activation response element
ZF	Zinc finger

ESCRT	Endosomal sorting complex required for transport
MIP	Macrophage inflammatory protein
TRIM5α	Tripartite motif 5 alpha
rAd5	Recombinant adenovirus serotype 5
ODN	Oligonucleotide
DC	Dendritic cell
IFN-α/β	Type I interferons
PKR	Protein kinase R
NF-κB	Nuclear factor κB
VSV	Vesicular stomatitis virus
AAV	Adenoassociated virus
VEE	Venezuelan equine encephalitis
CMV	Cytomegalovirus
HSV	Herpes simplex virus

General Introduction

General Introduction

Human immunodeficiency virus 1 (HIV-1) is the causative agent of AIDS (Acquired Immunodeficiency Syndrome), which leads to a reduction of the effectiveness of the immune system and leaves individuals susceptible to opportunistic infections and tumors. The transmission of the virus is mostly done by direct contact of a mucous membrane or the bloodstream with a body fluid containing HIV-1, such as blood, semen, vaginal fluid, and breast milk.

HIV-1 is an enveloped virus with a positive-strand RNA genome consisting of two identical 9.2 kb single stranded RNA. However, it can also contain fair amounts of minus-strand cDNA (Zhang, Dornadula et al. 1996) which synthesis appears to be promoted by microenvironment, notably by components of the seminal fluid such as nucleotides, spermine–spermidine, and small basic peptides derived from the prostatic acid phosphatase with nucleic acid binding and condensing activities (Zhang, Dornadula et al. 1998; Munch, Rucker et al. 2007).

Retroviral nucleocapsid protein (NC) is a major structural component of the infecting HIV-1 particles. About 1500–2000 NC molecules coating the gRNA in a dimeric form are found within the core structure, together with molecules of RT, integrase, viral protein R (Bachand, Yao et al. 1999) and molecules of cellular origin such as tRNAs, including replication primer tRNALys,3 (Kleiman, Halwani et al. 2004), ribosomal RNAs (Cimarelli and Darlix 2002) and proteins, such as the cellular factor apolipoprotein B mRNA editing enzyme, catalytic polypeptide-like 3G (APOBEC3G).

NC proteins are derived from the Gag structural polyprotein precursor, which consists of the matrix (MA), Capsid, and NC domains (Ganser, Li et al. 1999). During virus assembly at the plasma membrane, Gag and Gag-Pol precursor molecules are cleaved by the activated protease in a well-ordered manner (Adamson and Freed 2007) resulting in the generation of the mature structural proteins and enzymes, which in turn cause virion maturation, core condensation, and the gain of virus infectivity.

Retroviral nucleocapsid (NC) proteins are small, basic, NA binding proteins with one or two zinc-binding domains or zinc fingers, which are connected by a short flexible basic peptide linker. Each zinc finger contains the invariant metal-ion binding motif CX2CX4HX4C, more commonly referred to as a CCHC motif.

HIV-1 NC is a multifunctional protein. It binds NAs non-specifically through electrostatic interactions of the basic residues with the NA phosphodiester backbone and exhibits

sequence-specific binding to runs of Gs or T/UGs through interactions that involve the zinc fingers (Levin, Guo et al. 2005). Importantly, NC is a NA chaperone, which means that it facilitates remodeling of NA structures to form the most thermodynamically stable conformations. Mature NC plays a critical role in assuring the specificity and efficiency of reverse transcription and maturation of the genomic RNA dimer (Darlix, Lapadat-Tapolsky et al. 1995; Rein, Henderson et al. 1998; Thomas and Gorelick 2008). In addition, NC may be important for integration of viral DNA (vDNA) into the host chromosome (Carteau, Gorelick et al. 1999). The NC domain in Gag also exhibits NA chaperone activity, which is required for genomic RNA packaging and primer placement. i.e., annealing of the tRNALys 3 primer to the primer binding site (PBS) in genomic RNA. Moreover, the NC domain promotes genomic RNA dimerization (Darlix, Gabus et al. 1990; Kafaie, Song et al. 2008) and interacts with the Bro 1 domain of the host protein Alix during HIV-1 assembly (Dussupt, Javid et al. 2009; Popov, Popova et al. 2009). Thus, NC and the NC domain in Gag play a major role in almost every step in virus replication. The critical role of NC in the viral life cycle was further illustrated by the fact that point mutations disrupting the globular structure of the zinc fingers result in a complete loss of virus infectivity.

Due to the highly conserved sequence of NC and its crucial function during HIV-1 life cycle, molecules directed against NC are believed to be able to complement the highly active anti-retroviral therapies (HAART) based on drugs targeting the viral enzymes. Anti-NC drugs are thought to provide a sustained replication inhibition of a large panel of HIV-1 isolates including virus strains resistant to drugs targeting viral enzymes.

Bibliographic review

I. Retroviruses

I.1. Retrovirus, definition

Retroviridae is a large and diverse family defined by a common structure and composition as well as replicative properties (Coffin 1990). The members of this family replicate via reverse transcription using a single stranded RNA genome to produce DNA, later incorporated into the host genome. Based on the organization of their genomes, retroviruses can be divided into two categories – simple and complex.

In general, virions are 80-100 nm in diameter, having an outer lipid envelope that incorporates and displays the viral glycoproteins. The single-stranded, linear RNA is found to be 7-12 kb in size. All retroviruses contain three important coding domains:

I. gag - contains information to direct the synthesis of internal virion proteins that form the matrix, the capsid and the nucleoprotein structures.
II. pol - contains information for the reverse transcriptase and integrase enzymes. In Gamma and Lentiviruses domain pol encodes additional information for protease enzyme. Only in some cases e.g. Mause Mammary Tumor Virus (MMTV) domain pol is a distinct open reading frame (ORF) whereas in Alpharetroviruses like Avian Leucosis Virus (ALV) and Rous sarcoma virus (RSV) protease enzyme is a part of the Gag ORF.
III. env - contains the information for the surface and transmembrane components of the viral envelop.

Another significant coding domain present in this family is pro – a domain that encodes the virion protease. The differentiation between simple and complex retroviruses comes from the information that is carried in the genome. Simple retroviruses carry only the above mentioned regions in their genome. Rous sarcoma virus, however, is unique among simple Alpharetroviruses, in possessing its oncogene (src) outside the genes required for replication (Gifford and Tristem 2003). Moreover, Murine Leukaemia virus classified as a simple retrovirus, code for glycol-gag and glycol-pol domains, which makes Gammaretroviruses not so simple one.

On the contrary, complex retroviruses, including Lentiviruses, Spumaviruses, viruses of HTLV-BLV group and the fish viruses, have multiple splice donors in the genome causing a greater variety of gene products. HIV-1 virus, a member of Lentiviruses, encodes six additional proteins, often called accessory proteins, Vpr, Vif, Vpu, Tat, Rev and Nef. Among three first proteins only Vpr is found in the viral particle at the substancial amount. Two other

accessory proteins, Tat and Rev, provide essential gene regulatory functions, and the last protein, Vpu, indirectly assists in assembly of the virion (Frankel and Young 1998).

I.2. Retrovirus discovery

Thanks to the pioneering work of Beijernick on the Tabacco mosaic virus together with the work of Frosh and Loffler (1898) on the food-to-mouth diseases distinguishing virus from other microbes, members of the Retroviridae family have become a very interesting subject of studies all over the world even before discovery of the first human retrovirus in 1981. The first member of the Retroviridae family, the Equine Infectious Anemia virus, was discovered in 1904 by Carré and Vallée (Carré 1904). After this discovery, the Avian Leukemia Virus (ALV) was identified by Ellerman and Bang in 1908, Rous Sarcoma Virus (RSV) by Rous in 1911 and Murine leukemia virus (Gross 1957) in 1957 by Gross.
However, the notion of retroviruses was not officially introduced until 1970, when Howard Temin and David Baltimore (Nobel Prize in Medicine and Physiology 1975) independently published their discovery of reverse transcriptase, an enzyme capable of synthesizing DNA from an RNA template (Baltimore 1970; Temin and Mizutani 1970). This discovery was a revolution against the dogma in molecular biology according to which DNA was considered as the only carrier of genetic information and RNA as a simple vector. In addition, reverse transcriptase is a key enzyme involved in many human viral diseases. In 1979, the team of R. Gallo isolated the first human retrovirus, HTLV-1 (for the human T cell leukemia/lymphoma virus) (Poiesz, Ruscetti et al. 1980). Today, retroviruses are known to be the cause of many diseases, for example, HTLV-I and HTLV-II cause adult T-cell leukaemia, lymphoma and hairy cell leukaemia, HIV-1 and HIV-2 are indirect causes of lymphoma and Kaposi's sarcoma and human papilloma-viruses cause cervical and penile carcinomas (Weiss 2001). Human endogenous retroviruses (HERVs) have also been proposed to be the cause of human diseases, including carcinogenesis. Because of their high genetic variability, they are the subject of many biomedical research.

I.3. Classification

The taxonomy of retroviruses is based on the homologies of nucleotide sequences of the pol gene. According to the final classification of the Eighth Report of the International Committee on Taxonomy of Viruses published in 2005, they are two sub-families belonging to the Retroviridae: Orthoretrovirinae and Spumaretrovirinae.

Sub-family	*Genus*	*Examples*
ORTHORETROVIRINAE	*Betaretrovirus*	*Mouse mammary tumor virus*
	Gammaretrovirus	*Murine leukemia virus* *Feline leukemia virus* *Xenotropic murine leukemia-related virus*
	Alpharetrovirus	*Avian leukemia virus*
	Deltaretrovirus	*Human T-cell leukemia virus*
	Lentivirus	*HIV, SIV, FIV*
	Epsilonretrovirus	*Wall-eyed sarcoma virus*
SPUMARETROVIRINAE	*Spumavirus*	*No known associated diseases*

Table 1. Retrovirus taxonomy.

Spumaretrovirinae

Consisting of Spumaviruses (Table 1), which bring together viruses infecting mainly mammals (monkey, human, feline, bovine), *Spumaretrovirinae* were characterized for the first time in 1954 as a transmissible agent causing cytopathology in cell cultures of renal macaques (Enders 1954).

Although these viruses are apparently non-pathogenic, they could be linked to neurodegenerative diseases (Wick, Grubeckloebenstein et al. 1992; Meiering and Linial 2001).

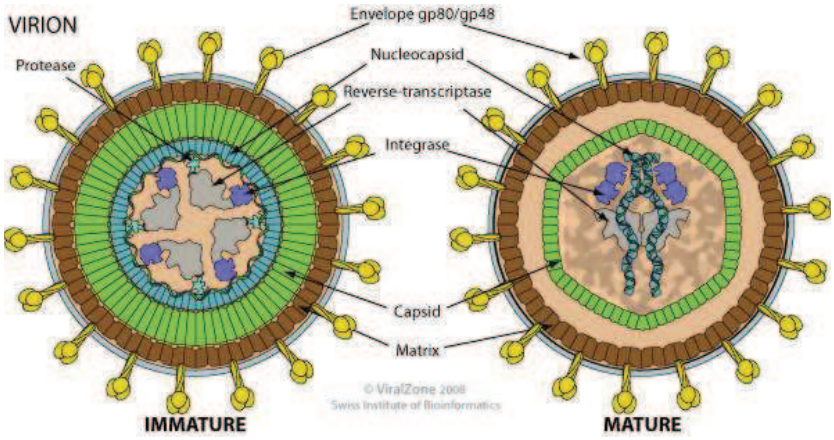

Fig.1. Schematic representation of Spumavirus virion in its immature and mature form (Viralzone.com)

Orthoretrovirinae

This subfamily consists of six genera among which five are known to cause tumor processes. The Alpharetroviruses infect primarily birds causing oncogenic diseases by insertion mutagenesis next to protooncogenes.

Another genera, Betaretroviruses, are not carriers of oncogenic sequences, but often are the origin of carcinomas in monkeys or mice.

The Gammaretroviruses are simple retroviruses infecting mammals, birds and reptiles.

The Deltaretroviruses are complex retroviruses (HTLV, BLV), being the origin of bovine and human leukemias. Although they are not carriers of oncogenic sequences, their genome contains coding sequences for the Tax protein, which acts as transactivator of cellular genes involved in cell growth (McArthur, Hoover et al. 1993; Johnson, Harrod et al. 2001; Okada, Nakae et al. 2005).

The Epsilonretroviruses are oncogenic retroviruses infecting mainly fish.

The Lentiviruses are a group of retroviruses causing the death of infected cells. Lentiviruses are unique in the fact that they can infect non-dividing cells by actively entering the nucleus of a cell through the nuclear envelope via the PIC (Preintegration complex). Other retroviruses such as the Moloney virus require cell division for infection due to the fact that it cannot enter the nuclear envelope of a non-dividing cell.

The most common example of this group of retroviruses is HIV-1. Although the clinical presentation of HIV-1-associated immune system dysfunction varies from individual to individual, the infection, without therapeutic intervention, generally unfolds in four phases over a period of approximately eight to ten years after initial exposure to the virus:

- Incubation period The virus replicates extensively in the absence of any detectable adaptive immune response (virion production between 1 and 10 billion per day). During this period that 70% of individuals experience clinical symptoms of acute infection or what is called acute retroviral syndrome. Several non-specific signs and symptoms have been reported in association with acute infection. Fever in the range of 38 to 40ºC is almost always present in addition lymphadenopathy concomitant with the emergence of a specific immune response to HIV occurs. A generalized rash is also common in symptomatic acute HIV-1 infection. The eruption typically occurs 48 to 72 hours after the onset of fever and persists for five to eight days. The upper thorax, collar region, and face are most affected with well-circumscribed, red colored macules or maculopapules. In addition, painful mucocutaneous oral, vaginal, anal or penal ulcerations are one of the most distinctive manifestations of the syndrome. Further common symptoms are arthralgia, pharyngitis, malaise, weight loss, aseptic meningitis and myalgia (Kahn and Walker 1998). Although none of these findings are specific, several features, combinations of symptoms and prolonged duration are suggestive of HIV-1. The highest sensitivity for a clinical diagnosis of acute HIV-1 infection are fever (80%) and malaise (68%), whereas weight loss (86%) and oral ulcers (85%) had the highest specificity (Hecht, Busch et al. 2002). In study Daar et all, fever, rash, myalgia, arthralgia and night sweats were the best predictors of acute infection (Daar, Little et al. 2001).
- Clinically asymptotic stage. This stage lasts from 3 to 10 years in absence of HAART (Highly Acitve Antiviral Theraphy) treatment and, as its name suggests, is free from major symptoms, although there may be swollen glands. The level of HIV-1 in the peripheral blood drops to very low levels but people remain infectious and HIV-1 antibodies are detectable in the blood, so that antibody tests will show a positive result. In this stage slow decline in the CD4 T-cell count is usually observd, being above 500 cells/mm3. However, some patients with a CD4 T-cell count below 500 cells/mm3 but usually above 350 cells/mm3 may also be within this phase.
- Symptomatic HIV-1 infection (1-2 years). Over time, the immune system becomes severely damaged by HIV. There are three main reasons: the lymph nodes and tissues become damaged or 'burnt out' because of the years of activity. HIV mutates and becomes more pathogenic, leading to more T helper cell destruction, the body fails to keep up replacing the T helper cells that are lost. As the immune system fails, symptoms develop. Initially, many of the symptoms are mild, but as the immune

system deteriorates, the symptoms worsen. Symptomatic HIV infection is mainly caused by the emergence of opportunistic infections that the immune system would normally prevent. This stage of HIV infection is often characterized by multi-system diseases and infections can occur in almost all the body.

System	Examples of Infection/Cancer
Respiratory system	Pneumocystis Carinii Pneumonia (PCP) Tuberculosis (TB) Kaposi's Sarcoma (KS)
Gastro-intestinal system	Cryptosporidiosis Candida Cytomegolavirus (CMV) Isosporiasis Kaposi's Sarcoma
Central/peripheral Nervous system	HIV Cytomegolavirus Toxoplasmosis Cryptococcosis Non Hodgkin's lymphoma Varicella Zoster Herpes simplex
Skin	Herpes simplex Kaposi's sarcoma Varicella Zoster

Table.2. Examples of opportunistic infections occurring in symptomatic HIV-1 infection stage.

- AIDS phase/opportunistic infections. The rapid decline of limpocytes T CD4 + is caused by an increase in viral replication. Indeed, this is the result of a co-infection with other viruses, bacteria, parasites. The clinical criteria used by WHO to diagnose the progression to AIDS, differ slightly between adults and children under five. In adults and children (aged 5 or over), the progression to AIDS is diagnosed when any condition listed in clinical stage 4 is diagnosed and/or the CD4 count is less than 200 cells/mm^3 or a CD4 percentage less than 15. In children younger than five, an AIDS diagnosis is based on having any stage 4 condition and/or a CD4 percentage less than 20 (children aged 12-35 months) and a CD4 percentage less than 25 (children less than 12 months).

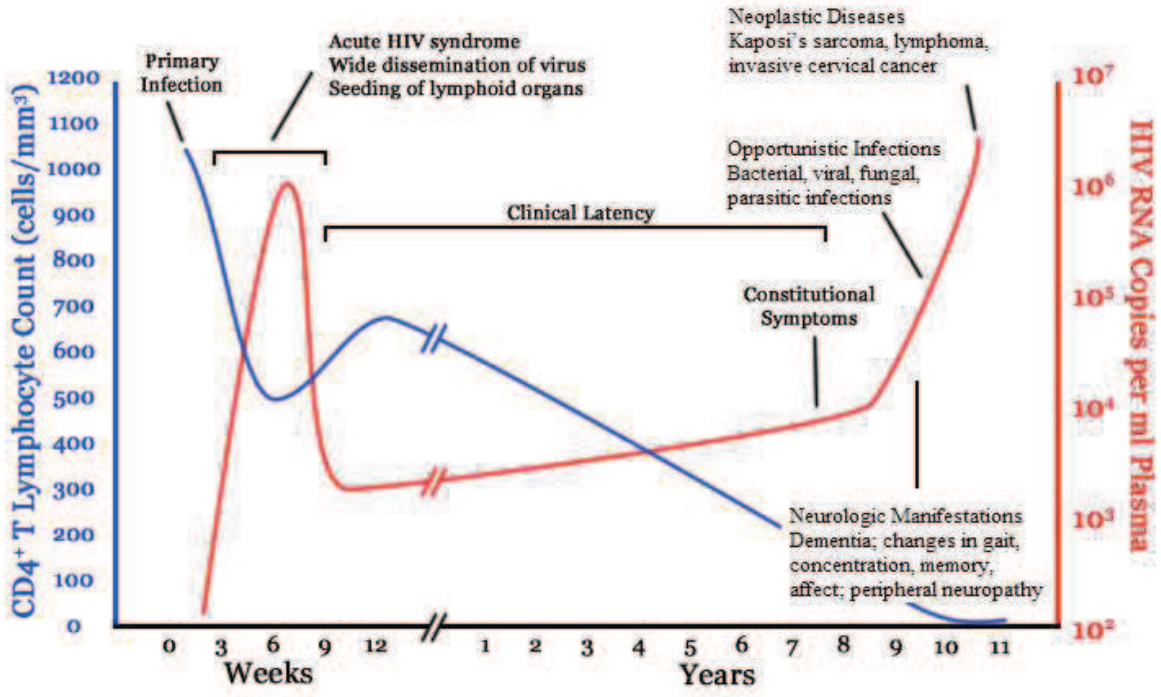

Fig.2. Schematic representation of the course of HIV-1 infection *in vivo* (Dewhurst, da Cruz et al. 2000).

As more HIV-1-infected patients were identified and diagnosed, an association between HIV-1 infection and the emergence of CNS pathologic and functional abnormalities became recognized. The spectrum of neurologic abnormalities associated with the nervous system infection was collectively referred as the AIDS dementia complex (ADC) or, more recently, HIV-1 dementia (HIVD). Approximately 30% to 60% of all HIV-1-infected individuals exhibit symptoms characteristic of HIVD (McArthur, Hoover et al. 1993), including dementia with progressive loss of cognitive functions, decreased memory, psychomotor retardation, headaches, motor deficits, seizures, and psychiatric dysfunction. Although HIVD may appear at any time during the progression of HIV-1 infection and is not necessarily temporally linked to the progression of the systemic immunologic dysfunction, it often appears late in the course of disease concurrent with low CD4-positive cell numbers and high viral titers in the peripheral circulation (Barresinoussi, Chermann et al. 1983).

II. HIV-1

II.1. Origin of the virus HIV-1

The analysis of two archival HIV-positive samples collected in 1959 and 1960 on territory of the Democratic Republic of the Congo (previously Zaire) showed that at that time the group M viruses had already diversified significantly suggesting that they had been evolving in humans since 1902–1921. Three hypotheses of global pandemic exist:

- The virus was transmitted to humans in the 1800s or early 1900s. It then would have remained isolated in a small, local human population until about 1930s, when it began spreading to other human populations and to diversify (Transmission Early Hypothesis).
- The virus was transmitted from chimpanzees to humans around 1930, and immediately began to spread and diversify in human populations (Transmission Causes Epidemic Hypothesis).
- Multiple strains of SIV were transmitted from chimpanzees to humans in the 1940s or 1950s (Parallel Late Transmisson Hypothesis).

It has been suggested that parallel transmission could have occured through oral poliovirus vaccinations adminestered in Central Africa between 1957 and 1960. Poliovirus was cultured in chimpanzee kidney cells that could have been contaminated with multiple SIVs.

The source of HIV-1 infection in humans was identified in a type of the West Africa chimpanzee (*Pan troglodytes troglodytes)*. It is believed that the chimpanzee version of the immunodeficiency virus (SIVcpz) most likely was transmitted to humans during the Civil War in Congo as a result of multiple determinants e.g. starvation and chimpanzee hunting. Normally, the hunter's body would have fought off SIV, but on a few occasions virus adapted itself within its new host and became HIV-1. Moreover, discovery of close simian relatives of HIV-1 and HIV-2 in chimpanzees (Huet, Cheynier et al. 1990) and sooty mangabeys (Hirsch, Olmsted et al. 1989) gave the evidence that AIDS had emerged in both humans and macaques as a consequence of cross-species infections with the lentiviruses from different primate species. It becomes clear that the HIV-1 and HIV-2 are the result of zoonotic transfer of viruses from infected primates in Africa (Hahn, Shaw et al. 2000).

A scooty mangabey origin of HIV-2 was proposed in 1989 (Hirsch, Olmsted et al. 1989) and subsequently confirmed by the presence of humans in Western Africa harboring HIV-2 strains resembling locally circulating SIVsmm infections (Gao, Yue et al. 1992).

On the other hand, it has been postulated that HIV-1 originated from three independent cross-species transmission of simian immunodeficiency virus (SIVcpz Ptt)

infecting chipmansees (*Pan troglodytes troglodytes)* in west-cntral Africa giving rise to pandemic (group M) and non-pandemic (groups N and O) clades of HIV-1 (Lihana, Ssemwanga et al.). The source of the less numbered group O of HIV-1 remains unclear since there are no ape viruses related to this group (Lemey, Pybus et al. 2004). The viruses from O group are likely originating from west central Africa and are believed to have either chimpanzee or gorilla origin.

More recently, new putative group designed P, was reported to be found in Cemeroonian patients (Vallari, Holzmayer et al.; Plantier, Leoz et al. 2009). The group P viral sequences, RBF168 and 06CMU14788, form a distinct HIV-1 lineage that includes SIV sequences from western gorillas (SIVgor; Gorilla gorilla gorilla), suggesting gropu P originated from gorillas (Van Heuverswyn, Li et al. 2007; Plantier, Leoz et al. 2009). Evolutionary analysis of the near-complete genome sequence further confirms that RBF168 strain is most closely related to SIVgor and similarity plotting further confirms relationship in all the regions of the genome (Lihana, Ssemwanga et al.).

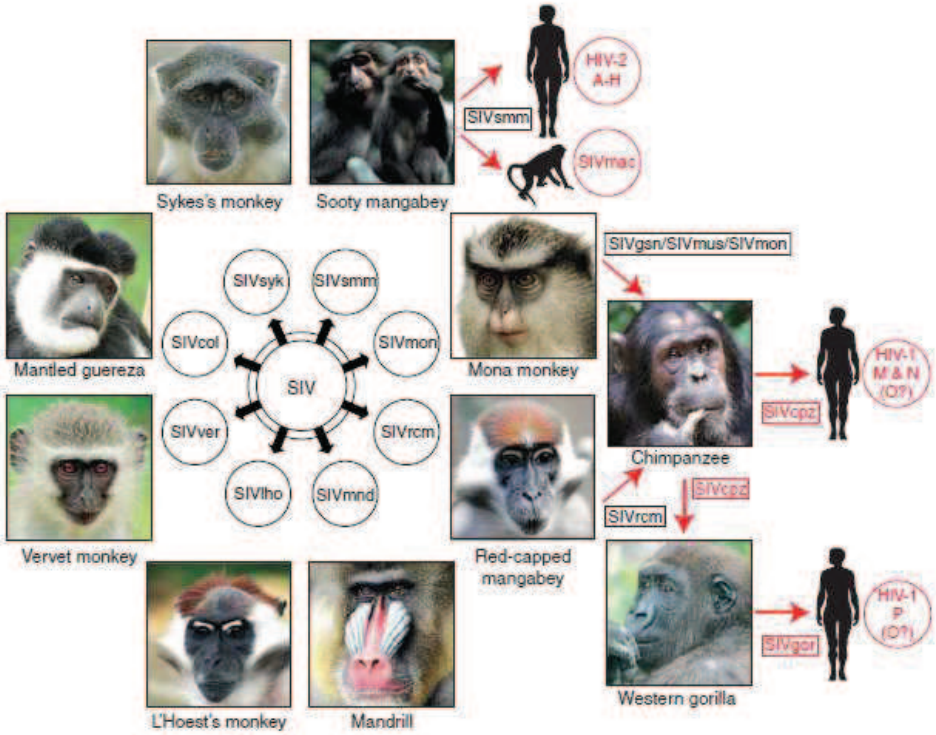

Fig.3. The origin of viruses causing human AIDS. The red circles represents known examples of cross-species transmissions together with the resulting viruses (Sharp and Hahn).

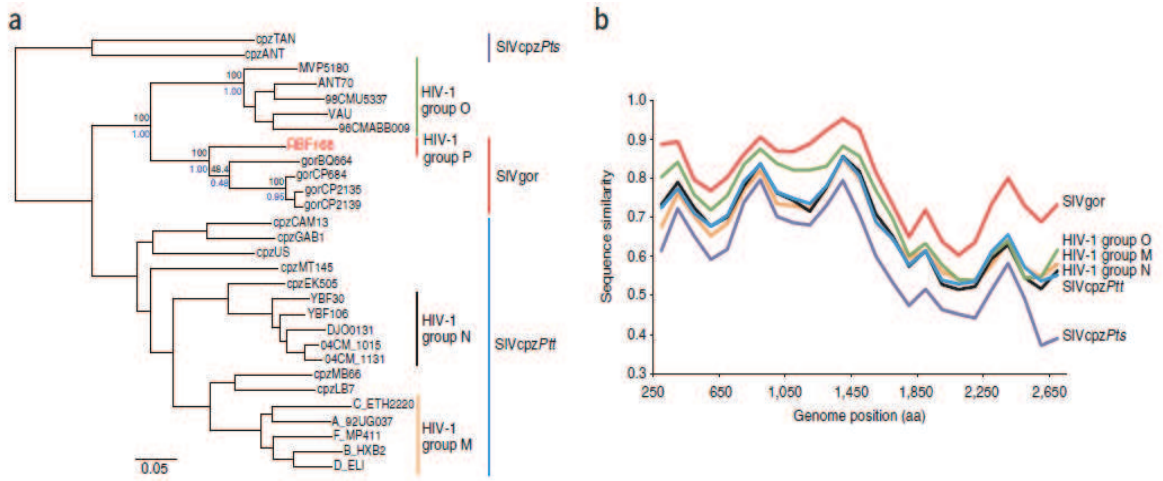

Fig.4. Evolutionary relationship of strain RBF168 to HIV-1, SIVcpz and SIVgor. (a) Maximum likelihood phylogeny inferred from concatenated amino acid alignments corresponding to the partial sequences available for SIVgorBQ664 (Takehisa, Kraus et al. 2009); 1,052 amino acid positions remained after stripping gap-containing sites. The support values (indicated for key nodes only) in black above the branches are from 1,000 maximum likelihood bootstraps (shown as percentages), whereas posterior probabilities from amino acid Bayesian analysis are shown in blue below the branches (shown as proportions). (b) Average sequence similarity (250 amino acid windows, 100–amino-acid increments) of RBF168 with representative strains of HIV-1 groups M, N and O, SIVgor, SIVcpz from Pan troglodytes schweinfurthii (SIVcpzPts) and Pan troglodytes troglodytes (SIVcpzPtt) across the concatenated translated gene sequence alignments (Plantier, Leoz et al. 2009).

Over decades, the virus slowly spread across Africa and later into other parts of the world. Scientists studying HIV-1 group M, responsible for almost 99% of all of the world's deaths from AIDS already had found many related subtypes, each with slightly different genetic structures and paths through the world. One, scientists discovered, had traveled east from Kinshasa toward Lake Victoria. One went south to Zambia, Botswana and South Africa. One spread all the way across the ocean to Haiti, then to the United States where it circulated during 10-12 years before first outbreak.

The earliest known case of HIV in human was a blood sample collected in 1959 from a man in Kinshasa, Democratic Republic of Congo. Genetic analysis of his blood sample suggested that HIV-1 may have stemmed from a single virus in the late 1940s or early 1950s. It is known that the virus has existed in the United States since at least the mid to late 1970s. From 1979-1981, rare types of pneumonia, cancer and other illnesses were reported in Los Angeles and New York. A number of gay male patients were presenting these uncommon illnesses and many died soon after. In 1982, public health officials began to use the term "acquired immunodeficiency syndrome" or AIDS to describe the occurrences of opportunistic infections, Kaposi's sarcoma and Pneumocystis carinii pneumonia in previously healthy men.

Formal tracking of AIDS cases began that year in the United States. The cause of AIDS is a virus isolated in 1983 (Coffin 1990). The virus was at first named HTLV-III/LAV (human T-cell lymphotropic virus-type III/lymphadenopathy- associated virus) by an international scientific committee. Later, this name was changed to HIV (human immunodeficiency virus).

II.2. Epidemiology

According to the World Health Organization since the beginning of the epidemic, more than 60 million people have been infected with the HIV virus and nearly 30 million people have died of AIDS. In 2009, there were an estimated 33.3 million people living with HIV, 2.6 million new infections and 1.8 million AIDS-related deaths. Africa and Asia have the highest reported prevalence rates while the lowest were found in industrialized countries such as Central and Western Europe and Australia. Since 2001, when the United Nations Declaration of Commitment on HIV/AIDS was signed, the number of new infections in sub-Saharan Africa is approximately 15% lower, with about 400,000 fewer infections in 2008. In East Asia new HIV infections declined by nearly 25% and in South and South East Asia by 10% in the same time period. In Eastern Europe, after a dramatic increase in new infections among injecting drug users, the epidemic has leveled off considerably. In the 2009 AIDS epidemic update, new HIV infections have been reduced by 17% over the past eight years. However, in some countries there are signs that new HIV infections are rising again (UNAIDS, 2010).

Fig.5. Number of adults and children living with HIV (source: UNAIDS, November 2010).

II.3. Classification of HIV

The virus HIV is a member of the *Lentivirus* genus, which is a part of the family of Retroviridae. The virus infects CD4 + lymphocytes causing their destruction with a half-lifetime of the less than two days. There are two types of HIV: HIV-1 and HIV-2. Both are transmitted by sexual contact, through blood and from mother to child and appear to cause clinically indistinguishable AIDS. However, it seems that HIV-2 is less easily transmitted and the period between initial infection and illness is longer than in the case of HIV-1. Worldwide, the predominant virus is HIV-1. The relatively uncommon HIV-2 type is concentrated in West Africa and is rarely found elsewhere.

The genetic analysis of HIV-1 showed great diversity. The strains of HIV-1 can be classified into four groups, which represent four separate cross-species transmission of simian immunodeficiency virus into humans:

- The group M, represents a pandemic form of HIV-1 Within this group at least nine genetically distinct subtypes of HIV-1are known: A, B, C, D, F, G, H, J and K. In the same group also belong 14 circulating recombinant forms (CRFs): CRF-01–AE, CRF-02–AG, CRF-03–AB, CRF-04–cpx, CRF-05–DF, CRF06–cpx, CRF07–BC, CRF08–BC, CRF-09–cpx, CRF-10–CD, CRF-11–cpx, CRF-12–BF, CRF-13–cpx, and CRF-14–BG. CRFs represent recombinant HIV-1 genomes that have infected two or more persons who are not epidemiologically related (Lihana, Ssemwanga et al.)
- The group O, discovered in 1990, represents less than 1 % of global HIV-1 infection and appears to be restricted to west-central Africa (Deleys, Vanderborght et al. 1990).
- The group N, a strain discovered in 1998 in Cameroon (Simon, Mauclere et al. 1998)- is extremely rare. So far only 13 cases of group N infection have been demonstrated (Vallari, Bodelle et al.).
- The group P, discovered in 2009 (Plantier, Leoz et al. 2009), is closely related to gorilla simian immunodeficiency virus.

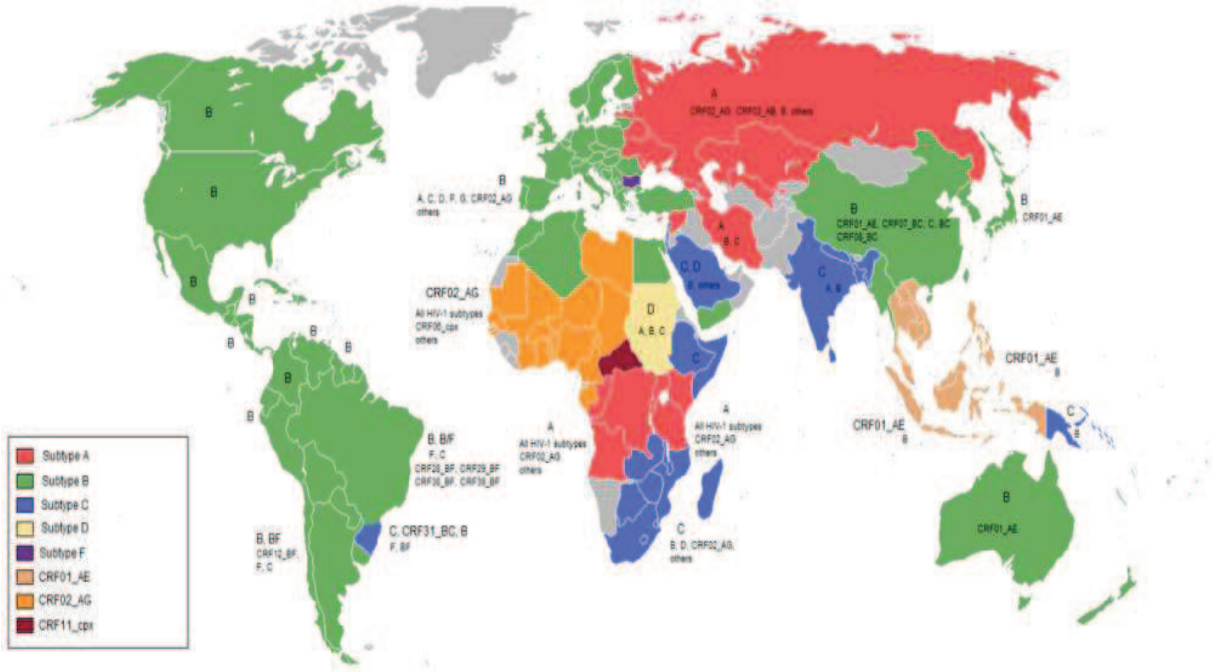

Fig.6. Worldwide prevalence of HIV-1 group M subtypes and CRF (Santos and Soares).

II.4. Structure of HIV-1 virus particles

Mature HIV-1 virions have spherical morphology of 100-120 nm in diameter. Each viral particle consists of 62% of proteins, 35% of phospholipids and 3% of nucleic acids.

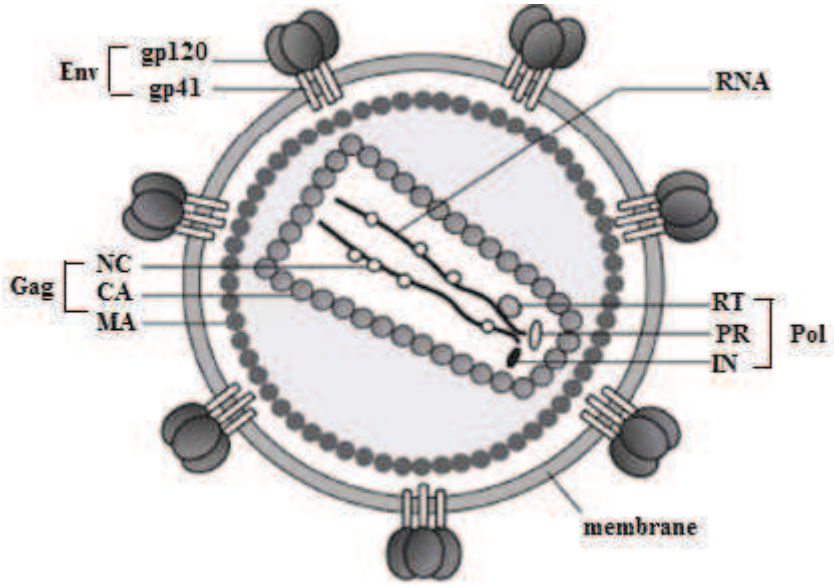

Fig.7. Schematic representation of a mature HIV-1 particle. Positions of the major viral proteins, the lipid bilayer, and the genomic RNA are indicated. Modified from Freed, 1998 (Freed 1998)

As all lentiviruses, the HIV-1 virus is enveloped by a lipid bilayer, derived from the membrane of the host cell. Exposed surface glycoproteins (SUgp120) are anchored to the virus via interactions with the transmembrane protein (TMgp41). The lipid bilayer also contains several cellular membrane proteins derived from the host cell, including major histocompatibility antigens, actin and ubiquitin (Arthur, Bess et al. 1992). A matrix shell comprising approximately 2000 copies of the matrix protein (MAp17) lines the inner surface of the viral membrane, and surrounds a conical capsid core particle comprising ca. 2000 copies of the capsid protein (CAp24). The capsid particle encapsidates two copies of the unspliced viral genome, which is stabilized as a ribonucleoprotein complex with ca. 2000 copies of the nucleocapsid protein (NCp7) and also contains three viral enzymes: protease (PR), integrase (IN) and reverse transcriptase (RT). HIV-1 encodes six additional proteins, often called accessory proteins – Vpr, Vif, Vpu, Nef ,Tat and Rev.

Both Vpr and Vif are incorporated into HIV-1 virions. Vpr is effectively packaged into the virions via interaction with p6 domain of Gag. According to a recent estimate the ratio of Vpr and capsid protein is 1:7 and HIV-1 particle contains about 275 molecules of Vpr and 1800 molecules of capsid (Muller, Tessmer et al. 2000). Vif is packaged into virions with genomic RNA as a nucleoprotein complex. While Vif is efficiently packaged into virions from acutely infected cells (60–100 copies per virion), packaging from chronically infected cells is very low (4–6 copies per virion) (Kao, Khan et al. 2003). Thus while the levels of viron associated Vpr are relatively high (100-400 copies per virion), the levels of virion associated Vif depend on type of infection and can be substantially lower (Okumura, Alce et al. 2008). As for Nef, little amount if any is incorporated into virions produced by chronically infected cells. Three additional accessory proteins that function in the host cell, Rev, Tat and Vpu, do not appear to be packaged.

IV. HIV-1 Genome

IV.1. Genome organization

The genome of HIV-1 consists of two (+) identical RNA strands of about 9.2 kb held together by noncovalent interactions involving a limited number of base pairs (Berkhout and Jeang 1989; Baudin, Marquet et al. 1993; Darlix, Lapadattapolsky et al. 1995). The genes in the viral RNA are flanked by 5'UTR and 3'UTRs. The unique sequences (U5 and U3) are located originally in the RNA genome only at the 5'- or 3'-end, respectively and the repetitive sequence (R) is located at both ends of the RNA genome.

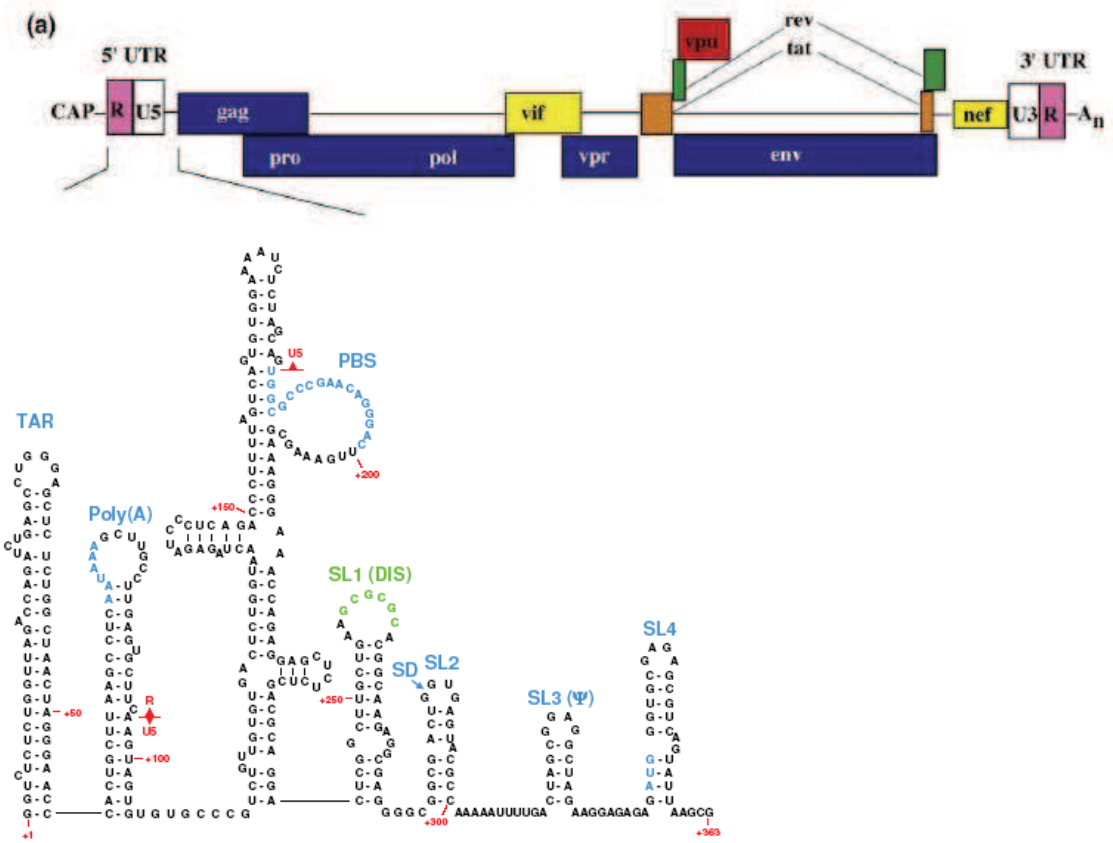

Fig.8. (a) Diagram of the HIV-1 genome showing location of the 5'-UTR and splice sites. (b) Representative secondary structures predicted for the HIV-1 5'-UTR (Lu, Heng et al.)

The repetitive sequence (R) of HIV-1 is relatively extended (97 nucleotides) as compared to other retroviruses. This sequence is present in two copies positioned at both ends of the viral genome. This region encodes two well-conserved stem-loop structures, the TAR and poly(A) hairpins.

The TAR (trans activation region) is essential for the Tat-mediated activation of transcription (Das, Klaver et al. 1999; Sarafianos, Das et al. 2001) and replication. However it does not play a major role in packaging (Das, Harwig et al. 2007) since effective genome packaging occurred for HIV-1 mutants, where the TAR hairpin and Tat gene were substituted by a tetracycline-inducible tetO-rtTA system (Verhoef, Marzio et al. 2001).

The TAR hairpin consists of a conserved 3-nt pyrimidine bulge able to bind to the viral Tat transactivator protein and an apical 6-nt loop that binds to the cyclin T1 subunits of the cellular transcriptional elongation factor (pTEFb)(Isel, Ehresmann et al. 1995; Wei, Garber et al. 1998; Richter, Ping et al. 2002).

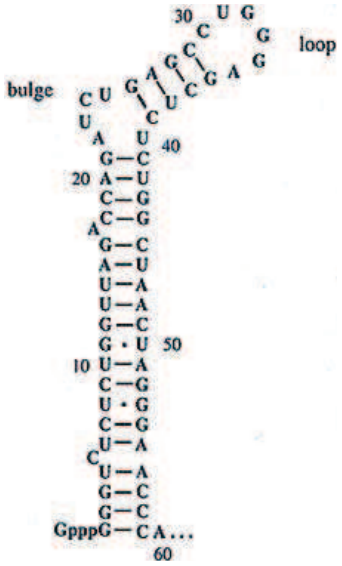

Fig.9.The HIV-1 TAR sequence and structure (Gottfredsson and Bohjanen 1997).

The poly(A) hairpin contains the AAUAAA polyadenylation signal and is important for the regulation of the polyadenylation process (Pollard and Malim 1998), which occurs within the 3'R region. Clever et al. showed that any mutation disrupting the poly(A) base paring leads to defects in genome packaging and viral replication (Clever, Eckstein et al. 1999). Although the 3'polyadenylation signal is known to function in mRNA maturation, little is known about the possible roles of poly(A) located at 5'UTR. The R region plays also a major role in reverse transcription, which is initiated near the 5'end of HIV-1 genome.

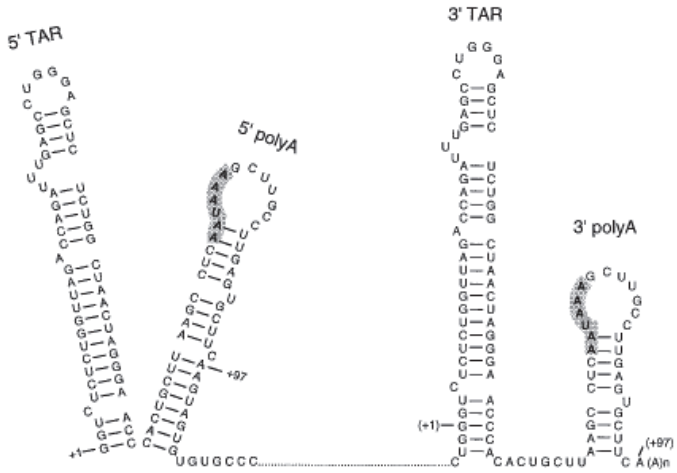

Fig.10. Tandem hairpin motifs at both ends of the HIV-1 genomic RNA (Das, Klaver et al. 1997).

The U5 region is a 84 nucleotides sequence firstly transcribed during the reverse transcription process. At 3' region of U5 is situated the PBS region (Prime Binding Site). It plays a critical

role in the replication by serving as the binding site for the human $tRNA^{Lys}$ RNA , the primer for reverse transcription. (Lu, Heng et al.).

Fig.11. Secondary structure of a portion of the 105 nt fragment of the HIV-1 genome containing the primer binding site (PBS) (Hargittai, Gorelick et al. 2004).

The unique region 3 (U3) is a 450 nucleotides long sequence, which contains the signals necessary for viral replication as well as sequences that promote and regulate transcription by RNA polymerase II, including binding sites for transcription activator SP1, TATA box and two copies of the 10 bp binding site for NF-κB factor. (Krebs et al.)

III.1.1. The Ψ domain

The retroviral Psi packaging element is a cis-acting RNA element identified in the genomes of the Human immunodeficiency virus (HIV) (Lever, Gottlinger et al. 1989) and Simian immunodeficiency virus (SIV). It is involved in regulating the packaging of the retroviral RNA genome into the viral capsid during replication (McBride and Panganiban 1996; McBride and Panganiban 1997; McBride, Schwartz et al. 1997). The 5'-UTR containing this domain is capable of directing the packaging of heterologous RNAs into VLPs (Hayashi, Shioda et al. 1992). Moreover Ψ deletion and mutations designed to disrupt base pairing in the stem led to a significant reduction in genome packaging (Luban and Goff 1994; McBride and Panganiban 1996; Clever and Parslow 1997). The Psi element is ~80–150 nucleotides in length, and located just upstream of the *gag* initiation codon (Lawrence, Stover et al. 2003). Its secondary structure is composed of four hairpins called SL1 to SL4 connected by relatively short linkers. All four stem loops are important for genome packaging and each of them, namely SL1, SL2, SL3 and SL4 have been independently expressed and structurally

characterized. Stem loop 1 (SL1) consists of a conserved hairpin structure with a palindromic loop sequence (Berkhout and vanWamel 1996). It is believed to promote dimerization of the viral genome through formation of a "kissing dimer" intermediate (Skripkin, Paillart et al. 1994). SL1 may also provide a secondary binding site for the viral Rev protein (Gallego, Greatorex et al. 2003). Stem-loop 2 (SL2) consists of a highly conserved 19 nt stem-loop which has been shown to modulate the splicing efficiency of HIV-1 mRNAs (Abbink and Berkhout 2008). Stem-loop 3 (SL3) consists of a highly conserved 14 nt stem-loop. HIV-1 SL3 is sufficient by itself to induce heterologous RNA into virus-like particles but its deletion does not completely eliminate encapsidation (Abbink and Berkhout 2008). Stem-loop 4 (SL4) consists of a highly conserved 14 nt stem-loop that is located just downstream of the *gag* start codon. It may exhibits both coding and non-coding roles.

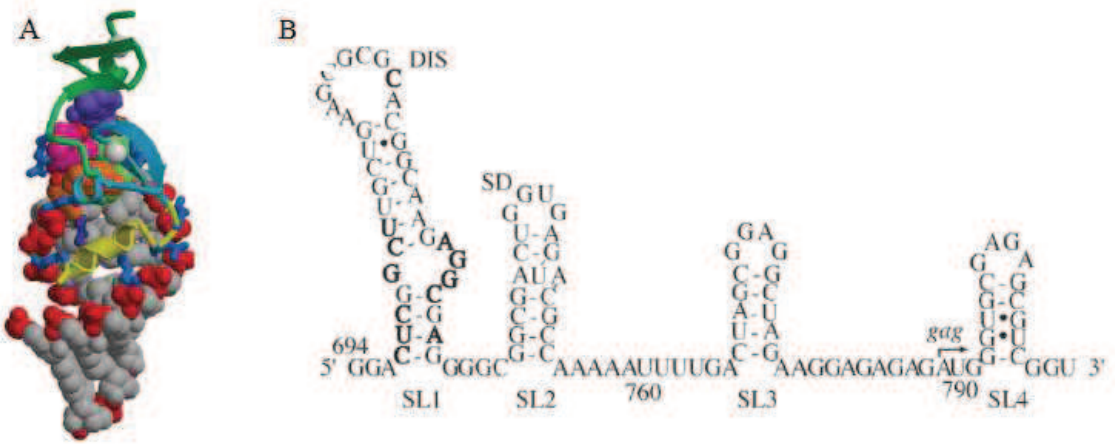

Fig.12. (A) NMR structure of Ψ hairpin bound to NC (in a ribbon format) (De Guzman, Wu et al. 1998). (B) Ψ signal of HIV-1 gRNA (Lawrence, Stover et al. 2003).

III.1.2. Other non coded regions among the viral genome

The PPT sequence

PPT is a 15-nt purine rich RNA sequence (5'-AAAAGAAAAGGGGGG-3') resistant to RNase H cleavage that serves as primer for plus (+) strand synthesis (Miles, Agresta et al. 2005; Welman, Lemay et al. 2007). While all retroviruses carry a PPT near the 3' end of the retroviral genome, defining the 5'boundary of the U3 region, several retroviruses, including lentiviruses, carry a second PPT near the center of the genome. Central polypurine tracts (cPPT) have mainly been described for lentiviruses, including visna virus, feline immunodeficiency virus, bovine immunodeficiency virus, equine infectious anemia virus, simian immunodeficiency virus (SIV), human immunodeficiency virus type 1 (HIV-1), and HIV-2, but they have also been found in spumaretroviruses and in the yeast retrotransposons

Ty1 and Ty3 (Blum, Harris et al. 1985; Heyman, Agoutin et al. 1995; Stetor, Rausch et al. 1999; Wurtzer, Goubard et al. 2008)

The RRE sequence

The Rev Response Element (RRE) resides within the env intron. According to computer-assisted RNA folding analyses, further confirmed by in vivo and in vitro structure probing analyses, this region is a 234-nt stem-and-loop structure. The RRE serves as docking site for Rev on RNAs that are confined to the nucleus (Freed and Martin 1995).

III.1.3. Coding regions

Through different open reading frames, three genes are transcribed:

The gag gene encodes a 55 kDa precursor called Pr55Gag. This polyprotein is proteolytically processed into the mature MA (matrix protein p17), apsid protein p24 (CA), nucleocapsid protein p7 (NC) and p6 protein. In addition, two peptides Sp1 and Sp2, are also generated by cleavage of Pr55Gag, on both sides of the coding region for NC.

The gag-pol gene encodes a large precursor: the Pr160Gag-pol that generates after cleavage, enzymatic viral proteins such as protease, integrase, and reverse transcriptase.

The env gene encodes the transmembrane Pr160env polyprotein precursor. Maturation occurs in the endoplasmic reticulum, and its cleavage by protease generates two cell membrane glycoproteins involved in virus-cell interactions: gp120 and gp41. By alternative splicing of mRNA, HIV-1 codes for proteins such as Tat, Rev, Vif, Vpu, Vpr, and Nef called "regulators" that contribute to the success of viral replication. .

IV. Viral proteins

IV.1. Envelope proteins

The envelope glycoproteins of HIV-1 are encoded by the viral env genes and synthesized as precursor proteins. Situated on the virus surface, envelope proteins are responsible for mediating virion attachment to cells and fusion of the viral and cellular membranes. This process is initiated by the interaction between SU and cell-surface CD4 receptors and the chemokine co-receptors, CCR5 and CXCR4. Sequential binding events are thought to trigger major structural rearrangements in the TM glycoprotein subunit that are critical for the membrane fusion process and viral entry (Roux and Taylor 2007)

The HIV-1 envelope glycoproteins consist of two noncovalently associated subunits, gp120 and gp41, that are generated by proteolytic cleavage of the precursor polypeptide gp 160 (Ashish, Garg et al. 2006).

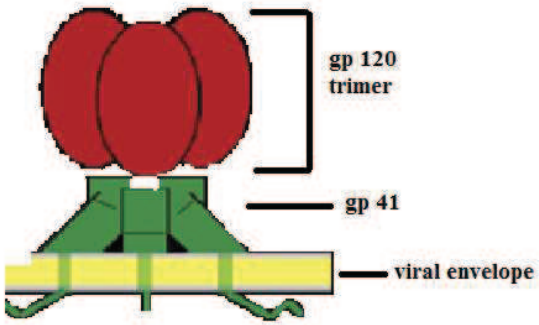

Fig.13. Schematic representation of a spike consisting of gp120 trimer and gp41 trimer (Leonard, Spellman et al. 1990).

The subunit SU (gp120) contains five variable regions (V1-V5), four of which (V1-V4) form surface-exposed loops with disulfide bonds at their bases (Frankel and Young 1998)

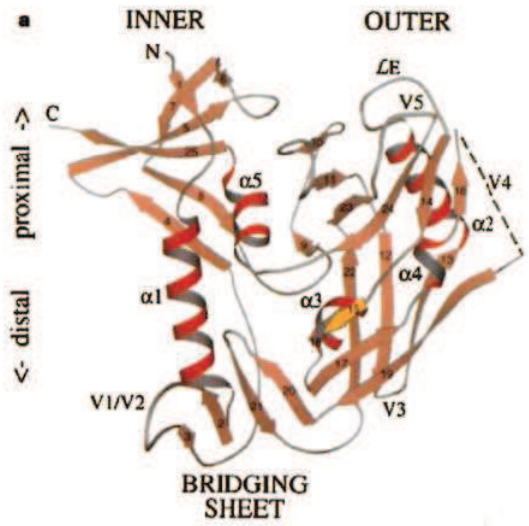

Fig.14. Structure of the HIV-1 SU core, determined for its complex with the two-domain fragment of CD4 and an antigen-binding fragment of a neutralizing antibody that blocks the chemokine-receptor binding. The yellow β-strand forms an antiparallel β-sheet with residues in CD4. (Kwong et al. 1998).

The ‘‘core’’ region of the HIV gp120 protein, for which crystal structures are known, lacks N- and C-terminal extensions, three variable (V1-V3) loops, and glycosylation (~50%). These

loop regions play an important role in molecular recognition and have been the limiting factor in resolving the crystal structure of the full-length gp120 molecule.

The gp120 glycoprotein binds sequentially to CD4 and chemokine receptors on cells to initiate virus entry. During natural infection, gp120 is a primary target of the humoral immune response, and it has evolved to resist antibody-mediated neutralization. Additionally, viral protein gp120 causes apoptosis of neuronal cells, inducing mitochondrial-death proteins like caspases which may influence the upregulation of the death receptor Fas leading to apoptosis of neuronal cells (Thomas, Mayer et al. 2009). Gp 120 is also known to activate STAT1 (Kwong, Wyatt et al. 2000) and to induce interleukins IL-6 and IL-8 secretion in neuronal cells (Yang, Akhter et al. 2009).

The subunit TM (gp41) protein consists of ectodomain transmembrane domain and a C-terminal segment interacting with MA. The TM glycoprotein is composed of 172 amino acids ectodomain, a 21 amino acid membrane-spanning domain (MSD) and 150 amino acid cytoplasmic tails. Three N-terminal helices have the capacity to form a triple-stranded coiled-coil that enables the hydrophobic fusion peptide to insert into the target cell membrane. The membrane spanning domain of gp41 is primary responsible for anchoring the envelope glycoproteins on the lipid bilayer (Gamble, Vajdos et al. 1996)

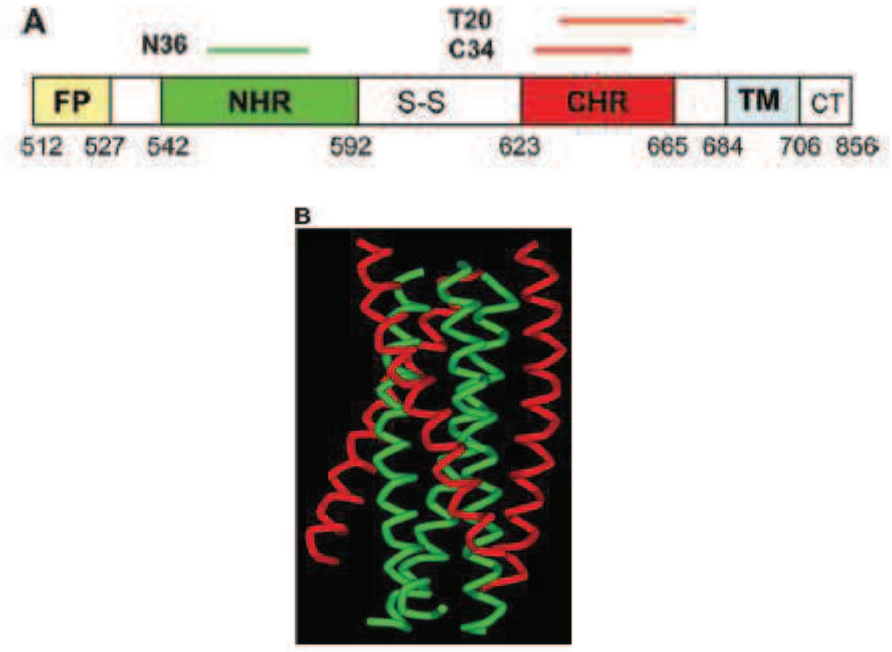

Fig.15. Structure of the HIV-1 gp41 core. (a) Schematic view of the gp41 functional regions. FP, fusion peptide; S-S, disulfide bond loop; TM, transmembrane domain; CT, cytoplasmic tail. The residue number of each region corresponds to its position in gp160 of HIV-1_{HXB2}. (B) Cristal structure of the six-helix bundle modeled by the peptides N36(green) and C34(red) (Turner and Summers 1999).

The fusion of the two membranes is the first step towards releasing the virion core into the cell for replication. Gp 41 also keeps gp 120 attached to the viral envelope. Situated in the membrane gp41 binds to gp 120, rather than gp 120 attaching to the envelope directly.
Small-angle X-ray scattering studies on a fully glycosylated recombinant soluble gp120-gp41 ectodomain showed a structure with several prominent protrusions, some of which (e.g.V3 loop) undergo significant conformational rearrangement upon CD4 binding (Turner and Summers 1999). Displays a highly variable sequence, V3 loops maintains a rather conserved β - turn structure, with a disulfide-stabilized base and minimal sequence variation at the tip of the loop. It is believed that V3 loop is partially occluded by the V1/V2 loop in the unliganded state and is an important target of neutralizing antibodies.

IV.2. Structural proteins

IV.2.1. Matrix protein (MA)

MA is the N-terminal component of the Gag polyprotein and is important for targeting Gag and Gag-Pol precursor proteins to the plasma membrane prior to viral assembly. In the mature viral particle, the 132-residue MA protein lines the inner surface of the virion membrane (Scarlata and Carter 2003). The HIV-1 matrix protein consists of five α-helices, two short 3_{10} helical stretches and a three-strand mixed β-sheet. Helices I-III and 3_{10} helices pack about a central helix (IV) to form a compact globular domain that is capped by the β-sheet (Turner and Summers 1999). Two discrete features of MA are involved in membrane targeting : an N-terminal myristate group and basic residues located within the first 50 amino acids. In addition to targeting Gag and Gag-Pol to the membrane, MA also helps incorporating Env glycoproteins with long cytoplasmic tails into viral particles.
In addition to its function in the viral assembly, MA facilitates the infection of non dividing cell types, principally macrophages. Bukrinsky et al. (Bukrinsky, Haggerty et al. 1993), proposed that first NLS (Nuclear localization signal) within the HIV-1 PIC is presented in the N-terminal region of p17gag MA. Mutation of two lysines at position 26 and 27 was shown to block HIV-1 replication in terminally differentiated primary macrophages but not in proliferating cells. However, three studies could not confirm the presence of an NLS in MA (Freed, Englund et al. 1995; Freed, Englund et al. 1997). The phenotype of HIV-1 mutants in the N-terminal MA NLS also remained controversial. More recently, MA has been reported to have a Chromosomal region maintenance 1 (CRM1)-dependent nuclear export signal (NES). Mutations in this NES at position 18 and 22 of MA were shown to cause nuclear

localisation/retention of viral RNA and severely impair HIV-1 infectivity. Furthermore, the NES has been proposed to override a presumably masked NLS in the context of the p55gag polyprotein. In summary, although there is no agreement on the existence of a NLS in HIV-1 MA (Bukrinsky, Haggerty et al. 1993; Fouchier, Meyer et al. 1997; Haffar, Popov et al. 2000), there appears to be some consensus that mutations in the N-terminal region of MA have a moderate effect on virus infectivity in macrophages as well as other dividing cell types. Since such an effect is also detected in single-cycle assays, it is likely to involve some early, post-entry event (Fassati 2006).

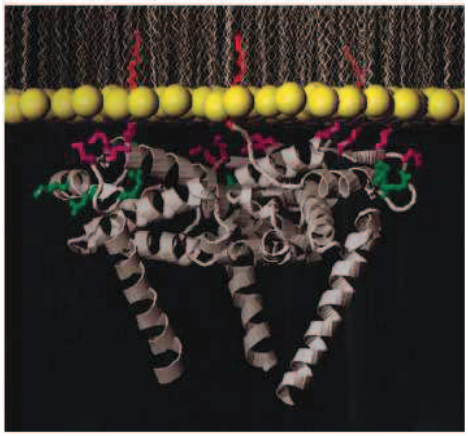

Fig.16.Model of the trimeric HIV-1 matrix protein interacting with a lipid membrane. Essential and nonessential basic residues are colored in magneta and green, respectively, and the N-terminal myristoyl groups are in red (Turner and Summers 1999).

IV.2.2. Capsid protein (CA)

CA is the second component of the Gag polyprotein and forms the core of the virus particle, with ~ 2000 molecules per virion. CA is subdivided into two domains, an N-terminal (residues 1-145) and a C-terminal (residues 146-231).

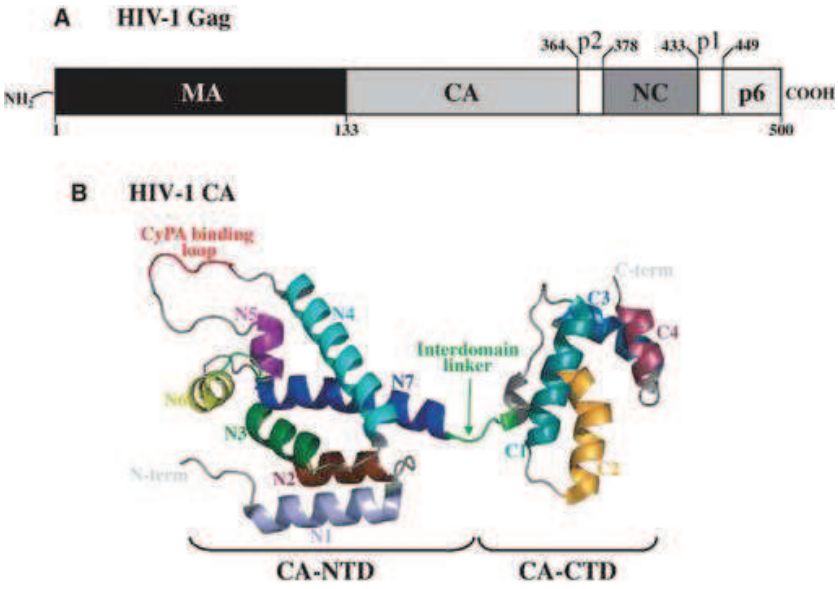

Fig.17. (A) Linear representation of the HIV Gag protein CA. (B) X-ray crystal structure of HIV-1 CA (Mascarenhas and Musier-Forsyth 2009).

The N-terminal domain (NTD) consists of five long helices forming a stable coiled-coil structure, two short ones, two λ-hairpins, and a Pro-rich loop. This domain is important for viral infectivity, by participating in viral uncoating through its association with a putative cellular chaperone, cyclophilin A (CypA) (Turner and Summers 1999).

CypA is the most abundant member of a ubiquitous family of peptidyl-prolyl isomerases and binds to the capsid (CA) domain of human immunodeficiency virus type 1 (HIV-1) and SIVcpz Gag proteins (Luban, Bossolt et al. 1993). Consequently, it is quite efficiently packaged into HIV-1 and SIVcpz virions, with about 1 molecule of CypA incorporated per 10 Gag molecules (Franke, Yuan et al. 1994; Thali, Bukovsky et al. 1994). The CypA-Gag interaction can be blocked by an immunosuppressive drug, cyclosporine A (CsA), and its analogues, and this manipulation inhibits the replication of most HIV-1 strains in most cells in vitro. In addition, mutation of residues G89 or P90 of HIV-1 CA, which constitute the core of the CypA binding site, both disrupt CypA binding and confer a substantial replication defect in human cells consistent with the notion that the CypA-CA interaction is important for HIV-1 replication (Hatziioannou, Perez-Caballero et al. 2005)

The C-terminal half (CTD) of CA contains four conserved helices and a highly conserved sequence among retroviruses known as the major homology region (MHR). The role of the MHR region has been investigated using mutagenesis strategies. Various mutations within the MHR block viral replication at different and distinct stages, such as assembly, maturation, and infectivity (Provitera, Goff et al. 2001), indicating that MHR may play a role in Gag interactions with the host membrane and/or with viral RNA (Provitera, Goff et al. 2001).

IV.2.3. Nucleocapsid protein (NC)

NC is the third component of the Gag polyprotein. In its mature form, NC coats the genomic RNA inside the virion core. NC is 55 residues long and contains two zinc fingers (of the CCHC type) flanked by basic amino acids. All three NC forms : NCp15 (NCp7-sp2-p6), NCp7(1-71) and NCp7(1-55) proteins have been detected in budding HIV-1 virions (Lapadattapolsky, Derocquigny et al. 1993)

NC plays a role in the dimerization (Navia, Fitzgerald et al. 1989) and selective encapsidation of genomic RNA. NC is also involved in reverse transcription and virus assembly. The NC structure and functions will be presented in section VIII.

IV.2.4. p6

The protein p6 comprises the C-terminal 51 amino acids of Gag and is important for incorporation of Vpr during viral assembly. This small peptide contains the late domain which is required for the pinching off of the newly assembled virion from the host membrane.

Within the p6 region of HIV-1, the prolin-rich motif PTAP(P) appears to play critical roles in the exocytosis of the assembled particles. Scarlata et al. discovered that this region directly interacts with Tsg101, a host component of the cellular endocytosis machinery (Scarlata and Carter 2003).

Tsg101 is an orthologue of the yeast vacuolar protein sorting protein 23 (Vps 23) and an inactive homologue of Ub conjugating (E2) enzymes (Scarlata et all, 2003). Its main function being recognizing ubiquitinated cargo, TSG101 also proved to be essential for the budding process of HIV-1 virions. In this process, TSG101 is recruited from internal site of the infected cell to the budding site to aid in the release of the HIV-1 virus particles (Chen, Liu et al.) The Tsg101 UEV domain features the PTAP binding pocket represented by amino acid residues: Thr 58, Val 61, Tyr 63, Tyr 68, Asn 69, Ile 70, Pro 71, Thr 92, Met 95, Pro 139, Val 141, Phe 142, Ser 143 and Arg 144. This binding pocket, which under normal conditions binds the protein Hrs (Hepatocyte growth factor-regulated tyrosine kinase substrate), can also

bind the HIV-1 Gag protein. The PTAP(P) motif recruits a multi-component complex containing proteins involved in the trafficking machinery (Garrus, von Schwedler et al. 2001). Another important feature on the Tsg101 that may be involved in the normal trafficking or viral budding process is the ubiquitin binding pocket. The ubiquitin binding pocket of the Tsg101 UEV domain has eight specific residues that are involved: residues 43 through 49; and residue 88. The flanking or end residues are Valine 43 and Phenylalanine 88. These residues are highlighted because they mark the beginning and end of the ubiquitin binding pocket. The binding of ubiquitin is thought to strengthen the Tsg101 - HIV-1 Gag interaction and it is speculated that it assists the complex into the trafficking lane and onto the membrane for budding. A third structural feature of the Tsg101 UEV domain that may be indirectly involved in the overall trafficking and viral budding is amino acid residues occupying the C-terminal end of the UEV domain

V. Viral enzymes

V.1. Protease

Protease is the first protein of HIV-1 structurally characterized (Debouck, Gorniak et al. 1987; Farmerie, Loeb et al. 1987; Wlodawer, Miller et al. 1989). All retroviral proteases are aspartic proteases. This class of enzymes contains a conserved active-site triplet Asp-Thr/Ser/Gly and includes such cell-derived enzymes as pepsin, renin, chymotrypsin, penicillopepsin, and cathepsin D and E (Davies 1990). In contrast to their cellular counterparts, retroviral proteases are smaller, less efficient, and act as symmetrical homodimers with two identical subunits contributing towards the active site (Tozser, Weber et al. 1992). Although retroviral PR generally function best at acidic pH 4.5-6.5, they display significant *in vitro* activity up to physiological pH 7.0-7.5 (Kotler, Danho et al. 1989). Recombinant forms of retroviral PR also require a specific solvent composition including high ionic strength and polyethylene glycol to enhance conformational stability, substrate affinity and catalytic activity (Jordan, Zugay et al. 1992).

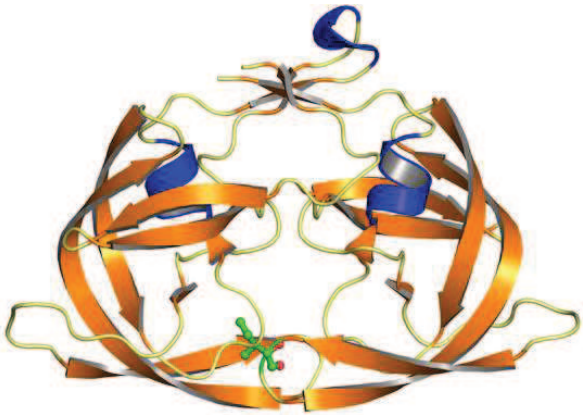

Fig.18. 3D structure of HIV-1 protease complexed with MVT 101 inhibitor (Torbeev, Raghuraman et al.).

During the late-phase of viral replication, HIV-1 PR cleaves viral Gag and Gag-Pol polyproteins at a limited number of sites to release mature structural and functional proteins. The role of HIV-1 PR during the early-phase remains controversial. Processing of cytoskeletal and sarcomeric proteins including vimentin, desmin, actin, myosin and tropomyosin (Shoeman, Honer et al. 1990) PR may be important in regulating the transport of PICs to the nucleus (Bukrinskaya, Brichacek et al. 1998).

V.2. Reverse transcriptase

HIV-1 RT is an asymmetric heterodimer composed of two subunits. The larger p66 subunit is 560 residues long and exhibits all the enzymatic activities of RT. The DNA polymerase domain of HIV-1 RT adopts in solution the right hand conformation with four defined subdomains (Kohlstaedt and Steitz 1992). The fingers are located at residues 1–85 and 118–155, the palm at residues 86–117 and 156–236, the thumb at residues 237–318, and the connection to the RNase H is located at residues 319–426 (Jacobo-Molina, Ding et al. 1993). The RNase H domain extends approximately beyond residue 440. The smaller p51 subunit is about 440 residues long and is identical to the N-terminal portion of the p66. The p51 is cleaved from a p66 subunit by the viral PR after association of two p66 subunits to generate p66/p66 homodimers (Sluis-Cremer, Arion et al. 2004) the p51 subunit stabilizes the heterodimer but may also participate in binding the tRNA primer. This subunit can also affect the RNase H activity (Sevilya, Loya et al. 2001; Sevilya, Loya et al. 2003). The fingers, palm, thumb and connection subdomains in the p51 subunit (except for the C-terminus of the connection, fold similarly to the corresponding subdomains in the p66. All p66 subdomains, along with the thumb and connection subdomains of p51, participate in binding the nucleic

acids, but the RNase H domain plays only a minor role in this binding. The connection subdomains of both subunits, together with the thumb of the p51 portion, form the ‘‘floor’’ of the binding cleft (Jacobo-Molina, Ding et al. 1993). HIV-1 RT binds the nucleic acid substrate in a configuration that places the substrate in direct contact simultaneously with both the DNA polymerase and RNase H active sites. The distance between the two active sites is about 60 Å (Sarafianos, Das et al. 2001). This allows positioning the substrate so that 17 nts (for DNA–DNA) or 18 nts (for RNA–DNA) separate the two sites on the nucleic acid substrate. DNA synthesis is an ordered reaction in which RT first binds its primer-template substrate and places the 3’-OH group of the primer terminus at the priming site (P site) that is located next to the polymerase active site. Comparison of crystal structures of the unliganded RT with structures of RT bound to its nucleic acid substrate shows that the binding results in a change of the position of the p66 thumb from ‘‘close’’ to ‘‘open’’ conformation (Hsiou, Ding et al. 1996). The flexibility of the thumb allows movements from the ‘‘close’’ position, in which the thumb touches the tip of the fingers to the ‘‘open’’ position, in which the thumb moves about 30^0 away from the fingers.

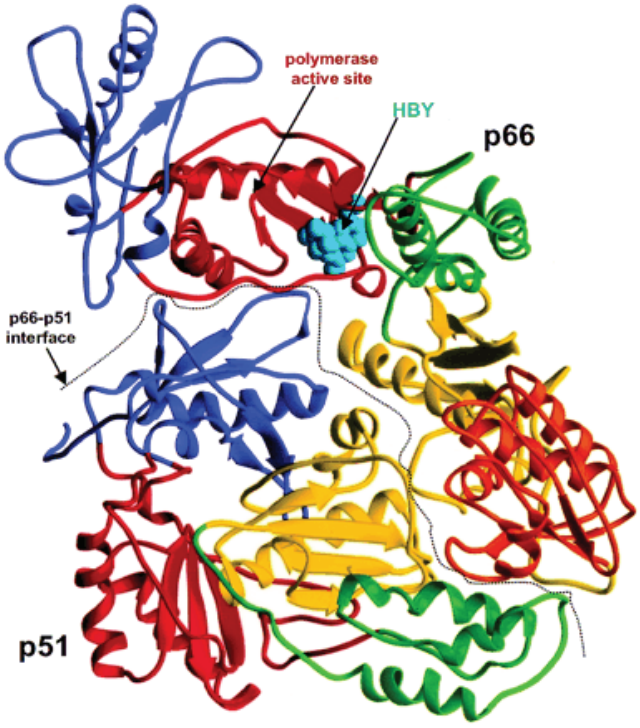

Fig.19.Sructure of HIV-1 RT with a bound NNRTI(Non-Nucleoside Reverse Transcriptase Inhibitors. The p66 subunit is on the upper right; the p51 subunit is on the lower left. The interface between the subunits is shown by a dotted line (Turner and Summers 1999).

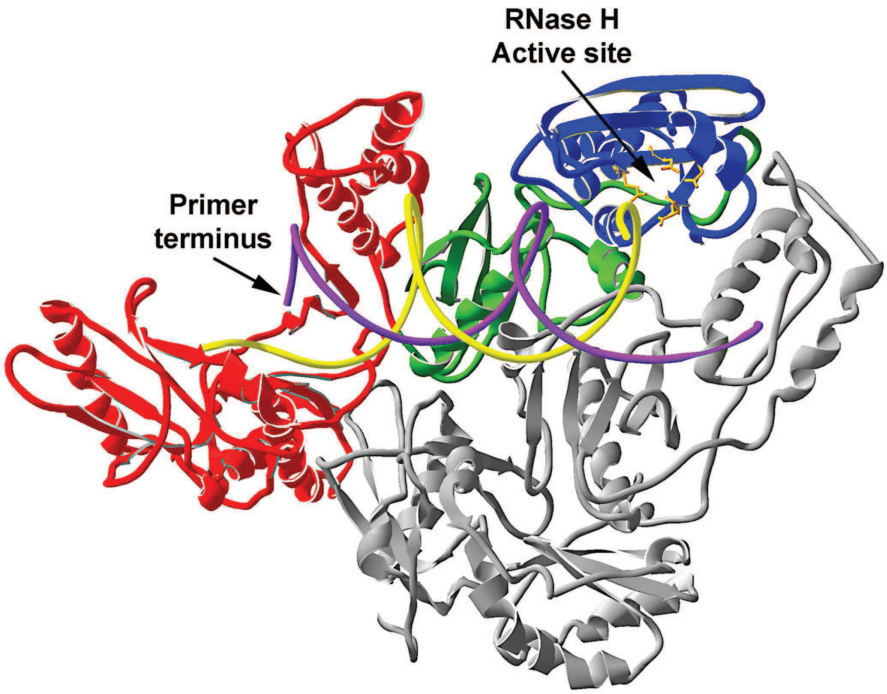

Fig.20. Ribbon diagram of the co-crystal structure of HIV-1 reverse transcriptase with a bound RNA template and DNA primer (pdb entry 1HYS) (Sarafianos, Das et al. 2001). The polymerase (p66 residues 1–318), connection (p66 residues 319–437) and RNase H (p66 residues 438–553) domains are drawn in red, green, and blue, respectively with the p51 subunit shown in gray. The RNase H active site is indicated with the four key acidic residues drawn in yellow ball and stick. The primer terminus of the DNA primer strand (purple) is indicated with the RNA template strand shown in yellow (Champoux and Schultz 2009)

The DNA polymerase active site is composed of three highly conserved Asp residues at positions 110, 185 and 186, located within the palm subdomain of p66. The carboxylate moieties bind two metal ions, probably Mg^{2+} in vivo, facilitating the incorporation of new dNTPs into the primer. The precise alignment of the catalytic residues of RT, the 3'-OH group of the primer and the phosphate of the incoming dNTP allows a nucleophilic attack of the 3'-OH on the a phosphate group, consequently liberating a pyrophosphate molecule that leaves the active site as the fingers open.

The RNase H activity of HIV-1 RT degrades the RNA strand in the RNA-DNA heteroduplex during DNA synthesis. In addition to the removal of the template RNA and the primer tRNA, it also produces the PPTs for the (+) DNA strand synthesis and eventually hydrolyses them (Nowotny, Gaidamakov et al. 2005). The structure of HIV-1 RT RNase H shows a high structural similarity to E. coli RNase H, most remarkably in the catalytic cores, despite the fact that the primary sequence identity between those two proteins is merely about 20% . However, it should be emphasized that the specific activity of the bacterial enzyme is at least 100-fold higher than that of the complete retroviral RTs. Moreover, the isolated HIV-1 RT

RNase H domain is by far less active than the intact RT molecule. This is probably due to the inherent low capacity of the RNase H to bind the primer-template substrate that is mostly bound during synthesis by the DNA polymerase domain (Herschhorn and Hizi 2010).

V.3. Integrase

Integrase (IN) is a 32-kDa protein with 288 amino acids, which is cleaved to its functional form from the pol polyprotein. Integrase catalyzes the viral and host DNA integration, involving: (i) 3′-processing, i.e. cleaving 3′-OH extremities of viral DNA, (ii) strand transfer process that leads to the integration of 3′-processed viral and host DNA by a trans-esterification reaction, resulting in a five base pair stagger in host DNA and (iii) gap filling and ligation, where the five base pair staggering is repaired by the host cell's repair mechanism (Delelis, Carayon et al. 2008).

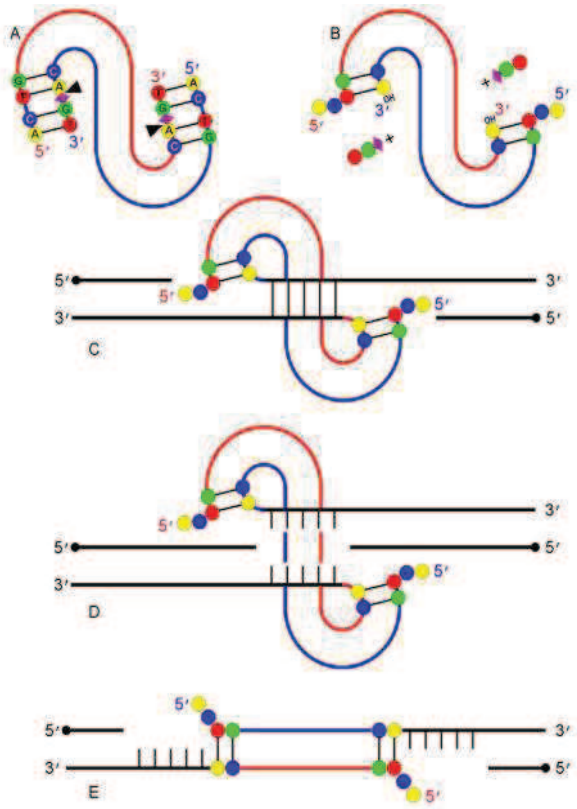

Fig.21. A schematic representation of the reaction catalyzed by retroviral IN during an infection cycle**.** In the processing step (A→B), the 3′ ends of viral DNA (colored molecule) are nicked (arrowheads) before the phosphate group (diamond) of the conserved terminal GT dinucleotide (colored beads, A=yellow, C=blue, G=green, T=red), leading to a DNA molecule with a 5′ overhang and a free 3′ OH group on each strand. In the joining step (B→C), host DNA (black) is nicked with a five-nucleotide stagger (vertical bars) on the two strands, and the free 3′ ends of the viral substrate are joined to both host strands, preserving DNA polarity. Panels D and E are equivalent to C and are presented to illustrate the topology of the final DNA product (not shown), which is

created from molecule E by cellular DNA repair enzymes, which remove the overhanging viral 5′ dinucleotides and seal the gaps on both sides of the integrated viral DNA. In the final product, the viral insert is flanked by the repeated stagger sequence, and begins with the conserved TG sequence at each 5′ end (Jaskolski, Alexandratos et al. 2009).

When the structural features are considered, IN possesses three distinct domains (Delelis, Carayon et al. 2008), the N-terminal zinc-binding domain (residues 1–50), which is required for 3' processing and strand transfer in vitro, binds viral DNA sequences and promotes IN multimerisation (Engelman, Bushman et al. 1993), catalytic core domain (CCD) from 55 to 212 amino acids responsible for the catalytic activity. This domain contains the D, D-35E triad coordinating divalent ions and is conserved in other retroviral integrases as well as in retrotransposon proteins such as the Tn5 transposase (Haren, Ton-Hoang et al. 1999).
The last, C-terminal domain (CTD) (Hung, Holbrook et al. 2000) from 220 to 288 amino acids, expresses non-specific DNA binding activity and also stabilizes the IN–DNA complex (Engelman, Hickman et al. 1994), while the residues 46–54 and 213– 219 form coiled linkers.
IN activity was shown to increased in the presence of cellular proteins (Turlure, Devroe et al. 2004), in particular, the transcriptional coactivator LEDGF/p75 interacting with HIV-1 IN (Cherepanov, Maertens et al. 2003) as well as with other lentiviral integrases (Cherepanov 2007) and its expression is required for proviral integration and subsequent production of HIV-1 virions (Emiliani, Mousnier et al. 2005). The function of LEDGF (Lens epithelium derived growth factor) is to target IN to chromosomes of infected cells (Maertens, Cherepanov et al. 2003). LEDGF tethers lentiviral IN to host chromatin in the nucleus (Llano, Vanegas et al. 2004; Llano, Vanegas et al. 2006) and plays a critical role in directing PICs to active genes during integration (Hare, Shun et al. 2009) LEDGF also protects IN from proteosomal degradation and can stimulate IN catalysis *in vitro* (Meehan and Poeschla)
LEDGF contains a pair of small structural domains: an ∼92 residue PWWP domain at its N-terminus, responsible for binding to an as yet unidentified component of chromatin, and the IN binding domain (IBD, residues 347–429) within its C-terminal portion. The CCD and NTD of IN were both implicated in LEDGF binding: while the CCD is minimally sufficient, the NTD is required for high affinity binding. Deletion of the HIV-1 IN NTD, or a mutation destabilizing zinc coordination within this domain (His-12 to Asn), greatly reduced the interaction with LEDGF. Mass spectrometry analysis and the fitting of known atomic structures in cryo negatively stain electron microscopy (EM) maps revealed that the

functional unit comprises two asymmetric integrase dimmers and two LEDGF/p75 molecules (Michel, Crucifix et al. 2009)

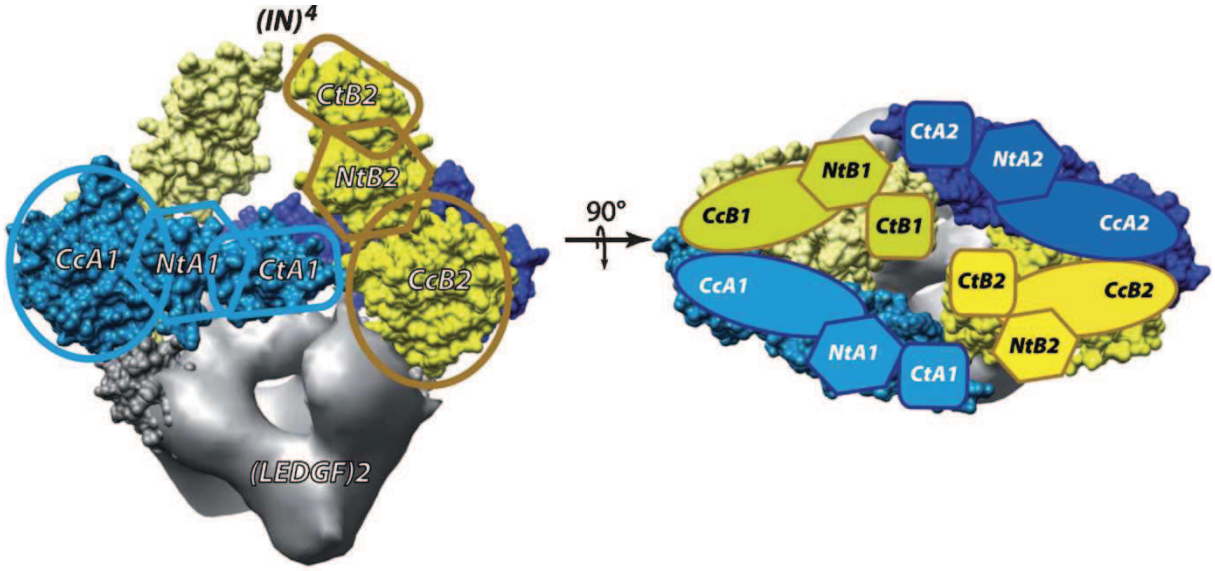

Fig.22. Integrase domain organization. (A) Two perpendicular views of the (IN)4–(LEGDF)2 complex. Each IN/LEDGF complex contains 4 IN molecules (A1, A2, B1 and B2) organized in two IN dimers (1 and 2). The different IN monomers are represented with different colors: monomer A1 in light blue, A2 in dark blue, B1 in light yellow and B2 in yellow. Monomers 1 and 2 are related by a two-fold axis. The density of LEDGF (grey) is obtained by subtracting the model from the EM map (Michel, Crucifix et al. 2009).

VI. Regulatory proteins

VI.1. Tat (TransActivator of Transcription)

The HIV-1 transactivator of transcription, a small basic protein with a variable length of 86-104 amnioacids (Daly, Cook et al. 1989), encoded by two exons, is one of the early regulators of the viral life cycle, which plays a pivotal role in HIV-1 replication because it enhances transcription through binding to the TAR hairpin at the 5'end of newly formed RNA transcripts. Important features in the TAR hairpin are the highly conserved 3-nucleotide (nt) pyrimidine bulge that binds the Tat protein and the apical 6-nt loop to which the transcriptional elongation factor pTEFb binds in a Tat-dependent manner (Ammerman, Fisk et al. 2008). Upon TAR binding, the kinase component of pTEFb, cyclin-dependent kinase 9 (CDK9), can phosphorylate the C-terminal domain of RNA polymerase II, which enhances the processivity of the elongating polymerase (Draper 1999; Mayer, Rajkowitsch et al. 2007). pTEFb also directs the recruitment of TATA box binding protein to the LTR promoter and thus stimulates the assembly of new transcription complexes (Doetsch, Furtig et al.).

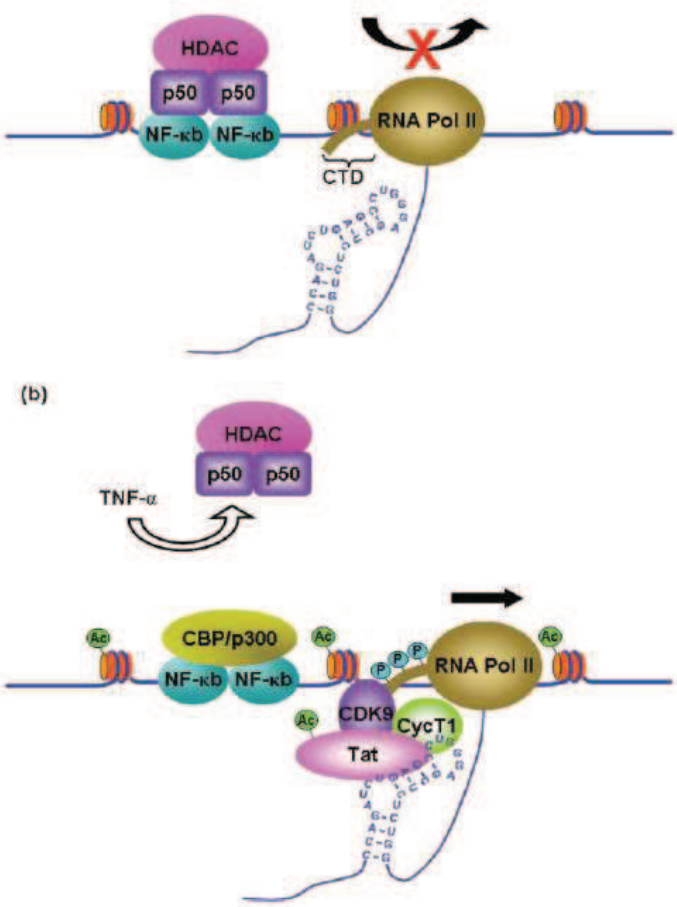

Fig. 23. Schematic representation of the role of HIV-1 Tat in the synthesis of full-length viral mRNA. (Romani, Glashoff et al.) (a) NF-κB, p50 and HDAC1 complexes bind to the latent HIV-1 LTR and induce histone deacetylation and repressive changes in chromatin structure of HIV-1 LTR. In the absence of Tat, althoght RNA polymerase II initates synthesis of the virus transcripts, it fails to complete synthesis of full-length transcripts. (b) In the presence of simulations e.g. TNF-α, the complex inducing latency, p50 and HDAC1, are removed from LTR. The CBP/p300 complex binds to promoter and acetylates surrounding histones. It also mediates acetylation of Tat by PCAF. Tat interacts with P-TEFb complex to recruit the stem-loop structure, TAR, which acts as promoter element in the transcribed 5' end of the viral LTR.

Several other, nontranscriptional functions of Tat in the viral life cycle have been suggested for example, Tat was shown to influence HIV-1 RNA splicing (Jablonski, Amelio et al.), capping (Chiu, Coronel et al. 2001), translation (Braddock, Powell et al. 1993) and reverse transcription. Moreover, Tat(1-86) was found to be as efficient as the nucleocapsid protein NCp7, a major nucleic acid chaperone of HIV-1, in promoting cTAR/dTAR annealing, and could act cooperatively with NCp7 during the annealing reaction (Boudier, Storchak et al.)
Tat has been proposed to interact with a large number of cellular proteins, and to inhibit the cellular RNA interference mechanism (Das, Harwig et al.)

Additionally, Tat has been suggested to modulate the expression of cellular genes (Li, Lee et al. 2005). For instance, it has been proposed that Tat up-regulates the expression of number of cytokines, as well as HIV-1 co-receptors CCR5 and CD25 receptors in HIV-1 infected cells (Zheng, Yang et al. 2005; Mayol, Munier et al. 2007; Stettner, Nance et al. 2009). Tat also down regulates the gene encoding the major histocompatibility complex (MHC) class I (Matsui, Warburton et al. 1996). However, the transactivation effect of Tat is not limited only to the infected cells since it was reported that Tat is able to enter uninfected cells and exert its activity on the responsive genes (Ju, Song et al. 2009), leading to the induction of apoptosis and immunosupression (Bennasser and Bahraoui 2002; Poggi and Zocchi 2006; Gupta, Boppana et al. 2008).

VI.2. Rev (Regulatory of virion expression)

Rev is a 19-kDa phosphoprotein located mostly in the nucleus/nucleoleus (Malim, Bohnlein et al. 1989) but it has been shown to shuttle between nucleus and cytoplasm (Daelemans, Costes et al. 2004). Rev consists of several distinct domains. :

The arginine-rich domain (RQARRNRRRRWRERQR), located at the N-terminus of Rev, acts as a nuclear localization signal (NLS). It is responsible for Rev nuclear location together with sequence specific interaction with a stem loop RNA target sequence RRE (Cochrane, Perkins et al. 1990; Pollard and Malim 1998).

Also at the N-terminus of Rev, a small domain of 15 aa (EDLLKAVRLIKFLYQ) was identified as the nuclear inhibitory signal (NIS). Its main function is to maintain the nuclear domain sub-cellular distribution and Rev activity (Kubota, Siomi et al. 1989).

A third essential domain, located between 73 and 84 amino acids of the C-terminal region of Rev, is a leucine-rich sequence (LQLPPLERLTLD) that serves as a nuclear export signal (NES) and interacts with cellular proteins involved in the export of viral mRNA.

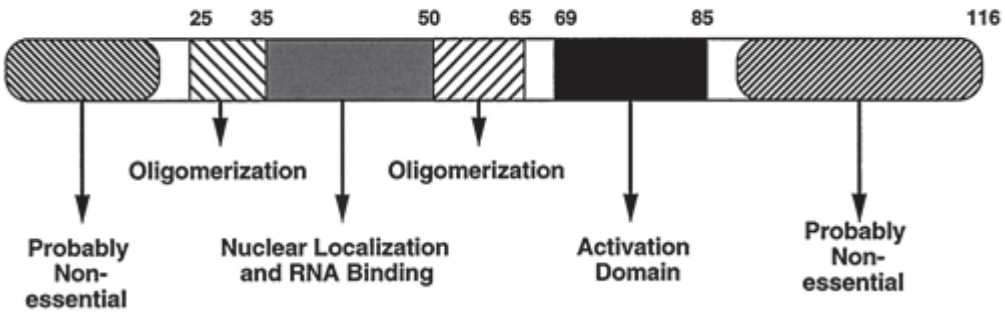

Fig.24. Schematic representation of Rev domains (Suhasini and Reddy 2009). The RRE binding domain is located between amino acid 35-50 in HIV-1 Rev, and is rich in arginine residues. This domain is flanked by

sequences important for oligomerization. The black box represents the activation domain (Van Ryk and Venkatesan 1999).

VI.3. Vpr (Viral Protein R)

Vpr is a 96 amino acid protein incorporated efficiently into virions. It contains three amphipathic helices spanning residues (17-33), (38-50) and (54-77) mutually oriented to generate a central hydrophobic core surrounded by two flexible N- and C-terminal domains (Morellet, Roques et al. 2009). This hydrophobic core is required for Vpr-Vpr interaction *in vitro* and in human cells (Chen, Kremer et al.; Singh, Tungaturthi et al. 2001; Bolton and Lenardo 2007; Fritz, Didier et al. 2008). Vpr plays a pivotal role in the HIV-1 physiopathology through the recruitment of a number of cellular proteins (Andersen and Planelles 2005; Le Rouzic and Benichou 2005). During the course of virion assembly, this regulatory protein is encapsidated in the nascent particle through a direct interaction with the p6 part of Gag (Paxton, Connor et al. 1993; Bachand, Yao et al. 1999; Muller, Tessmer et al. 2000). Vpr likely also participates to the nuclear import of the HIV-1 pre-integration complex (PIC) in nondividing cells e.g. macrophages (Fouchier, Meyer et al. 1998; Le Rouzic, Mousnier et al. 2002; Waldhuber, Bateson et al. 2003).

In addition to its nuclear uptake function, Vpr can also induce G2 cell cycle arrest prior to nuclear envelope breakdown and chromosome condensation, and sustained expression can lead to the death of T cells by apoptosis (Fletcher, Brichacek et al. 1996).

VI.4. Vif (Viral Infectivity Factor)

Vif is a 192-residue protein that is important for the production of infectious mature virions. Its primary function is to negate the action of APOBEC3G, a naturally occurring cellular inhibitor of HIV replication. Vif acts by binding to APOBEC3G, inducing its degradation within infected cells and reducing its level in progeny virions (Piguet, Chen et al. 1997). Moreover, Vif neutralizes a potent intercellular defense pathway that protects mammals from the retroviruses and retro-elements that continually invade their genomes (Rose, Marin et al. 2004). The expression of Vif is highly conserved among lentiviruses. Interestingly, the defective phenotype of Vif is cell-type dependent and is determined by the virus-producing cells e.g. the HeLa cell line is permissive for Vif mutants and virus produced from this cell line is fully infectious regardless of the target cells used. On the other hand, primary lymphocytes and macrophages are nonpermissive (Freed 2001).

VI.5. Nef (Negative Regulatory Factor)

Nef is a N-terminally myristoylated 206-amino acid protein that reduces the levels of cellular CD4. Nef facilitates the routing of the CD4 receptors from the cell surface and Golgi apparatus to lysosomes, resulting in receptor degradation and prevention of inappropriate interactions with Env (Greenway and McPhee 1997). It has been also proposed that Nef can serve as a direct bridge between CD4 and the cellular endocytic machinery by interacting with β-COP (β'-coatomer protein) and adaptins which link proteins in the Golgi apparatus and plasma membrane to clathrin-coated pits (Moarefi, Sicheri et al. 1997). By down regulation of CD4, Nef can enhance incorporation of Env into virions, promote virus particle release and possibly affect CD4+ T-cell signaling pathways. Nef can also down regulate the expression of MHC class I molecules, which may help protect infected cells from killing by cytotoxic T-cells (LeGall, Prevost et al. 1997). This can be probably achieved by impairing the ability of cytotoxic T lymphocytes to detect and eliminate virus-expressing cells (Collins, Chen et al. 1998). Nef contains a consensus SH3 domain binding sequence (PXXP) that mediates binding to several Src-family proteins e.g. Src, Lyn, Hck, Fyn, thus regulating their tyrosine kinase activities (Cohen, Subbramanian et al. 1996; Kerkau, Bacik et al. 1997). Although in general the effects of Nef deletion on virus replication in culture are limited, it has been reported that in a single-cycle assay, Nef stimulates virus infectivity (Frankel and Young 1998)

Nef mutant viruses exhibit decreased rates of viral DNA synthesis following infection . However, this defect can be overcome if Nef is supplied in *trans* in virus-producing cells but not in target cells, suggesting possible roles of Nef in virus assembly, maturation, or entry.

VI.6. Vpu (Viral Protein U)

Vpu is an 84-residue oligomeric integral transmembrane protein with a N-terminal 24-residue hydrophobic membrane-spanning domain, which functions both as a signal peptide and membrane anchor and a C-terminal cytoplasmic tail (Miyauchi, Kim et al. 2009). The cytoplasmic domain consists of two amphipathic α-helical domains of opposite polarity, separated by an unstructured region containing two conserved seryl residues which are phosphorylated by protein kinase CK-2. The cytoplasmic domain is crucial for CD4 degradation while the membrane anchor domain plays a crucial role in regulation of virus release and in formation of cation-selective ion channels (Opella, Park et al. 2005). Similarly to Nef, Vpu can down regulate cell surface expression of MHC class I proteins (Daecke, Fackler et al. 2005).

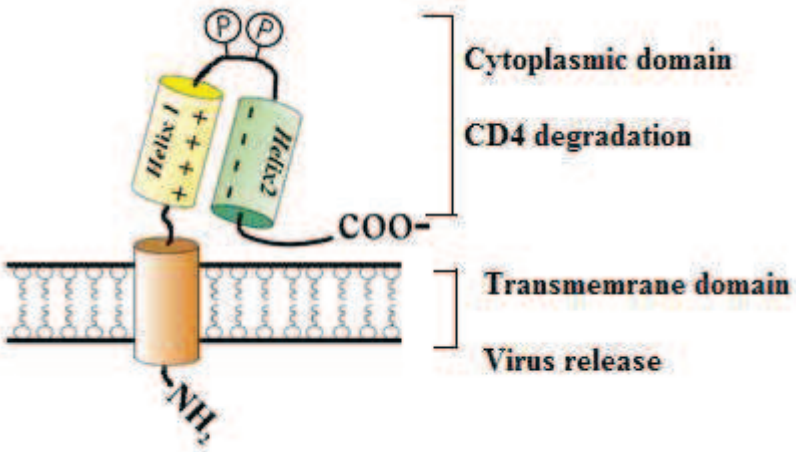

Fig.25. Structural domains of Vpu (Strebel K. 1996)

VII. The life cycle of HIV-1 virus

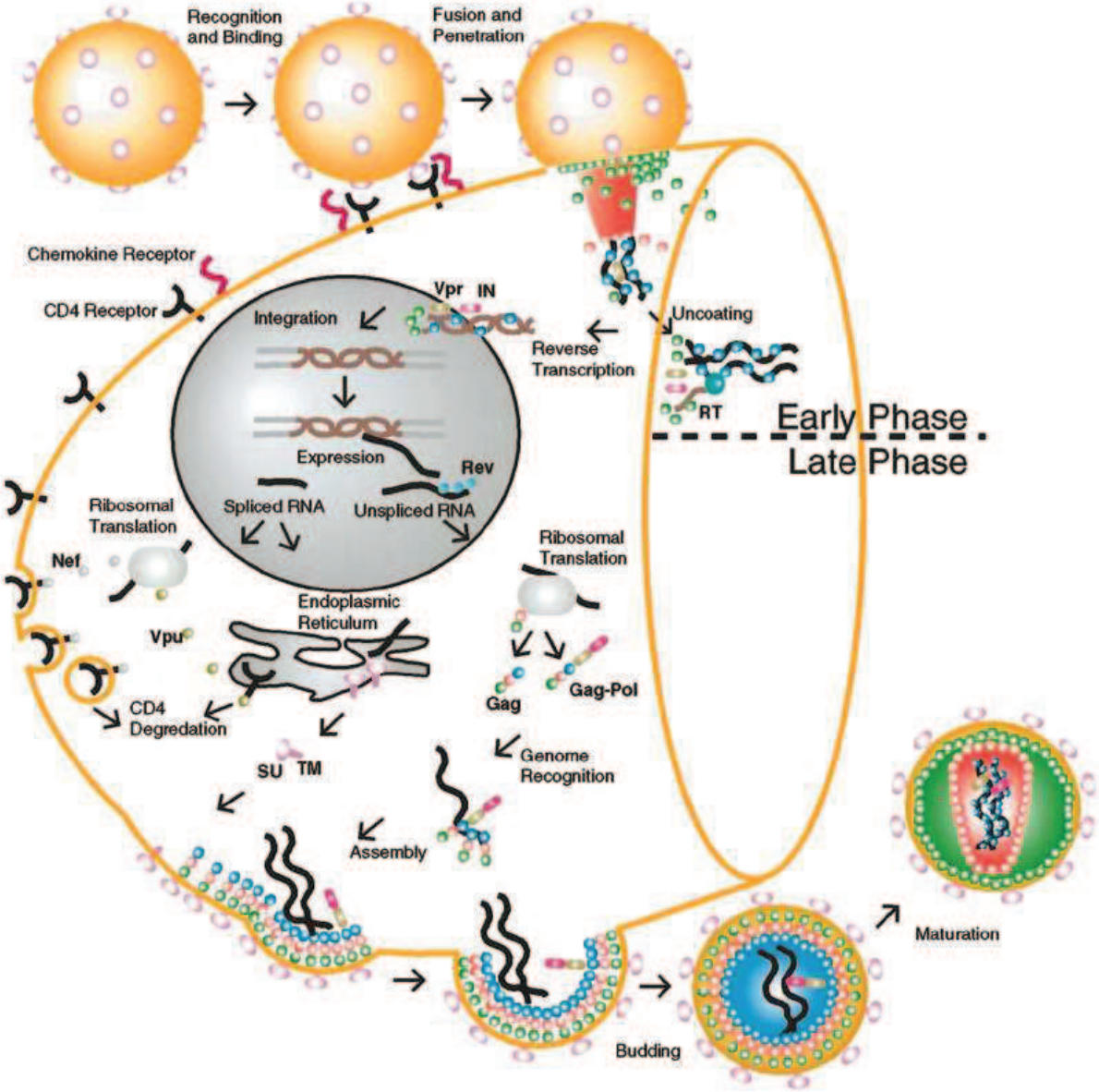

Fig.26. Main steps of the viral life cycle (Turner and Summers 1999)

The viral life cycle is divided into early and late phases. The early phase begins with the recognition of a target cell by the mature virion and involves all processes leading to integration of the genomic DNA into the chromosome of the host cell.

The late phase begins with the regulated expression of the integrated proviral genome and involves all processes up to virus budding and maturation. Studies of different group showed that non integrated proviral DNA can be also transcribed giving rise to proteins such as Tat (Wiskerchen and Muesing 1995)and Nef (Spina, Guatelli et al. 1995; Wu 2004)

VII.1. The early phase

VII.1.1. Virus entry

HIV-1 can efficiently infect cells that express two types of receptors: the CD4 receptor and co-receptors s from the chemokine receptor family, typically CCR5 or CXCR4. However, the most efficient infection process is mediated by direct cell to cell infection through the virological synapse (Jolly and Sattentau 2004).

The virus enters host cells through a pH-independent membrane fusion event, which results in the release of core particles into the cytoplasm. Then, HIV-1 entry and membrane fusion follow the endocytosis pathway (Gallaher 1987; Harter, James et al. 1989; Zhou, Xu et al. 2007).

When interacting with a new target cell, gp 120 initially contacts the N-terminus of CD4. This interaction results in the exposure of a highly conserved co-receptor binding site of the gp120 molecule (Lobritz, Ratcliff et al. 2010). This coreceptor binding site interacts with the N-terminal end of either the CCR5 or CXCR4 coreceptor (Freed 2001). Further coreceptor binding is mediated by the amino acids of the crown of the V3 loop.

Conformational changes in the envelope glycoprotein further expose the fusion peptide, a sequence of 15 hydrophobic amino acids located at the N-terminus of gp 41, which inserts into and destabilizes the host cell membrane (Arhel). At this stage, gp 41 becomes an integral component mutual to the viral envelop and host membrane. However, further structural transitions in gp41 are necessary to provide the significant change in free energy required to drive membrane fusion (Melikyan, Markosyan et al. 2000; Myszka, Sweet et al. 2000). Prior to fusion, gp41 folds back on itself forming a hairpin structure, the function of which is to bring into close proximity the fusion peptide associated cellular membrane and the integral gp41 associated viral membrane (Lobritz, Ratcliff et al.).

The process of hairpin structure formation is mediated by two helical regions in the ectodomain of gp41, HR1 and HR2 (N-terminal and C-terminal Heptad Repeat region, respectively). HR1 and HR2 form a stable 6-helix bundle, resulting in the localization of the fusion peptide and transmembrane domains at the same end of the molecule. This reorientation and release of free energy drive the fusion of the viral and host cell membranes.

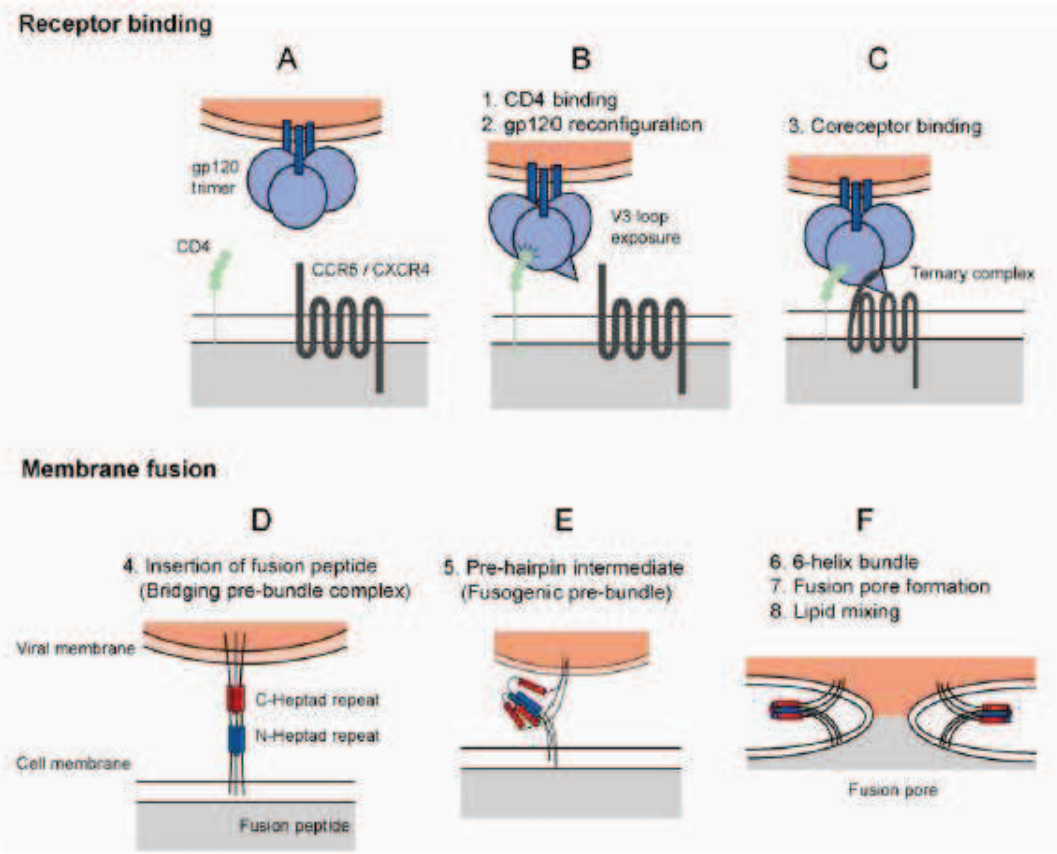

Fig.27. Schematic representation of virus HIV-1 entry (Lobritz, Ratcliff et al.) HIV-1 Entry. **(a)** Virus entry into host cells is mediated by the envelope glycoprotein. The functional unit of envelope is a trimer composed of three gp41 molecules (blue bars) and three gp120 molecules (blue spheres), which are associated by non-covalent interactions. **(b)** Virus entry is initiated by the attachment event, binding of gp120 to host cell CD4 (green spheres). Binding to CD4 results in reconfiguration of the gp120 molecule. The bridging sheet is formed and gp120 is primed for interaction with a coreceptor molecule. **(c)** CD4-bound gp120 interacts with a coreceptor, either CCR5 or CXCR4. **(d)** After interaction with the coreceptor, a hydrophobic gp41-derived peptide (the fusion peptide) is inserted into the host cell membrane. (HIV-1 gp120, CD4 molecules, and coreceptor molecules have been removed for simplification, and to allow focus on the transition in gp41 during fusion). This event anchors the virus to the host cell, and the gp41 molecule acts as a bridge between the viral and cellular membranes. Structural rearrangements within the gp41 molecule are mediated by two triple stranded coiled-coils, the C-terminal (red) and N-terminal (blue) heptad repeat domains. **(e)** Metastable prefusion intermediates occur during the reconfiguration of the gp41 domains. **(f)** The C- and N-terminal heptad repeat regions pack into one another forming a stable sixhelix bundle. This results in a close approximation of viral and host cell membrane and the formation of a fusion pore. The initial fusion pore enlarges as the membrane lipids mix, ultimately leading to a fusion pore of critical size for release of the viral core into the cytoplasm.

VII.1.2.Uncoating

HIV-1 and other lentiviruses are unique among orthoretroviruses in their ability to replicate efficiently in metabolically active non-dividing cells as a result of the active nuclear import of their genome across the nuclear membrane of interphasic nuclei (Bukrinsky, Sharova et al. 1992). Retroviruses such as the Murine Leukaemia Virus (MLV) gain access to the nuclear chromatin following the disassembly of the nuclear membrane that occurs during mitosis (Roe, Reynolds et al. 1993). For such retroviruses, evidence suggests that the viral capsid accompanies the viral genome into the nuclear compartment and participates in interaction with the chromatin indicating that uncoating is not required prior to nuclear import. HIV and other lentiviruses enter the nuclei via the nuclear pore and, although commonly assumed, it is by no means certain that they can use an alternative route of entry during mitosis. HIV-1 uncoating, defined as the loss of viral capsid occurring within the cytoplasm of infected cells before the viral genome enters into the nucleus, is an obligatory step of viral early infection. Uncoating accompanies the transition between reverse transcription complexes (RTCs) and pre-integration complexes (PICs). RTCs are simply defined as HIV-1 complexes that undergo reverse transcription, during which they convert their single-stranded positive RNA viral genome into double-stranded DNA (Telesnitsky and Goff 1993; Basu, Song et al. 2008). The RTC genomes are either RNA or RNA-DNA intermediates of reverse transcription. In contrast, PICs no longer contain any RNA but only the double-stranded DNA. PICs are per definition integration- competent HIV-1 complexes and can integrate efficiently into a target DNA in vitro (Arhel; Ellison, Abrams et al. 1990). The uncoating process is progressive and may occur several hours after the viral entry (Zennou, Petit et al. 2000).

VII.1.3. Reverse transcription

Reverse transcription proceeds in a series of steps, which utilize several cis-acting elements in the viral genome.

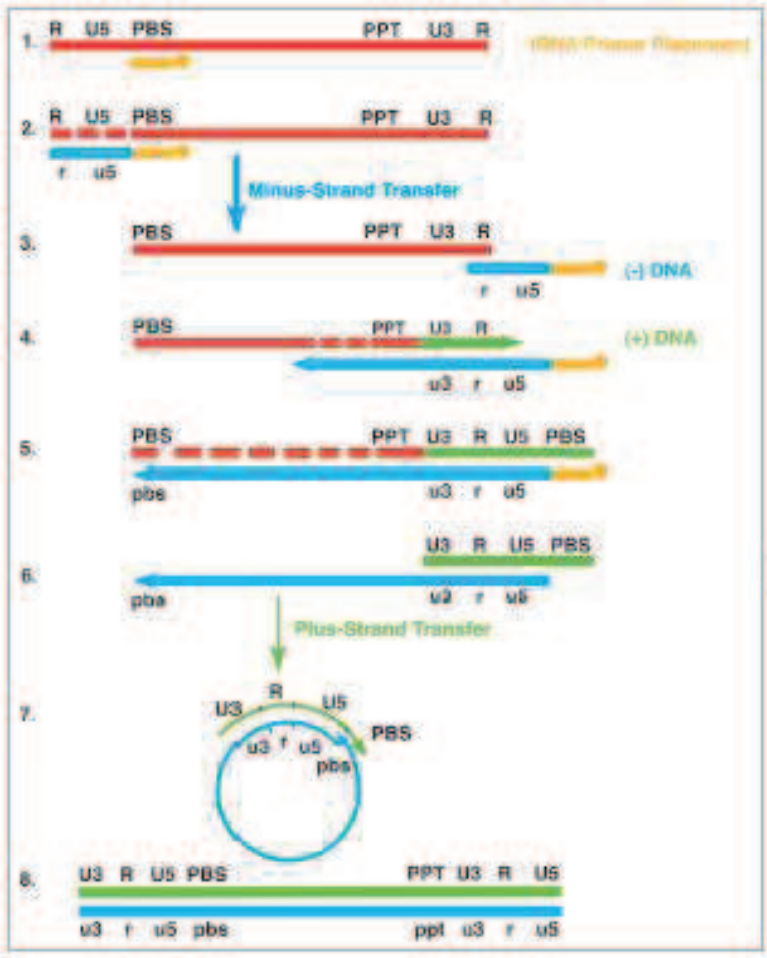

Fig.28. Process of reverse transcription of the HIV-1 genome. (Levin, Mitra et al.) The explanation is presented in the text.

Reverse transcription is initiated through a primer a tRNA molecule that binds to the primer binding site (PBS). Catalyzed by all LTR retroelements and retroviruses reverse transcription is initiated by the synthesis of the first (-) DNA strand that is complementary to the viral (+) strand RNA genome. This synthesis starts by extending the 3'-OH terminus of the RNA primer (either tRNA or self-primer) while copying the 5'-end of the viral RNA genome that contains the unique 5'-end sequence (U5) and the 5'-end repeat (R) region. The synthesized DNA strand and the viral RNA produce an RNA–DNA hybrid in which the RNA strand is then hydrolyzed by the RT-associated RNase H activity. The DNA 3'-end-directed cleavage leaves the nascent (-) DNA strand as single stranded that is designated (-) strand strong stop DNA (sssDNA), which contains a sequence complementary to the identical repeat (R)

sequences, located at both the 5' and 3' -ends of the viral RNA genome. Due to the fact that RT is only able to cleave on average only once for every polymerized 100–120 nts, multiple internal cleavages are probably required to generate gaps that allow a further degradation by the RNA 5'-end-directed mode of RNase H cleavage.

In the next step, the minus-strand strong stop DNA is transferred from the 5' end to the 3' end of the genome. It is well documented, that NC increases the efficiency of this minus-strand transfer by facilitating the annealing of the complementary R regions. Due to its destabilizing activity, NC increases also the specificity of the minus-strand transfer by suppression of non-specifc reverse transcription from self-primed RNA representing the 5' end or the 3' end of the genome, by extensive inhibition of the reverse transcription of cellular RNAs presented in virions and inhibition of self-primed replication of DNA templates (LapadatTapolsky, Gabus et al. 1997; Freed 2001).

Since there are two such RNA molecules in each virion, first (-) strand transfer can be either intermolecular by switching to the second RNA molecule, or intramolecular, by switching to the other end of the same RNA molecule. These two alternative switches occur during with different frequency (van Wamel and Berkhout 1998; Yu, Jetzt et al. 1998) and the intermolecular sscDNA(-) transfer was stated to be much more frequent (Hu and Temin 1990). After the nascent DNA hybridizes to 3'-end R region (-) strand DNA synthesis proceeds along the viral RNA, while the RNase H concomitantly degrades the already copied RNA.

Most cleavages by RNase H are not sequence-specific, however, specific purine-rich sequences (polypurine tracks, PPTs) show high resistance to RNase H hydrolysis. The major PPT, which is located close to the 3' end of the viral RNA (3' PPT) and is quite diverse in different retroviruses, serves as a major primer for the second (+) strand DNA synthesis after removing other RNA sequences (Rausch and Le Grice 2004). Nevertheless, other RNA segments that are left after partial RNA degradation can also serve as minor primers for (+) strand DNA synthesis. In contrast to other retroviruses, HIV priming also occurs efficiently from another site, known as the central PPT (cPPT). Synthesis of (+) DNA strand continues until RT starts copying the tRNA primer. The first 18 nts at the 3'-end, which are complementary to the viral PBS, are copied by RT, but the next nucleotide in the tRNA is a modified ''rA'' and cannot serve as a template for DNA synthesis. The synthesized DNA strand and the 3'-end of the tRNA generates a new RNA-DNA hybrid that can serve as substrate for the RNase H activity. In most retroviruses, the RT-associated RNase H removes the complete tRNA segment, while in HIV-1 the RNase H activity of RT cleaves exactly one

nucleotide from the junction between tRNA and DNA, thus leaving an extra ‘‘rA’’ at the 5’ end of the (-) DNA strand. The newly formed second DNA strand is named (+) strand strong stop DNA (sssDNA).

At this stage, the R region, the U5 sequence and the unique viral RNA sequence, located at the 3’-end (U3), have been brought all together to form the 3’ LTR of the (+) strand DNA. The (+) strand is discontinuous and is annealed to nearly a full length (-) DNA strand. Subsequently, a second (+) strand DNA transfer, is catalyzed by RT. This strand transfer is mediated by annealing of the single-stranded DNA form of the PBS sequence, located at the (+) sssDNA, to the complementary region at the 3’ of the (-) DNA. Priming from both sites involves discontinuous DNA synthesis, generating a 99 nt central DNA flap at the center of the double stranded viral DNA products (Charneau, Mirambeau et al. 1994). This flap is part of a triple-stranded structure containing two overlapping plus-strand DNA and a complementary minus-strand (Charneau, Mirambeau et al. 1994). It was proposed that this flap plays a role in the nuclear import of the PICs (Wei, Garber et al. 1998) whereas cPPT protects HIV-1 from the activity of the human APOBEC 3 (A3) restriction factor.

VII.1.4. Nuclear import and integration

Once near the nuclear membrane, HIV-1 most likely relies on the cellular nuclear import proteins to pass through the nuclear pore complexes (NPC) of the nuclear envelope. NPC have a pore-like, molecular sieve function, whereby molecules smaller than 40–45 kDa can diffuse into and out of the nucleus. Proteins larger than 40–45 kDa require a nuclear localization signal (NLS) to be targeted to the nucleus. Too large for passive diffusion through nuclear pore complexes, PICs are presumably dependent on host cell mechanisms to enter the nucleus (Fassati, 2006).An alternative mechanism based on the ability of Vpr to induce reversible ruptures of the nuclear membrane, which might serve as entry points for the PIC, has been suggested (de Noronha, Sherman et al. 2001), however, this possibility has not been tested experimentally in the context of HIV infection. The model favored by investigators working in the area of HIV nuclear import is that the HIV PIC itself is karyophilic. This implies that a component or components of the complex contain targeting signals that engage the cellular transport proteins, which direct the PIC through the nuclear pore. The most likely candidates for the role of karyophilic agents are viral proteins associated with the PIC (matrix (MA), Vpr, and integrase (IN), although they may regulate trafficking indirectly by binding host cell–derived karyophilic proteins (Gupta, Ott et al. 2000; Bukrinsky 2004). The cellular Lens Epithelium-Derived Growth Factor p75 (LEDGF/p75) protein as well as the DNA flap

structure of the viral cDNA have also been implicated in promoting the translocation of the PIC into nuclei of virally infected cells. Yamashipa et al. have proposed that the HIV capsid protein plays a crucial role in controlling the nuclear import of the HIV genome (Levin, Armon-Omer et al. 2009). CA dissociates from the HIV-1 reverse-transcription complex (RTC) prior to nuclear entry (Fassati and Goff, 2001; McDonald et al., 2002). The mechanism by which HIV-1 separates from its CA core before accessing the nuclear pore is unclear, but data suggest that substantial levels of CA may remain associated (Arhel et al., 2007; Dismuke and Aiken, 2006).

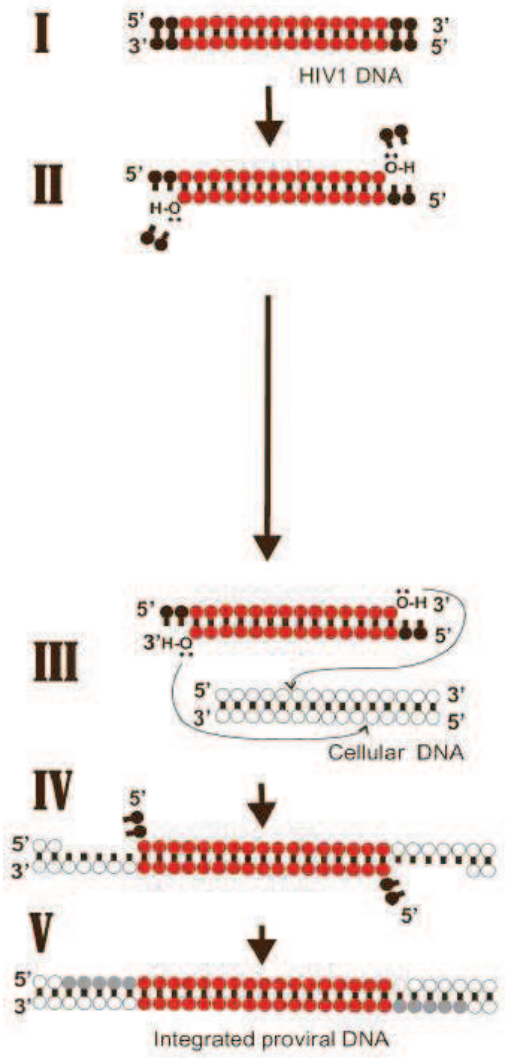

Fig.29. Sequences of events of HIV-1 integration: I) donor DNA; II) integrase-catalyzed 3' processing; III) integrase-catalyzed strand transfer; IV) product of strand transfer; V) DNA repair by cellular enzymes. (Savarino 2007).

Integration process, catalyzed by the 32 kDa IN protein, is an essential step in retrovirus replication. Like reverse transcription, integration proceeds via a series of steps. Based on the

available crystal structure information, it appears that at least a tetramer or even an octamer of IN would be necessary to accomplish concerted integration of both LTRs (Brown, Heuer 1998).

IN first clips off several nucleotides from the 3' terminus of both strands of the linear viral DNA (3'-end processing). This reaction generates double-stranded DNA with 3'-recessed ends. In the nucleus, IN makes a straggled cleavage in the cellular target DNA. The 3'-recessed ends of viral DNA formed in the 3'-end processing reaction are joined to the ends of the cleaved cellular DNA (strand transfer). The integration process is completed when cellular enzymes fill the gaps between the integrated viral DNA and the host target DNA (Freed 2001).

VII.2. The late phase

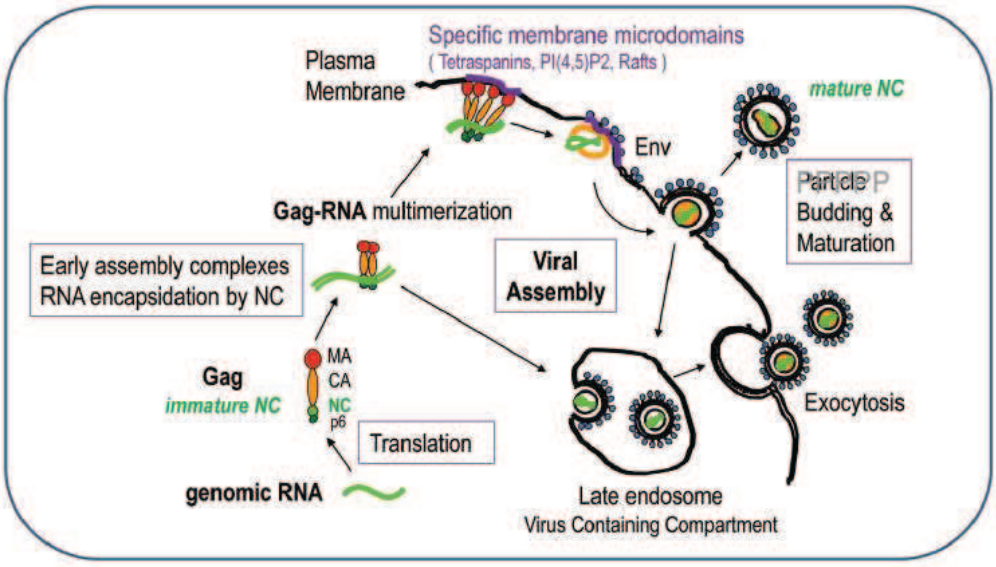

Fig.30. Late steps of retroviral particle formation (Muriaux and Darlix): traffic, assembly and budding. The different stages of NC: immature NC in Gag and mature NC in the viral particle. Scheme of Gag-gRNA complexes trafficking within the cell and viral particle assembly and release. Upon export of the genomic RNA from the nucleus, the gRNA is translated into Gag and GagPol proteins that recruit the genome and traffic through the cytoplasm onto the assembly site et the plasma membrane; few Gag complexes with the viral genome anchor into the plasma membrane; Gag recognizes the PM phospholipids PI(4,5)P2 which triggers the anchoring of the myristate into the inner leaflet of the membrane, multimers of Gag thus accumulate at the assembly site which can be rafts or tetraspanins enriched microdomains and will serve as a plateform for particle budding; other cellular determinant can intervene to promote budding and particle release, such as the ESCRT machinery. Some preformed or formed virions can undergo endocytosis from the plasma membrane and create new virus-containing compartment (VVC) in the cell that could be released by exocytosis upon cellular signal. During release, the particle undergoes a maturation process due to the viral protease that cuts Gag and GagPol to specific sites which releases the structural proteins and enzymes in order to form the mature infectious particle,

in which free NC proteins condensed on the genomic RNA inside the viral mature core. This phenomenon is a key determinant for particle morphogenesis and infectivity.

VII.2.1.Gene expression

Successful transcription leads to the generation of approximately 30 different viral transcripts from the provirus. All these transcripts are derived from a single full-length transcript by alternative splicing, which generates mRNA with common 5' and 3' ends. The spliced viral RNA can be grouped into three classes: the multiply spliced mRNA encoding early regulatory proteins such as Tat, Nef and Rev; the singly spliced mRNA encoding Vpu, Vpr, Vif and Env; the un-spliced, full-length mRNA encoding the Gag-Pol poly protein. HIV gene expression is also regulated at a second level by the nuclear export of intron-containing transcripts. This process is mediated by the viral encoded Rev protein (Pollard and Malim 1998). Both singly-spliced and un-spliced viral RNAs are intron-containing transcripts and carry a secondary structure called Rev Responsive Element (RRE) within the 3' end intron region. Like most pre-spliced transcripts in eukaryotic cells, intro-containing viral transcripts are retained in the nucleus by the interaction of splicing factors until they are spliced to completion or degraded. However, specific interaction between REV and RRE permits nuclear export of incompletely spliced viral transcripts in infected cells. The current model suggests that REV directly binds to RRE and multimerizes upon RRE binding. REV multimerization stablizes the formation of a complex between REV, cellular exportin-1(CRM-1) and the GTPase Ran. This complex targets the mRNA complex to the nuclear pore complex for export. After cytoplasmic translocation, Ran-GTP is converted to Ran-GDP, and dissociated along with exportin-1 from the mRNA complex. REV is also dissociated from mRNA by unknown mechanism and recycled back into the nucleus by cellular importin-β. REV interacts with importin-β in the cytoplasm and dissociates with it in the nucleoplasm due to the action of Ran-GTP. Several other host cofactors have also been implicated to interact with the REV/RRE nuclear export process. These include eIF-5A, Rip/Rab, B23, p32 (Kjems and Askjaer 2000). However, their distinctive roles in the process of REV/RRE mediated nuclear export still need to be defined (Wu 2004).

VII.2.2.Virus particle production

The assembly process begins with the synthesis of the viral proteins. Initiation of translation of most eukaryotic cellular messenger RNAs (mRNAs) occurs by a cap-dependent

mechanism that requires ribosomal scanning of their 5'UTR. The 40S ribosomal subunit bearing the initiator tRNA, Met-tRNA^{Met} i, interacts with the initiation factors bound at the cap (m^7GpppG) at the 5' end of the mRNA, and then scans the mRNA in the 5'–3' direction until it encounters an initiation codon in an appropriate context. The 60S ribosomal subunit joins the 40S subunit and translation of the mRNA begins. However, several groups of viruses and a minority of cellular mRNAs initiate translation in a cap-independent manner, using internal ribosome entry sites (IRESes). IRESes are structured RNA regions that are able to directly recruit the 40S ribosomal subunit at or near an initiation codon. This mode of initiation usually requires the participation of some canonical initiation factors and of host cell factors called IRES trans-acting factors (ITAFs).

IRESes were first discovered in picornaviruses (Jang, Krausslich et al. 1988), and have since been found in several other groups of viruses, including retroviruses (Bolinger and Boris-Lawrie 2009) such as simian immunodeficiency virus (Ohlmann, Lopez-Lastra et al. 2000), human immunodeficiency virus type 1 (HIV-1) (Brasey, Lopez-Lastra et al. 2003), human immunodeficiency virus type 2 (Weill, James et al.; Herbreteau, Weill et al. 2005), murine leukemia virus (Vagner, Waysbort et al. 1995), Rous sarcoma virus (Deffaud and Darlix 2000), feline immunodeficiency virus (FIV) (Camerini, Decimo et al. 2008) and mouse mammary tumor virus (Vallejos, Ramdohr et al.).

A major function in assembly is played by the Gag precursor polyprotein, Pr55^{Gag} (Freed 1998), which contains determinants that target it to the plasma membrane, bind the membrane itself, promote Gag-Gag interactions, encapsidate the viral RNA genome, associate with the viral Env glycoproteins and stimulate budding from the cell. The HIV-1 Gag associates with the membrane within few minutes of its synthesis. It appears that the membrane binding is largely specific for the host cell plasma membrane (Freed 2001).

VII.2.2.RNA encapsidation

Specific and efficient encapsidation of HIV-1 gRNA into viral particles is a multifaceted process of relocating the gRNA following transcription in the nucleus to sites of particle assembly at the plasma membrane. Cis packaging signals in the viral RNA confer specific selection among the milieu of host cell RNAs through interactions with trans factors encoded by the virus, and host cell (Cockrell, van Praag et al.).

The conventional canonical cis packaging signal (ψ) is a ~120 bp fragment comprised of four stem-loop structures located in the HIV-1 5' untranslated region (UTR), and extending into the 5' end of the HIV-1 Gag coding sequence (Kaye and Lever 1998). The packaging signal

of HIV-1, composed of four stem-loop structures, referred as SL1-SL4, is important for conferring RNA encapsidation specificity, since RNA lacking this signal is not efficiently encapsidated into viral particles.

Retroviral RNAs are linked together at a sequence near the 5' end of the genome known as the dimer linkage signal (DLS). Within the identified DLS, a single stem-loop structure (SL1) appeared to be responsible for the majority of the dimerization potential of the full-length HIV genomic RNA. The SL1 is a highly evolutionarily conserved hairpin from nt 236 to 282 nt (based on numbering with respect to the cap site of HIV-1_{HXB2} genomic transcripts), containing two internal bulges and an apical loop consisting of nine bases, of which six form a palindrome. Deletion of this motif prevents *in vitro* dimerization of the nt 1–707 fragment of HIV-1 genomic RNA (Skripkin, Paillart et al. 1994), and antisense oligonucleotides targeting the palindrome also prevent dimerization of sequences in this region (Muriaux, Girard et al. 1995). Thus, this motif is widely accepted as the dimerization initiation site (DIS). The palindromic nature of the DIS allows it to form classic Watson-Crick base pairs with another RNA containing the same DIS sequence in an antiparallel manner (Clever, Wong et al. 1996). This interaction, the result of which is termed the "kissing loop" dimer has been solved using nuclear magnetic resonance and X-ray crystallographic techniques (Moore and Hu 2009)

Although the important role of the DIS as the central element for initiation of RNA-RNA contact has been well demonstrated, one major caveat is that HIV-1 can replicate without the DIS, or even without the entire SL1, albeit at reduced levels in most cell types (Hill, Shehu-Xhilaga et al. 2003). Furthermore, the viral RNA extracted from such DIS mutants is dimeric, even though the dimers display heterogeneous migration by native gel electrophoresis (Moore, Fu et al. 2007). Interestingly, when DIS mutant viruses were placed in long-term culture, the compensatory mutations that arose were within Gag and resulted in an improved ability of Gag to distinguish full-length viral RNA from spliced RNA. This observation suggests that the DIS is not required for replication *per se*. Rather, it enhances dimerization and thereby potentially allows for better recognition of the genomic RNA species by Gag, whereas, in the absence of the DIS, dimerization can still occur, but with reduced kinetics and presumably through currently unidentified redundant mechanisms (Moore, Fu et al. 2007)

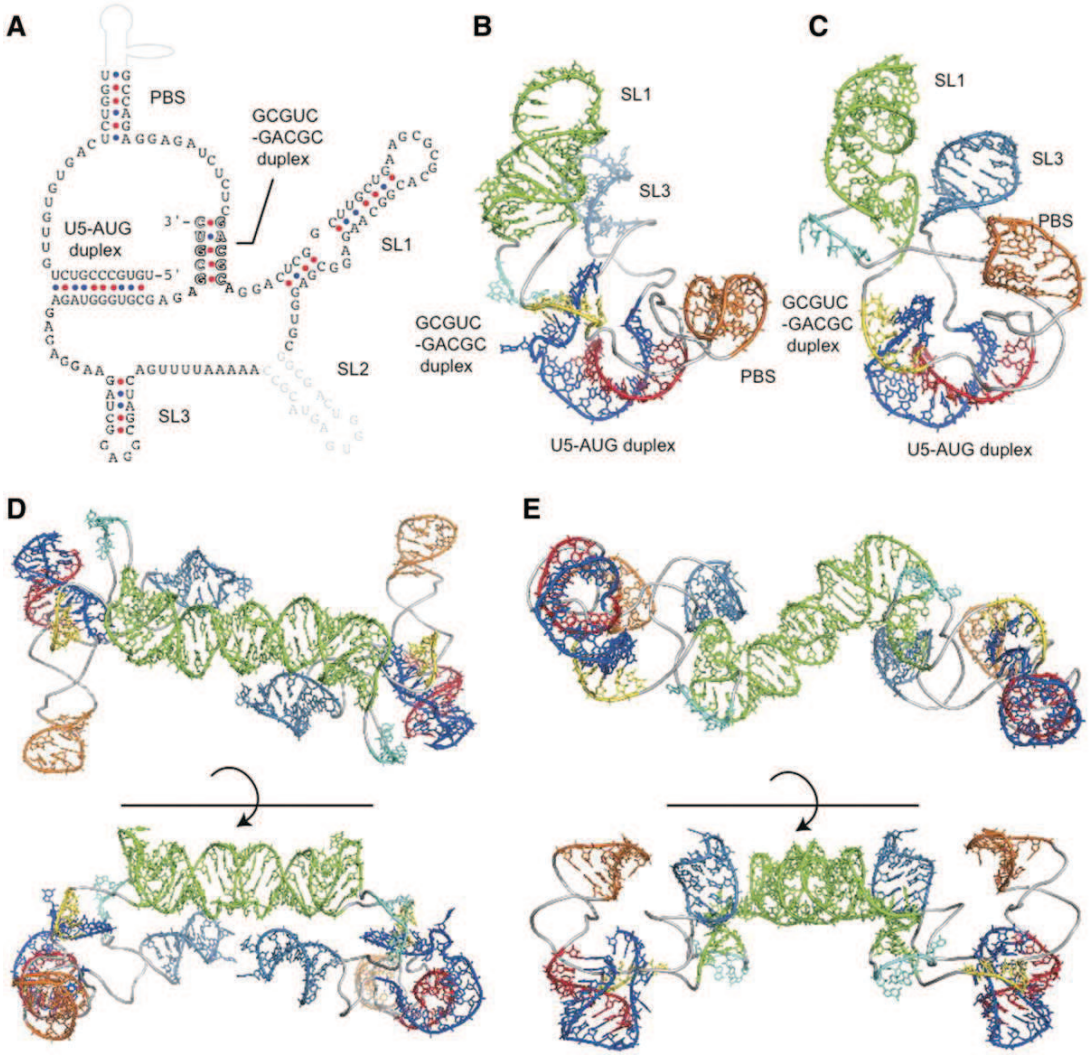

Fig.31. New models of 2D and 3D structure of the DLS. The 2D and 3D structures of the DLS. (Sakuragi, Ode et al.) **(**A**)** The 2D DLS schematic model that contains a previously unknown GCGUC-GACGC duplex. Other duplexes that were proposed previously and suggested to play roles in HIV-1 RNA dimerization within the virion in this and other studies (Clever, Sassetti et al. 1995; Huthoff and Berkhout 2001) are also indicated. **(**B**,** C**)** Two 3D structural models of the DLS monomer were predicted with the MC-Sym software (Parisien and Major 2008). Only two monomer models that were thermodynamically stable were obtained, due to the pseudoknot-like conformation that was formed with the two duplexes (GCGUC-GACGC and U5-AUG) restraining the conformational flexibility of the monomer. **(**D**,** E**)** Two 3D structural models of the DLS dimer were constructed by superposing 3D structure of SL1 with SL1 in a reported dimer structure [PDB code: 2D19] (Baba, Takahashi et al. 2005).

In general, retroviruses are able to package their own RNA genome, but not those of other retroviruses. In some cases, non-reciprocal packaging can be observed e.g. HIV-1 packages both HIV-1 and HIV-2 genomic RNAs, whereas HIV-2 does not efficiently encapsidate HIV-1 RNA (Freed 2001).

VII.2.4. Assembly and release

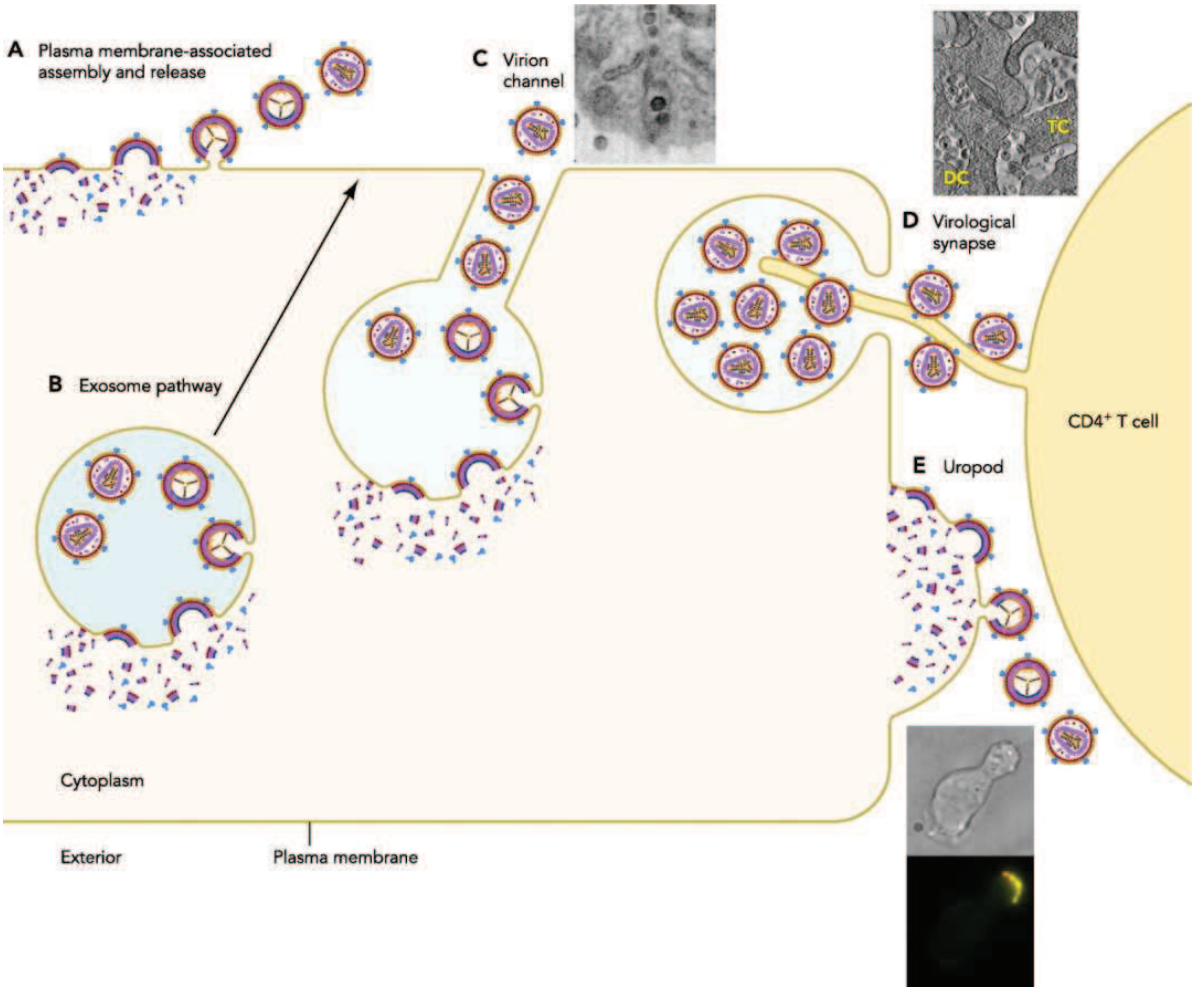

Fig.32. Schematic representation of the HIV-1 assembly and release associated with different membrane interfaces (Balasubramaniam and Freed).

There are different models explaining assembly and release of HIV-1.

According to the canonical one, Gag traffics to the inner leaflet of the plasma membrane where it initiates virus assembly and budding (Fig.32.A). This process is independent of the cell type.

An alternative model proposes that Gag molecules assemble, in a cell-dependent manner, on the cytoplasmic face of intracellular vesicles e.g. endosome/multivesicular bodies (LE/MVBs), and the ensuing virus particles bud into the intraluminal space. Virus-harboring vesicles then traffic to and fuse with the plasma membrane for example through the exosome pathway, resulting in the extracellular release of virus (fig.32. B). Another model claims that such intracellular compartments in macrophages, where HIV-1 Gag assembles at and buds into, are connected to the plasma membrane via nanoscale tubes (Fig.32.C). in another version of the cell-type-dependent HIV-1 assembly and release events, Gag trafficking and assembly

are proposed to target virological synapses that promote efficient virus transmission. (Fig.32.D) (Balasubramaniam and Freed).

The final step of viral assembly and release involves the budding of viral particles from the host cell plasma membrane. In contrast to what was believed before, retroviruses encode specific sequences promoting particle release, the "L" domains. In the case of HIV-1, the L domain is present in the p6, since deletion of p6 or mutations within a highly conserved Pro-Thr/Ser-Ala-Pro (P-T/S-A-P) motif of p6 impair particle release (Yeager, Wilson-Kubalek et al. 1998). Each day, up to 10^9-10^{10} HIV particles are produced.

VII.2.5.Maturation

Viral maturation begins concomitant with (or immediately following) budding, and is driven by viral PR cleavage of the Gag and Gag-Pro-Pol polyproteins at ten different sites, ultimately producing the fully processed MA, CA, NC, p6, PR, RT, and IN proteins (Sundquist and Krug).

Over the course of maturation, these processed proteins rearrange dramatically to create the mature infectious virion, with its characteristic conical core. MA remains associated with the inner leaflet of the viral membrane, forming a discontinuous matrix shell that lacks long-range order. The outer capsid shell of the core particle is composed of approximately 1200 copies of CA and is typically conical, although tubes and other aberrant assemblies, including double capsids, also form at lower frequencies (Briggs et al. 2003b; Benjamin et al. 2005). The capsid approaches the matrix closely at both ends (Benjamin et al. 2005; Briggs et al. 2006), particularly at the narrowend, which may represent the nucleation site for assembly (Briggs et al. 2006). The capsid surrounds the nucleocapsid, which typically resides at the wide end of the capsid and lacks obvious long-range order (Briggs et al. 2006).

Important changes that occur during HIV-1 maturation include activation of the fusogenic activity of the viral Env protein (Murakami et al. 2004; Wyma et al. 2004), capsid assembly, stabilization of the genomic RNA dimer, and rearrangement of the tRNALys,3 primer–genome complex (Moore et al. 2009; Rein 2010). Maturation is a dynamic, multistep process that involves a series of conformational switches and subunit rearrangements.

Temporal control of viral maturation is provided, at least in part, by the very different rates of processing at the five Gag processing sites, whose cleavage rates vary by up to 400-fold. These cleavage sites fall into three different categories: rapid (SP1/NC), intermediate (SP2/p6, MA/CA), and slow (CA/SP1) and extremely slow (NC/SP2) (Pettit et al. 1994). Analyses of mutant virions with blockages at the different Gag sites indicate that each cleavage event

performs a different function. SP1/NC cleavage activates Env (Wyma et al. 2004) and promotes condensation of the RNP particle (de Marco et al. 2010), SP2 processing frees NC to chaperone formation of the stable genomic RNA dimer (Kafaie et al. 2008; Ohishi et al. 2011), MA/CA cleavage disassembles the immature lattice and releases CA-SP1, and CA-SP1 cleavage frees CA to form the conical capsid (de Marco et al. 2010). around the RNA/protein complex within the core (Sundquist and Krug).

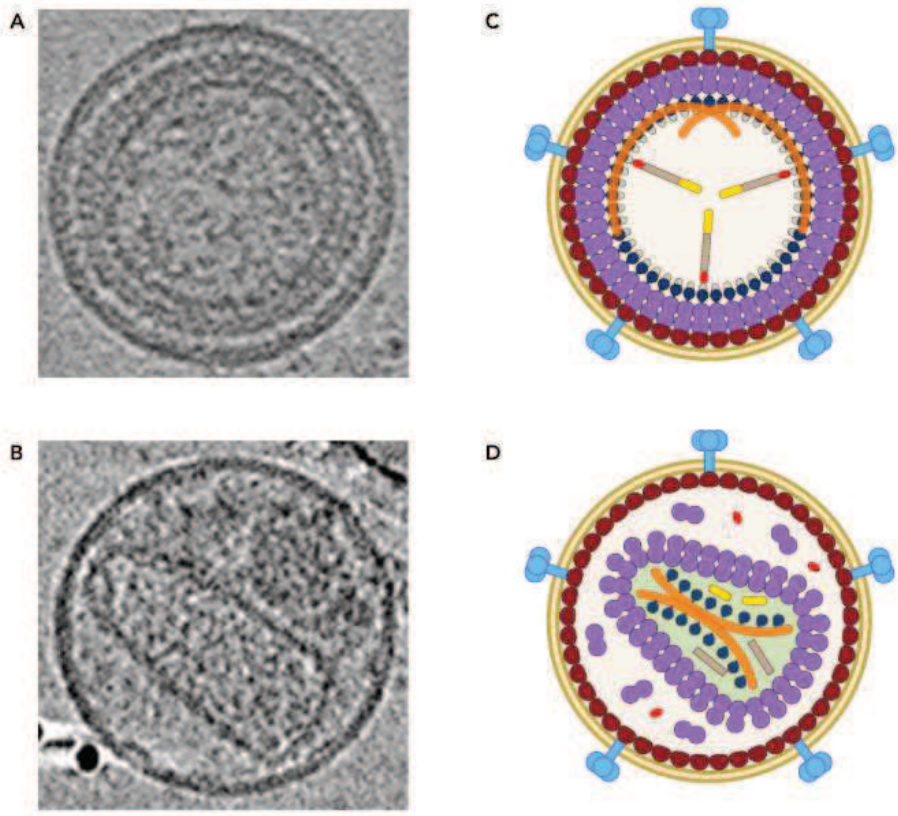

Fig.33. Cryoelectron micrographs and schematic representation of immature (A and C) and mature (B and D) HIV-1 particles (Balasubramaniam and Freed).

VIII. Nucleocapsid protein

VIII.1. Structure and properties of HIV-1 NC

NC is an abundant component of the HIV-1 retrovirus, associated with the two copies of genomic RNA in the interior of the mature viral particle (Mervis, Ahmad et al. 1988). NC is derived from the multidomain 55kDa Gag protein precursor ($Pr55^{Gag}$), which contains (from the N- to C-terminus) matrix (MA), capsid (CA), spacer peptide 1, NC, spacer peptide 2 and p6 (Henderson, Bowers et al. 1992). Mature NC is generated by a series of protease-mediated cleavages beginning during the assembly process (Kaplan, Krogstad et al. 1994; Ott, Coren et al. 2003). Interaction of the NC domain of Gag with the vRNA, which likely occurs initially in the cytosol promotes Gag multimerization (Balasubramaniam and Freed).

The initial protease cleavage of HIV-1 $Pr55^{Gag}$ leads to the formation of peptide $p15^{NC}$, which consists of $p7^{NC}$, p1(SP2) and p6 domains. Secondary cleavages, generating $p9^{NC}$, comprised of $p7^{NC}$and SP2 (Henderson, Bowers et al. 1992) occur with 10-fold lower rates than the initial one. The last PR cleavage results in the production of the 55-amino acid form of $p7^{NC}$, detected in mature viral HIV-1 particles. Thus, during proteolysis, NC exists in two intermediate forms, $p15^{NC}$ (partial cleavage product containing NC/SP2/p6) and $p9^{NC}$ (partial cleavage product containing NC/SP2) and the fully processed form, $p7^{NC}$ (Thomas, Bosche et al. 2008).

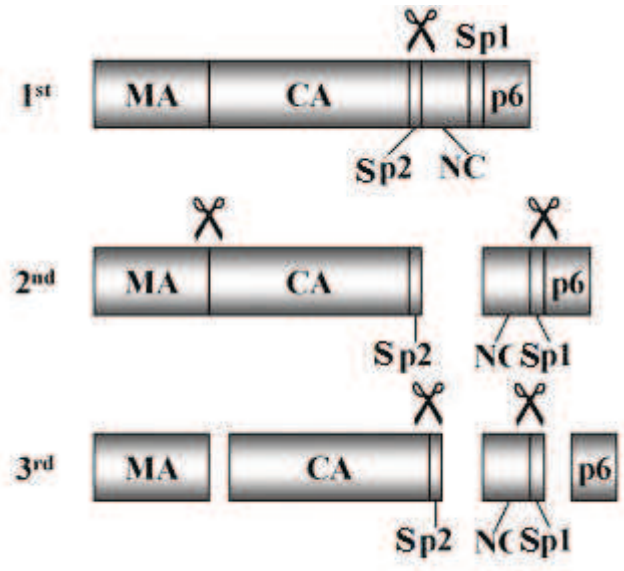

Figure.34. Schematic overview of the sequential proteolytic processing of the HIV-1 Gag precursor protein (Wensing, van Maarseveen et al.).

Retroviral nucleocapsid proteins are basic proteins, characterized by one or two copies of a highly conserved zinc finger motif of the CCHC type (Cys-X_2-Cys-X_4-His-X_4-Cys), flanked by basic regions (Berg 1986). In HIV-1 NC as well as other retroviral NCs with two zinc fingers, a short basic and flexible linker of 5-13 residues bridges the two ZFs. In the case of HIV-1 NC, the conformation of ^{29}RAPRKKG located downstream of the first CCHC box is responsible for the proximity of the two ZFs (Morellet, Jullian et al. 1992; Summers, Henderson et al. 1992).

(a)

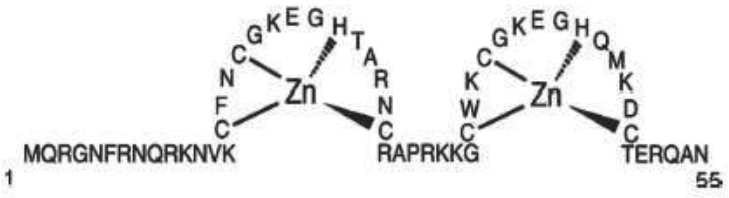

(b)

	N-Terminus	N-terminal zinc finger	Central	C-terminal zinc finger	C-Terminus
M-Group Consensus	MQRGNFKGQKRIIK	CFNCGKEGHIARNC	RAPRKKG	CWKCGKEGHQMKDC	TERQAN
Consensus-A1	------R----.--	---------L----	-------	--------------	------
Consensus-A2	------R----.--	---------L----	-------	--------------	------
Consensus-B	------RN-RKTV-	----------K--	-------	--------------	------
Consensus-C	---S----P---V-	--------------	-------	--------------	------
Consensus-D	--------PRK---	----------K--	-------	--------------	------
Consensus-F1	--KS-----R--V-	----------K--	-------	-----R--------	------
Consensus-G	--KS----PR-T--	---------L----	-------	--------------	------
Consensus-H	--K-----PRK-V-	--------------	-------	-----R--------	------
Consensus-K	---------RK---	--------------	-------	--------------	------
Consensus-01-AE	----------.--	---------L----	-------	--------------	------
Consensus-02-AG	------R--RT.--	---------L----	K------	--------------	------
Consensus-03-AB	--KS--R-P--.--	------D--L----	-------	--------------	------
Consensus-04-CPX	--KS-----R----	---------L----	-------	--------------	------
Consensus-06-CPX	--KS----P--S--	---------L----	-------	--------------	------
Consensus-07-BC	---S----S---V-	--------------	-------	--------------	------
Consensus-08-BC	---S----S---V-	----------K--	-------	--------------	------
Consensus-10-CD	--------P-K---	----------K--	-------	-----R--------	------
Consensus-11-CPX	---S-------.--	---------L----	-------	--------------	------
Consensus-12-BF	--KS-----R--V-	----------K--	-------	-----R--------	------
Consensus-14-BG	--KS----PR-N--	---------L----	-------	--------------	--SK--
NL4-3	I-----RN--KTV-	----------K--	-------	--------------	------

Fig.35.(a) Sequence of the HIV-1 Nucleocapsid protein from the MAL strain. (Mely, DeRocquigny et al. 1996) (b) Alignment of Group M HIV-1 NC protein sequences. The consensus sequence alignments shown above are from the Los Alamos HIV Sequence Database (http://www.hiv.lanl.gov) . The subtype is indicated by a letter, those that are preceded by a number are circulating recombinant forms (CRFs). Dashes indicate amino acid consensus identity, specified amino acids indicate variations, and the presence of a "." represents a one amino acid gap. The generation of the Consensus M-Group sequence does not include CRF; the total number of

sequences used to derive the Consensus M-Group is ~1100 (120 A; ~280 B; ~590 C; ~70 D; ~10 F1; ~20 G; 3 H).

Each ZF of the HIV-1 NC coordinates one zinc ion with high affinity through its 3 Cys and one His residues (K_a = 10^{13} - 10^{14} M^{-1}) (South, Blake et al. 1991; Gorelick, Chabot et al. 1993). Zinc binding acts as the main driving force for the folding of NC. Coordination of Zn^{2+} has been shown to be necessary for most NC functions since antiviral agents that disrupt the folding of the zinc binding motifs by ejecting Zn^{2+} and mutations that prevent zinc binding lead to noninfectious viruses (Aldovini and Young 1990; Gorelick, Nigida et al. 1990; Schwartz, Fiore et al. 1997).

NMR analysis reveals that the N-terminal part of each ZF adopts a rubredoxin-type run, while the central amino acids fold into a loop and NH…S hydrogen are established between amide protons of the backbone and the zinc-chelating Cys residues (Morellet, Jullian et al. 1992; Summers, Henderson et al. 1992; Darlix, Garrido et al. 2007). Close proximity between the two ZFs is achieved by the ^{29}RAPRKKG linker joining the two ZFs (Darlix, Garrido et al. 2007). Moreover, folding of ZF domain allows the formation on its top of hydrophobic plateau with the hydrophobic residues Val13, Phe16, Thr24 and Ala25 of the proximal finger and the hydrophobic residues Trp37, Gln45 and Met46 of the distal finger (Morellet, Jullian et al. 1992; Déméné et al, 1994, Summers et al, 1992).

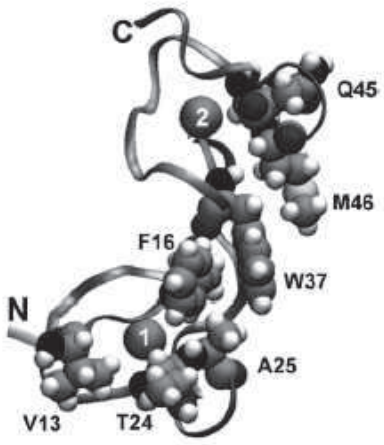

Fig.36. Primary structure and hydrophobic plateau of the nucleocapsid protein of HIV-1 (de Rocquigny, Shvadchak et al. 2008)

Structure of all oligonucleotide/NC complexes (de Guzman et al, 98; Morellet et al, 98; Amarasinghe et al, 01; Bourbigot et al, 08; Spriggs et al, 08; Bazzi et al, 11) showed that this hydrophobic plateau directs the nucleic acid binding properties of NC, through multiple

contacts with the oligonucleotide bases and backbone. Moreover Trp37 residue stacks with guanine bases, in line with the major contribution of this interaction to the NC/NA binding energy (Vuilleumier et al, 99). The complex is further stabilized by electrostatic interactions with the numerous basic amino acids scattered throughout the NC sequence.

VIII.1.1.Nucleic acid binding

Nucleocapsid proteins can bind either specifically or nonspecifically to nearly anyNAsequence. However, the binding constants strongly depend on the nature, the sequence, and the folding of the interacting sequences and can thus vary by several orders of magnitude. This strong variation in the binding constants confers on the protein the ability to exert different functions, depending on the nature of the interacting NA sequences and the respective concentrations of the protein and the NA sequences. In-line with the basic character of NCp7 and the strong ionic strength dependence of its binding to numerous oligonucleotides (Athavale 2010; Lapadattapolsky, 1995) NCp7 is able to bind, through an unspecific low-affinity electrostatic mode, to nearly any NA sequence of 5–8 nt in length. This binding mode is certainly the predominant one in the virus, where due to the small size of the viral core, the concentrations of NCp7 and the relevant NAs are in the millimolar range. As a consequence, an extensive coating of the gRNA by about 1500–2000 copies of NCp7 can be achieved, (Chertova, E.et al. 2006; Chen et al.2009) ensuring its protection against cellular nucleases (Lapadat-Tapolsky et al. 1993). NC also exhibits sequence- specific binding properties to a number of defined single-stranded sequences. These specific and strong binding properties play notably a critical role in the recognition, by the NC domain of Gag, of theΨ encapsidation signal of the gRNA, enabling its specific recognition and selection among a large excess of cellular RNAs during virus assembly (Cimarelli and Darlix 2002; Aldovini and Young 1990). A significant progress in the understanding of the underlying mechanism of this specific NC–gRNA recognition has been achieved through the NMR based determination of the structures of NCp7 complexed to the individual SLs of the Ψ encapsidation signal. A first important conclusion is that NCp7 bind with nanomolar affinity to the loop of both SL2 and SL3 (Paoletti et al. 2002). In sharp contrast, no strong affinity is observed for the stems of these sequences or for the SL4 domain. A second key feature provided by these studies is that the specific binding of NCp7 to these sequences is largely mediated through the hydrophobic platform formed at the top of the two folded ZFs by the V13, F16, T24, A25, W37, Q45, and M46 residues. This NCp7 hydrophobic platform allows

a mainly non-electrostatic interaction with the GGNG loops (N corresponds to either A, C, or U) of SL2 and SL3.

VIII.2. Chaperone properties of NC

The NC proteins belong to the large class of RNA chaperones that are ubiquitous in all living organisms and viruses where they are playing seminal functions from the gene transcription and regulation to RNA translation and maintenance. Their number is increasing constantly (Herschlag 1995; Cristofari and Darlix 2002; Semrad, Green et al. 2004). Many of these proteins have been characterized for their RNA binding properties and for their RNA chaperone activity in different assays, but little is know about their mode of action. Due to the lack of similarity between the individual protein families, the mechanisms they employ are likely to be diverse. However, some general principles can be derived from their shared features. Proteins with RNA chaperone activity bind RNAs only weakly and with low specificity, suggesting that the interaction of these proteins with RNA is transient and mainly of electrostatic nature (Mayer, Rajkowitsch et al. 2007). In line with this notion, for example a mutant version of the *E. coli* protein StpA with reduced RNA binding capacity displays a higher RNA chaperone activity than the wild-type, indicating that strong binding leads to RNA stabilization and is detrimental to RNA chaperone activity. The transient mode of action also entails that once the RNA is correctly folded, proteins with RNA chaperone activity are no longer required for the RNA to maintain its native structure. This has been shown for StpA (Zhang, Derbyshire et al. 1995) and S12 (Coetzee, Herschlag et al. 1994) in in vitro assays by means of protein digestion between the RNA folding step and the activity assay. Moreover, many of the chaperone proteins show a capability to oligomerize, such as the histone-like proteins H-NS (Dorman, Hinton et al. 1999) and StpA (Tanchou, Gabus et al. 1995; Rajkowitsch, Chen et al. 2007).

Through its chaperone properties, NC catalyses the folding of nucleic acids into their thermodynamically more stable structure. This is achieved by lowering the energy barrier for breakage and reformation of base pairs. Interactions between the nucleic acid molecules and NC proteins lead to transient un-pairing of bases available for re-pairing in alternative combinations.

All the forms of NC, from $Pr55^{Gag}$ to $p7^{NC}$, exhibit nucleic acid chaperone properties that increase greatly as the Gag precursor is progressively processed (Cruceanu, Urbaneja et al. 2006). Both NCp7 and Gag are affective in annealing PBS with $tRNA_3^{Lys}$, but Gag seems to

be even more effective than NC (Roldan, Warren et al. 2005). On the other hand, only processed NC facilitates minus-strand transfer (Guo, Wu et al. 2000).

Two main functions account for the NC chaperone properties. The first one corresponds to the transient destabilization of nucleic acid secondary structure upon binding of NC molecules (Bernacchi, Stoylov et al. 2002; Beltz, Azoulay et al. 2003; Beltz, Piemont et al. 2004). The second function corresponds to the ability of NC to promote annealing of complementary nucleic acid strands (Darlix, Vincent et al. 1993; Godet, de Rocquigny et al. 2006; Liu, Zeng et al. 2007).

As a result of the combined action of both annealing and melting activities, NC promotes also strand exchange during reverse transcription (Rascle, Ficheux et al. 1998). Due to this ability, NC causes destabilization of a nucleic acid duplex and formation of a more stable duplex with another nucleic acid strand where complementarities are more extended (Cristofari and Darlix 2002). Importantly, an optimal NC activity is reached at a protein to nucleic acid molar ratio between 1:8 and 1:6 nt, which corresponds to the "chaperoning mode", whereby the template is coated with NC molecules in a proportion similar to that existing in the virion (Darlix, Garrido et al. 2007).

Depending on the RNA occupancy level, three different modes of action were proposed for NC: The "Binding mode" occurs when the protein is in limiting concentration. Thus, NC binding to the RNA leads to the formulation of simple ribonucleoprotein complexes (RNP). The"Chaperoning mode" occurs when more protein is available and all RNA molecules can interact with chaperone molecules, resulting in the formation of high molecular weight RNPs. The "Unwinding mode" occurs when NC is present at saturating level and all RNA molecules are completely coated.

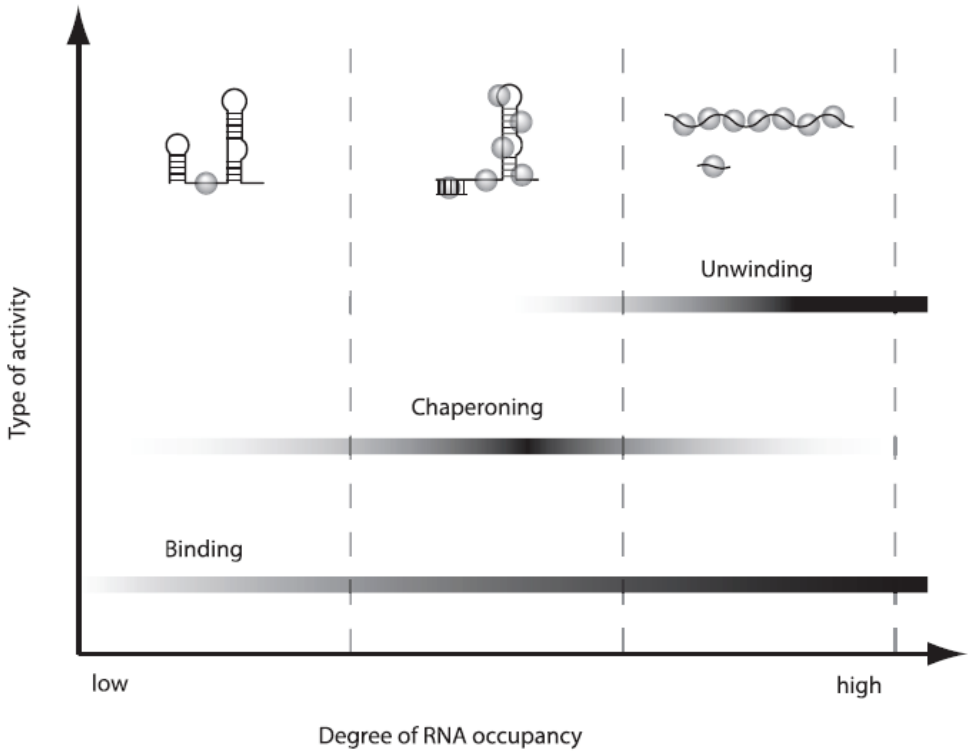

Fig.37. Schematic presentation of the connection between the degree of RNA occupancy by NC molecules (gray circles) and its possible activity (Cristofari and Darlix 2002). This scheme illustrates the different types of activity associated with RNA chaperone proteins according to the degree of RNA occupancy. The three modes depicted in the scheme can be classified with respect to the chaperone protein as noncrowded, crowded, and overcrowded.

VIII.2.1. Nucleic acid destabilization activity of NC

The chaperone properties of NC have been investigated with both DNA and RNA substrates (Tsuchihashi and Brown 1994; Lapadattapolsky, Pernelle et al. 1995; Urbaneja, Wu et al. 2002) and were found to be required for the two obligatory strand transfers during viral DNA synthesis (Darlix, Vincent et al. 1993; You and McHenry 1994). The initial and rate-limiting step of minus strand transfer is related to the destabilization of the transactivation response element TAR RNA and its cDNA copy, cTAR, upon binding of NC (You and McHenry 1994; Lapadattapolsky, Pernelle et al. 1995; Rein, Henderson et al. 1998).

NC activates the transient opening of cTAR terminal base-pairs (Azoulay, Clamme et al. 2003; Beltz, Azoulay et al. 2003) which leads to the partial melting of the cTAR ends, up to the T^{40} bulge or up to $^{10}C{\cdot}A^{44}$ mismatch (fig.38).

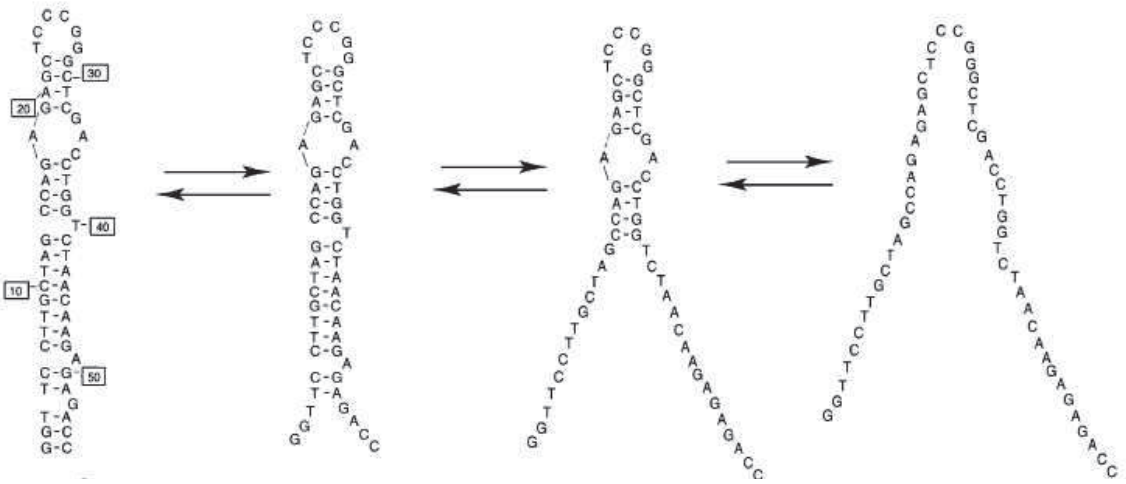

Fig.38. Equilibrium between the closed and opened form of cTAR sequence (Beltz, Clauss et al. 2005)

By the use of several NC derivatives, NC destabilization properties were shown to rely on the zinc fingers (Williams, Rouzina et al. 2001). Indeed, the inability of the fingerless NC(13-61)$_{dd}$ peptide and the non-structured (SSHS)$_2$NC(1-55) mutant to promote cTAR destabilization clearly indicated that the structural information required for destabilization is distributed among both folded motifs. The data with (SSHS)$_2$NC(1– 55) are consistent with the inability of this mutant to alter the cooperativity of the helix–coil transition of λ DNA molecules (Williams, Rouzina et al. 2001), and its limited effect in blocking cTAR-induced self-priming and promoting minus-strand transfer (Beltz, Clauss et al. 2005). Moreover, dramatic effects were observed with the Trp37 to Leu substitution on cTAR binding and destabilization, in line with the loss of NC-promoted tRNALys,3 annealing to the genomic primer binding site observed with the same mutation (Rong et al, 97) and may explain, at least in part, why HIV-1 containing the Trp37 to Ala mutation in NC is not infectious (Beltz, Clauss et al. 2005).

The requirement of the proper folding of both fingers together with the presence of Trp37 residue in the distal finger suggested that the hydrophobic plateau composed of Val13, Phe16, Thr24, Ala25 and Trp37 is a critical determinant for nucleic acid binding and destabilization (Beltz, Clauss et al. 2005). Moreover, NC-induced destabilization was found to be inversely dependent on the oligonucleotide stability and was more efficient for cTAR DNA than for the more stable TAR RNA sequence. Similarly, stabilization of the lower part of cTAR stem has been shown to impair the NC ability to destabilize cTAR and to block self-priming of (-)ssDNA (Driscoll and Hughes 2000). The NC-induced melting of the stem relies on the

presence of the terminal bulges within the stem, which cooperatively destabilize the cTAR secondary structure (Beltz, Azoulay et al. 2003).

The NC-induced promotion of the annealing between (+)PBS and its (−)PBS complement sequence involved in the second strand transfer was found to marginally depend on the limited destabilization of the PBS stem (Egele, Schaub et al. 2004). In contrast, through binding to the 5-CTG-7 sequence of (-)PBS, NC induces a stretching of the loop and perturbation of the C5-G11 base pair next to the loop, favoring the annealing reaction with the complementary (+)PBS sequence via an intermediate "kissing complex" (Ramalanjaona, de Rocquigny et al. 2007).

VIII.2.2. Nucleic acid annealing activity of NC

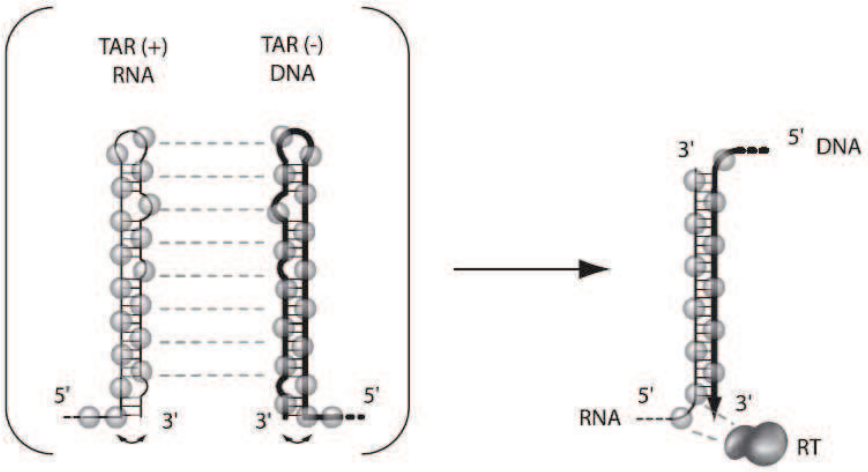

Fig.39. Nucleic acid annealing during HIV-1 minus strand DNA synthesis chaperoned by viral NC protein (Cristofari and Darlix 2002). The gray circles represent NC molecules.

The second step in NC chaperoning minus strand transfer corresponds to the hybridization of cTAR with TAR while being coated by NC molecules (Darlix, Vincent et al. 1993; Lapadattapolsky, Pernelle et al. 1995). In the absence of NC, the annealing rate of this reaction is extremely slow (You and McHenry 1994; Lapadattapolsky, Pernelle et al. 1995; Guo, Henderson et al. 1997; Godet, de Rocquigny et al. 2006) and the annealing reaction proceeds via loop-loop kissing intermediate, followed by a rate-limiting strand exchange between the terminal stems (Vo et al, 2009).

NC has been shown to chaperone this hybridization, accelerating the process by about 3000-fold in physiological temperature and salt conditions (Vo, Barany et al. 2009). This property of NC is mainly promoted by the numerous basic residues able to neutralize the negatively

charged DNA, thus decreasing the electrostatic repulsion between the nucleic acid molecules. NC facilitates the cTAR/TAR annealing reaction via the stem ends. According to the observed dependence of TAR/cTAR annealing reaction on the NC concentration it was proposed that NC can shift the annealing pathway from a loop-loop "kissing" to a "zipper" pathway as the concentration of protein increases. Such a mechanistic switch suggests that the annealing mechanism is both sequence and protein-concentration dependent with a fine balance between the local stability of nucleic acids and the destabilization induced by NC in these sequences (Vo, Barany et al. 2009).

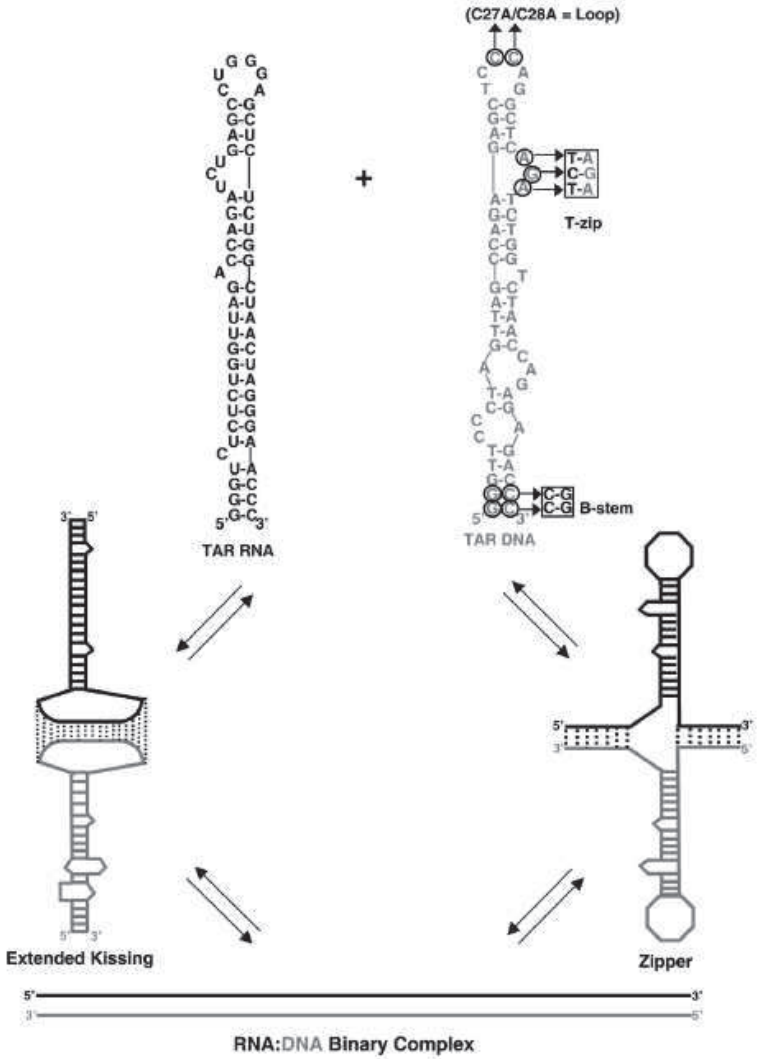

Fig.40. Schematic representation of the two pathways of TAR/cTAR annealing (Chen, Balakrishnan et al. 2003).

Negroni and Buc proposed an acceptor invasion-driven mechanism for the NC-promoted annealing of RNA and DNA substrates with strong homology. Briefly, in this mechanism the first interaction of the cDNA with the acceptor RNA occurs at a site upstream of the DNA primer terminus (Negroni and Buc, 2000). The site is a region cleared by RT RNaseHactivity

so that the acceptor can interact with the cDNA. An early model proposed by Negroni and Buc (2000) indicated that as synthesis proceeds, the chaperone activity of nucleocapsid protein (NC) (Tsuchihashi and Brown, 1994; You and McHenry, 1994; Rein et al., 1998; Guo et al., 2000) facilitates annealing of the acceptor RNA to the cDNA via complementary sequences of nucleic acids.

As synthesis progresses and the acceptor–cDNA interaction expands, the pre-existing hairpins in the acceptor are disrupted while new secondary structures are transiently formed. Ultimately, transfer is accomplished by displacement of the cDNA primer from the donor and completion of synthesis on the acceptor RNA template (Negroni and Buc,2000).

The nucleic acid annealing properties of NC were further demonstrated by the NC-induced annealing of small complementary DNA hairpins, PBS(+) and PBS(-), representing the rate-limiting step of the plus-strand transfer of reverse transcription (Ramalanjaona, de Rocquigny et al. 2007). In the absence of NC, (+)PBS was reported to spontaneously anneal to (−)PBS, mainly via a nucleation mediated by their single-stranded overhangs.(Darlix, Godet et al.) NC increases the (−)/(+)PBS annealing kinetics and switches the pathway of the reaction to a loop–loop kissing mechanism that does not occur in the absence of NC (Godet et al, 2011). Although the stem of the PBS is only slightly destabilized by NC, the NC-dependent destabilization of the PBS loop appears to play a critical role in the annealing reaction (Ramalanjaona, de Rocquigny et al. 2007).

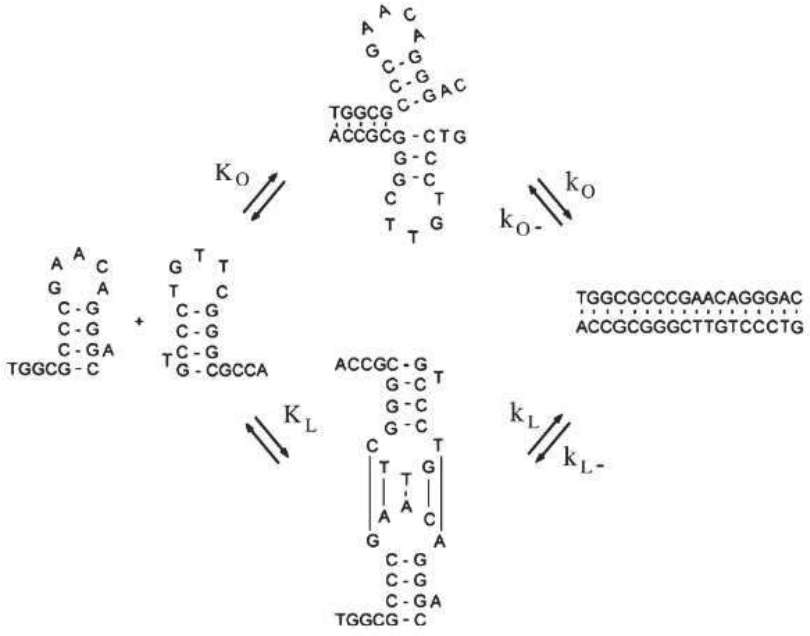

Fig.41. Proposed mechanism of PBS(+)/PBS(-) annealing (Godet and Mely; Khan and Giedroc 1992)

However, if the general action of NC is to enhance the annealing reaction between two complementary sequences, when the degree of RNA occupancy is very high, NC can promote reverse reaction e.g. addition of an excess of NCp7 to small (<20 nt) or imperfect duplexes can result in their destabilization (Barat, Schatz et al. 1993).

VIII.3 Role of NC during the viral lifecycle

VIII.3.1. Role of NC during the early phase of the viral lifecycle

Receptor binding and virus fusion with the cellular membrane result in the entry of the virion core into the cytoplasm. The virion core consists of a capsid shell surrounding the nucleocapsid core (dimerized RNA genome, $tRNA^{Lys,3}$ primers and around 2000 copies of NC). As the RTC uncoats, reverse transcription proceeds. NC is known to play at least three distinct roles in the process of reverse transcription. Firstly, it facilitates the annealing of the tRNA primer to the PBS of the viral RNA template (Guo, Henderson et al. 1997). Enhancement of tRNA/PBS annealing has been shown to occur with either mature NC, or NC in the context of the Gag precursor. A second role of the NC in the process of reverse transcription is the facilitation of viral DNA synthesis through reduction of self-primed reverse transcription (Peliska, Balasubramanian et al. 1994) or by enhancement of the efficiency and processivity (i.e. the ability of an enzyme to repetitively continue its catalytic function without dissociating from its substrate) of RT (Peliska et al. 1994; Druillennec et a. 1999) during the synthesis of viral minus- and plus-strand DNA. *In vitro* experiments using purified components to reconstruct reverse transcriptase reactions have shown that strand transfer is extremely inefficient. This is due to the occurrence of competing intramolecular self-priming reactions along the RNA template that result in the formation of secondary structures that interfere with the synthesis of high fidelity DNA copies of the viral RNA genome (Darlix, Vincent et al. 1993; Musah 2004). A third role of NC in reverse transcription is in the promotion of minus and plus strand transfers allowing complete synthesis of full-length DNA products (McGrath, Buckman et al. 2003)

An obligatory step in the establishment of retroviral infection is the integration of reverse transcribed viral DNA into the host cell genome. A number of reports demonstrated that NC is a required cofactor in integration. Mutations of the NC zinc fingers prevent proper 3'-end processing *via* viral IN (Musah 2004). It was also demonstrated that NC plays a role in stabilizing viral DNA produced during infection, and efficient removal of the 3'-terminal dinucleotides by IN *in vivo*. It has also been shown that IN activation relies not only on the intact NC zinc fingers, but also on its basic residues, since NC lacking the zinc fingers binds DNA but only moderately stimulates strand transfer by IN, whereas the zinc finger domain

binds DNA poorly and does not efficiently stimulate the IN activity (Thomas, Bosche et al. 2008).

During the first strand transfer, referred as a minus cDNA transfer, NC functions are associated with its chaperone properties. NC activates the transient opening of cTAR terminal base pairs and increases the speed of hybridization of the two complementary stem-loops, TAR and cTAR. Following minus-strand transfer, RT catalyzes the elongation of minus-strand DNA, and degrades the genomic RNA by its RNase H activity. Since the RNA template is highly structured, when RT encounters secondary structure it pauses at that site or prematurely stops polymerization. Through its ability to destabilize secondary structures, NC reduces pausing allowing RT to continue polymerization. NC is able to increase the amplitude of primer extension by 3-fold. Furthermore, NC enhances the stability of RT-nucleic acid substrate complexes by decreasing the dissociation rate constant of these complexes (Grohman et al, 2008).

Viruses with mutations in either or both of NC zinc fingers (NCH23C and/or NCH44C) are replication defective although, they are still able to enter cells and reverse transcribe their genomes. Thomas et al reported that after infection with these mutants, the principal defect appears to be at the integration step (Thomas, Bosche et al. 2008). Moreover, it was shown that premature reverse transcription occurs, resulting in nascent virions containing abnormally high levels of vDNA. Each virus particle contains minus-strand strong-stop DNA, in 1,000-fold excess over the amount observed in wild-type particles (Chertova, Chertov et al. 2006)**.** Furthermore, mutating or deleting the NC zinc fingers (Grigorov B 2007) caused an accumulation of Gag in the cytoplasm or at the plasma membrane, but not at the level of late endosomes as for wild-type Gag, probably due to the fact that Gag–NC interactions with genomic RNA and with the cellular budding factor ALIX were impaired (Popov S 2008). Thus, it favored the notion that late reverse transcription takes place in core structures formed of nonprocessed and processed Gag and Gag-Pol molecules.

In addition, tight interactions were found to take place between NC molecules, the cellular tRNA primer and the RT enzyme in reconstituted HIV-1 replicative complexes (Guo J 1997; Lener, Tanchou et al. 1998). These multiple RT-NC-RNA interactions contribute to the fidelity of the reverse transcripton reaction by inhibiting self-initiation of cDNA synthesis and providing excision-repair activities to the RT enzyme *in vitro.* (LapadatTapolsky, Gabus et al. 1997; Rein, Henderson et al. 1998).

It was proposed that the newly synthesized cDNA is at the interface between two hemispheres corresponding to bound NC molecules on one hand and RT heterodimer on the other hand. In

conclusion, RT converts the genomic template into cDNA in a reaction that NC enhances by increasing the time of RT residency on the template and by preventing false initiation and elongation events (fig.42) (Rein, Henderson et al. 1998).

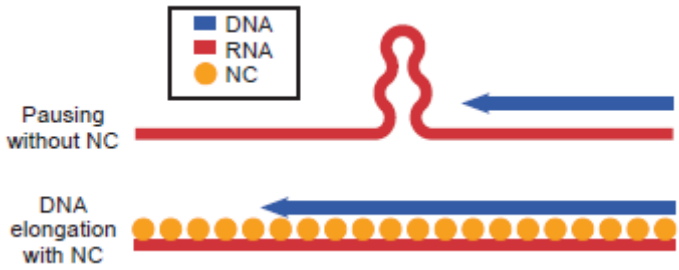

Fig.42. Effect of NC on DNA elongation during reverse transcription. Addition of NC reduces the pausing of RT and increases the efficiency of the full-length DNA products synthesis (Lapadattapolsky, Derocquigny et al. 1993).

As the reverse transcription process is ending, NC partially coats the newly synthesized viral DNA, which leads to the formation of a nucleoprotein complex partially resistant to enzyme degradation (Gorelick, Chabot et al. 1996; Krishnamoorthy, Roques et al. 2003). Numerous studies with different NC mutants revealed that all the NC functions during the early phase of the viral life cycle discussed above require the presence of the ZF hydrophobic plateau since structural changes in the first or second zinc finger caused strong defects in reverse transcription and integration processes. (Berthoux, Pechoux et al. 1997). On the other hand, mutations within the regions flanking the ZFs seem to be less detrimental to virus replication since several basic residues need to be replaced by neutral ones to cause a dramatic reduction in viral DNA synthesis (Berkowitz, Fisher et al. 1996).

VIII.3.2.Role of NC during the late steps of the virus life cycle

During particle assembly, NC plays an important role in the specific gRNA packaging into virus particles (Brasey, Lopez-Lastra et al. 2003). Gag-NC-RNA interactions were shown to be the major determinants in the switch from the messenger to genomic RNA. During synthesis, HIV-1 genomic RNA constitutes the messenger RNA for Gag production. Newly

made Gag molecules bind the gRNA via NC domain leading to a conformational rearrangement of the 5' leader. The structural modification of gRNA promoted by Gag-NC exposes cis-acting elements required for gRNA dimerization and packaging, occluding the RNA site required for protein synthesis (De Guzman, Wu et al. 1998). Thus, the overall effect of RNA structural rearrangement in the 5' leader results in the inhibition of translation and promotion of gRNA dimerization and packaging. NMR data gave clear evidence that ZFs are responsible for specific interaction with the Ψ-site sequence of the gRNA (Ott, Coren et al. 2003). Moreover, NC domain removal from Gag prevents specific packaging of HIV-1 gRNA (Thomas and Gorelick 2008).

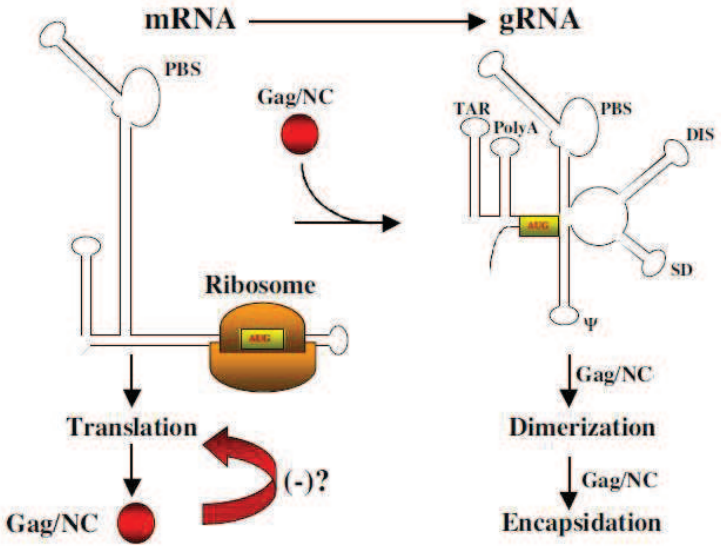

Fig.43. Gag-NC determinants in the switch from messenger to genomic RNA (Darlix, Cristofari et al. 2000) .

An important step in the virus particle maturation, in which NC participates is the formation of a stable dimer between the two molecules of gRNA present in the virus particle. Moreover, NC facilitates RNA maturation via its chaperone activity, assisting the RNA in finding its most stable annealed structure (Clavel and Orenstein 1990). Interestingly, studies with virus mutants, where the SL1/DIS sequence was deleted, causing reduction of gRNA dimerization, have shown that due to NC chaperone properties, NC-Gag formation of dimeric gRNA was far from totally abolished. On the other hand, deletion of a strong NC binding site, the A-U loop connecting SL2 and SL3 in Ψ, caused a marked inhibition of NC-mediated dimerization together with impairment of gRNA packaging (Cen, Huang et al. 1999; Feng, Campbell et al. 1999).

Another event occurring during particle assembly is tRNA molecule incorporation into virions. NC, both in its precursor and mature form, enables annealing of its cognate tRNA to gRNA sequences, resulting in the unfolding of 15 nucleotides of the tRNA (Hargittai,

Gorelick et al. 2004). Again, this function of NC is connected to its chaperone properties which increase the rate of annealing (Morita and Sundquist 2004). NC was also reported to cooperate with the budding pathway also dependent on the sp2 and p6 domain and its association with the ESCRT (Endosomal sorting complex required for transport) proteins Tsg101 required for virus budding (Buchbinder, Katz et al. 1994).

IX.Protective host responses towards HIV-1 infection

The pathogenesis of AIDS reflects the balance between viral replication and host response. It is believed that a critical role in controlling viral infection is played by the cellular response.

Soon after HIV-1 virus infection, an asymptomatic period of disease begins. Although it may last for about ten years, it varies greatly among infected subjects (Anastassopoulou and Kostrikis 2003). It is widely accepted that human allelic variants for certain genes can influence the sensitivity to HIV-1 infection (Amara, LeGall et al. 1997). Several studies have shown that susceptibility to HIV infection and progression of AIDS are dependent on environmental and genetic factors. In spite of the multifactorial nature of AIDS and the difficulties in isolating the effect of individual allelic variations in genetically diverse groups of patients, better understanding of the modulation by the host factors of HIV infection and disease progression could be used in the future to design viral vectors for gene therapy and search for novel antiviral drug targets. There are several different cellular factors inhibiting different stages of the HIV-1 lifecycle.

<u>Host factors modulating virus entry.</u>

The beta-chemokines, macrophage inflammatory protein 1-MIP-1α(CCL3) and MIP-1β(CCL4), RANTES (CCL5) are the natural ligands of CCR5. When bound to CCR5, β-chemokines induce internalization of the receptor, decreasing its ability to promote HIV-1 infection (Garzino-Demo, Moss et al. 1999). The high level of these chemokines in exposed-uninfected persons further confirmed their role in the resistance against infection (Gonzalez, Kulkarni et al. 2005).

The macrophage inflammatory proteins alpha (MIP-1α) were reported to be more potent as CCR5 agonist than beta-chomokines. They are also the strongest inhibitors of infection by R5 strains of HIV-1. Recent studies have shown the connection between a high number of copies of MIP-1s and the sensitivity to HIV infection and AIDS progression (Chang, Vargas et al. 2005). These findings strongly support the role of MIP-1 in disease progression.

Another group of cellular factors with anti-HIV-1 activity are human defensins, which are cationic cysteine-rich peptides produced by leucocytes and epithelial cells. Treatment with alpha defensins interferes with virus entry mostly by blocking or eliminating viral receptors from the cell surface (Daher, Selsted et al. 1986; Cole 2003; Mackewicz, Yuan et al. 2003; Weinberg, Quinones-Mateu et al. 2006).

Beta-defensins have been mostly identified in epithelial cells. They share the same way of action than alpha-defensins. Additionally, β-defensins can control HIV-1 replication by modulating the immune system (Armogida, Yannaras et al. 2004).

The fact that both α and β defensins have been found in breast milk indicates that they could play a role in protecting infants from viral infection (Nakayama and Shioda).

Host restriction factors involved in the early steps of HIV-1 replication

In 2004, the tripartite motif 5 alpha (TRIM5 alpha) was identified as a host factor important in the restricted host range of HIV-1 (Nakayama and Shioda 2004). This protein recognizes the multimerized capsid (viral core) of an incoming virus by its alpha-isoform specific SPRY domain and is believed to be involved in innate immunity controlling retroviral infection. TRIM5α carries a RING domain that was frequently found in E3 ubiquitin ligases and was shown to degrade the HIV core via the ubiquitin-proteasome pathway (Lama and Planelles 2007).

Unlike simian forms, the human form of TRIM5α appears to only marginally inhibit HIV-1 replication (Nakayama and Shioda).

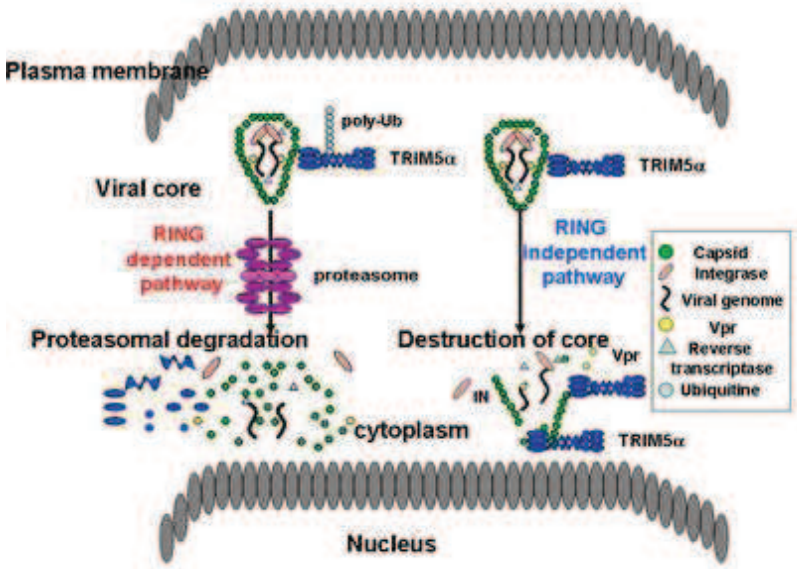

Fig.44. Anti-viral mechanism of action of TRIM5 alpha (Sheehy, Gaddis et al. 2002).

Another endogenous inhibitor of HIV-1 replication is APOBEC3G (apolipoprotein B mRNA-editing enzyme-catalytic polypeptide-like-3G), a host cystidine deaminase (Levin, Mitra et al.). APOBEC3G has two zinc-binding domains, each containing a conserved motif $HXE(X)_{23\text{-}28}CXXC$. APOBEC3G binds to ssRNA and ssDNA with similar affinities but the main substrate for deamination is ssDNA.

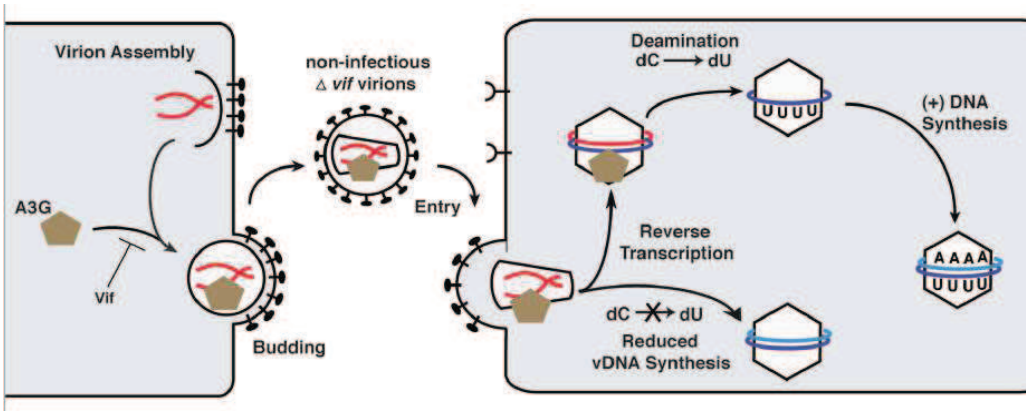

Fig.45. Effect of APOBEC 3G on HIV-1 replication (Luo, Wang et al. 2007).

In the absence of Vif protein, APOBEC3G proteins are packaged into newly formed virions. Viruses containing APOBEC3G infect other cells and undergo reverse transcription. The deaminase activity of APOBEC3G causes C to U mutation on exposed ssDNA regions

generated during reverse transcription. These mutations are harmful to the virus and lead to inhibition of virus replication. In addition to its effect on vDNA synthesis, APOBEC3G was also proposed to inhibit the integration step (Okumura, Lu et al. 2006). Moreover, APOBEC3G can disrupt the propagation of HIV by binding viral RNA, interfering with the obligatory strand transfers, physically blocking reverse transcriptase (RT), and obstructing integration into the host cell genome (Mbisa JL 2007). APOBEC3G has also been shown to block RT activity by decreasing tRNA priming, competing for binding to templates, and direct binding (Guo F 2007; Li XY 2007)..

However, studies on the APOBEC3G molecular properties have suggested that it may not inhibit the chaperone properties of NC during reverse transcription. The kinetics of $tRNA^{Lys}_3$ annealing to a viral RNA transcript was the same whether the reaction was performed in presence of NC alone or NC plus APOBEC3G. Similar results were observed when (-)ssDNA was annealed with the acceptor RNA. Thus, APOBEC3G shows marginal effect on the NC-promoted $tRNA^{Lys}_3$ or TAR annealing

Cellular factors modulating the late steps of HIV-1 replication.

As a key component of the innate response against viral infections, interferon-α has a great impact on HIV-1 particle release. The interferon-induced protein ISG15 appears to be a critical component of the interferon-α antiviral response. ISG15 inhibits ubiquitination of TSG101 and the late HIV-1 Gag domain, inhibiting the p6-TSG101 interaction required for viral budding (Biron 1998). Furthermore, IFN-α and IFN-β enhance the lytic activity of NK cells, making them very effective in killing cells infected with viruses (Zimmerman, Klein et al. 2002; Lingappa, Dooher et al. 2006).

Another host factor which regulates the late steps of the viral life cycle is HP68 (also known as ABCE1 and RNase L inhibitor). HP68 appears to be crucial in the assembly of the HIV-1 capsid proteins. HP68 interacts with the NC domain of Gag, and as proteolytic processing of the Gag polypeptide occurs, HP68 is released and viral particles acquire their mature conformation (Lama and Planelles 2007). However, the role of HP68 in HIV pathogenesis in vivo has not yet been evaluated.

Regarding HIV infection, there are two key groups of proteins participating in the innate immune response against HIV, namely cytokines and Tol-like receptors (Jacques, Gosset et al. 2006). The cytokine protein group can be divided into HIV-inducing (TNF-α, TNF-β, Il-1 and IL-6) and HIV-suppressing (IFN-α, IFN-β and IL-16) proteins. IL-1α and IL-1β are known to be co-stimulatory cytokines for T helper cells and promoter of B cell maturation and

clonal expansion (Kornfeld and Cruikshank 2001). IL-16 is a multifunctional cytokine, inducing both suppression of HIV-1 replication and enhancing expression of IL-2 receptors, making T cells responsive to IL-2 (Stylianou, Bjerkeli et al. 2003; Torre and Pugliese 2006). IL-18 is a pro-inflammatory cytokine mostly secreted by activated macrophages. IL-18 is known to play an important role in responses against viruses and intracellular pathogens, inducing IFN-γ production in T cells and enhancing NK cytotoxic activity. Increased levels of IL-18 have been found in late stage HIV-1 patients, and plasma levels of this cytokine correlate with viral load, constituting an excellent marker for disease progression (Biron 1998).

Proteins of the interferon family play essential roles in the innate response against viruses, including HIV-1. Type 1 interferons (IFN-α and IFN-β) induce expression of protein kinase R (PKR), which blocks protein synthesis in virus-infected cells. IFN-α/β also enhance lytic activity of NK cells, making them very effective in killing virally-infected cells (Lama and Planelles 2007).

Toll-like receptors are believed to modulate the extent of viral replication. Members of the TLR family recognize specific motifs expressed by pathogens such as lipid moieties, protein motifs and nucleotide sequences (Pomerantz, Feinberg et al. 1990). The first piece of evidence that TLRs have an impact in HIV pathogenesis dates back to 1990 when it was shown that bacterial lipopolisaccharide activates viral LTR, a process mediated by TLR4 (Lama and Planelles 2007) (Chen, Hoy et al. 2007).

X. Developments in antiretroviral therapy

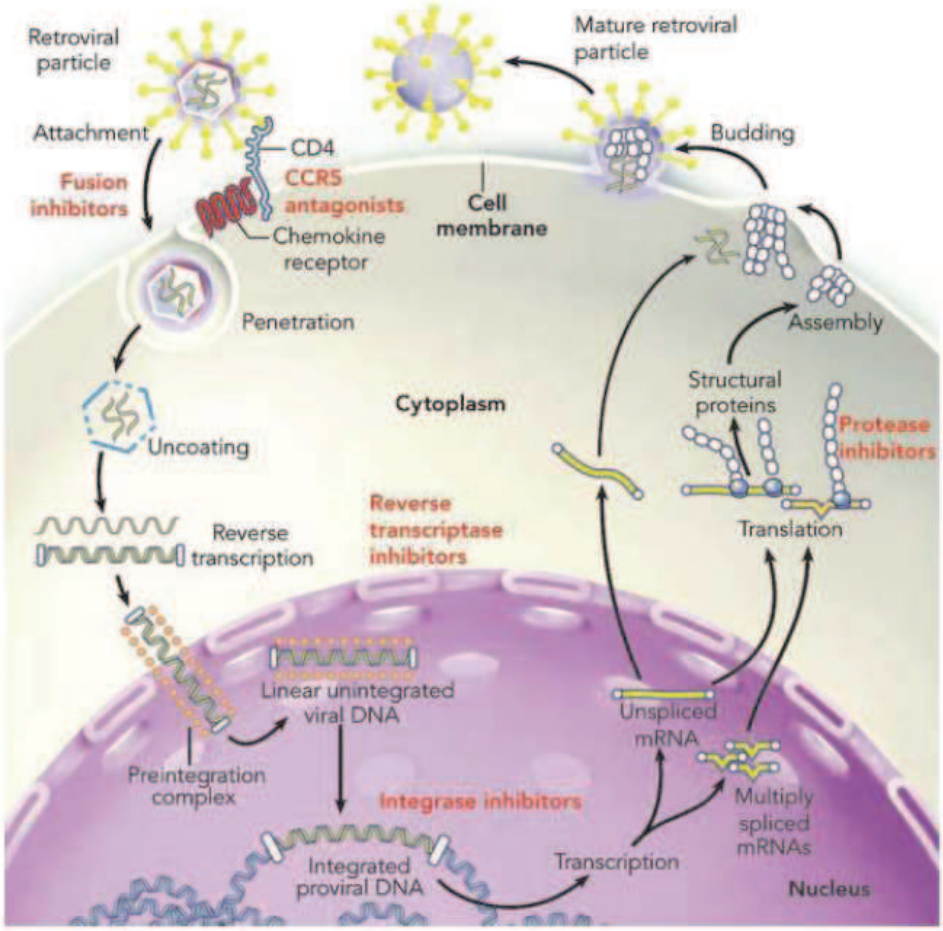

Fig.46. Life cycle and site of action of antiretroviral therapy (Palella, Delaney et al. 1998).

Nowadays with the use of the highly active antiretroviral therapy (HAART), HIV-1 infection is treated as a chronic disease (Shen, Peterson et al. 2008). Excess mortality among patients with AIDS was nearly halved in the HAART era, but it remains approximately 5 times higher in patients with AIDS than in HIV-infected patients without AIDS. There are currently six classes of antiretroviral agents, targeting different steps in the viral life cycle.

Antiretroviral drug class	**Abbreviations**	**First approved to treat HIV**	**How they attack HIV**
Nucleoside/Nucleotide Reverse Transcriptase Inhibitors	NRTIs, nucleoside analogues,	1987	Being analogue of naturally occurring purines and pirimidines, nucleosides are recognized by RT and incorporated in the nascent DNA, preventing viral DNA synthesis. NRTIs need to be activated by intercellular phosphorylation.
Non-Nucleoside Reverse Transcriptase Inhibitors	NNRTIs, non-nucleosides,	1997	Bind directly to reverse transcriptase noncompetitevely inhibiting enzymatic activity
Protease Inhibitors	PIs	1995	PIs inhibit HIV protease
Fusion or Entry Inhibitors		2003	Fusion or entry inhibitors prevent HIV from binding to or entering human immune cells.
Integrase Inhibitors		2007	Integrase inhibitors interfere with the HIV integrase enzyme, important for integration.

Table 3. Antiretroviral agents currently available.

X.1.1. Nucleoside/nucleotide reverse transcriptase inhibitors (NRTIs) were the first agents available for the treatment of HIV infection. Although less potent against HIV than nonnucleoside reverse transcriptase inhibitors (NNRTIs) and protease inhibitors (PIs), the NRTIs have had a central role in antiretroviral treatment and remain part of the current standard of care (Cox, Aperia et al. 1994). They exhibit activity against HIV-1 and HIV-2 (Cihlar and Ray).

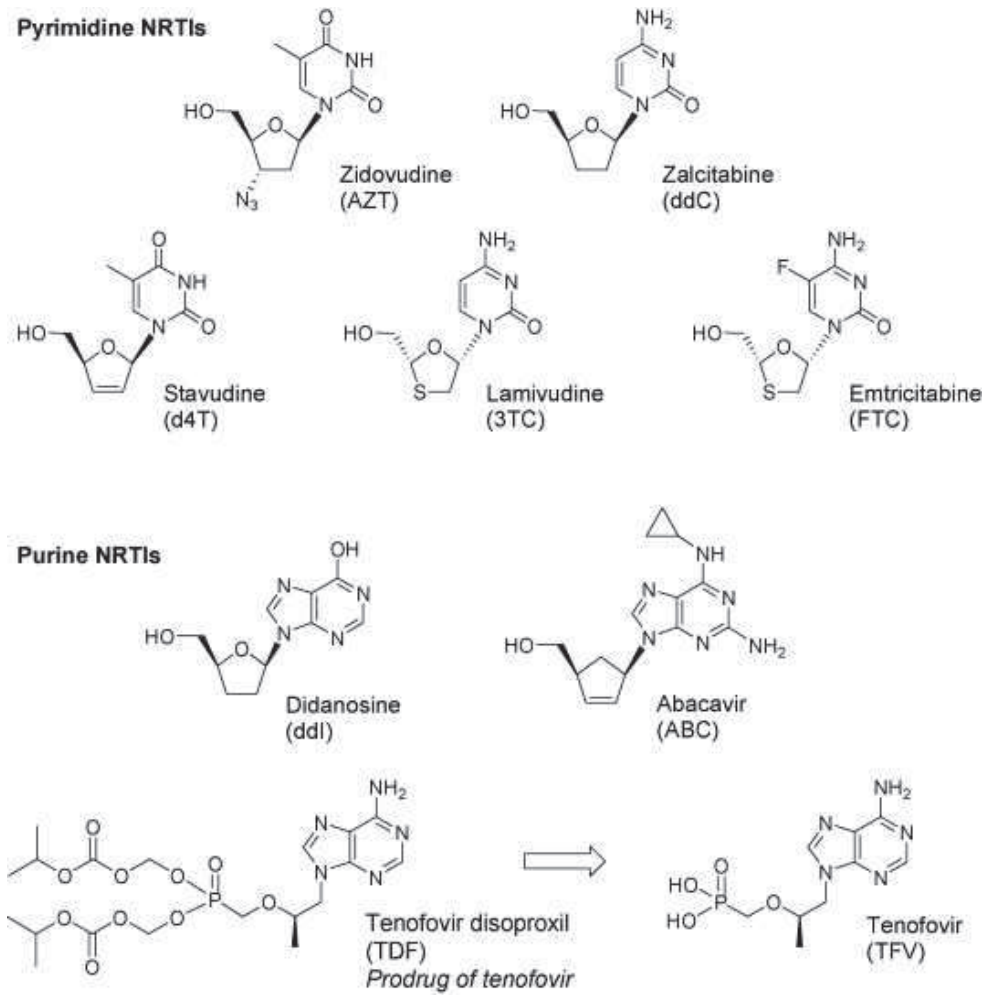

Fig.47. Structures of approved nucleoside/nucleotide reverse transcriptase inhibitors (Weller and Williams 2001)

Mechanism of action

NRTIs interrupt the HIV replication cycle via competitive inhibition of HIV reverse transcriptase (Clavel and Hance 2004). They are incorporated into the viral DNA, preventing reverse transcription and causing inhibition of viral DNA synthesis. Although this group was shown to be specific for RT, mitochondrial DNA polymerase γ inhibition was also observed.

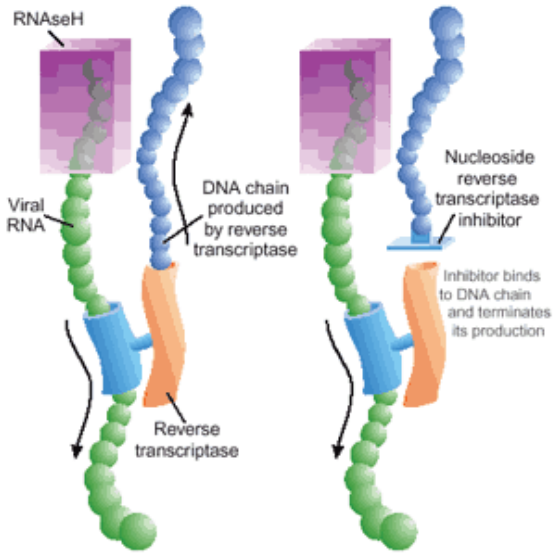

Fig.48. NRTIs : mechanisms of action.

However, resistance to NRTIs is observed. It occurs by either impaired incorporation into the proviral DNA chain or removal from the proviral DNA chain (Clavel and Hance 2004). Mutations typically occur gradually, with accumulation of several mutations before resistance develops. Thymidine analog mutations (mutations associated with zidovudine resistance (M41L, D67N, K70R, L210W, T215Y, T215F, K219Q, K219E) remove NRTIs from the DNA chain by fostering a conformational change in the reverse transcriptase domain that allows the addition of ATP or pyrophosphate to the end. This placement causes a break in the proviral DNA and NRTI bond, enabling continued elongation of the proviral DNA strand (Shen, Peterson et al. 2008).

X.1.2.Nonnucleoside reverse transcriptase inhibitors (NNRTIs) were introduced in 1996 with the approval of Nevirapine. NNRTIs exhibit potent activity against HIV-1 and are part of preferred initial regimens (Rimsky, Azijn et al. 2009).

First-generation NNRTIs include Delavirdine (Rescriptor), Efavirenz (Sustiva) and Nevirapine (Viramune). Second-generation NNRTIs currently include Etravirine (Intelence) and Rilpivirine (Edurant) approved in 2011.

All NNRTIs exhibit the same mechanism of action. First-generation NNRTIs share similar resistance patterns, whereas Etravirine and Rilpivirine display a more unique resistance profile (Sluis-Cremer, Temiz et al. 2004).

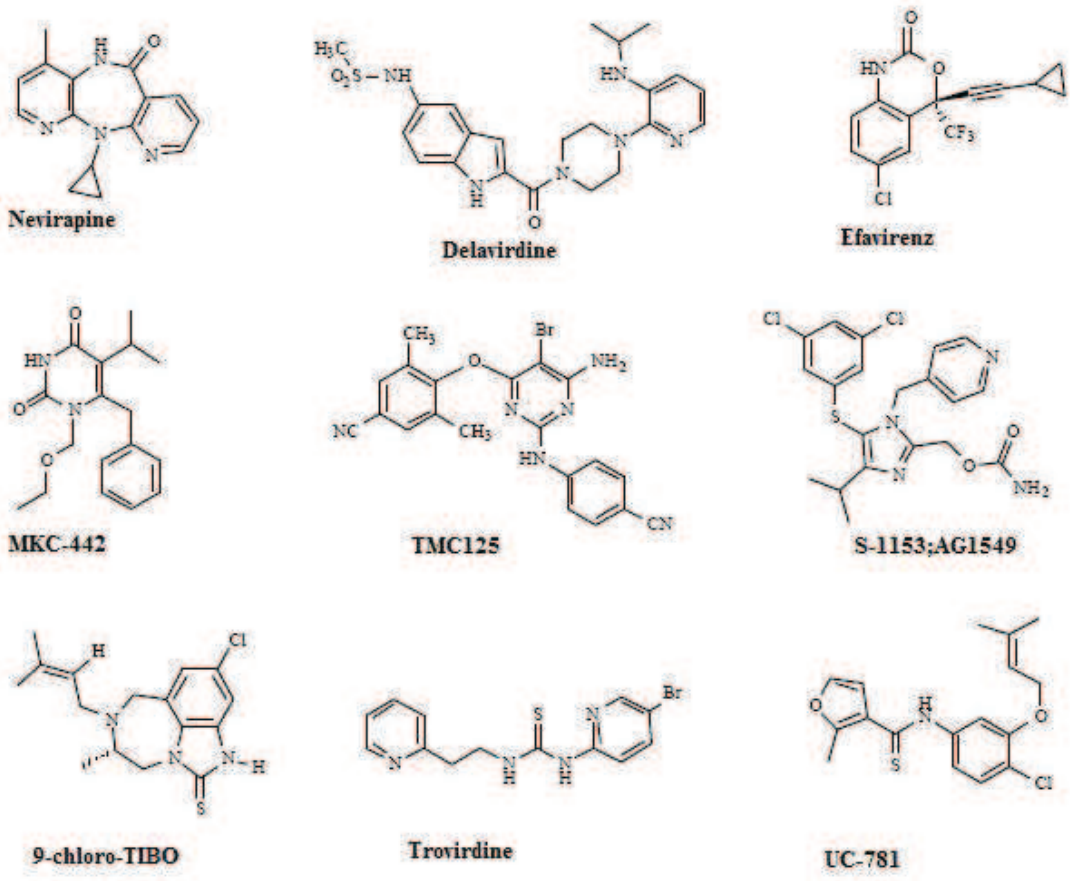

Fig.49. Some non-nucleoside inhibitors of HIV reverse transcriptase (NNRTIs) (Kroeger Smith MB 2003).

Mechanism of action

NNRTIs bind the p66 subunit at a hydrophobic pocket distant from the active site of the enzyme. This noncompetitive binding induces a conformational change in the enzyme that alters the active site and limits its activity (fig.50) (Vingerhoets, Azijn et al. 2005). Mutations within the reverse transcriptase gene domain alter the ability of the NNRTIs to bind to the enzyme. First-generation NNRTIs have a low genetic barrier to resistance, whereby a single mutation in the binding site can decrease the ability of the drug to bind, significantly diminishing its activity (Karacostas, Nagashima et al. 1989; Roberts, Martin et al. 1990). Etravirine differs from first-generation NNRTIs in its ability to bind at this site despite the presence of mutations that limit the efficacy of the first-generation agents. It is a highly flexible molecule able to rotate within the binding site to allow multiple binding

conformations. In vitro studies have shown that etravirine also shows activity against HIV-2 (Soriano and de Mendoza 2002).

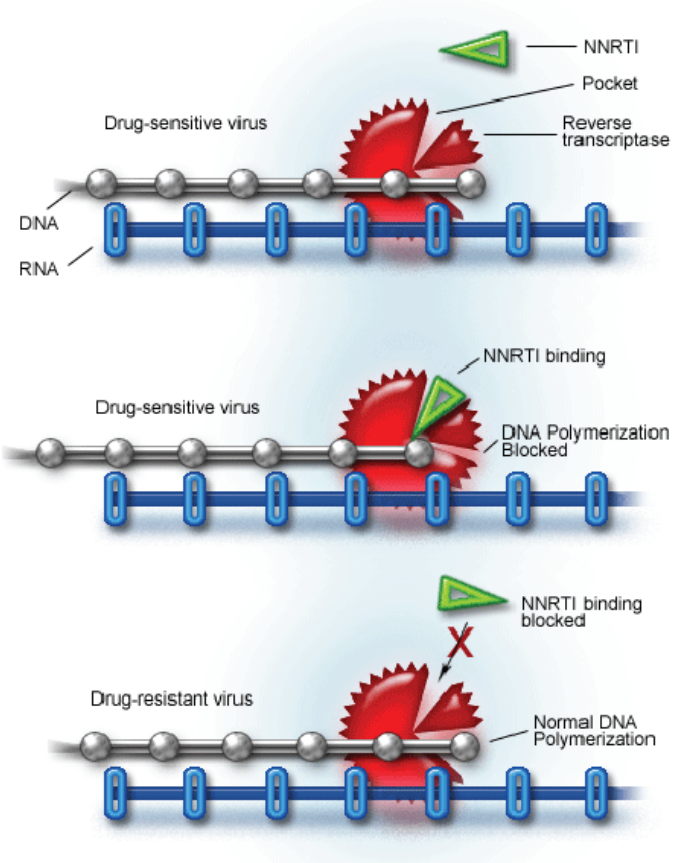

Fig.50. Mechanism of NNRTI activity and HIV NNRTI resistance

X.1.3. HIV protease inhibitors (PIs) were first introduced in 1995 and are an integral part of treatment of HIV infection. Although all protease inhibitors exhibit the same mechanism of action, they show important differences in pharmacokinetics, efficacy and adverse event profiles.

Mechanism of action

HIV protease systematically cleaves individual proteins from the *gag* and *gag -pol* polypeptide precursors into functional subunits for viral capsid formation during or shortly after viral budding from an infected cell. HIV protease inhibitors function as competitive inhibitors that directly bind to HIV protease and prevent subsequent cleavage of gag and gag-pol protein precursors in acutely and chronically infected cells, arresting maturation and thereby blocking the infectivity of nascent virions (Flexner 1998). They exhibit activity

against clinical isolates of both HIV-1 and HIV-2 (Roberts, Martin et al. 1990; Kempf, Marsh et al. 1995), with in vitro IC_{50} values ranging from 2 to 60 nM (Arts and Hazuda).

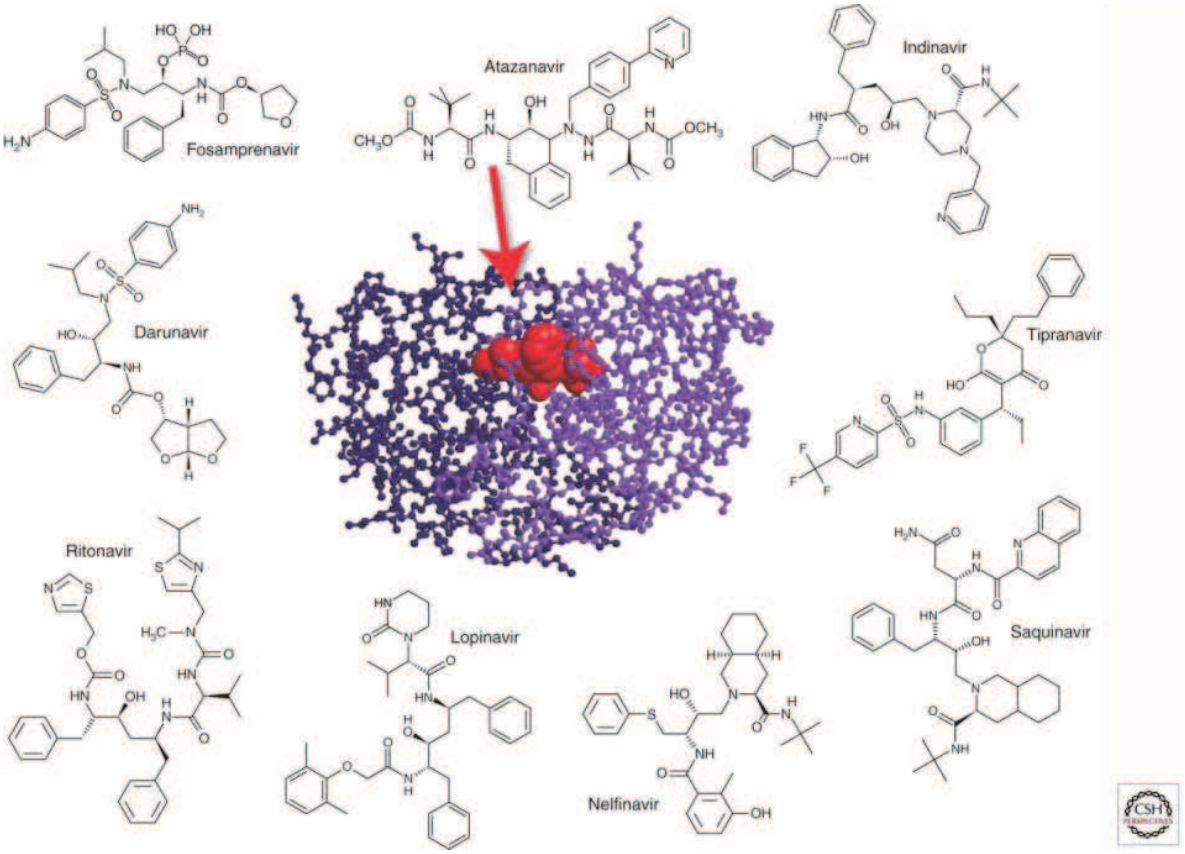

Fig.51. Protease inhibitors and crystal structure of HIV-1 protease complexed with atazanavir (Kim and Baxter 2008)

Resistance to HIV protease results from mutations both inside and outside the active protease domain (Kim and Baxter 2008). Resistance typically occurs through the development of one or more major mutations, which produce conformational changes in the protease binding site, followed by secondary compensatory mutations that improve enzymatic activity and, in some cases, viral fitness (Kim and Baxter 2008).

The second-generation protease inhibitors lopinavir/ritonavir, darunavir and tipranavir may retain activity in the presence of resistance to first-generation agents. Lopinavir/ritonavir requires the accumulation of 7 or more mutations before high-level resistance develops (Rhee, Taylor et al.). Darunavir and tipranavir typically retain activity against lopinavir/ritonavir and first-generation protease inhibitor–resistant strains.

A review of 2725 HIV isolates for protease inhibitor susceptibility revealed that certain mutations could result in increased susceptibility to a particular drug, and that some effects on resistance had been underestimated (Dyda, Hickman et al. 1994). The study concluded that

cross-resistance between the various protease inhibitors now and in the future may be missed without a systematic analysis of the effects of specific mutations.

Importantly, HIV-1 (M) shows wide resistance to NRTIs, NNRTIs and PRIs (Johnson VA 2011)

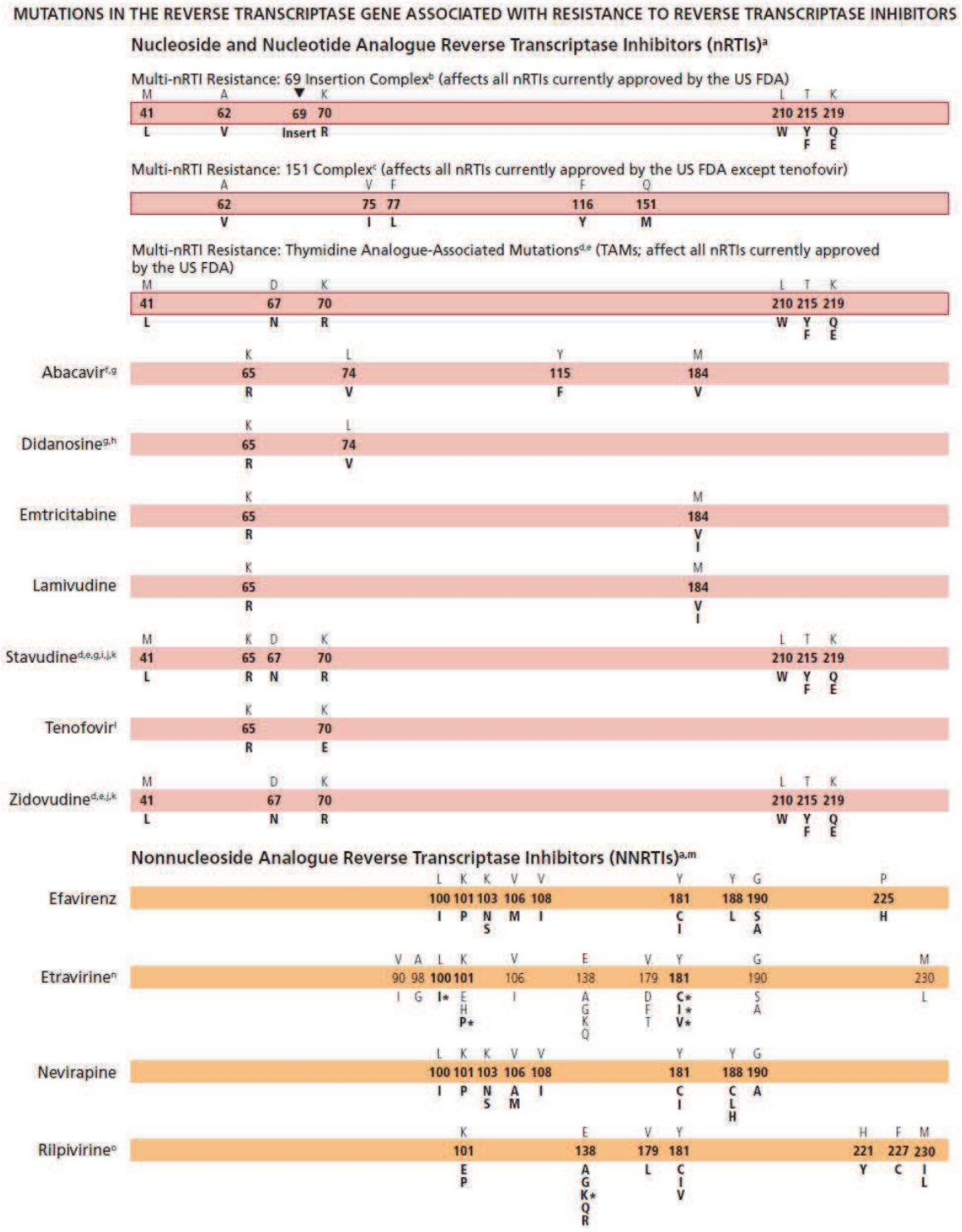

MUTATIONS IN THE PROTEASE GENE ASSOCIATED WITH RESISTANCE TO PROTEASE INHIBITORS[p,q,r]

Atazanavir +/– ritonavir[s]

L	G	K	L	V	L	E	M	M	G	I	F	I	D	I	I	A	G	V	I	I	N	L	I
10	16	20	24	32	33	34	36	46	48	**50**	53	54	60	62	64	71	73	82	**84**	85	**88**	90	93
I F V C	E	R M I T V	I	I	I F V	Q	I L V	I L	V	L	L Y	L V M T A	E	V	L M V	V I T L	C S T A	A T F I	V	V	S	M	L M

Darunavir/ ritonavir[t]

V	V	L	I	I	I	T	L	I	L
11	32	33	**47**	**50**	**54**	74	**76**	**84**	89
I	I	F	V	V	M L	P	V	V	V

Fosamprenavir/ ritonavir

L	V	M	I	I	I	G	L	V	I	L
10	32	46	47	**50**	54	73	76	82	**84**	90
F I R V	I	I L	V	V	L V M	S	V	A F S T	V	M

Indinavir/ ritonavir[u]

L	K	L	V	M	M	I	A	G	L	V	V	I	L
10	20	24	32	36	**46**	54	71	73	76	77	**82**	**84**	90
I R V	M R	I	I	I	I L	V	V T	S A	V	I	A F T	V	M

Lopinavir/ ritonavir[v]

L	K	L	V	L	M	I	I	F	I	L	A	G	L	V	I	L
10	20	24	**32**	33	46	**47**	50	53	54	63	71	73	**76**	**82**	84	90
F I R V	M R	I	I	F	I L	V A	V	L	V L A M T S	P	V T	S	V	A F T S	V	M

Nelfinavir[u,w]

L	D	M	M	A	V	V	I	N	L
10	**30**	36	46	71	77	82	84	88	**90**
F I	N	I	I L	V T	I	A F T S	V	D S	M

Saquinavir/ ritonavir[u]

L	L	G	I	I	A	G	V	V	I	L
10	24	**48**	54	62	71	73	77	82	84	**90**
I R V	I	V	V L	V	V T	S	I	A F T S	V	M

Tipranavir/ ritonavir[x]

L	L	M	K	M	I	I	Q	H	T	V	N	I	L
10	33	36	43	46	**47**	54	**58**	69	**74**	**82**	**83**	**84**	89
V	F	I L V	T	L	V	A M V	E	K R	P	L T	D	V	I M V

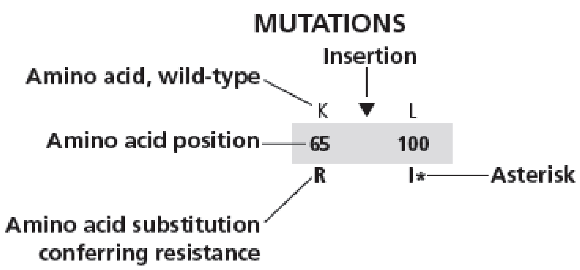

Table.4. The wide resistance to NRTIs, NNRTIs and PRIs of HIV-1(M) virus ((Johnson VA 2011). Amino acid abbreviations: A, alanine; C, cysteine; D, aspartate; E, glutamate; F, phenylalanine; G, glycine; H, histidine; I, isoleucine; K, lysine; L, leucine; M, methionine; N, asparagine; P, proline; Q, glutamine; R, arginine; S, serine; T, threonine; V, valine; W, tryptophan; Y, tyrosine.

X.1.4. Integrase Inhibitors

The crystal structure of HIV integrase was first described in 1994 and led to the identification of novel inhibitors (Anthony 2004; Kassahun, McIntosh et al. 2007). However, no homology for HIV integrase was observed in humans thus, identification of selective inhibitors is expected to result in a low frequency of adverse effects (Delelis, Carayon et al. 2008).

Using biochemical assays, several classes of IN inhibitors have been discovered over the past 17 years (Fesen, Kohn et al. 1993; Robinson, Reinecke et al. 1996). Hydroxylated natural products like dihydroxynaphtoquinones, isoflavones, chicoric acid and caffeic acid were reported in early biochemical studies (Marchand, Maddali et al. 2009). Derivatives were developed (CAPE, 5-CITEP, V-165) but the most important family of inhibitors that emerged was the diketo acids (DKA). L-870,810 (Merck & Co.) and S-1360 (Shionogi & Co. Ltd. and GlaxoSmithKline) were the first DKA-like IN inhibitors to reach clinical trials. DKA derivatives are Strand Transfer-selective inhibitors (INSTI) with high specificity for IN-DNA complexes and antiviral activity. Clinical trials with S-1360 and L-870,810 were terminated in phase I/II and II due to limited efficacy and toxicity, respectively (Andreola 2009). Peptides and nucleic acid inhibitors of IN *in vitro* have also been identified by screening (phage display, yeast 2-hybrids, SELEX) or rational design (derived from viral or cellular co-factors) (Semenova, Marchand et al. 2008). For instance, Zintevir (AR177) (Aronex Pharmaceuticals) is a G-quadruplex-forming oligonucleotide that inhibits both recombinant IN and HIV-1 replication at low nanomolar concentration. It entered clinical trials in 1996, before the DKA, but was shown to target viral entry in cells and clinical trials were discontinued. After years of sustained effort, Merck and Co. successfully developed raltegravir (RAL, Isentress® also known as MK-0518), which was approved by the FDA in late 2007 as the first IN inhibitor. As for DKA, RAL's inhibition mechanism is specific for the strand transfer step of integration and proposed to involve chelation of one or two metals within the IN active site, after processing of the bound viral DNA ends (Hare, Gupta et al.).

Crystal structures obtained recently with RAL bound to the full length PFV IN confirmed the binding of two metal ions. Binding of RAL also induces a displacement of the viral DNA within the IN active site, moving the terminal 3'-A of the conserved CA by more than 6 Å from its original position (2009). RAL also makes Van Der Waals (VDW) interactions with the conserved CA dinucleotide and the fourth guanine from the end of the non-cleaved strand (base paired with the conserved C). In addition, RAL contacts several amino acids, including P214 and Q215 (corresponding to P145 and Q146 for HIV-1 IN, respectively) by VDW interactions, and P214 (P145) by hydrophobic interaction and Y212 (Y143) by stacking

interaction. RAL also forms polar interactions with the catalytic triad (DDE) and the two Mg^{2+} ions. This binding mode is consistent with the interfacial inhibition paradigm whereby RAL was proposed to bind at the interface of IN and its DNA substrate.

First used in regimen of heavily treated patients, RAL is now approved (since July 2009) for first line therapy in combination with other drugs used in the HAART combination regimen (Markowitz, Nguyen et al. 2007). RAL has a remarkably low toxicity, exhibits high potency and favorable pharmacokinetics. In first line therapy, the oral formulation (400 mg twice a day) induces a large decrease of viral RNA load below detection levels within a few weeks (Marchand, Maddali et al. 2009).

Elvitegravir (EVG, GS-9137, JTK-303) is the next most advanced IN inhibitor. It is developed by Gilead Sciences and presently in phase III clinical trials. *In vitro*, EVG exhibits potent anti-IN and anti-HIV activity at low nanomolar IC50 and EC90 (Marinello, Marchand et al. 2008). EVG is a slightly more potent IN inhibitor than RAL (Correll and Klibanov 2008). However, it has also been reported to produce some non-specific toxicity in non-infected cells. EVG is metabolized *in vivo* by cytochrome P450 and glucuronidation (Metifiot, Marchand et al.), and co-administration with ritonavir (PR inhibitor) increases EVG systemic concentrations by about 20-fold, consistent with a possible once daily use of the drug (Chan, Fass et al. 1997; Weissenhorn, Dessen et al. 1997)

X.1.5.Fusion inhibitors (FIs) were the first class of antiretroviral medications targeting the HIV replication cycle extracellularly. Theyreceived accelerated FDA approval in 2003. Their unique mechanism of action provides additional options for therapy in patients who are highly treatment resistant. However, use of fusion inhibitors has been limited, because of the production time and costs, inconvenient administration (subcutaneous injection) and adverse effect profile. The discovery of additional antiretroviral classes and medications with activity against highly resistant viral strains has further limited the utility of the fusion inhibitors. Moreover, the only product proposed, Fuzeon was shown to cause injection site reactions with enfuvirtide, which usually are mild to moderate but occasionally can be severe.

Mechanism of action

Fusion inhibitors act extracellularly to prevent the fusion of HIV to f target cells. Enfuvirtide blocks the second step in the fusion pathway by binding to the HR1 region of the glycoprotein 41 (gp41). This mechanism does not allow HR1 and HR2 to fold properly, thereby preventing the conformational changes of gp41 required to complete the final step in the fusion process (Perez-Alvarez, Carmona et al. 2006).

Resistance to enfuvirtide has been well described and occurs in the HR1 domain of gp41. Amino acid substitutions in the 36-45 region result in a significant loss of enfuvirtide activity (Lalezari, Henry et al. 2003; Lazzarin, Clotet et al. 2003). The risk of resistance can be minimized by combining enfuvirtide with other antiretroviral agents that display genotypic or phenotypic activity, which is now more easily achieved with the availability of second-generation nonnucleoside reverse transcriptase inhibitors (NNRTIs) and protease inhibitors (PIs) and new antiretroviral classes (eg, integrase inhibitors and CCR5 inhibitors) (Lieberman-Blum, Fung et al. 2008).

X.1.6. Chemokine Receptor Antagonists

In August 2007, maraviroc (Selzentry) was approved by the FDA and was the first medication in a novel class of antiretroviral agents termed chemokine receptor 5 (CCR5) antagonists. It joins the fusion inhibitors (FIs) as another type of the general class of HIV-entry inhibitors.

Mechanism of action

The way by which HIV binds to CD4 cells and ultimately fuses with the host cell is a complex multistep process, which begins with binding of the gp120 HIV surface protein to the CD4 receptor. This binding induces a structural change that reveals the V3 loop of the protein. The V3 loop then binds with a chemokine co-receptor (principally either CCR5 or CXCR4), allowing gp41 to insert itself into the host cell and lead to fusion of the cell membranes. Maraviroc selectively and reversibly binds the CCR5 co-receptor, blocking the V3 loop interaction and inhibiting fusion of the cellular membranes. Maraviroc is active against HIV-1 CCR5 tropic viruses, but has no activity against CXCR4 tropic or dual/mixed tropic virus (Lieberman-Blum, Fung et al. 2008).

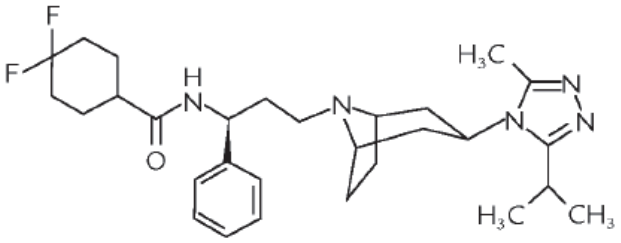

Fig.52. Chemical structure of Maraviroc (Li, Goila-Gaur et al. 2003).

Although experience with maraviroc is limited, treatment failure due to resistance has been observed. Resistance appears to occur via two mechanisms. The first mechanism is most

likely through amino acid substitutions in the V3 loop of gp120. Although specific mutations associated with resistance have not yet been described, they appear to allow HIV binding to the co-receptor despite the presence of maraviroc.

The second mechanism does not provide resistance but rather the inability of phenotypic tropism assays to detect small quantities of CXCR4 virus that may be present, leading to overgrowth of CXCR4 virus in the presence of maraviroc and loss of viral control.

X.2.Novel antiviral treatment

X.2.1. Maturation inhibitors.

This is a new class of inhibitors, targeting the Gag precursor protein and its function in virus assembly. Currently, there are no FDA approved maturation inhibitors available. However, there are few maturation inhibitors in trials. In 2007, 3-O-(3',3'-dimethylsuccinyl)-betulinic acid, known as Bevirimat gave promising results in early Phase I and Phase II trials, showing good antiviral activity even in patients with resistant virus.

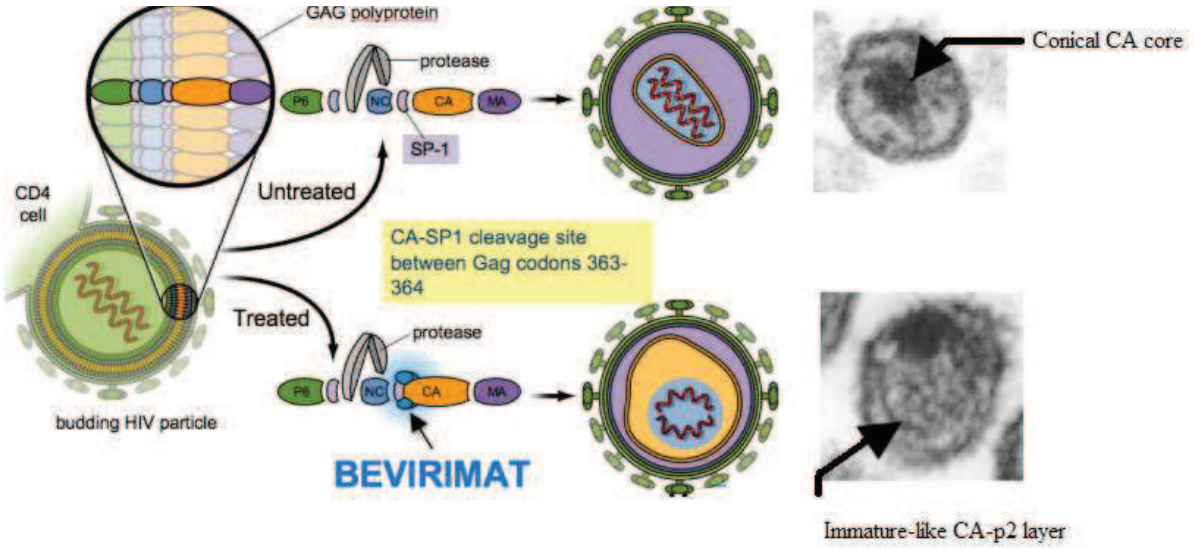

Fig.53. Proposed mechanism of action of Bevirimat (Panacos.com). Micrographs are reproduced from (Adamson, Ablan et al. 2006).

Additionally, a safety study showed that Bevirimat was safe to be taken with other established HIV medications. Specifically, when Berivimat was taken with Reyataz (protease inhibitor), bilirubin levels in the blood were not more elevated than with Reyataz alone. However, more extensive studies are needed before Berivimat would be ready for commercial use (Waheed

and Freed 2008). Although Berivimat seemed to be promising agent in anti-HIV therapy, on June 8, 2010, bevirimat's developer, Myriad Genetics, announced that it was suspending its HIV drug development program. While it is possible that bevirimat and another maturation inhibitor being developed by Myriad will be sold to another company for ongoing development, no licensing agreements have been announced.

PA1050040 is a second generation of HIV maturation inhibitor drug, chemically analogous to Bevirimat. PA10540040 also inhibits HIV replication by inhibiting the final step in the gag processing cascade thus causing production of a defective outer core and the release of noninfectious virus particles from infected CD4+ T cells. Additionally, PA1050040 was shown to be active against HIV isolates resistant to Bevirimat.

Another promising anti-maturation agent is Vivecon (MP-9055) which is now in Phase II trials. Phase I study showed that the doses of Vivecon studied achieved levels in the blood capable of inhibiting HIV when taken with food. Preliminary laboratory tests have already suggested that this drug is active against virus strains resistant to drugs from both the non-nucleoside reverse transcriptase and protease inhibitor classes.

X.2.2.Peptide inhibitors of HIV-1 egress.

A potential target for the development of new anti-HIV-1 agents seems to be the interaction between the p6 domain and Tsg101, a component of ESCRT complex. By the use of reverse two-hybrid strategy, new cyclic peptides disrupting this interaction have been identified (Tang, Loeliger et al. 2003). The most active inhibitor, IYWNVSGW, decreased virus-like particles by 2-3 fold with an IC_{50} of 7 μM. However, an effect of the tested peptide on the normal functions of Tsg101 was also observed.

A very promising peptide inhibiting CA was characterized for the first time in 2003 (Zhang, Zhao et al. 2008). Among two potent inhibitors, CAP-1 and CAP-2, only CAP-1 showed dose-dependent HIV-1 inhibition (Zhang, Zhao et al. 2008) whereas CAP-2 was highly cytotoxic. Unfortunately, CAP-1 was shown to interfere only with the maturation step of HIV-1 life cycle. Recently, by the use of phage-display techniques, a new 12-mer peptide CAI was identified and shown to disrupt the assembly of both immature and mature VLP in vitro by targeting the C-terminal domain of CA protein. Unfortunately, CAI was not able to inhibit HIV-1 in cell cultures mostly due to its lack of cell permeability.

Modification of CAI led to the design of a new cell-penetrating peptide, NYAD-1, which interacts with the C-terminal domain of CA, which is crucial in the dimerization process. NYAD-1 was shown to disrupt the formation of both immature and mature virus particles in

cell-free and cell-based in vitro systems. In addition, NYAD-1 was found to exhibit anti-HIV-1 activity in a large panel of both laboratory-adapted and primary HIV-1 isolates at the micromolar range (Domagala, Bader et al. 1997).

X.2.3. Anti-NC molecules

Nearly all currently available inhibitors of HIV replication target the enzymatic components of the virion. Due to the fact that NC does not have any enzymatic activity, HTS assays are not easy to design. This task is even further complicated by the fact that many of the NC functions rely on poorly specific interactions mediated through the basic domains of NC. Moreover, the genomic RNA coating by a large number of NC copies is causing high local concentration of NC in the viral particles and thus, likely requires high concentration of anti-NC molecules.

Despite all these difficulties, different classes of anti-NC molecules have been developed or selected.

X.2.3.1. Zinc ejectors

The proof of concept for zinc ejectors as anti-NC drugs was demonstrated in the 90's with a series of small compounds such as the benzamide family (NOBA, DIBA) (Vandevelde, Witvrouw et al. 1996), the pyrimidinioalkanoyl thioester (PATEs) and azodicarbonamide (ADA) (Huang et al. 1998). For these compounds, depletion of zinc begins at the level of the C-terminal zinc finger. In the case of DIBA, the nucleophilic attack of the cysteins (Cys39 and Cys49) of the second ZF leads to a covalent modification of NC with the formation of a disulfide bridge. This initial covalent link promotes the reaction of additional reactants with other Cys residues of the same motif and finally leads to zinc ejection and NC unfolding.

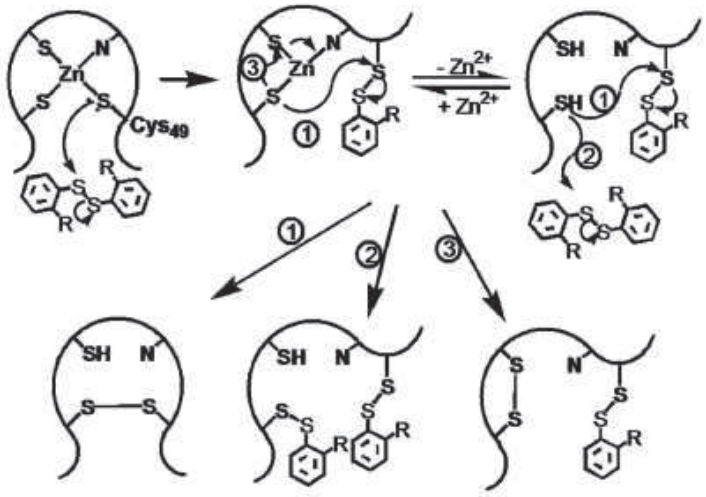

Fig.54. Proposed mechanism of zinc ejection by DIBA (Wu, Bishopric et al. 1996; Whittal, Benz et al. 2000).

Unlike DIBA compounds, thioester-based chemotypes including the pyridinioalkanoyl thioesters (PATE) do not use an oxidative mechanism. Instead, they acylate the cysteine residue and release a free thiol. The acylation of NC by PATEs results in the formation of thioester bond. Nevertheless, ZFs of cellular transcription factors such as Sp1, FOG-1, GATA-1 and the steroid-binding glucocorticoid receptor were also sensitive to thiol-reducing agents (Turpin, Terpening et al. 1996), which explains their toxicity.

In cellular assays, zinc ejectors inhibit a wide range of HIV-1 isolates (Turpin, Terpening et al. 1996). In spite of the importance of the NC ZF structure for the specific packaging of genomic RNA, a significant amount of gRNA was found in the treated virions (Berthoux, Pechoux et al. 1999) likely due to the protection afforded by the RNA from the attack by the zinc ejectors (Chertova, Kane et al. 1998; Berthoux, Pechoux et al. 1999; Bernacchi, Stoylov et al. 2002). Interestingly, DIBA also causes formation of heterogeneous populations of immature viral particles (Gillespie, Kuti et al. 2005), probably as a result of the DIBA-induced alteration of the viral assembly pathway (Grigorov et al. 2006).

Though the surface of the virion keeps a wild type conformation (Lifson et al. 2002; Chertova, Kane et al. 1998) proviral DNA synthesis was strongly impaired, resulting from the inability of oxidized NC to chaperone the initiation and elongation of cDNA synthesis (Levin and Gou 2005; Beltz 2005).

Complete inactivation of virus infectivity together with the preservation of the structure and functions of the viral envelope made these particles a potential attractive vaccine (Arthur, Bess et al. 1998; Chertova, Kane et al. 1998; Chertova, Chertov et al. 2006). This was tested with the simian immunodeficiency virus (SIV), closely related to HIV-2. The AT-2-

inactivated SIV was not infectious and elicited both humoral and cellular immune responses (Lifson et al. 2004). The resulting immunization facilitated effective containment of pathogenic homologous challenge viruses but failed to protect against heterologous SIV isolates. Based on DIBA compounds, thioester-based chemotypes, SAMT and PATE, were developed. Recently, due to the fact that SAMTs were able to prevent HIV transmission from infected cells to uninfected ones with EC_{50} below 100 nM, SAMT compounds were tested as a topical microbicides to prevent HIV transmission (Turpin, Schito et al. 2008).

ADA has been used for the unique clinical trial using zinc ejectors (Turpin 2003). An increase in the number of CD4 cells similar to that obtained with other antiretroviral agents and a decrease in the viral load were observed, but only in 1/3 of the treated patients. Unfortunately, the ratio of infectious to non infectious particles was not determined. A combination with other antiretrovirals could be possible, but the renal toxicity of the biurea metabolite of ADA would prevent a combination with PR inhibitors that are nephrotoxic (De Clercq 2002).

X.2.3.2. Non zinc ejecting NC binders.

The limited specificity of zinc ejectors for HIV NC prompted the search for compounds able to bind NC but with no zinc ejecting properties. A first screening assay (Stephen et al. 2002) based on the inhibition of the binding of NC to oligonucleotides containing TG repeats led to the identification of tetrachlorogallein derivatives, which stoichiometrically bind and inhibit NC chaperone properties. The most active compounds such as gallein were active in the nanomolar range but did not show any activity when added after DNA titration with NC, suggesting that they exhibit an antagonist effect against free NC only. It is thought that these compounds may interfere with NC ability to stack its aromatic residues with the bases of targeted nucleic acids.

More recently, a HTS based on NC-promoted destabilization of ODN, was used to detect a new group of hits able to inhibit this specific property of NC (Azoulay et al. 2003). Five positive hits with IC_{50} values in the low micromolar range have been selected (Shvadchak et al, 2009). On the basis of ESI-Mass Spectroscopy in nondenaturing conditions, which has been shown to be appropriate to characterize non-covalent complexes with proteins (Dhe-Paganon, Duda et al. 2002; Sanglier, Bourguet et al. 2004),Four out of the five hits were found to form a stable complex with NC(12-55). Interestingly, none of these compounds was able to eject zinc, in contrast with DIBAs, PATEs, N-ethylmaleimide (NEM) and SAMTs (Rein, Ott et al. 1997). Moreover, the inhibitory properties of the tested molecules were not modified in the presence of an excess of free zinc further suggesting that the hits do not

interact with the zinc bound to NC(12-55). The lack of zinc ejection by those compounds should avoid the targeting of cellular zinc binding proteins, which caused the toxicity of most anti-NCs based on zinc ejectors. Additionally, hits differ from the gallein derivatives, by their ability to inhibit NC(12-55) even when the protein is already bound to cTAR (Cruceanu, Stephen et al. 2006).

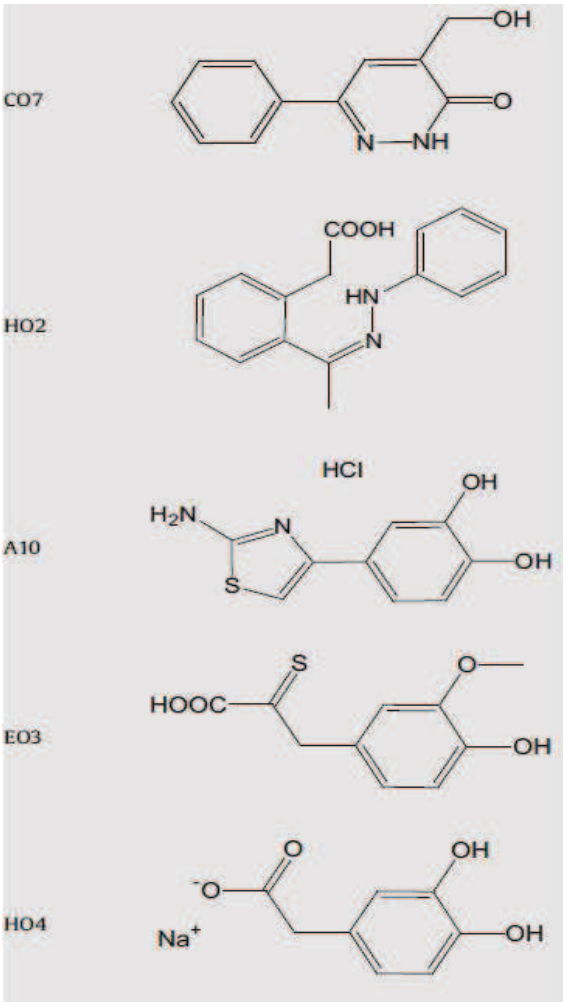

Fig.55. Structure of the positive hits (Shvadchak et al. 2009)

X.2.3.3. Nucleic acid intercalators and aptamers.

By homology with antibiotics targeting bacterial nucleic acids, actinomycin D was shown to inhibit HIV-1 minus strand transfer during reverse transcription, likely by blocking the nucleic acid chaperone activity of NC. Nevertheless, the use of Actinomycin D in HIV therapy is not a viable option due to poor specificity and high toxicity (Gillespie, Kuti et al. 2005).

More recently, aminoglycosides selected from a small library of nucleic acid binders were shown to dissociate NC/SL3 and NC/SL4 complexes, but not NC/SL2 complexes (Turner et

al. 2006). Aminoglycosides were also able to bind the DIS extended duplex, suggesting that they could target genomic RNA both before and after its maturation by NC (Bernacchi et al. 2007). Moreover, due to the ability of aminoglycosides to dissociate complexes between Tat and TAR, these molecules could simultaneously target two essential proteins of HIV-1 (Faber, Sticht et al. 2000). However, the use of this group of molecules remains questionable since they were found inefficient in inhibiting HIV-1 production in infected MT4 or CEMUSS cell lines (Ennifar, Paillart et al. 2006).

Meanwhile, different libraries of RNA apptamers were produced using the SELEX method, generating aptamers of about 40 nucleotides in length (Allen, Collins et al. 1996; Berglund, Charpentier et al. 1997). Their secondary structure corresponds to stem-loops containing G and U residues and rich in GC base pairs. Several aptamers exhibit a higher affinity for NC than the Ψ sequence itself and are thus able to fully abolish the binding of NC to Ψ and TAR *in vitro*. The proof of concept to use RNA aptamers as NC inhibitors was assessed by co-transfecting a plasmid expressing the aptamer and one expressing the HIV-1 DNA. As a consequence only a partial inhibition of the genomic RNA packaging was observed (Kim and Jeong 2004).

Recently, it was reported that the chaperoning activity of NC can be extensively inhibited in vitro by small 2'-O-methylated oligoribonucleotides (mODNs) mimicking the LTR end sequences (Grigorov, Bocquin et al.). Delivered intracellularly with the use of a cell penetrating peptide (CPP), mODNs were found to impede HIV-1 replication in primary human T lymphocytes and macrophages at concentrations below 1 nM. On the basis of data obtained for one of the most potent oligonucleotide – mODN-11, it was proposed that mODN mechanism of action is mediated by binding of NC hydrophobic plateau to the single-stranded mODN rich in GUs .

Moreover, mODN-11 inhibits HIV-1 replication in a manner similar to the NRTI AZT by impairing viral DNA synthesis which suggests that mODN targets the RTC. Addition of mODN-11 together with AZT at sub-nanomolar concentrations caused a complete inhibition of HIV-1 infection, indicating that mODN-11 targets an element of the RTC different from AZT. Furthermore, mODN-11 was shown to target cell-free virions by inhibiting their replication and thus, represent a potential microbicide.

Extensive analysis showed that viral cDNA synthesis was severely impaired by mODNs. Partially resistant viruses with mutations in NC and RT emerged after months of passaging in cell culture. A HIV-1 molecular clone (NL4.3) bearing these mutations was found to replicate at high concentrations of mODN, albeit with a reduced fitness further supporting the view that

the RT enzyme cooperates with NC during viral DNA synthesis in newly infected cells. This is also in agreement with prior in vitro results where NC was found to be an indispensable partner of the RT enzyme (Buckman, Bosche et al. 2003; Grohmann, Godet et al. 2008). Furthermore, it was shown that HIV-1 containing ZF mutations disrupting the NC hydrophobic plateau failed to complete viral DNA synthesis (Sarafianos, Marchand et al. 2009). Therefore, it is tempting to speculate that the NC binding site on RT encompasses the NNRTI binding pocket, which lies close to the polymerase primer grip and the polymerase active site driving cDNA synthesis (Grigorov, Bocquin et al.; Druillennec, Meudal et al. 1999).

X.2.3.4. Peptides

Another strategy to inhibit NC functions is to use peptides that directly compete with NC for binding to its RNA and DNA substrates. One first approach was to design cyclic peptides mimicking the spatial orientation of Phe 16 and Trp37 residues in the NC hydrophobic plateau (Druillennec, Meudal et al. 1999). To further strengthen the interaction of peptides with RNA and DNA substrates of NC, two basic residues thought to mimic Arg26 and Arg32 have been introduced into the cyclic peptides. The peptides were shown to compete with NC chaperone activities and interaction with RT (Druillennec and Roques 2000).

Both inhibitory activities led to a dose-dependent reduction in cDNA levels possibly explaining the inhibition of HIV-1 replication in CEM-4 cells. This result clearly indicates that small molecules able to mimic structural determinants of NC can impair virus replication (Lener, Tanchou et al. 1998). However, though these cyclic peptides were not cytotoxic up to 150 μM, their high IC50 value (30 μM) shows that their structure should be improved.

A different approach was to identify small peptides that specifically recognize NC RNA targets by the use of a phage-displayed library (Raja, Ferner et al. 2006). All selected peptides consist of a cluster of Trp residues surrounded by basic residues and bind to the Ψ sequence with micromolar affinities.

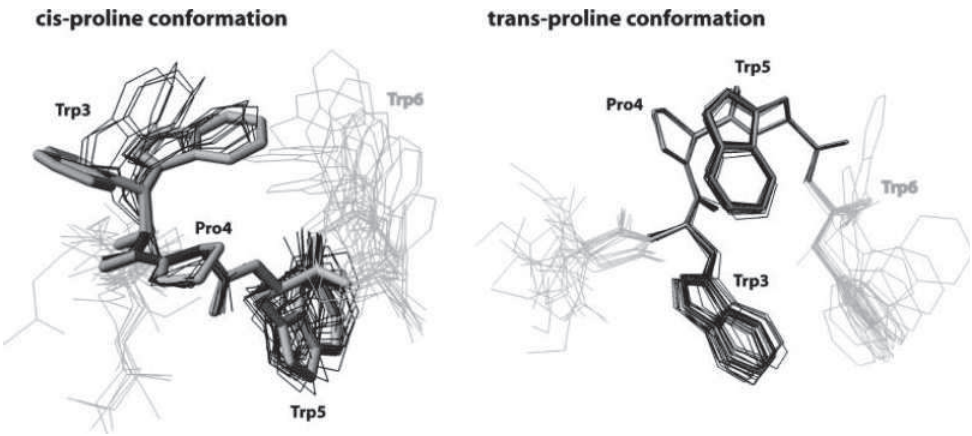

Fig.56. NMR-derived structures of HKWPWW peptide (Raja, Ferner et al. 2006).

The optimized peptide, HKWPWW was shown to adopt an equilibrium between cis and trans conformers (Fig 56) around the central Pro residue (Clarke, Taylor et al. 1993; Poss, Martin et al. 1995; vantWout, Ran et al. 1998). Moreover, the HKWPWW peptide was found to inhibit the NC-promoted cTAR destabilization. The HKWPWW peptide also inhibited RNA encapsidation and HIV-1 replication in cellular assays, likely via competition with NC to its target nucleic sequences (Dietz et al, 2008).

Interestingly, like RB2121, the leader of the aforementioned cyclic peptides, HKWPWW peptide likely mimics part of the NC hydrophobic plateau, confirming that this NC plateau is a promising starting point to develop agents with antiviral activities.

X.3. HIV-1 Vaccines

Although treatment of HIV-infected individuals with the HAART therapy can extend life and health of infected people by a complete control of the plasma viremia below detectable levels (less than 40 copies/mL plasma), HIV is able to council itself by creating its reservoirs in structures immunologically separated from the blood and lymphoid systems e.g. gastrointestinal tract, brain, central nervous system, genital tract and lung. Despite the access to treatment or use of infection preventing compounds such as topical microbicides, HIV vaccine is still the simplest and most direct strategy for prevention.

The goal of an HIV-1 vaccine would be either to prevent infection or to reduce viral loads and clinical disease progression following infection (Fig. 57).

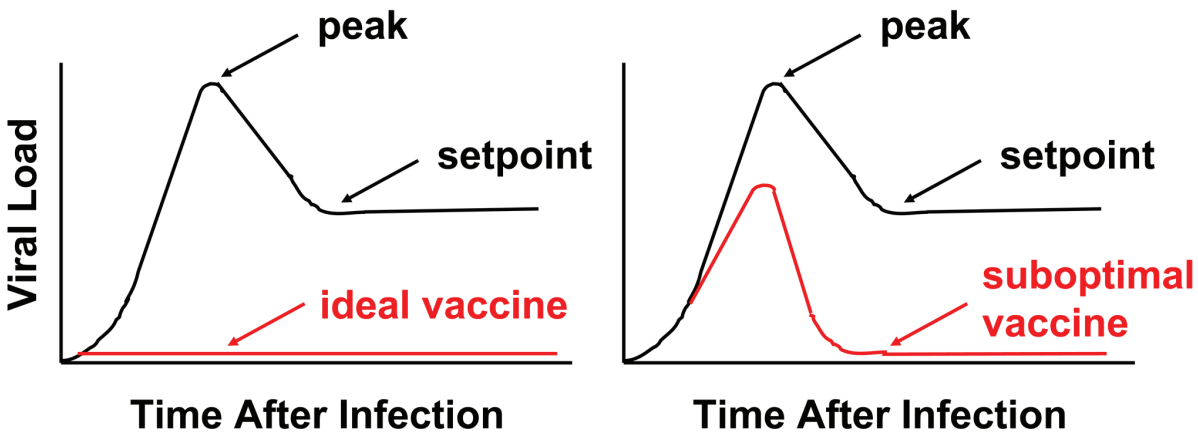

Fig.57. Goals of an HIV-1 vaccine**.** Following infection, HIV-1 replicates exponentially to a peak level and then is partially controlled to a viral setpoint level (black). Left, an ideal vaccine would protect against infection and afford sterilizing immunity (red). Right, a suboptimal vaccine would result in decreased peak and setpoint viral loads following infection (red) (Barouch 2008).

An ideal vaccine would completely block infection and provide sterilizing immunity. Although such a vaccine would be optimal, this degree of protection is not even achieved with the majority of clinically licensed vaccines. In contrast, most licensed viral vaccines appear to function by controlling subclinical viral replication and by preventing clinical disease. It may therefore be more realistic to develop a suboptimal HIV-1 vaccine that fails to prevent infection but that provides partial immune control of viral replication following infection. Such partial control, as exemplified by a reduction in peak and setpoint viral loads following infection, has been demonstrated in certain preclinical studies by vaccines that elicit T lymphocyte responses. Moreover, since viral loads represent a principal determinant of HIV-1 transmission (Quinn 2002), it is conceivable that such a partially protective vaccine might have substantial impact on a population level.

Despite numerous attempts in USA, Canada and Europe with the use of different vectors, there is no efficient HIV-1 vaccine available.

In general, vaccine strategies for HIV-1 can be divided into traditional and novel vaccine approaches. Traditional vaccine technologies include live attenuated viruses, whole killed viruses, and protein subunits. Although these approaches have proven successful for the development of vaccines against other viruses, they all have substantial limitations in terms of their utility for HIV-1. Live attenuated viruses have afforded substantial protective efficacy against SIV challenges in rhesus monkeys (Daniel, Kirchhoff et al. 1992), but are unlikely to be utilized in humans due to significant safety concerns (Baba, Jeong et al. 1995; Learmont, Geczy et al. 1999). In contrast, whole killed viruses and protein subunits (Murphey-Corb M,

et al. 1989) are limited by their inability to induce broadly reactive NAb responses as well as by their inability to elicit CD8+ T lymphocyte responses (Flynn, Forthal et al. 2005). Recent data, however, suggests that Toll-like receptor (TLR) adjuvants may increase the utility of protein subunit immunogens (Wille-Reece, Flynn et al. 2005).

Novel vaccine strategies include gene delivery technologies such as plasmid DNA vaccines and live recombinant vectors engineered to express HIV-1 antigens. Plasmid DNA vaccines offer considerable promise in terms of simplicity but multiple injections of high doses of DNA vaccines are typically required to elicit detectable immune responses in nonhuman primates and humans (Casimiro, Wang et al. 2005). Substantial research is therefore focused on the development of adjuvants for DNA vaccines (Barouch, Santra et al. 2000; Chong, Egan et al. 2007) and improved delivery technologies such as in vivo electroporation. Recombinant vectors include attenuated or replication incompetent viruses, most notably adenoviruses (Priddy, Brown et al. 2008) and poxviruses (Amara, Villinger et al. 2001). Viral vectors either alone or in the context of heterologous DNA primer, represent the majority of HIV-1 vaccine candidates that are currently in clinical trials. Other viral vectors that are being evaluated include vesicular stomatitis virus (VSV), adenoassociated virus (AAV), Venezuelan equine encephalitis (VEE) virus, cytomegalovirus (CMV), herpes simplex virus (HSV), and measles virus. Bacterial and mycobacterial vectors are also being explored, including *Salmonella*, *Listeria*, and BCG.

Only two vaccine concepts have completed clinical efficacy studies. The first concept utilized monomeric HIV-1 Env gp120 protein vaccine candidates. In early phase clinical trials, gp120 immunogens elicited type-specific binding antibodies but failed to induce broadly reactive neutralizing antibodies (NAbs) (Connor et al. 1998) affording no detectable protective efficacy (Priddy, Brown et al. 2008). Another phase 3 study evaluating the efficacy of a recombinant canarypox vector prime, gp120 protein boost vaccine regimen showed no efficacy against HIV-1 infection in humans (Flynn, Forthal et al. 2005; Pitisuttithum, Gilbert et al. 2006).

The second vaccine concept that has completed clinical efficacy studies involved recombinant adenovirus serotype 5 (rAd5) vectors expressing HIV-1 Gag, Pol, and Nef. The aim of this strategy was to elicit HIV-1-specific cellular immune responses. Early phase clinical trials demonstrated that rAd5 vector-based vaccines elicited cellular immune responses in the majority of subjects, although these responses were partially suppressed in individuals with pre-existing Ad5-specific Nabs (Priddy et al. 2008). The efficacy trials were unexpectedly terminated as the vaccine failed to protect against infection or to reduce viral loads following

infection and that vaccines with pre-existing Ad5-specific NAbs exhibited an enhanced rate of HIV-1 acquisition.

Until recently (Munier, Andersen et al.), the hopes for an effective vaccine were thwarted by the disappointing results and early termination in September 2007 of the study, which saw a subgroup of male vaccine recipients at an increased risk of HIV-1 infection, and the failure of earlier trials of vaccines based on recombinant envelope proteins to provide any level of protection. The study of neutralizing antibodies has demonstrated that the induction of high-titre, broadly neutralizing antibodies in the majority of recipients is likely to be highly problematic.

In September 2009 Sanofi Pasteur, the vaccine division of the Sanofi-Aventis Group presented the results of the collaborative HIV vaccine trial that has been conducted in Thailand over the past six years (RV144 Thai trial). The Phase III clinical trial involving more than 16,000 adult volunteers in Thailand has demonstrated that an investigational HIV vaccine regimen was safe but modestly effective in preventing HIV infection. According to the final results released by the U.S. Army Surgeon General, combination of ALVAC® HIV and AIDSVAX® B/E vaccines lowered the rate of HIV infection by 31.2% compared with placebo.

This study employed envelope-based immunogens delivered as a priming vaccination with a recombinant poxvirus vector and boosting with recombinant proteins. This regimen provided modest protection to HIV-1 infection in a low-risk population. Although the correlates of protection are currently unknown, extensive studies are underway to try to determine these. The current paradigm for an optimal HIV-1 vaccine is to design immunogens and vaccination protocols that allow the induction of both broadly neutralizing humoral and broadly reactive and effective cell-mediated immunity, to act at sites of possible infection and post-infection, respectively. However, this is challenged by the results of the RV144 trial as neither of these responses was induced but modest protection was observed. Understanding the biology and immunopathology of HIV-1 early following infection, its modes of transmission and the human immune system's response to the virus should aid in the rational design of vaccines of increased efficacy.

Different strategies are currently being explored to develop antigens to contend more effectively with viral diversity and to elicit substantially more potent and more cross-reactive immune responses than those achieved in the previous study.

Several groups have fused the most conserved parts of the viral protesome to form an artificial protein immunogen (Létourneau et al. 2007). Connecting short regions from different proteins

into one antigen can have undesirable immunologic consequences. For example, polyepitope vaccines have to date failed to produce robust T cell responses in phase 1 clinical studies (Korber et al. 2009). In scenarios where somewhat longer conserved peptide regions are linked (Létourneau et al. 2007), rather than linking narrowly defined optimal epitopes, cleavage signals for epitope processing may be preserved (Nielsen et al. 2005), allowing more natural epitope processing and presentation than in a polyepitope construct. In addition, in many regions there is extensive overlap of known epitopes. A conserved region approach thus enables responses to any of the overlapping epitopes within the included regions, which represents an advantage over the polyepitope strategy of narrowly focusing on optimally defined epitopes.

There are two theoretical virtues of "immunofocusing" host vaccine responses onto conserved regions. The first is that limiting the immune responses to conserved epitopes may enhance cross-reactivity at the population level. The second is that potent immune responses in conserved regions are more likely to force escape pathways that reduce viral fitness (Létourneau et al. 2007; Rolland et al. 2007; Nielsen et al.2005).

Another approach is vaccination simultaneously with multiple variants of the same protein which may increase the breadth of population coverage as well as the depth of coverage of variants of a single epitope. If more T cell receptor clonotypes are expanded simultaneously, each recognizing the epitope and its variants differently, then this may effectively block common and fit viral escape routes. The use of multiple natural Env immunogens has been shown to elicit responses against all antigens without antigenic interference in rhesus monkeys. Phase 1 clinical trials have also indicated enhanced breadth of responses with the use of polyvalent cocktails of natural proteins.

X.4.Recent developments in HIV-1 vaccines

In September 2011, Inovio Pharmaceuticals, Inc. (NYSE Amex: INO), a leader in the development of synthetic immunogens against cancers and infectious diseases, announced that it has achieved best-in-class immune responses in a Phase I clinical study of PENNVAX™-B, its product for the prevention of the HIV sub-type prevalent in the US and Europe. In that study (named HVTN-080), three doses of the vaccine delivered together with an IL-12 cytokine plasmid via electroporation resulted in over 89% of the vaccinated subjects mounting an antigen-specific CD4+ or CD8+ T cell response against at least one of the vaccine antigens. The HIV-001 study did not include the IL-12 cytokine plasmid. Inovio plans

to further study the impact of cytokines as well as the impact of therapeutic vaccination on HIV viral load in future clinical trials.

In December 2011, a group of scientists under the supervision of Dr. Chil-Yong Kang from The University of Western Ontario got an approval from the FDA to test vaccine based on attenuated viruses on humans (Chip Martin, QMI Agency). Initiated in January 2012, trials will be followed in three phases of human clinical trials:
Phase I, already started in January 2012, will double check the safety of the vaccine in humans, involving only 40 HIV-positive volunteers.
Phase II will measure immune responses in humans, involving approximately 600 HIV-negative volunteers who are in the high-risk category for HIV infection.
Phase III will measure the efficacy of the vaccine, involving approximately 6,000 HIV-negative volunteers who are also in the high-risk category for HIV infection.
The vaccine holds big promise since it was already proven to stimulate strong immune responses with no adverse effects or safety risks. It is the only HIV vaccine currently under development in Canada and one of only a few in the world.

In March 2012, Inovio Pharmaceuticals, Inc. (NYSE Amex: INO) announced that it has achieved strong T cell immune responses in a Phase I clinical study of PENNVAX®-B,
Overall, significant vaccine-specific T-cell responses were observed in 75% (9 out of 12) of subjects against at least one of the three vaccine antigens (gag. pol, or env) following vaccination. Fifty percent of the subjects (6 out of 12) had strong vaccine induced antigen-specific responses above the pre-vaccination levels to at least two of the antigens. Importantly, the responses induced by vaccination were predominantly antigen-specific (i.e. gag, pol and env) CD8+ T-cells, which are considered to be paramount in clearing chronic viral infections and an important measurement of the performance of a therapeutic vaccine. These results are in contrast to previously reported studies with other DNA vaccines delivered without electroporation that yielded poor overall T cell immune responses (Inovio Pharmaceuticals, Inc 2012).

Due to the fact that there is no efficiently working anti-HIV-1 vaccine, efforts have been made to better educate people in HIV-1 prevention. The main one, since HIV-1 is mostly transmitted by sexual contacts, is use of condoms which reduces risc of HIV transmission by 80% over the long term. For women, a vaginal gel containing tenofovir, a reverse

transcriptase inhibitor, has beed proposed. When used immediately before sex, tenofovir reduces infection rates by approximately 40% among Africa women.

Based on various studies, the World Health Organizatio and UNAIDS both recommended male circumcision as a method of preventing female-to-male HIV transmission in 2007 since in sub-Saharan Africa, it reduces the risk of HIV infection in heterosexual men by between 38 percent and 66 percent over two years. However whether it protects against male-to-female transmission is disputed. Programs encouraging sexual abstinence do not appear to effect subsequent HIV risk. Comprehensive sexual education provided at school is believed to decrease high risk behavior.

Early treatment of HIV-infected people with antiretrovirals protected 96% of partners from infection. Pre-exposure prophylaxis with a daily dose of tenofovir with or without emtricitabine is effective in a number of groups including: homosexual men, by couples where one is HIV positive, and by young heterosexuals in Africa.

Antiretrovirals administered within 48 to 72 hours after exposure to HIV positive blood or genital secretions is referred to post-exposure prophylaxis. The use of the single agent zidovudine reduces the risk of subsequent HIV infection fivefold following a needle stick injury. This kind of treatment is recommended after sexual assault when the perpetrator is known to be HIV positive. Current treatment regimes typically use lopinavir/ritonavir and lamivudine/zidovudine or emtricitabine/tenofovir and may decrease the risk further. The duration of treatment is usually four weeks and is associated with significant rates of adverse effects (for zidovudine ~70% including: nausea 24%, fatigue 22%, emotional distress 13%, headaches 9%) (Kripke 2007). Much effort has been also done to prevent transmission of HIV from mothers to children. This primarily involves the use of a combination of antivirals during pregnancy and after birth in the infant but also potentially include bottle feeding rather than breastfeeding.

Research Aim

Due to the highly conserved sequence of NCp7 and its critical function during HIV-1 life cycle, several different classes of anti-NC compounds have already been developed. Among the different classes of anti-NC molecules, the most interesting one is the zinc ejector class, which fully inactivates NCp7 by ejecting the zinc ions. These molecules lead to a complete loss of viral infectivity, but are poorly specific due to their interaction with the zinc fingers of cellular proteins. As a consequence, these molecules have been restricted for inactivation of viral particles in vaccine approaches or used as microbicides.

Recently, within the European consortium TRIoH (Targeting Replication and Integration of HIV), new strategies to specifically target the nucleic acid chaperone properties of NCp7 were developed. A series of peptides has been designed to act as competitors for NCp7 and thus, inhibit virus replication. Among this series, several peptides were found to efficiently inhibit the nucleic acid destabilization properties of NCp7. Four of them have been tested in the cellular context and three out of them were found to efficiently inhibit the replication of HIV-1 in lymphocytes. In this context, the objective of this thesis was to characterize in depth the properties of these peptides by the use of fluorescence-based techniques.

Since the antiviral peptides include residues of the NCp7 hydrophobic plateau, we first checked if these peptides are able to reproduce the nucleic acid chaperone properties of NCp7. To this end, we monitored the ability of the peptides to destabilize the secondary structure of cTAR and promote the annealing of cTAR with its complementary TAR sequence.

Next, we characterized the possible cytotoxicity of the peptides. In addition, by confocal microscopy, we characterized the cell entry and intracellular pathway of the labelled antiviral peptides either in their free form or complexed with carrier (Nanovepep). We notably addressed the importance of the endocytosis pathway in peptide internalization and the possibility for the formulated peptide to directly enter the cytosol.

Furthermore, we tested the formulated peptides for their ability to inhibit HIV-1 based lentivector transduction of HeLa cells.

The obtained results should enable us to better understand the possible role of peptides as anti-NC molecules and explain the way these peptides reduce HIV-1 replication.

In parallel, we also investigated the molecular mechanism in respect to NCp7 of small antiviral drugs developed by the groups of D. Daelemans (Leuven) and M. Botta (Siena).

By the use of fluorescence-based techniques we characterized ability of tested compounds to remove zinc from NC zinc fingers structure and thus inhibit NC-induced cTAR destabilization. The obtained results together with data from in vitro assays provided by

groups of Daelemans and Botta help us to understand mechanism of action of tested compounds as anti-NC drugs.

Materials and Methods

1. MATERIALS

1.1. Peptide synthesis

All the used anti-NC peptides were synthesized by PEPSCAN (Netherland). The model peptide, pE and NC(11-55) were synthesized in the host laboratory by solid phase synthesis on a 433A synthesizer (ABI,Foster City, CA). Labeling of peptide pE with chromophore was performed by a Phd student Volodomyr Schvadchak.

Cleavage of the peptides from solid-phase support and amino acid side chain deprotection were performed in 95% trifluoroacetic acid (TFA) containing water (5%, v/v), phenol (2%, w/v), thioanisole (5%, v/v) and ethanedithiol (2.5%, v/v). After the cleavage, the peptide was precipitated, filtered, purified by reverse-phase HPLC and characterized by mass-spectroscopy. Prior to use, the peptides were dissolved in buffer, aliquoted and stored at -20°C.

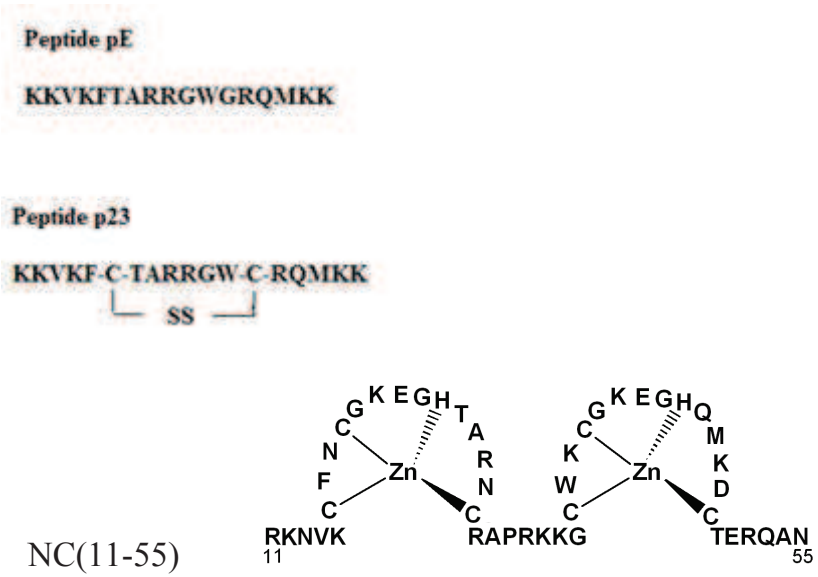

Fig. 58. Amino acid sequence of anti-NC peptides used in the thesis.

1.2. Preparation of peptide/protein solutions

The lyophilized peptides were dissolved in 25mM Tris, 30mM NaCl and 0,2mM $MgCl_2$, pH 7.5. The concentration of proteins was determined by measuring the absorbance A, at 280nm, using the Beer-Lambert law :

$$A = \varepsilon \cdot l \cdot C \qquad \text{Equation 1}$$

Where,

Ɛ is the molar absorption coefficient

l is the path length (cm)

C is the protein concentration

An absorption coefficient of 5700 M^{-1} cm^{-1} at 280 nm was used to determine the peptide concentrations.

All absorption spectra were recorded on a spectrophotometer Cary 4000 (Varian). Spectra were corrected for buffer absorption with the use of a baseline measured in cuvettes filled only with the used buffer.

NC(11-55) preparation

The lyophilized peptide was dissolved in water and its concentration was determined using an extinction coefficient of 5700 M^{-1} x cm^{-1} at 280 nm. Next, 2.5 molar equivalents of $ZnSO_4$ were added to the peptide and pH was raised to its final value, by adding buffer. The increase of pH was done only after zinc addition to avoid oxidization of the zinc-free peptide. Zinc binding by the protein was verified by the variation of the tryptophan fluorescence quantum yield induced by the addition of an excess of EDTA, acting as zinc ejector.

1.3. Nucleic acid sequences

Synthesis

All used oligonucleotides were synthesized at a 0.2 μmol scale and purified by reverse-phase HPLC and polyacrylamide gel electrophoresis by IBA GmbH Nucleic Acids Product Supply (Göttingen, Germany). The doubly labeled ODNs were labeled at their 5' terminus with carboxytetramethylrhodamine (TMR) or ethyl 2-[3-(ethylamino)-6-ethylimino-2,7-dimethylxanthen-9-yl]benzoate hydrochloride (Rh6G) via an amino-linker with a six carbon spacer arm, whereas the 3' terminus was labelled with either 4-(4'-dimethylaminophenylazo) benzoic acid (Dabcyl) or 5(and 6)-carboxyfluorescein (Fl).

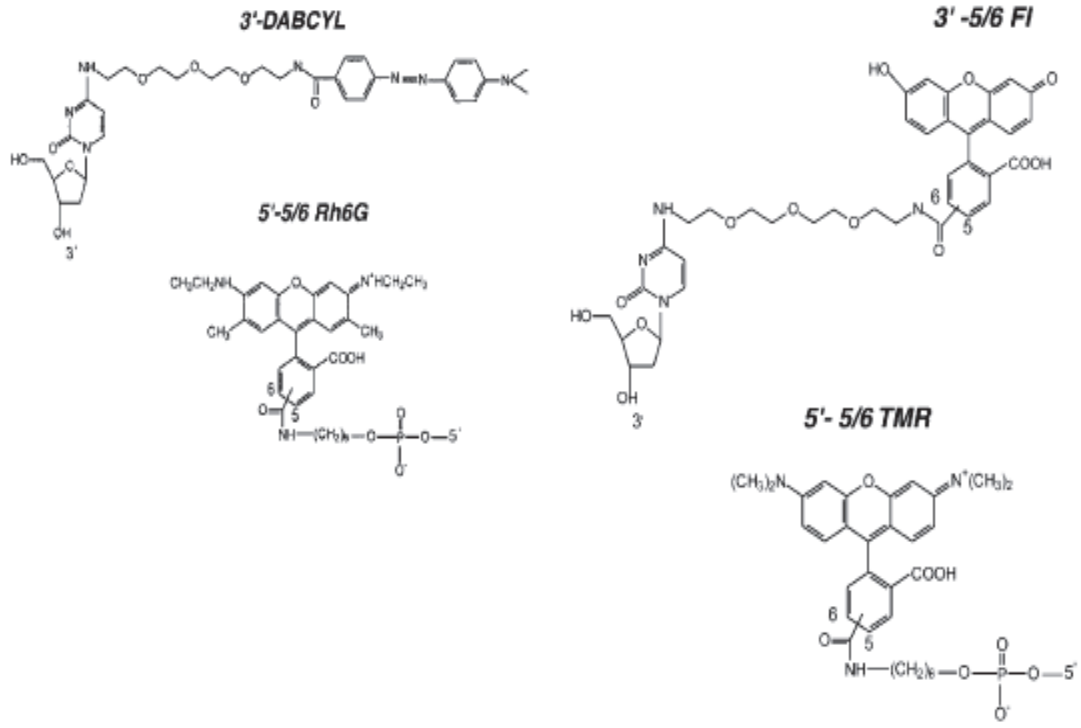

Fig.59. Chemical structures of the dyes.

Oligonucleotide sequences used in the thesis

To study the anti-NC properties of the peptides, we used complementary DNA sequences represented by the HIV-1 transactivation response (TAR) element in a DNA form (dTAR) and the complementary sequence cTAR, as well as several mutated sequences.

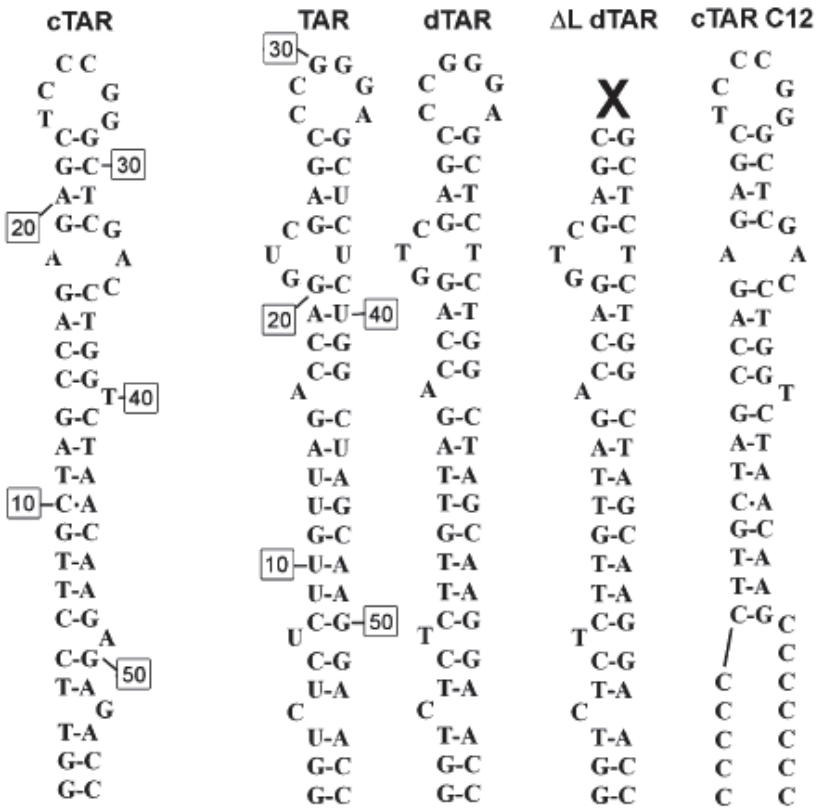

Fig.60. Structure of the oligonucleotides used in this study. The TAR RNA and cTAR DNA sequences are from the HIV-1 MAL strain. The secondary structures of the oligonucleotides were predicted from the structure of TAR27 and the mfold program (http//www.bioinfo.rpi.edu/applications/mfold/old/dna/form1.cgi).

To characterize the properties of the peptides in strand exchange reactions, we used oligonucleotides originally studied by Tsuchihashi and Brown (Tsuchihashi and Brown 1994). The numbers in their names indicate the lengths of these oligonucleotides. 28(+) ODN contains 19 bases from the 3'end of region U5. 28(+) and 28(-) have opposite polarity and are able to form complete duplex structures. Twenty nucleotides of 21(-) are identical to the 20 central nucleotides of the 28(-) oligonucleotide.

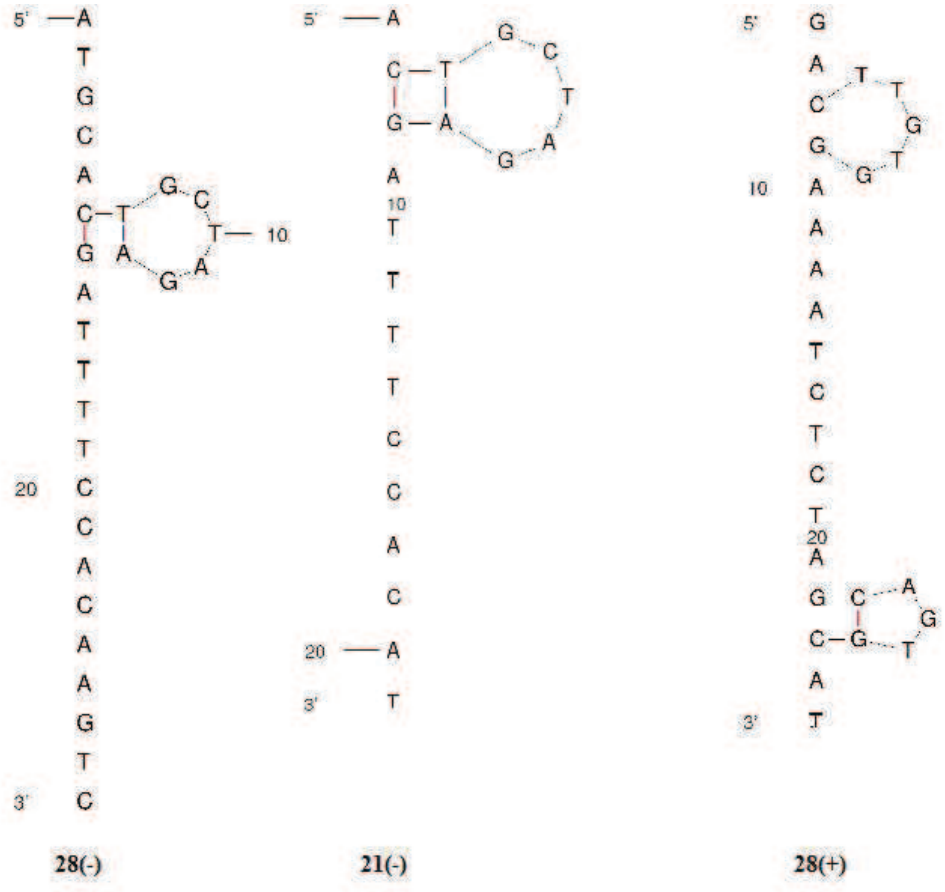

Fig.61. Oligonucleotide sequences used in this study for strand exchange reactions. Oligonucleotide secondary structures were predicted by using the mfold program (http//www.bioinfo.rpi.edu/applications/mfold/old/dna/form1.cgi).

Preparation of oligonucleotide solutions

All lyophilized oligonucleotides were dissolved in Milli-Q water and stored at -20 °C. The concentration of oligonucleotides was determined by their absorbance at 260 nm by using the extinction coefficient provided by the producer.

1.4. Chemical compounds inhibiting NC

Synthesis

The compounds given in Fig.62 were synthesized by group of Dr Daelemans (Leuven, Belgium).

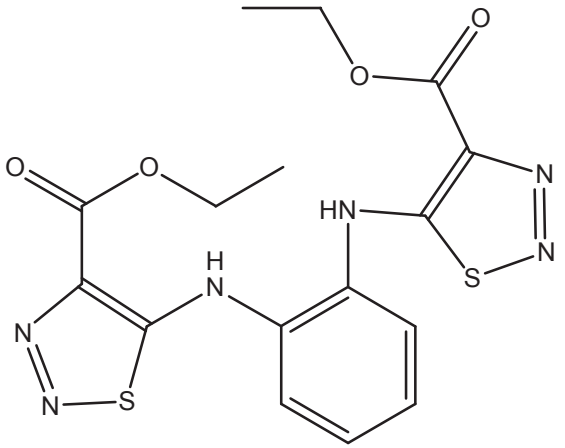

N,N'-bis(1,2,3-thiadiazol-5-yl)benzene-1,2-diamine

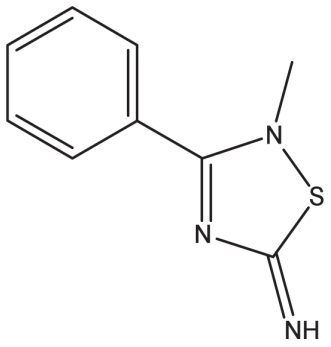

2-methyl-3-phenyl-2H-[1,2,4]thiadiazol-5- ylideneamine

Fig.62. Chemical structures of tested compounds.

The compounds were dissolved in 1mM DMSO (Dimethyl sulfoxide), an polar aprotic solvent and their concentration was estimated on the basis of their weight and molecular mass. Since the compounds were dissolved in DMSO, we checked its possible influence on the interaction between NC(11-55) and cTAR. For this purpose, we titrated the complex of NC and Rh6G-5'-cTAR-3'-Dabcyl (with NC added to ODN at 10-fold molar excess) with increasing concentrations of DMSO up to 100 μM.

A decrease in rhodamine (Rh6G) fluorescence was observed in the presence of increasing concentrations of DMSO, indicating either a direct effect of the solvent on rhodamine fluorescence or an indirect effect through an alteration of the NC/cTAR interaction (fig.63).

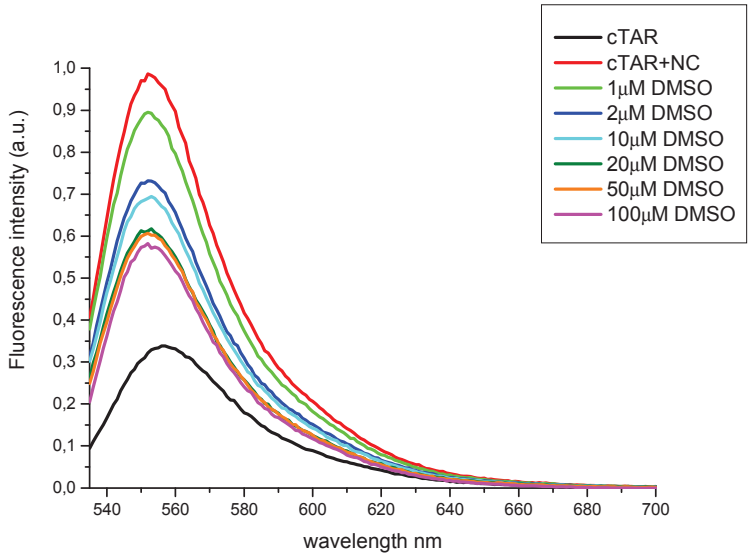

Fig.63. Effect of DMSO on the fluorescence of the complex of NC(11-55) complexed with doubly labeled cTAR. Emission spectra of NC(11-55)/cTAR were recorded in the presence of DMSO at different concentrations. Concentration of NC(11-55) and Rh6G-5'-cTAR-3'-Dabcyl were 1 µM and 0.1 µM, respectively.

To discriminate between these two hypotheses, we checked the influence of DMSO on the signal of Rh6G-5'-cTAR-3'-Dabcyl alone. For this purpose, we prepared two samples where ODN was mixed with DMSO at concentrations equal to the final solvent concentrations used when tested compounds were added at 10µM and 100µM.

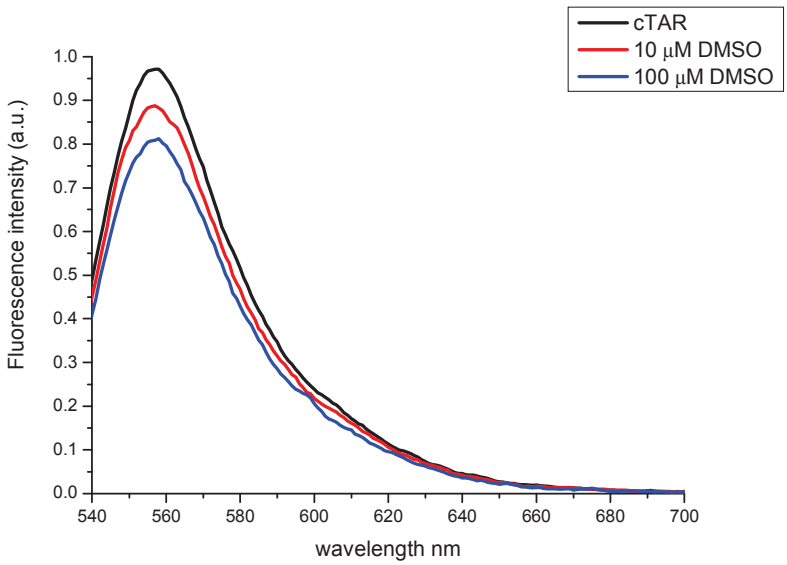

Fig.64. Emission spectra of doubly labeled Rh6G-5'-cTAR-3'-Dabcyl recorded in the presence of DMSO at the concentrations indicated on the graph.

The limited decrease observed in Rhodamine fluorescence suggested that the effect of DMSO on the fluorescence of the NC/ODN complex may be due to conformational changes or partial dissociation of complex. Thus, to limit the incidence of DMSO, all further experiments with tested compounds were performed with DMSO concentrations of 10 μM.

1.5. Lentiviral vectors

In order to determine the ability of the tested anti-NC peptides to inhibit lentiviral infection, lentiviral vectors based on HIV-1 were produced in the laboratory by co-transfection of 3 plasmids into 293-T cells. 48 h post-transfection, the cellular supernatants were harvested and the virus was quantified at 5.7 ng / ml of protein p24 (capsid) using the HIV Antigen mAb kit Innotest (Innogenetics, Belgium).

The transfer vector plasmid harbors the transgene (eGFP) under the control of the CMV promoter and all of the essential *cis*-acting elements (LTRs, Ψ and RRE) for packaging/reverse transcription/integration, but do not encodes any HIV proteins. The packaging plasmid express gag/pol and is deleted of the non essential genes as Vif, Vpu, Vpr and Nef. The third plasmid encodes the vesicular stomatitis virus envelope glycoprotein G (VSV-G). Because of the splitting into several plasmids and the removal of several HIV-1 the lentiviruses produced can be manipulated into a BSL-2 safety laboratory. By consequence of the absence of HIV-1 genes into the incorporated pseudo-genome these pseudo-viruses can only perform a single round of infection. The infection is followed by the expression of the eGFP after insertion of the lentiviral pseudo-genome into the genome of the cell. By pseudotyping the lentivirus, by substitution of the HIV-1 Env glycoprotein by the viral attachment protein of VSV-G **(**vesicular stomatitis virus envelope glycoprotein G), we obtain lentiviruses able to infect a large range of cells including HeLa cells used in this study (Sakuma, Barry et al.).

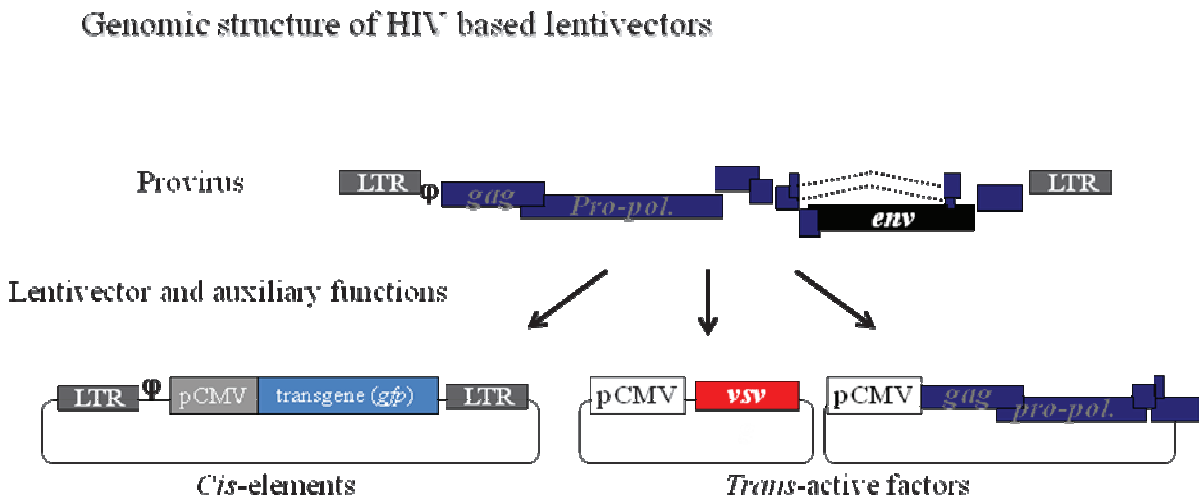

Fig.65. Schematic representation of HIV based lentivectors.

2. METHODS

2.1. Fluorescence correlation spectroscopy (FCS)

FCS measurements were used to determine non-aggregative experimental conditions.

2.1.1. Principle of FCS

FCS is an experimental technique developed to study both the Brownian diffusion and equilibrium kinetics of chemical systems. As molecules diffuse through a focal volume, the number of particles in this volume varies around its equilibrium value. Two major results can be extracted by tracking the emission of the moving particles : the time scale of diffusion and the average number of fluorescent molecules in the detection volume. These data provide information that can be used to determine diffusion coefficients, rate constants and sample concentration.

Since the method is based on the observation of a small number of molecules in a very tiny spot, FCS is a very sensitive analytical tool. In contrast to other methods, it does not need a physical separation process and has a good spatial resolution determined by the optics. Moreover, this method allows observing fluorescence-tagged-molecules in intact living cells.

2.1.2. Processing and analysis of FCS data

FCS measurements were performed on a two-photon laser scanning system. Photon excitation required for focal volume generation, was obtained by focusing a femto-second pulsed titanium-sapphire laser beam (Tsunami, Spectra Physics). Beam focusing on the sample was obtained by the use of an Olympus 60x 1.2 NA water immersion objective mounted on an Olympus IX70 inverted microscope. The emitted photons were collected with an Avalanche Photodiode (APD SPCM-AQR-14-FC, Perkin Elmer) connected to an on-line hardware correlator (ALV GmbH, Germany). The focal spot was set about 20 µm above the coverslip.

To determine the size of the focal volume, a calibration step is necessary. Carboxytetramethylrhodamine (TMR) in water was taken as a reference. The diffusion coefficient of TMR in water is 2.8×10^{-16} cm^2 s^{-1} (Egele, Schaub et al. 2005). The excitation volume is about 0.3 μm^3.

The fluctuations of the fluorescence signal were quantified by an autocorrelation curve that provides a measure for the self-similarity of the signal after a lag time (τ). It displays the

conditional probability of finding a molecule in the focal volume at a later time, τ, given it was there at t=0. Decaying with time, the autocorrelation function measures the average duration of a fluorescence fluctuation.

The number of molecules within the focal volume at any time is governed by a Poissonian distribution. Thus, the root mean square fluctuation of the number of particles (N) is given by:

$$\frac{\sqrt{\left\langle (\partial N)^2 \right\rangle}}{\langle N \rangle} = \frac{\sqrt{\left\langle \left(N - \langle N \rangle\right)^2 \right\rangle}}{\langle N \rangle} = \frac{1}{\sqrt{\langle N \rangle}} \qquad \text{Equation 4}$$

The fluorescence emitted by molecules in the focal volume is recorded photon by photon. Assuming a constant excitation power, the fluctuations of the fluorescence signal are defined as deviations from the temporal average of the signal :

$$\partial F(t) = F(t) - \langle F(t) \rangle \qquad \text{Equation 5}$$

$$\langle F(t) \rangle = \frac{1}{T} \int_0^T F(t) dt \qquad \text{Equation 6}$$

The normalized autocorrelation function is defined as :

$$G(\tau) = \frac{\langle \partial F(t) \cdot \partial F(t+\tau) \rangle}{\langle F(t) \rangle^2} \qquad \text{Equation 7}$$

Where :

<F(t)> represents the average fluorescence signal

∂F (t) represents is the difference between the fluorescence signal, $F(t)$, at a given time and the average fluorescence signal,$<F(t)>$

τ is the lag time.

For an ideal case of freely diffusing fluorescent particles undergoing triplet blinking in a Gaussian excitation volume, the correlation function G(τ), calculated from the fluorescence fluctuations can be fitted according to the following equation :

$$G(\tau) = \frac{1}{N}\left(1 + \frac{\tau}{\tau_d}\right)^{-1}\left(1 + \frac{1}{s^2}\frac{\tau}{\tau_d}\right)^{-\frac{1}{2}} \times \left(1 + \left(\frac{f_t}{1-f_t}\right)\exp\left(-\frac{\tau}{\tau_t}\right)\right) \qquad \text{Equation 8}$$

Where,

τ_d is the diffusion time

N is the mean number of molecules within the sample volume

S is the ratio between the axial and lateral radii of the sample volume

f_t is the mean fraction of fluorophores in their triplet state

τ_t is the triplet lifetime.

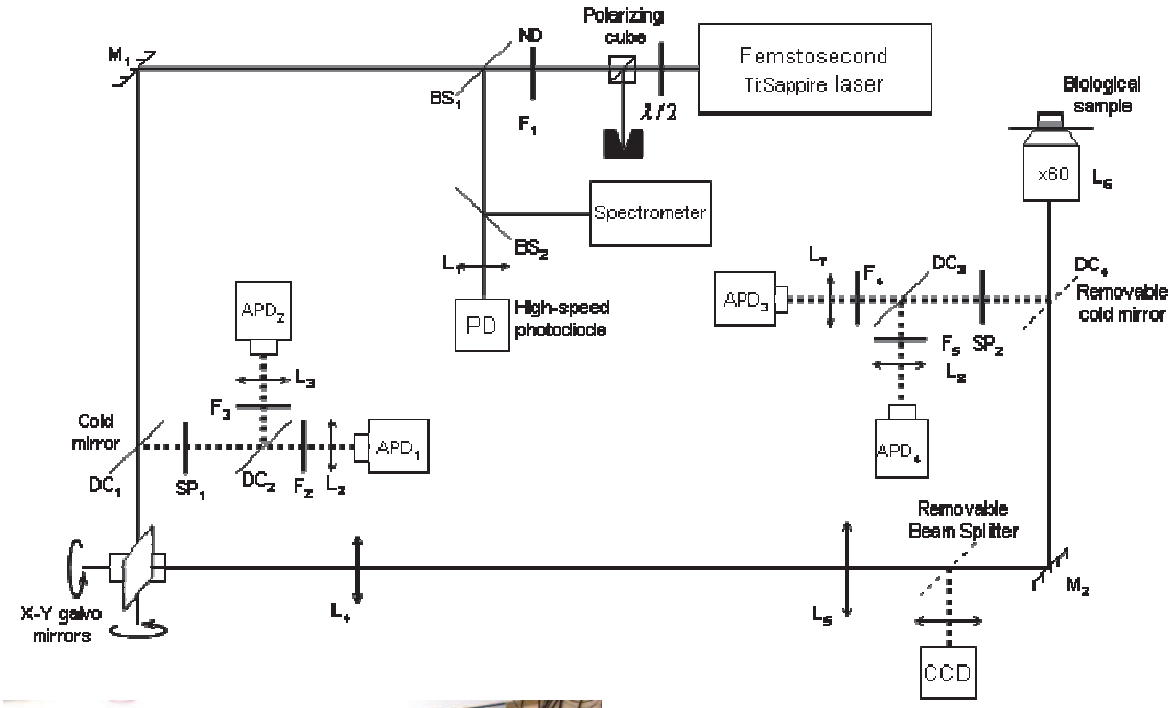

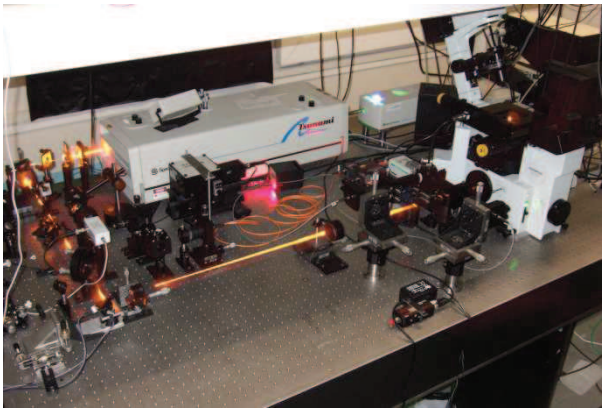

Fig.66. Schematic representation of the instrumental FCS set up.

2.1.3. Experimental

The measurements were carried out in an 96-well glass plate, using a 100 µl sample solution per well. Peptides were added to the labeled oligonucleotides at different ratios. To avoid high local concentrations during mixing, both reactants were of the same volume.
Typical data recording time was 10 min. An average autocorrelation curve was calculated from the sum of the autocorrelation curves obtained during the measurement time and then fitted by a one or two population model.

2.2. Flow cytometry

This method was used to characterize the effect of the tested peptides on HeLa cell viability and their ability to inhibit lentiviral infection.

2.2.1. Principle

Flow cytometry is a technique that simultaneously measures and then analyzes multiple physical characteristics of single cells as they flow in a fluid stream through a beam of light. The relative fluorescence intensities and light scattering of individual cells are determined using an optical-to-electronic coupling system.

2.2.2. Processing and analyzing data

A flow cytometer (BD FACSCalibur™) is made up of three mains systems:

- The fluidics system that transports particles in a stream to the laser beam for interrogation.
- The optics system consists of lasers to illuminate the particles in the sample stream and optical filters to direct the resulting light signal to the appropriate detectors.
- The electronic system converts the detected light signals into electronic signals that can be processed by the computer.

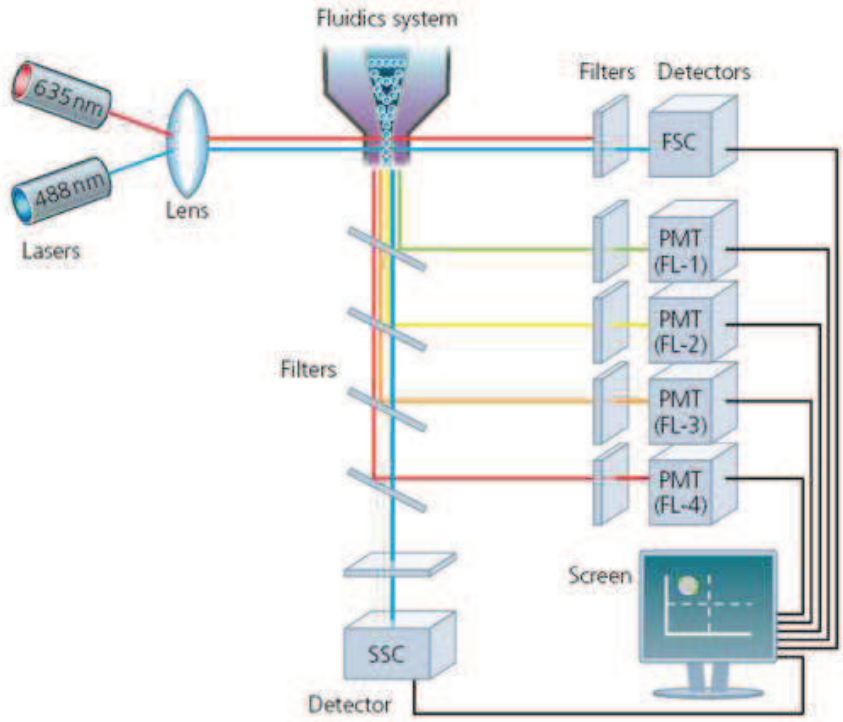

Fig.67. Scheme of a typical flow cytometer setup.

The flow cytometer (FACSCalibur) uses an air-cooled argon gas laser regulated at 15 mW of power and a fixed wavelength emission of 488 nm. The instrument is capable of detecting six parameters : forward scatter direction (FCS, correlated with cell size), side scatter direction (SSC, correlated with granularity and cell density) and three fluorescent emissions (green, yellow-orange and red).

2.2.3. Experimental

Cytotoxicity assay

Analysis of apoptosis in HeLa cells was performed by the use of the Annexin V-Biotin staining protocol, used to quantitatively determine the percentage of cells within a population that are actively undergoing apoptosis. It relies on the property of cells to lose membrane asymmetry in the early phases of apoptosis. In apoptotic cells, the membrane phospholipid phosphatidylserine (PS) is translocated from the inner leaflet of the plasma membrane to the outer leaflet, exposing PS to the external environment.

Annexin V is a Ca^{2+}-dependent phospholipid-binding protein that has a high affinity for PS, and is useful for identifying apoptotic cells with exposed PS. Propidium Iodide (PI) is a

standard viability probe. Viable cells with intact membranes exclude PI, whereas the membranes of dead and damaged cells are permeable to PI. Cells that stain positive for Annexin V-Biotin and negative for PI are undergoing apoptosis. Cells that stain positive for both Annexin V- Biotin and PI are either in the end stage of apoptosis, are undergoing necrosis, or are already dead. Cells that stain negative for both Annexin V- Biotin and PI are alive and do not undergo apoptosis.

HeLa cells were seeded in a 12-well plate at a concentration of $0.08x10^6$ cells per mL in Gibco DMEM + Glutamax medium 24 hours before performing the experiment. To achieve proper cell growth conditions, DMEM was mixed with 10% Fetal Bovine Serum (Invitrogen Corporation, Cergy Pontoise, France) and antibiotics (Streptavidine/Peniciline).

After 24 hours, the medium was removed and cells were transfected with peptides at concentrations varying from 10 to 100 μM and incubated up to 48 hours at 37°C and 5% CO_2. After this time, cells were stained using the Annexin V-Biotin staining protocol. One hour after sample preparation, cells were sorted by FACS with a rate of 10.000 cells per sample.

Actinomycin D (0.5 μg/mL) was used for the positive apoptotic control and untreated cells were used as negative control. Each experiment was repeated three times.

Inhibition of viral infection

HeLa cells were seeded in 6-well plates at $0.9x10^5$ cells per well 24 h before performing experiment. After this time cells were incubated with peptide, Nanovepep or complexes of peptide/Nanovepep for 2 h. Next, cells were washed once with PBS and infected with lentivirus (per well: 100 μL of virus stock in 1900 μL of complete DMEM supplemented with polybrene, 8μg/mL). After 24h, medium was changed and cells were incubated for another 24 hours. 48 h after treatment, cells were prepared for analysis by FACS as follows: cells were washed twice with 1X PBS, trypsinized with 500 μL of trypsin/well for 3 min at 37°C the reaction was stopped by addition of 3 ml of complete DMEM. After centrifugation (1200g 5 min) cells were washed once with 1 mL of PBS and fixed in 1 mL of 4% PFA in PBS for 15 min in the dark at RT. After two washes with PBS, cells were then counted and resuspend in PBS at 10^6 cells/mL. Samples were analyzed on a BDFACS AriaTM II. Rhodamine was excited by the laser "Yellow-Green" to 561 nm and was detected by a photomultiplier in front of which are placed optical filters. The eGFP was excited with the laser 488 nm and in this case a filter is used "long pass" filter and a 505 nm "band pass" 525/50. The level of infection was directly estimated by quantifying the number of eGFP positive cells.

Additionally, since the anti-viral activity of the peptides requires peptide vectorization, cell viability was also tested when cells were incubated with complexes of peptide (cargo) and NANOVEPEP (carrier).

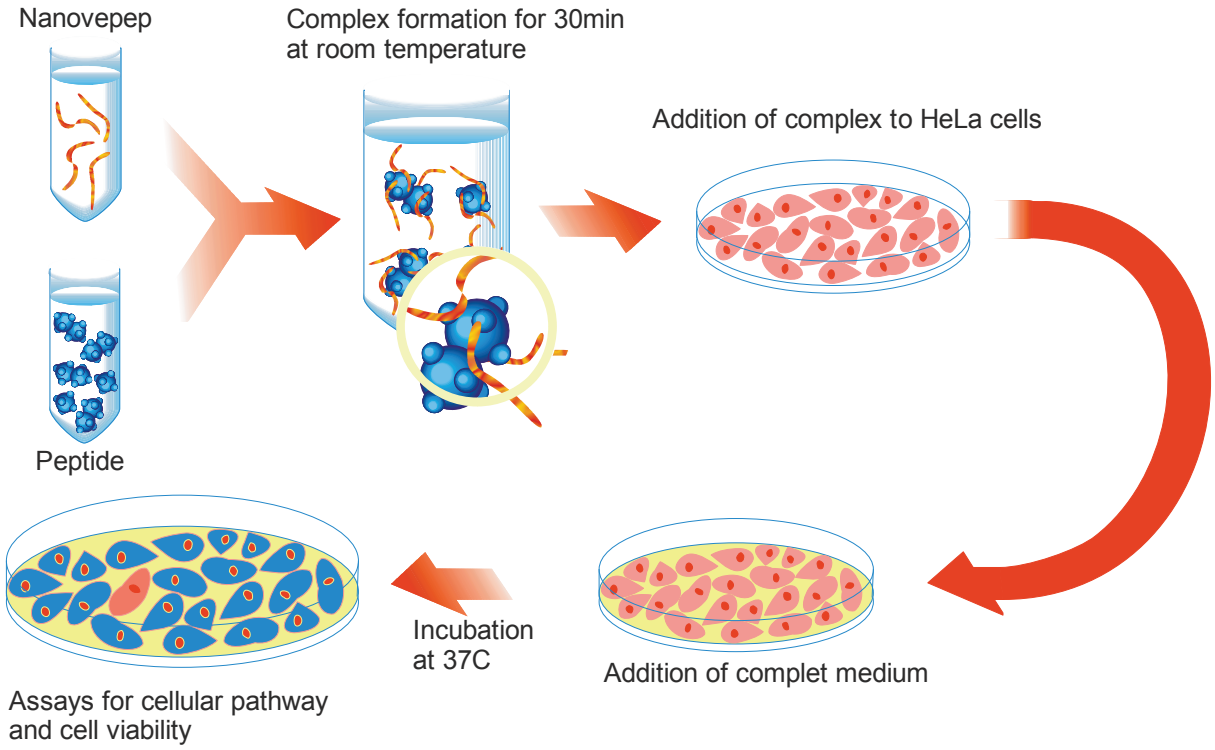

Fig.68. NANOVEPEP/peptide formation and testing.

Peptide vectorization

NANOVEPEP was provided as a lyophilized powder by Dr Gilles Divita (CNRS, Montpellier). NANOVEPEP forms non-covalent bonds with peptides, protecting them from degradation and preserving their characteristics during the transfection process. After delivery, the complex dissociates, leaving the biologically active peptides free to interact with their targets.

NANOVEPEP was resuspended in sterile H_2O and sonicated for 5 min in a water bath sonicator (BRANSONIC 220). The solution of tested peptides was prepared in (1x) PBS. Next, the diluted peptide solution was added to the diluted carrier solution and incubated at RT for 30 min. The ratio between NANOVEPEP and peptide was 1:1.

2.3. Confocal microscopy

Confocal microscopy was used to characterize the cellular pathway of the peptide alone and complexed with carrier, NANOVEPEP.

2.3.1. Principle

Confocal microscope creates sharp images of a specimen that would appear blurred when viewed with a conventional microscope. This is achieved by excluding most of the light from the specimen that is not from the microscope focal plane. The image has better contrast and represents a thin cross-section of the specimen. Thus, apart allowing better observation of details it is possible to create three-dimensional reconstructions of a volume of the specimen by assembling a series of thin slices taken along the vertical axis. Confocal microscopy also offers a modest increase in resolution.

2.3.2. Processing and analysis data

The coherent light emitted by the laser system (excitation source) passes through a pinhole aperture that is situated in a plane (confocal) conjugated with a scanning point on the specimen and a second pinhole aperture positioned in front of the detector (a photomultiplier tube). As the laser is reflected by a dichromatic mirror and scanned across the specimen in a defined focal plane, secondary fluorescence emitted from points on the specimen (in the same focal plane) passes back through the dichromatic mirror and is focused as a confocal point at the detector pinhole aperture.

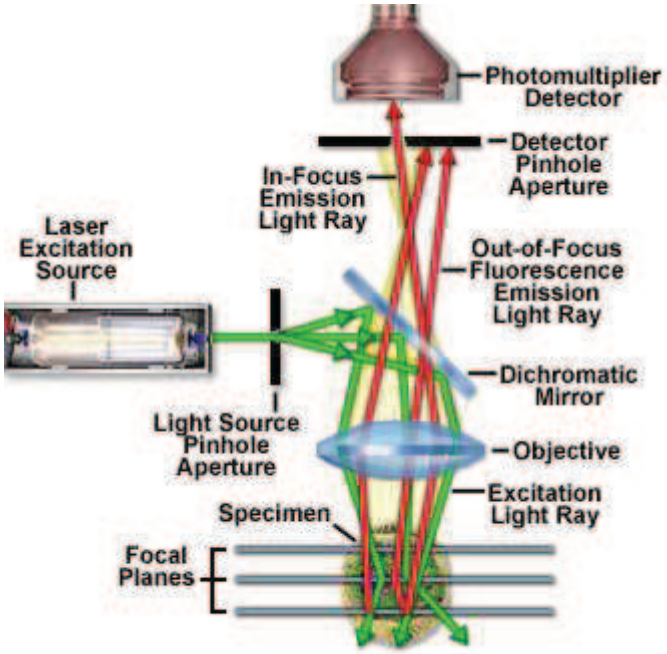

Fig.69. Schematic presentation of a basic confocal microscope.

2.3.3. Experimental

The HeLa cells (0.08×10^6/ml) were cultured on 35 mm glass coverslips (μ-Dish IBIDI, Biovalley, France) in Gibco DMEM + Glutamax medium supplemented with 10% fetal calf serum (Invitrogen Corporation, Cergy Pontoise, France) at 37°C in a 5% CO_2 atmosphere. After 24h, to visualize the cellular uptake, cells were incubated for one hour either with transferrin-Alexa 488 (Invitrogen Corporation, France) (Loh, Yeung et al. 1977) or 5 mM methyl-β-cyclodextrin (MβCD) (Sigma-Aldrich France) (Rodal, Skretting et al. 1999), rinsed with Opti-MEM and then incubated for two hours with 0.1μM pE-Rh alone or complexed with NANOVEPEP (ratio peptide/NANOVEPEP equal 1:1). To study the ATP-dependent cellular uptake, HeLa cells were incubated for one hour at 4°C with 0.1 μM peptide alone or complexed with NANOVEPEP.

When time of incubation was finished, cells were washed three times with PBS (Phosphate Buffer Solution), fixed with 4% PFA (Paraformaldehyde) and analyzed under the confocal microscope.

The cellular pictures were taken with an acquisition speed of 7.2 frames per second at 512x512 resolution. To ensure the correct view of the cellular localization of peptide and peptide/NANOVEPEP complexes, three-dimensional images were taken. For each

experimental condition, two separate samples were prepared. Untreated cells were used as a control.

2.4. Steady state fluorescence spectroscopy

Steady state fluorescence spectroscopy was used to characterize the ability of the tested peptides to promote the annealing between complementary oligonucleotides, to destabilize oligonucleotides (cTAR) and to inhibit the NC-induced cTAR destabilization. Additionally, this method was used to characterize the zinc ejection abilities of WDO-217 and NV038.

Steady state fluorescence experiments (both spectra and kinetics) were recorded either on a FluoroLog or FluoroMax (Jobin Yvon Instruments SA Inc.) spectrofluorimeter equipped with a thermostated cell compartment. The excitation source was a 450 W xenon lamp. The excitation and emission wavelengths were selected by two monochromators with adjustable slits. All fluorescence intensities were corrected for lamp fluctuations using a calibrated photodiode and for the wavelength-dependent photomultiplier response by factors provided by the producer.

2.4.1. Tryptophan fluorescence

Among the aromatic amino acids, tryptophan is the most interesting one since it has absorption properties superior to those of tyrosine and phenylalanine. Moreover, tryptophan can be selectively excited and is very sensitive to the physico-chemical properties of its environment. Due to its high environment sensitivity, Trp emission was used to monitor the conformational changes of NC provoked by zinc ejection.

Depending on the solvent, tryptophan absorbs with two transitions So → 1La and So → 1Lb. In polar solvents, 1La has lower energy than 1Lb and its emission is supposed to be observed from this lower state. The two excited states are characterized by very similar energies, but their transition dipole are almost perpendicular. Up to now, there are no studies revealing the correlation between the two transitions and fluorescence lifetimes. The tryptophan characteristic absorption peak around 280 nm is mainly due to the ^1L_b state whereas the ^1L_a state is responsible for absorption around 300 nm. The emission maximum is strongly dependent on solvent polarity. Moreover, the fluorescence quantum yield (Φ) of Trp in

proteins varies from 0.13 in water at neutral pH to near 0.35 in the nonpolar aprotic solvent dioxane (Muino and Callis 2009)

At neutral pH, the fluorescence decay of Trp is characterized by two lifetimes, a dominant component of 3 ns and a shorter 0.6 ns which emits at shorter wavelengths. This heterogeneity is due to a distribution of conformational states, each with its own lifetime (Rosato, Gratton et al. 1990) or to the presence of ground state conformers (rotamers) that are quenched to varying degrees by functional groups in the microenvironment surrounding the indole ring (Szabo and Rayner 1980; Petrich J. W. 1983; Dahms and Szabo 1995).

Most of the intrinsic fluorescence emission of folded proteins is due to excitation of tryptophan residues which can be selectively excited at 295-305 nm, with limited emission due to tyrosine (ε_{274}=1.300 $M^{-1}cm^{-1}$) and phenylalanine (ε_{250}=200 $M^{-1}cm^{-1}$). However, disulfide bridges (ε_{250}= 300$M^{-1}.cm^{-1}$) and thiol groups ($\varepsilon_{230\text{-}240}$= 4.500 $M^{-1}.cm^{-1}$) also have appreciable absorption in this wavelength range. Furthermore, tryptophan fluorescence is strongly influenced by the proximity of other residues (i.e. nearby protonated groups such as Asp or Glu, but also disulfide bonds and carbonyl groups can cause quenching of Trp fluorescence).

2.4.2. Experimental

In order to optimize the measurements of the fluorescence signal, a number of precautions were taken during sample preparation. To limit the adsorption of tested peptides to the walls of the measurement cells, experiments were performed with eppendorf vials and tips with low surface adhesion.

The destabilization experiments were performed at room temperature in 25 mM TRIS pH 7.5, 30 mM NaCl, 0.2 mM $MgCl_2$ buffer. The emission spectra with excitation at 520 nm were corrected for dilution and buffer fluorescence. The protein spectra were additionally corrected for screening effects, using:

$$I_P = I_m * \frac{(d_p + d_s + d_r/2)(1-10^{-d_p})}{d_p(1-10^{-(d_p+d_s+d_r/2)})}$$

Equation 10

where I_m is the measured fluorescence of the protein, I_p is the fluorescence intensity of the protein in the absence of inner filter, d_p is the absorbance of the protein, d_s is the absorbance

of the inner filter agent at the excitation wavelength, and d_r is the absorbance of this agent at the emission wavelengths.

To characterize the nucleic acid destabilizing properties of peptides and proteins, cTAR labelled at its 5‘ and 3‘ ends by 2-[3-(ethylamino)-6-ethylimino-2,7-dimethylxanthen-9-yl]benzoate hydrochloride (Rh6G) and 4-(4’-dimethylaminophenylazo) benzoic acid (Dabcyl), respectively, was used. In their closed form, the very low fluorescence of these labeled oligonucleotides is explained by the strong coupling between the chromophore transition dipoles (Bernacchi and Mely 2001). As soon as the two chromophores are separated from each other, the strong coupling is probably substituted by a weak dipolar coupling that permits a radiationless transfer of the electronic excitation energy (FRET) from the donor to the acceptor (Bernacchi, Stoylov et al. 2002; Beltz, Azoulay et al. 2003). The destabilization properties of the peptides were evaluated from the ratio between the fluorescence intensity of Rh6G in the presence and in the absence of the tested compounds. In the presence of saturating concentrations of NC, the ratio I_f/I_0 is equal to 7, while in the absence of destabilization, the ratio is equal to 1.

Zinc ejection experiments were performed in 25 mM TRIS pH 7.5, 30 mM NaCl, 0.2 mM $MgCl_2$ buffer with an excitation wavelength of 295 nm.
The zinc ejection ability of the tested compounds was monitored through the intrinsic fluorescence of the Trp37 residue of NC(11-55). Trp37 belongs to the distal zinc finger motif and shows a 3-fold increase in fluorescence quantum yield on zinc binding.
The effect of the peptides on the hybridization reactions between two complementary ODNs was investigated using cTAR and dTAR derivatives. Experiments were performed at 20°C in 25 mM TRIS pH 7.5, 30 mM NaCl, 0.2 mM $MgCl_2$, in pseudo first-order conditions by mixing nonlabelled dTAR with cTAR labelled at its 3’ and 5’ ends by two chromophores exhibiting fluorescence resonance energy transfer (FRET). The pair of chromophores chosen for the experiments were carboxytetramethylrhodamine (TMR) at the 5’ terminus and 5(and 6)-carboxyfluorescein (Fl) at the 3’terminus. Excitation and emission wavelengths were 480 nm and 520 nm, respectively, to monitor the Fluorescein emission peak. All reported concentrations of reactants correspond to those after mixing. To avoid high local concentrations during mixing, both reactants were prepared in the same volume. For all measurements, the concentration of cTAR was 10 nM and the concentration of dTAR varied

from 200 nM to 1.6 μM for pE and 4.5 μM for p23. Peptides were added to each reactant separately, and then the reaction was initiated by mixing the peptide-coated ODNs together. The kinetics was fast enough to monitor the fluorescence intensities continuously without photobleaching. The apparent rate constants k_{obs} and the amplitudes were determined from the kinetic traces by including a dead-time correction t_0 to take into account the delay between the mixing of reactants and the start of the measurements. The best estimates of the apparent kinetic rate constants for cTAR to dTAR hybridization were recovered from the progress curves by non-linear regression analysis using:

$$I(t) = I_f - (I_f - I_0) \times a \times e^{-kobs_1(t-to)} - (I_f - I_0) \times (1-a) \times e^{-k_{obs2}(t-to)} \quad \text{Equation 11}$$

where I_0, I_f and I are the initial (in the presence of peptide), final and actual fluorescence intensity, respectively; k_{obs1} and k_{2obs2} are the apparent kinetic rate constants; t_0 is the dead time and a is the relative amplitude of the fast component.

The rate constants of association, k_{ass}, and dissociation, k_{off}, for both the fast and slow components are determined by:

$$k_{obs} = k_{ass}[dTAR] + k_{diss} \quad \text{Equation 12}$$

To further characterize the kinetic reactions, the temperature dependence of the k_{obs} values was monitored as a function of the temperature and analyzed using the Arrhenius equation:

$$k(T) = A \exp\left(-\frac{E_a}{RT}\right) \quad \text{Equation 13}$$

where k(T) represents the rate constant determined at the temperature T, A is the pre-exponential factor of Arrhenius, E_a is the activation energy and R is the gas constant (8.314 J $\cdot$ mol $^{-1}$ $\cdot$ K $^{-1}$). T is the absolute temperature at which the reaction was carried out (in degrees Kelvin).

The Arrhenius plot is obtained by plotting the logarithmic value of the rate constant versus the inverse temperature 1/T. The resulting straight line is useful for finding the Arrhenius pre-exponential factor (A) and the activation energy (E_A).

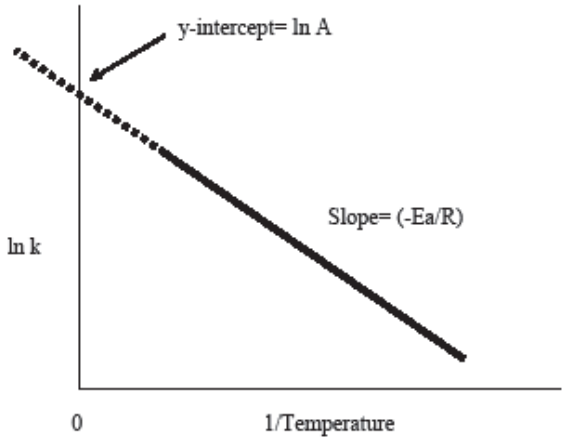

Fig.70. Arrhenius plot.

The temperature dependence of the annealing kinetics was carried out with 10 nM doubly labeled cTAR and a fixed excess of non-labelled dTAR, at different temperatures (15°C, 20°C, 25°C, 30°C, 35°C and 40°C) in the presence of the tested peptides.

To complete our data on the properties of the tested peptides and notably their ability to mimic the NC chaperone properties, we analyzed the peptide-promoted strand exchange kinetics (Urbaneja, Wu et al. 2002).

The experiments were performed with a 28(+) oligomer labeled at its 5' end with the fluorescein-6-carboxamidohexyl (FAM) group, its complementary 28(-) strand and a partially complementary strand 21(-) labeled at its 3' end with a 4-[[(4-dimethylamino)phenyl]-azo]benzenesulfonicamino (DABCYL) group. Excitation and emission wavelengths were 460 nm and 515 nm, respectively to monitor the FAM fluorescence.

A typical strand exchange experiment involved the formation of the perfect 28 base-pair duplex from a 28(+)/21(-) base-pair hybrid in the presence of the complementary 28-mer (28(-)). The reaction was monitored with the FAM group joined to the 5' end of the 28(+) component of the imperfect 28(+)/21(-) duplex. The exchange reaction was triggered by the addition of the nonlabeled 28-mer(-). Thus, the dissociation of the duplex 28(+)/21(-) was monitored through the fluorescence emission enhancement due to the recovery of FAM fluorescence upon displacement of the Dabcyl labeled 21-mer(-). The reactions in the presence of peptides were fast enough to monitor the fluorescence intensities continuously in real time whereas in the absence of peptide, the strand exchange was slow, so that the reaction was monitored only at certain time points.

2.4.3 Fluorescence Resonance Energy Transfer (FRET)

The Fluorescence Resonance Energy Transfer (FRET) between two molecules is an important physical phenomenon. Due to its sensitivity to distance, FRET has been used to investigate molecular interactions.

The mechanism of FRET involves a donor fluorophore in an excited electronic state, which may transfer its excitation energy to a nearby acceptor chromophore in a non-radiative fashion through long-range dipole-dipole interactions. The theory supporting energy transfer is based on the concept of treating an excited fluorophore as an oscillating dipole that can undergo an energy exchange with a second dipole having a similar resonance frequency. FRET can yield structural information on the donor-acceptor pair. Resonance energy transfer is not sensitive to the surrounding solvent shell of the fluorophore, and thus, produces molecular information unique to that revealed by solvent-dependent events, such as fluorescence quenching, excited-state reactions, solvent relaxation, or anisotropic measurements.

There are a few criteria that must be satisfied in order for FRET to occur : (i) the fluorescence emission spectrum of the donor molecule must overlap the absorption or excitation spectrum of the acceptor chromophore. (ii) The two fluorophores (donor and acceptor) must be in close proximity (typically 1 to 10 nanometer). (iii) The transition dipole of the donor and acceptor must be properly oriented to each other. (iv) The fluorescence lifetime of the donor molecule must be of sufficient duration to allow the FRET to occur.

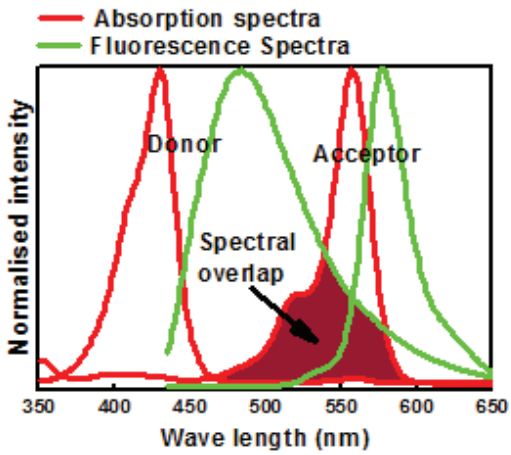

Fig.71. Absorption and fluorescence spectra of an ideal donor-acceptor pair. Brown colored region is the spectral overlap between the fluorescence spectrum of the donor and absorption spectrum of acceptor.

The FRET efficiency (E) describes the yield of the energy transfer i.e. the fraction of energy transfer event occurring per donor excitation event :

$$E = \frac{k_{ET}}{k_f + k_{ET} + \sum k_i} \qquad \text{Equation 14}$$

Where, k_{ET} is the rate of energy transfer, k_f is the radiative decay rate and k_i is the rate constant of any other de-excitation pathway.

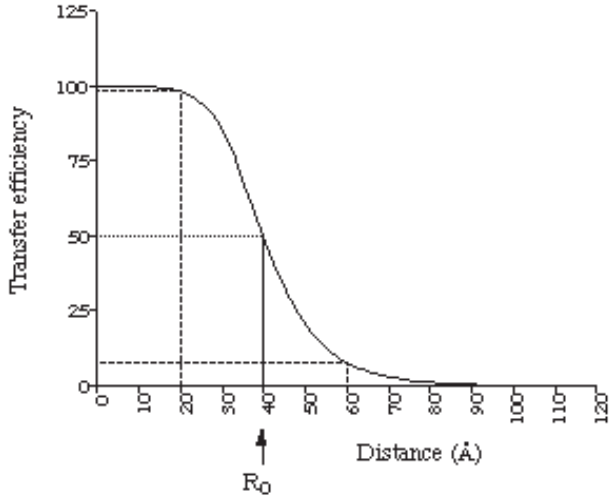

Fig.72. Relationship between the efficiency of the fluorescence resonance energy transfer and the distance separating the donor and the acceptor.

The efficiency of the FRET process (E) depends on the donor-to-acceptor separation distance r with an inverse sixth power of the distance between the donor and acceptor pair and is given by:

$$E = \frac{R_6^0}{\left(R_0^6 + r^6\right)} \qquad \text{Equation 15}$$

Where, R_0 is the Förster radius at which half of the excitation energy of the donor is transferred to the acceptor chromophore. Therefore, the Förster radius (R_0) is referred to as the distance at which the efficiency of energy transfer is 50%.

The Förster radius (R_0) depends on the fluorescence quantum yield of the donor in the absence of acceptor (QY_D), the refractive index of the solution (η) , the dipole angular

orientation of each molecule (κ^2) and the spectral overlap integral of the donor-acceptor pair ($J(\lambda)$).

This dependence is given by following equation:

$$R_0 = \left[8.8\times10^{23}\cdot\kappa^2\cdot n^{-4}\cdot QY_D\cdot J(\lambda)\right]^{\frac{1}{6}} A \qquad \text{Equation 16}$$

The strong distance-dependence of the FRET efficiency has been widely utilized in studying the structure and dynamics of proteins and nucleic acids, in the detection and visualization of intermolecular associations and in the development of intermolecular binding assays (Willard, Carillo et al. 2001) FRET is a particularly useful tool in molecular biology as the fraction of energy that is transferred can be measured (Jares-Erijman and Jovin 2006) and depends on the distance between the two fluorophores. The distance over which energy can be transferred is dependent on the spectral characteristics of the fluorophores, but is generally in the range 10–100A°.Thus, if fluorophores can be attached to known sites within molecules, measurement of the efficiency of energy transfer provides an ideal probe of inter- or intramolecular distances over macromolecular length scales. Techniques for measuring FRET are becoming more sophisticated and accurate, making them suitable for a range of applications such as measuring intramolecular distances (Haas, Wilchek et al. 1975), conformational changes (Heyduk 2002) and interactions between molecules (Hink, Bisseling et al. 2002).

Characterization of N,N'-bis (1,2,3-thiadiazol-5-yl) benzene-1,2-diamine chelating zinc ions from the retroviral nucleocapsid zinc fingers

The nucleocapsid protein NCp7 of human immunodeficiency virus type 1 (HIV-1) is a small basic protein tightly associated with genomic RNA in the mature infectious virus. It is characterized by two copies of highly conserved zinc finger motifs (CCHC). During the viral life cycle, NCp7 plays several crucial roles either as the full mature protein or the Pr55 polyprotein precursor. Due to the dependence of the chaperone activity of NCp7 on the proper folding of its zinc fingers, much effort has been made to develop compounds that target the NCp7 zinc fingers. The most promising ones are the zinc ejectors agents, which are generally efficient but suffer from limited selectivity (de Rocquigny, Shvadchak et al. 2008).

Here we reported on the characterization of the inhibitory mechanism of N,N'-bis(1,2,3-thiadiazol-5-yl)benzene-1,2-diamine (NV038) that efficiently blocks the replication of a wide spectrum of HIV-1, HIV-2 and SIV strains, by interfering with the early reverse transcription reaction coinciding with an early function of NCp7 protein and chelates Zn^{2+} from it.

In first step, we characterized the antiviral effect of NV038. For this purpose, we monitored the inhibition of viral replication in the presence of NV038 by measuring the MT-4 cells viability 5 days after infection with HIV-1, HIV-2, and simian immunodeficiency virus (SIV) strains. Interestingly, NV038 was found equally active against HIV-1_{IIIB}, HIV-2_{ROD} and SIV_{MAC251}. Additionally, the antiviral activity of NV038 was also tested against HIV-1 strains resistant either to the entry antagonist dextran sulfate, the CXCR4 inhibitor AMD3100 or the NNRTI navirapine. NV038 retained its antiviral activity while dextran sulfate, AMD3100 and navirapine were inactive against HIV-1 mutants (fig.73).

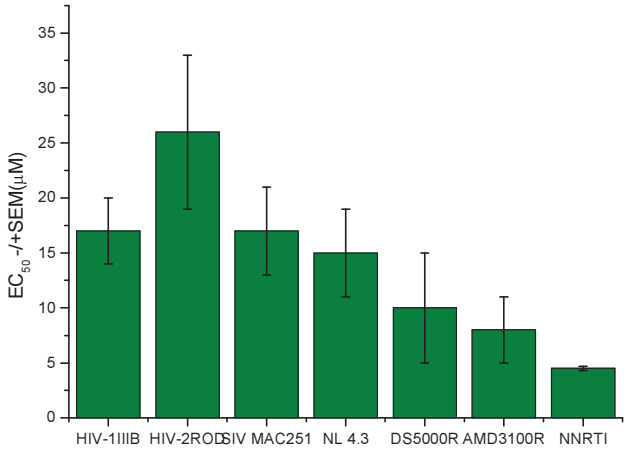

Fig.73. Antiviral effect of N,N'-bis(1,2,3-thiadiazol-5-yl)benzene-1,2-diamine and inhibitors of tested HIV-1 resistant strains. The number on the Y axis represents mean value of EC_{50} in µM range. The values represent means from at least 3 separate experiments.

To identify the viral step targeted by NV038, time of addition experiment was performed (fig74). To this end, cells were infected at a high multiplicity of infection and either NV038 or one of the control compounds (AZT, Dextran sulfate and Navirapine) was added at different times after infection. Virus replication was monitored by expression of p24 capsid at 31h after infection. Depending on the drug target, the addition of the compound could be delayed for hours specifically for each compound without losing its antiviral activity. Dextran sulfate, which interacts with virus adsorption to the cell, should be added together with the virus (at 0 h) to be active, its addition at 1 h postinfection or later did not block viral replication because adsorption had already occurred at this time. For zidovudine (AZT) and nevirapine, their addition could be delayed for 3 and 4 h postinfection, respectively. The addition of NV038 could be postponed for only 1 h, favoring the notion that it targets the incoming core or the early reverse transcription complex (RTC), thus making NCp7 a potential target of this compound.

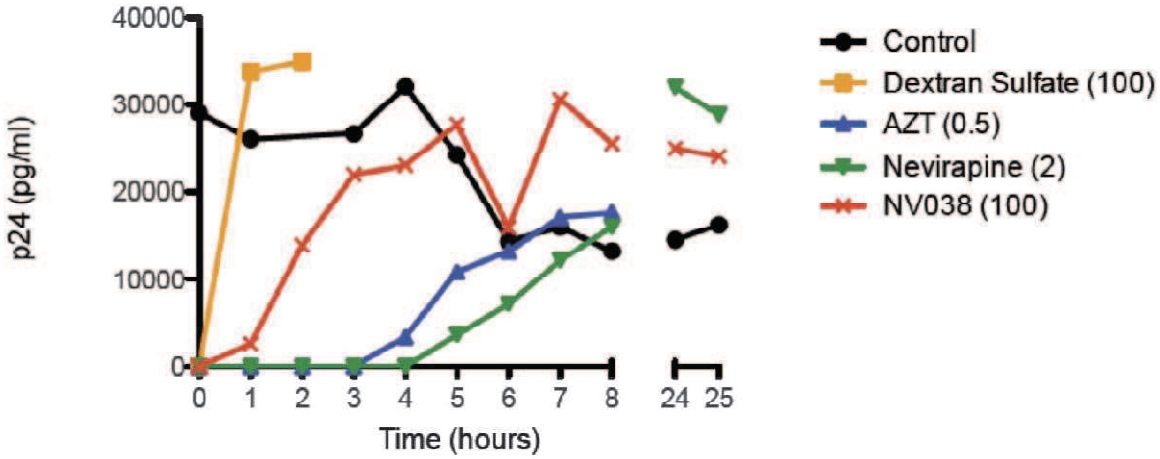

Fig.74. Time-of-addition experiment. MT-4 cells were infected with HIV-1, and the test compounds were added at different time points after infection. Virus production was determined by p24 Ag production in the supernatant at 31 h postinfection. Circles, control; squares, dextran sulfate (20 μM); triangles, AZT (1.9 μM); inverted triangles, nevirapine (7.5 μM); crosses, NV038 (297.5 μM). The graph is representative of data for 2 independent experiments.

Due to the fact that NCp7 contains two zinc fingers required for specific recognition of genomic RNA and viral DNA synthesis, we next characterized the zinc chelating properties of NV038 by monitoring the decrease in the fluorescence of a zinc-selective fluorophore, Newport Green (NPG) upon binding the Zn^{2+} ions released from NCp7. As most fluorimetric metal indicators, NPG signals metal chelation by suppressing an electron transfer in the

excited state which in the absence of zinc quenches the fluorescence of the fluorophore (Valeur and Leray 2000).

We further analyzed the zinc ejection properties of NV038 *in vitro*. Zinc ejection from the NCp7 zinc finger by NV038 was monitored through the intrinsic fluorescence of residue Trp37 of NC(11-55). This residue belongs to the distal zinc finger motif and shows a 3.0-fold increase of its fluorescence quantum yield upon zinc binding (Mely, DeRocquigny et al. 1996). The addition of a 10-fold excess of NV038 was found to induce a rapid decrease of Trp37 fluorescence, suggesting that NV038 efficiently removes zinc from NC(11-55). After 3h, the fluorescence dropped to a level close to that observed in the presence of 1 mM EDTA, indicating a nearly full ejection of zinc. Thus, we confirmed that NV038 is able to eject zinc from NCp7 and lead to its unfolding. As a consequence, NCp7 was no more able to destabilize cTAR, the complementary DNA sequence of TAR, in line with the strong dependence of the NCp7 destabilization activity on the folded fingers.

In conclusion, we presented a new lead compound inhibiting HIV-1, HIV-2 and SIV retroviruses. Data from mechanism of action studies indicates that NV038 targets early stage function of NC by chelating Zn^{2+} ions from zinc fingers. The mode of action analysis of different, already reported classes of NC inhibitors by nuclear magnetic resonance (NMR) and mass spectroscopy prompted us to speculate a different mechanism of action for NV038 since its structural features do not allow an acetyl transfer to Cys or a thiol-disulfide interchange. However to confirm this, further structure activity relationship experiments need to be performed.

Additionally, as compared to the efficiency of AZT or Nevirapine, the current EC_{50} of NV038 does not predict sufficient potency for good efficacy in clinical studies. Nevertheless, its potency might be increased. By the use of molecular modeling, a rational design of new analogues that will enable improved activity and selectivity is planned.

Furthermore, to better characterize the structural requirement for zinc chelation, series of compounds different in their chemical structure will be synthesized. The obtained results will help us to better understand the relationship between the structure and anti-NC activity and thus create new generation of NC inhibitors with improved activity.

ANTIMICROBIAL AGENTS AND CHEMOTHERAPY, Apr. 2010, p. 1461–1468 Vol. 54, No. 4
0066-4804/10/$12.00 doi:10.1128/AAC.01671-09

Inhibition of HIV-1 Replication by a Bis-Thiadiazolbenzene-1,2-Diamine That Chelates Zinc Ions from Retroviral Nucleocapsid Zinc Fingers▽

Christophe Pannecouque,[1] Beata Szafarowicz,[2] Natalia Volkova,[3] Vasiliy Bakulev,[3] Wim Dehaen,[4] Yves Mély,[2] and Dirk Daelemans[1]*

Rega Institute for Medical Research, Katholieke Universiteit Leuven, Minderbroedersstraat 10, B-3000 Leuven, Belgium[1]; Laboratoire de Biophotonique et Pharmacologie, UMR 7213 du CNRS, Université de Strasbourg, Faculté de Pharmacie, 74 route du Rhin, 67401 Illkirch, France[2]; Urals State Technical University, Mira Str. 19, Ekaterinburg 620002, Russia[3]; and Chemistry Department, Katholieke Universiteit Leuven, Celestijnenlaan 200F, 3001 Leuven, Belgium[4]

Received 25 November 2009/Returned for modification 28 December 2009/Accepted 11 January 2010

The human immunodeficiency virus type 1 (HIV-1) nucleocapsid p7 (NCp7) protein holds two highly conserved "CCHC" zinc finger domains that are required for several phases of viral replication. Basic residues flank the zinc fingers, and both determinants are required for high-affinity binding to RNA. Several compounds were previously found to target NCp7 by reacting with the sulfhydryl group of cysteine residues from the zinc fingers. Here, we have identified an *N*,*N*′-bis(1,2,3-thiadiazol-5-yl)benzene-1,2-diamine (NV038) that efficiently blocks the replication of a wide spectrum of HIV-1, HIV-2, and simian immunodeficiency virus (SIV) strains. Time-of-addition experiments indicate that NV038 interferes with a step of the viral replication cycle following the viral entry but preceding or coinciding with the early reverse transcription reaction, pointing toward an interaction with the nucleocapsid protein p7. In fact, *in vitro*, NV038 efficiently depletes zinc from NCp7, which is paralleled by the inhibition of the NCp7-induced destabilization of cTAR (complementary DNA sequence of TAR). A chemical model suggests that the two carbonyl oxygens of the esters in this compound are involved in the chelation of the Zn^{2+} ion. This compound thus acts via a different mechanism than the previously reported zinc ejectors, as its structural features do not allow an acyl transfer to Cys or a thiol-disulfide interchange. This new lead and the mechanistic study presented provide insight into the design of a future generation of anti-NCp7 compounds.

Human immunodeficiency virus type 1 (HIV-1) is the causative agent of AIDS and still represents a serious global public health problem. Shortly after the isolation of the virus, an intensive search for compounds that would inhibit the infectivity and replication of the virus was initiated. Although in the last 25 years, 25 compounds were licensed for the treatment of AIDS, and significant progress has been made in the treatment of HIV-infected individuals, there is presently no curative treatment for HIV/AIDS. Although established anti-HIV treatments are relatively effective, they are sometimes poorly tolerated, highlighting the need for a further refinement of existing antiviral drugs and the development of drugs with other mechanisms of antiviral action.

In order to replicate, HIV has to undergo several major steps. First, infectious virions bind to the cellular receptors on the surface of susceptible cells. The fusion of the viral envelope with the cellular membrane ensues, and the viral core penetrates into the cytoplasm (11). The single-stranded RNA genome of the virus is copied into a double-stranded linear DNA molecule by the viral enzyme reverse transcriptase (RT) assisted by nucleocapsid molecules in the core structure (13, 28). The DNA is then transported to the nucleus as a nucleic acid-protein complex (the preintegration complex [PIC]) and is integrated into the host cell's genome by the action of a second viral enzyme, integrase (IN), assisted by the NC protein (2). The covalently integrated form of viral DNA, which is defined as the provirus, serves as the template for transcription. Retroviral RNAs are synthesized, processed, and then transported to the cytoplasm, where they are translated by an internal ribosome entry site (IRES)-based mechanism (4) to produce viral proteins. The proteins that form the viral core, encoded by the *gag* and *pol* genes, initially assemble into immature cores together with two copies of the full-length viral RNA. As these structures bud through the plasma membrane, they become enveloped by a lipid bilayer from the cell membrane that also harbors the viral Env glycoproteins in the form of trimers. Coincident with virus assembly and budding, the viral protease (PR) cleaves the Gag and Gag-Pol precursors to release the structural core proteins and Pol enzymes in their final processed forms.

The development of anti-HIV compounds continues to be very active, and many lead compounds still emerge from initial antiviral screens. Compounds with a novel mechanism of action targeting mutation-intolerant targets are of special interest. The CCHC zinc fingers and the HIV nucleocapsid NCp7 protein are examples of such targets. The zinc finger motif is essential for virus replication, and the mutation of cysteine residues, which functions as zinc binding ligands, resulted in noninfectious virus particles (15, 17, 18), further underlining the importance of NCp7 in the viral life cycle. Several classes of compounds targeting the retroviral NCp7 have been described, including 3-nitrosobenzamide (NOBA) (30), 2,2′-dithiobisbenzamide (DIBA) (31), cyclic 2,2′-dithiobisbenzamide (e.g., SRR-SB3) (37), 1,2-dithiane-4,5-diol-1,1-dioxide (29), azadicarbonamide (ADA) (32), pyridinioalkanoyl thiolesters

* Corresponding author. Mailing address: Rega Institute, Katholieke Universiteit Leuven, Minderbroedersstraat 10, 3000 Leuven, Belgium. Phone: 32-16-337367. Fax: 32-16-337340. E-mail: dirk.daelemans@rega.kuleuven.be.

▽ Published ahead of print on 1 February 2010.

(PATEs) (35), and *S*-acyl-2-mercaptobenzamide thioesters (SAMTs) (20). These compounds react with the sulfhydryl group of cysteine residues from the NCp7 zinc fingers. On the other hand, zinc chelation by a general zinc chelator, TPEN [*N*,*N*,*N*′,*N*′-tetrakis(2-pyridylmethyl)ethylenediamine], inhibits Vif function and enhances the APOBEC3G (A3G)-mediated degradation of HIV; however, this effect is unrelated to the interaction of Vif with A3G (25, 38). Here we report the characterization of an *N*,*N*′-bis(4-ethoxycarbonyl-1,2,3-thiadiazol-5-yl)benzene-1,2-diamine (NV038) that efficiently inhibits the replication of HIV-1, HIV-2, and simian immunodeficiency virus (SIV). Studies of the mechanism of action indicate that this compound interferes with an early stage of the replication cycle coinciding with an early function of the NCp7 protein of Gag and chelates the Zn^{2+} from NCp7.

MATERIALS AND METHODS

Cells, viruses, and virus-like particles (VLPs). MT-4 and C8166 cells were grown and maintained in RPMI 1640 medium supplemented with 10% heat-inactivated fetal calf serum, 2 mM L-glutamine, 0.1% sodium bicarbonate, and 20 μg gentamicin per ml.

The HIV-1_{IIIB} strain was provided by R. C. Gallo and M. Popovic. The NL4-3.GFP11 strain expressing an enhanced version of green fluorescent protein (GFP) in place of Nef was a kind gift of A. Valentin and G. N. Pavlakis (National Cancer Institute at Frederick, Frederick, MD). For all tests described, the NL4-3.GFP11 virus was obtained by DNA transfection of 293T cells with the molecular clone. Next, 1 ml of virus-containing supernatant was used to infect 8×10^6 MT-4 cells in 40 ml of culture medium. Three days after infection, the supernatant was collected and used as a viral input in the respective assays.

Vesicular stomatitis virus G protein (VSV-G)-pseudotyped HIV-1 cells containing the envelope glycoprotein of the vesicular stomatitis virus instead of the wild-type HIV-1 envelope protein were produced by cotransfecting 293T cells with a NL4.3 molecular clone lacking a functional SUgp120 (pNL4.3-ΔE-GFP) (39) and a construct encoding VSV-G.

HIV-1 VLPs were generated by the cotransfection of a codon-optimized Gag p55 polyprotein expression plasmid (33) with pVSV-g in 293T cells. These plasmids were a kind gift of M. Rosati and G. N. Pavlakis (National Cancer Institute at Frederick, Frederick, MD). To obviate specific cell surface receptor requirements, VLPs were pseudotyped with the pantropic VSV-G envelope protein.

***In vitro* antiviral assays.** Evaluation of the antiviral activity of the compounds against HIV-1_{IIIB} in MT-4 cells was performed by using a 3-(4,5-dimethylthiazol-2-yl)-2,5-diphenyltetrazolium bromide (MTT) assay as previously described (27). Stock solutions (10× final concentration) of test compounds were added in 25-μl volumes to two series of triplicate wells to allow the simultaneous evaluation of their effects on mock- and HIV-infected cells at the beginning of each experiment. Serial 5-fold dilutions of test compounds were made directly in flat-bottomed 96-well microtiter trays using a Biomek 3000 robot (Beckman Instruments, Fullerton, CA). Untreated HIV- and mock-infected cell samples were included as controls. An HIV-1_{IIIB} stock (50 μl) at 100 to 300 50% cell culture infectious doses ($CCID_{50}$) or culture medium was added to either the infected or mock-infected wells of the microtiter tray. Mock-infected cells were used to evaluate the effects of the test compound on uninfected cells in order to assess the cytotoxicity of the test compounds. Exponentially growing MT-4 cells were centrifuged for 5 min at 1,000 rpm, and the supernatant was discarded. The MT-4 cells were resuspended at 6×10^5 cells/ml, and 50-μl volumes were transferred into the microtiter tray wells. Five days after infection, the viability of mock- and HIV-infected cells was examined spectrophotometrically by using the MTT assay. The MTT assay is based on the reduction of yellow MTT (Acros Organics, Geel, Belgium) by the mitochondrial dehydrogenase of metabolically active cells to a blue-purple formazan that can be measured spectrophotometrically. The absorbances were read in an eight-channel computer-controlled photometer (Multiscan Ascent reader; Labsystems, Helsinki, Finland) at two wavelengths (540 and 690 nm). All data were calculated by using the median optical density (OD) value of three wells. The 50% cytotoxic concentration (CC_{50}) was defined as the concentration of the test compound that reduced the absorbance (OD at 540 nm [OD_{540}]) of the mock-infected control sample by 50%. The concentration achieving 50% protection against the cytopathic effect of the virus in infected cells was defined as the 50% effective concentration (EC_{50}).

Evaluation of the antiviral activity of the compounds against NL4-3.GFP11 in C8166 cells was performed by using flow cytometry (see below), and HIV-1 core antigen (p24 antigen [Ag]) in the supernatant was analyzed by a p24 Ag enzyme-linked immunosorbent assay (Perkin-Elmer).

Flow cytometry. Flow cytometric analysis was performed with a FACSCanto II flow cytometry system (Becton Dickinson, Erembodegem, Belgium) equipped with a 488-nm argon-ion laser and a 530-nm/30-nm-bandpass filter (FL1, detection of GFP-associated fluorescence) (Becton Dickinson). Before acquisition, cells were pelleted at 1,000 rpm for 10 min and fixed in 3% paraformaldehyde solution. Acquisition was stopped when 10,000 events were counted. Data analysis was carried out with Cell Quest software (BD Biosciences). Cell debris were excluded from the analysis by gating on forward- versus side-scatter dot plots.

Time-of-addition experiments. MT-4 cells were infected with HIV-1_{IIIB} at a multiplicity of infection (MOI) of 0.5. Following a 1-h adsorption period, cells were distributed into a 96-well tray at 45,000 cells/well and incubated at 37°C. Test compounds were added at different times (0, 1, 2, 3, 4, 5, 6, 7, 8, 24, and 25 h) after infection. HIV-1 production was determined at 31 h postinfection via a p24 enzyme-linked immunosorbent assay (Perkin-Elmer, Brussels, Belgium).

Zinc chelation monitored by NPG fluorescence. The zinc chelation assay buffer consisted of 20 mM HEPES and 10 μM $ZnCl_2$ (pH 7.4). Zinc chelation was monitored by monitoring the decrease in the fluorescence of a zinc-selective fluorophore, Newport Green (NPG) (Molecular Probes), in the assay buffer at room temperature. Zinc chelation was initiated by the addition of different concentrations of test compounds in dimethyl sulfoxide to the zinc chelation assay buffer and incubation for 20 min at room temperature. An equal volume of 1 μM NPG in 20 mM HEPES (pH 7.4) was then added, and the increase fluorescence was monitored at 530 nm (excitation wavelength = 485 nm) by using the Saffire^2 fluorescence reader (Tecan).

Zinc ejection and inhibition of NC(11-55) destabilization of cTAR (complementary DNA sequence of TAR). The NC(11-55) peptide was synthesized by solid-phase peptide synthesis on a 433A synthesizer (ABI, Foster City, CA) as previously described (34). The lyophilized peptide was dissolved in water, and its concentration was determined by using an extinction coefficient of 5,700 $M^{-1} \cdot cm^{-1}$ at 280 nm. Next, 2.5 molar equivalents of $ZnSO_4$ were added to the peptide, and the pH was raised to its final value by adding buffer. The increase of pH was done only after the addition of zinc to avoid the oxidization of the zinc-free peptide.

Doubly labeled cTAR was synthesized at a 0.2 μmol scale by IBA GmbH Nucleic Acids Product Supply (Göttingen, Germany). The 5′ terminus of cTAR was labeled with 6-carboxyrhodamine (Rh6G) via an amino linker with a six-carbon spacer arm. The 3′ terminus of cTAR was labeled with 4-(4′-dimethylaminophenylazo)benzoic acid (Dabcyl) using a special solid support with the dye already attached. Doubly labeled cTAR was purified by reverse-phase high-performance liquid chromatography (HPLC) and polyacrylamide gel electrophoresis. An extinction coefficient at 260 nm of 521,910 $M^{-1} \cdot cm^{-1}$ was used for cTAR. All experiments were performed at 20°C with a solution containing 25 mM Tris-HCl (pH 7.5), 30 mM NaCl, and 0.2 mM $MgCl_2$ (8). Absorption spectra were recorded with a Cary 400 spectrophotometer. Fluorescence spectra were recorded at 20°C with a Fluorolog spectrofluorometer (Horiba Jobin-Yvon) equipped with a thermostated cell compartment. Excitation wavelengths were 295 nm and 520 nm for NC(11-55) and Rh6G-5′-cTAR-3′-Dabcyl, respectively. The spectra were corrected for dilution and buffer fluorescence. The protein spectra were additionally corrected for screening effects due to the zinc-ejecting agent with the following equation:

$$I_P = \frac{I_m \times (d_p + d_s + d_r/2)(1 - 10^{-d_p})}{d_p\,(1 - 10^{-d_p + d_s + d_r/2})}$$

where I_m is the measured fluorescence of the protein, I_p is the fluorescence intensity of the protein in the absence of inner filter, d_p is the absorbance of the protein, d_s is the absorbance of NV038 at the excitation wavelength, and d_r is the absorbance of NV038 at the emission wavelengths.

RESULTS

Inhibition of HIV and SIV in cell culture. We have discovered an *N*,*N*′-bis(4-ethoxycarbonyl-1,2,3-thiadiazol-5-yl)benzene-1,2-diamine (NV038) with anti-HIV and anti-SIV activities in cell culture (Fig. 1 and Table 1). The inhibition of viral replication was monitored by measuring the viability of MT-4 cells 5 days after infection (27). The cytotoxicity of the compound was assessed in parallel by monitoring the viability of mock-infected cells. Inter-

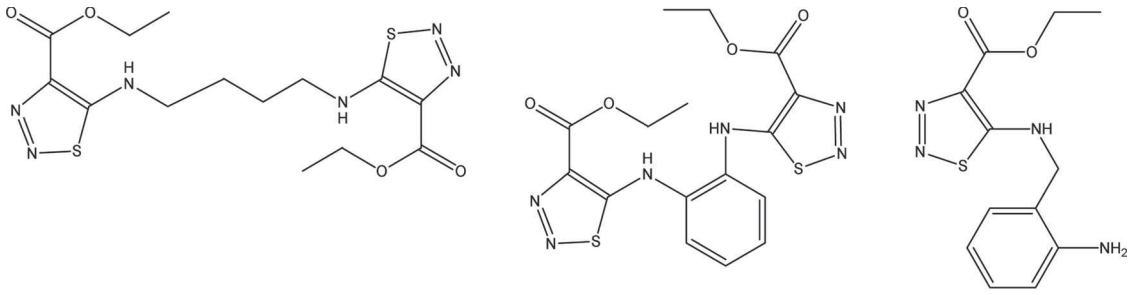

FIG. 1. Chemical structures of tested compounds. MW, molecular weight (in thousands).

estingly, NV038 was equally active against HIV-1_{IIIB}, HIV-2_{ROD}, and SIV_{Mac251}, while compounds lacking the benzenediamine moiety (NV037) or carrying only one 4-ethoxycarbonyl-1,2,3-thiadiazyle substitution (NV039) were completely inactive. The well-characterized nonnucleoside reverse transcriptase inhibitor (NNRTI) nevirapine did not inhibit the replication of HIV-2 or SIV at concentrations of up to 7.5 μM tested. The 50% cytotoxic concentration of NV038 was greater than 297.5 μM tested, resulting in a selective range value of more than 17.

To assess the potential of NV038 against drug-resistant HIV-1 strains, its antiviral activity was tested against strains that are resistant to either the entry antagonist dextran sulfate, the CXCR4 inhibitor AMD3100, or the NNRTI nevirapine. NV038 retained its activity against these strains (Table 1), whereas dextran sulfate, AMD3100, and nevirapine were inactive against their respective resistant HIV-1 mutants. These results provide evidences that NV038 does not interfere with virus-cell (coreceptor) binding or the catalytic reverse transcription activity of viral replication and prompted us to carry out a more detailed study of the NV038 mechanism of action.

Mechanism-of-action studies: determination of the step in the virus life cycle affected by the action of NV038. In the NL4-3.GFP11 molecular clone (36), enhanced GFP (eGFP) is expressed from multiply spliced *nef* mRNAs. Therefore, eGFP expression from this recombinant clone enabled us to determine whether an inhibitor interferes with a target before or after the expression of multiply spliced mRNA (12, 12a). To study the effect of NV038 during a single round of infection, C8166 cells were infected with NL4-3.GFP11 in the presence of inhibitors. Cells were harvested 24 h after infection (time required for a single round of replication), and the number of eGFP-expressing cells was monitored by flow cytometry (Fig. 2). The toxicity of the compounds was assessed from the forward- versus side-scatter dot plots. As expected, the well-characterized HIV inhibitors dextran sulfate and nevirapine and the integrase inhibitor L-870,810 caused a dramatic decrease in numbers of eGFP-expressing cells compared to the untreated control. In contrast, in cultures treated with the HIV-1 protease inhibitor ritonavir, the number of eGFP-expressing cells was similar to that for the untreated control. These results are consistent with the fact that in a single round of infection, molecules interfering with a viral component implicated in the early steps of virus replication inhibit the expression of eGFP, while molecules targeting a viral component essential for virus assembly do not inhibit eGFP expression. NV038 behaved like dextran sulfate, nevirapine, and L-870,810 in that it inhibited the expression of eGFP (by 94.5% compared to the control), thus targeting a viral component playing a key role during the early steps of virus replication.

The above-described results were confirmed when NV038 was evaluated for its inhibitory effect on virus production by chronically HIV-1-infected HuT-78 cells (data not shown). We noticed no inhibitory effect on the release of infectious virus at subtoxic concentrations, while, as expected, the control compound ritonavir, targeting the viral protease, efficiently inhibited the production of infectious viruses. Taken together, such data suggest that the compound NV038 targets an early viral function.

Time of drug addition. To identify the viral component targeted by this compound, a time-of-addition experiment was set up. This experiment determines how long the addition of a compound can be postponed before its antiviral activity is lost. Indeed, when an inhibitor that interferes with the binding of the virus to the host cell is present at the time of virus addition,

TABLE 1. Antiviral effect of *N*,*N*′-bis(4-ethoxycarbonyl-1,2,3-thiadiazol-5-yl)benzene-1,2-diamine and analogues[a]

Compound	Mean EC_{50} ± SEM (μM)							Mean CC_{50} ± SEM (μM)
	HIV-1_{IIIB}	NL4.3/WT	NL4.3/DS5000^R (165-fold)	NL4.3/AMD3100^R (>100-fold)	$NNRTI^R_{K103N:Y181C}$ (>85-fold)	HIV-2_{ROD}	SIV_{Mac251}	
NV037	>105	ND	ND	ND	ND	>105	ND	105 ± 20
NV038	17 ± 3	15 ± 4.0	10 ± 5	8 ± 3	4.5 ± 0.2	26 ± 7	17 ± 4	>297.5
NV039	>290	ND	ND	ND	ND	>290	ND	>290

[a] Values are from at least 3 independent experiments. The fold resistance toward the respective inhibitor of resistant strains is given in parentheses (with the EC_{50} for the NL4.3 wild type [WT] set as 1). EC_{50}, 50% effective concentration (concentration of inhibitor required for 50% inhibition of viral replication); CC_{50}, 50% cytotoxic concentration (concentration of inhibitor that kills 50% of the cells); ND, not determined.

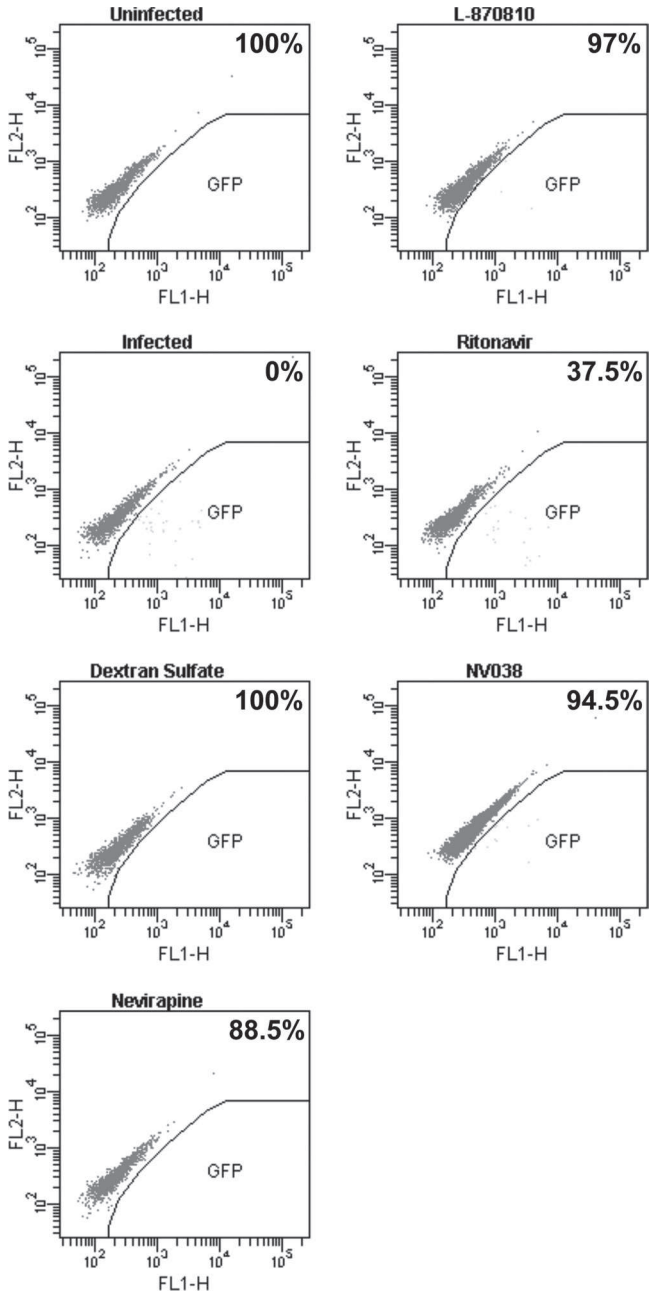

FIG. 2. NV038 targets a pretranscriptional step of the HIV-1 life cycle. Cells were infected with NL4-3.GFP11 in the presence of the test compound, and 24 h after infection, cells were analyzed for GFP expression as a marker for infection. The amount of GFP-expressing cells (gated as indicated) were quantified by flow cytometry analysis, and the percentage of inhibition of GFP-expressing cells compared to that of the untreated control (0%) is given in the upper right corner of each plot. Concentrations used were as follows: dextran sulfate, 20 μM; nevirapine, 7.5 μM; L-870,810, 0.3 μM; ritonavir, 2.8 μM; NV038, 297.5 μM.

it will inhibit virus replication. However, when this binding inhibitor is added after virus delivery to the host cell, it will not interfere with replication. To that end, cells were infected at a high multiplicity of infection, and either one of the compounds was added at 1, 2, 3, 4, 5, 6, 7, and 8 h after infection, as indicated in Fig. 3. Virus replication was monitored by p24

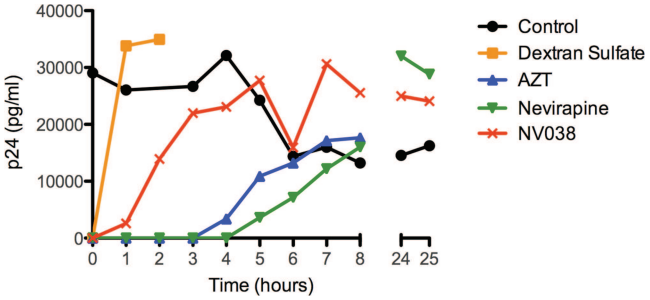

FIG. 3. Time-of-addition experiment. MT-4 cells were infected with HIV-1, and the test compounds were added at different time points after infection. Virus production was determined by p24 Ag production in the supernatant at 31 h postinfection. Circles, control; squares, dextran sulfate (20 μM); triangles, AZT (1.9 μM); inverted triangles, nevirapine (7.5 μM); crosses, NV038 (297.5 μM). This graph is representative of data for 2 independent experiments.

capsid expression at 31 h after infection. Depending on the drug target, the addition of the compound could be delayed for hours specifically for each compound without losing its antiviral activity. Dextran sulfate, which interacts with virus adsorption to the cell, should be added together with the virus (at 0 h) to be active; its addition at 1 h postinfection or later did not block viral replication because adsorption had already occurred at this time. For zidovudine (AZT) and nevirapine, their addition could be delayed for 3 and 4 h postinfection, respectively. The addition of NV038 could be postponed for only 1 h, favoring the notion that it targets the incoming core or the early reverse transcription complex (RTC).

NV038 did not interfere with the virus entry process as measured with a classical virus-binding assay (data not shown). The compound also retained full antiretroviral activity against VSV-G-pseudotyped HIV-1 replication (data not shown), confirming that it is not interfering with the specific binding or fusion processes of HIV-1.

***N,N′*-Bis(4-ethoxycarbonyl-1,2,3-thiadiazol-5-yl)benzene-1,2-diamine targets one of the Gag proteins.** The above-described data suggest that this new compound interacts with one or more essential viral components soon after virus entry into cells. In that respect, NCp7 is a likely candidate since it plays a critical role in the viral core structure and in DNA synthesis and maintenance, notably by chaperoning the RT enzyme during the obligatory minus- and plus-strand DNA transfers to generate long terminal repeats (LTRs) (13, 21).

To test whether the anti-HIV-1 activity of NV038 is targeting one of the Gag proteins (including NCp7), we examined whether the anti-HIV-1 effect of NV038 could be suppressed by saturating target cells with HIV-1 virus-like particles (VLPs) containing Gag and pseudotyped with VSV-G. The anti-HIV-1 activity of NV038 decreased in the presence of VLPs, while VLPs had no effect on AMD3100 or on nevirapine (Fig. 4). These results indicate that the inhibitory effect exhibited by NV038 is saturable and is caused by an interaction with one or more of the Gag structural proteins.

NCp7, which is one of the Gag proteins, contains two CCHC zinc fingers required for the specific recognition of genomic RNA and viral DNA synthesis (reviewed in reference 13). Using Newport Green (NPG) as a specific zinc indicator, we have found that *N,N′*-bis(4-ethoxycarbonyl-1,2,3-thiadiazol-5-

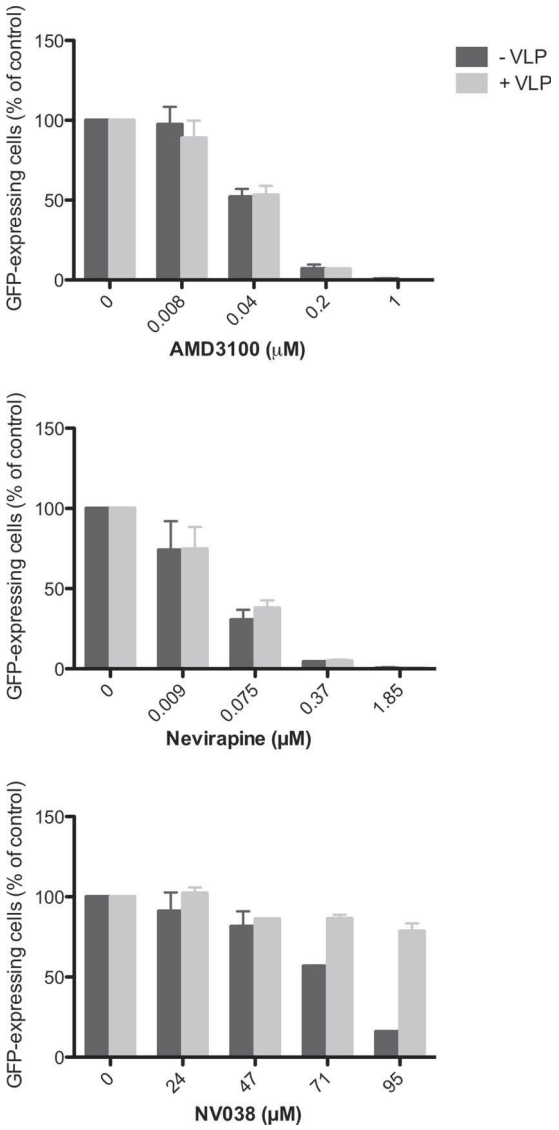

FIG. 4. NV038 inhibition of HIV-1 NL4-3.GFP11 replication is decreased in the presence of VLPs expressing the Gag p55 polyprotein. Human T-lymphocyte C8166 cells were infected with GFP-encoding HIV-1 in the presence or absence of Gag p55-containing VLPs as indicated. Viral replication in the presence of different concentrations of compound was measured by virus-dependent GFP expression using flow cytometry.

yl)benzene-1,2-diamine is able to efficiently chelate zinc (Fig. 5). The assay is based on the increase in Newport Green fluorescence intensity upon binding Zn^{2+}. In this experiment, NV038 was incubated with 10 μM $ZnCl_2$ for 30 min, and free Zn^{2+} was then quantified by using Newport Green. Figure 5 shows the decrease of Zn^{2+}-dependent Newport Green fluorescence in the presence of NV038, suggesting that NV038 is chelating Zn^{2+} ions. NV037 and NV039 had no effect on Newport Green fluorescence in the presence of Zn^{2+}. Altogether, these experiments provide strong evidence that NV038 is interfering with an early step in viral replication by targeting HIV-1 NCp7 function and chelating the Zn^{2+} ions from the zinc fingers.

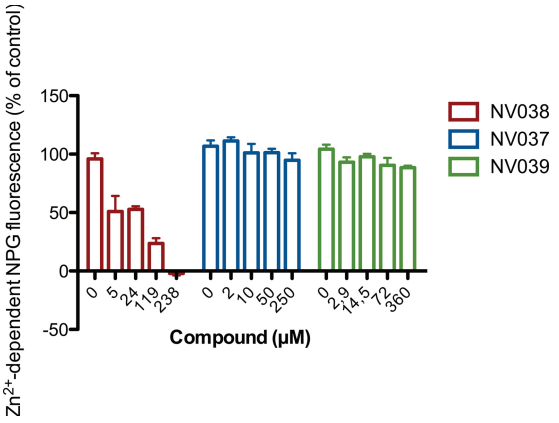

FIG. 5. Zn^{2+}-dependent Newport Green (NPG) fluorescence in the presence of *N*,*N*′-bis(1,2,3-thiadiazol-5-yl)benzene-1,2-diamine derivatives. Zinc chelation of the compounds was monitored by measuring the decrease in the fluorescence of the zinc-selective fluorophore Newport Green.

Zinc ejection and inhibition of NCp7(11-55) destabilization of cTAR. Zinc ejection from the NCp7 zinc finger by NV038 was monitored through the intrinsic fluorescence of residue Trp37 of NC(11-55). This residue belongs to the distal zinc finger motif and shows a 3.0-fold increase of its fluorescence quantum yield upon zinc binding (9, 24). The addition of a 10-fold excess of NV038 was found to induce a rapid decrease of Trp37 fluorescence (Fig. 6A), suggesting that NV038 efficiently removes zinc from NC(11-55). After 3 h, the fluorescence dropped to a level close to that observed in the presence of 1 mM EDTA, indicating a nearly full ejection of zinc.

To confirm the zinc ejection, we then monitored, in the presence of NV038, the NC(11-55)-induced destabilization of the secondary structure of cTAR DNA (Fig. 6B, inset), the complementary sequence of the transactivation response element, involved in minus-strand DNA transfer during reverse transcription (3, 5, 8). Indeed, this destabilization is exquisitely sensitive to the proper folding of the zinc-bound finger motifs and totally disappears when zinc ions are removed (6). Sensitive monitoring of the NCp7-induced destabilization of cTAR can be obtained by using the doubly labeled Rh6G-5′-cTAR-3′-Dabcyl derivative. In the absence of NC, cTAR is mainly in a nonfluorescent closed form, where the Rh6G and Dabcyl labels at the 5′ and 3′ termini, respectively, of the cTAR stem are close together, giving excitonic coupling (7). As previously reported (8), NC(11-55) added to cTAR at a 10-fold molar excess led to a melting of the bottom of the cTAR stem, which increases the distance between the two fluorophores and thus restores Rh6G fluorescence (Fig. 6B). In line with the zinc ejection hypothesis, the addition of NV038 to the NC(11-55)/cTAR complex at a molar ratio of 10:1 with respect to NC(11-55) led to a strong decrease in Rh6G emission and, thus, in cTAR destabilization. The NC(11-55)-induced destabilization of cTAR further decreased with time, and the peptide became almost fully inactive after 3 h of incubation with NV038. Moreover, the loss of the ability of NC(11-55) to destabilize cTAR was found to closely match the ejection of zinc from the fingers (Fig. 6C), further confirming that NV038 efficiently removes bound zinc ions from NCp7.

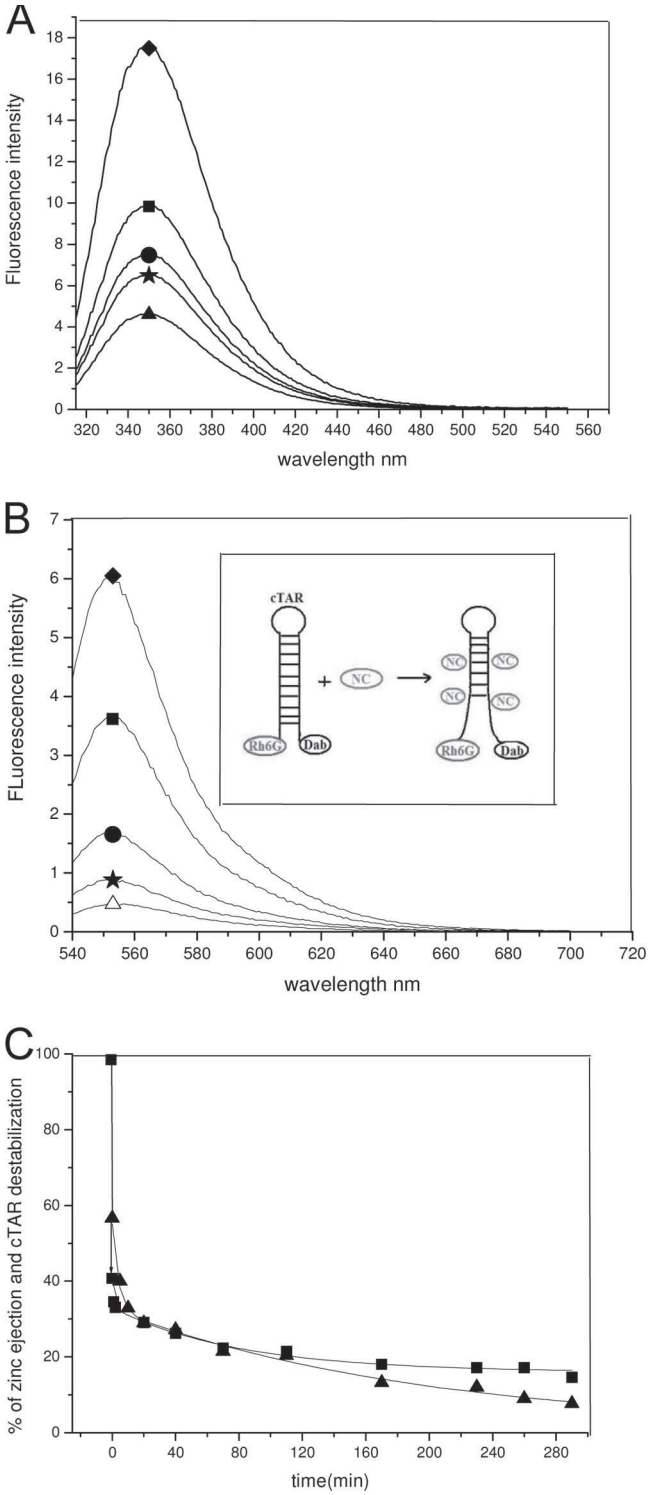

FIG. 6. Zn ejection and inhibition of NC(11-55)-promoted cTAR destabilization by NV038. (A) Ejection of the zinc ions bound to NC(11-55) by NV038. The emission spectrum of 1 μM NCp7 was recorded either in the absence (diamond) or in the presence of 4.2 μg/ml (10 μM) NV038 after 1 min (square), 1 h (circle), and 3 h (star) of incubation. Triangle, emission spectrum of NC(11-55) after the addition of 1 mM EDTA. (B) Inhibition of NC(11-55)-induced cTAR destabilization by NV038. The emission spectrum of 0.1 μM Rh6G-5′-cTAR-3′-Dabcyl was recorded either in the absence (open triangle) or in the presence of 1 μM NC(11-55) before (diamond) and after incubation with 10 μM of the NV038 compound for 1 min (square), 1 h (circle), and 3 h (star). (Inset) Scheme of the NC(11-55)-induced destabilization of cTAR and the resulting fluorescence increase of Rh6G. (C) Correlation between zinc ejection and inhibition of NC(11-55)-promoted cTAR destabilization. The percentages of Zn^{2+} ejection (squares) and inhibition of cTAR destabilization (triangles) induced by 10 μM NV038 are reported as a function of time. Solid lines represent double-exponential fits to the data.

DISCUSSION

We have identified *N*,*N*′-bis(4-ethoxycarbonyl-1,2,3-thiadiazol-5-yl)benzene-1,2-diamine (NV038), a new lead compound that efficiently interferes with the replication of HIV-1, HIV-2, and SIV and resistant HIV-1 strains. The compound was tested with different acute and chronic HIV infection models in order to establish its time of effect and mode of action. Its effectiveness in inhibiting HIV replication in acute infection models as opposed to its inability to block virus production from chronically infected cells indicates that the target of NV038 encompasses a preintegrational process. Furthermore, time-of-addition experiments even refined the time of intervention to a time frame situated after entry and prior to the completion of the reverse transcription step, indicating that NV038 targets the incoming core complex. However, compared to the efficiency of AZT or nevirapine, its current EC_{50} does not predict sufficient potency for good efficacy in clinical studies. Indeed, in comparison to these extremely potent inhibitors, the antiretroviral activity of NV038 is almost insignificant. However, one of the keystones of actual anti-HIV treatment, namely, the phosphonate acyclic nucleotide analogue (R)-PMPA (tenofovir), has a 50% inhibitory concentration (IC_{50}) of 7 μM when assessed with the same biological system. This is only about half the value observed for NV038. Nevertheless, its potency might be increased by chemical modification. By using molecular modeling, a rational design of new analogues that will enable an improvement of activity and selectivity is planned.

As NCp7 is one of the possible targets occurring after entry and prior to the completion of the RT step, the effect of loading infected cells with an excess of Gag p55 on the inhibitory activity of NV038 was tested. The observed loss of the anti-HIV-1-inhibitory effect of NV038 in the presence of Gag p55-containing VLPs suggested a stoichiometric interaction of the compound with a protein derived from Gag p55. *In vitro*, we demonstrated that NV038 is able to chelate zinc ions. Interestingly, the zinc chelation ability of NV038 and its analogues correlates well with their inhibitory capacity on retroviral replication. Indeed, the compound NV038 is able to chelate zinc and inhibit HIV replication, while the related compounds NV037 (having a 1,3-proylenediamine linker instead of the 1,2-benzenediamine linker) and NV039 (having only one 4-ethoxycarbonyl-1,2,3-thiadiazol-5-yl moiety) did not inhibit HIV *in vitro*, nor did they chelate zinc. We also demonstrated that NV038 efficiently ejects zinc from NCp7. Noticeably, our data (Fig. 6A) indicate that the distal finger motif releases zinc in the presence of NV038. Moreover, the loss of the ability of NCp7 to destabilize cTAR was correlated with the ejection of zinc from the fingers, further confirming that NV038 efficiently removes the bound zinc ions from NCp7.

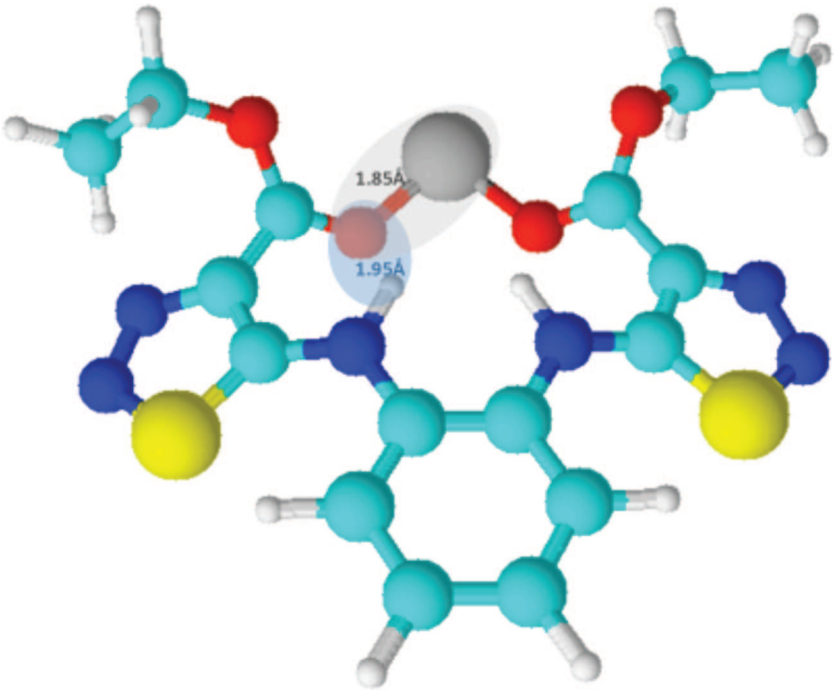

FIG. 7. Chemical model for chelation of Zn^{2+} by the two carbonyl oxygens of the esters from NV038. Bond lengths for a Zn-oxygen complex (1.85 Å) and the interatomic distance for N-H···O (1.95 Å) are given. This figure was created by using ACD/Chemsketch 12.0 software. Red, oxygen; dark blue, nitrogen; yellow, sulfur; gray, zinc; green, carbon; white, hydrogen.

Altogether, these experiments unambiguously pinpoint NCp7 as the target for this new lead compound.

It was reported previously that compounds with zinc ejection properties can inhibit a postintegration stage of HIV-1 replication (31). However, the *N*,*N*′-bis(4-ethoxycarbonyl-1,2,3-thiadiazol-5-yl)benzene-1,2-diamine described here clearly interferes with an early step happening after viral entry and before reverse transcription. Other compounds with zinc-ejecting properties were previously shown to inhibit an early step of the HIV-1 life cycle (14). Furthermore, the reported zinc-ejecting compounds that are interfering with HIV-1 replication, whether they act on an early or a late stage of the viral life cycle, have been shown to target one of the functions of the nucleocapsid (NCp7) protein. Indeed, retroviral nucleocapsid proteins harbor a multiplicity of functions, including viral RNA binding and packaging (1, 40), virus infectivity (15, 18), reverse transcription promotion (16, 19, 22, 26), and the stimulation of retroviral integration (10). Since these processes are happening in both early and late stages of the viral life cycle, different inhibitors targeting different functions of NCp7 could have an early or a late effect on HIV-1 replication. Further molecular analysis of how these different classes of NCp7 inhibitors act and how they structurally interact with NCp7 could be useful to draw the different functional regions within NCp7 responsible for early and late functions. At least for the thioester zinc ejectors, nuclear magnetic resonance (NMR) and mass spectroscopy studies showed that they act by the covalent modification of Cys39 (20). Also, for DIBA compounds, the proposed reaction mechanism is a thiol-disulfide interchange between DIBA and NCp7 at Cys36 and Cys49 (23). We speculate that the *N*,*N*′-bis(1,2,3-thiadiazol-5-yl)benzene-1,2-diamine described here acts via a different mechanism, as its structural features do not allow an acyl transfer to Cys or a thiol-disulfide interchange. Future research, such as structure-activity relationship experiments, is needed to confirm this hypothesis. However, the limited series of compounds reported here already indicates that the anti-HIV activity is linked to the Zn^{2+}-chelating capacity of the compound. It is likely that the conformation adopted by NV038 is determined by the chelation of the Zn^{2+} ion by the two carbonyl oxygens of the esters and furthermore by a hydrogen bond between the NH and the carbonyl of the esters. This model is depicted in Fig. 7 and is in agreement with the typical bond lengths for a Zn-oxygen complex (≈1.85 Å) and the interatomic distance for N-H···O (≈1.95 Å). The selectivity of the compound reveals a possible specific chelation of zinc at the zinc fingers. This implies that NV038 harbors structural features that direct the molecule to the zinc fingers of NCp7. In an ongoing effort to study the structural requirements for Zn^{2+} chelation at the zinc fingers, a series of molecules that will shed light on the structure-activity relationship is now being synthesized.

In conclusion, we present a new lead compound inhibiting HIV-1, HIV-2, as well as SIV retroviruses. Data from mechanism-of-action studies indicate that this compound targets an early-stage function of the nucleocapsid protein and chelates Zn^{2+} from the NCp7 zinc fingers. This lead compound and the study of its mechanism of action are useful for the development of a future generation of NCp7 inhibitors with improved activity.

ACKNOWLEDGMENTS

We thank L. Bral, L. De Dier, K. Erven, C. Heens, and K. Uytterspot for excellent technical assistance; G. Pavlakis and B. Felber for plasmids; and J.-L. Darlix for helpful discussions and comments on the

manuscript. A number of reagents were obtained through the NIH AIDS Reagent Program.

The work was supported by grant number 1.5.104.07 from the Belgian Fonds voor Wetenschappelijk Onderzoek (FWO), a Geconcerteerde Onderzoeksacties grant (grant number GOA 10/014) to the Katholieke Universiteit Leuven, the French ANRS (Agence Nationale de la Recherche sur le SIDA), and the Russian Foundation for Basic Research (grant numbers RFBR 08-03-00376 a and RFBR/NNSF 08-03-92208 a).

REFERENCES

1. **Aldovini, A., and R. A. Young.** 1990. Mutations of RNA and protein sequences involved in human immunodeficiency virus type 1 packaging result in production of noninfectious virus. J. Virol. **64:**1920–1926.
2. **Al-Mawsawi, L. Q., and N. Neamati.** 2007. Blocking interactions between HIV-1 integrase and cellular cofactors: an emerging anti-retroviral strategy. Trends Pharmacol. Sci. **28:**526–535.
3. **Azoulay, J., J. P. Clamme, J. L. Darlix, B. P. Roques, and Y. Mely.** 2003. Destabilization of the HIV-1 complementary sequence of TAR by the nucleocapsid protein through activation of conformational fluctuations. J. Mol. Biol. **326:**691–700.
4. **Balvay, L., M. Lopez Lastra, B. Sargueil, J. L. Darlix, and T. Ohlmann.** 2007. Translational control of retroviruses. Nat. Rev. Microbiol. **5:**128–140.
5. **Beltz, H., J. Azoulay, S. Bernacchi, J. P. Clamme, D. Ficheux, B. Roques, J. L. Darlix, and Y. Mely.** 2003. Impact of the terminal bulges of HIV-1 cTAR DNA on its stability and the destabilizing activity of the nucleocapsid protein NCp7. J. Mol. Biol. **328:**95–108.
6. **Beltz, H., C. Clauss, E. Piemont, D. Ficheux, R. J. Gorelick, B. Roques, C. Gabus, J. L. Darlix, H. de Rocquigny, and Y. Mely.** 2005. Structural determinants of HIV-1 nucleocapsid protein for cTAR DNA binding and destabilization, and correlation with inhibition of self-primed DNA synthesis. J. Mol. Biol. **348:**1113–1126.
7. **Bernacchi, S., and Y. Mely.** 2001. Exciton interaction in molecular beacons: a sensitive sensor for short range modifications of the nucleic acid structure. Nucleic Acids Res. **29:**E62.
8. **Bernacchi, S., S. Stoylov, E. Piemont, D. Ficheux, B. P. Roques, J. L. Darlix, and Y. Mely.** 2002. HIV-1 nucleocapsid protein activates transient melting of least stable parts of the secondary structure of TAR and its complementary sequence. J. Mol. Biol. **317:**385–399.
9. **Bombarda, E., N. Morellet, H. Cherradi, B. Spiess, S. Bouaziz, E. Grell, B. P. Roques, and Y. Mely.** 2001. Determination of the pK(a) of the four Zn2+-coordinating residues of the distal finger motif of the HIV-1 nucleocapsid protein: consequences on the binding of Zn2+. J. Mol. Biol. **310:**659–672.
10. **Carteau, S., R. J. Gorelick, and F. D. Bushman.** 1999. Coupled integration of human immunodeficiency virus type 1 cDNA ends by purified integrase in vitro: stimulation by the viral nucleocapsid protein. J. Virol. **73:**6670–6679.
11. **Clapham, P. R., and A. McKnight.** 2002. Cell surface receptors, virus entry and tropism of primate lentiviruses. J. Gen. Virol. **83:**1809–1829.
12. **Daelemans, D., C. Pannecouque, G. N. Pavlakis, O. Tabarrini, and E. De Clercq.** 2005. A novel and efficient approach to discriminate between pre- and post-transcription HIV inhibitors. Mol. Pharmacol. **67:**1574–1580.

12a. **Daelemans, D., E. De Clercq, and A. M. Vandamme.** 2001. A quantitative GFP-based bioassay for the detection of HIV-1 Tat transactivation inhibitors. J. Virol. Methods **96:**183–188.

13. **Darlix, J. L., J. L. Garrido, N. Morellet, Y. Mely, and H. de Rocquigny.** 2007. Properties, functions, and drug targeting of the multifunctional nucleocapsid protein of the human immunodeficiency virus. Adv. Pharmacol. **55:**299–346.
14. **de Rocquigny, H., V. Shvadchak, S. Avilov, C. Z. Dong, U. Dietrich, J. L. Darlix, and Y. Mely.** 2008. Targeting the viral nucleocapsid protein in anti-HIV-1 therapy. Mini Rev. Med. Chem. **8:**24–35.
15. **Dorfman, T., J. Luban, S. P. Goff, W. A. Haseltine, and H. G. Gottlinger.** 1993. Mapping of functionally important residues of a cysteine-histidine box in the human immunodeficiency virus type 1 nucleocapsid protein. J. Virol. **67:**6159–6169.
16. **Driscoll, M. D., and S. H. Hughes.** 2000. Human immunodeficiency virus type 1 nucleocapsid protein can prevent self-priming of minus-strand strong stop DNA by promoting the annealing of short oligonucleotides to hairpin sequences. J. Virol. **74:**8785–8792.
17. **Gorelick, R. J., W. Fu, T. D. Gagliardi, W. J. Bosche, A. Rein, L. E. Henderson, and L. O. Arthur.** 1999. Characterization of the block in replication of nucleocapsid protein zinc finger mutants from Moloney murine leukemia virus. J. Virol. **73:**8185–8195.
18. **Gorelick, R. J., S. M. Nigida, Jr., J. W. Bess, Jr., L. O. Arthur, L. E. Henderson, and A. Rein.** 1990. Noninfectious human immunodeficiency virus type 1 mutants deficient in genomic RNA. J. Virol. **64:**3207–3211.
19. **Guo, J., T. Wu, J. Anderson, B. F. Kane, D. G. Johnson, R. J. Gorelick, L. E. Henderson, and J. G. Levin.** 2000. Zinc finger structures in the human immunodeficiency virus type 1 nucleocapsid protein facilitate efficient minus- and plus-strand transfer. J. Virol. **74:**8980–8988.
20. **Jenkins, L. M., J. C. Byrd, T. Hara, P. Srivastava, S. J. Mazur, S. J. Stahl, J. K. Inman, E. Appella, J. G. Omichinski, and P. Legault.** 2005. Studies on the mechanism of inactivation of the HIV-1 nucleocapsid protein NCp7 with 2-mercaptobenzamide thioesters. J. Med. Chem. **48:**2847–2858.
21. **Levin, J. G., J. Guo, I. Rouzina, and K. Musier-Forsyth.** 2005. Nucleic acid chaperone activity of HIV-1 nucleocapsid protein: critical role in reverse transcription and molecular mechanism. Prog. Nucleic Acid Res. Mol. Biol. **80:**217–286.
22. **Li, X., Y. Quan, E. J. Arts, Z. Li, B. D. Preston, H. de Rocquigny, B. P. Roques, J. L. Darlix, L. Kleiman, M. A. Parniak, and M. A. Wainberg.** 1996. Human immunodeficiency virus type 1 nucleocapsid protein (NCp7) directs specific initiation of minus-strand DNA synthesis primed by human tRNA(Lys3) in vitro: studies of viral RNA molecules mutated in regions that flank the primer binding site. J. Virol. **70:**4996–5004.
23. **Loo, J. A., T. P. Holler, J. Sanchez, R. Gogliotti, L. Maloney, and M. D. Reily.** 1996. Biophysical characterization of zinc ejection from HIV nucleocapsid protein by anti-HIV 2,2′-dithiobis[benzamides] and benzisothiazolones. J. Med. Chem. **39:**4313–4320.
24. **Mely, Y., H. De Rocquigny, N. Morellet, B. P. Roques, and D. Gerad.** 1996. Zinc binding to the HIV-1 nucleocapsid protein: a thermodynamic investigation by fluorescence spectroscopy. Biochemistry **35:**5175–5182.
25. **Nathans, R., H. Cao, N. Sharova, A. Ali, M. Sharkey, R. Stranska, M. Stevenson, and T. M. Rana.** 2008. Small-molecule inhibition of HIV-1 Vif. Nat. Biotechnol. **26:**1187–1192.
26. **Ottmann, M., C. Gabus, and J. L. Darlix.** 1995. The central globular domain of the nucleocapsid protein of human immunodeficiency virus type 1 is critical for virion structure and infectivity. J. Virol. **69:**1778–1784.
27. **Pannecouque, C., D. Daelemans, and E. De Clercq.** 2008. Tetrazolium-based colorimetric assay for the detection of HIV replication inhibitors: revisited 20 years later. Nat. Protoc. **3:**427–434.
28. **Ren, J., and D. K. Stammers.** 2005. HIV reverse transcriptase structures: designing new inhibitors and understanding mechanisms of drug resistance. Trends Pharmacol. Sci. **26:**4–7.
29. **Rice, W. G., D. C. Baker, C. A. Schaeffer, L. Graham, M. Bu, S. Terpening, D. Clanton, R. Schultz, J. P. Bader, R. W. Buckheit, Jr., L. Field, P. K. Singh, and J. A. Turpin.** 1997. Inhibition of multiple phases of human immunodeficiency virus type 1 replication by a dithiane compound that attacks the conserved zinc fingers of retroviral nucleocapsid proteins. Antimicrob. Agents Chemother. **41:**419–426.
30. **Rice, W. G., C. A. Schaeffer, B. Harten, F. Villinger, T. L. South, M. F. Summers, L. E. Henderson, J. W. Bess, Jr., L. O. Arthur, J. S. McDougal, et al.** 1993. Inhibition of HIV-1 infectivity by zinc-ejecting aromatic C-nitroso compounds. Nature **361:**473–475.
31. **Rice, W. G., J. G. Supko, L. Malspeis, R. W. Buckheit, Jr., D. Clanton, M. Bu, L. Graham, C. A. Schaeffer, J. A. Turpin, J. Domagala, R. Gogliotti, J. P. Bader, S. M. Halliday, L. Coren, R. C. Sowder II, L. O. Arthur, and L. E. Henderson.** 1995. Inhibitors of HIV nucleocapsid protein zinc fingers as candidates for the treatment of AIDS. Science **270:**1194–1197.
32. **Rice, W. G., J. A. Turpin, M. Huang, D. Clanton, R. W. Buckheit, Jr., D. G. Covell, A. Wallqvist, N. B. McDonnell, R. N. DeGuzman, M. F. Summers, L. Zalkow, J. P. Bader, R. D. Haugwitz, and E. A. Sausville.** 1997. Azodicarbonamide inhibits HIV-1 replication by targeting the nucleocapsid protein. Nat. Med. **3:**341–345.
33. **Schneider, R., M. Campbell, G. Nasioulas, B. K. Felber, and G. N. Pavlakis.** 1997. Inactivation of the human immunodeficiency virus type 1 inhibitory elements allows Rev-independent expression of Gag and Gag/protease and particle formation. J. Virol. **71:**4892–4903.
34. **Shvadchak, V., S. Sanglier, S. Rocle, P. Villa, J. Haiech, M. Hibert, A. Van Dorsselaer, Y. Mely, and H. de Rocquigny.** 2009. Identification by high throughput screening of small compounds inhibiting the nucleic acid destabilization activity of the HIV-1 nucleocapsid protein. Biochimie **91:**916–923.
35. **Turpin, J. A., Y. Song, J. K. Inman, M. Huang, A. Wallqvist, A. Maynard, D. G. Covell, W. G. Rice, and E. Appella.** 1999. Synthesis and biological properties of novel pyridinioalkanoyl thiolesters (PATE) as anti-HIV-1 agents that target the viral nucleocapsid protein zinc fingers. J. Med. Chem. **42:**67–86.
36. **Valentin, A., W. Lu, M. Rosati, R. Schneider, J. Albert, A. Karlsson, and G. N. Pavlakis.** 1998. Dual effect of interleukin 4 on HIV-1 expression: implications for viral phenotypic switch and disease progression. Proc. Natl. Acad. Sci. U. S. A. **95:**8886–8891.
37. **Witvrouw, M., J. Balzarini, C. Pannecouque, S. Jhaumeer-Laulloo, J. A. Este, D. Schols, P. Cherepanov, J. C. Schmit, Z. Debyser, A. M. Vandamme, J. Desmyter, S. R. Ramadas, and E. de Clercq.** 1997. SRR-SB3, a disulfide-containing macrolide that inhibits a late stage of the replicative cycle of human immunodeficiency virus. Antimicrob. Agents Chemother. **41:**262–268.
38. **Xiao, Z., E. Ehrlich, K. Luo, Y. Xiong, and X. F. Yu.** 2007. Zinc chelation inhibits HIV Vif activity and liberates antiviral function of the cytidine deaminase APOBEC3G. FASEB J. **21:**217–222.
39. **Zhang, H., Y. Zhou, C. Alcock, T. Kiefer, D. Monie, J. Siliciano, Q. Li, P. Pham, J. Cofrancesco, D. Persaud, and R. F. Siliciano.** 2004. Novel single-cell-level phenotypic assay for residual drug susceptibility and reduced replication capacity of drug-resistant human immunodeficiency virus type 1. J. Virol. **78:**1718–1729.
40. **Zhang, Y., and E. Barklis.** 1995. Nucleocapsid protein effects on the specificity of retrovirus RNA encapsidation. J. Virol. **69:**5716–5722.

Characterization of a phenyl-thiadiazolylidene-amine derivative chelating zinc ions from retroviral nucleocapsid zinc fingers

The viral nucleocapsid protein (NC) plays crucial roles in the HIV-1 virus replication, mainly through its nucleic acid chaperone properties. These properties mostly rely on its highly conserved 'CCHC' zinc fingers. Due to its highly conserved structure, NC is a promising target for anti-HIV-1 therapy. Different classes of anti-NC molecules have already been developed. The most promising ones are likely those acting as microbicides, preventing viral transmission. In collaboration with the group of Dr. Daelemans (Belgium), a low-molecular-weight molecule, 2-methyl-3-phenyl-2H-[1,2,4]thiadiazol-5-ylideneamine (WDO-217) acting as a microbicide was identified.

The aim of this work was to characterize the molecular mechanism of the antiviral properties of WDO-217, and notably, to determine whether this compound targets the NC protein.

In first step, by monitoring MT-4 cell viability after viral infection in presence of the tested compound, we examined its anti-HIV and anti-SIV activity. Interestingly, WDO-217 was equally active against HIV-1_{IIIB}, HIV-2_{ROD} and $SIV_{MAC251,}$ while its CC_{50} was around 72µM resulting in an average selective range value of 17. In addition, WDO-217 was also tested against HIV-1 strains resistant either to the entry antagonist dextran sulfate, the CXCR4 inhibitor AMD3100, the NNRTI nevirapine or the NRTI AZT.

WDO-217 retained it antiviral activity whereas dextran sulfate, AMD3100, nevirapine and AZT were inactive against their respective resistant HIV-1 mutants (fig.75).

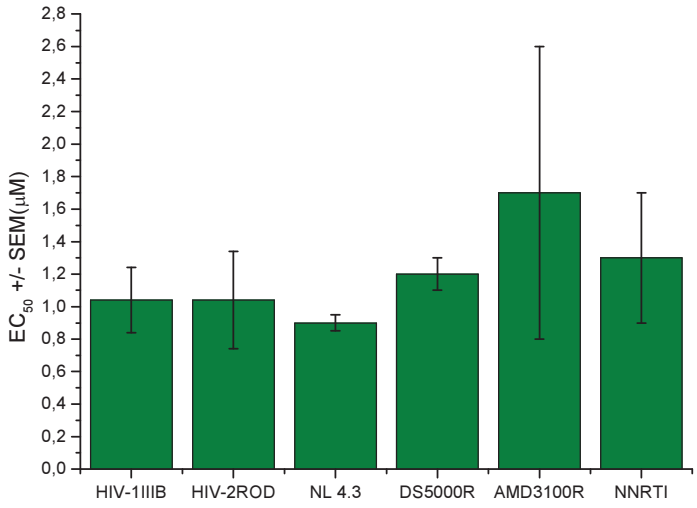

Fig.75. Antiviral effect of WDO-217 and inhibitors of HIV-1 resistant strains. The number on the Y axis represents mean value of EC_{50} in µM range. The values represents data from at least 3 separate experiments.

In a next step we examined the direct effect of WDO-217 on virus HIV-1 $_{IIIB}$ or HIV-2 $_{ROD}$ particles. To that end, the virus stock was incubated for one hour at 37 ^{0} C in presence of different concentrations of compound and virus infectivity was determined by titration and $CCID_{50}$/ml (50% of cell culture infectious dose) calculation. When tested at concentrations above 26 μM, WDO-217 attenuated HIV-1 and HIV-2 infectivity, presenting same results as commonly used detergent, Triton X-100.

In next step, due to its virucidal properties and potential use as microbicide component, WDO-217 was investigated for its ability to prevent DC-SIGN cells-mediated transmission to CD4+ cells. Although obtained results demonstrated that the tested compound does not inhibit viral capture by DC-SIGN cells, WDO-217 was able to efficiently prevent viral transmission from DC-SIGN to CD4+ cells underlining its potential use as microicide.

To investigate the mechanism of HIV inactivation in more detail, we tested the effect of the compound on different viral structural components. Pre-treated with WDO-217 virus stock was assessed for both core p24 antigen protein and viral genomic RNA content. Treatment with WDO-217 did not affect the amount of virus-associated p2 protein as compared with the untreated or AZT-treated control. On the other hand, we observed a clear decrease in viral RNA when HIV-1 virions were treated with WDO-217, suggesting that in one or the other way our compound reduces virion-associated RNA stability. Due to the fact that inside the virion genomic RNA is protected by nucleocapisd protein in next step we examined the effect of 2-methyl-3-phenyl-2H-[1,2,4]thiadiazol-5-ylideneamine on NC in vitro.

Using the intrinsic fluorescence of Trp37 of NC(11-55), we found that WDO-217 efficiently removes zinc from the peptide leading to its unfolding. Zinc ejection was confirmed by the inability of the peptide in the presence of WDO-217 to destabilize the secondary structure of cTAR, the complementary sequence of the transactivation response element. In addition, by monitoring the changes in the emission spectra of 3-hydroxyflavone (3HC) labelled NC preincubated with oligonucleotide, we study the WDO-217 effect on NC binding properties. The lack of changes in the emission spectra of the NC/oligonucleotide complexes after treatment with WDO-217 suggests that the compound does not dissociate the complexes but that zinc ejection leads to rearrangement of the zinc-free peptide in the complexes, causing even stronger interaction of the 3HC probe with the oligonucleotide. Similar final complexes were obtained with the zinc-depleted form of NC confirming that WDO-217 is able to eject zinc from the NC/oligonucleotide complex.

In a last step we investigated the influence of WDO-217 on the processing of the Gag precursor. In contrast to NCp7 zinc ejecting compounds, SRR-SB3 or SAMTs, WDO-217 did not cause accumulation of unprocessed Gag polyprotein.

In conclusion, we present a new lead compound able to efficiently inactivate HIV-1 and HIV-2 retroviruses by targeting the nucleocapsid protein. This leads to a decrease in the viral RNA in cell free virions, likely as a consequence of a defective protection by the zinc-depleted form of NC protein. This new mechanism of action makes WDO 217 useful for the design a future generation of NC inhibitors that could be applied in microbicide formulations.

A phenyl-thiadiazolylidene-amine derivative potently ejects zinc from retroviral nucleocapsid zinc fingers and inactivates HIV virions

Thomas Vercruysse[1*], Beata Basta[2*], Wim Dehaen[3], Jan Balzarini[1], Francois Debaene[4], Sarah Sanglier-Cianférani[4], Christophe Pannecouque[1], Yves Mély[2], and Dirk Daelemans[1¶]

[1]Rega Institute for Medical Research, KU Leuven, Minderbroedersstraat 10, B-3000 Leuven, Belgium, [2]Laboratoire de Biophotonique et Pharmacologie, UMR 7213 du CNRS, Université de Strasbourg, Faculté de Pharmacie, 74 route du Rhin, 67401, Illkirch, France, [3]Chemistry Department, KU Leuven, Celestijnenlaan 200F, B-3001 Leuven, Belgium, [4]Laboratoire de Spectrométrie de Masse BioOrganique (LSMBO), Université de Strasbourg, IPHC, 25 rue Becquerel 67087 Strasbourg, France. CNRS, UMR7178, 67037 Strasbourg, France.

*both authors contributed equally to this work

Running title: A new potent NCp7 zinc ejector inactivates HIV virions

text pages: 34
tables: 5
figures: 8
references: 46
words in abstract: 188
words in introduction: 406
words in discussion : 551

¶Corresponding authors: Dirk Daelemans: Rega Institute, KU Leuven, Minderbroedersstraat 10, 3000 Leuven, Belgium. Phone: 32-16-337367. Fax: 32-16 337340. E-mail: dirk.daelemans@rega.kuleuven.be

Yves Mély: Laboratoire de Biophotonique et Pharmacologie, UMR 7213 CNRS, Université de Strasbourg, 74 route du Rhin, 67401 ILLKIRCH, France. Phone: 33-3-68854263. Fax: 33-3-68854312. E-mail: yves.mely@unistra.fr

ABSTRACT

Sexual acquisition of the human immunodeficiency virus (HIV) through mucosal transmission may be prevented by using topically applied agents that block HIV transmission from one individual to another. Here, we have identified 2-methyl-3-phenyl-2*H*-[1,2,4]thiadiazol-5-ylideneamine (WDO-217) as a low-molecular-weight molecule that inactivates HIV particles. Both HIV-1 and HIV-2 virions pretreated with this compound were unable to infect permissive cells. Moreover, WDO-217 was able to inhibit infections of a wide spectrum of wild-type and drug-resistant HIV-1, HIV-2 and SIV strains. Whereas the capture of virus by DC-SIGN was unaffected by the compound, it efficiently prevented the transmission of DC-SIGN-captured virus to $CD4^+$ T-lymphocytes. Interestingly, exposure of virions to WDO-217 reduced the amount of virion-associated genomic RNA as measured by real-time RT-qPCR. Further mechanism of action studies demonstrated that WDO-217 efficiently ejects zinc from the zinc fingers of the retroviral nucleocapsid protein NCp7 and inhibits the nucleic acid destabilization properties of this protein. Importantly, WDO-217 was able to eject zinc from both zinc fingers, even when NCp7 was bound to oligonucleotides. This new lead compound opens opportunities for the development of a new series of zinc ejectors as candidate topical microbicide agents.

INTRODUCTION

Human immunodeficiency virus type 1 (HIV-1), the causative agent of AIDS (Acquired Immune Deficiency Syndrome), still represents a serious global public health problem. Although established anti-HIV treatments are relatively effective, they are sometimes poorly tolerated, highlighting the need for further refinement of the existing antiviral drugs and the development of novel anti-HIV strategies. In this respect, the use of topical virucides would be an interesting therapeutic strategy to prevent HIV transmission. Several topical agents for preventing HIV transmission have been described, including i) agents that inactivate HIV such as detergents (e.g. Nonoxynol-9 or Savvy) or *p*H modifiers (e.g. BufferGel; ReProtect (Mayer et al., 2001)), ii) agents that target viral replication (e.g. the reverse transcriptase inhibitors UC-781, TMC-120, tenofovir) and iii) agents that target viral entry (e.g. PRO 2000, cellulose sulfate). With the exception of tenofovir (Andrei et al., 2011), most microbicide candidate drugs that have been subject of large clinical trials, proved non-effective or even toxic upon long-term exposure to the vaginal environment.

The HIV-1 nucleocapsid NCp7 is essential for and plays multiple roles in virus replication (Thomas and Gorelick, 2008). NCp7 contains two CCHC zinc-finger motifs and binds the viral genomic RNA in the interior of the virion. The binding of NCp7 to nucleic acids results in their condensation and protection from nuclease degradation (Krishnamoorthy et al., 2003; Lapadat-Tapolsky et al., 1993; Tanchou et al., 1995). Therefore, this nucleoprotein complex protects the genomic RNA ensuring viral stability. A number of classes of compounds targeting the retroviral NCp7 has been described, including, 3-nitrosobenzamide (NOBA) (Rice et al., 1993a), 2,2'-dithiobisbenzamides (DIBA) (Rice et al., 1995), cyclic 2,2'-dithiobisbenzamides (e.g. SRR-SB3) (Witvrouw et al., 1997), 1,2-dithiane-4,5-diol-1,1-

dioxide (Rice et al., 1997a), azadicarbonamide (ADA) (Goebel et al., 2001; Rice et al., 1997b), pyridinioalkanoyl thiolesters (PATEs) (Turpin et al., 1999), bis-thiadiazolbenzene-1,2-diamines (Pannecouque et al., 2010) and S-acyl-2-mercaptobenzamide thioesters (SAMTs) (Jenkins et al., 2005). The latter class of compounds was recently considered for testing as topical microbicide for the prevention of HIV transmission (Turpin et al., 2008). These SAMT compounds were able to efficiently prevent vaginal transmission of SHIV upon exposure to nonhuman primates (Wallace et al., 2009). Here, we have identified a low-molecular-weight molecule, 2-methyl-3-phenyl-2*H*-[1,2,4]thiadiazol-5-ylideneamine, WDO-217, that inhibits HIV replication. Mechanism of action studies reveal WDO-217 a potent NCp7 zinc ejector that directly inactivates HIV-1 and HIV-2 virions and inhibits the transmission of DC-SIGN captured virus to $CD4^+$ lymphocytes. WDO-217 qualifies as a usual potential microbicide lead compound for further (pre)clinical studies.

MATERIALS AND METHODS

Cells and Viruses. MT-4, Jurkat A72, CEM, HuT-78 and Raji/DC-SIGN cells were grown and maintained in RPMI 1640 supplemented with 10% heat-inactivated fetal calf serum, 2 mM L-glutamine, 0.1% sodium bicarbonate and 20 µg gentamicin per ml. The HIV-1(III_B) strain was provided by R.C. Gallo and M. Popovic (at that time at the NIH, Bethesda, MD, USA). HIV-2(ROD) was obtained from L. Montagnier (at that time at the Pasteur Institute, Paris, France) and SIV(Mac251) from C. Bruck. Raji/DC-SIGN were kindly provided by L Burleigh (Paris, France)

In Vitro **Antiviral Assays.** Evaluation of the antiviral activity of the compounds against HIV-1 strain III_B in MT-4 cells was performed using the MTT assay as previously described (Pannecouque et al., 2008; Pauwels et al., 1988). Stock solutions (10 x final concentration) of test compounds were added in 25 µl volumes to two series of triplicate wells so as to allow simultaneous evaluation of their effects on mock- and HIV-infected cells at the beginning of each experiment. Serial 5-fold dilutions of test compounds were made directly in flat-bottomed 96-well microtiter trays using a Biomek 3000 robot (Beckman instruments, Fullerton, CA). Untreated HIV- and mock-infected cell samples were included as controls. HIV-1(III_B) stock (50 µl) at 100-300 $CCID_{50}$ (50 % cell culture infectious doses) or culture medium was added to either the infected or mock-infected wells of the microtiter tray. Mock-infected cells were used to evaluate the effects of test compound on uninfected cells in order to assess the cytotoxicity of the test compounds. Exponentially growing MT-4 cells were centrifuged for 5 minutes at 1000 rpm and the supernatant was discarded. The MT-4 cells were resuspended at 6 x 10^5 cells/ml and 50 µl volumes were transferred to the microtiter tray wells. Five days after infection, the viability of mock-and HIV-infected cells

was examined spectrophotometrically using the MTT assay. The MTT assay is based on the reduction of yellow coloured 3-(4,5-dimethylthiazol-2-yl)-2,5-diphenyltetrazolium bromide (MTT) (Acros Organics) by mitochondrial dehydrogenase activity in metabolically active cells to a blue-purple formazan that can be measured spectrophotometrically. The absorbances were read in an eight-channel computer-controlled photometer (Infinite M1000, Tecan), at two wavelengths (540 and 690 nm). All data were calculated using the median absorbance value of three wells. The 50% cytotoxic concentration (CC_{50}) was defined as the concentration of the test compound that reduced the absorbance (OD_{540}) of the mock-infected control sample by 50%. The concentration achieving 50% protection against the cytopathic effect of the virus in infected cells was defined as the 50% effective concentration (EC_{50}).

The antiviral activity of the compounds against HIV was evaluated in Jurkat cells stably transformed to express the LTR-GFP (A72 cells) (Jordan et al., 2003; Jordan et al., 2001). In 96-well plates, 3×10^4 A72 cells were infected with HIV in the presence of various concentrations of test compound. Three days post infection, cells were harvested and fixed in 3% paraformaldehyde. GFP-expression was quantified on a single cell basis by flow cytometry (Daelemans et al., 2001; Daelemans et al., 2005). Toxicity of the compounds was tested using an MTT-based method.

HIV-1 core antigen (p24 Ag) in the supernatant was analyzed by the p24 Ag enzyme-linked immunosorbent assay (Perkin Elmer).

Virucidal assay. Aliquots of a HIV stock (III_B or ROD) were incubated with various concentrations of compound in a final volume of 100 µl RPMI-1640 culture medium with 10% FCS for 1 hour at 37°C. Subsequently, the samples were diluted 4000 times with complete medium so that the residual concentration of compound present was far below its IC_{50}. The drug-treated and diluted virus was then used to infect susceptible MT-4 T-cells to

quantify the viral infectivity by titration and $CCID_{50}$ determination (Daelemans et al., 2011). Control experiments with AZT indicated that this procedure effectively diluted the compound to concentrations well below its effective antiviral concentration.

Treatment of HuT-78/III_B persistently infected cells, virion analysis and western blot. Chronically-infected HIV-1_{IIIB} HuT-78 cells (HuT-78/III_B) were washed four times with PBS to remove all free virions before treatment and $2x10^5$ cells were resuspended in 1 ml compound-containing medium for 43 hours at 37°C. Then, virions were prepared from clarified supernatants (10 min at 300 g) by centrifugation at 36 670 g for 2 hours at 4°C. Protein from lysed virions were separated by SDS-PAGE on a NuPage® Novex 4-12% Bis-Tris gel (Invitrogen) and transferred to a hydrophobic polyvinylidene difluoride (PVDF) membrane (Amersham Hybond™-P). The blot was blocked overnight at 4°C by 5% dry milk powder in western blot wash solution (WBWS; PBS + 0,5% Tween 20), washed three times for 5 minutes with WBWS and incubated with a mouse anti-HIV-1 p24 antibody (1:5000) from Abcam. The blot was then washed three times for 5 minutes with WBWS and incubated for 1 h with a goat anti-mouse IgG-HRP secondary antibody (1:2500) from Santa Cruz Biotechnology. The blot was washed three times for 5 minutes with WBWS and after 5 minutes of incubation with SuperSignal West Pico Chemiluminescent Substrate (Thermo Scientific) it was developed.

Effect of WDO-217 on the exposure of HIV-1 to Raji/DC-SIGN cells. In a first set of experiments (procedure A), HIV-1 (NL4.3) was exposed to WDO-217 at 105 µM (in 0.5 ml culture medium) for 60 min at 37°C. Then, 0.5 ml exponentially growing Raji/DC-SIGN cells (10^6 cells) was added, and the suspension further incubated at 37°C for 60 min. Subsequently, 39 ml medium was added to the cell suspension and centrifugated at 1,200 rpm for 10 min. The pellet was washed again with 40 ml medium and after centrifugation, the cell

pellet (containing DC-SIGN-bound virus) was analysed for p24 antigen content by ELISA. In a second set of experiments (procedure B), Raji/DC-SIGN cells treated as in procedure A were co-cultured in the presence of an equal amount of C8166 cells (10^6 cells) (total volume of 1 ml). Replication in C8166 was measured after ~ 20 hr of incubation. In a third set of experiments (procedure C), Raji/DC-SIGN cells were given the opportunity to capture HIV-1/NL4.3 by mixing Raji/DC-SIGN cells with virus (10^6 cells/ml). After one hour incubation at 37°C, C8166 cells (10^6 cells/ml) were added in the presence of WDO-217 at different concentrations and giant cell formation in the cultures was examined microscopically after ~24 hr. In the above-described experiments, the mannose-binding entry inhibitor HHA was included as a reference drug.

Quantitative RT-PCR. Total mRNA from virus stock was extracted using the QIamp viral RNA kit (Qiagen) followed by DNA digestion using RNase-free DNase I (Invitrogen). DNase I treated mRNA was used to generate cDNA along with Thermoscript reverse transcriptase (Invitrogen) and oligo$(dT)_{20}$. qRT-PCR for genomic unspliced HIV mRNA was performed according to a protocol described earlier (Vercruysse et al., 2010), using 0.2 mM primers TCAGCCCAGAAGTAATACCCATGT and TGCTATGTCAGTTCCCCTTGGTTCTCT, and 0.2 mM FAM-BHQ1 fluorescent probe ATTAACAGAAGGAGCCACCCCACAAGA. Control reactions omitted reverse transcriptase, and the number of cDNA copies was determined using a HIV-$1_{NL4.3}$ molecular clone DNA standard.

Zinc ejection and inhibition of NC(11-55)-induced destabilization of cTAR monitored by fluorescence techniques. The NC(11-55) peptide was synthesized by solid phase peptide synthesis on a 433A synthesizer (ABI, Foster City, CA), as previously described (Shvadchak et al., 2009). The lyophilized peptide was dissolved in water and its

concentration was determined using an extinction coefficient of 5,700 M^{-1} x cm^{-1} at 280 nm. Next, 2.5 molar equivalents of $ZnSO_4$ were added to the peptide and pH was raised to its final value, by adding buffer. The increase of pH was done only after zinc addition to avoid oxidization of the zinc-free peptide. Zinc ejection was monitored through the changes in the intrinsic fluorescence of the Trp37 residue of NC(11-55) (Bombarda et al., 2007; Mely et al., 1996), after addition of a 10-fold excess of WDO-217 (10 μM) to 1 μM NC(11-55).

To monitor the inhibition by WDO-217 of the NC(11-55)-induced destabilization of cTAR, we used doubly labelled cTAR, synthesized at a 0.2 μmol scale by IBA GmbH Nucleic Acids Product Supply (Göttingen, Germany). The 5‘ terminus of cTAR was labelled with 6-carboxyrhodamine (Rh6G) via an amino-linker with a six carbon spacer arm. The 3‘ terminus of cTAR was labelled with 4-(4‘-dimethylaminophenylazo)benzoic acid (Dabcyl) using a special solid support with the dye already attached. The doubly labelled cTAR was purified by reverse-phase HPLC and polyacrylamide gel electrophoresis. An extinction coefficient at 260 nm of 521,910 M^{-1} x cm^{-1} was used for cTAR. All experiments were performed at 20°C in 25 mM Tris-HCl, pH 7.5, 30 mM NaCl, and 0.2 mM $MgCl_2$ (Bernacchi et al., 2002). The effect of WDO-217 on the NC(11-55)-induced destabilization of cTAR was observed after addition of 10 μM WDO-217 to 0.1 μM Rh6G-cTAR-Dabcyl preincubated with 1 μM NC(11-55)

Absorption spectra were recorded on a Cary 400 spectrophotometer. Fluorescence spectra were recorded at 20°C on a Fluorolog spectrofluorometer (Horiba, Jobin-Yvon), equipped with a thermostated cell compartment. Excitation wavelength was 295 nm and 520 nm, for NC(11-55) and Rh6G-5’-cTAR-3’-Dabcyl, respectively. The spectra were corrected for dilution and buffer fluorescence. The protein spectra were additionally corrected for screening effects due to the zinc ejecting agent, using:

$$I_P = I_m * \frac{(d_p + d_s + d_r/2)(1-10^{-d_p})}{d_p(1-10^{-(d_p+d_s+d_r/2)})} \qquad (1)$$

where I_m is the measured fluorescence of the protein, I_p is the fluorescence intensity of the protein in the absence of inner filter, d_p is the absorbance of the protein, d_s is the absorbance of WDO-217 at the excitation wavelength, and d_r is the absorbance of WDO-217 at the emission wavelengths.

Zinc ejection monitored by supramolecular mass spectrometry. Before mass spectrometry (MS) analysis, NC(11-55) was dissolved and buffer exchanged with 50 mM ammonium acetate pH 7.0 using 4 cycles of microcentrifuge size exclusion filtering (Vivaspin 500 5kD, Sartorius Stedim biotech, Aubagne, France) and peptide concentration was measured by a Bradford assay.

ESI-MS measurements were performed in the positive ion mode on an electrospray time-on-flight mass spectrometer (LCT, Waters, Manchester, UK) equipped with an automated chip-based nanoESI source (Triversa Nanomate, Advion Biosciences, Ithaca, NY). Calibration of the instrument was performed using multiply charged ions of a 2 µM horse heart myoglobine solution. For analysis in denaturing conditions, samples were diluted to 2 µM in a 1/1 water/acetonitrile mixture (v/v) acidified with 1% formic acid and standard interface parameters were used to obtain best mass accuracy. In these conditions, noncovalent interactions are disrupted, allowing the measurement of the molecular weight of the monomer with a good accuracy (better than 0.01%).

Analyses under non-denaturing conditions were carried out after careful optimization of instrumental settings to avoid dissociation of noncovalent bonds and obtain sensible detection of protein/zinc complexation states. The accelerating voltage (Vc) was fixed to 20 V and the pressure in the first pumping stage of the instrument (Pi) to 6 mbar. Zinc ejection

measurements were performed after 30 min incubation at room temperature of a 20 μM solution of NC(11-55) with either 40 μM or 100 μM WDO-217. Data analysis was performed with the MassLynx 3.5 software (Waters, Manchester, UK). Peak intensities were used to estimate the ratios of the different ions detected.

RESULTS

Inhibition of HIV and SIV in Cell Culture. 2-Methyl-3-phenyl-2*H*-[1,2,4]thiadiazol-5-ylideneamine (WDO-217) (**Fig. 1**) was identified in a high-throughput screen for anti-HIV and anti-SIV activity in cell culture (**Fig. 2** and Table 1) (Pannecouque et al., 2008; Pauwels et al., 1988). WDO-217 was equally active against HIV-1 (III_B) (EC_{50}: 5 ± 3 μM), HIV-2 (ROD) (EC_{50}: 2.3 ± 0.3 μM), and SIV (Mac251) (EC_{50}: 5 ± 1 μM), while its 50% cytotoxic concentration in MT-4 cell cultures was around 72 μM resulting in an average selective index of ~20. Its antiretroviral activity was confirmed in human T-lymphocyte CEM cell cultures (Table 2).

To assess the potential of WDO-217 against drug-resistant HIV-1 strains, its antiviral activity was examined against virus strains that are resistant to either the entry inhibitor dextran sulfate, the CXCR4 antagonist AMD3100, the NRTI AZT, or the NNRTI nevirapine. Therefore, Jurkat A72 cells containing LTR-GFP (Jordan et al., 2001) were infected with the respective drug-resistant virus strains in the presence of the test compound. Production of Tat protein as a result of viral replication drives the integrated LTR to produce GFP. Infected cells became brightly fluorescent when measured by flow cytometry, providing a direct and quantitative marker for HIV-1 infection in individual live cells. Cells were harvested 5 days after infection and the number of GFP-expressing cells was monitored. Toxicity of the compounds was assessed from an MTT-based viability assay. WDO-217 invariably retained its full anti-HIV activity against the different virus strains (Table 3) whereas dextran sulphate, AMD3100, AZT, and nevirapine markedly lost inhibitory potential against their respective resistant HIV-1 mutants. These results incited us to carry out a detailed study on the target of antiviral action of WDO-217.

Inactivation of HIV-1 as well as HIV-2 virions by 2-methyl-3-phenyl-2*H*-[1,2,4]thiadiazol-5-ylideneamine. To explore the direct effect of WDO-217 on virus particles, HIV-1_{IIIB} was incubated for 1h at 37°C in the presence or absence of different concentrations of the compound. Then the virus was diluted to such extent that the residual compound concentration was far below its antivirally effective concentration and this diluted virus amount was used to infect MT-4 cell cultures. Virus infectivity was determined by titration and $CCID_{50}$ calculation (Table 4). WDO-217 attenuated both HIV-1 and HIV-2 infectivity, as did the Triton X-100 control, a detergent commonly used in laboratory practice to inactivate HIV. When the virus was incubated at drug concentrations of 26, 130 and 650 μM WDO-217, it was unable to infect cells, indicating that these concentrations were able to entirely inactivate the HIV virions. Similar results were obtained with 0.5% Triton-X-100. In contrast, AZT an inhibitor of the HIV reverse transcription that is inhibiting the viral replication (Yarchoan et al., 1986) but not directly inactivating HIV virions was completely inactive. This demonstrates that the compound is sufficiently diluted during the procedure and no significant amount of residual AZT is retained in the sample during titration and $CCID_{50}$ determination.

Effect of 2-methyl-3-phenyl-2*H*-[1,2,4]thiadiazol-5-ylideneamine on the capture of HIV-1 by Raji/DC-SIGN cells and on subsequent virus transmission to $CD4^+$ T cells. Because WDO-217 has virucidal properties, we next investigated whether it was able to prevent the DC-SIGN-mediated virus capture and subsequent transmission to $CD4^+$ T cells in view of its potential use as a microbicide candidate drug. First, the capability of WDO-217 to prevent capture of HIV-1 (III_B) by DC-SIGN was evaluated using Raji/DC-SIGN cells abundantly expressing DC-SIGN in their cell membranes. Exposure of Raji/DC-SIGN cells to HIV-1 captured the virus to their cell membranes, while wild-type Raji/0 cells did not

(Bertaux et al., 2007). Virus was pre-exposed to different concentrations of WDO-217 before it was administered to the Raji/DC-SIGN cell cultures. After 60 min of pre-incubationwith the Raji/DC-SIGN cells, unadsorbed virus and test compound were carefully removed by serial washing steps and the amount of captured virus was determined by measurement of the virus-associated p24 content on the Raji/DC-SIGN cell surface. The α(1-3)/(1-6)-mannose-specific plant lectin HHA was included as a positive control for inhibition of virus capture by Raji/DC-SIGN cells. In contrast to HHA, WDO-217 was not able to prevent binding of HIV-1 to the Raji/DC-SIGN cells (Table 5, procedure A), suggesting that the compound does not negatively affect the surface glycoproteins of the virus particles.

Next, we evaluated whether WDO-217 could prevent the transmission of captured HIV-1 from DC-SIGN-expressing cells to $CD4^+$ T cells. Therefore, the $DC\text{-}SIGN^+$ cells that efficiently captured drug-treated virus were co-cultured with uninfected C8166 cells. In these co-cultures, WDO-217 dose-dependently inhibited syncytium formation at an IC_{50} of 2.2 μM, whereas abundant syncytium formation occurred within 24 to 48 h post co-cultivation when the captured virus had not been pre-exposed to the drug (Table 5, procedure B). When virus was first given the opportunity to be captured by Raji/DC-SIGN cells in the absence of compound and then the Raji/DC-SIGN cells were co-cultured with C8166 cells in the presence of various concentrations of compound, WDO-217 still prevented the transmission of DC-SIGN-captured virus with an IC_{50} value of 8.3 μM. This suggests that WDO-217 can inactivate virus particles when they are bound to DC-SIGN (Table 5, procedure C). All together, these results demonstrate that 2-methyl-3-phenyl-2*H*-[1,2,4]thiadiazol-5-ylideneamine does not inhibit the viral capture by DC-SIGN but is able to inactivate captured virus and efficiently prevent the transmission of HIV-1 from DC-SIGN-expressing cells to $CD4^+$ T-lymphocytes, underlining its potential use as a microbicide agent.

Treatment of HIV-1 with WDO-217 decreases the virion-associated viral RNA content. To explore the mechanism of HIV inactivation by WDO-217 in more detail, we investigated the effect of WDO-217 on different viral structural components. Therefore, a pre-treated and subsequently compound-cleared virus stock was assessed for both its core p24 antigen protein as well as its viral genomic RNA content (**Fig. 3**). As expected, the detergent Triton-X-100 disturbs the structure of the virions and no p24 core protein nor viral genomic RNA could be detected in the isolated virus stock after treatment and subsequent washing. In contrast, treatment with WDO-217 did not affect the amount of virus-associated p24 core protein as for the untreated or AZT-treated control. However, when the viral genomic RNA content of the pre-treated virus stock was quantified by real-time RT-qPCR, there was a clear decrease in viral RNA for the WDO-treated HIV-1 virions as compared to the untreated control (**Fig. 3**), indicating that WDO-217 somehow reduces the virion-associated RNA stability. Since inside the virion the genomic RNA is protected by the viral nucleocapsid protein (NCp7), this prompted us to investigate the effect of WDO-217 on the nucleocapsid protein.

Zinc ejection from the retroviral zinc fingers. The zinc-ejecting properties from the NCp7 zinc fingers by WDO-217 was investigated by monitoring the intrinsic fluorescence of the Trp37 residue of NCp7(11-55), which shows a 3-fold decrease in its fluorescence quantum yield on zinc removal (Bombarda et al., 2007; Mely et al., 1996). Addition of a 10-fold excess of WDO-217 (10 μM) induced the same decrease of Trp37 fluorescence as observed for 1 mM EDTA, indicating that WDO-217 efficiently ejects zinc from NCp7(11-55) (**Fig. 4A**). Subsequently, the zinc ejection from NCp7(11-55) by WDO-217 exposure was investigated in function of time (**Fig 4B** and **C**). The compound induced a progressive decrease in Trp37 fluorescence and zinc ejection was complete after 35 min.

Ejection of 50% of the zinc is observed in less than 5 min (**Fig. 4C**). A large excess of Zn^{2+} ions (100-fold excess of zinc sulphate) did not prevent the zinc ejecting capacity of WDO-217, since nearly complete ejection of zinc from NCp7(11-55) was observed after 30 min (**Fig. 4D**). This result suggests that WDO-217 does not directly chelate zinc ions but progressively ejects the zinc ions from the NCp7 zinc fingers. All together, our results indicate that WDO-217 is a very efficient zinc ejector from NCp7.

To further investigate the zinc ejection properties of WDO-217, we analyzed the changes in the mass of NC(11-55) by supramolecular mass spectrometry (MS). Purity and homogeneity of NC(11-55) were verified by mass analysis in denaturing conditions. In these acidic conditions, zinc is released from the peptide and a molecular weight of 5137. 7 ± 0.4 Da was measured, in agreement with the expected mass of the zinc-free NC form (5137.9). In non-denaturing conditions, NC(11-55) analysis revealed the presence of a unique ion series of 5164.0 ± 0.4 Da corresponding to NC(11-55) with 2 zinc ions attached (Fig. 5A). Similar MS experiments were then performed in the presence of increasing WDO-217 amounts in order to assess the WDO-127 effect on NC/zinc complexes (Fig 5B and 5C). In the presence of a 2-fold excess of WDO-127, three different peaks corresponding to the native form of NC(11-55) with 2 zinc ions (MW = 5264.0 ± 0.4 Da), NC(11-55) with one zinc ion (MW = 5195.7 ± 0.1 Da) and the zinc free form of NC(11-55) (MW = 5131.8 ± 0.3 Da) were observed, confirming that WDO-217 was able to eject zinc (Fig. 5B). Using higher WDO-217 concentrations (five-fold excess of WDO-127 over NC) led to more efficient zinc ejection, as the major species detected (80 %) corresponded to the zinc-free form of NC(11-55). Noticeably, zinc ejection leads to the formation of three disulfide bridges as suggested from the differences in molecular weights in denaturing conditions for NC(11-55) in the absence (5137. 4 ± 0.4 Da) and the presence (5131. 4 ± 0.6 Da) of WDO-127. Altogether

these MS results unambiguously confirmed that WDO-217 acts as a zinc-ejector. Interestingly, no noncovalent complex between NC(11-55) and WDO-217 was observed in our experimental conditions (even in very mild MS conditions, Vc = 20 V and Pi = 6 mbar), suggesting that the interaction between the two species is likely transient.

Inhibition of NCp7(11-55)-induced destabilization of cTAR. To confirm the zinc ejection, we measured the ability of NC(11-55) to induce the destabilization of the secondary structure of cTAR DNA in the presence of WDO-217. cTAR is the complementary sequence of the transactivation response element, involved in the minus strand DNA transfer during reverse transcription (Azoulay et al., 2003; Beltz et al., 2003; Bernacchi et al., 2002). The NC(11-55)-induced destabilization is exquisitely sensitive to the proper folding of the zinc-bound finger motifs and totally disappears when zinc ions are removed (Beltz et al., 2005). The NCp7-induced destabilization of cTAR can be sensitively monitored by using the doubly labeled Rh6G-5'-cTAR-3'-Dabcyl derivative. In the absence of NCp7, cTAR is mainly in a non-fluorescent closed form where the Rh6G and Dabcyl labels, respectively at the 5' and 3' termini of the cTAR stem are in close proximity of each other (Bernacchi and Mely, 2001). As can be noticed from Figure 6A, and in agreement with previous data (Bernacchi and Mely, 2001), NC(11-55) added to cTAR at a 10-fold molar excess led to a melting of the bottom of the cTAR stem, which increases the distance between the two fluorophores and thus increases the Rh6G fluorescence. In line with the zinc ejection hypothesis, preincubation of NC(11-55) with WDO-217 at a molar ratio of 10:1 in respect with NC(11-55), led to a full loss of NC(11-55) ability to destabilize cTAR. Interestingly, there was no difference in activity on NCp7-induced cTAR destabilization by WDO-217 when the compound was preincubated first with NCp7 or first with cTAR (**Fig. 6A**). This suggests that WDO-217 can dissociate zinc from NCp7 even when the protein is bound to nucleic acids.

The inhibition of the NC(11-55)-induced destabilization of cTAR by WDO-217 was further monitored as a function of time (**Fig 6B**). A complete inhibition was observed after 50 min of incubation with WDO-217 and 50% inhibition was reached in less than 5 minutes in close correlation with its zinc ejection profile (**Fig. 6D**), further confirming the effect of WDO-217 on NC(11-55).

Effect of WDO-217 on the interaction of NCp7(11-55) with SL3 or PBS. To explore the effect of WDO-217 on the nucleic acid binding properties of NCp7(11-55), we used 3-hydroxyflavone (3HC) labelled NC(11-55) peptide. The 3HC probe shows a two-band emission highly sensitive to the binding of nucleic acids (Shvadchak et al., 2009). This two-band emission is the result of a proton transfer reaction that generates two excited states: a normal one (N*) and a tautomeric one (T*). Due to their different dipole moments, these two forms are differently sensitive to the environment. To test the binding properties of 3HC-NCp7(11-55), the SL3 RNA and Δ(-)PBS DNA sequences were selected since they preferentially bind one NCp7 per oligonucleotide (ODN) (Bourbigot et al., 2008; De Guzman et al., 1998). SL3 corresponds to the third stem-loop sequence of the HIV-1 encapsidation sequence, while Δ(-)PBS DNA corresponds to the (-) Primer Binding Site sequence lacking its 3' single strand overhang. Accordingly, we examined the changes in the emission spectra of 3HC-NCp7(11-55)/oligonucleotide complexes after treatment with WDO-217. Addition of Δ(-)PBS DNA or SL3 RNA to 3HC-NCp7(11-55) was found to decrease the overall intensity of the 3HC probe as well as the N*/T* ratio of its two emission bands in respect to the free 3HC-NCp7(11-55) peptide (**Fig. 7A and B**). This is a result of the stacking of the probe with the bases and its contact with the ODN backbone in the peptide/ODN complexes (Shvadchak et al., 2009). Addition of WDO-217 induces a further decrease in the intensity of the spectrum, suggesting that WDO-217 does not dissociate the NCp7/oligonucleotide

complex. This additional decrease in fluorescence accompanied by a slight increase in the N*/T* ratio is likely due to a rearrangement of the zinc-free peptide on the ODN sequence, which leads to a change in the interaction of the 3HC probe with the ODN. The increase in the N*/T* ratio observed with the zinc-depleted complex indicates that the environment of the 3HC probe is more polar than in the initial 3HC-NCp7(11-55)/oligonucleotide complex, suggesting a shift from stacking interactions towards more polar interactions with the backbone.

Next, we monitored the changes in the emission spectrum of 3HC-NCp7(11-55) that was preincubated with WDO-217 for 30 minutes, before addition to SL3 (**Fig. 7C**). The incubation of 3HC-NCp7(11-55) with WDO-217 for 30 minutes leads to a decrease in the overall intensity of the 3HC probe as well as its N*/T* ratio (from 1.0 to 0.86) in respect with the free 3HC-NCp7(11-55). This is likely the result of a stronger interaction of the 3HC probe with the peptide backbone when it is in the zinc-free form. Addition of SL3 to the zinc-depleted 3HC-NC(11-55) induced a further decrease of the fluorescence emission resulting in a spectrum similar to that obtained when WDO-217 was added to the preformed 3HC-NC(11-55)/SL3 complex (**Fig. 7B**). This result confirms that WDO-217 is able to eject zinc from the NC/ODN complex.

WDO-217 does not cause accumulation of unprocessed Gag polyprotein. When added to infected cells, several NCp7 zinc ejecting compounds, such as SRR-SB3 (Mahmood et al., 1998) and SAMTs (Miller Jenkins et al., 2010), have been demonstrated to inhibit HIV replication by preventing Gag precursor protein processing and causing accumulation of aggregated, unprocessed Gag polyprotein. Recently, it has been shown that this new mechanism involves acetylation of the NCp7 region of Gag, thereby blocking Gag processing (Miller Jenkins et al., 2010). We investigated whether WDO-217 was able to induce a

similar effect when added to virus-infected cells. For this experiment, HIV-1 III_B chronically-infected HuT-78 cells were treated with different WDO-217 concentrations. Analysis of the progeny virus in the supernatant demonstrated that treatment with WDO-217 did not result in a drastic accumulation of unprocessed Gag polyprotein (**Fig. 8**). In contrast, ritonavir (a protease inhibitor) and the zinc ejector SRR-SB3 did effectively increase the appearance of unprocessed Gag.

DISCUSSION

The retroviral zinc fingers of the HIV-1 NCp7 are highly conserved and functionally obligatory in the viral replication and virion stability. Early studies have demonstrated that disruption of the zinc fingers by removal of the zinc led to a loss of viral replication (Rice et al., 1993b). Different classes of zinc ejectors have been reported to efficiently eject zinc from the NCp7 zinc fingers. More specifically, the *N*-substituted *S*-acyl-2-mercaptobenzamides (SAMTs) are suggested as candidate pluripotent, HIV-specific, virucidal microbicides (Turpin et al., 2008). Such nucleocapsid inhibitors were directly virucidal by preventing the initiation of reverse transcription and modifying the CCHC amino acid domain conformation within Gag (Rice et al., 1997b; Schito et al., 2006). Here, we have identified 2-methyl-3-phenyl-2*H*-[1,2,4]thiadiazol-5-ylideneamine (WDO-217) as a very potent ejector of zinc ions from the HIV-1 NCp7 zinc fingers, inactivating HIV-1 and HIV-2 virions relieving the protection of the viral RNA by the retroviral nucleocapsid protein. The detailed mechanism by which the RNA is degraded is currently under study. Interestingly, WDO-217 is able to dissociate zinc ions from NCp7 even when it is bound to nucleic acids. In agreement with the strong affinity of the zinc-depleted NCp7 for oligonucleotides (Beltz et al., 2005; Urbaneja et al., 1999; Vuilleumier et al., 1999), ejection of zinc from NCp7 by WDO-217 does not dissociate the protein from the oligonucleotide, but likely changes its binding mode. Although its antiviral selectivity is somewhat moderate, WDO-217 represents the first lead compound among zinc-ejecting compounds with a unique mode of action. Future structure activity relationship studies and molecular modeling studies will likely enable improvement on activity and selectivity.

Interestingly, WDO-217 treatment does not inhibit the direct gp120-mediated capture

of virus on DC-SIGN suggesting that it is able to inactivate HIV but with a preservation of the conformational and functional integrity of the surface envelope proteins. This preservation of surface proteins has earlier been demonstrated with the prototypical NCp7 zinc ejector AT-2 (Rossio et al., 1998). Moreover, WDO-217 inactivates virus particles even when they are bound to DC-SIGN and prevents the transmission of DC-SIGN-captured HIV to $CD4^+$ cells. This makes WDO-217 suitable, not only as a valuable component in topical microbicides, but also for the inactivation of virions to be used as vaccine antigens (Rossio et al., 1998). Indeed, HIV vaccine strategies using DCs are currently being investigated. DCs detect viruses in peripheral tissues and, following activation and virus capture/uptake, migrate to lymph nodes to trigger adaptive immune responses (Altfeld et al., 2011). However, HIV is able to modulate these DCs to facilitate infection and transmission to T-cells causing their dysregulation (van der Vlist et al., 2011). This justifies the need to develop strategies that prevent this modulation and dysregulation. In this respect, WDO-217 appears of high interest, since it does not prevent the capture by DC SIGN but prevents subsequent transmission and infection.

In conclusion, a new lead compound that inactivates HIV-1 and HIV-2 strains by targeting the NCp7 zinc fingers has been discovered. It differs from other zinc ejectors like SAMTs or SRR-SB3 in that it does not prevent processing of the Gag precursor polyprotein. The novel mechanism of action of this new compound makes it useful as a lead for the design of a future new generation NCp7 inhibitors that could be applied as an agent in microbicide formulations and vaccine strategies.

ACKNOWLEDGEMENTS

We thank L. Bral, C. Heens, K. Erven and L. Ingels for excellent technical assistance; a number of reagents were obtained through the NIH AIDS Reagent Program.

Authorship Contributions

Participated in research design: Vercruysse, Basta, Pannecouque, Mély, Daelemans.

Conducted experiments: Vercruysse, Basta, Debaene, Sanglier-Cianféraini.

Contributed new reagents or analytic tools: Dehaen.

Performed data analysis: Vercruysse, Basta, Balzarini, Mély, Daelemans

Wrote or contributed to the writing of the manuscript: Daelemans and Mély

References

Altfeld M, Fadda L, Frleta D and Bhardwaj N (2011) DCs and NK cells: critical effectors in the immune response to HIV-1. *Nat Rev Immunol* **11**(3): 176-186.

Andrei G, Lisco A, Vanpouille C, Introini A, Balestra E, van den Oord J, Cihlar T, Perno CF, Snoeck R, Margolis L and Balzarini J (2011) Topical tenofovir, a microbicide effective against HIV, inhibits herpes simplex virus-2 replication. *Cell Host Microbe* **10**(4): 379-389.

Azoulay J, Clamme JP, Darlix JL, Roques BP and Mely Y (2003) Destabilization of the HIV-1 complementary sequence of TAR by the nucleocapsid protein through activation of conformational fluctuations. *J Mol Biol* **326**(3): 691-700.

Beltz H, Azoulay J, Bernacchi S, Clamme JP, Ficheux D, Roques B, Darlix JL and Mely Y (2003) Impact of the terminal bulges of HIV-1 cTAR DNA on its stability and the destabilizing activity of the nucleocapsid protein NCp7. *J Mol Biol* **328**(1): 95-108.

Beltz H, Clauss C, Piemont E, Ficheux D, Gorelick RJ, Roques B, Gabus C, Darlix JL, de Rocquigny H and Mely Y (2005) Structural determinants of HIV-1 nucleocapsid protein for cTAR DNA binding and destabilization, and correlation with inhibition of self-primed DNA synthesis. *J Mol Biol* **348**(5): 1113-1126.

Bernacchi S and Mely Y (2001) Exciton interaction in molecular beacons: a sensitive sensor for short range modifications of the nucleic acid structure. *Nucleic Acids Res* **29**(13): E62-62.

Bernacchi S, Stoylov S, Piemont E, Ficheux D, Roques BP, Darlix JL and Mely Y (2002) HIV-1 nucleocapsid protein activates transient melting of least stable parts of the secondary structure of TAR and its complementary sequence. *J Mol Biol* **317**(3): 385-399.

Bertaux C, Daelemans D, Meertens L, Cormier EG, Reinus JF, Peumans WJ, Van Damme EJ, Igarashi Y, Oki T, Schols D, Dragic T and Balzarini J (2007) Entry of hepatitis C virus and human immunodeficiency virus is selectively inhibited by carbohydrate-binding agents but not by polyanions. *Virology* **366**(1): 40-50.

Bombarda E, Grell E, Roques BP and Mely Y (2007) Molecular mechanism of the Zn2+-induced folding of the distal CCHC finger motif of the HIV-1 nucleocapsid protein. *Biophys J* **93**(1): 208-217.

Bourbigot S, Ramalanjaona N, Boudier C, Salgado GF, Roques BP, Mely Y, Bouaziz S and Morellet N (2008) How the HIV-1 nucleocapsid protein binds and destabilises the (-)primer binding site during reverse transcription. *J Mol Biol* **383**(5): 1112-1128.

Daelemans D, De Clercq E and Vandamme AM (2001) A quantitative GFP-based bioassay for the detection of HIV-1 Tat transactivation inhibitors. *J Virol Methods* **96**(2): 183-188.

Daelemans D, Pannecouque C, Pavlakis GN, Tabarrini O and De Clercq E (2005) A novel and efficient approach to discriminate between pre- and post-transcription HIV inhibitors. *Mol Pharmacol* **67**(5): 1574-1580.

Daelemans D, Pauwels R, De Clercq E and Pannecouque C (2011) A time-of-drug addition approach to target identification of antiviral compounds. *Nat Protoc* **6**(6): 925-933.

De Guzman RN, Wu ZR, Stalling CC, Pappalardo L, Borer PN and Summers MF (1998) Structure of the HIV-1 nucleocapsid protein bound to the SL3 psi-RNA recognition element. *Science* **279**(5349): 384-388.

Goebel FD, Hemmer R, Schmit JC, Bogner JR, de Clercq E, Witvrouw M, Pannecouque C, Valeyev R, Vandevelde M, Margery H and Tassignon JP (2001) Phase I/II dose escalation and randomized withdrawal study with add-on azodicarbonamide in patients failing on current antiretroviral therapy. *AIDS* **15**(1): 33-45.

Jenkins LM, Byrd JC, Hara T, Srivastava P, Mazur SJ, Stahl SJ, Inman JK, Appella E, Omichinski JG and Legault P (2005) Studies on the mechanism of inactivation of the HIV-1 nucleocapsid protein NCp7 with 2-mercaptobenzamide thioesters. *J Med Chem* **48**(8): 2847-2858.

Jordan A, Bisgrove D and Verdin E (2003) HIV reproducibly establishes a latent infection after acute infection of T cells in vitro. *EMBO J* **22**(8): 1868-1877.

Jordan A, Defechereux P and Verdin E (2001) The site of HIV-1 integration in the human genome determines basal transcriptional activity and response to Tat transactivation. *EMBO J* **20**(7): 1726-1738.

Krishnamoorthy G, Roques B, Darlix JL and Mely Y (2003) DNA condensation by the nucleocapsid protein of HIV-1: a mechanism ensuring DNA protection. *Nucleic Acids Res* **31**(18): 5425-5432.

Lapadat-Tapolsky M, De Rocquigny H, Van Gent D, Roques B, Plasterk R and Darlix JL (1993) Interactions between HIV-1 nucleocapsid protein and viral DNA may have important functions in the viral life cycle. *Nucleic Acids Res* **21**(4): 831-839.

Mahmood N, Jhaumeer-Lauloo S, Sampson J and Houghton PJ (1998) Anti-HIV activity and mechanism of action of macrocyclic diamide SRR-SB3. *J Pharm Pharmacol* **50**(12): 1339-1342.

Mayer KH, Peipert J, Fleming T, Fullem A, Moench T, Cu-Uvin S, Bentley M, Chesney M and Rosenberg Z (2001) Safety and tolerability of BufferGel, a novel vaginal microbicide, in women in the United States. *Clin Infect Dis* **32**(3): 476-482.

Mely Y, De Rocquigny H, Morellet N, Roques BP and Gerad D (1996) Zinc binding to the HIV-1 nucleocapsid protein: a thermodynamic investigation by fluorescence spectroscopy. *Biochemistry* **35**(16): 5175-5182.

Miller Jenkins LM, Ott DE, Hayashi R, Coren LV, Wang D, Xu Q, Schito ML, Inman JK, Appella DH and Appella E (2010) Small-molecule inactivation of HIV-1 NCp7 by repetitive intracellular acyl transfer. *Nat Chem Biol* **6**(12): 887-889.

Pannecouque C, Daelemans D and De Clercq E (2008) Tetrazolium-based colorimetric assay for the detection of HIV replication inhibitors: revisited 20 years later. *Nat Protoc* **3**(3): 427-434.

Pannecouque C, Szafarowicz B, Volkova N, Bakulev V, Dehaen W, Mely Y and Daelemans D (2010) Inhibition of HIV-1 replication by a bis-thiadiazolbenzene-1,2-diamine that chelates zinc ions from retroviral nucleocapsid zinc fingers. *Antimicrob Agents Chemother* **54**(4): 1461-1468.

Pauwels R, Balzarini J, Baba M, Snoeck R, Schols D, Herdewijn P, Desmyter J and De Clercq E (1988) Rapid and automated tetrazolium-based colorimetric assay for the detection of anti-HIV compounds. *J Virol Methods* **20**(4): 309-321.

Rice WG, Baker DC, Schaeffer CA, Graham L, Bu M, Terpening S, Clanton D, Schultz R, Bader JP, Buckheit RW, Jr., Field L, Singh PK and Turpin JA (1997a) Inhibition of multiple phases of human immunodeficiency virus type 1 replication by a dithiane compound that attacks the conserved zinc fingers of retroviral nucleocapsid proteins. *Antimicrob Agents Chemother* **41**(2): 419-426.

Rice WG, Schaeffer CA, Graham L, Bu M, McDougal JS, Orloff SL, Villinger F, Young M, Oroszlan S, Fesen MR and et al. (1993a) The site of antiviral action of 3-nitrosobenzamide on the infectivity process of human immunodeficiency virus in human lymphocytes. *Proc Natl Acad Sci U S A* **90**(20): 9721-9724.

Rice WG, Schaeffer CA, Harten B, Villinger F, South TL, Summers MF, Henderson LE, Bess JW, Jr., Arthur LO, McDougal JS and et al. (1993b) Inhibition of HIV-1 infectivity by zinc-ejecting aromatic C-nitroso compounds. *Nature* **361**(6411): 473-475.

Rice WG, Supko JG, Malspeis L, Buckheit RW, Jr., Clanton D, Bu M, Graham L, Schaeffer CA, Turpin JA, Domagala J, Gogliotti R, Bader JP, Halliday SM, Coren L, Sowder RC, 2nd, Arthur LO and Henderson LE (1995) Inhibitors of HIV nucleocapsid protein zinc fingers as candidates for the treatment of AIDS. *Science* **270**(5239): 1194-1197.

Rice WG, Turpin JA, Huang M, Clanton D, Buckheit RW, Jr., Covell DG, Wallqvist A, McDonnell NB, DeGuzman RN, Summers MF, Zalkow L, Bader JP, Haugwitz RD and Sausville EA (1997b) Azodicarbonamide inhibits HIV-1 replication by targeting the nucleocapsid protein. *Nat Med* **3**(3): 341-345.

Rossio JL, Esser MT, Suryanarayana K, Schneider DK, Bess JW, Jr., Vasquez GM, Wiltrout TA, Chertova E, Grimes MK, Sattentau Q, Arthur LO, Henderson LE and Lifson JD (1998) Inactivation of human immunodeficiency virus type 1 infectivity with preservation of conformational and functional integrity of virion surface proteins. *J Virol* **72**(10): 7992-8001.

Schito ML, Soloff AC, Slovitz D, Trichel A, Inman JK, Appella E, Turpin JA and Barratt-Boyes SM (2006) Preclinical evaluation of a zinc finger inhibitor targeting lentivirus nucleocapsid protein in SIV-infected monkeys. *Curr HIV Res* **4**(3): 379-386.

Shvadchak VV, Klymchenko AS, de Rocquigny H and Mely Y (2009) Sensing peptide-oligonucleotide interactions by a two-color fluorescence label: application to the HIV-1 nucleocapsid protein. *Nucleic Acids Res* **37**(3): e25.

Tanchou V, Gabus C, Rogemond V and Darlix JL (1995) Formation of stable and functional HIV-1 nucleoprotein complexes in vitro. *J Mol Biol* **252**(5): 563-571.

Thomas JA and Gorelick RJ (2008) Nucleocapsid protein function in early infection processes. *Virus Res* **134**(1-2): 39-63.

Turpin JA, Schito ML, Jenkins LM, Inman JK and Appella E (2008) Topical microbicides: a promising approach for controlling the AIDS pandemic via retroviral zinc finger inhibitors. *Adv Pharmacol* **56**: 229-256.

Turpin JA, Song Y, Inman JK, Huang M, Wallqvist A, Maynard A, Covell DG, Rice WG and Appella E (1999) Synthesis and biological properties of novel pyridinioalkanoyl thiolesters (PATE) as anti-HIV-1 agents that target the viral nucleocapsid protein zinc fingers. *J Med Chem* **42**(1): 67-86.

Urbaneja MA, Kane BP, Johnson DG, Gorelick RJ, Henderson LE and Casas-Finet JR (1999) Binding properties of the human immunodeficiency virus type 1 nucleocapsid protein p7 to a model RNA: elucidation of the structural determinants for function. *J Mol Biol* **287**(1): 59-75.

van der Vlist M, van der Aar AM, Gringhuis SI and Geijtenbeek TB (2011) Innate signaling in HIV-1 infection of dendritic cells. *Curr Opin HIV AIDS* **6**(5): 348-352.

Vercruysse T, Pardon E, Vanstreels E, Steyaert J and Daelemans D (2010) An intrabody based on a llama single-domain antibody targeting the N-terminal alpha-helical

multimerization domain of HIV-1 rev prevents viral production. *J Biol Chem* **285**(28): 21768-21780.

Vuilleumier C, Bombarda E, Morellet N, Gerard D, Roques BP and Mely Y (1999) Nucleic acid sequence discrimination by the HIV-1 nucleocapsid protein NCp7: a fluorescence study. *Biochemistry* **38**(51): 16816-16825.

Wallace GS, Cheng-Mayer C, Schito ML, Fletcher P, Miller Jenkins LM, Hayashi R, Neurath AR, Appella E and Shattock RJ (2009) Human immunodeficiency virus type 1 nucleocapsid inhibitors impede trans infection in cellular and explant models and protect nonhuman primates from infection. *J Virol* **83**(18): 9175-9182.

Witvrouw M, Balzarini J, Pannecouque C, Jhaumeer-Laulloo S, Este JA, Schols D, Cherepanov P, Schmit JC, Debyser Z, Vandamme AM, Desmyter J, Ramadas SR and de Clercq E (1997) SRR-SB3, a disulfide-containing macrolide that inhibits a late stage of the replicative cycle of human immunodeficiency virus. *Antimicrob Agents Chemother* **41**(2): 262-268.

Yarchoan R, Klecker RW, Weinhold KJ, Markham PD, Lyerly HK, Durack DT, Gelmann E, Lehrman SN, Blum RM, Barry DW and et al. (1986) Administration of 3'-azido-3'-deoxythymidine, an inhibitor of HTLV-III/LAV replication, to patients with AIDS or AIDS-related complex. *Lancet* **1**(8481): 575-580.

FOOTNOTES

The work was supported by grants from the KU Leuven (GOA 10/14 and PF 10/18) and the Agence Nationale de la Recherche sur le Sida (ANRS). BB is supported by an ANRS fellowship.

FIGURE LEGENDS

Fig. 1. Chemical structure of WDO-217. Molecular weight: 191.25

Fig. 2. Dose-dependent Inhibitory effect of WDO-217 on the replication of HIV-1 III_B, HIV-2 ROD, and SIV Mac251. MT-4 T-cells were infected with the respective viruses and incubated in the presence of compound. Protection against HIV-induced cytophatic effect was monitored 5 days after infection using the MTT-assay (Pannecouque et al., 2008). Cell viability in the presence of compound but in the absence of virus was measured in parallel. Results are presented as mean ± sem from at least 2 independent experiments each in triplicate.

Fig. 3. Effects of WDO-217 on virion-associated Gag p24 CA and genomic mRNA content of HIV-1 virus particles. Isolated HIV-1 particles were incubated with different concentrations of compounds and subsequently cleared from excess compound by multiple washing and centrifugation steps. The amount of virion-associated p24 was quantified by ELISA and the total virus-associated genomic RNA was quantified by RT-qPCR. Concentration of compound used is given between brackets. Results are mean ± st dev with n=3.

Fig. 4. Zinc ejection from the NCp7(11-55) zinc fingers by WDO-217. *A*, emission spectra of NCp7(11-55) (1 μM) recorded in the absence (disks) and the presence of 10 μM WDO-217 (star). As a reference, NCp7(11-55) was treated with 1 mM EDTA, a well known zinc chelatant (triangle). Preincubation time of WDO-217 with NCp7(11-55) was 1 hour. *B*,

time-dependent zinc ejection from NCp7(11-55). The emission spectra of NCp7(11-55) (1μM) were recorded in the absence (disks) and presence of WDO-217 (10 μM) at the different time points as indicated. *C*, kinetics of zinc ejection after addition of 10 μM WDO-217. The data points (stars) corresponded to the fluorescence intensity at the maximum emission wavelength from panel B. Solid line represents a double-exponential fit to the data. *D,* zinc ejection from NCp7(11-55) in the presence of an excess of zinc. Emission spectra of the NCp7(11-55) (1 μM) in the presence of an excess of 100 μM zinc (triangle). Then, 10 μM of WDO-217 was added and the spectrum was recorded after 30 min of incubation (square). The emission spectrum of NCp7(11-55) incubated with 1 mM EDTA (triangle) for one hour is given as a reference.

Fig. 5 Zinc ejection as monitored by mass spectrometry. Supramolecular mass spectrometry analysis on 20 μM NCp7(11-55) (A) in the absence of WDO-217 or after 30 min incubation at room temperature with either (B) 40μM WDO-217 or (C) 100 μM WDO-217 in 50 mM ammonium acetate, pH7.0. Under non-denaturing conditions (Vc = 20V, Psi = 6mbar), the mass measured for NCp7(11-55) alone is 5264.0 Da corresponding to the NC peptide complexed with two zinc ions. Five times molar excess of WDO-217 leads to approximately 80% zinc ejection.

Fig. 6. Inhibition of NCp7(11-55)-induced cTAR destabilization by WDO-217. *A*, emission spectra of Rh6G-cTAR-Dabcyl (0.1μM) recorded in the absence (circle) or in the presence of NCp7(11-55) (1 μM) (square). To determine the importance of the order of addition of the compounds, the emission spectra of Rh6G-cTAR-Dabcyl (0.1 μM) were recorded either after addition of NCp7(11-55) preincubated with 10 μM WD0-217 (open

triangle) or after preincubation with 10 μM WDO-217 and then, addition of 10 μM NCp7(11-55) (closed triangles). Excitation wavelength was 520 nm. *B*, Inhibition kinetics of NC-induced cTAR destabilization by WDO-217. Emission spectra of Rh6G-cTAR-Dabcyl (0.1μM) were recorded in the absence (circle) and in the presence of NCp7(11-55) (1μM) (square) and at different times after addition of WDO-217 (10 μM) as indicated. Excitation wavelength was 520 nm. *C*, correlation between the kinetics of Zn^{2+} ejection and inhibition of NC-induced cTAR destabilization by WDO-217 (10 μM). Inhibition of cTAR destabilization (triangle) correlates well with zinc ejection (star).

Fig. 7. Effect of WDO-217 on the interaction of NCp7(11-55) with SL3 or PBS. A, effect of WDO-217 on the emission spectra of 3HC-NC(11-55) complexed with ΔP(-)PBS. Emission spectra of 3HC-NC (0.2μM) in the absence (square) and in the presence of ΔP(-)PBS (0.2 μM)(disk). For monitoring the effect of 10 μM WDO-217, the spectra were recorded immediately after its addition to the complex (triangle) and after 30 minutes (star). B, effect of WDO-217 on the emission spectra of 3HC-NCp7(11-55) complexed with SL3 RNA. Conditions and symbols are as in A. C, importance of the order of addition of the reactants on the emission spectra of 3HC-NCp7(11-55) complexed with SL3. The emission spectra of 3HC-NC(11-55) (0.2μM) in the absence (square) and in the presence of WDO-217 (10 μM) (circle). SL3 (0.2 μM) was added to 3HC-NCp7(11-55) (0.2μM) pre-incubated with WDO-217 (10 μM) for 30 min (triangle). Spectra were recorded in 10 mM phosphate buffer, 100 mM NaCl, pH 7.0. Excitation wavelength was 340 nm.

Fig. 8. WDO-217 does not cause accumulation of unprocessed Gag polyprotein. HIV-1 III_B virions from persistently infected HuT-78 cells treated with different concentrations of

compound were analysed by gel electrophoresis and immunoblotting with antibody against capsid. 1: untreated; 2: AZT (3.7 μM); 3: ritonavir (2.7 μM); 4: WDO-217 (50 μM); 5: WDO-217 (26 μM); 6: SRR-SB3 (75 μM); 7: SRR-SB3 (15 μM).

Table 1

Antiretroviral activity and cytotoxicity of WDO-217 in the MT-4/MTT-assay

Compound	EC_{50} (μM)			CC_{50} (μM)
	HIV-1 III_B	HIV-2 ROD	SIV Mac251	
WDO-217	7.9 ± 3.3	2.3 ± 0.3	5.3 ± 1.5	72 ± 11

Values are presented as mean ± std dev from at least 3 independent experiments
EC_{50}: 50% effective concentration, concentration of inhibitor required for 50% inhibition of viral replication
CC_{50}: 50% cytotoxic concentration, concentration of inhibitor that kills 50% of the cells

Table 2

Anti-HIV-1 and -HIV-2 activity and cytostatic properties of WDO-217 in human T-lymphocyte (CEM) cells

	EC_{50} (μM)		CC_{50} (μM)
Compound	HIV-1 III_B	HIV-2 ROD	
WDO-217	8.3 ± 1.8	15 ± 6.7	94 ± 15

EC_{50}: effective concentration or concentration required to protect CEM cells against the cytopathogenicity of HIV by 50 %
CC_{50}: cytotoxic concentration or concentration compound required to reduce CEM cell proliferation by 50 %
Values are the mean ± std dev of about 2 to 3 independent experiments.

Table 3
Antiretroviral activity and cytotoxicity of WDO-217 in the anti-HIV.GFP-assay in Jurkat cells

Compound	EC_{50} µM							CC_{50} µM
	HIV-1 III_B	NL4.3/WT	NL4.3/DS5000^R (165)	NL4.3/AMD3100^R (>100)	AZT^R (>30)	NNRTI$^R_{K103N:Y181C}$ (>85)	HIV-2 ROD	
WDO-217	1.04 ± 0.2	0.9 ± 0.05	1.2 ± 0.1	1.7 ± 0.9	1.5 ± 0.6	1.3 ± 0.4	1.04 ± 0.3	75 ± 11

Values are presented as mean ± std dev from at least 3 independent experiments. Fold resistance of mutant strains towards the respective inhibitor of resistant strains is given in parenthesis (EC_{50} for NL4.3 wild-type as 1)
EC_{50}: 50% effective concentration, concentration of inhibitor required for 50% inhibition of viral replication
CC_{50}: 50% cytotoxic concentration, concentration of inhibitor that kills 50% of the cells

Table 4

Inactivation of isolated HIV particles by WDO-217

Compound	$CCID_{50}$/ml	
	HIV-1 III_B	HIV-2 ROD
No drug	1×10^6	5.4×10^6
AZT (3.7 μM)	1×10^6	5.4×10^6
Triton X-100 (0.5%)	0	0
WDO-217 (0.2 μM)	5.4×10^6	1.6×10^6
WDO-217 (1 μM)	1.6×10^6	1×10^6
WDO-217 (5 μM)	1×10^6	2.1×10^6
WDO-217 (26 μM)	0	0
WDO-217 (130 μM)	0	0
WDO-217 (650 μM)	0	0

$CCID_{50}$: 50% cell culture infectious dose as determined by the Reed and Muench method

Table 5

Inhibition of HIV-1 NL4.3 capture and transmission* by Raji/DC-SIGN cells, quantified by p24-ELISA

	IC_{50} (μM)		
Compound	HIV-capture Procedure A	Transmission Procedure B	Transmission Procedure C
WDO-217	>105	2.2 ± 1	8.3 ± 0.4
HHA	0.014 ± 0.01	0.002 ± 0.001	≤0.003

*In cocultivation with C8166 cells; samples examined after 42 hours of incubation

Procedure A: HIV was pretreated (1h) with compound before it was added to Raji/DC-SIGN cells. Capture was measured by p24 analysis of the washed cell pellet

Procedure B: Raji/DC-SIGN cells were exposed to compound-pretreated (1h) HIV after which compound was removed and the cells were cocultured in the presence of C8166 cells. The read-out of this experiment was the replication capacity of virus in C8166 as monitored by p24 analysis

Procedure C: HIV-captured Raji/DC-SIGN cells were cocultivated with C8166 cells in the presence of compound (microscopic measurement of giant cell formation)

Zinc ejection from HIV-1 nucleocapsid affects virion associated genomic RNA stability

In our previous study, we showed the ability of WDO 217 to disrupt NC zinc fingers and decrease the level of viral genomic RNA.

In the present work, we investigated the mechanism of action and antiviral efficiency of WDO-217 in comparison with well-known zinc ejectors targeting the NC zinc fingers e.g. SAMT-89, SAMT-247, Aldrithiol (AT-2) and macrocyclic disulfide (SRR-SB3).

Treatment of isolated HIV-1_{IIIB} particles with these compounds abrogated the virus infectivity, making virus unable to replicate in MT-4 cells. In addition, real-time RT-qPCR quantification of viral RNA level showed that WDO-217 as well as AT-2 and SRR-SB3 led to almost complete depletion of viral genomic RNA while SAMT-89 and SAMT-247 reduce the RNA level by only 50%, as compared with non treated virions.

Since the observed differences between compounds on the level of viral genomic RNA might be related to their ability to eject zinc from NC complexed to viral RNA, we compared their effect on NC when it is bound with nucleic acids.

Zinc ejection was confirmed by the inability of NC in the presence of WDO-217 and other tested compounds to destabilize the secondary structure of cTAR, the complementary sequence of the transactivation response element. Thus, comparison between compounds gave the following order of efficiency: WDO-217>AT-2, SRR-RB3>SAMT-89>SAMT-247.

The observed increased accessibility of viral RNA to degradation is likely a consequence of the different binding modes to nucleic acid of the zinc-bound and zinc-depleted NC forms.

The zinc bound form of NC was reported to bind with either DNA or RNA by two alternative binding modes. In the first mode characterized with DNA oligonucleotides (Morellet 1998), the C-terminal zinc finger interacts with a guanine residue whereas the N-terminal zinc finger interacts with the residue (C or T) immediately upstream to the guanine residue. In the second mode reported for the three NC:RNA complexes (De Guzman 1998; Amarasinghe 2000), both zinc fingers interact (through both hydrogen bonding and stacking interactions) with two guanine residues separated by a third residue, i.e. the recognized sequence is GNG.

On the other hand, the zinc-depleted forms of NCp7 were reported to have limited ability to restrict the ODN flexibility, in line with a binding of the unfolded peptide mainly to the phosphate backbones. This binding is likely mediated mainly through electrostatic interactions that compensate for the loss of hydrophobic interactions with the bases.

The loss of proper folding of the NC finger domain together with increased RNA degradation observed after treatment with WDO-217, provides also further explanation for earlier studies where HIV-1 virions treated with zinc ejectors arrested replication. Based on its ability to

efficiently inactivate virions, WDO-217 may be a lead compound for a new class of microbicides.

Moreover, in line with previous observations showing that virions stopped their replication when treated with zinc ejectors, our study is the first direct visualization of viral RNA degradation inside virus particles treated with anti-NC compounds.

Zinc ejection from HIV-1 nucleocapsid affects virion-associated genomic RNA stability

Thomas Vercruysse[1], Nicolas Humbert[2], Beata Basta[2], Wim Dehaen[3], Lisa M Miller Jenkins[4], Christophe Pannecouque[1], Yves Mély[2#], and Dirk Daelemans[1#]

[1]Rega Institute for Medical Research, KU Leuven, Minderbroedersstraat 10, B-3000 Leuven, Belgium, [2]Laboratoire de Biophotonique et Pharmacologie, UMR 7213 du CNRS, Université de Strasbourg, Faculté de Pharmacie, 74 route du Rhin, 67401, Illkirch, France, [3]Chemistry Department, KU Leuven, Celestijnenlaan 200F, 3001 Leuven, Belgium, [4]Laboratory of Cell Biology, National Cancer Institute, National Institutes of Health, Bethesda, Maryland, USA

Running title: NCp7 zinc ejectors decrease viral RNA stability

[#]co-last authors; address correspondence to: Dirk Daelemans, phone.: ++32-16-332164, Fax: ++32-16-332131, E-mail: dirk.daelemans@rega.kuleuven.be or Yves Mély phone: ++ 33-368854263; fax: ++ 33-368854312, E-mail: yves.mely@unistra.fr

The retroviral nucleocapsid (NCp7) protein of HIV-1 is a structural protein that contains two highly conserved zinc-finger motifs. Here we provide the first experimental evidence that targeting the NCp7 by zinc ejectors decreases viral genomic RNA stability inside the virus particle. In addition to the known direct effect of zinc ejectors on NCp7, this new mechanism explains the inactivation of virions and provides additional rationale for the development of NCp7 inhibitors as candidate microbicide component.

The retroviral nucleocapsid protein of HIV-1 (NCp7) is characterized by two strictly conserved zinc finger CCHC motifs that bind Zn^{2+} with high affinity (16) and are critical for function and virion stability (7). NCp7 plays multiple roles in virus replication (26) and its function depends on its specific interactions with nucleic acids. NCp7 interacts notably with the psi sequence of the viral genomic RNA to promote selective encapsidation into viral particles; and also is important for efficient proviral DNA synthesis. Inside the infectious virus particle, NCp7 molecules coat and condense the genomic RNA (14, 15, 25).

Early studies have demonstrated that disruption of the zinc fingers by removal of the zinc led to a loss of viral replication (20). A number of classes of compounds targeting the retroviral NCp7 have been described, including, 3-nitrosobenzamide (NOBA) (20), 2,2'-dithiobisbenzamides (DIBA) (21), cyclic 2,2'-dithiobisbenzamides (e.g. SRR-SB3) (30), 1,2-dithiane-4,5-diol-1,1-dioxide (22), azadicarbonamide (ADA) (12, 22), pyridinioalkanoyl thiolesters (PATEs) (28), bis-thiadiazolbenzene-1,2-diamines (19) and *N*-substituted *S*-acyl-2-mercaptobenzamide thioesters (SAMTs) that were presented as

56 candidate, HIV-specific, virucidal microbicides (13, 17, 27). These nucleocapsid inhibitor
57 compounds eject or chelate the zinc from the CCHC domains within Gag resulting in
58 unfolding of the NCp7 structure, inactivation of virus particles and inhibition of the viral
59 replication (9, 22-24). In addition to this direct effect on NCp7 structure, we now
60 demonstrate that treatment of virus particles with zinc ejectors also decreases the viral
61 genomic RNA content.

62 As NCp7 wraps the genomic viral RNA inside the HIV particle, we investigated
63 whether ejecting zinc from NCp7 would affect genomic RNA stability inside HIV virions.
64 Therefore, we analyzed the effect of NCp7 zinc ejectors on the viral genomic RNA
65 content of isolated HIV-1_{IIIB} particles. For these experiments, we used the prototypical
66 NC zinc finger-targeting compound aldrithiol-2 (AT-2), the well-characterized SAMTs
67 (13), the macrocyclic disulfide SRR-SB3 (30) and a new highly-efficient zinc-ejecting
68 compound 2-methyl-3-phenyl-2H-[1,2,4]thiadiazol-5-ylideneamine (WDO-217) (Fig. 1)
69 that was identified as a hit (IC_{50}: 4.9 ± 3.3 μM; CC_{50}: 72 ± 10 μM) in an anti-HIV high-
70 throughput screen (18). Treatment of isolated HIV-1 particles with these zinc ejectors
71 abrogated the infectivity (as measured by $CCID_{50}$ determination) of the virus, as shown
72 by the inability of the virus to replicate in highly susceptible MT-4 cells (Fig. 2). When
73 virions were treated with the zinc ejectors and viral genomic RNA was subsequently
74 quantified by real-time RT-qPCR (29), we observed a clear reduction of virus-associated
75 genomic RNA (Fig. 3A). Treatment with 200 μM AT-2, 375 μM SRR-SB3, and 125 μM
76 WDO-217 caused a nearly complete depletion of viral genomic RNA while treatment
77 with the SAMT-89 or SAMT-247 only produced a 50% reduction at a concentration of
78 300 μM and 470 μM, respectively; while the compound preparations did not have a direct

79 effect on yet isolated RNA (Supplemental Figure S1). This result was corroborated by
80 northern blot analysis (Fig. 3B). We hypothesized that the difference between the effects
81 of the various compounds might be related to their power to eject zinc from NCp7 when it
82 is complexed to the viral genomic RNA inside the virus particle.

83 Therefore, we compared the effect of the compounds on NCp7 alone or when it is
84 bound to nucleic acid. Zinc ejection from NCp7 alone was monitored through the intrinsic
85 fluorescence of the Trp37 residue of NC(11-55) (16). Addition of the zinc ejecting
86 compounds to NC(11-55) alone at a molar ratio of 10:1 resulted in a decrease in Trp37
87 fluorescence but we observed a clear difference in the ability of the compounds to eject
88 zinc from NCp7 (Fig. 4A and C). After 1 hour of incubation of 1 μM NC(11-55) with 10
89 μM of compound, SAMT-247 was the least efficient compound while WDO-217 was the
90 most potent one [SAMT-247 (20 %) < SAMT-89 (30 %) < SRR-SB3 (70 %) < AT-2 (80
91 %) < WDO-217 (100 %)]. These results also show that the new compound WDO-217 is
92 very efficient zinc ejector as compared to the yet known zinc ejectors.

93 Next, we investigated the effect of the zinc ejectors on NCp7 in complex with
94 nucleic acids by monitoring the NCp7-induced destabilization of the secondary structure
95 of cTAR (3, 6, 10). Indeed, this destabilization is exquisitely sensitive to the proper
96 folding of the zinc-bound finger motifs and totally disappears when zinc ions are removed
97 (5). The NCp-7-induced destabilization of cTAR can be sensitively monitored by using a
98 doubly labeled Rh6G-5'-cTAR-3'-Dabcyl derivative (6). Addition of the zinc ejectors to
99 the NC(11-55)/cTAR complex at a molar ratio of 10:1 led to a decrease in Rh6G emission
100 as a result of zinc ejection from NCp7 (Fig. 4B and D). After 1h incubation, the inhibitory
101 effect of the various zinc ejectors on the NC-induced destabilization of cTAR varied in

102 the following order: WDO-217 > AT-2, SRR-SB3 > SAMT-89 > SAMT-247, showing
103 that again WDO-217 was the most potent compound. Interestingly, at a given time, the
104 percentages of inhibition of cTAR destabilization by these compounds are lower than the
105 percentages of zinc ejection (Fig. 4 C and D). This is especially the case for the two
106 SAMT compounds that inhibit the NC-induced destabilization of cTAR by only 7-18%
107 after 300 minutes of incubation, suggesting that these two compounds can hardly access
108 NCp7 when it is complexed to oligonucleotides (13). In contrast, the NC-induced
109 destabilization of cTAR was fully inhibited after 120 and 180 minutes for WDO-217 and
110 AT-2, respectively, indicating that these compounds efficiently eject zinc from NCp7
111 even when it is bound to nucleic acids. These results correlate well with the superior
112 reduction in genomic RNA content caused by AT-2 and WDO-217 as compared to
113 SAMT-89 and SAMT-247 (Fig. 3) and suggest that unfolding the NCp7 structure when
114 bound to genomic RNA makes it accessible to degradation. This increased accessibility is
115 likely a consequence of the different binding modes of the zinc-bound and zinc-depleted
116 NCp7 forms to nucleic acids. Whereas the zinc-bound fingers of NCp7 were reported to
117 mainly interact with the RNA or DNA bases through their hydrophobic amino acids (1, 4,
118 8), the zinc-depleted NCp7 form is thought to interact mainly with the RNA of DNA
119 backbone through electrostatic interactions (2, 11). Our results also explain the
120 observations from earlier studies that virions treated with zinc ejectors arrest replication at
121 a stage before the initiation of reverse transcription (23).

122 The results presented here are the first direct visualization of viral genomic RNA
123 degradation inside isolated virus particles when treated with anti-NCP7 compounds. This
124 new mechanism provides further motivation for the design of future generation NCp7

inhibitors that could be applied in microbicide formulations.

We thank L Bral, C Heens and Maarten Jacquemyn for excellent technical assistance. Thomas Vercruysse acknowledges a grant from the “Instituut voor de Aanmoediging van Innovatie door Wetenschap en Technologie (IWT)”; Beata Basta acknowledges a grant from the French agency against AIDS (ANRS). This work was supported by grants from the “Fonds voor Weteschappelijk Onderzoek-Vlaanderen (FWO)” numbers 1.5.104.07 and 1.5.165.10 ”, the KU Leuven (GOA No. 10/14) and the French agency against AIDS (ANRS).

148

FIGURE LEGENDS

Fig. 1. Chemical structure and anti-HIV-1 activity in μM of the zinc ejectors used. NA: not active at subtoxic concentration.

Fig. 2. Reduction in infectivity of isolated HIV particles by zinc ejectors. Virions were treated with compound for 1h at 37°C. Then, virus was diluted 4000-times so that the remaining compound concentration dropped well below its antiviral active concentration. Infectivity ($CCID_{50}$) of the treated and diluted virus stock was determined by titration on MT-4 cells and monitoring the replication-induced cytopathogenic effect.

Fig. 3. Zinc ejectors decrease the virion-associated genomic mRNA content in HIV-1 virus particles. Isolated HIV-1 particles were incubated with different concentrations of compounds and the amount of virus-associated genomic RNA was (A) quantified by real-time RT-qPCR or (B) visualized by northern blot, 1: virus control, 2: Triton X-100 (0.5%), 3: WDO-217 (125 μM), 4: SAMT-89 (300 μM), 5: SAMT-247 (470 μM), 6: AT-2 (200 μM), 7: SRR-SB3 (375 μM).

Fig. 4. The ability of the zinc ejectors to decrease the virion-associated genomic mRNA content in HIV-1 virus particles is correlated with their property to eject zinc from NCp7 when complexed to oligonucleotides. (A) Ejection of the zinc ions bound to NC(11-55) by SAMT-89 (closed square), SAMT-247 (closed triangle), SRR-SB3 (closed disk), AT-2 (star), or WDO-217 (closed diamond). The emission spectrum of 1 μM

NC(11-55) was recorded either in the absence (open square) or in the presence of 10 μM zinc ejectors after 1 h of incubation. Open triangle, emission spectrum of NC(11-55) after 1h incubation with 1 mM EDTA. (B) Inhibition of NC(11-55)-induced cTAR destabilization. The emission spectrum of 0.1 μM Rh6G-5'-cTAR-3'-Dabcyl was recorded either in the absence (open triangle) or in the presence of 1 μM NC(11-55) before (open square) and after 1h incubation with 10 μM of zinc ejectors. Symbols are as in (A). (C) Time-dependence of zinc ejection and (D) of inhibition of cTAR destabilization by the various compounds. The percentages of zinc ejection and inhibition of cTAR destabilization induced by 10 μM of the inhibitors (symbols are as in (A)) are reported as a function of time. Solid lines represent double-exponential fits to the data.

REFERENCES

1. **Amarasinghe, G. K., R. N. De Guzman, R. B. Turner, K. J. Chancellor, Z. R. Wu, and M. F. Summers.** 2000. NMR structure of the HIV-1 nucleocapsid protein bound to stem-loop SL2 of the psi-RNA packaging signal. Implications for genome recognition. J Mol Biol **301:**491-511.
2. **Avilov, S. V., E. Piemont, V. Shvadchak, H. de Rocquigny, and Y. Mely.** 2008. Probing dynamics of HIV-1 nucleocapsid protein/target hexanucleotide complexes by 2-aminopurine. Nucleic Acids Res **36:**885-96.
3. **Azoulay, J., J. P. Clamme, J. L. Darlix, B. P. Roques, and Y. Mely.** 2003. Destabilization of the HIV-1 complementary sequence of TAR by the nucleocapsid protein through activation of conformational fluctuations. J Mol Biol **326:**691-700.
4. **Bazzi, A., L. Zargarian, F. Chaminade, C. Boudier, H. De Rocquigny, B. Rene, Y. Mely, P. Fosse, and O. Mauffret.** 2011. Structural insights into the cTAR DNA recognition by the HIV-1 nucleocapsid protein: role of sugar deoxyriboses in the binding polarity of NC. Nucleic Acids Res **39:**3903-16.
5. **Beltz, H., C. Clauss, E. Piemont, D. Ficheux, R. J. Gorelick, B. Roques, C. Gabus, J. L. Darlix, H. de Rocquigny, and Y. Mely.** 2005. Structural determinants of HIV-1 nucleocapsid protein for cTAR DNA binding and destabilization, and correlation with inhibition of self-primed DNA synthesis. J Mol Biol **348:**1113-26.
6. **Bernacchi, S., S. Stoylov, E. Piemont, D. Ficheux, B. P. Roques, J. L. Darlix, and Y. Mely.** 2002. HIV-1 nucleocapsid protein activates transient melting of least stable parts of the secondary structure of TAR and its complementary sequence. J Mol Biol **317:**385-99.
7. **Darlix, J. L., J. Godet, R. Ivanyi-Nagy, P. Fosse, O. Mauffret, and Y. Mely.** 2011. Flexible Nature and Specific Functions of the HIV-1 Nucleocapsid Protein. J Mol Biol **410:**565-81.
8. **De Guzman, R. N., Z. R. Wu, C. C. Stalling, L. Pappalardo, P. N. Borer, and M. F. Summers.** 1998. Structure of the HIV-1 nucleocapsid protein bound to the SL3 psi-RNA recognition element. Science **279:**384-8.
9. **de Rocquigny, H., V. Shvadchak, S. Avilov, C. Z. Dong, U. Dietrich, J. L. Darlix, and Y. Mely.** 2008. Targeting the viral nucleocapsid protein in anti-HIV-1 therapy. Mini Rev Med Chem **8:**24-35.
10. **Godet, J., and Y. Mely.** 2010. Biophysical studies of the nucleic acid chaperone properties of the HIV-1 nucleocapsid protein. RNA Biol **7:**687-99.
11. **Godet, J., N. Ramalanjaona, K. K. Sharma, L. Richert, H. de Rocquigny, J. L. Darlix, G. Duportail, and Y. Mely.** 2011. Specific implications of the HIV-1 nucleocapsid zinc fingers in the annealing of the primer binding site complementary sequences during the obligatory plus strand transfer. Nucleic Acids Res **39:**6633-45.
12. **Goebel, F. D., R. Hemmer, J. C. Schmit, J. R. Bogner, E. de Clercq, M. Witvrouw, C. Pannecouque, R. Valeyev, M. Vandevelde, H. Margery, and J. P. Tassignon.** 2001. Phase I/II dose escalation and randomized withdrawal study

with add-on azodicarbonamide in patients failing on current antiretroviral therapy. AIDS **15:**33-45.

13. **Jenkins, L. M., J. C. Byrd, T. Hara, P. Srivastava, S. J. Mazur, S. J. Stahl, J. K. Inman, E. Appella, J. G. Omichinski, and P. Legault.** 2005. Studies on the mechanism of inactivation of the HIV-1 nucleocapsid protein NCp7 with 2-mercaptobenzamide thioesters. J Med Chem **48:**2847-58.
14. **Krishnamoorthy, G., B. Roques, J. L. Darlix, and Y. Mely.** 2003. DNA condensation by the nucleocapsid protein of HIV-1: a mechanism ensuring DNA protection. Nucleic Acids Res **31:**5425-32.
15. **Lapadat-Tapolsky, M., H. De Rocquigny, D. Van Gent, B. Roques, R. Plasterk, and J. L. Darlix.** 1993. Interactions between HIV-1 nucleocapsid protein and viral DNA may have important functions in the viral life cycle. Nucleic Acids Res **21:**831-9.
16. **Mely, Y., H. De Rocquigny, N. Morellet, B. P. Roques, and D. Gerad.** 1996. Zinc binding to the HIV-1 nucleocapsid protein: a thermodynamic investigation by fluorescence spectroscopy. Biochemistry **35:**5175-82.
17. **Miller Jenkins, L. M., D. E. Ott, R. Hayashi, L. V. Coren, D. Wang, Q. Xu, M. L. Schito, J. K. Inman, D. H. Appella, and E. Appella.** 2010. Small-molecule inactivation of HIV-1 NCp7 by repetitive intracellular acyl transfer. Nat Chem Biol **6:**887-9.
18. **Pannecouque, C., D. Daelemans, and E. De Clercq.** 2008. Tetrazolium-based colorimetric assay for the detection of HIV replication inhibitors: revisited 20 years later. Nat Protoc **3:**427-34.
19. **Pannecouque, C., B. Szafarowicz, N. Volkova, V. Bakulev, W. Dehaen, Y. Mely, and D. Daelemans.** 2010. Inhibition of HIV-1 replication by a bis-thiadiazolbenzene-1,2-diamine that chelates zinc ions from retroviral nucleocapsid zinc fingers. Antimicrob Agents Chemother **54:**1461-8.
20. **Rice, W. G., C. A. Schaeffer, B. Harten, F. Villinger, T. L. South, M. F. Summers, L. E. Henderson, J. W. Bess, Jr., L. O. Arthur, J. S. McDougal, and et al.** 1993. Inhibition of HIV-1 infectivity by zinc-ejecting aromatic C-nitroso compounds. Nature **361:**473-5.
21. **Rice, W. G., J. G. Supko, L. Malspeis, R. W. Buckheit, Jr., D. Clanton, M. Bu, L. Graham, C. A. Schaeffer, J. A. Turpin, J. Domagala, R. Gogliotti, J. P. Bader, S. M. Halliday, L. Coren, R. C. Sowder, 2nd, L. O. Arthur, and L. E. Henderson.** 1995. Inhibitors of HIV nucleocapsid protein zinc fingers as candidates for the treatment of AIDS. Science **270:**1194-7.
22. **Rice, W. G., J. A. Turpin, M. Huang, D. Clanton, R. W. Buckheit, Jr., D. G. Covell, A. Wallqvist, N. B. McDonnell, R. N. DeGuzman, M. F. Summers, L. Zalkow, J. P. Bader, R. D. Haugwitz, and E. A. Sausville.** 1997. Azodicarbonamide inhibits HIV-1 replication by targeting the nucleocapsid protein. Nat Med **3:**341-5.
23. **Rossio, J. L., M. T. Esser, K. Suryanarayana, D. K. Schneider, J. W. Bess, Jr., G. M. Vasquez, T. A. Wiltrout, E. Chertova, M. K. Grimes, Q. Sattentau, L. O. Arthur, L. E. Henderson, and J. D. Lifson.** 1998. Inactivation of human immunodeficiency virus type 1 infectivity with preservation of conformational and functional integrity of virion surface proteins. J Virol **72:**7992-8001.

24. **Schito, M. L., A. C. Soloff, D. Slovitz, A. Trichel, J. K. Inman, E. Appella, J. A. Turpin, and S. M. Barratt-Boyes.** 2006. Preclinical evaluation of a zinc finger inhibitor targeting lentivirus nucleocapsid protein in SIV-infected monkeys. Curr HIV Res **4:**379-86.
25. **Tanchou, V., C. Gabus, V. Rogemond, and J. L. Darlix.** 1995. Formation of stable and functional HIV-1 nucleoprotein complexes in vitro. J Mol Biol **252:**563-71.
26. **Thomas, J. A., and R. J. Gorelick.** 2008. Nucleocapsid protein function in early infection processes. Virus Res **134:**39-63.
27. **Turpin, J. A., M. L. Schito, L. M. Jenkins, J. K. Inman, and E. Appella.** 2008. Topical microbicides: a promising approach for controlling the AIDS pandemic via retroviral zinc finger inhibitors. Adv Pharmacol **56:**229-56.
28. **Turpin, J. A., Y. Song, J. K. Inman, M. Huang, A. Wallqvist, A. Maynard, D. G. Covell, W. G. Rice, and E. Appella.** 1999. Synthesis and biological properties of novel pyridinioalkanoyl thiolesters (PATE) as anti-HIV-1 agents that target the viral nucleocapsid protein zinc fingers. J Med Chem **42:**67-86.
29. **Vercruysse, T., E. Pardon, E. Vanstreels, J. Steyaert, and D. Daelemans.** 2010. An intrabody based on a llama single-domain antibody targeting the N-terminal alpha-helical multimerization domain of HIV-1 rev prevents viral production. J Biol Chem **285:**21768-80.
30. **Witvrouw, M., J. Balzarini, C. Pannecouque, S. Jhaumeer-Laulloo, J. A. Este, D. Schols, P. Cherepanov, J. C. Schmit, Z. Debyser, A. M. Vandamme, J. Desmyter, S. R. Ramadas, and E. de Clercq.** 1997. SRR-SB3, a disulfide-containing macrolide that inhibits a late stage of the replicative cycle of human immunodeficiency virus. Antimicrob Agents Chemother **41:**262-8.

Figure 1

Aldrithiol-2	IC_{50}: NA CC_{50}: 17	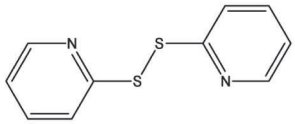
SAMT-89	IC_{50}: 5.5 ± 0.6 CC_{50}: 170 ± 15	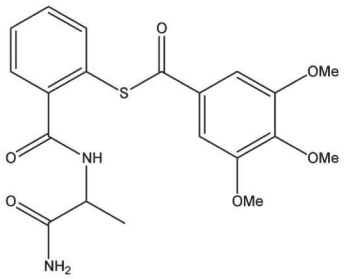
SAMT-247	IC_{50}: 8 ± 1.5 CC_{50}: 210 ± 10	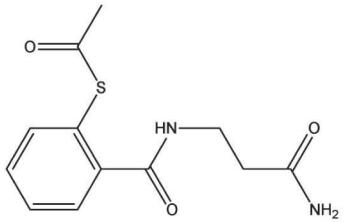
WDO-217	IC_{50}: 4.9 ± 3.3 CC_{50}: 72 ± 10	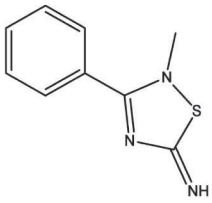
SRR-SB3	IC_{50}: 6.7 ± 4.7 CC_{50}: 42 ± 25	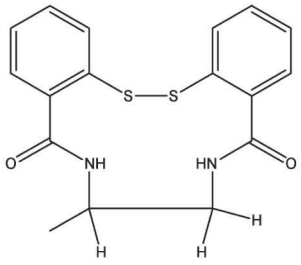

Figure 2

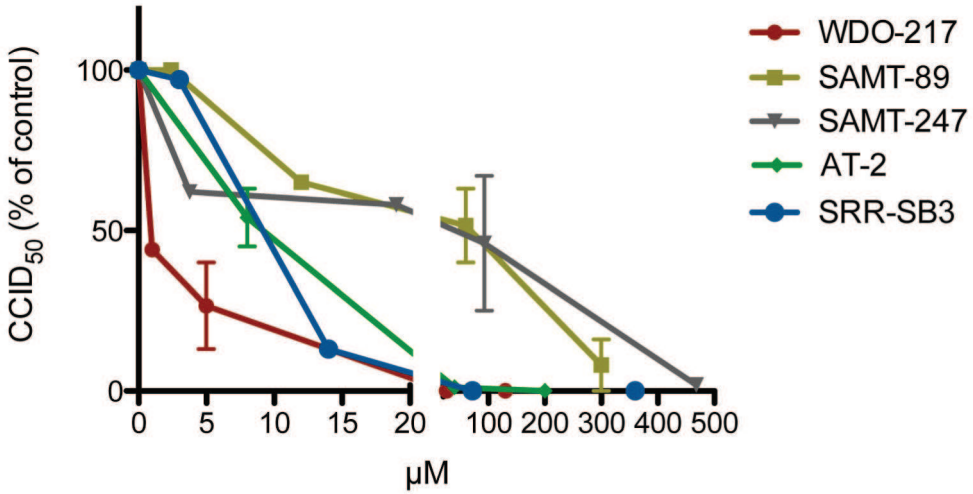
CCID50 (% of control)
100
50
0
0
5
10
15
20
100
200
300
400
500
μM
WDO-217
SAMT-89
SAMT-247
AT-2
SRR-SB3

Figure 3A

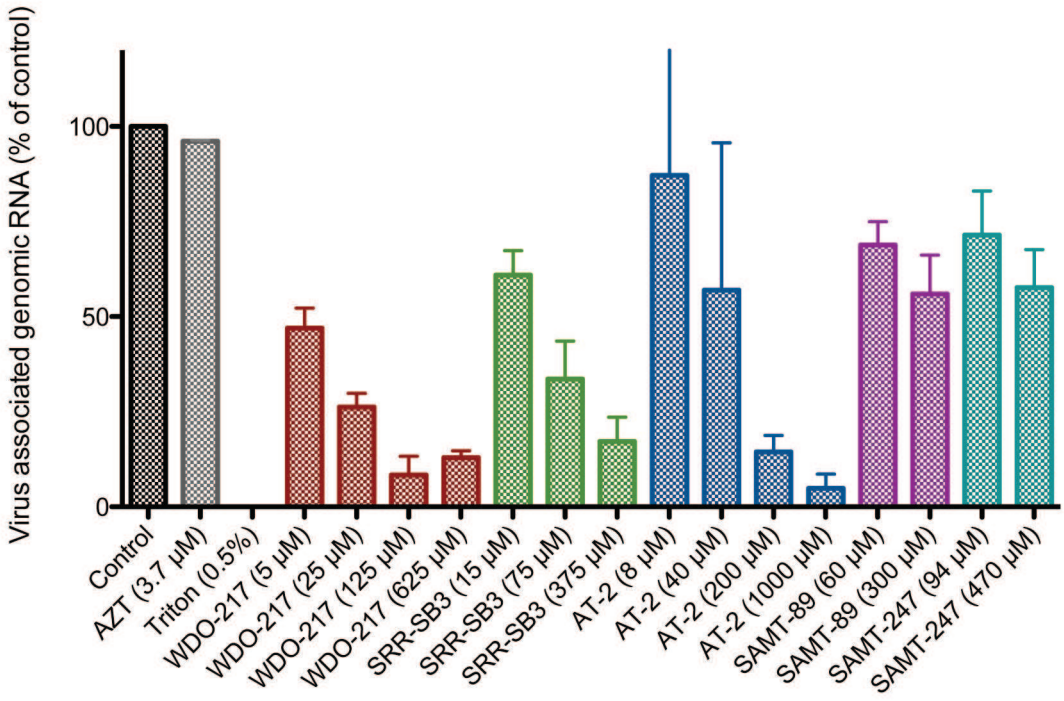

Figure 3B

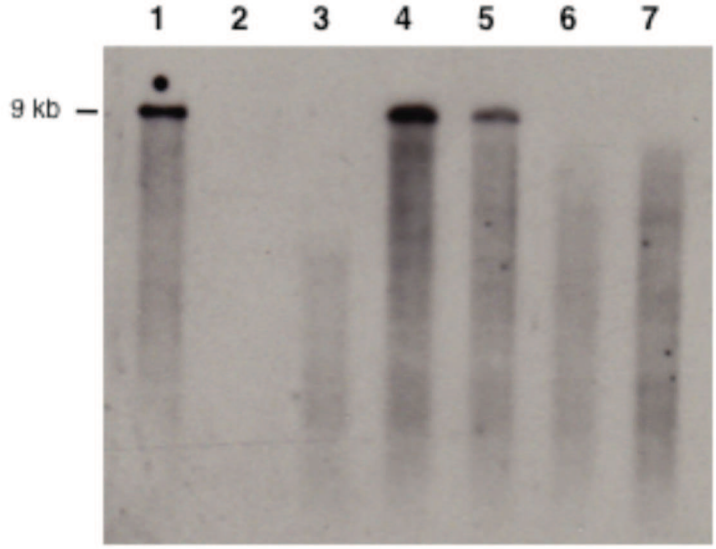

Figure 4

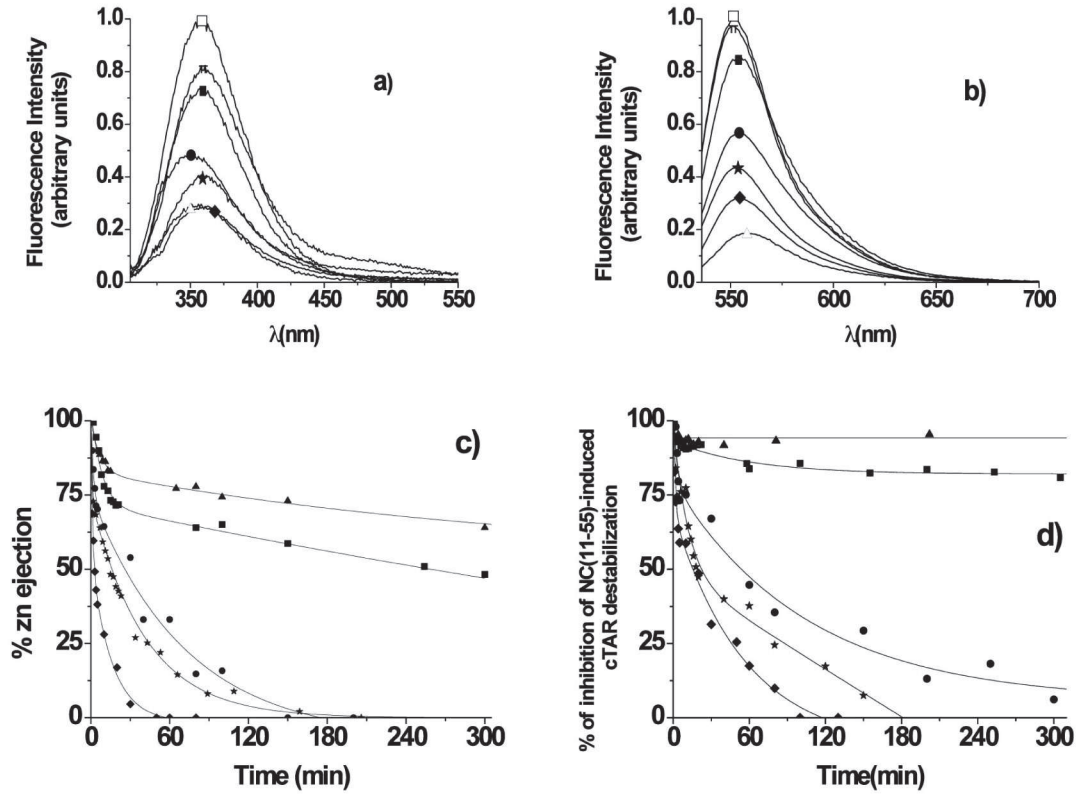
a)
Fluorescence Intensity (arbitrary units)
λ(nm)
b)
Fluorescence Intensity (arbitrary units)
λ(nm)
c)
% zn ejection
Time (min)
d)
% of inhibition of NC(11-55)-induced cTAR destabilization
Time(min)

Figure 1

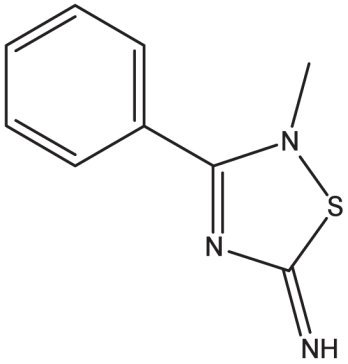

Figure 2

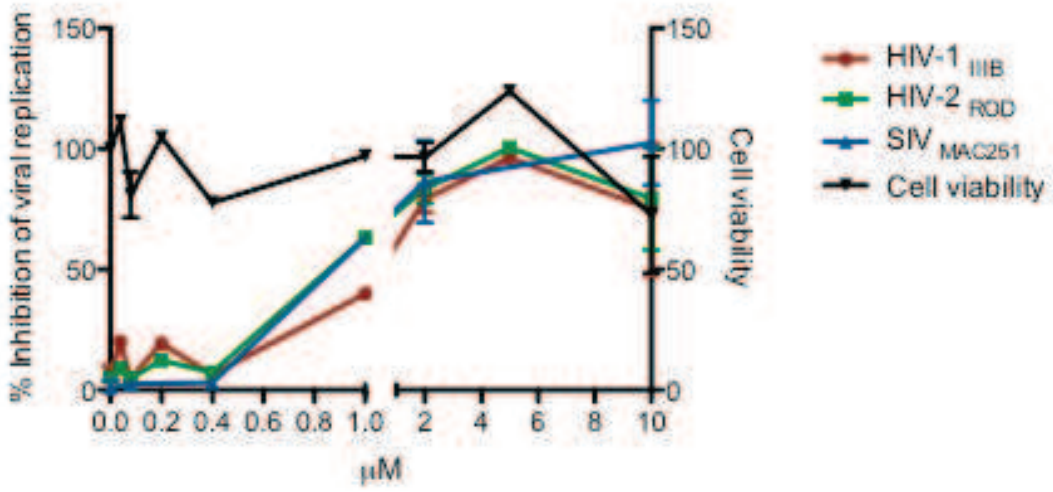
% Inhibition of viral replication
150
100
50
0
0.0 0.2 0.4 0.6 0.8 1.0
2 4 6 8 10
µM
Cell viability
HIV-1 IIIB
HIV-2 ROD
SIV MAC251
Cell viability

Figure 3

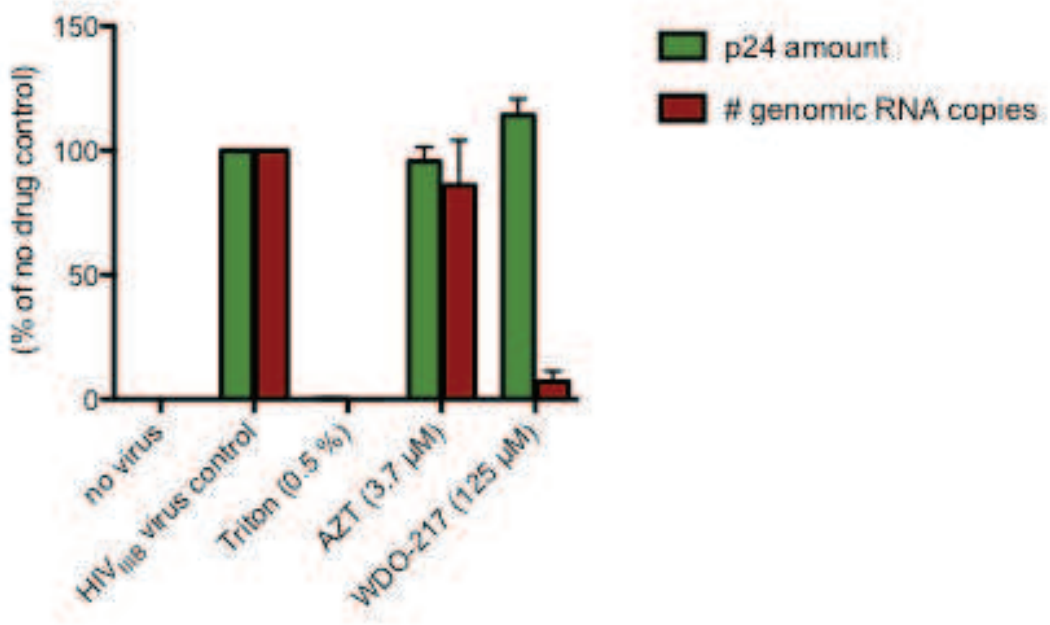
150
100
50
0
(% of no drug control)
p24 amount
genomic RNA copies
no virus
HIV IIIB virus control
Triton (0.5 %)
AZT (3.7 µM)
WDO-217 (125 µM)

Figure 4

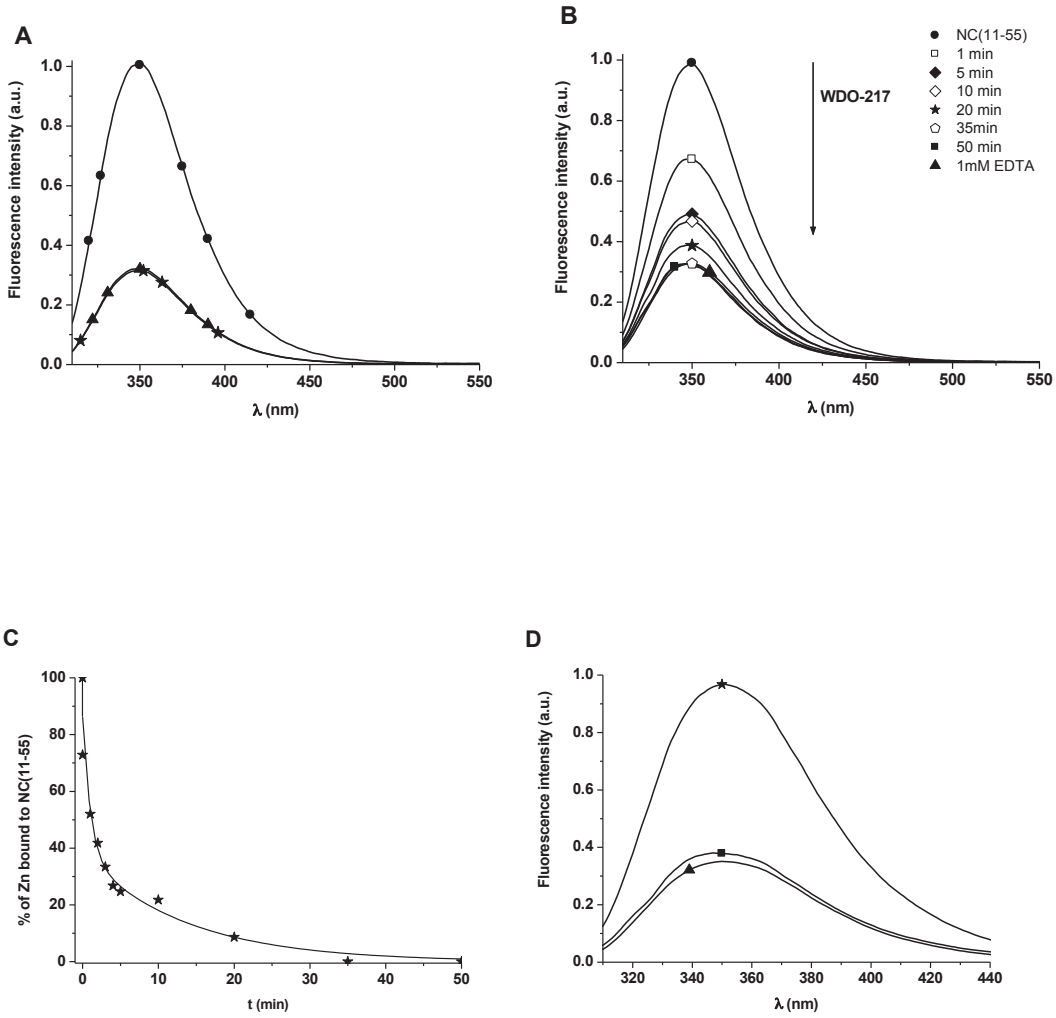
A
Fluorescence intensity (a.u.)
λ (nm)
B
Fluorescence intensity (a.u.)
λ (nm)
WDO-217
NC(11-55)
1 min
5 min
10 min
20 min
35min
50 min
1mM EDTA
C
% of Zn bound to NC(11-55)
t (min)
D
Fluorescence intensity (a.u.)
λ (nm)

Figure 5

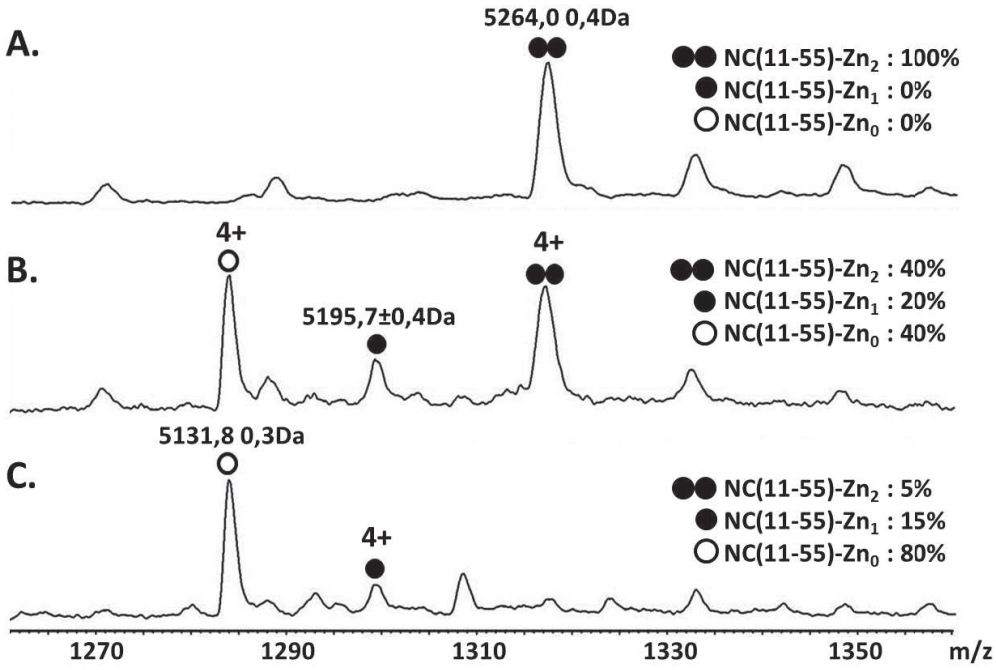
A.
5264,0 0,4Da
NC(11-55)-Zn2 : 100%
NC(11-55)-Zn1 : 0%
NC(11-55)-Zn0 : 0%
B.
4+
4+
5195,7±0,4Da
NC(11-55)-Zn2 : 40%
NC(11-55)-Zn1 : 20%
NC(11-55)-Zn0 : 40%
C.
5131,8 0,3Da
4+
NC(11-55)-Zn2 : 5%
NC(11-55)-Zn1 : 15%
NC(11-55)-Zn0 : 80%
1270
1290
1310
1330
1350
m/z

Figure 6

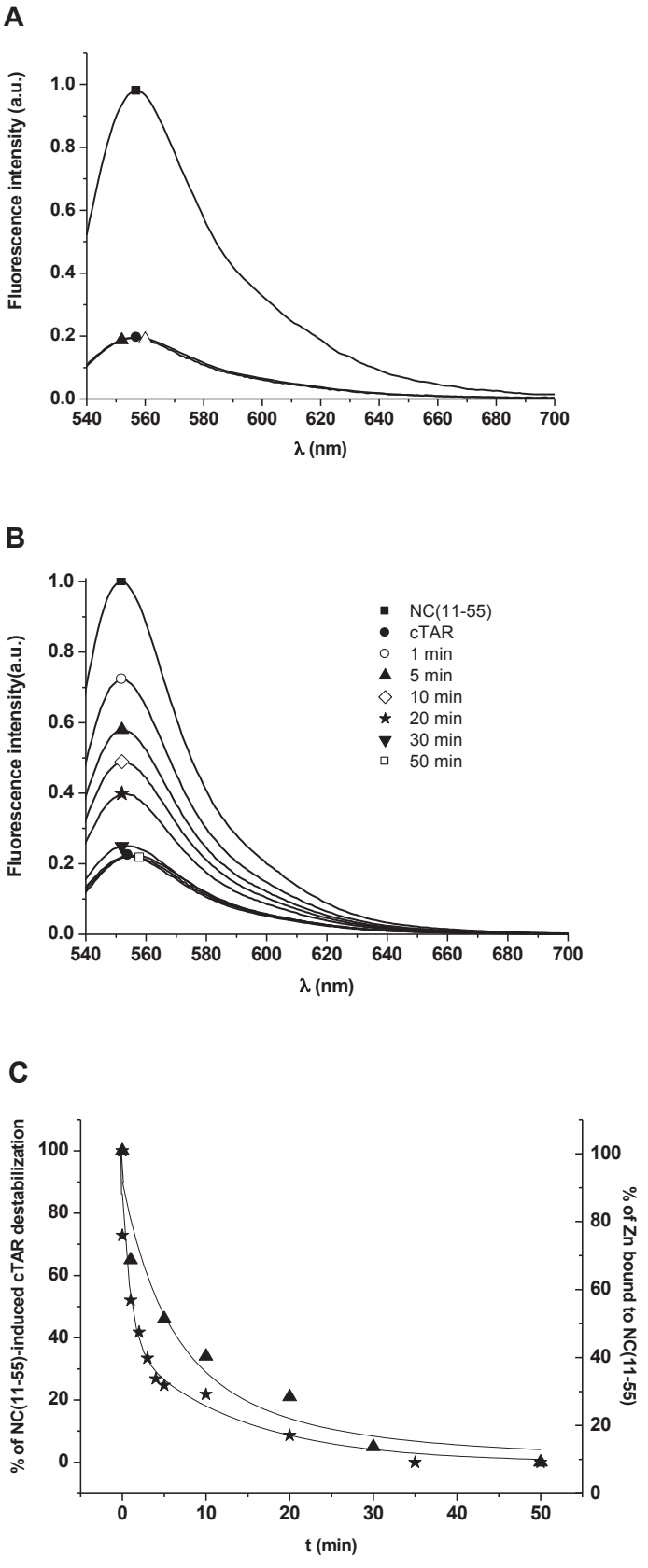
A
Fluorescence intensity (a.u.)
λ (nm)
B
Fluorescence intensity(a.u.)
λ (nm)
NC(11-55)
cTAR
1 min
5 min
10 min
20 min
30 min
50 min
C
% of NC(11-55)-induced cTAR destabilization
% of Zn bound to NC(11-55)
t (min)

Figure 7

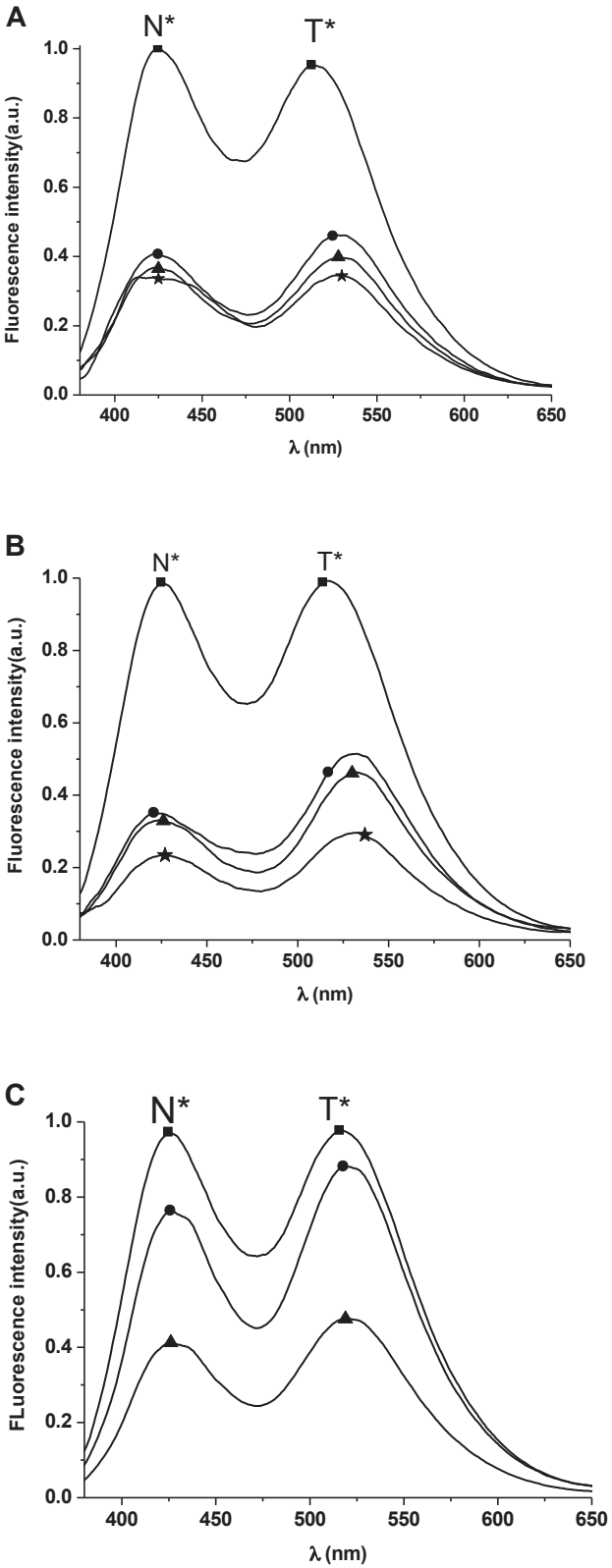
A
N*
T*
Fluorescence intensity(a.u.)
λ (nm)
B
N*
T*
Fluorescence intensity(a.u.)
λ (nm)
C
N*
T*
FLuorescence intensity(a.u.)
λ (nm)

Figure 8

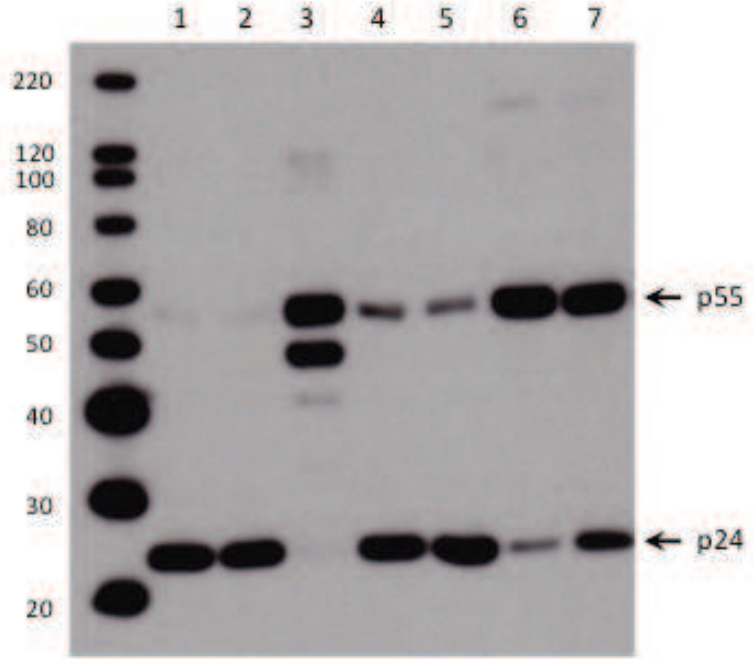

Use of virtual screening for discovering antiretroviral compounds interacting with HIV-1 nucleocapsid protein

In order to provide drug-candidates which interfere with NC functions, we developed in a collaboration with the group of prof. M.Botta, a new multidisciplinary approach consisting of molecular modeling, cellular assays and biophysical studies for discovering small molecule inhibitors of the NC protein.

In a first step, using molecular dynamic simulations, a series of pharmacophores was generated on the basis of the binding modes of PBS–DNA and PSI–RNA, with a special focus on the interactions of NC with the central guanine. Ten of them were generated on the NC/PBS-DNA complex and further merged in a single representative, pharm-D. An additional pharmacophore, referred as pharm-R, was generated for NC/Psi-RNA interactions.

Using the Discovery Studio 3.0 software and the two pharmacophores, pharm-D and pharm-R, the virtual library ASINEX was screened by. Compounds fitting to the pharmacophores with a Fit-Value higher than 1.5 were selected for the further docking step.

Molecular docking of the selected compounds on the NC structure in its binding conformation in PBS–DNA in NC/Psi-RNA was performed. This docking step helped us to select 500 top ranking hits, among which 10 show the highest chemical diversity to each other and against nucleotides and known NCp7 inhibitors. These 10 hits were then purchased from ASINEX and submitted to in vitro and biophysical testing.

By monitoring the amount of produced infectious viruses from cells, we estimated the antiviral activity of the selected compounds. Seven out of ten compounds show antiviral activity. The two most interesting compounds, namely 6 and 8 gave IC_{50} values of 2 and 100µM, respectively. To eliminate the possibility that cytotoxicity cause positive antiviral results, we checked that no toxicity was observed for both compounds. Then, using the intrinsic fluorescence of Trp37 of NC(11-55), we tested whether both compounds were able to eject zinc from the peptide and unfold it. We found that none of them was able to efficiently eject zinc from NC(11-55). In contrast, we observed a reproducible decrease of the Trp37 fluorescence on addition of compounds 6 and 8, suggesting an interaction of the compound with NC at the level of Trp37. To further investigate this interaction, we used NC(11-55) labelled at its N-terminus by a two colour 3HC probe developed in the laboratory. The significant change in the ratio of the two emission bands of 3HC observed after addition of the tested molecules further confirmed the binding of the compounds to NC. Finally, molecular modelling performed by the Italian group rationalized these observations, by showing that the compounds can bind at the level of the hydrophobic platform at the top of the zinc fingers.

In conclusion, in this work we characterized two non-toxic small molecules, 6 and 8, capable to interact with NC and showing antiretroviral activity at micromolar concentrations These compounds do no eject zinc from NC zinc fingers but are able to interact with the hydrophobic platform at the top of the folded fingers. This appears thus, as new clue to develop small molecules against NC.

G Model
VIRUS-95727; No. of Pages 11
ARTICLE IN PRESS

Virus Research xxx (2012) xxx–xxx

Contents lists available at SciVerse ScienceDirect

Virus Research

journal homepage: www.elsevier.com/locate/virusres

Use of virtual screening for discovering antiretroviral compounds interacting with the HIV-1 nucleocapsid protein

Mattia Mori[a,b], Patrizia Schult-Dietrich[c], Beata Szafarowicz[d], Nicolas Humbert[d], Francois Debaene[e], Sarah Sanglier-Cianferani[e], Ursula Dietrich[c], Yves Mely[d], Maurizio Botta[b,f,*]

[a] Università di Roma "La Sapienza", Dipartimento di Chimica e Tecnologie del Farmaco, piazzale A. Moro 5, I-00185 Roma, Italy
[b] Università degli Studi di Siena, Dipartimento Farmaco Chimico Tecnologico, via A. Moro, I-53100 Siena, Italy
[c] Georg-Speyer-Haus, Institute for Biomedical Research, Paul-Ehrlich-Str. 42-44, 60596 Frankfurt, Germany
[d] Laboratoire de Biophotonique et Pharmacologie, UMR 7213 CNRS, Faculté de Pharmacie, Université de Strasbourg, Cedex, Fr., 67401 Illkirch, France
[e] Laboratoire de spectrométrie de masse bio-organique, UMR 7178 CNRS, ECPM, 25 rue Becquerel, Bât. R5, 67087 Strasbourg, France
[f] Sbarro Institute for Cancer Research and Molecular Medicine, Center for Biotechnology, College of Science and Technology, Temple University, BioLife. Science Bldg., Suite 333, 1900 N 12th Street, Philadelphia, PA 19122, USA

ARTICLE INFO

Article history:
Available online xxx

Keywords:
Nucleocapsid protein
Antiretroviral activity
Virtual screening
HIV-1
Biophysical techniques
NC inhibitors

ABSTRACT

The HIV-1 nucleocapsid protein (NC) is considered as an emerging drug target for the therapy of AIDS. Several studies have highlighted the crucial role of NC within the viral replication cycle. However, although NC inhibition has provided *in vitro* and *in vivo* antiretroviral activity, drug-candidates which interfere with NC functions are still missing in the therapeutic arsenal against HIV. Based on previous studies, where the dynamic behavior of NC and its ligand binding properties have been investigated by means of computational methods, here we used a virtual screening protocol for discovering novel antiretroviral compounds which interact with NC. The antiretroviral activity of virtual hits was tested *in vitro*, whereas biophysical studies elucidated the direct interaction of most active compounds with NC(11–55), a peptide corresponding to the zinc finger domain of NC. Two novel antiretroviral small molecules capable of interacting with NC are presented here.

1. Introduction

AIDS is one of the most serious pandemic diseases of the modern era. According to the Joint United Nations Programme on HIV/AIDS (UNAIDS), at the end of 2010 there were approximately 34 million people infected by HIV-1 and about 30 million people have died of AIDS-related causes since the beginning of the epidemic (2011e). Most of the commonly available drugs, although potent and selective, experienced clinical failures due to the emergence of drug resistance across multiple HIV-1 strains. Hence, there is an urgent need of novel drugs and/or alternative therapeutic strategies.

The HIV-1 nucleocapsid protein (NC) is a basic, small zinc-binding protein which is highly conserved among several HIV-1 strains and thus potentially represents an ideal drug target. NC is involved in both the early and late phases of the HIV-1 replication cycle within the host cell mainly due to its nucleic acid chaperone activity (Darlix et al., 2011; Mirambeau et al., 2010; Thomas and Gorelick, 2008), and assists the reverse transcriptase during reverse transcription by promoting the annealing of the cellular primer tRNA to the primer binding site (PBS) and the two obligatory DNA strand transfers necessary for the synthesis of a complete double-stranded viral DNA (Darlix et al., 1993; Godet and Mely, 2010; Lapadat-Tapolsky et al., 1997; Levin et al., 2005; Rein et al., 1998; Tisne et al., 2004). NC is also thought to protect the nascent viral DNA against nucleases and to assist the HIV-1 integrase for the integration of the viral DNA into the host genome (Buckman et al., 2003; Carteau et al., 1997; Lapadat-Tapolsky et al., 1993; Krishnamoorthy et al., 2003). Finally, as a domain of the Gag structural polyprotein precursor, NC selects the genomic RNA and promotes its dimerization and packaging into newly formed viral particles (Clever et al., 1995; Darlix et al., 1993; Rist and Marino, 2002).

Due to its central role in the HIV-1 replication cycle, NC inhibition/inactivation has interfered with HIV-1 replication (Mirambeau et al., 2010; Thomas and Gorelick, 2008). Single point mutation of any of the zinc-coordinating residues, or aromatic residues Phe16 and Trp37 has led to a total loss of viral infectivity (Dorfman et al., 1993), whereas multiple strategies have been adopted for inhibiting NC by using small molecules or oligonucleotides (de Rocquigny et al., 2008; Goldschmidt et al., 2010). For example, electrophilic small molecules have provided *in vitro* and *in vivo* zinc ejection by

* Corresponding author at: Faculty of Pharmacy Università degli Studi di Siena, Dipartimento Farmaco Chimico Tecnologico, Università degli Studi di Siena, Via Aldo Moro 2, 53100 Siena, Italy. Tel.: +39 0577 234306; fax: +39 0577 234333.
E-mail address: botta.maurizio@gmail.com (M. Botta).

0168-1702/$ – see front matter © 2012 Published by Elsevier B.V.
http://dx.doi.org/10.1016/j.virusres.2012.05.011

targeting the zinc-coordinating cysteines of NC zinc fingers, thus inducing NC unfolding and the subsequent activity drop (Jenkins et al., 2005; Loo et al., 1996; Mayasundari et al., 2003; Miller Jenkins et al., 2007; Pannecouque et al., 2010; Rice et al., 1993). Zinc ejection has been also promoted by platinum nucleobases through the formation of a Zn–S–Pt intermediate within the C-terminal zinc finger of NC (Anzellotti et al., 2006; Quintal et al., 2011). However, both electrophilic compounds and platinum nucleobases suffer from limited selectively and significant toxicity, and have been therefore mainly explored as topical microbicide candidates. Antiretroviral small peptides, RNA aptamers and oligonucleotides inhibiting the NC functions have been also developed (Kim et al., 2002; Jeong et al., 2008; Raja et al., 2006). Of particular interest are the recently characterized methylated oligonucleotides that strongly inhibit NC binding on nucleic acids by a competitive mechanism (Avilov et al., 2012; Grigorov et al., 2011). Finally, the first small molecular inhibitors of the interaction between NC and TG-rich oligonucleotides have been identified in 2002 among the NCI diversity chemical library (Stephen et al., 2002), while active compounds with a xanthenyl ring have been later found to bind stoichiometrically to NC and exhibit an anti-HIV activity in the micromolar range, even if their antiviral mechanism is still unclear (Cruceanu et al., 2006). More recently, five low molecular weight compounds have been identified by screening a chemical library of 4800 compounds, based on their ability to inhibit the NC-mediated destabilization of the secondary structure of the cTAR sequence involved in the first obligatory strand transfer (Shvadchak et al., 2009a). However, these molecules were not able to cross the cell membrane (Godet and Mely, 2010). Although these strategies have significantly contributed to emphasize the potential role of NC as drug target, further efforts are needed to discover anti-NC agents endowed with drug-like properties (Mori et al., 2011b).

Recently, we have refined available NMR structures of NC in complex with nucleic acids (PBS–DNA and PSI–RNA) by means of molecular dynamics (MD) simulations. Such computational structures were in agreement with experimental data and have been used as target receptors for the structure-based modeling of the five hit compounds described by Shvadchak, as well as to develop a computational protocol for enriching NC inhibitors by virtual screening (Mori et al., 2010, 2011a; Shvadchak et al., 2009a). Starting from these checkpoints, here we combined pharmacophore modeling, molecular docking and free energy calculations into a virtual screening cascade for the identification of potential NC inhibitors among the ASINEX database. Ten chemically diverse hits were purchased and tested on P4.R5 MAGI cells infected with HIV-1 Lai for assessing their cytotoxicity and antiretroviral activity *in vitro*. None of the tested compounds was toxic below 100 μM. The two most active compounds designed as **6** and **8** (IC_{50} of 2 μM and 100 μM, respectively) were further investigated by biophysical methods which proved their capability to interact with NC. The multidisciplinary work-flow used in this work is summarized in Fig. 1.

2. Materials and methods

2.1. Generation of pharmacophores from MD snapshots

The conformation of NC in complex with PBS–DNA and PSI–RNA has been previously analyzed by means of molecular dynamics (MD) simulations (Mori et al., 2010). All MD frames were grouped in ten clusters by using the *ptraj* script of the AMBER10 package (Case et al., 2010), and the representative member of each cluster was selected. Coordinates of nucleotides were manually removed from representative frames with the exception of the guanine base of central deoxyguanosine 7 (DG7) and riboguanosine 10 (RG10) nucleotide of PBS–DNA and PSI–RNA respectively, whose binding mode to NC was used to generate structure-based pharmacophores by the Ligandscout 3.0 software (Wolber and Langer, 2005). A pharmacophore was generated from each representative frame. These models were further merged in two final pharmacophores, designed as pharm-D and pharm-R, which accounted for the interaction of DG10 and RG7 guanine base toward NC, respectively (Fig. 2). Pharmacophores were converted in a format compatible with Discovery Studio 3.0 (2010).

2.2. Preparation of the virtual library

The emerald, gold, platinum and synergy collections of the ASINEX database, consisting of 391,535 single entries, were screened in this work. Duplicates and molecules having metal ions, more than three chiral centres, less than 15 heavy atoms or a molecular weight lower than 150 or higher than 650 Da were removed. Ligands were then prepared by means of the Ligprep application of the Schrodinger Maestro suite (2011b,d). Energy minimization was done with Macromodel by using the OPLS2005 force field (2011c), while Epik was used to generate possible tautomers and ionization states at pH 7.0 ± 1.0 (2011a; Greenwood et al., 2010; Shelley et al., 2007). Only structures endowed with a normalized probability higher than 0.8 were retained in the final form of the library, which was composed of 648,465 unique structures. Only for pharmacophore screening, the conformational analysis of the entire library was done by using the "Build 3D Database" protocol with the CAESAR method implemented in Discovery Studio 3.0.

2.3. Preparation of NC structures for docking

Coordinates of the NC protein in complex with PBS–DNA and PSI–RNA were taken from a previous MD study (Mori et al., 2010, 2011a). The structure of NC in the binding conformation to PBS–DNA is thereafter referred as NC(DNA), while that to PSI–RNA is referred as NC(RNA).

2.4. Virtual screening

A structure-based virtual screening cascade composed of pharmacophore screening, molecular docking, rescoring, visual inspection and chemical diversity analysis was used. Pharmacophores generated as described in Section 2.1 were used as three-dimensional queries to filter the virtual library described in Section 2.2 by means of the "Search 3D Database" and the "Ligand Pharmacophore Mapping" protocols of Discovery Studio 3.0. Compounds fitting to pharmacophores with a FitValue higher than 1.5 were then docked by using the enrichment procedure already described (Mori et al., 2011a). More precisely, compounds filtered by the pharm-D model were docked toward the NC(DNA) structure whereas the NC(RNA) structure was used as receptor for docking compounds filtered by the pharm-R (see Fig. 1). Results obtained by docking toward both protein conformations were then merged by a consensus "rank by rank" approach.

2.5. In vitro analysis of selected compounds for antiviral activity

Antiviral assays were essentially performed as described previously (Dietz et al., 2008). Briefly, 1×10^4 P4.R5 MAGI cells were seeded and infected over night with HIV-1 Lai (MOI of 0.3) at 37 °C. The next day, after extensive washing, serial dilutions of the compounds in serum-free medium were added for 4 h and then DMEM medium (10% FCS) was added. The next day, cells were washed and incubated for further 24 h in fresh medium at 37 °C. Then supernatants were collected and infectious virus was quantified on TZM-bl cells expressing the firefly luciferase gene under the control of the HIV-1 LTR. 1×10^4 TZM-bl cells were seeded and infected

Please cite this article in press as: Mori, M., et al., Use of virtual screening for discovering antiretroviral compounds interacting with the HIV-1 nucleocapsid protein. Virus Res. (2012), http://dx.doi.org/10.1016/j.virusres.2012.05.011

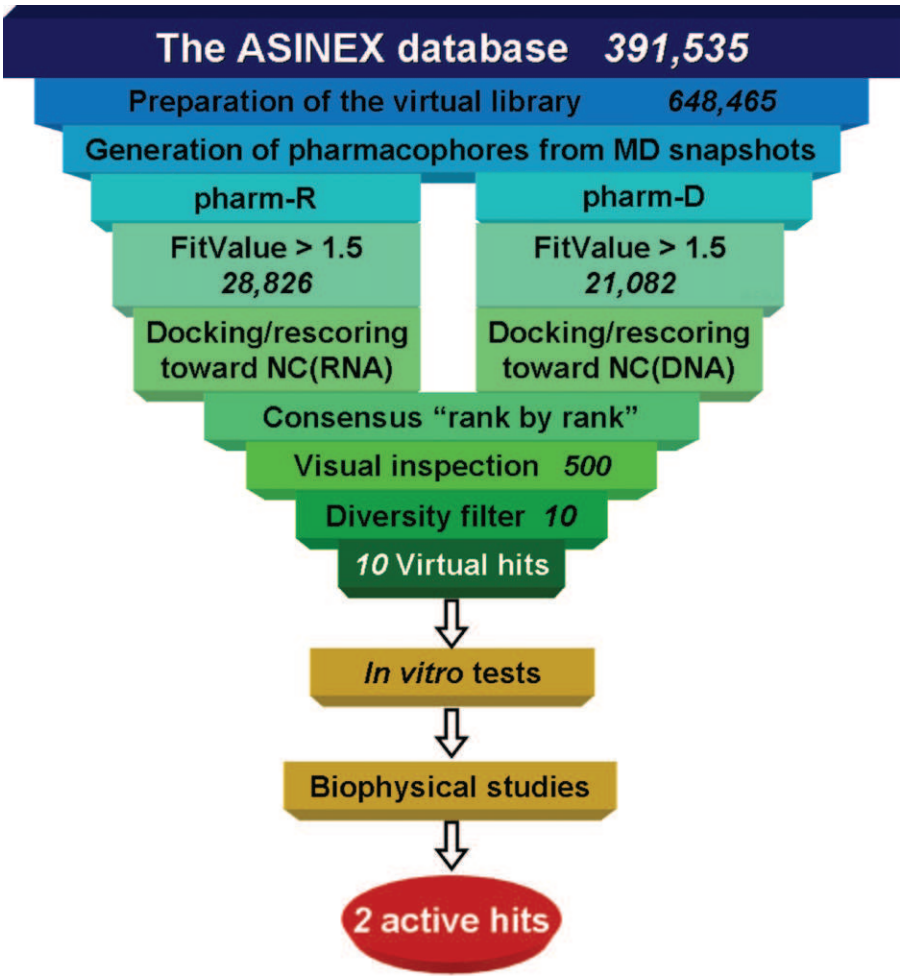

Fig. 1. Work-flow used for discovering new putative NC inhibitors. The number of individual compounds managed at each step is indicated.

with the viral supernatants in the presence of polybrene (8 μg/mL) for 44 h. Virus was quantified by measuring the luciferase activity in the infected cells. Cells were washed with PBS, lysed with harvest buffer (0.5 M Mes–Tris, 1 M DTT, 10% Triton 100× and glycerol) and frozen. Subsequently, light emission was measured on a Lumistar Galaxy Luminometer.

2.6. *In vitro analysis of selected compounds for cytotoxicity*

The viability of uninfected P4.R5 MAGI cells treated with the compounds as described above was determined by measuring ATP in living cells by luminometry with the ViaLight Plus kit according to the instructions of the manufacturer (Lonza).

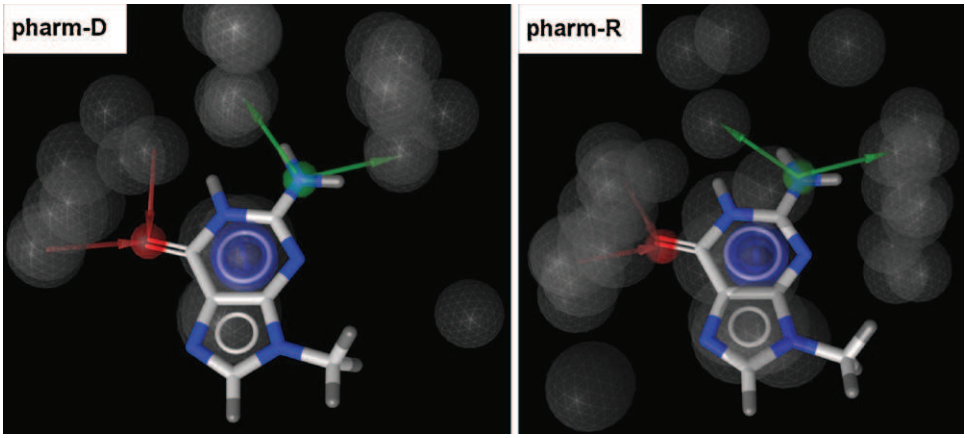

Fig. 2. The structure-based pharmacophores representing the interactions of the guanine base with the NC protein in the DNA (left) or RNA (right) binding conformation. Pharmacophoric features are colored: green, hydrogen bond donor; red, hydrogen bond acceptor; blue, aromatic ring; grey, excluded volumes. (For interpretation of the references to color in this figure legend, the reader is referred to the web version of the article.)

Please cite this article in press as: Mori, M., et al., Use of virtual screening for discovering antiretroviral compounds interacting with the HIV-1 nucleocapsid protein. Virus Res. (2012), http://dx.doi.org/10.1016/j.virusres.2012.05.011

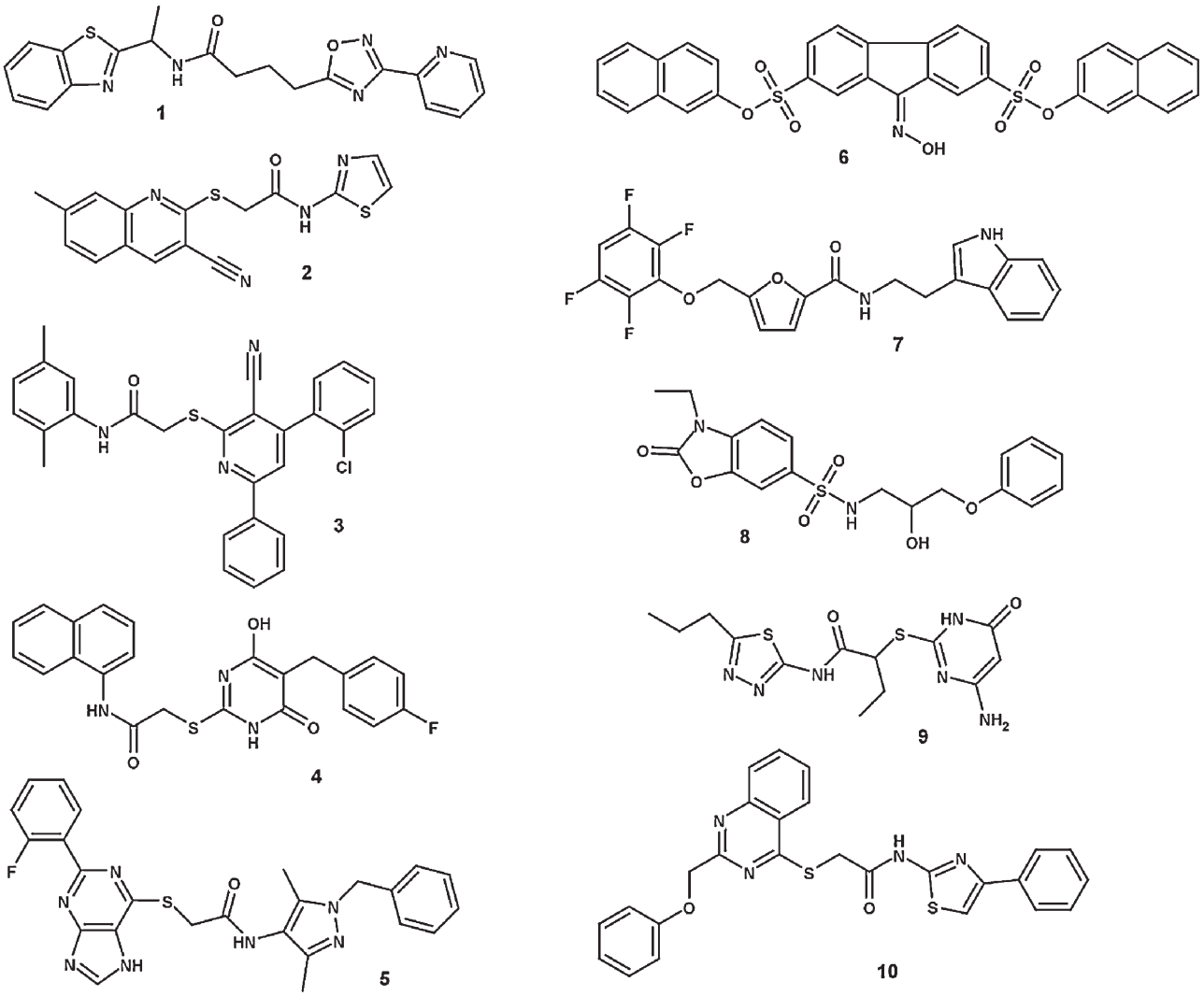

Fig. 3. Chemical structures of hit compounds selected by means of virtual screening.

2.7. Preparation of molecules and NC(11–55) peptide synthesis

All solvents for spectroscopic measurements were from Sigma–Aldrich. Purity of compounds **1**–**10** was higher than 95%. The DMSO solutions of all compounds were prepared freshly before all the experiments. The NC(11–55) peptide was synthesized by solid-phase peptide synthesis on a 433A synthesizer (ABI, Foster City, CA) as previously described (Shvadchak et al., 2009a). The lyophilized peptide was dissolved in water, and its concentration was determined by using an extinction coefficient of (5.7×10^3) M^{-1} cm^{-1} at 280 nm. Next, 2.5 M equivalents of $ZnSO_4$ were added to the peptide, and the pH was raised to its final value by adding buffer. The pH was increased only after the addition of zinc to avoid the oxidation of the zinc-free peptide. The NC(11–55) peptide labeled at its N-terminus by *N*-(2-furan-2-yl-3-hydroxychromon-6-yl)-succinamic acid was prepared, as previously described (Shvadchak et al., 2009b). The extinction coefficient of this peptide, referred as 3HC–NC(11–55), is 15,000 M^{-1} cm^{-1} at 350 nm, due to the absorbance of the 3-hydroxychrome (3HC) dye.

2.8. Binding affinity measurements

All experiments were performed at 20 °C with a solution containing 25 mM Tris–HCl (pH 7.5), 30 mM NaCl, and 0.2 mM $MgCl_2$ or 10 mM PBS (pH 6.5) and 30 mM NaCl (Bernacchi et al., 2002). Absorption spectra were recorded with a Cary 400 or a Cary 4000 spectrophotometer (Varian). Steady-state fluorescence emission spectra were measured on either a Fluorolog or a Fluoromax spectrofluorometer (Horiba Jobin-Yvon) equipped with a thermostated cell compartment. Excitation wavelength was 295 nm for NC(11–55) and 350 nm for 3HC-labeled NC(11–55). The spectra were corrected for dilution and buffer fluorescence. Extinction coefficients at 269 nm and at 280 nm of (5.54×10^4) M^{-1} cm^{-1} and of (1.11×10^4) M^{-1} cm^{-1} were used for **6** and for **8**, respectively.

Titration of 3HC–NC(11–55) by compound **6** was performed by adding increasing concentrations of **6**–1 μM of peptide, and monitoring the emission of the 3HC probe at 517 nm. Excitation was at 350 nm. As a consequence of the direct excitation of compound **6** at this wavelength, the emission spectra of 3HC–NC(11–55) was corrected from the emission of compound **6** in the titration, as well as from the screening effect due to the absorbance of **6** at the excitation wavelength.

The fluorescence data were fitted to Eq. (1) to recover the equilibrium association constant K_a:

$$I = I_0 - \frac{(I_0 - I_t)}{L_t} \cdot \frac{[1 + (L_t + nN_t)K_a] - \sqrt{[1 + (L_t + nN_t)K_a]^2 - 4L_t nN_t K_a^2}}{2K_a} \quad (1)$$

where L_t and N_t designate the total concentration of compound **6** and NC peptide, respectively; I_t represents the fluorescence at

the plateau when all the compound **6** is bound, whereas I_0 and I correspond to the fluorescence intensities of the NC peptide in the absence and in the presence of a given concentration of compound **6**, respectively; n represents the number of NC binding sites for compound **6**. The parameters were recorded from nonlinear fits of Eq. (1) to the experimental data sets by using the Origin software (Microcal).

2.9. Mass spectrometry experiments

NanoESI–MS analysis was performed in positive mode on an electrospray time-of-flight mass spectrometer (LCT, Waters, Manchester, UK) equipped with a nanoESI source (Triversa Nanomate, Advion Biosciences, Ithaca, NY). Calibration was performed with a 2 μM horse heart myoglobin solution prepared in a mixture of water:acetonitrile (1:1) acidified with 1% of formic acid. MS data were acquired and processed using MassLynx^{TM} 4.1 (Waters). Deconvolutions of the peptide mass spectra were performed with MaxEnt1 deconvolution software with optimized parameters.

Prior to mass spectrometry analysis, NC(11–55) peptide was buffer exchanged using 5 cycles of dilution/concentration steps on size exclusion column (Vivaspin 3 kD, Sartorius, Goettingen, Germany) against a 50 mM ammonium acetate ($AcNH_4$) solution buffered at pH 7.5. Peptide concentration was further determined by absorption spectrometry using an extinction coefficient of 5.700 M^{-1} cm^{-1} at 280 nm. Purity and integrity of the NC(11–55) peptide was first checked in denaturing conditions by diluting the peptide at 2 μM in a water:acetonitrile (1:1) mixture acidified with 1% of formic acid. Noncovalent mass spectrometry analyses were performed by diluting NC(11–55) peptide at 5 μM in $AcNH_4$ (50 mM, pH 7.5). Mass spectrometer interface conditions were carefully optimized in order to detect protein/ligand interaction. Ligands (**6** or **8**) were diluted to 250 mM in $AcNH_4$ (50 mM, pH 7.5) and incubated with NC(11–55) peptide for 30 min at 20 °C.

3. Results

Here we present a multidisciplinary approach consisting of molecular modeling, cellular assays and biophysical studies for discovering small molecule inhibitors of the HIV-1 NC protein. Biological and biophysical methods were essential to test the *in vitro* antiretroviral activity of virtual hits, and to prove the direct binding of active compounds on NC(11–55).

3.1. Pharmacophore modeling and screening

A pharmacophore model is an intuitive three-dimensional representation of the most relevant polar and hydrophobic interactions performed by active ligands toward a target receptor, which is often used for the *in silico* screening of large chemical libraries. In a previous work, the most relevant interactions occurring between NC and PBS–DNA or PSI–RNA have been analyzed by MD (Mori et al., 2010). Starting from representative MD frames, the Ligandscout software was herein used to generate pharmacophores accounting for H-bond interactions made by the central guanine with the backbone atoms of Phe16, Lys33, Gly35, Trp37, Met46, and hydrophobic/aromatic interactions made with the side-chain of Trp37. The crucial role of these residues for NC activity has been elucidated in several studies (Raja et al., 2006; Amarasinghe et al., 2000a,b; Morellet et al., 1992; South and Summers, 1993; Bazzi et al., 2011). In particular, ten pharmacophores were generated on the NC/PBS–DNA complex and were merged in a single representative pharmacophore, thereafter referred as pharm-D (Fig. 2). The same procedure was followed to generate a single representative pharmacophore for the NC/PSI–RNA interaction, thereafter referred as pharm-R (Fig. 2).

Notably, although these pharmacophores were derived from significantly different NC structures, they shared a RMS difference of 1.73 Å which suggests that the NC, despite its large structural flexibility, could present a similar interaction pattern for the guanine base of PBS–DNA and PSI–RNA (Fig. 2).

The ASINEX database, prepared as described in Section 2.2, was then filtered by pharm-D and pharm-R pharmacophores using Discovery Studio 3.0. The "Search 3D Database" protocol was used for identifying ligands in the initial library that map each pharmacophore, whereas the "Ligand Pharmacophore Mapping" protocol was used to align selected ligands to the query pharmacophore and for calculating the relative FitValue as a measure of how well the ligand fits the pharmacophore. Then, ligands mapping with a FitValue higher than 1.5, which correspond to the 3.2% and the 4.4% of the initial library for pharm-D and pharm-R, respectively, were selected for the further docking step.

3.2. Docking, rescoring and compounds selection

Molecular docking is a computational tool for predicting the binding conformation of a ligand to a target receptor, and represents the core of our virtual screening cascade. The reliability of docking simulations strictly depends on the quality or resolution of the target receptor coordinates and on the type of docking or scoring function used. In this work we used docking parameters already optimized for the NC target (Mori et al., 2010, 2011a). NC structures extracted from MD trajectories were used for docking: the NC(DNA) describes the NC in its binding conformation to PBS–DNA and was used for docking compounds filtered by the pharm-D model, whereas the NC(RNA) was used for docking compounds filtered by the pharm-R model. With the aim of reducing as much as possible the number of false positives, docking poses were rescored by means of the Molecular Mechanics Poisson–Boltzmann Surface Area (MMPBSA) approach implemented in AMBER10. This method has been also found to enrich the number of active compounds identified by docking toward different receptor systems (Brown and Muchmore, 2007; Thompson et al., 2008; Li et al., 2010).

Since the NC binding conformation to small molecules is still unknown, in this work we aimed at discovering molecules that could interact *in vitro* with both NC conformations known from computational and experimental studies. Accordingly, a consensus "rank by rank" analysis of rescoring results was performed. Docking poses of 500 top ranking hits were visually analyzed and the ten most interesting molecules, **1**–**10** in Fig. 3, showing the highest chemical diversity to each other and against nucleotides and known NCp7 inhibitors (Avilov et al., 2012; Shvadchak et al., 2009a) were purchased from ASINEX and submitted to *in vitro* and biophysical testing.

3.3. Antiviral activity of the selected compounds

All compounds were analyzed for antiviral activity in P4.R5 MAGI cells. The antiviral activity was assessed by quantifying the amount of infectious virus produced from these cells in the presence of serial dilutions of the compounds. This approach was chosen to include antiviral effects mediated by inhibiting late NC functions in the replication cycle. Overall, seven compounds out of ten showed antiretroviral activity at tested concentrations. Compounds **6** and **8** showed nice concentration-dependent antiviral activity (Fig. 4). The IC_{50} was around 2 μM for compound **6** and about 100 μM for compound **8**. Compounds **3**, **5**, **7**, **9** and **10** were tested several times, but did not show consistent concentration dependent inhibition, whereas no antiviral activity was observed in the concentration range tested for compounds **1**, **2** and

Please cite this article in press as: Mori, M., et al., Use of virtual screening for discovering antiretroviral compounds interacting with the HIV-1 nucleocapsid protein. Virus Res. (2012), http://dx.doi.org/10.1016/j.virusres.2012.05.011

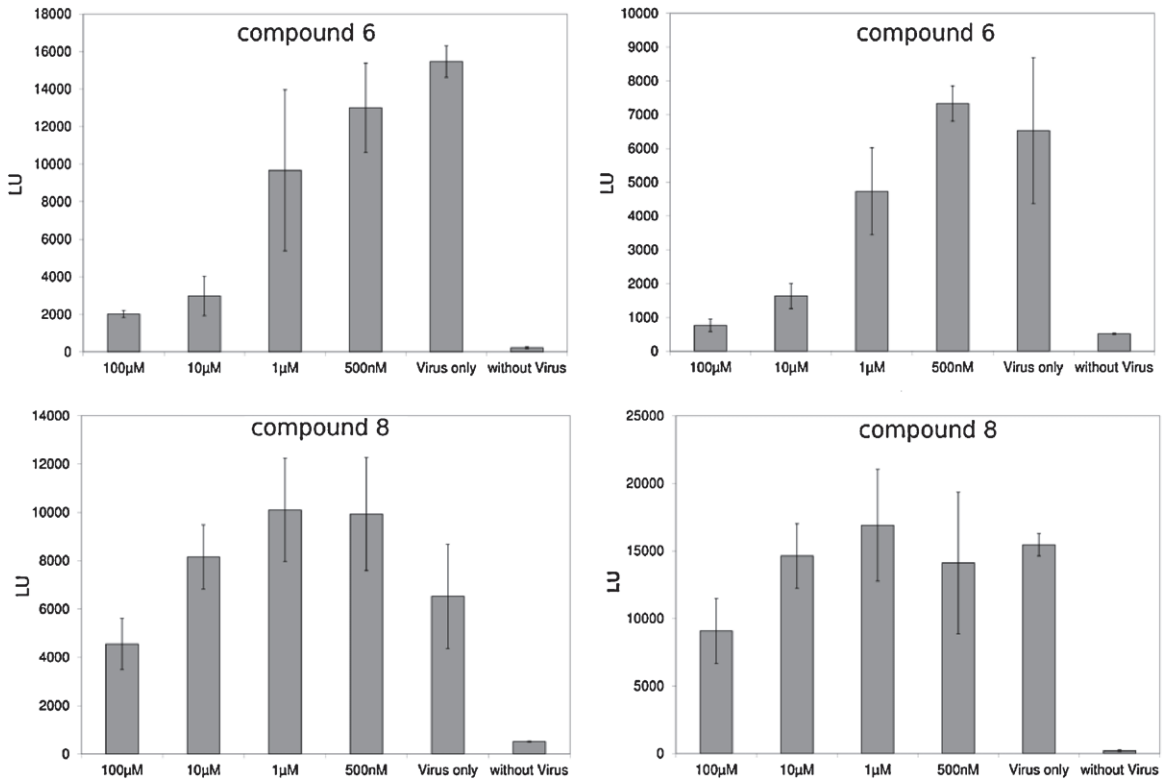

Fig. 4. Compounds **6** and **8** showed a concentration-dependent antiviral activity *in vitro*. This was seen by the reduction of infectious virus produced from P4.R5 MAGI cells, measured by luminometry (LU), in the presence of the compounds compared to virus only. Two independent experiments are shown for both compounds and the mean of triplicates is shown with standard deviations.

4. Saquinavir, a known protease inhibitor added as positive control, inhibited with an IC_{50} of 20 nM in this assay (data not shown).

3.4. *In vitro cytotoxicity of the selected compounds*

To exclude cytotoxic effects of compounds **6** and **8** potentially resulting in reduced virus production, cytotoxicity assays were performed with the compounds using the same assay conditions as in the infectivity assays, but in the absence of HIV-1 infection. No toxicity was observed for compounds **6** and **8** at the inhibitory concentration (Fig. 5).

3.5. *Zinc ejection from NC(11–55)*

The zinc ejection property of selected compounds was first characterized by using the intrinsic fluorescence of the Trp37 residue of NC(11–55), which belongs to the distal zinc finger motif and shows a 3-fold decrease in its fluorescence quantum yield upon zinc removal (Bombarda et al., 2001; Mely et al., 1996). Addition of **1**–**10** to the zinc-bound NC(11–55) at a molar ratio of 1:1 and 10:1 was found to induce no or small changes in the Trp37 fluorescence when compared with the spectrum obtained after addition of 1 mM EDTA (Fig. 6). Thus, none of the tested compounds is able to significantly eject zinc from NC(11–55). Nevertheless, it could be noted that a small, but reproducible decrease (~10–15%) of the Trp37 fluorescence was observed with compound **8**, suggesting either limited zinc ejection or interaction of compound **8** with Trp37. Indeed, it is well known that interactions and notably stacking interactions of Trp with aromatic moieties lead to substantial decrease in Trp fluorescence (Montenay-Garestier et al., 1993; Mely et al., 1993).

To further check the zinc ejection, mass spectrometry of NC(11–55) was performed in the presence of **6** or **8**, added at a

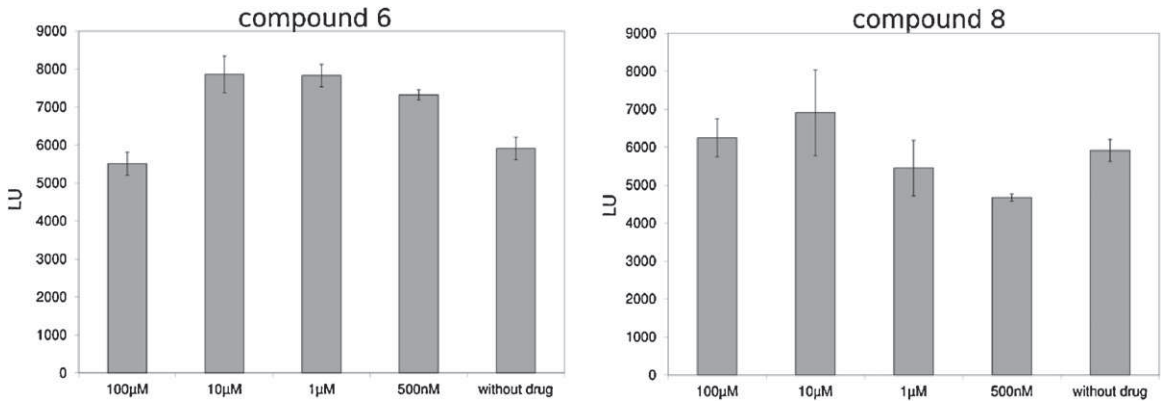

Fig. 5. Compounds **6** and **8** were non-toxic in P4.R5 MAGI cells, as measured in a luminometric assay for ATP quantification in living cells (LU).

Please cite this article in press as: Mori, M., et al., Use of virtual screening for discovering antiretroviral compounds interacting with the HIV-1 nucleocapsid protein. Virus Res. (2012), http://dx.doi.org/10.1016/j.virusres.2012.05.011

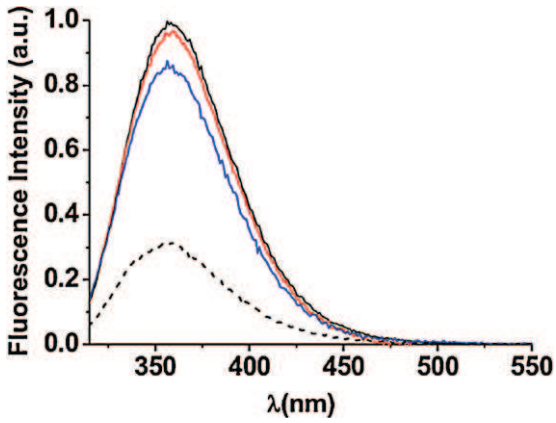

Fig. 6. Absence of zinc ejection from NC(11–55) by **6** and **8**, as monitored by the intrinsic fluorescence of NC(11–55). The emission spectrum of NC(11–55) (1 μM) was recorded in the absence (solid black) and in the presence of 10 μM **6** (red) or **8** (blue). Spectrum of NC(11–55) in the presence of 1 mM EDTA (dash black) is given as a control. Buffer: 25 mM Tris (pH = 7.5), 30 mM NaCl and 0.2 mM $MgCl_2$, T = 20 °C. λ_{exc} = 295 nm. Spectra of NC(11–55) in the presence of all other compounds **1**–**5**, **7**, **9**, **10** were superimposable to the spectrum of the zinc-bound NC(11–55) (solid black) and were not represented. (For interpretation of the references to color in this figure legend, the reader is referred to the web version of the article.)

ratio of 50:1. As shown in Fig. 7A, mass spectrometry analysis of native NC(11–55) peptide revealed a measured mass of 5264.8 Da ±0.3, which corresponds to the NC(Zn_2) complex (expected mass: 5264.6 Da). Neither compound **6** (Fig. 7B) or **8** (Fig. 7C) was able to eject zinc ion from the NC(11–55) peptide, since no complex with NC(Zn_1) or NC(Zn_0) could be detected, even with very low energetic measurement parameters (data not shown). Moreover, no complexes between these two compounds and NC(11–55) could be observed, suggesting that they are probably dissociated by the mass spectrometry conditions.

From the absence of zinc ejection observed by mass spectrometry, it could be deduced that the small decrease in Trp37 fluorescence observed with compound **8** is related to a direct interaction of this compound with the Trp37 residue of NC(11–55).

3.6. Binding of 6 and 8 on 3HC-labeled NC(11–55)

Compounds **6** and **8** were the most promising from *in vitro* tests. To investigate their interaction with NC we used the NC(11–55) labeled at its N-terminus by a 3-hydroxychrome (3HC) probe (Fig. 8) that shows two emission bands highly sensitive to the binding of nucleic acids, giving the unique opportunity to monitor environment changes (Shvadchak et al., 2009b). These two emission bands are due to an excited state proton transfer reaction that generates two excited states: a normal one (N^*) and a tautomer one (T^*), giving two well-separated emission bands. The N^*/T^* ratio between the two emission bands was about 0.87, indicating a high exposure of the 3HC probe to the solvent.

Addition of increasing concentrations of compound **6** was found to induce a large decrease of the overall intensity of the emission spectrum of 3HC–NC(11–55) (Fig. 9a), suggesting a direct interaction of **6** with the N-terminus of NC(11–55) that induces a subsequent change of the 3HC environment. Moreover, a significant change in the N^*/T^* ratio (from 0.87 to 0.65) accompanied the binding of **6** to 3HC–NC(11–55), indicating a partial screening of 3HC from the solvent as a consequence of the binding of compound **6**.

By plotting the changes in the intensity of the T^* band maximum at 517 nm, we could monitor the binding of **6** to the peptide (Fig. 9b) and by fitting the data with a Scatchard equation, determine an affinity of $(1.8 \pm 0.3) \times 10^5\ M^{-1}$, assuming a 1:1 stoichiometry.

In contrast to compound **6**, addition of **8** induced only a negligibly small decrease of the overall intensity of 3HC–NC(11–55), with nearly no change in the N^*/T^* ratio (data not shown), suggesting that **8** may bind only with low affinity to the NC peptide

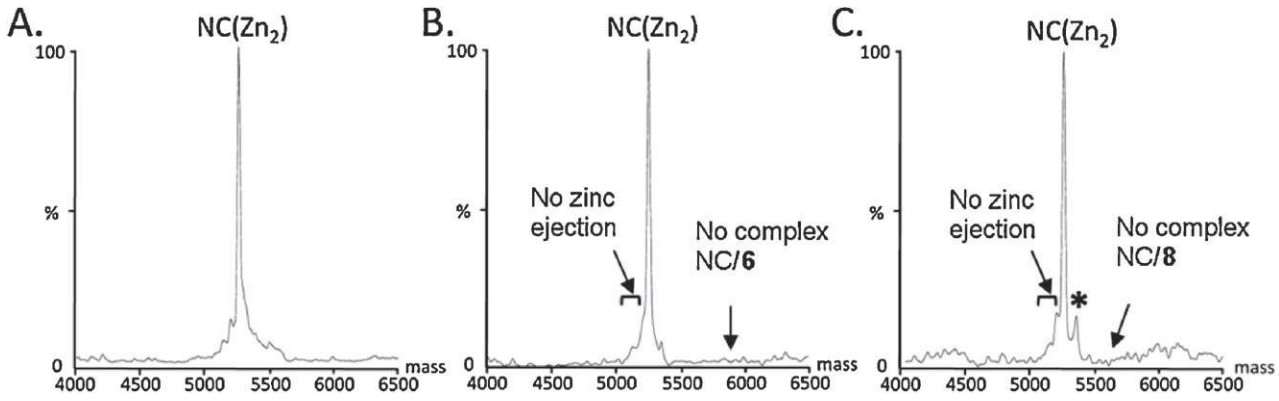

Fig. 7. Absence of zinc ejection from NC(11–55) by **6** and **8**, as monitored by mass spectrometry. Non-denaturing mass spectra of 5 μM NC(11–55) in $AcNH_4$ 50 mM, pH 7.5, in the absence (A) or in the presence of 250 μM of compound **6** (B) or 250 μM of compound **8** (C). Measured mass (5264.8 Da ±0.3) corresponds to NC(11–55) complexed with 2 zinc ions (NC(Zn_2)). *DMSO adduct.

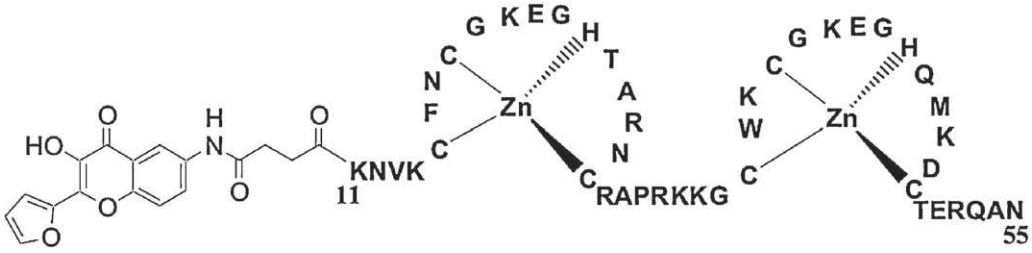

Fig. 8. Sequence of NC(11–55) labeled by the 3HC probe at its N-terminus.

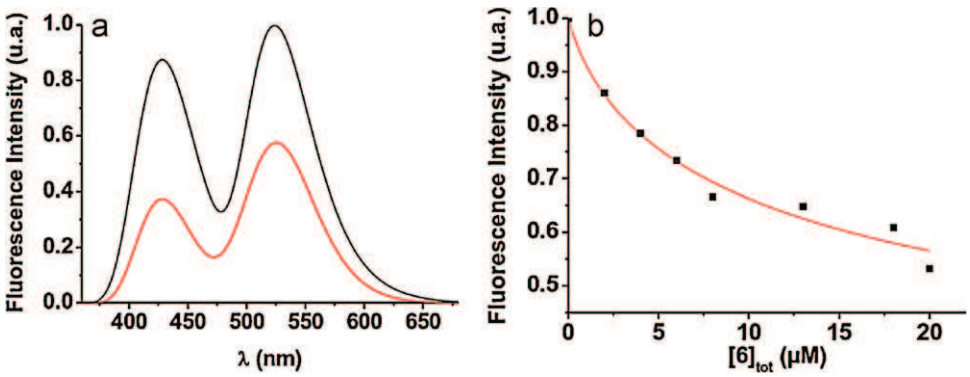

Fig. 9. Interaction of 6 with 3HC–NC(11–55), as monitored by the 3HC fluorescence. (a) Emission spectra of 1 μM 3HC–NC(11–55) recorded in the absence (black) or in the presence of 20 μM **6** (red). The left and right emission bands correspond to the emission of the N^* and T^* tautomers of the 3HC probe, respectively. (b) Titration of 3HC–NC(11–55) by **6**. The fluorescence intensities of 3HC–NC(11–55) were monitored at 517 nm as a function of the added concentrations of compound **6**. The data points (squares) were fitted with the equation 1 (solid line), using a 1:1 stoichiometry and a binding constant of $(1.7 \pm 0.5) \times 10^5\ M^{-1}$. All spectra were corrected from the **6** fluorescence. Buffer: 10 mM PBS (pH = 6.5), 30 mM NaCl, $T = 20\ ^\circ C$, $\lambda_{exc} = 350$ nm. (For interpretation of the references to color in this figure legend, the reader is referred to the web version of the article.)

or alternatively, that **8** interacts with NC at a site distant from its N-terminus.

3.7. Predicted binding modes of 6 and 8 toward NC

Compounds survived to the pharmacophoric screening were docked as described in Section 2.4. Docking results showed that **6** mostly performed hydrophobic interactions within the guanine binding site with Trp37, Met46 and Phe16 (Fig. 10A and B), this latter being involved only in the NC(RNA) protein conformation. A significant portion of **6** was docked in the polar groove formed by basic residues that link the two zinc fingers. Even if the overall binding conformation of **6** looks different within the two protein conformations, a common salt bridge with Lys47 and a hydrophobic interaction of stacking nature with Phe16 were observed. The predicted binding mode of **6** on the NC(RNA) included an additional H-bond with the backbone of Lys34 (Fig. 10B).

On the contrary, docking-based binding mode of **8** showed that a significant contribution was given by polar contacts within the guanine binding site. In particular, two H-bond interactions were performed in both protein conformations with the backbone of Met46 and Trp37 (Fig. 11A and B). As observed for **6**, a hydrophobic interaction of stacking nature occurred between the aromatic moiety and the side-chain of Trp37, while the Phe16 was not contacted by **8**. The sulphonamide group was H-bonded with Arg32 of NC(DNA) and Lys47 of NC(RNA), whereas the hydroxyl group was H-bonded with Gln45 side-chain of NC(DNA).

These predicted binding modes could account for the antiretroviral activity observed *in vitro*, since residues mostly contacted by **6** and **8** through docking simulations have been highlighted by mutagenesis studies as critical for NC activity (Dannull et al., 1994; Schmalzbauer et al., 1996; Dorfman et al., 1993; Ottmann et al., 1995). Moreover, the stronger activity of **6** as compared to **8** is likely related to the more hydrophobic character of its interactions with NC, in line with the major role played by hydrophobic interactions in the binding of NC with its target nucleic acid sequences as well as with the very strong inhibitory activity observed for methylated oligonucleotides (Amarasinghe et al., 2000a; Bazzi et al., 2011; De Guzman et al., 1998; Bourbigot et al., 2008; Beltz et al., 2005; Avilov et al., 2008, 2012; Godet et al., 2011).

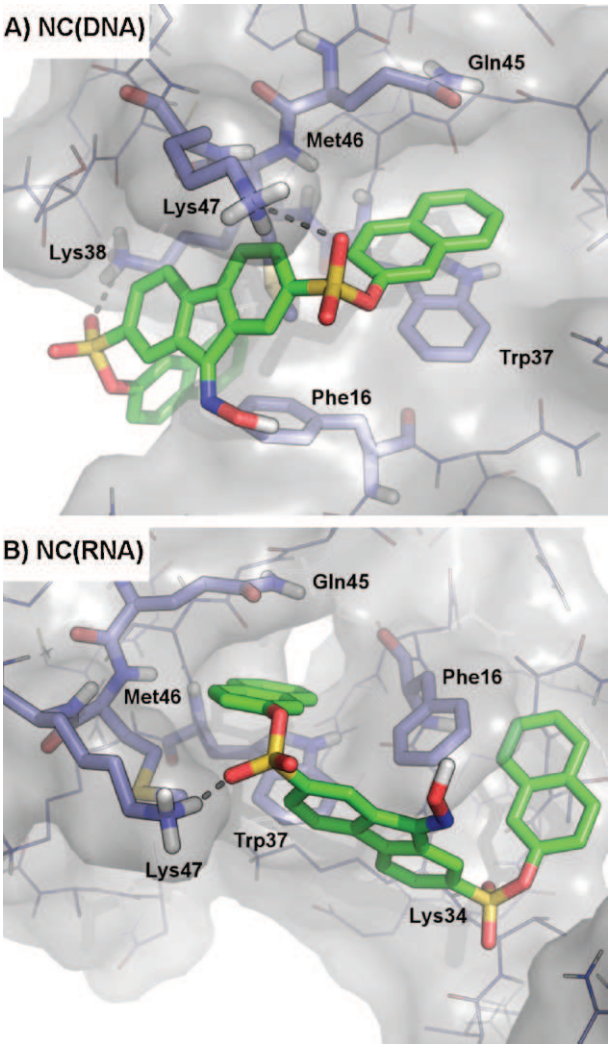

Fig. 10. Docking of **6** on (A) the NC(DNA) and (B) the NC(RNA) conformations of the protein. NC residues involved in binding to **6** are labeled and shown as sticks. Polar contacts are highlighted as dashed lines. The NC protein is showed as lines, sticks and surface. **6** is shown as green sticks. White, polar hydrogen; red, oxygen; deep blue, nitrogen; yellow, sulphur. (For interpretation of the references to color in this figure legend, the reader is referred to the web version of the article.)

4. Discussion

The HIV-1 nucleocapsid protein (NC) is being considered a potential drug target for the therapy of AIDS. Discovering small

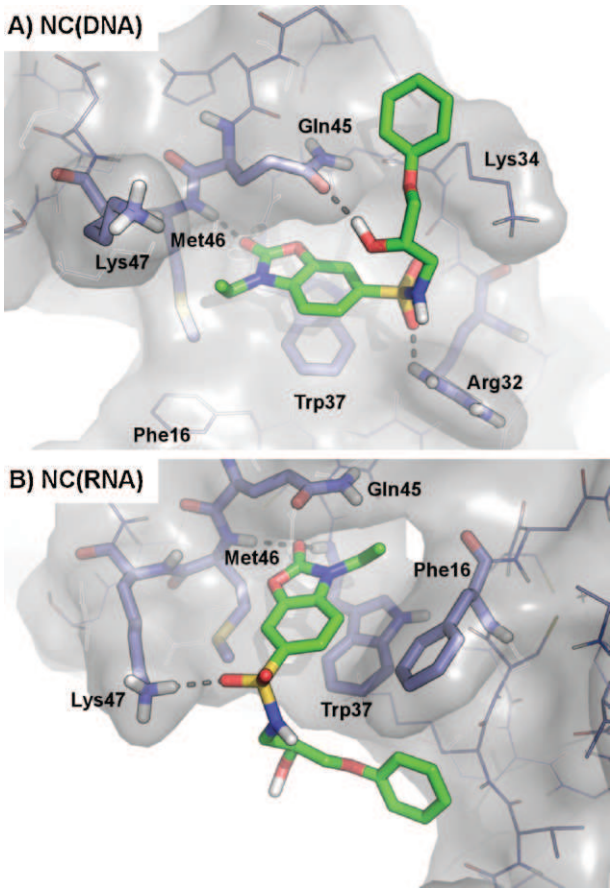

Fig. 11. Docking of **8** on (A) the NC(DNA) and (B) the NC(RNA) conformation of the protein. NC residues involved in binding to **8** are labeled and shown as sticks. Polar contacts are highlighted as dashed lines. The NC protein is showed as lines, sticks and surface. **8** is shown as green sticks. White, polar hydrogen; red, oxygen; deep blue, nitrogen; yellow, sulphur. (For interpretation of the references to color in this figure legend, the reader is referred to the web version of the article.)

molecules able to inhibit, or at least to modulate, the NC activity is of key importance for understanding the NC ligand binding properties and would promote the development of focused drug discovery campaigns.

Recently, we have used computational methods to study the conformational behavior and the energy profile of NC in complex with PBS–DNA and PSI–RNA. Moreover, we have established a molecular modeling protocol for exploring the molecular basis of NC inhibition by small molecules, to be used *in silico* for screening large chemical libraries. Starting from these checkpoints, in this work we performed a virtual screening of 391,535 compounds extracted from the ASINEX database, with the aim of discovering novel antiretroviral compounds that interfere with NC. To the best of our knowledge this is the first structure-based virtual screening approach targeting NC.

The ten most promising hits from virtual screening were purchased from ASINEX and their *in vitro* antiretroviral activity was tested. Seven compounds were active and the two most potent, namely **6** and **8**, showed an IC_{50} of 2 μM and around 100 μM without toxicity. The binding mode of **6** and **8** toward the NC(DNA) and the NC(RNA) structures was investigated by docking.

To try to elucidate the mechanism of action of **6** and **8** biophysical studies were performed, showing that tested compounds were not able to promote zinc ejection. Moreover, a direct interaction was evidenced between **6** and a NC(11–55) peptide labeled by a 3HC dye at its N-terminus. In contrast with docking studies, from the absence of changes in the Trp37 emission no direct stacking between Trp37 and **6** was observed in the complex, probably because of the very high intrinsic fluorescence of **6**. However, the measured binding affinity of **6** for NC(11–55), though weak, was comparable with the IC_{50} measured in cell culture. In the case of **8**, the interaction appears either of lower affinity or less perturbing than with compound **6** for the 3HC probe environment at the peptide N-terminus. In contrast, the small but reproducible decrease of Trp37 emission in the presence of **8** is consistent with a stacking of Trp37 with the aromatic moiety of compound **8**, in full line with the docking. The agreement between these data and docking studies supports the reliability of the computational protocol discussed here for designing NC inhibitors. This approach could be further used for trying to enhance the binding affinity of **6** and **8** toward NC by focused chemical optimization and for screening larger chemical libraries.

5. Conclusions

The multidisciplinary pipeline used in this work led us to discover two non-toxic small molecules, **6** and **8**, showing antiretroviral activity at micromolar concentrations and capable of interacting with NC. Their binding mode to NC was investigated by docking and was in agreement with biophysical evidences. These active compounds could be considered as tools for deepening the knowledge on NC functions as well as profitable lead compounds for further rational optimization. Taken together, our work represents a step forward for the chemical validation of NC as drug target.

Acknowledgments

This work was supported by grants from the Italian Fondazione Roma and the French Agency against AIDS (ANRS). This work was also supported by the European Union: "THINC", Collaborative Project, grant number HEALTH-2007-2.3.2-1;"CHAARM", Collaborative Project, grant number HEALTHF3-2009-242135.

References

Accelrys Discovery Studio 3.0, 2010. Accelrys, San Diego, CA.
Anonymous, 2011a. Epik, version 2.2. Schrodinger, LLC, New York.
Anonymous, 2011b. LigPrep, version 2.5. Schrodinger, LLC, New York.
Anonymous, 2011c. MacroModel, version 9.9. Schrodinger, LLC, New York.
Anonymous, 2011d. Maestro, version 9.2. Schrodinger, LLC, New York.
Anonymous, 2011. The 2011 UNAIDS World AIDS Day report.
Amarasinghe, G.K., De Guzman, R.N., Turner, R.B., Chancellor, K.J., Wu, Z.R., Summers, M.F., 2000a. NMR structure of the HIV-1 nucleocapsid protein bound to stem-loop SL2 of the PSI–RNA packaging signal. Implications for genome recognition. Journal of Molecular Biology 301, 491–511.
Amarasinghe, G.K., De Guzman, R.N., Turner, R.B., Summers, M.F., 2000b. NMR structure of stem-loop SL2 of the HIV-1 psi RNA packaging signal reveals a novel A-U-A base-triple platform. Journal of Molecular Biology 299, 145–156.
Anzellotti, A.I., Liu, Q., Bloemink, M.J., Scarsdale, J.N., Farrell, N., 2006. Targeting retroviral Zn finger–DNA interactions: a small-molecule approach using the electrophilic nature of trans-platinum–nucleobase compounds. Chemistry and Biology 13, 539–548.
Avilov, S.V., Boudier, C., Gottikh, M., Darlix, J.L., Mely, Y., 2012. Characterization of the inhibition mechanism of HIV-1 nucleocapsid protein chaperone activities by methylated oligoribonucleotides. Antimicrobial Agents and Chemotherapy 56, 1010–1018.
Avilov, S.V., Piemont, E., Shvadchak, V., de Rocquigny, H., Mely, Y., 2008. Probing dynamics of HIV-1 nucleocapsid protein/target hexanucleotide complexes by 2-aminopurine. Nucleic Acids Research 36, 885–896.
Bazzi, A., Zargarian, L., Chaminade, F., Boudier, C., de Rocquigny, H., Rene, B., Mely, Y., Fosse, P., Mauffret, O., 2011. Structural insights into the cTAR DNA recognition by the HIV-1 nucleocapsid protein: role of sugar deoxyriboses in the binding polarity of NC. Nucleic Acids Research 39, 3903–3916.
Beltz, H., Clauss, C., Piemont, E., Ficheux, D., Gorelick, R.J., Roques, B., Gabus, C., Darlix, J.L., de Rocquigny, H., Mely, Y., 2005. Structural determinants of HIV-1 nucleocapsid protein for cTAR DNA binding and destabilization, and correlation with inhibition of self-primed DNA synthesis. Journal of Molecular Biology 348, 1113–1126.
Bernacchi, S., Stoylov, S., Piemont, E., Ficheux, D., Roques, B.P., Darlix, J.L., Mely, Y., 2002. HIV-1 nucleocapsid protein activates transient melting of least stable parts

of the secondary structure of TAR and its complementary sequence. Journal of Molecular Biology 317, 385–399.
Bombarda, E., Morellet, N., Cherradi, H., Spiess, B., Bouaziz, S., Grell, E., Roques, B.P., Mely, Y., 2001. Determination of the pK(a) of the four Zn^{2+}-coordinating residues of the distal finger motif of the HIV-1 nucleocapsid protein: consequences on the binding of Zn^{2+}. Journal of Molecular Biology 310, 659–672.
Bourbigot, S., Ramalanjaona, N., Boudier, C., Salgado, G.F., Roques, B.P., Mely, Y., Bouaziz, S., Morellet, N., 2008. How the HIV-1 nucleocapsid protein binds and destabilises the (−)primer binding site during reverse transcription. Journal of Molecular Biology 383, 1112–1128.
Brown, S.P., Muchmore, S.W., 2007. Rapid estimation of relative protein–ligand binding affinities using a high-throughput version of MM–PBSA. Journal of Chemical Information and Modeling 47, 1493–1503.
Buckman, J.S., Bosche, W.J., Gorelick, R.J., 2003. Human immunodeficiency virus type 1 nucleocapsid Zn(2+) fingers are required for efficient reverse transcription, initial integration processes, and protection of newly synthesized viral DNA. Journal of Virology 77, 1469–1480.
Carteau, S., Batson, S.C., Poljak, L., Mouscadet, J.F., de Rocquigny, H., Darlix, J.L., Roques, B.P., Kas, E., Auclair, C., 1997. Human immunodeficiency virus type 1 nucleocapsid protein specifically stimulates Mg^{2+}-dependent DNA integration *in vitro*. Journal of Virology 71, 6225–6229.
Case, D.A., Darden, T.A., Cheatham, T.E., Simmerling, C.L., Wang, J., Duke, R.E., Luo, R., Walker, R.C., Zhang, W., Merz, K.M., Roberts, B.P., Wang, B., Hayik, S., Roitberg, A., Seabra, G., Kolossvary, I., Wong, K.F., Paesani, F., Vanichek, J., Liu, J., Wu, X., Brozell, S.R., Steinbrecher, T., Gohlke, H., Cai, Q., Ye, X., Wang, J., Hsieh, M.J., Cui, G., Roe, D.R., Mathews, D.H., Seetin, M.G., Sagui, C., Babin, V., Luchko, T., Gusarov, S., Kovalenko, A., Kollman, P.A., 2010. AMBER, 11. University of California, San Francisco.
Clever, J., Sassetti, C., Parslow, T.G., 1995. RNA secondary structure and binding sites for gag gene products in the 5′ packaging signal of human immunodeficiency virus type 1. Journal of Virology 69, 2101–2109.
Cruceanu, M., Stephen, A.G., Beuning, P.J., Gorelick, R.J., Fisher, R.J., Williams, M.C., 2006. Single DNA molecule stretching measures the activity of chemicals that target the HIV-1 nucleocapsid protein. Analytical Biochemistry 358, 159–170.
Dannull, J., Surovoy, A., Jung, G., Moelling, K., 1994. Specific binding of HIV-1 nucleocapsid protein to PSI RNA *in vitro* requires N-terminal zinc finger and flanking basic amino acid residues. EMBO Journal 13, 1525–1533.
Darlix, J.L., Godet, J., Ivanyi-Nagy, R., Fosse, P., Mauffret, O., Mely, Y., 2011. Flexible nature and specific functions of the HIV-1 nucleocapsid protein. Journal of Molecular Biology 410, 565–581.
Darlix, J.L., Vincent, A., Gabus, C., de Rocquigny, H., Roques, B., 1993. Trans-activation of the 5′–3′ viral DNA strand transfer by nucleocapsid protein during reverse transcription of HIV1 RNA. Comptes Rendus de l′ Academie des Sciences Serie III: Sciences de la Vie 316, 763–771.
De Guzman, R.N., Wu, Z.R., Stalling, C.C., Pappalardo, L., Borer, P.N., Summers, M.F., 1998. Structure of the HIV-1 nucleocapsid protein bound to the SL3 PSI–RNA recognition element. Science 279, 384–388.
de Rocquigny, H., Shvadchak, V., Avilov, S., Dong, C.Z., Dietrich, U., Darlix, J.L., Mely, Y., 2008. Targeting the viral nucleocapsid protein in anti-HIV-1 therapy. Mini Reviews in Medicinal Chemistry 8, 24–35.
Dietz, J., Koch, J., Kaur, A., Raja, C., Stein, S., Grez, M., Pustowka, A., Mensch, S., Ferner, J., Moller, L., Bannert, N., Tampe, R., Divita, G., Mely, Y., Schwalbe, H., Dietrich, U., 2008. Inhibition of HIV-1 by a peptide ligand of the genomic RNA packaging signal Psi. ChemMedChem 3, 749–755.
Dorfman, T., Luban, J., Goff, S.P., Haseltine, W.A., Gottlinger, H.G., 1993. Mapping of functionally important residues of a cysteine-histidine box in the human immunodeficiency virus type 1 nucleocapsid protein. Journal of Virology 67, 6159–6169.
Godet, J., Mely, Y., 2010. Biophysical studies of the nucleic acid chaperone properties of the HIV-1 nucleocapsid protein. RNA Biology 7, 687–699.
Godet, J., Ramalanjaona, N., Sharma, K.K., Richert, L., de Rocquigny, H., Darlix, J.L., Duportail, G., Mely, Y., 2011. Specific implications of the HIV-1 nucleocapsid zinc fingers in the annealing of the primer binding site complementary sequences during the obligatory plus strand transfer. Nucleic Acids Research 39, 6633–6645.
Goldschmidt, V., Miller Jenkins, L.M., de Rocquigny, H., Darlix, J.L., Mely, Y., 2010. The nucleocapsid protein of HIV-1 as a promising therapeutic target for antiviral drugs. HIV Therapy 4, 179–198.
Greenwood, J.R., Calkins, D., Sullivan, A.P., Shelley, J.C., 2010. Towards the comprehensive, rapid, and accurate prediction of the favorable tautomeric states of drug-like molecules in aqueous solution. Journal of Computer-Aided Molecular Design 24, 591–604.
Grigorov, B., Bocquin, A., Gabus, C., Avilov, S., Mely, Y., Agopian, A., Divita, G., Gottikh, M., Witvrouw, M., Darlix, J.L., 2011. Identification of a methylated oligoribonucleotide as a potent inhibitor of HIV-1 reverse transcription complex. Nucleic Acids Research 39, 5586–5596.
Jenkins, L.M., Byrd, J.C., Hara, T., Srivastava, P., Mazur, S.J., Stahl, S.J., Inman, J.K., Appella, E., Omichinski, J.G., Legault, P., 2005. Studies on the mechanism of inactivation of the HIV-1 nucleocapsid protein NCp7 with 2-mercaptobenzamide thioesters. Journal of Medicinal Chemistry 48, 2847–2858.
Jeong, Y.Y., Kim, S.H., Jang, S.I., You, J.C., 2008. Examination of specific binding activity of aptamer RNAs to the HIV-NC by using a cell-based *in vivo* assay for protein–RNA interaction. BMB Reports 41, 511–515.
Kim, S.J., Kim, M.Y., Lee, J.H., You, J.C., Jeong, S., 2002. Selection and stabilization of the RNA aptamers against the human immunodeficiency virus type-1 nucleocapsid protein. Biochemical and Biophysical Research Communications 291, 925–931.
Krishnamoorthy, G., Roques, B., Darlix, J.L., Mely, Y., 2003. DNA condensation by the nucleocapsid protein of HIV-1: a mechanism ensuring DNA protection. Nucleic Acids Research 31, 5425–5432.
Lapadat-Tapolsky, M., de Rocquigny, H., Van, G.D., Roques, B., Plasterk, R., Darlix, J.L., 1993. Interactions between HIV-1 nucleocapsid protein and viral DNA may have important functions in the viral life cycle. Nucleic Acids Research 21, 831–839.
Lapadat-Tapolsky, M., Gabus, C., Rau, M., Darlix, J.L., 1997. Possible roles of HIV-1 nucleocapsid protein in the specificity of proviral DNA synthesis and in its variability. Journal of Molecular Biology 268, 250–260.
Levin, J.G., Guo, J., Rouzina, I., Musier-Forsyth, K., 2005. Nucleic acid chaperone activity of HIV-1 nucleocapsid protein: critical role in reverse transcription and molecular mechanism. Progress in Nucleic Acid Research and Molecular Biology 80, 217–286.
Li, Y., Liu, Z., Wang, R., 2010. Test MM-PB/SA on true conformational ensembles of protein–ligand complexes. Journal of Chemical Information and Modeling 50, 1682–1692.
Loo, J.A., Holler, T.P., Sanchez, J., Gogliotti, R., Maloney, L., Reily, M.D., 1996. Biophysical characterization of zinc ejection from HIV nucleocapsid protein by anti-HIV 2,2′-dithiobis[benzamides] and benzisothiazolones. Journal of Medicinal Chemistry 39, 4313–4320.
Mayasundari, A., Rice, W.G., Diminnie, J.B., Baker, D.C., 2003. Synthesis, resolution, and determination of the absolute configuration of the enantiomers of cis-4,5-dihydroxy-1,2-dithiane 1,1-dioxide, an HIV-1NCp7 inhibitor. Bioorganic and Medicinal Chemistry 11, 3215–3219.
Mely, Y., de Rocquigny, H., Morellet, N., Roques, B.P., Gerad, D., 1996. Zinc binding to the HIV-1 nucleocapsid protein: a thermodynamic investigation by fluorescence spectroscopy. Biochemistry 35, 5175–5182.
Mely, Y., Piemont, E., Sorinas-Jimeno, M., de Rocquigny, H., Jullian, N., Morellet, N., Roques, B.P., Gerard, D., 1993. Structural and dynamic characterization of the aromatic amino acids of the human immunodeficiency virus type I nucleocapsid protein zinc fingers and their involvement in heterologous tRNA(Phe) binding: a steady-state and time-resolved fluorescence study. Biophysical Journal 65, 1513–1522.
Miller Jenkins, L.M., Hara, T., Durell, S.R., Hayashi, R., Inman, J.K., Piquemal, J.P., Gresh, N., Appella, E., 2007. Specificity of acyl transfer from 2-mercaptobenzamide thioesters to the HIV-1 nucleocapsid protein. Journal of the American Chemical Society 129, 11067–11078.
Mirambeau, G., Lyonnais, S., Gorelick, R.J., 2010. Features, processing states, and heterologous protein interactions in the modulation of the retroviral nucleocapsid protein function. RNA Biology 7, 724–734.
Montenay-Garestier, T., Toulme, F., Fidy, J., Toulme, J.J., Le Doan, T., Helene, C., 1993. Structure and dynamics of peptide-nucleic acid complexes. In: Helene, C. (Ed.), Structure, Dynamics, Interactions and Evolution of Biological Macromolecules D. Reidel Publishing Company, Dordrecht, the Netherlands, pp. 113–128.
Morellet, N., Jullian, N., de Rocquigny, H., Maigret, B., Darlix, J.L., Roques, B.P., 1992. Determination of the structure of the nucleocapsid protein NCp7 from the human immunodeficiency virus type 1 by 1H NMR. EMBO Journal 11, 3059–3065.
Mori, M., Dietrich, U., Manetti, F., Botta, M., 2010. Molecular dynamics and DFT study on HIV-1 nucleocapsid protein-7 in complex with viral genome. Journal of Chemical Information and Modeling 50, 638–650.
Mori, M., Manetti, F., Botta, M., 2011a. Predicting the binding mode of known NCp7 inhibitors to facilitate the design of novel modulators. Journal of Chemical Information and Modeling 51, 446–454.
Mori, M., Manetti, F., Botta, M., 2011b. Targeting protein–protein and protein–nucleic acid interactions for anti-HIV therapy. Current Pharmaceutical Design 17, 3713–3728.
Ottmann, M., Gabus, C., Darlix, J.L., 1995. The central globular domain of the nucleocapsid protein of human immunodeficiency virus type 1 is critical for virion structure and infectivity. Journal of Virology 69, 1778–1784.
Pannecouque, C., Szafarowicz, B., Volkova, N., Bakulev, V., Dehaen, W., Mely, Y., Daelemans, D., 2010. Inhibition of HIV-1 replication by a bis-thiadiazolbenzene-1,2-diamine that chelates zinc ions from retroviral nucleocapsid zinc fingers. Antimicrobial Agents and Chemotherapy 54, 1461–1468.
Quintal, S.M., dePaula, Q.A., Farrell, N.P., 2011. Zinc finger proteins as templates for metal ion exchange and ligand reactivity. Chemical and biological consequences. Metallomics 3, 121–139.
Raja, C., Ferner, J., Dietrich, U., Avilov, S., Ficheux, D., Darlix, J.L., de Rocquigny, H., Schwalbe, H., Mely, Y., 2006. A tryptophan-rich hexapeptide inhibits nucleic acid destabilization chaperoned by the HIV-1 nucleocapsid protein. Biochemistry 45, 9254–9265.
Rein, A., Henderson, L.E., Levin, J.G., 1998. Nucleic-acid-chaperone activity of retroviral nucleocapsid proteins: significance for viral replication. Trends in Biochemical Sciences 23, 297–301.
Rice, W.G., Schaeffer, C.A., Harten, B., Villinger, F., South, T.L., Summers, M.F., Henderson, L.E., Bess Jr., J.W., Arthur, L.O., McDougal, J.S., 1993. Inhibition of HIV-1 infectivity by zinc-ejecting aromatic C-nitroso compounds. Nature 361, 473–475.
Rist, M.J., Marino, J.P., 2002. Mechanism of nucleocapsid protein catalyzed structural isomerization of the dimerization initiation site of HIV-1. Biochemistry 41, 14762–14770.
Schmalzbauer, E., Strack, B., Dannull, J., Guehmann, S., Moelling, K., 1996. Mutations of basic amino acids of NCp7 of human immunodeficiency virus type 1 affect RNA binding *in vitro*. Journal of Virology 70, 771–777.
Shelley, J.C., Cholleti, A., Frye, L.L., Greenwood, J.R., Timlin, M.R., Uchimaya, M., 2007. Epik: a software program for pK(a) prediction and protonation state

Please cite this article in press as: Mori, M., et al., Use of virtual screening for discovering antiretroviral compounds interacting with the HIV-1 nucleocapsid protein. Virus Res. (2012), http://dx.doi.org/10.1016/j.virusres.2012.05.011

generation for drug-like molecules. Journal of Computer-Aided Molecular Design 21, 681–691.
Shvadchak, V., Sanglier, S., Rocle, S., Villa, P., Haiech, J., Hibert, M., Van, D.A., Mely, Y., de Rocquigny, H., 2009a. Identification by high throughput screening of small compounds inhibiting the nucleic acid destabilization activity of the HIV-1 nucleocapsid protein. Biochimie 91, 916–923.
Shvadchak, V.V., Klymchenko, A.S., de Rocquigny, H., Mely, Y., 2009b. Sensing peptide-oligonucleotide interactions by a two-color fluorescence label: application to the HIV-1 nucleocapsid protein. Nucleic Acids Research 37, e25.
South, T.L., Summers, M.F., 1993. Zinc- and sequence-dependent binding to nucleic acids by the N-terminal zinc finger of the HIV-1 nucleocapsid protein: NMR structure of the complex with the PSI-site analog, dACGCC. Protein Science 2, 3–19.
Stephen, A.G., Worthy, K.M., Towler, E., Mikovits, J.A., Sei, S., Roberts, P., Yang, Q.E., Akee, R.K., Klausmeyer, P., McCloud, T.G., Henderson, L., Rein, A., Covell, D.G., Currens, M., Shoemaker, R.H., Fisher, R.J., 2002. Identification of HIV-1 nucleocapsid protein: nucleic acid antagonists with cellular anti-HIV activity. Biochemical and Biophysical Research Communications 296, 1228– 1237.
Thomas, J.A., Gorelick, R.J., 2008. Nucleocapsid protein function in early infection processes. Virus Research 134, 39–63.
Thompson, D.C., Humblet, C., Joseph-McCarthy, D., 2008. Investigation of MM-PBSA rescoring of docking poses. Journal of Chemical Information and Modeling 48, 1081–1091.
Tisne, C., Roques, B.P., Dardel, F., 2004. The annealing mechanism of HIV-1 reverse transcription primer onto the viral genome. Journal of Biological Chemistry 279, 3588–3595.
Wolber, G., Langer, T., 2005. LigandScout: 3-D pharmacophores derived from protein-bound ligands and their use as virtual screening filters. Journal of Chemical Information and Modeling 45, 160–169.

Please cite this article in press as: Mori, M., et al., Use of virtual screening for discovering antiretroviral compounds interacting with the HIV-1 nucleocapsid protein. Virus Res. (2012), http://dx.doi.org/10.1016/j.virusres.2012.05.011

Antiviral Peptides: physicochemical properties

The nucleocapsid protein, either as a domain of the Gag polyprotein precursor or as a mature protein, is critical for several steps in the viral life cycle. NC is involved in viral genomic RNA packaging, particle assembly, reverse transcription and integration (Darlix, Cristofari et al. 2000). For example, selection of viral RNA for packaging is mediated by binding between the NC domain within Gag and the Ψ encapsidation sequence within the untranslated region of the HIV-1 genome. Moreover, NC is a nucleic acid chaperone, driving nucleic acids into their thermodynamically most stable conformation and favoring annealing of complementary structures. NC notably chaperones the two obligatory strand transfers necessary for the synthesis of a complete proviral DNA by reverse transcriptase (Clever, Sassetti et al. 1995). The critical role of NC in the viral life cycle is illustrated by the fact that point mutations disrupting the globular structure of the zinc fingers result in a complete loss of virus infectivity.

Due to the highly conserved sequence of NC and its crucial function during HIV-1 life cycle, molecules directed against NC are believed to be able to complement the highly active anti-retroviral therapies (HAART) based on drugs targeting the viral enzymes. Anti-NC drugs are thought to provide a sustained replication inhibition of a large panel of HIV-1 isolates including virus strains resistant to drugs targeting viral enzymes. Recently, within the European consortium TRIoH, new strategies to specifically target the nucleic acid chaperone properties of NC were developed. According to a strategy protected by a submitted patent, a series of peptides have been designed to act as competitors for NC and thus, inhibit virus replication. Among this series, several peptides were found to efficiently inhibit the nucleic acid destabilization properties of NC.

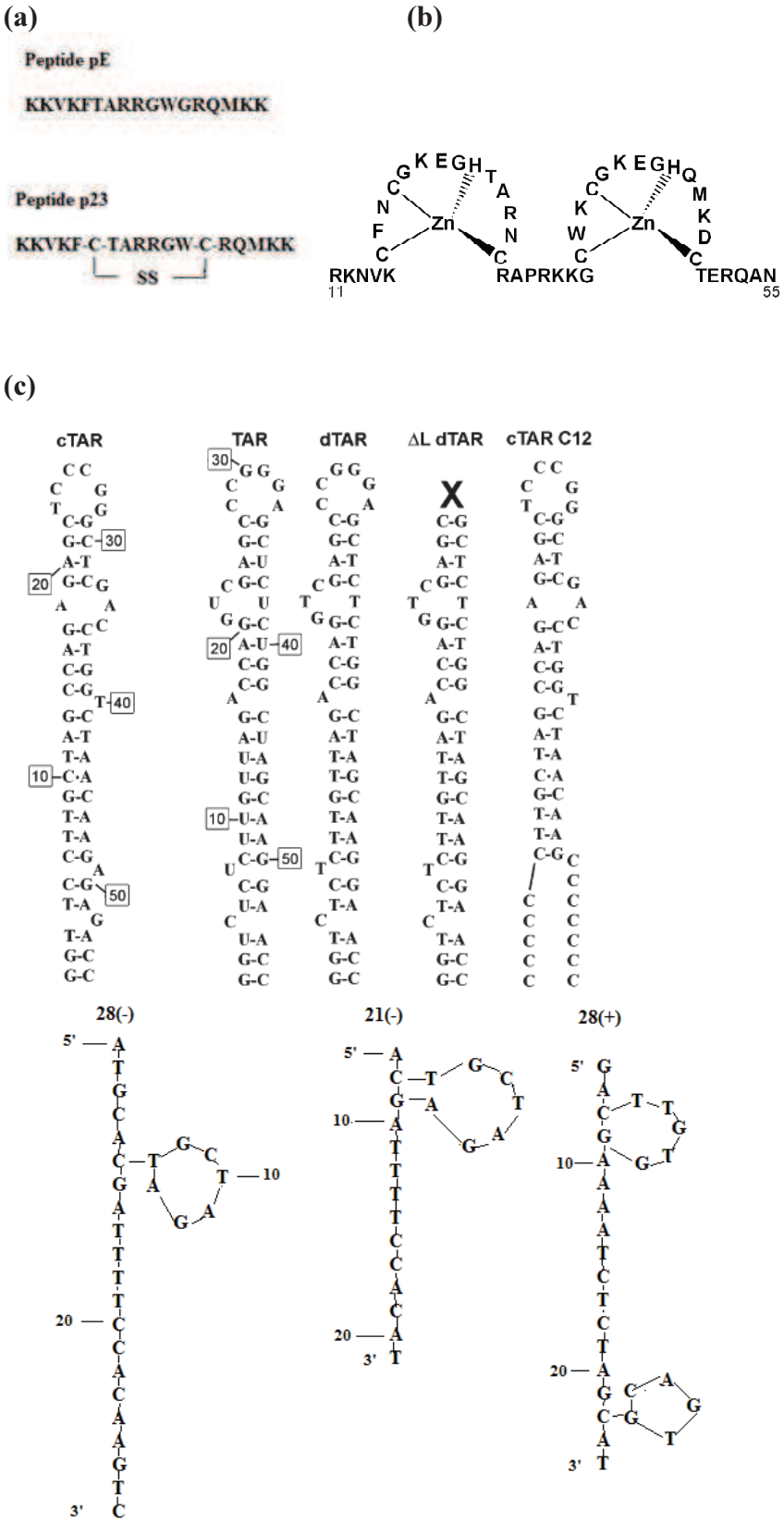

Fig.76. Structure of the tested antiviral peptides (a), nucleocapsid protein (b) and oligonucleotides (c) used in this study. The cTAR and dTAR sequences are from the HIV-1 MAL strain. The secondary structures of the

oligonucleotides were predicted from the structure of TAR and the mfold program (http://mfold.rna.albany.edu/?q=mfold/DNA-Folding-Form).

Due to the fact that positively charged peptides are known to aggregate nucleic acids in a concentration-dependent manner, we first determined aggregation-free conditions by using Fluorescence Correlation Spectroscopy and performed further experiments in these conditions.

Peptide pE or peptide p23 was added to the labeled cTAR sequences at different nucleotide to peptide ratios. To avoid high local concentrations during mixing, both reactants were of the same volume. Assuming that peptide pE diffuses freely in a Gaussian excitation volume, the normalized autocorrelation function, G(τ), calculated from the fluorescence fluctuations was fitted according to equation 8 (see Materials and Methods).

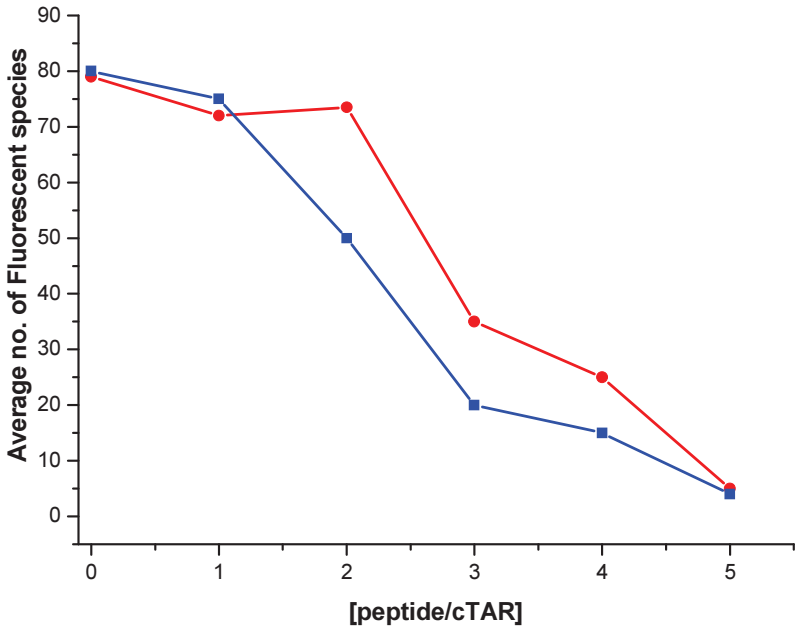

Fig.77. Evidence by fluorescence correlation spectroscopy of peptide-induced aggregation of TMR-5'-cTAR. The average number of fluorescent species, N, for 300 nM of TMR-5'-cTAR within the excitation volume was obtained by fitting the autocorrelation curves to Equation 8. The curves are given with peptide pE (red) and p23 (blue).

Aggregation of the TMR-labeled 5'-cTAR molecules by the tested peptides is expected to decrease the number of fluorescent species. In the absence of peptide, the number of fluorescent TAR molecules was in full agreement with the theoretical number of molecules

expected from their concentration. By adding increasing concentrations of either p23 or pE peptide, we found no change in the number of fluorescent species up to a peptide/ODN molar ratio of 1:1 or 2:1, for p23 and pE, respectively. This indicates that no aggregation occurred under these conditions. In contrast, aggregation took place at higher ratios as evidenced by the sharp drop in the number of fluorescent species. As a consequence, we selected a peptide/ODN molar ratio of 1:1 and 2:1 for p23 and pE, respectively, to characterize the properties of the peptides. Since the peptides share some structural features with NC, we first determined whether the two peptides exhibit nucleic acid chaperone properties analogous to NC.

Destabilization properties of the examined peptides

To characterize the nucleic acid destabilizing properties of the peptides, cTAR labelled at its 5' and 3' ends either by Rh6G and DABCYL, as a fluorophore and a quencher respectively, were used. The dyes form a nonfluorescent heterodimer when the cTAR stem is closed, while melting of the stem restores the fluorophore fluorescence. Thus, the destabilizing ability of the peptides can be evaluated from the ratio of the fluorescence intensity in the presence versus in the absence of the peptide.

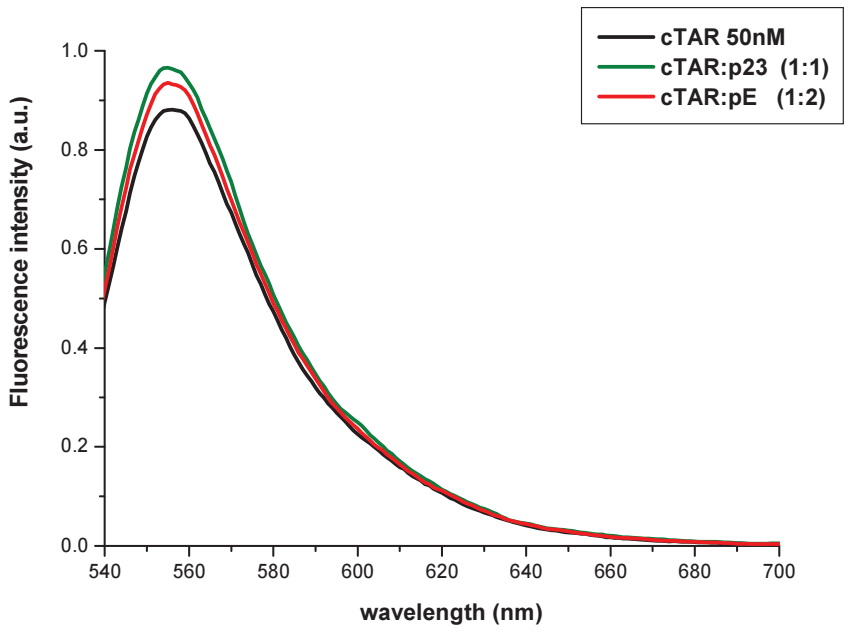

Fig.78. Absence of destabilization of cTAR secondary structure by peptides p23 and pE. Fluorescence emission spectra of 50 nM Rh6G-5′-cTAR-3′-Dabcyl in the absence (black line) and in the presence of 100 nM pE (red), or 50 nM p23 peptide (green), in 25 mM Tris–HCl (pH 7.5), 30 mM NaCl, 0.2 mM $MgCl_2$ at 20 °C. Excitation wavelength was 520 nm.

The fluorescence spectra of the doubly labeled cTAR mixed with an equimolar concentration of peptide p23 or a two-fold molar excess of peptide pE at 20^0C were nearly superimposable with the emission spectrum of the free cTAR species (Fig.78). This indicates that both peptides were not able to destabilize the secondary structure of cTAR, under the present conditions. Our data is in a agreement with the results obtained for the $(SSHS)_2$NC(1–55) peptide (Beltz, Clauss et al. 2005) further indicating that the folded zinc fingers are essential determinants for the NC destabilizing activity.

Next, the inhibition properties of tested peptides towards the NC-induced cTAR destabilization were investigated. Peptides were observed to strongly inhibit NC destabilization activity, likely by competing with NC for the binding to its DNA substrates. Both peptides caused almost 90% of NC inhibition in the first 20 minutes of treatment whereas full inhibition was achieved in less than 70 minutes of incubation (fig.79).

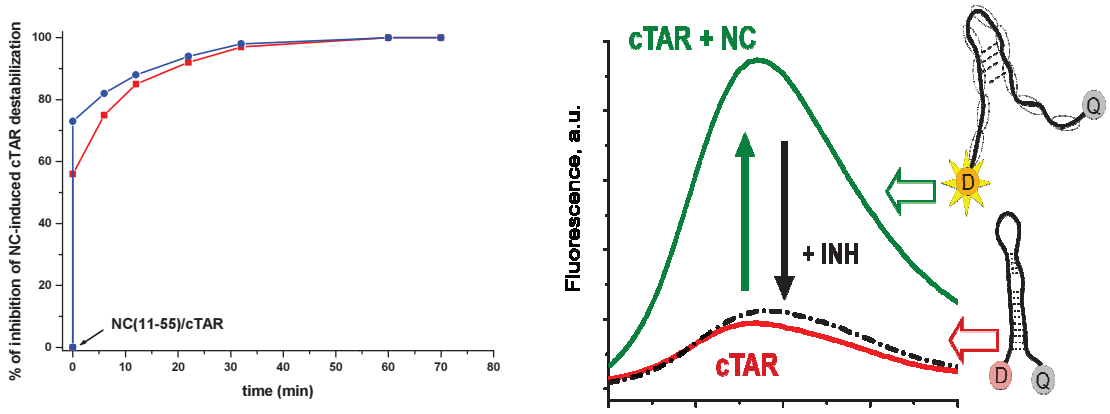

Fig.79. Peptides p23 and pE inhibit the nucleic acid destabilization properties of NC. (On the left) Percentage of inhibition of cTAR destabilization induced by NC(11-55) as a function of incubation time with p23 (blue) and pE (red) peptides. The doubly labeled cTAR (0.1μM) was mixed with 10 molar excess of NC(11-55). Next, tested peptides at 1μM concentration were added to the mixture of ODN/NC. (On the right) schematic representation of peptide-induced inhibition of NC-induced cTAR destabilization.

Kinetics of cTAR-dTAR annealing in the presence of peptide pE.

To determine the ability of pE to promote the annealing of two complementary oligonucleotides, the real-time annealing kinetics of cTAR with dTAR was monitored by mixing TMR-5'-cTAR-3'-Fl with an excess of non-labeled dTAR, in the presence of peptide pE added at a peptide/ODN ratio of 2:1. Formation of the 55-bp cTAR/dTAR extended

duplex (ED) strongly increases the interchromophore distance, leading to a full recovery of Fl emission.

Peptide pE strongly accelerated the annealing reaction, since it was complete in less than 90 min, while it needed more than 36 h in the absence of peptide. The final plateau was independent of the dTAR concentration, suggesting that pE was not able to dissociate the final ED. The annealing kinetic traces were fitted using the biexponential equation 11.

The experiments with various dTAR concentrations indicated a linear and saturation behaviour for k_{obs1} and k_{obs2} values, respectively (Fig.80). This behaviour is consistent with the two-step reaction scheme already described for the HIV-1 NCp7- or Tat- promoted cTAR/dTAR annealing where a rate-limiting interconversion (k_f and k_b) step is coupled to a much faster, preceding binding step, considered as a fast pre-equilibrium, governed by the equilibrium constant K_M:

$$\text{cTAR+dTAR} \overset{K_M}{\rightleftharpoons} \text{IC} \underset{k_b}{\overset{k_f}{\rightleftharpoons}} \text{ED}$$

Scheme 1

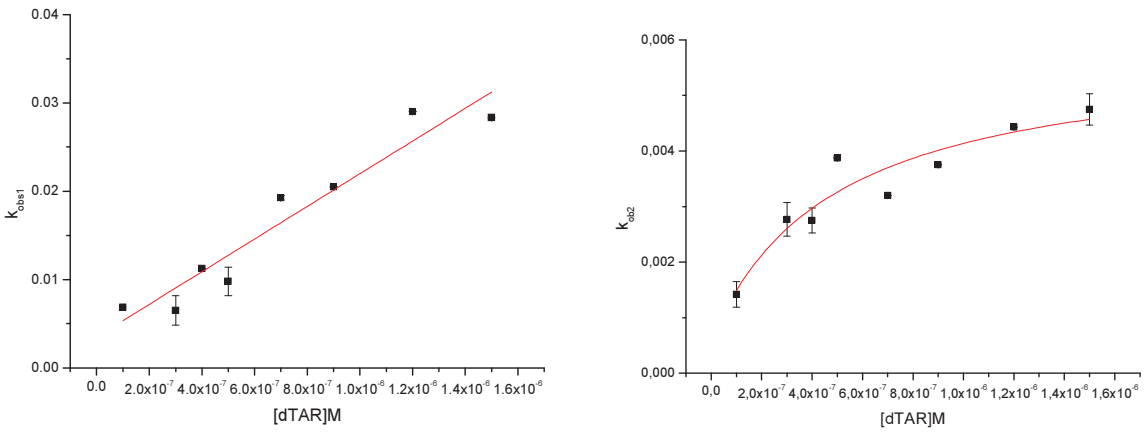

Fig.80. Kinetic parameters of the peptide pE- promoted cTAR/dTAR annealing. The observed rate constants for the fast kinetic phase (k_{obs1}) and the slow one (k_{obs2}) were plotted as a function of dTAR concentration. Each data point represents the mean of 3 measurements.

The hyperbolic dependence of k_{obs2} may be ascribed to IC accumulation as a consequence of its slow conversion into ED which likely constitutes the rate-limiting step of the annealing pathway. If the pre-equilibrium is rapidly reached, scheme 1 predicts a linear variation of k_{obs1} according to:

$k_{obs1} = k_{ass}[\mathrm{dTAR}] + k_{diss}$ equation 17

where, k_{ass} is the second order association rate constant and k_{diss} is the first order dissociation rate constant. On the other hand, the hyperbolic variation of k_{obs2} can be described by:

$$k_{obs} = \frac{k_f K_M [dTAR]}{1 + K_M [dTAR]} + k_b$$ equation 18

By fitting the data of Fig 70a with eq. 17, from the slope and the intercept with the Y axis, we found k_{ass} = 1,8×10^4 M^{-1}s^{-1} and k_{diss} = 3,5×10^{-3} s^{-1}. Non-linear regression of the k_{obs2} data (Fig.80b) with equation 18 yielded k_f = 5×10^{-3} s^{-1} and K_M = 2×10^{6}M^{-1}.

Taken together, a reaction mechanism with a single kinetic pathway can be proposed for the pE-promoted reaction:

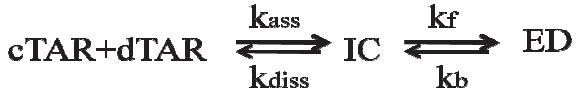

Formation of IC is governed by the second order association rate constant, k_{ass}, and the first order dissociation rate constant, k_{diss}, while the interconversion of IC to ED is governed by the forward and backward interconversion rate constants, k_f and k_b.

To check the validity of the postulated two-step annealing mechanism, we used the Dynafit numerical resolution software. This program analyses chemical systems on the basis of the written reaction mechanism, using the differential equations derived for the mechanism. By fitting simultaneously the experimental progress curves obtained at different complementary sequence concentrations, we obtained an excellent agreement with the experimental values for all variables, thus strengthening the proposed reaction mechanism.

From the DynaFit analysis, it was also observed that the IC fluorescence intensity corresponds to 87% of the ED fluorescence. This result was close to that reported for the HIV-1 Tat protein (Boudier, Storchak et al.), where the IC fluorescence intensity corresponded to 93% of the final fluorescence intensity. Based on the degree of ODN melting, the mechanism by which pE promotes the annealing reaction is likely similar to the one proposed for the Tat

protein with the IC formation requiring premelting of approximately three to five base pairs of the terminal double-stranded segments of cTAR.

Furthermore, the binding constant of the intermediate is about two orders of magnitude lower than that with NC(1-55), added at a ratio of 10 peptides per oligonucleotide ($K=10^8$ M^{-1}) (Vo, Barany et al. 2009). This difference may in part be explained by the incomplete coating of the oligonucleotides by pE, since the binding equilibrium constant of the intermediate was shown to be strongly dependent on the level of protein coating in the case of NCp7 (with an about 3 orders of magnitude difference between low and full coating). Interestingly, comparison with HCV core protein and HIV-1 Tat at similar coating level showed strong similarity for the binding constant of the intermediate complex (Sharma K 2010). Interestingly, the k_f value was only 6 times lower than the 0.03 s^{-1} value of the corresponding parameter obtained with NC (1-55). The comparison of this parameter for the two proteins is much easier, since this parameter was found poorly dependent on the level of protein coating. Thus, pE appears to promote the conversion of the intermediate to the final extended duplex, with an efficiency only slightly lower than NCp7.

Effect of the oligonucleotide sequence on the peptide pE-promoted annealing kinetics

Next, we characterized the molecular determinants of the annealing reaction promoted by pE. To characterize the possible role of the central loops, we used ΔL dTAR, a dTAR mutant where the loop was replaced by a flexible hexaethylenglycol tether. No change in the time course of the formation of the extended duplex was observed with this mutant, indicating that loop-loop interactions do not play a significant role in the pE-promoted cTAR/dTAR annealing reaction. This confirms that the annealing process is most probably initiated through the cTAR and dTAR stems. To confirm the role of the stems in the initiation of the annealing reaction, cTAR was substituted with the cTAR1,2 derivative where bases complementary to the bulged bases at position 49 and 52 have been introduced in order to stabilize the lower half of the stem. The reaction of TMR-5'-cTAR1,2-3′-Fl with dTAR in the presence of the peptide pE was much slower than with cTAR.

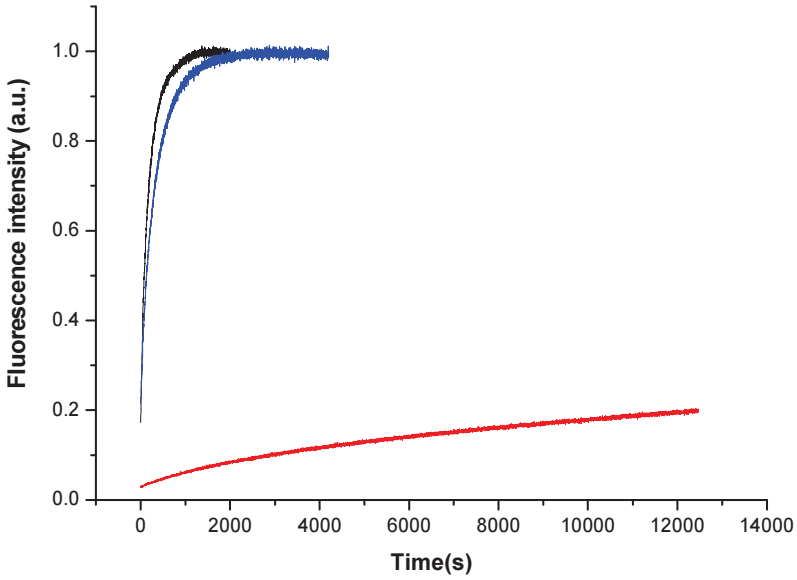

Fig.81. Kinetics of the peptide pE-promoted annealing of cTAR derivatives with TAR or dTAR derivatives. Kinetic traces of 10 nM doubly labeled cTAR derivatives with 300 nM nonlabeled TAR or dTAR derivatives. cTAR/dTAR (blue), cTAR/dTAR-TL (black) and cTAR1,2/dTAR (red). Peptide pE was added at a peptide/oligonucleotide ratio of 2:1 in all the cases. All the experiments were performed in 25 mM Tris–HCl (pH 7.5), 30 mM NaCl and 0.2 mM $MgCl_2$, at 20 °C.

These results proved that the kinetic pathway of the peptide pE-promoted annealing reaction is primarily mediated through the stems of cTAR and dTAR.

To get further insight into the reaction pathway, the temperature dependence of the k_{obs} values was monitored as a function of the temperature and analyzed using the Arrhenius equation (equation 13, Material and Methods)

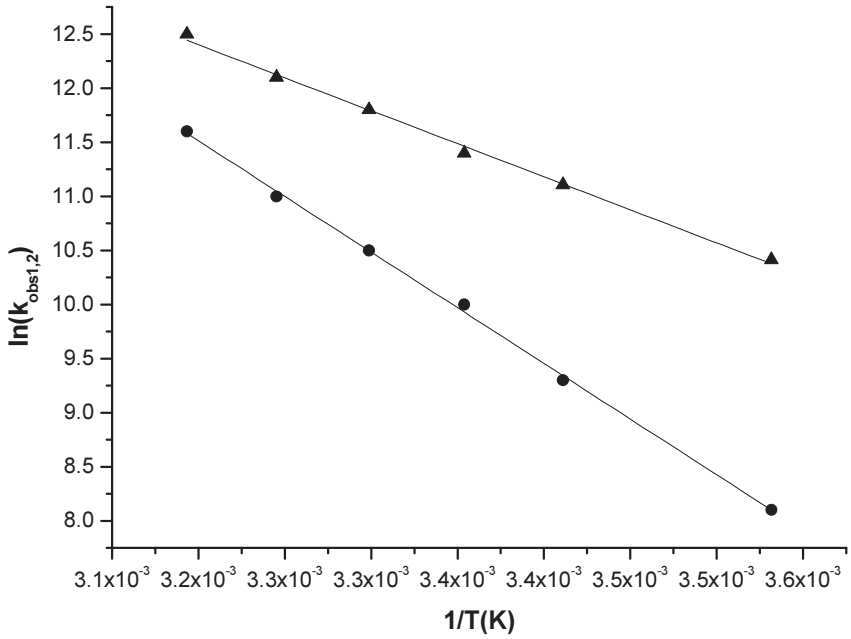

Fig.82. Temperature dependence of the cTAR/dTAR annealing kinetics promoted by peptide pE at a peptide to oligonucleotide ratio of 2:1. 10 nM of doubly-labeled cTAR was reacted with 300 nM dTAR in 25 mM Tris–HCl (pH 7.5), 30 mM NaCl, 0.2 mM $MgCl_2$. The fast (▲) and slow (•) kinetic rate constants were fitted according to the Arrhenius equation.

Both reaction rates increased with temperature, giving positive enthalpy values for the transition state of 12.2 ± 1 kcal /mol and 25.5 ± 1 kcal/mol for the fast and slow components, respectively. These values indicate that the pE-promoted cTAR/dTAR annealing involves premelting of three base pairs for the fast component and five-six base pairs for the slow component.

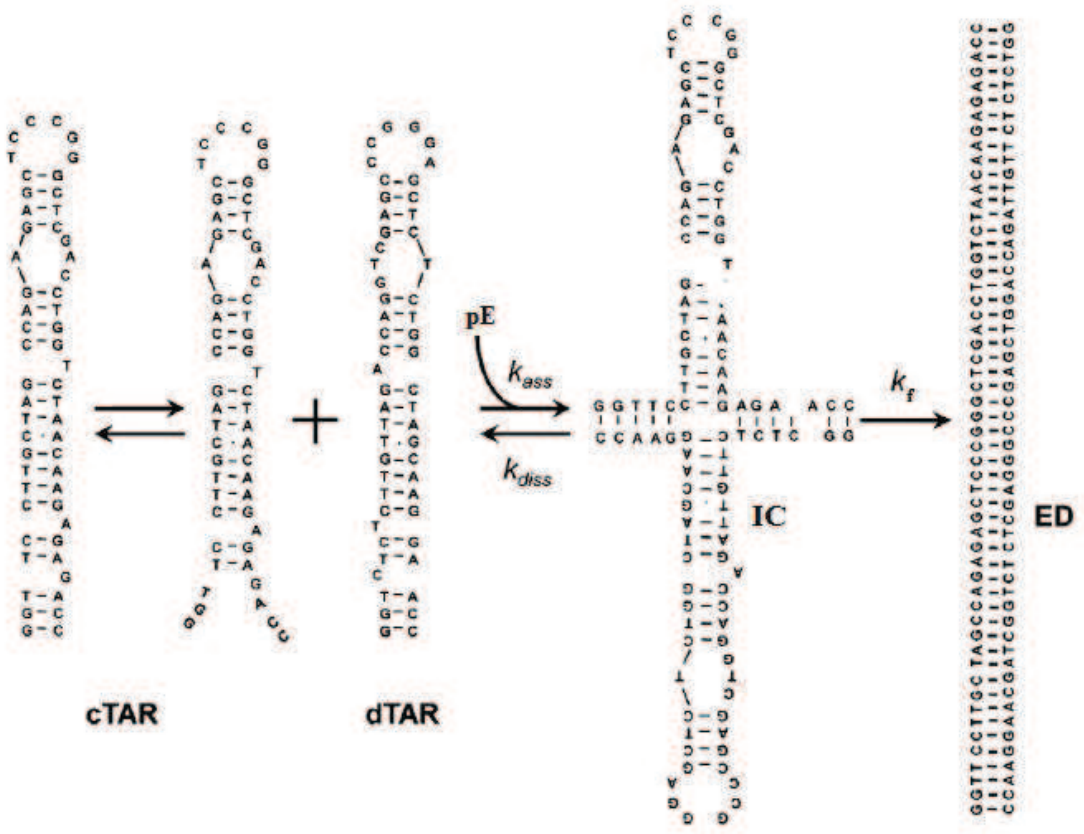

Fig. 83. Proposed reaction scheme for the pE-directed cTAR/dTAR annealing. In the presence of the peptide, the reactive cTAR conformer, spontaneously generated by thermal fraying, anneals to its complementary sequence through their stem termini. This leads to a reversible intermediate IC which further converts into the final extended duplex (ED), in a step rate-limited by the melting of the more stable upper portion of the stems.

Comparison of the nucleic acid annealing activity of peptide pE and NCp7

To further investigate the annealing properties of pE, we compared them to those of NC (11-55), a truncated NC peptide with a nucleic acid destabilizing activity similar to that of the full length protein, but with lower nucleic acid aggregating properties. The annealing kinetics of the doubly labelled cTAR to dTAR (10 and 100 nM, respectively) in the presence of pE at a peptide to ODN molar ratio of 2:1 was compared to the annealing kinetics with NC(11-55) added at ratios of 4:1, 5:1 and 7:1 (Fig.84a). It was observed that two molecules of pE exhibited the same annealing activity as seven molecules of NC (11-55). This was confirmed by experiments with peptide mixtures, since the kinetic curves with pE added at a ratio of 2:1 and NC(11-55) at a ratio of 3:1 were almost perfectly superimposable to those obtained in the presence of NC(11-55) alone at the ratio of 10:1, respectively (Fig.84b). In contrast, the kinetic curves with pE added at a ratio of 1:1 and NC (11-55) at a ratio of 3:1 seems to be much faster when compared with those obtained with NC (11-55) alone at ratio 7:1. Thus

depending on the respective concentrations of NC (11-55) and pE, the effect of the two peptides is synergistic or additive.

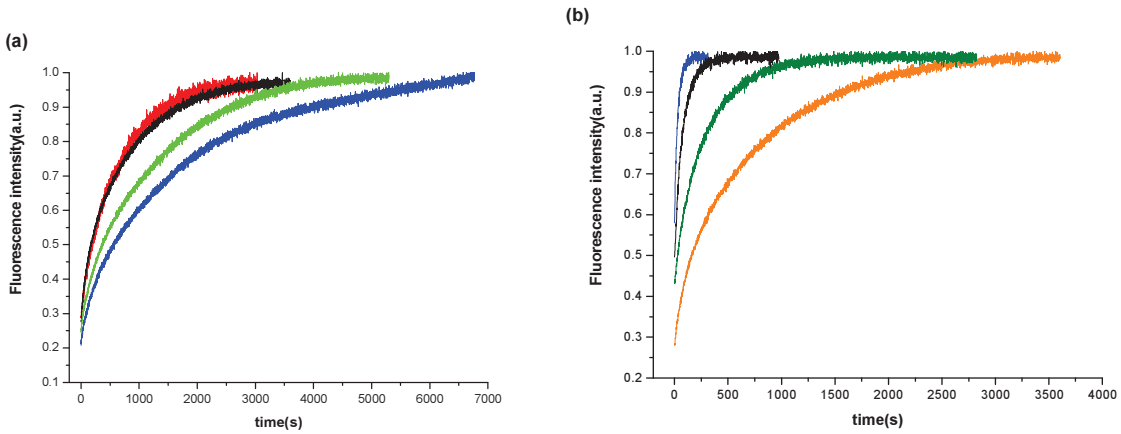

Fig.84. Comparison of the annealing properties of pE and NC(11-55) peptides. All progress curves shown describe the peptide-promoted reactions of 10 nM doubly labelled cTAR with 100 nM dTAR. (a) Comparison of the cTAR/dTAR annealing kinetics obtained in the presence of peptide pE at peptide to oligonucleotide molar ratio of 2:1 (red curve) and NC(11-55) at ratio of 4:1 (blue), 6:1 (green) and 7:1 (black). (b) cTAR/dTAR annealing kinetics observed in the presence of a mixture of pE and NC(11-55), added at molar ratio 3:1 and 2:1, respectively (green trace) and in the presence of NC(11-55) alone (molar ratio 7:1, orange trace). Similar annealing kinetics were also recorded in the presence of a mixture of peptide pE and NC(11-55) (ratio 1:1 and 3:1, respectively, black trace) and NC(11-55) alone (ratio 10:1, blue trace).

cTAR/dTAR annealing promoted by peptide p23

Next, we investigated the effect of the peptide p23 on the annealing of cTAR with dTAR, to determine whether it promotes the annealing reaction through the same mechanism as peptide pE (Fig.85). The annealing kinetics in presence of p23 was also biphasic with a linear and hyperbolic dependence of k_{obs1} and k_{obs2}, respectively, on the concentration of dTAR.

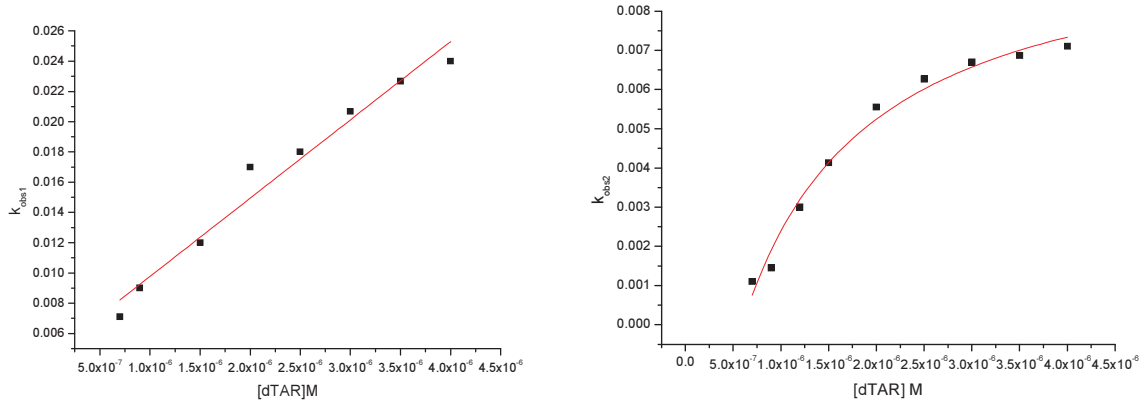

Fig.85. Kinetic parameters of the p23-promoted cTAR/dTAR annealing. The observed rate constants for the fast kinetic phase (k_{obs1}) and the slow one (k_{obs2}) were plotted as a function of dTAR concentration. Each data point represents the mean of 3 measurements.

Since the Km value depends strongly on the coating level of ODN by peptides, comparison of this parameter for pE and p23 is not possible. In contrast, the comparison of the k_f parameter is relevant, since this parameter was found poorly dependent on the level of protein coating. The k_f value for p23 was found only 2 times lower than that for pE. Thus, p23 appears to promote the conversion of the intermediate to the final extended duplex, with an efficiency slightly lower than pE.

In all cases, the k_b value was found to be close to zero indicating that dissociation of the ED was negligible. Once the intermediate complex is formed, it is converted by the p23 and pE peptides into the ED.

Labelled sequence	Complementary sequence	Peptide	Ratio of peptide/ ODN	k_{diss} (s^{-1})	k_f (s^{-1})	K_M (M^{-1})
cTAR	dTAR	pE	2	$3.5x10^4$	$5x10^3$	$2.05x10^{-6}$
cTAR	dTAR	p23	1	$4.5x10^3$	$1.8x10^3$	$9.4x10^{-4}$

Table 5. Kinetic rate constants for the annealing of cTAR to dTAR in the presence of peptides pE and p23.

As in the case of peptide pE, we characterized the molecular determinants of the annealing reaction promoted by p23. We used the previously described DNA mutants : ΔL dTAR, to characterize the possible role of the central loops and cTAR 1,2 to characterize the possible role of stems. Again, the reaction of TMR-5'-cTAR1,2-3′-Fl with dTAR in the presence of peptide p23 was much slower than with cTAR, indicating an annealing reaction via the stems. In contrast, the p23-promoted annealing of cTAR with ΔL dTAR was very similar to that of cTAR with dTAR, confirming that the loops play only a marginal role in the p23-directed annealing of cTAR with dTAR. The same mechanism was reported for NC(12-55) (Godet, de Rocquigny et al. 2006), indicating that the antiviral peptides, which include the residues of NCp7 hydrophobic plateau, reproduce to some extent, the ODN annealing properties of NCp7.

Comparison of the annealing properties of p23 and NC(11-55) peptides further revealed that peptide p23 added to ODN at a molar ratio 1:1 exhibited the same annealing activity as four molecules of NC (11-55). This was further confirmed by experiments with peptide mixtures, since the kinetic curves with p23 added at a ratio of 1:1 and NC(11-55) at a ratio of 3:1 were almost perfectly superimposable to those obtained in the presence of NC(11-55) alone at the ratio of 7:1, respectively (Fig.86). In the same way, the kinetics curves with p23 added at a ratio of 1:1 and NC (11-55) at a ratio of 7:1 seem to be superimposable to those obtained with NC (11-55) alone at ratio 10:1. Thus the effect of the two peptides is additive.

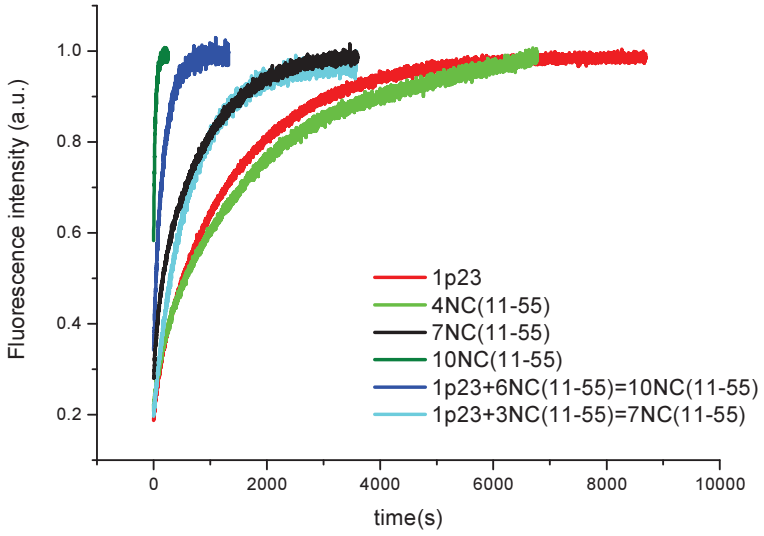

Fig.86. Comparison of the annealing properties of p23 and NC(11-55) peptides. All progress curves were obtained with 10 nM doubly labelled cTAR and 100 nM dTAR in 25mM Tris,pH 7.5, 30 mM NaCl and 0.2 mM $MgCl_2$ buffer.

Effect of peptide pE on the dynamics of the 2Ap-labeled oligonucleotides

Since the native NC and the truncated NC(11-55) were reported to freeze the dynamics of the ODN dynamics at the pico-nanosecond level, we further site-selectively investigated the interactions of peptide pE with 2Ap-labeled cTAR sequences, by using ODNs labeled by 2-aminopurine (2Ap), a fluorescent analog of adenine that can be selectively excited at 315–320 nm, where Trp does not absorb (Mollova 2002). The quantum yield of free 2Ap at pH 7.0 is 0.68 (Ward, Reich et al. 1969) but within ODNs, it is significantly quenched due to interactions with its neighbor bases.

To this end, we selected labelling positions all along the cTAR sequence: 2-Ap in position 9 forms a mismatch with C within the lower part of the stem, positions 28 and 35 are within the central and the internal loop, respectively. Positions 53 flanking the G54 bulge and position 49 are distributed within the double stranded segments (fig.87a).

In the absence of peptide pE, the 2Ap-labeled oligonucleotides exhibit a rather low quantum yield in comparison to that of free 2-Ap, as a consequence of the dynamic quenching of 2Ap fluorescence by the neighboring bases, and notably the flanking G residues which are the strongest quenchers among the bases (Guest CR 1991). Binding of peptide pE to various 2-Ap labeled oligonucleotides led to marginal changes in the quantum yield (fig.87b.), suggesting that peptide pE does not restrict the dynamic interactions of the 2-Ap residues with their neighboring bases. The absence of any effect for the quantum yield of 2-Ap inserted all over

the stem within the different double stranded segments of cTAR (2-Ap9, 2-Ap49 and 2-Ap53) can hardly be connected with an absence of binding of peptide pE to this region, since the annealing reaction for these oligonucleotides was shown to be promoted by peptide pE through the stems. This suggests that as the SSHS NCp7 mutant, pE binds mainly through its basic residues to the phosphate backbone of cTAR.

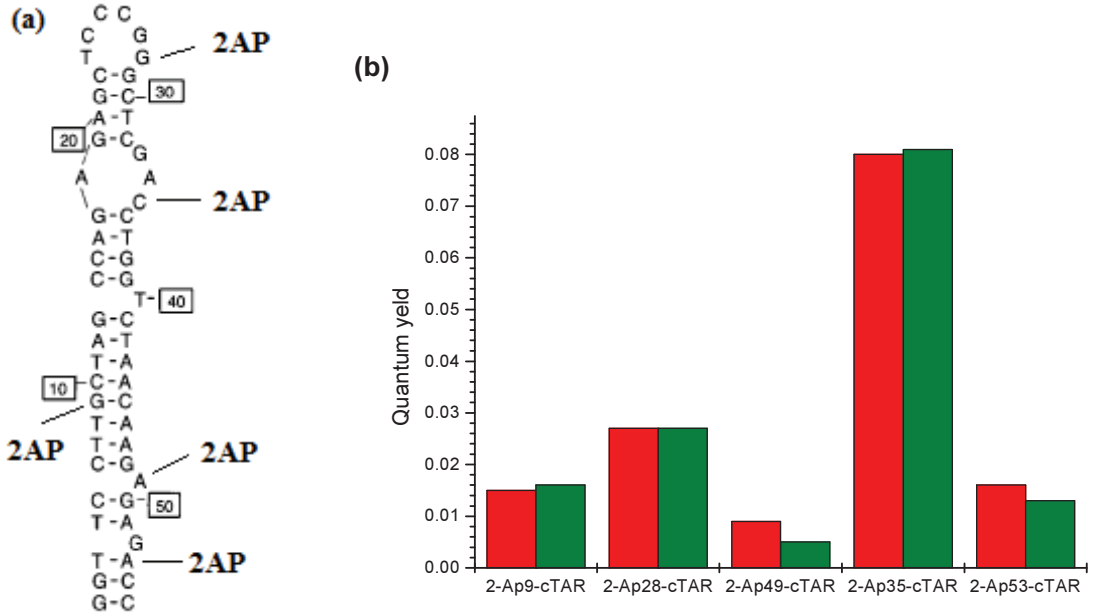

Fig.87. Site-selective monitoring of the interaction of peptide pE with cTAR sequences labeled with 2-Ap. (a) Labeled positions in cTAR oligonucleotides. The sequences were labeled by 2-Ap at position 9, 28, 35, 49 and 53. (b) Quantum yields of cTAR9Ap, cTAR28Ap, cTAR35Ap, cTAR49Ap and cTAR53Ap in the absence (orange) and presence (green) of peptide pE. Quantum yields were calculated assuming a quantum yield of 0.68 for free 2Ap (Ward, Reich et al. 1969). Excitation wavelength was 315 nm and all experiments were performed in 25 mM Tris (pH 7.5), 30 mM NaCl, 0.2 mM $MgCl_2$ at 20°C.

Strand exchange in the presence of peptides pE and p23

Since NC was found to stimulate both single-strand to double-strand (ss->ds) and the reverse ds->ss transitions, we tested whether both of these transitions could be promoted by p23 and pE, by monitoring strand exchange between complementary single-stranded DNA oligonucleotides. To study the effects of p23 and pE on strand exchange kinetics, simple strand transfer experiments involving displacement of a partially complementary strand in a double-stranded sequence by the fully complementary one, was performed. The reaction proceeds slowly in the absence of peptides (fig.88), whereas it is significantly enhanced when peptides were added. Kinetics were monitored in real time with the use of complementary oligonucleotides with end-labeled fluorophores that serve as donor–acceptor pairs.

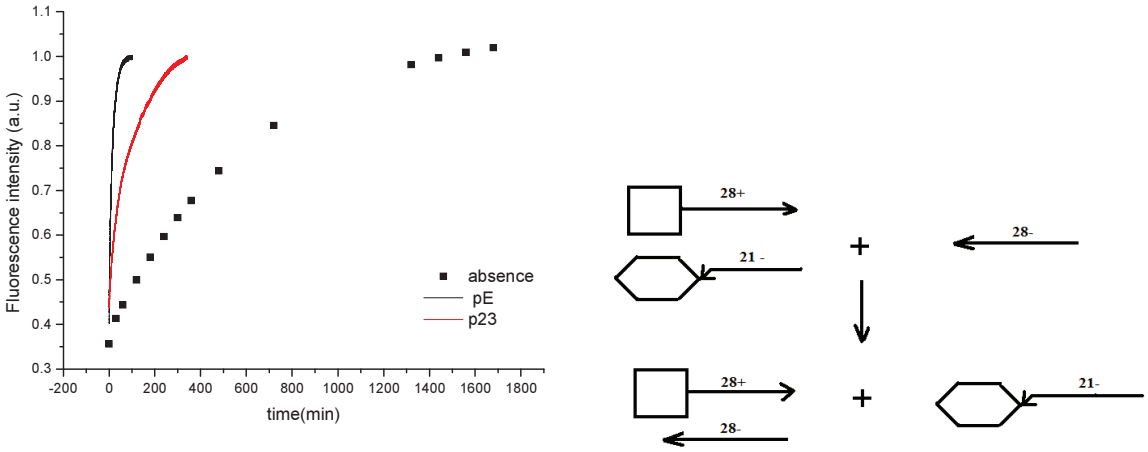

Fig.88. Strand exchange reaction in the absence (dotted line) and the presence of peptide pE (black line) and peptide p23 (red line). (Right) schematic representation of the strand exchange reaction.

Both peptides were found to strongly accelerate the strand exchange reaction which in absence of any peptide took more than 24 hours. The observed strand exchange promotion ability of the two peptides is in agreement with the fact that this NC property does not rely on the properly folded zinc fingers but mostly upon the basic domains flanking the zinc fingers (Darlix, Vincent et al. 1993; Lapadattapolsky, Pernelle et al. 1995). These findings confirmed the ability of the peptides to mimic the NC chaperone properties and may thus compete with NC.

The aim of this work was to characterize the physicochemical properties of antiviral peptides with respect to DNA sequences represented by the canonical model of the HIV-1 transactivation response (TAR) element in a DNA sequence (dTAR) and the complementary sequence cTAR.

When compared with HIV-1 NCp7, antiviral peptides exhibit only a negligible ODN destabilizing activity similar to what was obtained for $(SSHS)_2$NC(11-55) mutants, where all the cysteins were substituted by serines, leading to the loss of zinc finger folding (Godet J 2011).

Moreover, antiviral peptides were shown to accelerate the annealing reaction between complementary ODN sequences, confirming the poor correlation between ODN destabilizing activity and annealing enhancement (Godet J 2011). Similar data obtained for NC mutants and other non specific ODN annealing agents suggest that the annealing promotion is likely

related to the ability of pE to non-specifically stimulate the rearrangement of nucleic acids through pathways already existing in the absence of peptides.

However, it was reported that binding of wild-type NC either to TAR/cTAR or PBS(-)/PBS(+) loops induces a switch of the annealing pathway during the first and second strand transfer, respectively (Egele, Schaub et al. 2004; Vo, Barany et al. 2009). These two switches, from the loop to the stem for TAR/cTAR and from the overhangs to the loop for (+)/(-)PBS, are clearly related to the ability of NCp7 to locally destabilize these sequences. In the case of cTAR/TAR annealing, the contribution of the zinc fingers is quite subtle. Indeed, while both non specific nucleic annealing proteins and native NCp7 induce a mechanistic switch, only the native NCp7 induces an extended destabilization of cTAR stem that permits an efficient invasion of the TAR stem.

The specific ability of NCp7 to funnel nucleic acid rearrangements towards different routes appears to be strongly dependent on the sequence/structure context and is probably of importance for the control of reverse transcription timing and ultimately for the generation of stable vDNA products. This was further proven in vivo where even single point mutations within the ZFs was shown to cause production of non-infectious particles (Dorfman T 1993; Gorelick, Chabot et al. 1993) resulting in lower plus strand transfer efficiency, defective viral DNA (vDNA) sequences and profound modifications of the spatio-temporal control of the reverse transcription process.

The inability of antiviral peptides to promote a specific annealing reaction during minus strand transfer suggests that competition with NC in binding to its DNA substrates should affect the efficiency and fidelity of the reverse transcription process

Antiviral peptide: intracellular pathway and cytotoxicity

Next, we characterized the internalization and intracellular pathway in HeLa cells of peptide pE, taken as a representative. pE was chosen on the basis of its high efficiency in inhibiting the NC-induced cTAR destabilization

Preliminary experiments showed that when incubated alone with cells peptide, pE was found in punctuate structures that accumulated with time around the nucleus. This is typical of internalization through endosomes. In contrast, no diffuse fluorescence appeared in the cytoplasm, suggesting that pE could not escape from endosomes. As a consequence, it appears that the peptide pE should be vectorized in order to be released in the cytoplasm. In this respect, we used the peptide preparations of Gilles Divita (Montpellier) which are known to efficiently deliver cargoes into mammalian cells (Gros E. and Depollier J. 2006). Thus, unless it is stated, in all the following experiments, pE was complexed with a carrier (Nanovepep). The complex of carrier/cargo was prepared with the use of Nanovepep on the basis of the protocol provided by Dr Divita (see Materials and Methods).

Nanovepep represents a new strategy for delivering peptides into cells, and thus, appears as an alternative to the covalent PTD (Protein Transduction Domains) technology. PTDs have been shown to cross biological membranes efficiently, and promote the delivery of peptides and proteins into both cultured cells and animals (Wadia J.S. 2002). Although the covalent PTD technology has a number of advantages e.g. rationalization and reproducibility of the procedure, it is limited from the chemical point of view, as it is mainly performed via disulfide bonds, and risks thus to alter the biological activity of the cargoes. In contrast, Nanovepep, being an example of non-covalent peptide-based strategy of peptide transduction, improves the delivery of several proteins and peptides in their fully biologically active form into a variety of cell lines, without the need for prior chemical covalent coupling or denaturation steps.

Based on both structural and biophysical investigations, a four-step mechanism of cellular internalization of carrier/cargo was proposed with Nanovepep (Fig.89): (i) formation of the Nanovepep/cargo complexes through hydrophobic and electrostatic interactions depending on the nature of the cargo, (ii) interaction of the complex with the external side of the cell through electrostatic contacts with the phospholipid head groups (iii) insertion of the complex into the membrane, associated with conformational changes which induce membrane structure perturbation and (iv) release of the complex into the cytoplasm with partial “de-caging” of the cargo.

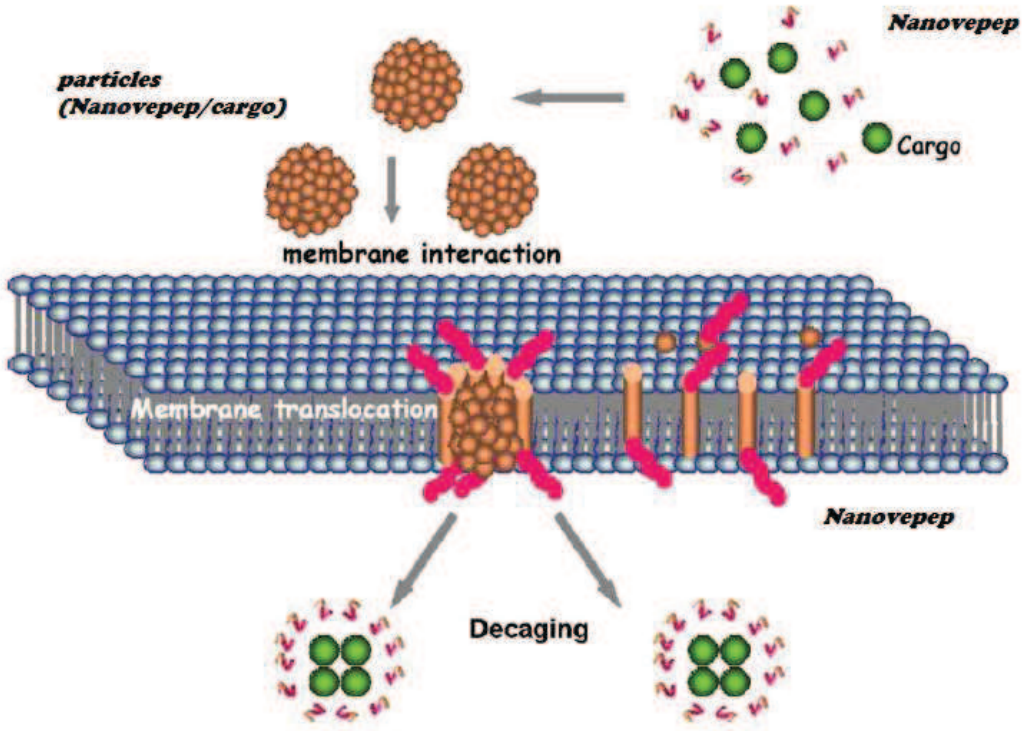

Fig.89. Mechanism of cellular internalization of Nanovepep (modified from Gross, Morris et al. 2006).

At first, to investigate the possible cytotoxicity of the peptide and carrier, we characterized the effect of both on HeLa cell viability with the use of the Annexin V/Propidium iodide assay and flow cytometry (see Material and Methods). Toxicity of the compounds was assessed from the Annexin V FITC-versus Propidium iodide dot plots. Using this system, we were able to distinguish by flow cytometry, viable cells (AnnV-/PI-), early apoptotic (AnnV+/PI-), late apoptotic (AnnV+/ PI+) and necrotic (AnnV-/ PI +) cells.

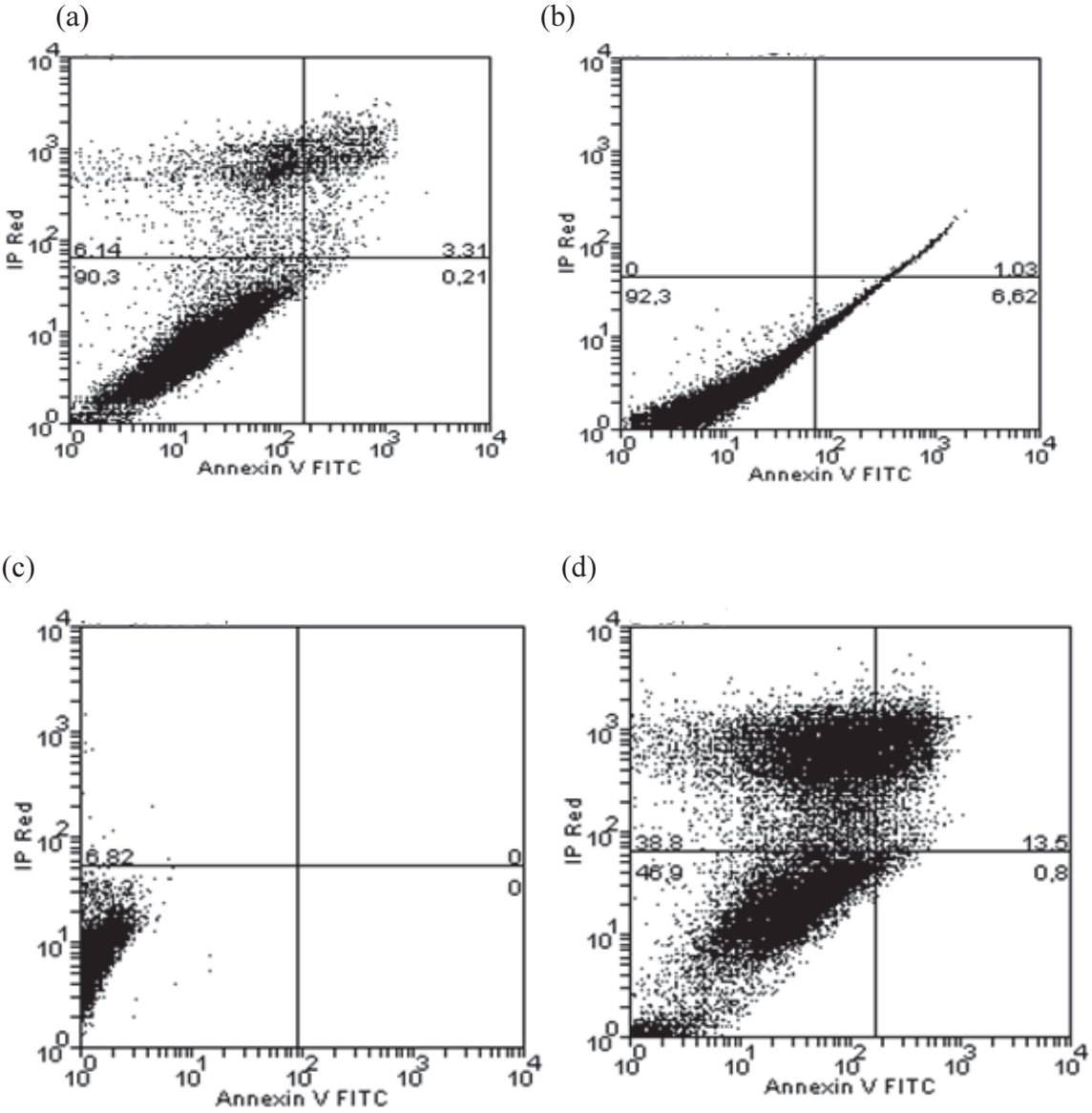

(e)

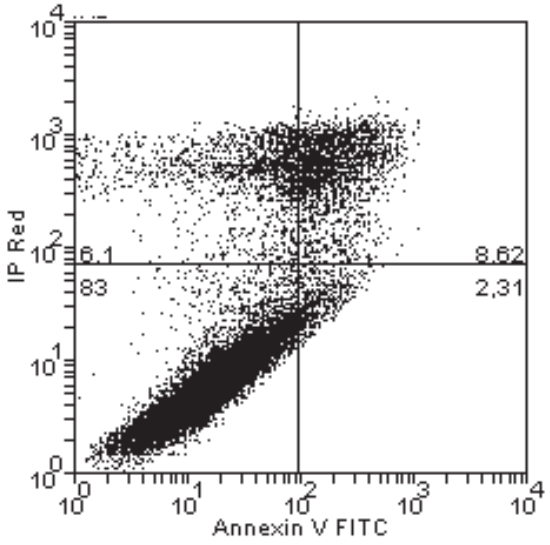

(f)

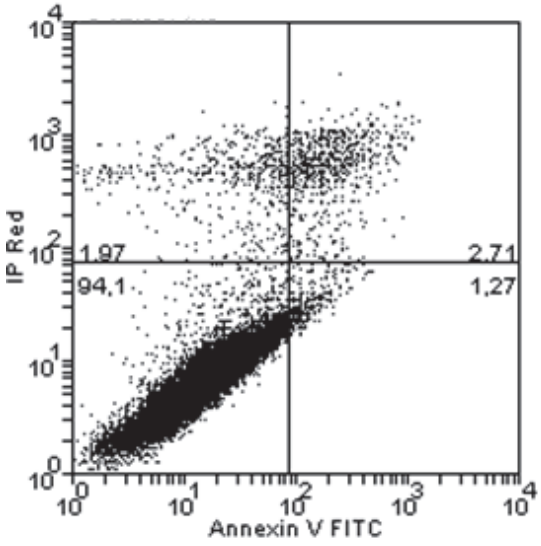

(g)

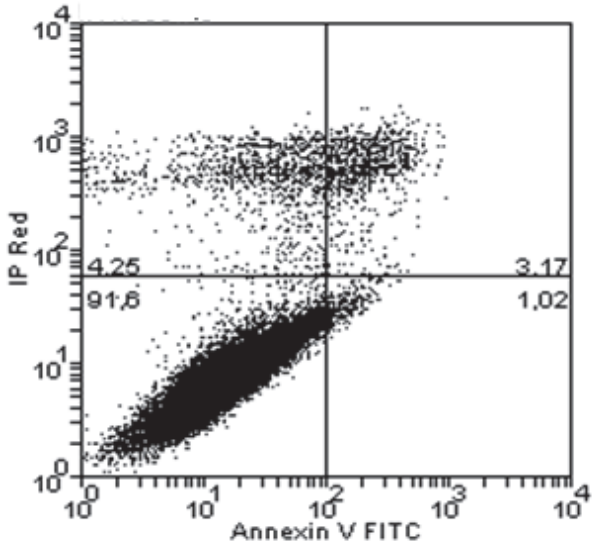

Fig.90. Flow cytometry for monitoring the effect of peptide pE alone and vectorized with Nanovepep on cell viability**. a-c,** Dual-staining of negative control cells (nontreated HeLa cells) and apoptotic cells (d) stained with propidium iodide (PI) (*y*-axis) and Annexin V-FITC (*x*-axis). Dual staining of cells incubated with Nanovepep alone (e), peptide pE alone (**f**) or complexed with Nanovepep (**g**). The quadrant analysis shows viable cells negative for annexin V and excluding PI **(lower left)**. Apoptotic cells stained with annexin V but excluding PI **(lower right)**. Secondary necrotic cells (i.e., necrosis after apoptosis) are positive for both PI and annexin V **(upper right)**. Necrotic or mechanically damaged cells positive for PI only are shown in the **upper left** quadrant.

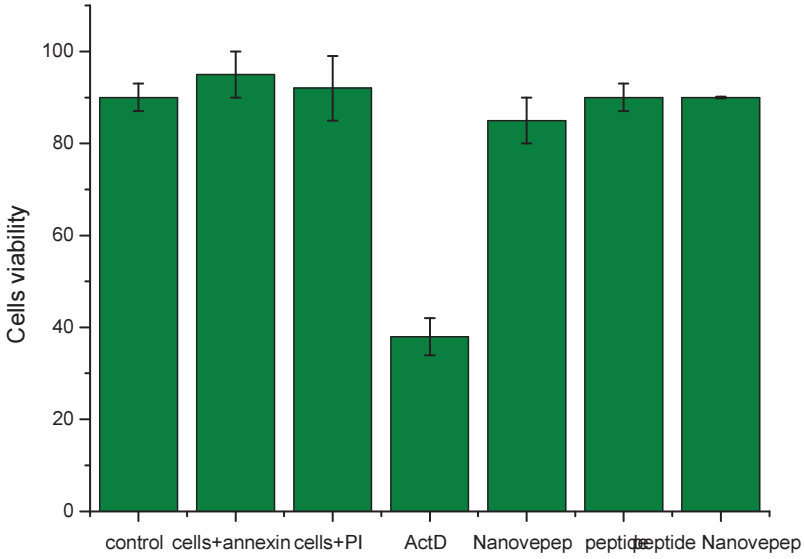

Fig.91. Cytotoxicity of peptide pE alone and vectorized, controlled by FACS using AnnexinV-FITC/PI staining. 18 hours before FACS analysis, one of the cell control group was treated with Actinomycin D (0.5µg/ml). Nanovepep and pE were mixed at a molar ratio 1:1, where concentration of peptide pE was 0.1 µM, Nanovepep and peptide alone were tested at 100µM each. The number on the Y axis represents the percentage of cells in the different states. Untreated cells were used as a control.

As expected, the well-characterized cell viability inhibitor, Actinomycin D caused a dramatic decrease in the number of living cells as compared to the untreated control. In contrast, in cultures treated with either peptide alone (100 µM), Nanovepep alone (100 µM) or complex carrier/cargo (ratio 1:1) no significant decrease in cell viability was observed (fig.91), which confirms the marginal toxicity of the tested peptide and Nanovepep.

To evaluate the mechanism of the cellular uptake of peptide pE alone or complexed with Nanovepep 0,1µM of the rhodamine labelled peptide alone or complexed with carrier (ratio 1:1) was incubated for two hours with adherent HeLa cells. Then, cells were quickly washed with trypsin to remove the background and fixed with paraformaldehyde (4%) before image analysis.

The cellular uptake mechanism of PTDs has been suggested to be associated with the endosomal pathway (Richard J.P. and Chernomordik L.V. 2003). However, the mechanism of uptake of PTD-cargo remains controversial. For most carriers, several routes of cell entry have been evidenced, some of which are independent of the endosomal pathway and involve a

trans-membrane potential (Alves ID 2010; Brasseur R 2010; Räägel H 2010). In non-covalent strategies, there are also evidences for several routes of cellular uptake, some of which being independent of the endosomal pathway. Thus, by monitoring the colocalization of the fluorescently labelled peptide and endocytosis markers we investigate the uptake mechanism of pE alone or vectorized with Nanovepep.

Endocytosis is the vesicle-mediated process used by all cells to internalize extracellular macromolecules, plasma membrane lipids, and plasma membrane proteins. There are several endocytosis pathways that utilize different mechanisms to internalize portions of the plasma membrane. The best studied endocytosis pathway in mammalian cells is the clathrin-coated pit pathway (Fig. 92). Many receptors and their associated ligands cluster into clathrin-coated pits by association with clathrin adaptor proteins such as the four-subunit complex AP2. Clathrin adaptors in turn bind to the clathrin lattice which is thought to provide the force required to deform the membrane into a curved bud. The large GTPase dynamin is then involved in pinching off the coated pit to form a clathrin-coated vesicle. Such vesicles are then uncoated by the chaperone hsc70 and the DNA-J domain co-chaperone auxillin. Uncoated endocytic vesicles then fuse with one another and with early endosomes in a reaction requiring the small GTPase Rab5. In early endosomes, ligand-receptor complexes dissociate due to the reduced pH of the endosomal lumen. Many receptors then recycle to the plasma membrane either directly or indirectly via recycling endosomes. However, many ligands do not recycle but instead are transported from early to late endosomes and eventually to lysosomes where they are degraded. Early to late endosome transport may be mediated by small vesicular intermediates, or through a maturation process whereby early endosomes lose components through recycling pathways and gain components through fusion with vesicles derived from the secretory pathway. Late endosomes are then thought to fuse with pre-lysosomes to form “hybrid” organelles, which mature back into lysosomes through sorting and fission.

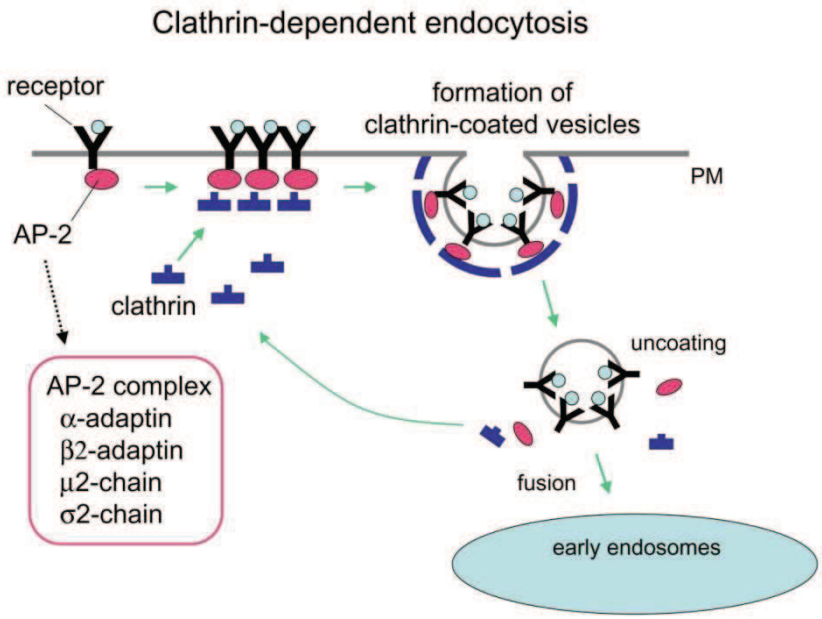

Fig.92. Mechanism of the clathrin-dependent endocytosis. Clathrin and cargo molecules are assembled into clathrin-coated pits on the plasma membrane together with an adaptor complex called AP-2 that links clathrin with transmembrane receptors, leading to the formation of mature clathrin-coated vesicles (CCVs). CCVs are then actively uncoated and transported to early/sorting endosomes (Brodsky 2001).

To test whether pE vectorized with Nanovepep enters into cells by an energy-dependent endocytosis, we added both fluorescein labelled transferrin (AlexaFluor488) and pE-Rhodamine to the cells. Transferrin binds to its cell surface receptor and is internalized through clathrin-associated endocytosis. Superimposition of the green and red images (fig.93A) revealed the presence of transferrin-positive vesicles in green that do not contain pE-Rh and pE-Rh-positive vesicles in red that do not contain transferrin and yellow coloured vesicles where the two proteins co-localize. The observed yellow vesicles suggest that clathrin-dependent endocytosis is partially responsible for the internalization of peptide/Nanovepep.

The same experiment was performed with the peptide alone (fig.93B). We did not observe yellow vesicles which suggest that clathrin-dependent endocytosis is not responsible for the internalization of the peptide..

Endocytosis could also be mediated through a caveolae-dependent pathway. This endocytic process involves clustering of lipid raft components on the plasma membrane into caveolae and signal transduction pathways leading to invagination and internalization. The caveolae vesicles are then delivered to pre-existing caveolin-1-enriched organelles, the caveosomes, which are cholesterol-rich structures that are devoid of markers of the classical endocytic pathway.

To investigate the role of caveolae for the internalization of peptide/Nanovepep, we incubated the fluorescent peptide complexed with Nanovepep with HeLa cells in the presence of methyl-β-cyclodextrin (MβCD) (fig.93C). This compound depletes the cholesterol from the plasma membrane, disrupting the lipid rafts needed for the caveolin-coated vesicles. With MβCD, only moderate effect on complex internalization was observed (compare fig.93 A and C), indicating that caveolae-dependent endocytosis is marginally responsible for internalization of the complex. Similar effect was observed when the peptide was incubated alone with HeLa cells (fig.93D) Thus, cholesterol in the cytoplasmic membrane appeared to be nonessential for an efficient transduction of the either the peptide alone or the pE/Nanovepep complex.

Meanwhile, internalization through an energy-independent mechanism has also been reported for small peptides such as penetratin, $(Arg)_9$ and transportan (Joliot A 1991; Pooga M 1998; Richard J.P. and Chernomordik L.V. 2003) which are efficiently internalized at both 37°C and 4°C. To check whether this mechanism plays a role in the internalization of the peptide pE, we incubated the rhodamine-labelled peptide complexed with Nanovepep with HeLa cells at 4°C. As shown in figure 93 E, pE-Rh/Nanovepep is detected as a diffuse fluorescence at the level of the plasma membrane, suggesting that at least a part of pE-Rh/Nanovepep internalization is not receptor-dependent but could result from an energy independent membrane crossing. Similar results were obtained when peptide was incubated alone with cells (fig.93F).

A

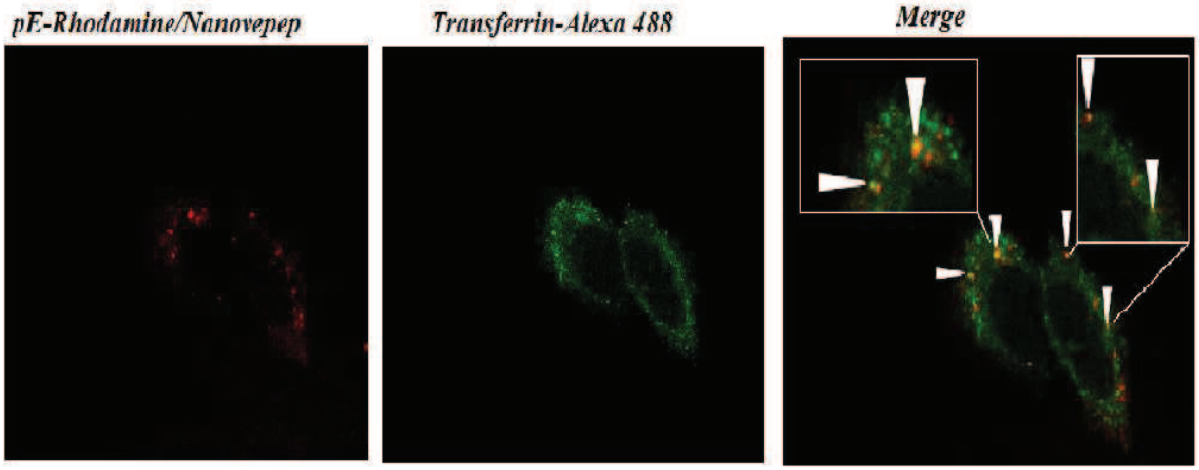
pE-Rhodamine/Nanovepep
Transferrin-Alexa 488
Merge

B

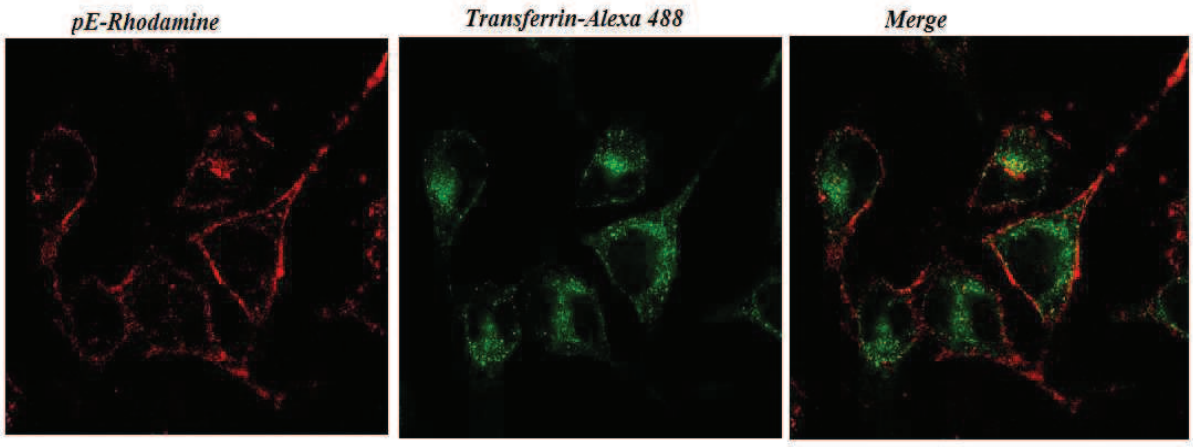
pE-Rhodamine
Transferrin-Alexa 488
Merge

C

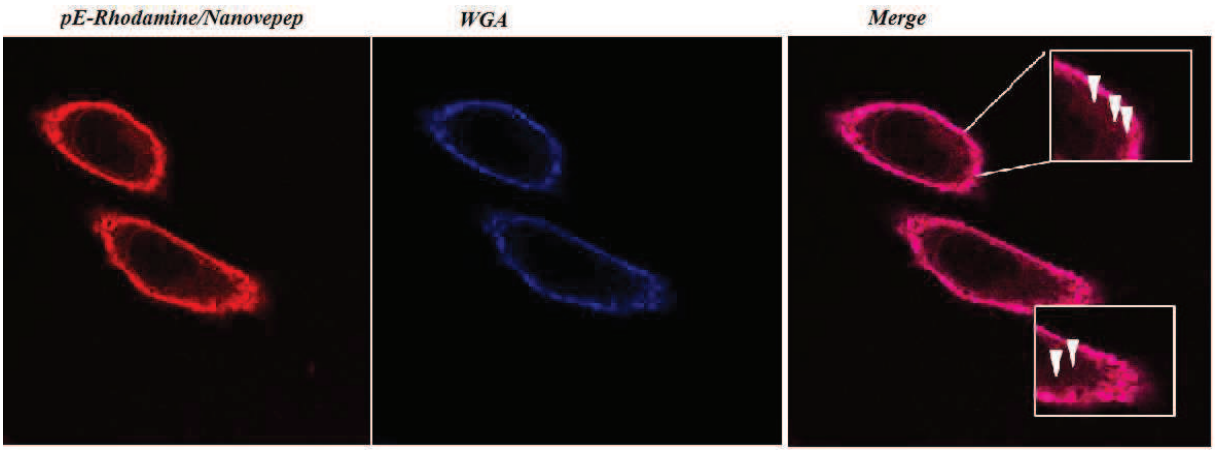
pE-Rhodamine/Nanovepep
WGA
Merge

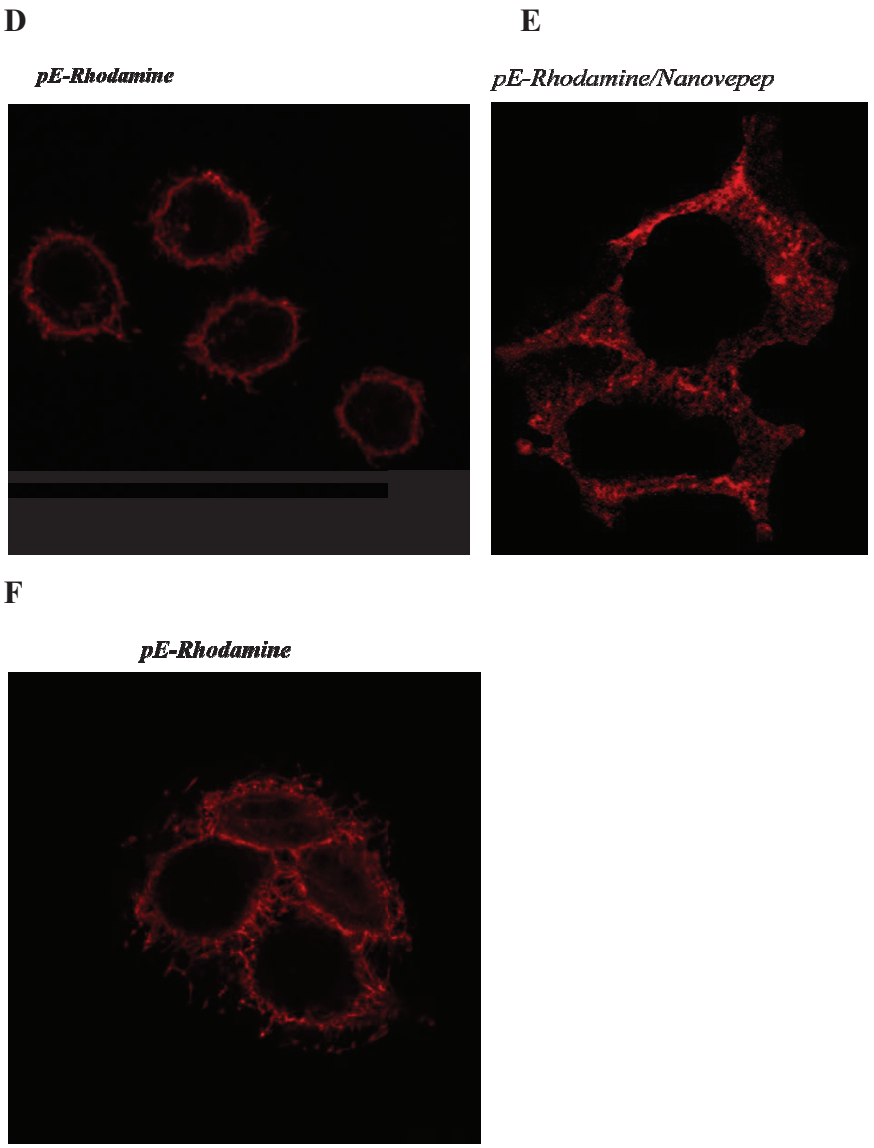

Fig.93. Internalization of pE/Nanovepep complexes and pE in HeLa cells. (**A**) Clathrin-mediated endocytosis. Hela cells were incubated with pE/Nanovepep complexes and transferrin labeled with Alexa 488. Superimposition of the green and red images revealed the presence of Fl-transferrin-positive vesicles in green that do not contain Rh-pE, Rh-pE-positive vesicles in red that do not contain Fl-transferrin and yellow coloured vesicles where the two proteins co-localize (Arrows). **(B)** Role of clathrin-dependent endocytosis in internalization of pE-rhodamine alone. **(C)** Caveolae mediated endocytosis. Hela cells were incubated with pE/Nanovepep complexes and MβCD, an inhibitor of caveolae uptake. The cellular membrane was additionally stained with WGA (Wheat Germ Agglutinin) labeled with AlexaFluor 594 (5µg/ml). **(D)** Role of caveolae mediated endocytosis in internalization of peptide alone. **(E)** Energy-dependence of endocytosis. The Hela cells were incubated with pE/Nanovepep complexes at 4 ^{0}C. (**F**) Energy-dependence of internalization of peptide pE alone at 4^{0}C.

In conclusion, our data show that pE competes with NC in binding to its DNA analogues and is non toxic. Microscopy data further show that when vectorized with Nanovepep, pE is

delivered inside the cell, but it is remains to be established whether it can be present in the same compartments than NCp7 to compete with it.

Antiviral activity of peptide pE

For single-round infections with lentiviral vectors coding for GFP, HeLa cells were prepared as described in material and methods. Cells were infected at a MOI (Multiplicity of infection) of 1, two hours after peptide/Nanovepep addition to the medium. Infected cells express eGFP, which provides a direct and quantitative marker for HIV-1 infection in individual live cells. Two days after infection, HeLa cells were harvested and the number of GFP-expressing cells was monitored.

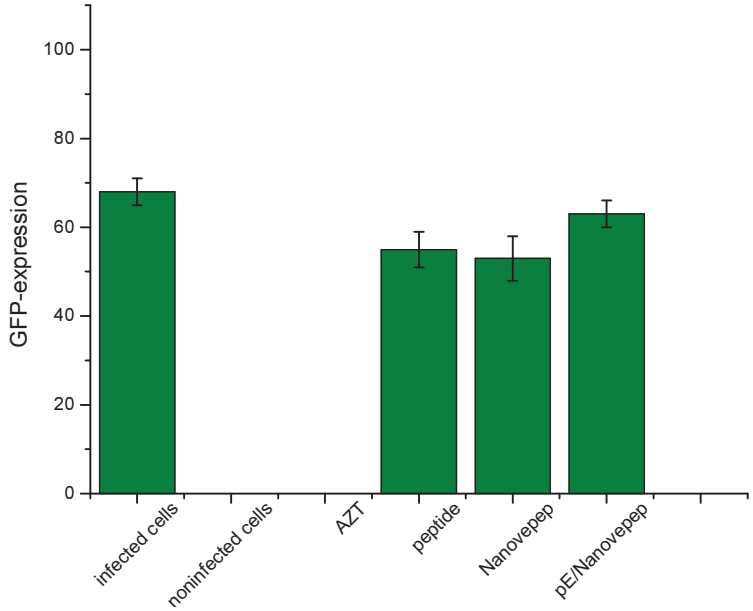

Fig.94. Inhibition of HIV-1 infection by peptide pE. The peptide and Nanovepep were added at 0.1μM concentration each, whereas AZT was added at 0.5μM.

As expected, the well characterized nucleoside reverse transcriptase inhibitor (NRTI), AZT caused a dramatic decrease in numbers of GFP-expressing cells as compared to the untreated control. In contrast, in cultures treated with peptide vectorized with Nanovepep (ratio 1:1), the number of GFP-expressing cells was similar to that for untreated control (fig.94), suggesting that peptide pE was not able to inhibit HIV-1 infection in HeLa cells. The negative results obtained with cells pretreated with peptide pE alone or peptide/Nanovepep could be caused by not proper concentration of peptide, which is delivered into the cell.

Thus, in next step we monitor the number of GFP-expressing cells in presence of peptide pE/Nanovepep, added at increasing concentrations (e.g. 5, 10 and 25μM).

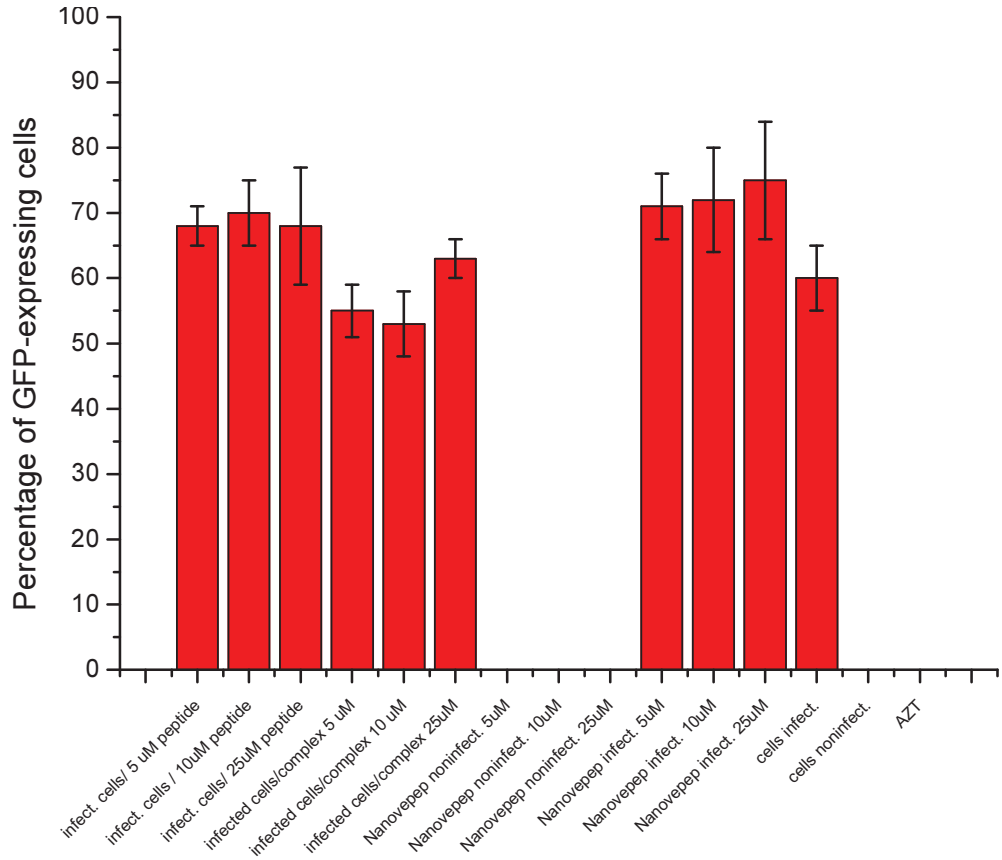

Fig.95. Inhibition of HIV-1 infection by peptide pE. The peptide and Nanovepep were added at concentrations indicated on the graph, whereas AZT was added at 0.5μM. Peptide pE was vectorized with Nanovepep at a ratio 1:1,where peptide concentration was 5, 10 or 25 μM.

As can been seen from fig.95, increasing concentrations of peptide pE complexed with Nanovepep did not cause changes in the number of GFP-expressing cells, giving similar results to those obtained for the untreated control. This suggests that peptide pE was not able to inhibit HIV-1 infection of HeLa cells even at high concentration.

Due to the fact that NCp7 is involved in reverse transcription, in viral DNA integration and virus assembly, we expect the antiviral activity to take place at more than one step. Thus, it is possible that peptide pE was not able to inhibit HIV-1 infection because it was not available in the places where NCp7 performs its role of chaperone e.g. during reverse transcription in the cytoplasm. We are on the way to develop new strategies of improving internalization of peptide pE (see Future perspectives).

General Conclusions

The nucleocapsid protein (NCp7) of human immunodeficiency virus type 1 (HIV-1) is formed of two highly conserved CCHC zinc fingers flanked by small basic domains. During virus life cycle, NCp7 acts as a nucleic acid chaperone, assisting the rearrangement of nucleic acid molecules into their most stable conformation notably during genomic RNA dimerization, encapsidation and replication. Due to the fact that NCp7 is highly conserved in all HIV-1 subtypes, a major benefit of anti-NC drugs should be to provide a sustained replication inhibition of a large panel of HIV-1 strains including those species that are resistant to anti-RT and anti-PR drugs.

In the host lab, several series of peptides have been designed to act as competitors for NC and thus, inhibit virus replication. Among these series, several of them were found to efficiently inhibit the nucleic acid destabilization properties of NC. Four of them have been tested for their antiviral activity and three of them were found to efficiently inhibit the replication of HIV-1 in lymphocytes. In this context, this work was aimed to further explore the mechanism of these peptides. During these studies, we mainly used peptide pE, as a representative with high efficiency in inhibiting the NC-induced cTAR destabilization.

In the first part, we focused on the in vitro properties of peptide pE and notably its ability to compete with NCp7. Since NC chaperone properties can be divided into 3 main components e.g. nucleic acid destabilization, promotion of annealing reaction between complementary sequences and strand exchange, we examine the pE ability to inhibit or mimic these NC features. Using a doubly labeled oligonucleotide (cTAR), pE was found to exhibit marginal nucleic acid destabilizing activity, in line with the fact that this NC property is strongly correlated with folded zinc fingers.

Next, we characterized the chaperone activity of the peptide on complementary cTAR and dTAR DNA sequences from HIV-1, as a model. It was observed that peptide pE activates the annealing of these complementary sequences by a two-step reaction mechanism that includes a distinct intermediate complex (IC). The formation of IC was found to be nucleated through the stem ends of cTAR and dTAR. Then, peptide pE was shown to promote the conversion of the IC to the final extended duplex, with an efficiency only slightly lower than NCp7.

Peptide pE was also shown to enhance the strand exchange reaction between complementary single-stranded DNA oligonucleotides, in line with the fact that this property mostly rely upon the basic domains flanking the zinc fingers. Together, with the ability of pE to compete with NC binding sites on nucleic acids, it is likely that pE acts as a non specific nucleic acid annealer that prevents NC to promote the specific pathways required in reverse transcription.

Therefore, pE may lead to perturbations in the spatiotemporal process of reverse transcription, with inefficient and non faithful production of viral DNA.

In a next step, we examined the intracellular trafficking and antiviral properties of peptide pE. With the use of Annexin-FITC/PI cytotoxicity assay, we eliminate the possibility of any toxic effect of the peptide on cells. Next, using fluorescently-labelled peptide pE vectorized with the Nanovepep carrier, we found out an efficient delivery in the cell, but got not clear answer on its concentration as a free peptide in the cytoplasm. In the last part of this work, we performed antiviral assays, but did not succeed to reproduce its antiviral activity in the tested conditions. This work is still in progress.

In parallel, we participated in the characterization of the mechanism of small antiviral drugs directed against NC, developed by the groups of Dr Daelemans (Leuven) and Prof. Botta (Sienna).

In collaboration with the group of Dr Daelemans (Belgium), we analyzed the mechanism of WDO-217 and NV038, two compounds that were selected by high throughput screening. The results obtained by the Belgian group showed that both components strongly decrease the viral activity of most drug-resistant virus strains e.g. HIV-2_{ROD}, HIV-1_{IIIB} and SIV_{MAC} (EC_{50} for WDO-217 < 7 μM and for NV038 < 20 μM). Moreover, according to the data obtained from time of addition experiments, NV038 was found to target the early step of reverse transcription. WDO-217 showed a similar behavior and also efficiently prevented the transmission of HIV-1 to $CD4^+$ T lymphocytes. Moreover, WDO-217 showed also strong microbicide effects on cell-free virions. To determine whether both compounds are potential anti-NC drugs, we examined their ability to eject Zn ions from NC and their effect on the ability of NC to destabilize ODNs. NV038 was found to expel Zn^{2+} ions very efficiently, leading to full ejection in a few hours. In line with this observation, the nucleic acid destabilization properties of NC that strongly rely on the proper folding of zinc fingers, were also efficiently inhibited by NV038.

Similarly, for WDO-217, full zinc ejection as well as nearly 100% of inhibition of ODN destabilization were observed. The zinc ejection property of the tested compounds was further proven by the use of the zinc selective fluorophore-Newport Green and mass spectroscopy. Next, we tested the influence of WDO-217 on the interaction between NC and two different oligonucleotides, PBS and SL3, selected based on their selective binding to NC. By the use of a two colour 3-hydroxychrome (3HC) probe developed in the laboratory, a probe highly sensitive to the environment, we monitored the changes in the emission of NC labelled with the 3HC probe after treatment with WDO-217. We noticed a decrease in the

emission of the probe when the protein was bound to the ODN. A further decrease after addition of WDO-217 suggested a shift from stacking interactions between protein and oligonuclotides towards a more polar interaction with the phosphate backbone. Thus, the observed decrease of the viral RNA in cell-free virions induced by WDO-217 is probably a consequence of the defective protection by the zinc-free NC protein. To our knowledge, this is the first time that this mechanism is proposed.

Finally, in a collaboration with the group of Prof. Botta (Italy) we participated in the discovery and validation of new inhibitors of NC, exhibiting antiretroviral activity through direct interaction with NC. The tested compounds were selected by the Italian group through virtual screening. Two of these compounds were found to exhibit an antiviral activity in the μM range. In our laboratory, we examined the possible zinc ejection properties of the tested molecules and found that none of the tested compounds was able to efficiently eject zinc from NC(11-55). In contrast, we observed a reproducible decrease of the Trp37 fluorescence on addition of the compounds, suggesting an interaction of the compounds with NC at the level of Trp37. To further investigate this interaction , we used NC(11-55) labelled at its N-terminus by a two colour 3HC probe. The significant change in the ratio of the two emission bands of 3HC observed after addition of the tested molecules further confirmed the binding of the compounds to NC. Finally, molecular modelling performed by the Italian group rationalized these observations, by showing that the compounds can bind at the level of the hydrophobic platform at the top of the zinc fingers. Through this collaboration, we demonstrated the potency of combining virtual screening, molecular modelling, in vitro tests and biophysical studies to discover new NC targeting drugs.

In conclusion, we proposed different strategies that can be used to inhibit NC and thus, lead to non infectious viruses. Either by competing with NC to its DNA substrates or by zinc removal, we were able to inhibit the NC properties and HIV-1 replication. All these findings make us believe that anti-NC drugs created on the basis of our strategies could help to further improve the therapy against HIV. Additionally, the virtual screening used to characterize the potential anti-NC drugs appears as the first structure-based screening directed against the nucleocapsid protein.

Future Perspectives

The present work on peptides with antiviral properties can be extended in the following directions:

- To ensure that peptide pE vectorized with Nanovepep is delivered in sufficient amounts for viral inhibition, we will add pE/Nanovepep complexes at different time points after infection (2, 5 and 24h). This should lead to accumulation of pE inside the cells and thus, give a better chance to monitor the antiviral properties of pE.
- In parallel to test another way of peptide internalization, we will use the N-succinyl-dioctadecylamine (SDODA), an anionic amphiphile previously described as an intermediate in the synthesis of polymeric lipids (Laschewsky et al., 1987) and used for gene transfection (Sainlos et al.,2003). Again, by monitoring the number of cells expressing eGFP, we will examine pE inhibition properties towards HIV-1 infection.
- Positive results from one of the above experiments will allow us to start a more detailed study on the viral steps targeted by pE. This will be done by time of addition assays. By comparison with linear peptides inactive in NCp7-based tests and well known antiviral molecules (i.e. AZT, Efavirenz, Raltegravir) used as negative and positive controls, respectively we will be able to determine whether pE targets reverse transcription, integration or viral assembly.

Furthermore, to identify the molecular target(s) of the antiviral peptide, HIV-1 resistance to this peptide will be elicited. To this end, we will perform multiple parallel selection experiments using the lymphotropic HIV-1 strain NL4-3. The selection will be initiated from infecting SupT1 lymphocytes at an MOI of 0.1. Next, peptides at the initial concentration close to the IC_{50} value will be added and cell cultures will be monitored for the occurrence of syncytia. Next, virus supernatants will be used to infect naive SupT1 cells and thus carry out virus passaging. The peptide concentration will be gradually raised in the course of virus passaging according to virus production as monitored by RT activity on supernatant containing virus. In a next step, we will assess the virus resistance pattern on naïve SupT1 cells in the presence of increasing concentrations of peptide pE. This experiment should help us to obtain peptide- resistant viruses.

In addition, we will also test the antiviral activity of the peptide on viral isolates resistant to anti-RT (AZT - 41L 215Y 181C, 41L 215Y 184V and Efavirenz –103N 190A, resistant virus), and anti-IN (raltegravir N155H, Q148H/G140S and Y143R/C and elvitegravir E92Q resistant virus) compounds in SupT1 cells. This should give important information regarding the ability of such antiviral peptides to be active against circulating drug-resistant HIV-1 isolates.

Moreover, we will characterize the molecular mechanism of peptide pE (complexed with Nanovepep). For this purpose we will express the target protein(s) both in their native and resistant forms tagged with GFP derivatives. Using FRET- FLIM (fluorescence lifetime imaging microscopy), we will monitor whether a direct interaction between the labelled antiviral peptides (added to the cells with Nanovepep) and their overexpressed molecular targets occurs, since a FRET signal requires that the two labels are less than 10 nm apart. Furthermore, by comparison with the resistant molecular targets, we will examine whether the mutation affects the binding process or the spatio-temporal distribution of the interactions in living cells.

The obtained results from in vitro molecular assays and photonic-based techniques should provide an overall view of the inhibitory mechanism of this promising anti-NC compound. This should also allow us to design rational modifications of the structure of peptide, in order to optimize its anti-viral activity and thus, propose compounds that could be tested in clinical trials.

References

A

Abbink, T. E. M. and B. Berkhout (2008). "RNA structure modulates splicing efficiency at the human immunodeficiency virus type I major splice donor." Journal Of Virology **82**(6): 3090-3098.

Adamson, C. S., S. D. Ablan, et al. (2006). "In vitro resistance to the human immunodeficiency virus type 1 maturation inhibitor PA-457 (Bevirimat)." Journal Of Virology **80**(22): 10957-10971.

Adamson, C. S. and E. O. Freed (2007). "Human immunodeficiency virus type 1 assembly, release, and maturation." Advances in pharmacology (San Diego, Calif.) **55**: 347-87.

Aldovini, A. and R. A. Young (1990). "Mutations Of Rna And Protein Sequences Involved In Human-Immunodeficiency-Virus Type-1 Packaging Result In Production Of Noninfectious Virus." Journal Of Virology **64**(5): 1920-1926.

Allen, P., B. Collins, et al. (1996). "A specific RNA structural motif mediates high affinity binding by the HIV-1 nucleocapsid protein (NCp7)." Virology **225**(2): 306-315.

Alves ID, J. C., Aubry S, Aussedat B, Burlina F, Chassaing G, Sagan S. (2010). "Cell biology meets biophysics to unveil the different mechanisms of penetratin internalization in cells." biochimica et biophysica acta **1798**: 2231-9.

Amara, A., S. LeGall, et al. (1997). "HIV coreceptor downregulation as antiviral principle: SDF-1 alpha-dependent internalization of the chemokine receptor CXCR4 contributes to inhibition of HIV replication." Journal Of Experimental Medicine **186**(1): 139-146.

Amara, R. R., F. Villinger, et al. (2001). "Control of a mucosal challenge and prevention of AIDS by a multiprotein DNA/MVA vaccine." Science **292**(5514): 69-74.

Ammerman, M. L., J. C. Fisk, et al. (2008). "gRNA/pre-mRNA annealing and RNA chaperone activities of RBP16." Rna **14**(6): 1069-80.

Amarasinghe, G. K., De Guzman,R.N., Turner,R.B., Chancellor,K.J., Wu,Z.R. and Summers,M.F (2000). "NMR structure of the HIV-1 nucleocapsid protein bound to stem-loop SL2 of the psi-RNA packaging signal. Implications for genome recognition." Journal Of Molecular Biology **301**: 491-511.

Anastassopoulou, C. G. and L. G. Kostrikis (2003). "The impact of human allelic variation on HIV-1 disease." Current Hiv Research **1**(2): 185-203.

Andersen, J. L. and V. Planelles (2005). "The role of Vpr in HIV-1 pathogenesis." Current Hiv Research **3**(1): 43-51.

Andreola, M. L. (2009). "Therapeutic potential of peptide motifs against HIV-1 reverse transcriptase and integrase." Curr Pharm Des **15**(21): 2508-19.

Anthony, N. J. (2004). "HIV-1 integrase: A target for new AIDS chemotherapeutics." Current Topics In Medicinal Chemistry **4**(9): 979-990.

Arhel, N. (2010) "Revisiting HIV-1 uncoating." Retrovirology **7**.

Armogida, S. A., N. M. Yannaras, et al. (2004). "Identification and quantification of innate immune system mediators in human breast milk." Allergy And Asthma Proceedings **25**(5): 297-304.

Arthur, L. O., J. W. Bess, et al. (1998). "Chemical inactivation of retroviral infectivity by targeting nucleocapsid protein zinc fingers: A candidate SIV vaccine." Aids Research And Human Retroviruses **14**: S311-S319.

Arthur, L. O., J. W. Bess, et al. (1992). "Cellular Proteins Bound To Immunodeficiency Viruses - Implications For Pathogenesis And Vaccines." Science **258**(5090): 1935-1938.

Arts, E. J. and D. J. Hazuda (2012) "HIV-1 Antiretroviral Drug Therapy." Cold Spring Harb Perspect Med **2**(4): a007161.

Ashish, R. Garg, et al. (2006). "Binding of full-length HIV-1 gp120 to CD4 induces structural reorientation around the gp120 core." Biophysical Journal **91**(6): L69-L71.

Athavale, S., S., Ouyang, W. et al.(2010) " Effects on the nature and concentration of salt on the interaction of the HIV-1 nucleocapsid protein with SL3 RNA." Biochemistry **49**: 3525-33.

Azoulay, J., J. P. Clamme, et al. (2003). "Destabilization of the HIV-1 complementary sequence of TAR by the nucleocapsid protein through activation of conformational fluctuations." Journal Of Molecular Biology **326**(3): 691-700.

B

Baba, S., K. Takahashi, et al. (2005). "Solution RNA structures of the HIV-1 dimerization initiation site in the kissing-loop and extended-duplex dimers." Journal Of Biochemistry **138**(5): 583-592.

Baba, T. W., Y. S. Jeong, et al. (1995). "Pathogenicity of live, attenuated SIV after mucosal infection of neonatal macaques." Science **267**(5205): 1820-5.

Bachand, F., X. J. Yao, et al. (1999). "Incorporation of Vpr into human immunodeficiency virus type 1 requires a direct interaction with the p6 domain of the p55 Gag precursor." Journal Of Biological Chemistry **274**(13): 9083-9091.

Balasubramaniam, M. and E. O. Freed (2011) "New Insights into HIV Assembly and Trafficking." Physiology **26**(4): 236-251.

Baltimore, D. (1970). "RNA-dependent DNA polymerase in virions of RNA tumour viruses." Nature **226**(5252): 1209-11.

Barat, C., O. Schatz, et al. (1993). "Analysis of the interactions of HIV1 replication primer tRNA(Lys,3) with nucleocapsid protein and reverse transcriptase." J Mol Biol **231**(2): 185-90.

C Barat, V Lullien, O Schatz et al. (1989) "HIV-1 reverse transcriptase specifically interacts with the anticodon domain of its cognate primer tRNA." EMBO **8**: 3279-85.

Barouch, D. H. (2008). "Challenges in the development of an HIV-1 vaccine." Nature **455**(7213): 613-9.

Barouch, D. H., S. Santra, et al. (2000). "Control of viremia and prevention of clinical AIDS in rhesus monkeys by cytokine-augmented DNA vaccination." Science **290**(5491): 486-92.

Barresinoussi, F., J. C. Chermann, et al. (1983). "Isolation Of A T-Lymphotropic Retrovirus From A Patient At Risk For Acquired Immune-Deficiency Syndrome (Aids)." Science **220**(4599): 868-871.

Basu, V. P., M. Song, et al. (2008). "Strand transfer events during HIV-1 reverse transcription." Virus Research **134**(1-2): 19-38.

Baudin, F., R. Marquet, et al. (1993). "Functional Sites In The 5' Region Of Human-Immunodeficiency-Virus Type-1 Rna Form Defined Structural Domains." Journal Of Molecular Biology **229**(2): 382-397.

Beltz, H., J. Azoulay, et al. (2003). "Impact of the terminal bulges of HIV-1 cTAR DNA on its stability and the destabilizing activity of the nucleocapsid protein NCp7." Journal Of Molecular Biology **328**(1): 95-108.

Beltz, H., C. Clauss, et al. (2005). "Structural determinants of HIV-1 nucleocapsid protein for cTAR DNA binding and destabilization, and correlation with inhibition of self-primed DNA synthesis." Journal Of Molecular Biology **348**(5): 1113-1126.

Beltz, H., E. Piemont, et al. (2004). "Role of the structure of the top half of HIV-1 cTAR DNA on the nucleic acid destabilizing activity of the nucleocapsid protein NCp7." Journal Of Molecular Biology **338**(4): 711-723.

Bennasser, Y. and E. Bahraoui (2002). "HIV-1 Tat protein induces interleukin-10 in human peripheral blood monocytes: involvement of protein kinase C-beta II and -delta." Faseb Journal **16**(6): 546-554.

Berg, J. M. (1986). "Potential Metal-Binding Domains In Nucleic-Acid Binding-Proteins." Science **232**(4749): 485-487.

Berglund, J. A., B. Charpentier, et al. (1997). "A high affinity binding site for the HIV-1 nucleocapsid protein." Nucleic Acids Research **25**(5): 1042-1049.

Berkhout, B. and K. T. Jeang (1989). "Trans-Activation Of Human Immunodeficiency Virus Type-1 Is Sequence Specific For Both The Single-Stranded Bulge And Loop Of The Trans-Acting-Responsive Hairpin - A Quantitative-Analysis." Journal Of Virology **63**(12): 5501-5504.

Berkhout, B. and J. L. B. vanWamel (1996). "Role of the DIS hairpin in replication of human immunodeficiency virus type 1." Journal Of Virology **70**(10): 6723-6732.

Berkowitz, R., J. Fisher, et al. (1996). "RNA packaging." Morphogenesis And Maturation Of Retroviruses **214**: 177-218.

Bernacchi, S. and Y. Mely (2001). "Exciton interaction in molecular beacons: a sensitive sensor for short range modifications of the nucleic acid structure." Nucleic acids research **29**(13): E62-2.

Bernacchi, S., S. Stoylov, et al. (2002). "HIV-1 nucleocapsid protein activates transient melting of least stable parts of the secondary structure of TAR and its complementary sequence." Journal Of Molecular Biology **317**(3): 385-399.

Bernacchi,S., Freisz, S. Maechling, C., Spiess, B., Marquet,R., Dumas,P. and Ennifar, E.(2007) "Aminoglycoside binding to the HIV-1 RNA dimerization initiation site: thermodynamics and effect on the kissing-loop to duplex conversion." Nucleic acids research **35:**7128-39.

Berthoux, L., C. Pechoux, et al. (1999). "Multiple effects of an anti-human immunodeficiency virus nucleocapsid inhibitor on virus morphology and replication." Journal Of Virology **73**(12): 10000-10009.

Berthoux, L., C. Pechoux, et al. (1997). "Mutations in the N-terminal domain of human immunodeficiency virus type 1 nucleocapsid protein affect virion core structure and proviral DNA synthesis." Journal Of Virology **71**(9): 6973-6981.

Biron, C. A. (1998). "Role of early cytokines, including alpha and beta interferons (IFN-alpha/beta), in innate and adaptive immune responses to viral infections." Seminars In Immunology **10**(5): 383-390.

Blum, H. E., J. D. Harris, et al. (1985). "Synthesis In Cell-Culture Of The Gapped Linear Duplex Dna Of The Slow Virus Visna." Virology **142**(2): 270-277.

Bolinger, C. and K. Boris-Lawrie (2009). "Mechanisms employed by retroviruses to exploit host factors for translational control of a complicated proteome." Retrovirology **6**.

Bolton, D. L. and M. J. Lenardo (2007). "Vpr cytopathicity independent of G(2)/M cell cycle arrest in human immunodeficiency virus type 1-infected CD4(+) T cells." Journal Of Virology **81**(17): 8878-8890.

Boudier, C., R. Storchak, et al.(2010) "The Mechanism of HIV-1 Tat-Directed Nucleic Acid Annealing Supports its Role in Reverse Transcription." Journal Of Molecular Biology **400**(3): 487-501.

Bourbigot, S., N. Ramalanjaona, et al. (2008). "How the HIV-1 nucleocapsid protein binds and destabilises the (-)primer binding site during reverse transcription." J Mol Biol **383**(5): 1112-28.

Braddock, M., R. Powell, et al. (1993). "HIV-1 TAR RNA-binding proteins control TAT activation of translation in Xenopus oocytes." Faseb J **7**(1): 214-22.

Brasey, A., M. Lopez-Lastra, et al. (2003). "The leader of human immunodeficiency virus type 1 genomic RNA harbors an internal ribosome entry segment that is active during the G(2)/M phase of the cell cycle." Journal Of Virology **77**(7): 3939-3949.

Brasseur R, D. G. (2010). "Happy birthday cell penetrating peptides: Already 20 years." biochimica et biophysica acta **1798**: 2177-81.

Brodsky, F. M., Chen, C.Y., Knuehl, C., Towler, M.C., and Wakeham, D.E. (2001). "Biological basket weaving: formation and function of clathrin-coated vesicles." Annu. Rev. Cell Dev. Biol. **17**: 517–568.

Brown P.O., Heuer T.S. (1998) Photo-crossing link studies suggest a model for the architecture of an active human immunodeficiency virus type I integrase - DNA complex. Biochemistry **37**: 6667-6678.

Buchbinder, S. P., M. H. Katz, et al. (1994). "Long-Term Hiv-1 Infection without Immunological Progression." Aids **8**(8): 1123-1128.

Buckman, J. S., W. J. Bosche, et al. (2003). "Human immunodeficiency virus type 1 nucleocapsid zn(2+) fingers are required for efficient reverse transcription, initial integration processes, and protection of newly synthesized viral DNA." J Virol **77**(2): 1469-80.

Bukrinskaya, A., B. Brichacek, et al. (1998). "Establishment of a functional human immunodeficiency virus type 1 (HIV-1) reverse transcription complex involves the cytoskeleton." J Exp Med **188**(11): 2113-25.

Bukrinsky, M. (2004). "A hard way to the nucleus." Mol Med **10**(1-6): 1-5.

Bukrinsky, M. I., S. Haggerty, et al. (1993). "A nuclear localization signal within HIV-1 matrix protein that governs infection of non-dividing cells." Nature **365**(6447): 666-9.

Bukrinsky, M. I., N. Sharova, et al. (1992). "Active Nuclear Import Of Human-Immunodeficiency-Virus Type-1 Preintegration Complexes." Proceedings Of The National Academy Of Sciences Of The United States Of America **89**(14): 6580-6584.

C

Camerini, V., D. Decimo, et al. (2008). "A dormant internal ribosome entry site controls translation of feline immunodeficiency virus." Journal Of Virology **82**(7): 3574-3583.

Carré, V. a. (1904). "Sur la nature infectieuse de l'anémie du cheval." Acad.Sci. **139**: 331-333.

Carteau, S., R. J. Gorelick, et al. (1999). "Coupled integration of human immunodeficiency virus type 1 cDNA ends by purified integrase in vitro: Stimulation by the viral nucleocapsid protein." Journal Of Virology **73**(8): 6670-6679.

Casimiro, D. R., F. Wang, et al. (2005). "Attenuation of simian immunodeficiency virus SIVmac239 infection by prophylactic immunization with dna and recombinant adenoviral vaccine vectors expressing Gag." J Virol **79**(24): 15547-55.

Catanzaro, A. T., R. A. Koup, et al. (2006). "Phase 1 safety and immunogenicity evaluation of a multiclade HIV-1 candidate vaccine delivered by a replication-defective recombinant adenovirus vector." J Infect Dis **194**(12): 1638-49.

Cen, S., Y. E. Huang, et al. (1999). "The role of Pr55(gag) in the annealing of tRNA44(3)(Lys) to human immunodeficiency virus type 1 genomic RNA." Journal Of Virology **73**(5): 4485-4488.

Champoux, J. J. and S. J. Schultz (2009). "Ribonuclease H: properties, substrate specificity and roles in retroviral reverse transcription." Febs Journal **276**(6): 1506-1516.

Chan, D. C., D. Fass, et al. (1997). "Core structure of gp41 from the HIV envelope glycoprotein." Cell **89**(2): 263-273.

Chang, T. L., J. Vargas, et al. (2005). "Dual role of alpha-defensin-1 in anti-HIV-1 innate immunity." Journal Of Clinical Investigation **115**(3): 765-773.

Charneau, P., G. Mirambeau, et al. (1994). "Hiv-1 Reverse Transcription - A Termination Step At The Center Of The Genome." Journal Of Molecular Biology **241**(5): 651-662.

Chen, C. P., C. Kremer, et al. (2010) "Modulating the activity of the channel-forming segment of Vpr protein from HIV-1." European Biophysics Journal With Biophysics Letters **39**(7): 1089-1095.

Chen, H., X. Liu, et al. (2010)"TSG101: a novel anti-HIV-1 drug target." Curr Med Chem **17**(8): 750-8.

Chen, L. F., J. Hoy, et al. (2007). "Ten years of highly active antiretroviral therapy for HIV infection." Medical Journal Of Australia **186**(3): 146-151.

Chen, Y., M. Balakrishnan, et al. (2003). "Mechanism of minus strand strong stop transfer in HIV-1 reverse transcription." Journal Of Biological Chemistry **278**(10): 8006-8017.

Cherepanov, P. (2007). "LEDGF/p75 interacts with divergent lentiviral integrases and modulates their enzymatic activity in vitro." Nucleic Acids Res **35**(1): 113-24.

Cherepanov, P., G. Maertens, et al. (2003). "HIV-1 integrase forms stable tetramers and associates with LEDGF/p75 protein in human cells." J Biol Chem **278**(1): 372-81.

Chertova, E., O. Chertov, et al. (2006). "Proteomic and biochemical analysis of purified human immunodeficiency virus type 1 produced from infected monocyte-derived macrophages." Journal Of Virology **80**(18): 9039-9052.

Chertova, E. N., B. P. Kane, et al. (1998). "Probing the topography of HIV-1 nucleocapsid protein with the alkylating agent N-ethylmaleimide." Biochemistry **37**(51): 17890-17897.

Chiu, Y. L., E. Coronel, et al. (2001). "HIV-1 Tat protein interacts with mammalian capping enzyme and stimulates capping of TAR RNA." J Biol Chem **276**(16): 12959-66.

Chong, S. Y., M. A. Egan, et al. (2007). "Comparative ability of plasmid IL-12 and IL-15 to enhance cellular and humoral immune responses elicited by a SIVgag plasmid DNA vaccine and alter disease progression following SHIV(89.6P) challenge in rhesus macaques." Vaccine **25**(26): 4967-82.

Cihlar, T. and A. S. Ray (2010) "Nucleoside and nucleotide HIV reverse transcriptase inhibitors: 25 years after zidovudine." Antiviral Res **85**(1): 39-58.

Cimarelli, A. and J. L. Darlix (2002). "Assembling the human immunodeficiency virus type 1." Cellular And Molecular Life Sciences **59**(7): 1166-1184.

Clarke, J. R., I. K. Taylor, et al. (1993). "The Epidemiology Of Hiv-1 Infection Of The Lung In Aids Patients." Aids **7**(4): 555-560.

Clavel, F. and A. J. Hance (2004). "Medical progress: HIV drug resistance." New England Journal Of Medicine **350**(10): 1023-1035.

Clavel, F. and J. M. Orenstein (1990). "A Mutant Of Human-Immunodeficiency-Virus With Reduced Rna Packaging And Abnormal Particle Morphology." Journal Of Virology **64**(10): 5230-5234.

Clever, J., C. Sassetti, et al. (1995). "Rna Secondary Structure And Binding-Sites For Gag Gene-Products In The 5'-Packaging Signal Of Human-Immunodeficiency-Virus Type-1." Journal Of Virology **69**(4): 2101-2109.

Clever, J. L., D. A. Eckstein, et al. (1999). "Genetic dissociation of the encapsidation and reverse transcription functions in the 5 ' R region of human immunodeficiency virus type 1." Journal Of Virology **73**(1): 101-109.

Clever, J. L. and T. G. Parslow (1997). "Mutant human immunodeficiency virus type 1 genomes with defects in RNA dimerization or encapsidation." Journal Of Virology **71**(5): 3407-3414.

Clever, J. L., M. L. Wong, et al. (1996). "Requirements for kissing-loop-mediated dimerization of human immunodeficiency virus RNA." J Virol **70**(9): 5902-8.

Cochrane, A. W., A. Perkins, et al. (1990). "Identification Of Sequences Important In The Nucleolar Localization Of Human Immunodeficiency Virus Rev - Relevance Of Nucleolar Localization To Function." Journal Of Virology **64**(2): 881-885.

Cockrell, A. S., H. van Praag, et al. (2011) "The HIV-1 Rev/RRE system is required for HIV-1 5' UTR cis elements to augment encapsidation of heterologous RNA into HIV-1 viral particles." Retrovirology **8**: 51.

Coetzee, T., D. Herschlag, et al. (1994). "Escherichia-Coli Proteins, Including Ribosomal-Protein S12, Facilitate In-Vitro Splicing Of Phage-T4 Introns By Acting As Rna Chaperones." Genes & Development **8**(13): 1575-1588.

Coffin, J. M. (1990). "The virology of AIDS: 1990." AIDS (London, England) **4 Suppl 1**: S1-8.

Cohen, E. A., R. A. Subbramanian, et al. (1996). "Role of auxiliary proteins in retroviral morphogenesis." Morphogenesis And Maturation Of Retroviruses **214**: 219-235.

Cole, A. M. (2003). "Minidefensins and other antimicrobial peptides: candidate anti-HIV microbicides." Expert Opinion On Therapeutic Targets **7**(3): 329-341.

Collins, K. L., B. K. Chen, et al. (1998). "HIV-1 Nef protein protects infected primary cells against killing by cytotoxic T lymphocytes." Nature **391**(6665): 397-401.

Correll, T. and O. M. Klibanov (2008). "Integrase inhibitors: a new treatment option for patients with human immunodeficiency virus infection." Pharmacotherapy **28**(1): 90-101.

Cox, S. W., K. Aperia, et al. (1994). "Comparison Of The Sensitivities Of Primary Isolates Of Hiv Type-2 And Hiv Type-1 To Antiviral Drugs And Drug-Combinations." Aids Research And Human Retroviruses **10**(12): 1725-1729.

Cristofari, G. and J. L. Darlix (2002). The ubiquitous nature of RNA chaperone proteins. Progress In Nucleic Acid Research And Molecular Biology, Vol 72. San Diego, Elsevier Academic Press Inc. **72:** 223-268.

Cruceanu, M., A. G. Stephen, et al. (2006). "Single DNA molecule stretching measures the activity of chemicals that target the HIV-1 nucleocapsid protein." Anal Biochem **358**(2): 159-70.

Cruceanu, M., M. A. Urbaneja, et al. (2006). "Nucleic acid binding and chaperone properties of HIV-1 Gag and nucleocapsid proteins." Nucleic Acids Research **34**(2): 593-605.

D

Daar, E. S., S. Little, et al. (2001). "Diagnosis of primary HIV-1 infection." Annals Of Internal Medicine **134**(1): 25-29.

Daecke, J., O. T. Fackler, et al. (2005). "Involvement of clathrin-mediated endocytosis in human immunodeficiency virus type 1 entry." Journal Of Virology **79**(3): 1581-1594.

Daelemans, D., S. V. Costes, et al. (2004). "In vivo HIV-1 rev multimerization in the nucleolus and cytoplasm identified by fluorescence resonance energy transfer." Journal Of Biological Chemistry **279**(48): 50167-50175.

Daher, K. A., M. E. Selsted, et al. (1986). "Direct Inactivation Of Viruses By Human Granulocyte Defensins." Journal Of Virology **60**(3): 1068-1074.

Dahms, T. E. S. and A. G. Szabo (1995). "Probing Local Secondary Structure By Fluorescence - Time-Resolved And Circular-Dichroism Studies Of Highly Purified Neurotoxins." Biophysical Journal **69**(2): 569-576.

Daly, T. J., K. S. Cook, et al. (1989). "Specific Binding Of Hiv-1 Recombinant Rev Protein To The Rev-Responsive Element Invitro." Nature **342**(6251): 816-819.

Daniel, M. D., F. Kirchhoff, et al. (1992). "Protective effects of a live attenuated SIV vaccine with a deletion in the nef gene." Science **258**(5090): 1938-41.

Darlix, J.-L., J. L. Garrido, et al. (2007). "Properties, functions, and drug targeting of the multifunctional nucleocapsid protein of the human immunodeficiency virus." Advances in pharmacology (San Diego, Calif.) **55**: 299-346.

Darlix, J. L., G. Cristofari, et al. (2000). "Nucleocapsid protein of human immunodeficiency virus as a model protein with chaperoning functions and as a target for antiviral drugs." Advances in pharmacology (San Diego, Calif.) **48**: 345-72.

Darlix, J. L., C. Gabus, et al. (1990). "Cis Elements And Trans-Acting Factors Involved In The Rna Dimerization Of The Human-Immunodeficiency-Virus Hiv-1." Journal Of Molecular Biology **216**(3): 689-699.

Darlix, J. L., J. Godet, et al. (2011) "Flexible nature and specific functions of the HIV-1 nucleocapsid protein." J Mol Biol **410**(4): 565-81.

Darlix, J. L., M. Lapadattapolsky, et al. (1995). "First Glimpses At Structure-Function-Relationships Of The Nucleocapsid Protein Of Retroviruses." Journal Of Molecular Biology **254**(4): 523-537.

Darlix, J. L., A. Vincent, et al. (1993). "Trans-activation of the 5' to 3' viral DNA strand transfer by nucleocapsid protein during reverse transcription of HIV1 RNA." C R Acad Sci III **316**(8): 763-71.

Das, A. T., A. Harwig, et al. (2011) "The HIV-1 Tat protein has a versatile role in activating viral transcription." J Virol **85**(18): 9506-16.

Das, A. T., A. Harwig, et al. (2007). "The TAR hairpin of human immunodeficiency virus type 1 can be deleted when not required for Tat-mediated activation of transcription." Journal Of Virology **81**(14): 7742-7748.

Das, A. T., B. Klaver, et al. (1999). "A hairpin structure in the R region of the human immunodeficiency virus type 1 RNA genome is instrumental in polyadenylation site selection." Journal Of Virology **73**(1): 81-91.

Das, A. T., B. Klaver, et al. (1997). "A conserved hairpin motif in the R-U5 region of the human immunodeficiency virus type 1 RNA genome is essential for replication." Journal Of Virology **71**(3): 2346-2356.

Davies, D. R. (1990). "The structure and function of the aspartic proteinases." Annu Rev Biophys Biophys Chem **19**: 189-215.

Davis, W. R., S. Gabbara, et al. (1998). "Actinomycin D inhibition of DNA strand transfer reactions catalyzed by HIV-1 reverse transcriptase and nucleocapsid protein." Biochemistry **37**(40): 14213-14221.

De Clercq, E. (2002). "New anti-HIV agents and targets." Medicinal Research Reviews **22**(6): 531-565.

De Guzman, R. N., Z. R. Wu, et al. (1998). "Structure of the HIV-1 nucleocapsid protein bound to the SL3 Psi-RNA recognition element." Science **279**(5349): 384-388.

de Noronha, C. M., M. P. Sherman, et al. (2001). "Dynamic disruptions in nuclear envelope architecture and integrity induced by HIV-1 Vpr." Science **294**(5544): 1105-8.

de Rocquigny, H., V. Shvadchak, et al. (2008). "Targeting the viral nucleocapsid protein in anti-HIV-1 therapy." Mini Rev Med Chem **8**(1): 24-35.

Debouck, C., J. G. Gorniak, et al. (1987). "Human Immunodeficiency Virus Protease Expressed In Escherichia-Coli Exhibits Autoprocessing And Specific Maturation Of The Gag Precursor." Proceedings Of The National Academy Of Sciences Of The United States Of America **84**(24): 8903-8906.

Deffaud, C. and J. L. Darlix (2000). "Rous sarcoma virus translation revisited: Characterization of an internal ribosome entry segment in the 5 ' leader of the genomic RNA." Journal Of Virology **74**(24): 11581-11588.

Delelis, O., K. Carayon, et al. (2008). "Insight into the integrase-DNA recognition mechanism. A specific DNA-binding mode revealed by an enzymatically labeled integrase." J Biol Chem **283**(41): 27838-49.

Deleys, R., B. Vanderborght, et al. (1990). "Isolation And Partial Characterization Of An Unusual Human Immunodeficiency Retrovirus From 2 Persons Of West-Central African Origin." Journal Of Virology **64**(3): 1207-1216.

Demene, H., C. Z. Dong, et al. (1994). "H-1-Nmr Structure And Biological Studies Of The His(23)-]Cys Mutant Nucleocapsid Protein Of Hiv-1 Indicate That The Conformation Of The First Zinc-Finger Is Critical For Virus Infectivity." Biochemistry **33**(39): 11707-11716.

Dewhurst, S., R. L. W. da Cruz, et al. (2000). "Pathogenesis and treatment of HIV-1 infection: Recent developments (y2K update)." Frontiers In Bioscience **5**: D30-D49.

Dhe-Paganon, S., K. Duda, et al. (2002). "Crystal structure of the HNF4 alpha ligand binding domain in complex with endogenous fatty acid ligand." J Biol Chem **277**(41): 37973-6.

Doetsch, M., B. Furtig, et al. (2011) "The RNA annealing mechanism of the HIV-1 Tat peptide: conversion of the RNA into an annealing-competent conformation." Nucleic Acids Res **39**(10): 4405-18.

Domagala, J. M., J. P. Bader, et al. (1997). "A new class of anti-HIV-1 agents targeted toward the nucleocapsid protein NCp7: The 2,2'-dithiobisbenzamides." Bioorganic & Medicinal Chemistry **5**(3): 569-579.

Dorfman T, L. J., Goff SP, Haseltine WA, Göttlinger HG. (1993). "Mapping of functionally important residues of a cysteine-histidine box in the human immunodeficiency virus type 1 nucleocapsid protein." Journal Of Virology **67**: 6159-69

Dorman, C. J., J. C. D. Hinton, et al. (1999). "Domain organization and oligomerization among H-NS-like nucleoid-associated proteins in bacteria." Trends In Microbiology **7**(3): 124-128.

Draper, D. E. (1999). "Themes in RNA-protein recognition." J Mol Biol **293**(2): 255-70.

Driscoll, M. D. and S. H. Hughes (2000). "Human immunodeficiency virus type 1 nucleocapsid protein can prevent self-priming of minus-strand strong stop DNA by promoting the annealing of short oligonucleotides to hairpin sequences." Journal Of Virology **74**(19): 8785-8792.

Druillennec, S., H. Meudal, et al. (1999). "Nucleomimetic strategy for the inhibition of HIV-1 nucleocapsid protein NCp7 activities." Bioorganic & Medicinal Chemistry Letters **9**(4): 627-632.

Druillennec, S. and B. P. Roques (2000). "HIV-1NCp7 as a target for the design of novel antiviral agents." Drug News & Perspectives **13**(6): 337-349.

Dussupt, V., M. P. Javid, et al. (2009). "The Nucleocapsid Region of HIV-1 Gag Cooperates with the PTAP and LYPXnL Late Domains to Recruit the Cellular Machinery Necessary for Viral Budding." Plos Pathogens **5**(3).

Dyda, F., A. B. Hickman, et al. (1994). "Crystal-Structure Of The Catalytic Domain Of Hiv-1 Integrase - Similarity To Other Polynucleotidyl Transferases." Science **266**(5193): 1981-1986.

E

Egele, C., E. Schaub, et al. (2004). "HIV-1 nucleocapsid protein binds to the viral DNA initiation sequences and chaperones their kissing interactions." Journal Of Molecular Biology **342**(2): 453-466.

Egele, C., E. Schaub, et al. (2005). "Investigation by fluorescence correlation spectroscopy of the chaperoning interactions of HIV-1 nucleocapsid protein with the viral DNA initiation sequences." Comptes Rendus Biologies **328**(12): 1041-1051.

Ellison, V., H. Abrams, et al. (1990). "Human-Immunodeficiency-Virus Integration In A Cell-Free System." Journal Of Virology **64**(6): 2711-2715.

Emiliani, S., A. Mousnier, et al. (2005). "Integrase mutants defective for interaction with LEDGF/p75 are impaired in chromosome tethering and HIV-1 replication." J Biol Chem **280**(27): 25517-23.

Enders, J. F. (1954). "Cytopathology of virus infections: particular reference to tissue culture studies." Annual review of microbiology **8**: 473-502.

Engelman, A., F. D. Bushman, et al. (1993). "Identification of discrete functional domains of HIV-1 integrase and their organization within an active multimeric complex." Embo J **12**(8): 3269-75.

Engelman, A., A. B. Hickman, et al. (1994). "The core and carboxyl-terminal domains of the integrase protein of human immunodeficiency virus type 1 each contribute to nonspecific DNA binding." J Virol **68**(9): 5911-7.

Ennifar, E., J. C. Paillart, et al. (2006). "Targeting the dimerization initiation site of HIV-1 RNA with aminoglycosides: from crystal to cell." Nucleic Acids Research **34**(8): 2328-2339.

F

Faber, C., H. Sticht, et al. (2000). "Structural rearrangements of HIV-1 Tat-responsive RNA upon binding of neomycin B." Journal Of Biological Chemistry **275**(27): 20660-20666.

Farmerie, W. G., D. D. Loeb, et al. (1987). "Expression And Processing Of The Aids Virus Reverse-Transcriptase In Escherichia-Coli." Science **236**(4799): 305-308.

Fassati, A. (2006). "HIV infection of non-dividing cells: a divisive problem." Retrovirology **3**: 74.

"FDA notifications. FDA approves raltegravir for HIV-1 treatment-naive patients."(2009) AIDS Alert **24**(9): 106-7.

Feng, Y. X., S. Campbell, et al. (1999). "The human immunodeficiency virus type 1 Gag polyprotein has nucleic acid chaperone activity: Possible role in dimerization of genomic RNA and placement of tRNA on the primer binding site." Journal Of Virology **73**(5): 4251-4256.

Fesen, M. R., K. W. Kohn, et al. (1993). "Inhibitors of human immunodeficiency virus integrase." Proc Natl Acad Sci U S A **90**(6): 2399-403.

Fletcher, T. M., B. Brichacek, et al. (1996). "Nuclear import and cell cycle arrest functions of the HIV-1 Vpr protein are encoded by two separate genes in HIV-2/SIVSM." Embo Journal **15**(22): 6155-6165.

Flexner, C. (1998). "HIV-protease inhibitors." New England Journal Of Medicine **338**(18): 1281-1292.

Flynn, N. M., D. N. Forthal, et al. (2005). "Placebo-controlled phase 3 trial of a recombinant glycoprotein 120 vaccine to prevent HIV-1 infection." J Infect Dis **191**(5): 654-65.

Fouchier, R. A., B. E. Meyer, et al. (1997). "HIV-1 infection of non-dividing cells: evidence that the amino-terminal basic region of the viral matrix protein is important for Gag processing but not for post-entry nuclear import." Embo J **16**(15): 4531-9.

Fouchier, R. A. M., B. E. Meyer, et al. (1998). "Interaction of the human immunodeficiency virus type 1 Vpr protein with the nuclear pore complex." Journal Of Virology **72**(7): 6004-6013.

Franke, E. K., H. E. Yuan, et al. (1994). "Specific incorporation of cyclophilin A into HIV-1 virions." Nature **372**(6504): 359-62.

Frankel, A. D. and J. A. Young (1998). "HIV-1: fifteen proteins and an RNA." Annu Rev Biochem **67**: 1-25.

Freed, E. O. (1998). "HIV-1 Gag proteins: Diverse functions in the virus life cycle." Virology **251**(1): 1-15.

Freed, E. O. (2001). "HIV-1 replication." Somatic cell and molecular genetics **26**(1-6): 13-33.

Freed, E. O., G. Englund, et al. (1997). "Phosphorylation of residue 131 of HIV-1 matrix is not required for macrophage infection." Cell **88**(2): 171-3; discussion 173-4.

Freed, E. O., G. Englund, et al. (1995). "Role of the basic domain of human immunodeficiency virus type 1 matrix in macrophage infection." J Virol **69**(6): 3949-54.

Freed, E. O. and M. A. Martin (1995). "The Role of Human-Immunodeficiency-Virus Type-1 Envelope Glycoproteins In Virus-Infection." Journal Of Biological Chemistry **270**(41): 23883-23886.

Freisz, S., K. Lang, et al. (2008). "Binding of aminoglycoside antibiotics to the duplex form of the HIV-1 genomic RNA dimerization initiation site." Angewandte Chemie-International Edition **47**(22): 4110-4113.

Fritz, J. V., P. Didier, et al. (2008). "Direct Vpr-Vpr Interaction in Cells monitored by two Photon Fluorescence Correlation Spectroscopy and Fluorescence Lifetime Imaging." Retrovirology **5**.

G

Gallaher, W. R. (1987). "Detection Of A Fusion Peptide Sequence In The Transmembrane Protein Of Human-Immunodeficiency-Virus." Cell **50**(3): 327-328.

Gallego, J., J. Greatorex, et al. (2003). "Rev binds specifically to a purine loop in the SL1 region of the HIV-1 leader RNA." Journal Of Biological Chemistry **278**(41): 40385-40391.

Gamble, T. R., F. F. Vajdos, et al. (1996). "Crystal structure of human cyclophilin A bound to the amino-terminal domain of HIV-1 capsid." Cell **87**(7): 1285-1294.

Ganser, B. K., S. Li, et al. (1999). "Assembly and analysis of conical models for the HIV-1 core." Science **283**(5398): 80-83.

Gao, F., L. Yue, et al. (1992). "Human Infection By Genetically Diverse Sivsm-Related Hiv-2 In West Africa." Nature **358**(6386): 495-499.

Garrus, J. E., U. K. von Schwedler, et al. (2001). "Tsg101 and the vacuolar protein sorting pathway are essential for HIV-1 budding." Cell **107**(1): 55-65.

Garzino-Demo, A., R. B. Moss, et al. (1999). "Spontaneous and antigen-induced production of HIV-inhibitory beta-chemokines are associated with AIDS-free status." Proceedings Of The National Academy Of Sciences Of The United States Of America **96**(21): 11986-11991.

Gifford, R. and M. Tristem (2003). "The evolution, distribution and diversity of endogenous retroviruses." Virus Genes **26**(3): 291-316.

Gillespie, E. L., J. L. Kuti, et al. (2005). "Pharmacodynamics of antimicrobials: treatment optimisation." Expert opinion on drug metabolism & toxicology **1**(3): 351-61.

Godet, J., H. de Rocquigny, et al. (2006). "During the early phase of HIV-1 DNA synthesis, nucleocapsid protein directs hybridization of the TAR complementary sequences via the ends of their double-stranded stem." Journal Of Molecular Biology **356**(5): 1180-1192.

Godet, J. and Y. Mely (2010). "Biophysical studies of the nucleic acid chaperone properties of the HIV-1 nucleocapsid protein." Rna Biology **7**(6): 687-699.

Godet J, R. N., Sharma KK, Richert L, de Rocquigny H, Darlix JL, Duportail G, Mély Y. (2011). "Specific implications of the HIV-1 nucleocapsid zinc fingers in the annealing of the primer binding site complementary sequences during the obligatory plus strand transfer." Nucleic Acids Research **39**: 6633-6645.

Goebel, F. D., R. Hemmer, et al. (2001). "Phase I/II dose escalation and randomized withdrawal study with add-on azodicarbonamide in patients failing on current antiretroviral therapy." Aids **15**(1): 33-45.

Gonzalez, E., H. Kulkarni, et al. (2005). "The influence of CCL3L1 gene-containing segmental duplications on HIV-1/AIDS susceptibility." Science **307**(5714): 1434-1440.

Gorelick, R. J., D. J. Chabot, et al. (1996). "Genetic analysis of the zinc finger in the Moloney murine leukemia virus nucleocapsid domain: Replacement of zinc-coordinating residues with other zinc-coordinating residues yields noninfectious particles containing genomic RNA." Journal Of Virology **70**(4): 2593-2597.

Gorelick, R. J., D. J. Chabot, et al. (1993). "The 2 Zinc Fingers In The Human-Immunodeficiency-Virus Type-1 Nucleocapsid Protein Are Not Functionally Equivalent." Journal Of Virology **67**(7): 4027-4036.

Gorelick, R. J., S. M. Nigida, et al. (1990). "Noninfectious Human-Immunodeficiency-Virus Type-1 Mutants Deficient In Genomic Rna." Journal Of Virology **64**(7): 3207-3211.

Gottfredsson, M. and P. R. Bohjanen (1997). "Human immunodeficiency virus type I as a target for gene therapy." Frontiers in bioscience: a journal and virtual library **2**: d619-34.

Greenway, A. and D. McPhee (1997). "HIV1 Nef: The Machiavelli of cellular activation." Research In Virology **148**(1): 58-64.

Gregoire, C. J., D. Gautheret, et al. (1997). "No tRNA(3)(Lys) unwinding in a complex with HIV NCp7." Journal Of Biological Chemistry **272**(40): 25143-25148.

Grigorov, B., A. Bocquin, et al.(2011) "Identification of a methylated oligoribonucleotide as a potent inhibitor of HIV-1 reverse transcription complex." Nucleic Acids Res **39**(13): 5586-96.

Grigorov B, D. D., Smagulova F, Pechoux C, Mougel M, Muriaux D, Darlix JL (2007). "Intracellular HIV-1 Gag localization is impaired by mutations in the nucleocapsid zinc fingers." Retrovirology **4**(54).

Grigorov, B., Arcanger, F., Roingeard, P., Darlix, J.L., Muriaux, D (2006) "Assembly of infectious HIV-1 in human epithelial and lymphoblastic cell lines."Journal of Molecular Biology **359**: 848-62.

Grohmann, D., J. Godet, et al. (2008). "HIV-1 nucleocapsid traps reverse transcriptase on nucleic acid substrates." Biochemistry **47**(46): 12230-40.

Gros E., D. S., Morris May C., Aldrian-Herrada G, and H. F. Depollier J., Divita G. (2006). "A non-covalent peptide-based strategy for
protein and peptide nucleic acid transduction." Biochimica et Biophysica Acta **1758**: 384–393.

Gross, L. (1957). "Development and serial cellfree passage of a highly potent strain of mouse leukemia virus." Proceedings of the Society for Experimental Biology and Medicine. Society for Experimental Biology and Medicine (New York, N.Y.) **94**(4): 767-71.

Guo F, C. S., Niu M, Yang Y, Gorelick RJ, Kleiman L. (2007). "The interaction of APOBEC3G with human immunodeficiency virus type 1 nucleocapsid inhibits tRNA3Lys annealing to viral RNA." Journal Of Virology **81**: 11322-31.

Guest CR, H. R., Sowers LC, Millar DP. (1991). "Dynamics of mismatched base pairs in DNA." Biochemistry **30**: 3271-9

Guo, J., L. E. Henderson, et al. (1997). "Human immunodeficiency virus type 1 nucleocapsid protein promotes efficient strand transfer and specific viral DNA synthesis by inhibiting TAR-dependent self-priming from minus-strand strong-stop DNA." J Virol **71**(7): 5178-88.

Guo, J. H., T. Y. Wu, et al. (2000). "Zinc finger structures in the human immunodeficiency virus type 1 nucleocapsid protein facilitate efficient minus- and plus-strand transfer." Journal Of Virology **74**(19): 8980-8988.

Guo, J. H., T. Y. Wu, et al. (1998). "Actinomycin D inhibits human immunodeficiency virus type 1 minus-strand transfer in in vitro and endogenous reverse transcriptase assays." Journal Of Virology **72**(8): 6716-6724.

Gupta, K., T. Diamond, et al.(2010) "Structural Properties of HIV Integrase.Lens Epithelium-derived Growth Factor Oligomers." Journal Of Biological Chemistry **285**(26): 20303-20315.

Gupta, K., D. Ott, et al. (2000). "A human nuclear shuttling protein that interacts with human immunodeficiency virus type 1 matrix is packaged into virions." J Virol **74**(24): 11811-24.

Gupta, S., R. Boppana, et al. (2008). "HIV-1 tat suppresses gp120-specific T cell response in IL-10-dependent manner." Journal Of Immunology **180**(1): 79-88.

H

Haas, E., M. Wilchek, et al. (1975). "Distribution Of End-To-End Distances Of Oligopeptides In Solution As Estimated By Energy-Transfer." Proceedings Of The National Academy Of Sciences Of The United States Of America **72**(5): 1807-1811.

Haffar, O. K., S. Popov, et al. (2000). "Two nuclear localization signals in the HIV-1 matrix protein regulate nuclear import of the HIV-1 pre-integration complex." J Mol Biol **299**(2): 359-68.

Hahn, B. H., G. M. Shaw, et al. (2000). "AIDS - AIDS as a zoonosis: Scientific and public health implications." Science **287**(5453): 607-614.

Harari, A., P. A. Bart, et al. (2008). "An HIV-1 clade C DNA prime, NYVAC boost vaccine regimen induces reliable, polyfunctional, and long-lasting T cell responses." J Exp Med **205**(1): 63-77.

Hare, S., S. S. Gupta, et al. (2010) "Retroviral intasome assembly and inhibition of DNA strand transfer." Nature **464**(7286): 232-6.

Hare, S., M. C. Shun, et al. (2009). "A novel co-crystal structure affords the design of gain-of-function lentiviral integrase mutants in the presence of modified PSIP1/LEDGF/p75." PLoS Pathog **5**(1): e1000259.

Haren, L., B. Ton-Hoang, et al. (1999). "Integrating DNA: transposases and retroviral integrases." Annu Rev Microbiol **53**: 245-81.

Hargittai, M. R. S., R. J. Gorelick, et al. (2004). "Mechanistic insights into the kinetics of HIV-1 nucleocapsid protein-facilitated tRNA annealing to the primer binding site." Journal Of Molecular Biology **337**(4): 951-968.

Harter, C., P. James, et al. (1989). "Hydrophobic Binding Of The Ectodomain Of Influenza Hemagglutinin To Membranes Occurs Through The Fusion Peptide." Journal Of Biological Chemistry **264**(11): 6459-6464.

Hatziioannou, T., D. Perez-Caballero, et al. (2005). "Cyclophilin interactions with incoming human immunodeficiency virus type 1 capsids with opposing effects on infectivity in human cells." J Virol **79**(1): 176-83.

Hayashi, T., T. Shioda, et al. (1992). "Rna Packaging Signal Of Human-Immunodeficiency-Virus Type-1." Virology **188**(2): 590-599.

Hecht, F. M., M. P. Busch, et al. (2002). "Use of laboratory tests and clinical symptoms for identification of primary HIV infection." Aids **16**(8): 1119-1129.

Henderson, L. E., M. A. Bowers, et al. (1992). "Gag Proteins Of The Highly Replicative Mn Strain Of Human-Immunodeficiency-Virus Type-1 - Posttranslational Modifications, Proteolytic Processings, And Complete Amino-Acid-Sequences." Journal Of Virology **66**(4): 1856-1865.

Herbreteau, C. H., L. Weill, et al. (2005). "HIV-2 genomic RNA contains a novel type of IRES located downstream of its initiation codon." Nature Structural & Molecular Biology **12**(11): 1001-1007.

Herschhorn, A. and A. Hizi (2010) "Retroviral reverse transcriptases." Cell Mol Life Sci **67**(16): 2717-47.

Herschlag, D. (1995). "Rna Chaperones And The Rna Folding Problem." Journal Of Biological Chemistry **270**(36): 20871-20874.

Heyduk, T. (2002). "Measuring protein conformational changes by FRET/LRET." Current Opinion In Biotechnology **13**(4): 292-296.

Heyman, T., B. Agoutin, et al. (1995). "Plus-Strand Dna-Synthesis Of The Yeast Retrotransposon Ty1 Is Initiated At 2 Sites, Ppt1 Next To The 3'-Ltr And Ppt2 Within The Pol Gene - Ppt1 Is Sufficient For Ty1 Transposition." Journal Of Molecular Biology **253**(2): 291-303.

Hill, M. K., M. Shehu-Xhilaga, et al. (2003). "The dimer initiation sequence stem-loop of human immunodeficiency virus type 1 is dispensable for viral replication in peripheral blood mononuclear cells." J Virol **77**(15): 8329-35.

Hink, M. A., T. Bisseling, et al. (2002). "Imaging protein-protein interactions in living cells." Plant Molecular Biology **50**(6): 871-883.

Hirsch, V. M., R. A. Olmsted, et al. (1989). "An African Primate Lentivirus (Sivsm) Closely Related To Hiv-2." Nature **339**(6223): 389-392.

Hsiou, Y., J. Ding, et al. (1996). "Structure of unliganded HIV-1 reverse transcriptase at 2.7 A resolution: implications of conformational changes for polymerization and inhibition mechanisms." Structure **4**(7): 853-60.

Hu, W. S. and H. M. Temin (1990). "Retroviral Recombination And Reverse Transcription." Science **250**(4985): 1227-1233.

Huet, T., R. Cheynier, et al. (1990). "Genetic Organization Of A Chimpanzee Lentivirus Related To Hiv-1." Nature **345**(6273): 356-359.

Hung, L. W., E. L. Holbrook, et al. (2000). "The crystal structure of the Rev binding element of HIV-1 reveals novel base pairing and conformational variability." Proc Natl Acad Sci U S A **97**(10): 5107-12.

Huang M, Maynard A, et al. (1998) "Anti-HIV agents that selectively target retroviral nucleocapsid protein zinc fingers without affecting cellular zinc finger proteins." J Med Chem. **141**:1371-81.

Huthoff, H. and B. Berkhout (2001). "Two alternating structures of the HIV-1 leader RNA." Rna-A Publication Of The Rna Society **7**(1): 143-157.

I

Isel, C., C. Ehresmann, et al. (1995). "Initiation Of Reverse Transcription Of Hiv-1 - Secondary Structure Of The Hiv-1 Rna/Trna(3)(Lys) (Template/Primer) Complex." Journal Of Molecular Biology **247**(2): 236-250.

J

Jablonski, J. A., A. L. Amelio, et al.(2010) "The transcriptional transactivator Tat selectively regulates viral splicing." Nucleic Acids Res **38**(4): 1249-60.

Jacobo-Molina, A., J. Ding, et al. (1993). "Crystal structure of human immunodeficiency virus type 1 reverse transcriptase complexed with double-stranded DNA at 3.0 A resolution shows bent DNA." Proc Natl Acad Sci U S A **90**(13): 6320-4.

Jacques, C., M. Gosset, et al. (2006). The role of IL-1 and IL-1RA in joint inflammation and cartilage degradation. Interleukins. San Diego, Elsevier Academic Press Inc. **74:** 371-403.

Jang, S. K., H. G. Krausslich, et al. (1988). "A Segment Of The 5' Nontranslated Region Of Encephalomyocarditis Virus-Rna Directs Internal Entry Of Ribosomes During Invitro Translation." Journal Of Virology **62**(8): 2636-2643.

Jares-Erijman, E. A. and T. M. Jovin (2006). "Imaging molecular interactions in living cells by FRET microscopy." Current Opinion In Chemical Biology **10**(5): 409-416.

Jaskolski, M., J. N. Alexandratos, et al. (2009). "Piecing together the structure of retroviral integrase, an important target in AIDS therapy." Febs J **276**(11): 2926-46.

Johnson, J. M., R. Harrod, et al. (2001). "Molecular biology and pathogenesis of the human T-cell leukaemia/lymphotropic virus type-1 (HTLV-1)." International Journal Of Experimental Pathology **82**(3): 135-147.

Johnson VA, C. V., Günthard HF, Paredes R, Pillay D, Shafer R, Wensing AM, Richman DD. (2011). "2011 update of the drug resistance mutations in HIV-1." Topics in antiviral medicine **19**: 156-64.

Joliot A, P. C., Deagostini-Bazin H, Prochiantz A. (1991). "Antennapedia homeobox peptide regulates neural morphogenesis." Proc Natl Acad Sci U S A **88**: 1864-8.

Jolly, C. and Q. J. Sattentau (2004). "Retroviral spread by induction of virological synapses." Traffic **5**(9): 643-650.

Jordan, S. P., J. Zugay, et al. (1992). "Activity and dimerization of human immunodeficiency virus protease as a function of solvent composition and enzyme concentration." J Biol Chem **267**(28): 20028-32.

Ju, S. M., H. Y. Song, et al. (2009). "Extracellular HIV-1 Tat up-regulates expression of matrix metalloproteinase-9 via a MAPK-NF-kappa B dependent pathway in human astrocytes." Experimental And Molecular Medicine **41**(2): 86-93.

K

Kafaie, J., R. J. Song, et al. (2008). "Mapping of nucleocapsid residues important for HIV-1 genomic RNA dimerization and packaging." Virology **375**(2): 592-610.

Kahn, J. O. and B. D. Walker (1998). "Acute human immunodeficiency virus type 1 infection." New England Journal Of Medicine **339**(1): 33-39.

Kao, S., M. A. Khan, et al. (2003). "The human immunodeficiency virus type 1 Vif protein reduces intracellular expression and inhibits packaging of APOBEC3G (CEM15), a cellular inhibitor of virus infectivity." Journal Of Virology **77**(21): 11398-11407.

Kaplan, A. H., P. Krogstad, et al. (1994). "Human-Immunodeficiency-Virus Type-1 Virions Composed Of Unprocessed Gag And Gag-Pol Precursors Are Capable Of Reverse Transcribing Viral Genomic Rna." Antimicrobial Agents And Chemotherapy **38**(12): 2929-2933.

Karacostas, V., K. Nagashima, et al. (1989). "Human Immunodeficiency Virus-Like Particles Produced By A Vaccinia Virus Expression Vector." Proceedings Of The National Academy Of Sciences Of The United States Of America **86**(22): 8964-8967.

Kassahun, K., I. McIntosh, et al. (2007). "Metabolism and disposition in humans of raltegravir (MK-0518), an Anti-AIDS drug targeting the human immunodeficiency virus 1 integrase enzyme." Drug Metabolism And Disposition **35**(9): 1657-1663.

Kaye, J. F. and A. M. L. Lever (1998). "Nonreciprocal packaging of human immunodeficiency virus type 1 and type 2 RNA: a possible role for the p2 domain of Gag in RNA encapsidation." Journal Of Virology **72**(7): 5877-5885.

Kempf, D. J., K. C. Marsh, et al. (1995). "Abt-538 Is A Potent Inhibitor Of Human-Immunodeficiency-Virus Protease And Has High Oral Bioavailability In Humans." Proceedings Of The National Academy Of Sciences Of The United States Of America **92**(7): 2484-2488.

Kerkau, T., I. Bacik, et al. (1997). "The human immunodeficiency virus type 1 (HIV-1) vpu protein interferes with an early step in the biosynthesis of major histocompatibility complex (MHC) class I molecules." Journal Of Experimental Medicine **185**(7): 1295-1305.

Khan, R. and D. P. Giedroc (1992). "Recombinant human immunodeficiency virus type 1 nucleocapsid (NCp7) protein unwinds tRNA." J Biol Chem **267**(10): 6689-95.

Kim, M. Y. and S. Jeong (2004). "Inhibition of the functions of the nucleocapsid protein of human immunodeficiency virus-1 by an RNA aptamer." Biochemical And Biophysical Research Communications **320**(4): 1181-1186.

Kim, R. and J. D. Baxter (2008). "Protease inhibitor resistance update: Where are we now?" Aids Patient Care And Stds **22**(4): 267-277.

Kjems, J. and P. Askjaer (2000). "Rev protein and its cellular partners." Adv Pharmacol **48**: 251-98.

Kleiman, L., R. Halwani, et al. (2004). "The selective packaging and annealing of primer tRNA(Lys3) in HIV-1." Current Hiv Research **2**(2): 163-175.

Kohlstaedt, L. A. and T. A. Steitz (1992). "Reverse transcriptase of human immunodeficiency virus can use either human tRNA(3Lys) or Escherichia coli tRNA(2Gln) as a primer in an in vitro primer-utilization assay." Proc Natl Acad Sci U S A **89**(20): 9652-6.

Korber BT, Letvin NL, Haynes BF. (2009) "T cell Vaccine Strategies for HIV, the Virus With a Thousand Faces". Journal of virology. **83**: 8300-14.

Kornfeld, H. and W. W. Cruikshank (2001). "Prospects for IL-16 in the treatment of AIDS." Expert Opinion On Biological Therapy **1**(3): 425-432.

Kotler, M., W. Danho, et al. (1989). "Avian retroviral protease and cellular aspartic proteases are distinguished by activities on peptide substrates." J Biol Chem **264**(6): 3428-35.

Kripke (2007). "Antiretroviral prophylaxis for occupational exposure to HIV." American family physician **76**: 375-6.

Krishnamoorthy, G., B. Roques, et al. (2003). "DNA condensation by the nucleocapsid protein of HIV-1: a mechanism ensuring DNA protection." Nucleic Acids Res **31**(18): 5425-32.

Kroeger Smith MB, H. B., Hawkins A, Lipchock J, Farnsworth DW, Rizzo RC, Tirado-Rives J, Arnold E, Zhang W, Hughes SH, Jorgensen WL, Michejda CJ, Smith RH Jr. (2003). "Molecular modeling calculations of HIV-1 reverse transcriptase nonnucleoside inhibitors: correlation of binding energy with biological activity for novel 2-aryl-substituted benzimidazole analogues." Journal of medicinal chemistry **46**: 1940-7.

Kubota, S., H. Siomi, et al. (1989). "Functional Similarity Of Hiv-I Rev And Htlv-I Rex Proteins - Identification Of A New Nucleolar-Targeting Signal In Rev Protein." Biochemical And Biophysical Research Communications **162**(3): 963-970.

Kutluay, S. B. and P. D. Bieniasz (2010) "Analysis of the Initiating Events in HIV-1 Particle Assembly and Genome Packaging." Plos Pathogens **6**(11).

Kwong, P. D., R. Wyatt, et al. (2000). "Structures of HIV-1 gp120 envelope glycoproteins from laboratory-adapted and primary isolates." Structure **8**(12): 1329-39.

L

Lalezari, J. P., K. Henry, et al. (2003). "Enfuvirtide, an HIV-1 fusion inhibitor, for drug-resistant HIV infection in North and South America." New England Journal Of Medicine **348**(22): 2175-2185.

Lama, J. and V. Planelles (2007). "Host factors influencing susceptibility to HIV infection and AIDS progression." Retrovirology **4**: 52.

Lapadattapolsky, M., H. Derocquigny, et al. (1993). "Interactions Between Hiv-1 Nucleocapsid Protein And Viral-Dna May Have Important Functions In The Viral Life-Cycle (Vol 21, Pg 831, 1993)." Nucleic Acids Research **21**(8): 2024-2024.

LapadatTapolsky, M., C. Gabus, et al. (1997). "Possible roles of HIV-1 nucleocapsid protein in the specificity of proviral DNA synthesis and in its variability." Journal Of Molecular Biology **268**(2): 250-260.

Lapadattapolsky, M., C. Pernelle, et al. (1995). "Analysis Of The Nucleic-Acid Annealing Activities Of Nucleocapsid Protein From Hiv-1." Nucleic Acids Research **23**(13): 2434-2441.

Laschewsky A, Ringsdorf H, Schmidt G, Schneider J. (1987). "Self-organization of polymeric lipids with hydrophilic spacers in side groups and main chain: Investigation in monolayers and multilayers". J Am Chem Soc **109**:788–796.

Lawrence, D. C., C. C. Stover, et al. (2003). "Structure of the intact stem and bulge of HIV-1 psi-RNA stem-loop SL1." Journal Of Molecular Biology **326**(2): 529-542.

Lazzarin, A., B. Clotet, et al. (2003). "Efficacy of enfuvirtide in patients infected with drug-resistant HIV-1 in Europe and Australia." New England Journal Of Medicine **348**(22): 2186-2195.

Le Rouzic, E. and S. Benichou (2005). "The Vpr protein from HIV-1: distinct roles along the viral life cycle." Retrovirology **2**.

Le Rouzic, E., A. Mousnier, et al. (2002). "Docking of HIV-1 Vpr to the nuclear envelope is mediated by the interaction with the nucleoporin hCG1." Journal Of Biological Chemistry **277**(47): 45091-45098.

Learmont, J. C., A. F. Geczy, et al. (1999). "Immunologic and virologic status after 14 to 18 years of infection with an attenuated strain of HIV-1. A report from the Sydney Blood Bank Cohort." N Engl J Med **340**(22): 1715-22.

LeGall, S., M. C. Prevost, et al. (1997). "Human immunodeficiency virus type I Nef independently affects virion incorporation of major histocompatibility complex class I molecules and virus infectivity." Virology **229**(1): 295-301.

Lemey, P., O. G. Pybus, et al. (2004). "The molecular population genetics of HIV-1 group O." Genetics **167**(3): 1059-1068.

Lener, D., V. Tanchou, et al. (1998). "Involvement of HIV-1 nucleocapsid protein in the recruitment of reverse transcriptase into nucleoprotein complexes formed in vitro." Journal Of Biological Chemistry **273**(50): 33781-33786.

Leonard, C. K., M. W. Spellman, et al. (1990). "Assignment Of Intrachain Disulfide Bonds And Characterization Of Potential Glycosylation Sites Of The Type-1 Recombinant Human-Immunodeficiency-Virus Envelope Glycoprotein (Gp120) Expressed In Chinese Hamster Ovary Cells." Journal Of Biological Chemistry **265**(18): 10373-10382.

Létourneau,S., Im,E. Mashishi, T., Brereton,C., Bridgeman,A.,Yang,H. Dorrell,H., Dong,T. et al.(2007) "Design and Pre-Clinical Evaluation of a Universal HIV-1 Vaccine." Plos one **10**: 1-11.

Lever, A., H. Gottlinger, et al. (1989). "Identification Of A Sequence Required For Efficient Packaging Of Human Immunodeficiency Virus Type-1 Rna Into Virions." Journal Of Virology **63**(9): 4085-4087.

Levin, A., A. Armon-Omer, et al. (2009). "Inhibition of HIV-1 integrase nuclear import and replication by a peptide bearing integrase putative nuclear localization signal." Retrovirology **6**: 112.

Levin, J. G., J. H. Guo, et al. (2005). Nucleic acid chaperone activity of HIV-1 nucleocapsid protein: Critical role in reverse transcription and molecular mechanism. Progress In Nucleic Acid Research And Molecular Biology, Vol 80. San Diego, Elsevier Academic Press Inc. **80:** 217-286.

Levin, J. G., M. Mitra, et al. "Role of HIV-1 nucleocapsid protein in HIV-1 reverse transcription." Rna Biology **7**(6): 754-774.

Li, F., R. Goila-Gaur, et al. (2003). "PA-457: A potent HIV inhibitor that disrupts core condensation by targeting a late step in Gag processing." Proceedings Of The National Academy Of Sciences Of The United States Of America **100**(23): 13555-13560.

Li, J. C. B., D. C. W. Lee, et al. (2005). "Mechanisms for HIV Tat upregulation of IL-10 and other cytokine expression: Kinase signaling and PKR-mediated immune response." Febs Letters **579**(14): 3055-3062.

Li XY, G. F., Zhang L, Kleiman L, Cen S. (2007). "APOBEC3G inhibits DNA strand transfer during HIV-1 reverse transcription." Journal Of Biological Chemistry **282**: 32065-74.

Lieberman-Blum, S. S., H. B. Fung, et al. (2008). "Maraviroc: A CCR5-receptor antagonist for the treatment of HIV-1 infection." Clinical Therapeutics **30**(7): 1228-1250.

Lifson, J. D., M. Piatak, et al. (2002). "Whole inactivated SIV virion vaccines with functional envelope glycoproteins: safety, immunogenicity, and activity against intrarectal challenge." Journal Of Medical Primatology **31**(4-5): 205-216.

Lifson, J. D., J. L. Rossio, et al. (2004). "Evaluation of the safety, immunogenicity, and protective efficacy of whole inactivated simian immunodeficiency virus (SIV) vaccines with conformationally and functionally intact envelope glycoproteins." Aids Research And Human Retroviruses **20**(7): 772-787.

Lihana, R. W., D. Ssemwanga, et al.(2012) "Update on HIV-1 Diversity in Africa: A Decade in Review." Aids Reviews **14**(2): 83-100.

Lingappa, J. R., J. E. Dooher, et al. (2006). "Basic residues in the nucleocapsid domain of gag are required for interaction of HIV-1 Gag with ABCE1 (HP68), a cellular protein important for HIV-1 capsid assembly." Journal Of Biological Chemistry **281**(7): 3773-3784.

Litvak S, Sarih-Cottin L et al. (1994) "Priming of HIV replication by tRNA(Lys3): role of reverse transcriptase." Trends Biochem Sci. **19**:114-8.

Liu, H. W., Y. N. Zeng, et al. (2007). "Insights on the role of nucleic acid/protein interactions in chaperoned nucleic acid rearrangements of HIV-1 reverse transcription." Proceedings Of The National Academy Of Sciences Of The United States Of America **104**(13): 5261-5267.

Liu, J., R. Kjeken, et al. (2008). "Recruitment of antigen-presenting cells to the site of inoculation and augmentation of human immunodeficiency virus type 1 DNA vaccine immunogenicity by in vivo electroporation." J Virol **82**(11): 5643-9.

Llano, M., M. Vanegas, et al. (2004). "LEDGF/p75 determines cellular trafficking of diverse lentiviral but not murine oncoretroviral integrase proteins and is a component of functional lentiviral preintegration complexes." J Virol **78**(17): 9524-37.

Lobritz, M. A., A. N. Ratcliff, et al. (2010). "HIV-1 Entry, Inhibitors, and Resistance." Viruses-Basel **2**(5): 1069-1105.

Loh, T. T., Y. G. Yeung, et al. (1977). "Transferrin And Iron Uptake By Rabbit Reticulocytes." Biochimica Et Biophysica Acta **471**(1): 118-124.

Lu, K., X. Heng, et al. (2011) "NMR Detection of Structures in the HIV-1 5 '-Leader RNA That Regulate Genome Packaging." Science **334**(6053): 242-245.

Lu, K., X. Heng, et al.(2011) "Structural Determinants and Mechanism of HIV-1 Genome Packaging." Journal Of Molecular Biology **410**(4): 609-633.

Luban, J., K. L. Bossolt, et al. (1993). "Human immunodeficiency virus type 1 Gag protein binds to cyclophilins A and B." Cell **73**(6): 1067-78.

Luban, J. and S. P. Goff (1994). "Mutational Analysis Of Cis-Acting Packaging Signals In Human-Immunodeficiency-Virus Type-1 Rna." Journal Of Virology **68**(6): 3784-3793.

Luo, K., T. Wang, et al. (2007). "Cytidine deaminases APOBEC3G and APOBEC3F interact with human immunodeficiency virus type 1 integrase and inhibit proviral DNA formation." Journal Of Virology **81**(13): 7238-7248.

M

Mackewicz, C. E., J. Yuan, et al. (2003). "alpha-Defensins can have anti-HIV activity but are not CD8 cell anti-HIV factors." Aids **17**(14): F23-F32.

Maertens, G., P. Cherepanov, et al. (2003). "LEDGF/p75 is essential for nuclear and chromosomal targeting of HIV-1 integrase in human cells." J Biol Chem **278**(35): 33528-39.

Malim, M. H., S. Bohnlein, et al. (1989). "Functional Dissection Of The Hiv-1 Rev Trans-Activator - Derivation Of A Trans-Dominant Repressor Of Rev Function." Cell **58**(1): 205-214.

Marchand, C., K. Maddali, et al. (2009). "HIV-1 IN inhibitors: 2010 update and perspectives." Curr Top Med Chem **9**(11): 1016-37.

Marinello, J., C. Marchand, et al. (2008). "Comparison of raltegravir and elvitegravir on HIV-1 integrase catalytic reactions and on a series of drug-resistant integrase mutants." Biochemistry **47**(36): 9345-54.

Markowitz, M., B. Y. Nguyen, et al. (2007). "Rapid and durable antiretroviral effect of the HIV-1 Integrase inhibitor raltegravir as part of combination therapy in treatment-naive patients with HIV-1 infection: results of a 48-week controlled study." J Acquir Immune Defic Syndr **46**(2): 125-33.

Mascarenhas, A. P. and K. Musier-Forsyth (2009). "The capsid protein of human immunodeficiency virus: interactions of HIV-1 capsid with host protein factors." Febs Journal **276**(21): 6118-6127.

Mascola, J. R., S. W. Snyder, et al. (1996). "Immunization with envelope subunit vaccine products elicits neutralizing antibodies against laboratory-adapted but not primary isolates of human immunodeficiency virus type 1. The National Institute of Allergy and Infectious Diseases AIDS Vaccine Evaluation Group." J Infect Dis **173**(2): 340-8.

Matsui, M., R. J. Warburton, et al. (1996). "Effects of HIV-1 tat on expression of HLA class I molecules." Journal Of Acquired Immune Deficiency Syndromes And Human Retrovirology **11**(3): 233-240.

Maria A. Munoz-Morris, Gilles Divita, May C. Morris (2007). "The peptide carrier Pep-1 forms biologically efficient
nanoparticle complexes." Biochemical and Biophysical Research Communications **355**: 877–882.

Mayer, O., L. Rajkowitsch, et al. (2007). "RNA chaperone activity and RNA-binding properties of the E-coli protein StpA." Nucleic Acids Research **35**(4): 1257-1269.

Mayol, K., S. Munier, et al. (2007). "Design and characterization of an HIV-1 Tat mutant: Inactivation of viral and cellular functions but not antigenicity." Vaccine **25**(32): 6047-6060.

Mbisa JL, B. R., Thomas JA, Vandegraaff N, Dorweiler IJ, Svarovskaia ES, Brown WL, Mansky LM, Gorelick RJ, Harris RS, Engelman A, Pathak VK. (2007). "Human immunodeficiency virus type 1 cDNAs produced in the presence of APOBEC3G exhibit defects in plus-strand DNA transfer and integration." journal Of Virology **81**: 7099-110.

McArthur, J. C., D. R. Hoover, et al. (1993). "Dementia In Aids Patients - Incidence And Risk-Factors." Neurology **43**(11): 2245-2252.

McBride, M. S. and A. T. Panganiban (1996). "The human immunodeficiency virus type 1 encapsidation site is a multipartite RNA element composed of functional hairpin structures." Journal Of Virology **70**(5): 2963-2973.

McBride, M. S. and A. T. Panganiban (1997). "Position dependence of functional hairpins important for human immunodeficiency virus type 1 RNA encapsidation in vivo." Journal Of Virology **71**(3): 2050-2058.

McBride, M. S., M. D. Schwartz, et al. (1997). "Efficient encapsidation of human immunodeficiency virus type 1 vectors and further characterization of cis elements required for encapsidation." Journal Of Virology **71**(6): 4544-4554.

McGrath, C. F., J. S. Buckman, et al. (2003). "Human cellular nucleic acid-binding protein Zn2+ fingers support replication of human immunodeficiency virus type 1 when they are substituted in the nucleocapsid protein." J Virol **77**(15): 8524-31.

Meehan, A. M. and E. M. Poeschla (2010) "Chromatin tethering and retroviral integration: recent discoveries and parallels with DNA viruses." Biochim Biophys Acta **1799**(3-4): 182-91.

Meiering, C. D. and M. L. Linial (2001). "Historical perspective of foamy virus epidemiology and infection." Clinical Microbiology Reviews **14**(1): 165-+.

Melikyan, G. B., R. M. Markosyan, et al. (2000). "Evidence that the transition of HIV-1 gp41 into a six-helix bundle, not the bundle configuration, induces membrane fusion." J Cell Biol **151**(2): 413-23.

Mely, Y., H. DeRocquigny, et al. (1996). "Zinc binding to the HIV-1 nucleocapsid protein: A thermodynamic investigation by fluorescence spectroscopy." Biochemistry **35**(16): 5175-5182.

Mervis, R. J., N. Ahmad, et al. (1988). "The Gag Gene-Products Of Human Immunodeficiency Virus Type-1 - Alignment Within The Gag Open Reading Frame, Identification Of Posttranslational Modifications, And Evidence For Alternative Gag Precursors." Journal Of Virology **62**(11): 3993-4002.

Metifiot, M., C. Marchand, et al. (2012) "Resistance to integrase inhibitors." Viruses **2**(7): 1347-66.

Michel, F., C. Crucifix, et al. (2009). "Structural basis for HIV-1 DNA integration in the human genome, role of the LEDGF/P75 cofactor." Embo J **28**(7): 980-91.

Miles, L. R., B. E. Agresta, et al. (2005). "Effect of polypurine tract (PPT) mutations on human immunodeficiency virus type 1 replication: A virus with a completely randomized PPT retains low infectivity." Journal Of Virology **79**(11): 6859-6867.

Miyauchi, K., Y. Kim, et al. (2009). "HIV Enters Cells via Endocytosis and Dynamin-Dependent Fusion with Endosomes." Cell **137**(3): 433-444.

Moarefi, I., F. Sicheri, et al. (1997). "Structure and regulation of the Src family tyrosine kinases." Abstracts Of Papers Of The American Chemical Society **214**: 163-COMP.

Mollova, E. T. (2002). "Single-molecule fluorescence of nucleic acids." Current Opinion In Chemical Biology **6**(6): 823-828.

Monajemi M, W. C., Benkaroun J, Grant M, Larijani M. (2012). "Emerging complexities of APOBEC3G action on immunity and viral fitness during HIV infection and treatment." Retrovirology **9**.

Moore, M. D., W. Fu, et al. (2007). "Dimer initiation signal of human immunodeficiency virus type 1: its role in partner selection during RNA copackaging and its effects on recombination." J Virol **81**(8): 4002-11.

Moore, M. D. and W. S. Hu (2009). "HIV-1 RNA dimerization: It takes two to tango." AIDS Rev **11**(2): 91-102.

Morellet, N., N. Jullian, et al. (1992). "Determination Of The Structure Of The Nucleocapsid Protein Ncp7 From The Human-Immunodeficiency-Virus Type-1 By H-1-Nmr." Embo Journal **11**(8): 3059-3065.

Morellet, N., Demene,H., Teilleux,V., Huynh-Dinh,T., de Rocquigny,H., Fournie-Zaluski,M.C. and Roques,B.P (1998). "Structure of the complex between the HIV-1 nucleocapsid protein NCp7 and the single-stranded pentanucleotide d(ACGCC)." Journal Of Molecular Biology **283**: 419-34.

Morellet, N., B. P. Roques, et al. (2009). "Structure-Function Relationship of Vpr: Biological Implications." Current Hiv Research **7**(2): 184-210.

Morita, E. and W. I. Sundquist (2004). "Retrovirus budding." Annual Review Of Cell And Developmental Biology **20**: 395-425.

Muino, P. L. and P. R. Callis (2009). "Solvent Effects on the Fluorescence Quenching of Tryptophan by Amides via Electron Transfer. Experimental and Computational Studies." Journal Of Physical Chemistry B **113**(9): 2572-2577

Muller, B., U. Tessmer, et al. (2000). "Human immunodeficiency virus type 1 Vpr protein is incorporated into the virion in significantly smaller amounts than Gag and is phosphorylated in infected cells." Journal Of Virology **74**(20): 9727-9731.

Munch, J., E. Rucker, et al. (2007). "Semen-derived amyloid fibrils drastically enhance HIV infection." Cell **131**(6): 1059-1071.

Munier, C. M., C. R. Andersen, et al.(2011) "HIV vaccines: progress to date." Drugs **71**(4): 387-414.

Muriaux, D. and J. L. Darlix (2010) "Properties and functions of the nucleocapsid protein in virus assembly." Rna Biology **7**(6): 744-753.

Muriaux, D., P. M. Girard, et al. (1995). "Dimerization of HIV-1Lai RNA at low ionic strength. An autocomplementary sequence in the 5' leader region is evidenced by an antisense oligonucleotide." J Biol Chem **270**(14): 8209-16.

Musah, R. A. (2004). "The HIV-1 nucleocapsid zinc finger protein as a target of antiretroviral therapy." Curr Top Med Chem **4**(15): 1605-22.

Myszka, D. G., R. W. Sweet, et al. (2000). "Energetics of the HIV gp120-CD4 binding reaction." Proc Natl Acad Sci U S A **97**(16): 9026-31.

N

Nakayama, E. E. and T. Shioda (2010) "Anti-retroviral activity of TRIM5 alpha." Reviews In Medical Virology **20**(2): 77-92.

Navia, M. A., P. M. D. Fitzgerald, et al. (1989). "3-Dimensional Structure Of Aspartyl Protease From Human Immunodeficiency Virus Hiv-1." Nature **337**(6208): 615-620.

Negroni, M., Buc, H., (2000)."Copy-choice recombination by reverse transcriptases: reshuffling of genetic markers mediated by RNA chaperones". Proc. Natl. Acad. Sci. U.S.A. **97**, 6385–6390.

Nielsen M, Lundegaard C, Lund O, Kesmir C.(2005) "The role of the proteasome in generating cytotoxic Tcell epitopes: insights obtained from improved predictions of proteasomal cleavage." Immunogenetics **57**:33–41.

Nowotny, M., S. A. Gaidamakov, et al. (2005). "Crystal structures of RNase H bound to an RNA/DNA hybrid: substrate specificity and metal-dependent catalysis." Cell **121**(7): 1005-16.

O

Ohlmann, T., M. Lopez-Lastra, et al. (2000). "An internal ribosome entry segment promotes translation of the simian immunodeficiency virus genomic RNA." Journal Of Biological Chemistry **275**(16): 11899-11906.

Okada, K., N. Nakae, et al. (2005). "Bovine leukemia virus high tax molecular clone experimentally induces leukemia/lymphoma in sheep." Journal Of Veterinary Medical Science **67**(12): 1231-1235.

Okumura, A., T. Alce, et al. (2008). "HIV-1 accessory proteins VPR and Vif modulate antiviral response by targeting IRF-3 for degradation." Virology **373**(1): 85-97.

Okumura, A., G. S. Lu, et al. (2006). "Innate antiviral response targets HIV-1 release by the induction of ubiquitin-like protein ISG15." Proceedings Of The National Academy Of Sciences Of The United States Of America **103**(5): 1440-1445.

Opella, S. J., S. H. Park, et al. (2005). "Structure and function of Vpu from HIV-1." Viral Membrane Proteins: Structure, Function, And Drug Design **1**: 147-163.

Ott, D. E., L. V. Coren, et al. (2003). "Elimination of protease activity restores efficient virion production to a human immunodeficiency virus type 1 nucleocapsid deletion mutant." Journal Of Virology **77**(10): 5547-5556.

P

Palella, F. J., K. M. Delaney, et al. (1998). "Declining morbidity and mortality among patients with advanced human immunodeficiency virus infection." New England Journal Of Medicine **338**(13): 853-860.

Parisien, M. and F. Major (2008). "The MC-Fold and MC-Sym pipeline infers RNA structure from sequence data." Nature **452**(7183): 51-55.

Paoletti A.C., Schubsda, M., F. et al. (2002) "Affinities of the nucleocapsid protein for variants of SL3 RNA in HIV-1". Biochemistry **41**: 15423-428.

Paxton, W., R. I. Connor, et al. (1993). "Incorporation Of Vpr Into Human-Immunodeficiency-Virus Type-1 Virions - Requirement For The P6 Region Of Gag And Mutational Analysis." Journal Of Virology **67**(12): 7229-7237.

Peliska, J. A., S. Balasubramanian, et al. (1994). "Recombinant HIV-1 nucleocapsid protein accelerates HIV-1 reverse transcriptase catalyzed DNA strand transfer reactions and modulates RNase H activity." Biochemistry **33**(46): 13817-23.

Perez-Alvarez, L., R. Carmona, et al. (2006). "Long-term monitoring of genotypic and phenotypic resistance to T20 in treated patients infected with HIV-1." Journal Of Medical Virology **78**(2): 141-147.

Petrich J. W., C. M. C., McDonald D. B., Fleming G. R. (1983). "On the origin of nonexponential fluorescence decay in tryptophan and its derivatives." J.Am.Chem.Soc. **105**: 3824-3832.

Piguet, V., Y. L. Chen, et al. (1997). "Mechanisms of Nef-induced MHCI and CD4 downregulation: Nef acts as a connector with the mu chain of adaptor complexes." Molecular Biology Of The Cell **8**: 2452-2452.

Pitisuttithum, P., P. Gilbert, et al. (2006). "Randomized, double-blind, placebo-controlled efficacy trial of a bivalent recombinant glycoprotein 120 HIV-1 vaccine among injection drug users in Bangkok, Thailand." J Infect Dis **194**(12): 1661-71.

Plantier, J. C., M. Leoz, et al. (2009). "A new human immunodeficiency virus derived from gorillas." Nat Med **15**(8): 871-2.

Plantier, J. C., M. Leoz, et al. (2009). "A new human immunodeficiency virus derived from gorillas." Nature Medicine **15**(8): 871-872.

Poggi, A. and M. R. Zocchi (2006). "HIV-1 Tat triggers TGF-beta production and NK cell apoptosis that is prevented by pertussis toxin B." Clinical & Developmental Immunology **13**(2-4): 369-372.

Pooga M, H. M., Zorko M, Langel U. (1998). "Cell penetration by transportan." Faseb Journal **12**: 67-77

Poiesz, B. J., F. W. Ruscetti, et al. (1980). "Detection And Isolation Of Type-C Retrovirus Particles From Fresh And Cultured Lymphocytes Of A Patient With Cutaneous T-Cell Lymphoma." Proceedings Of The National Academy Of Sciences Of The United States Of America-Biological Sciences **77**(12): 7415-7419.

Pollard, V. W. and M. H. Malim (1998). "The HIV-1 Rev protein." Annual Review Of Microbiology **52**: 491-532.

Pomerantz, R. J., M. B. Feinberg, et al. (1990). "Lipopolysaccharide Is A Potent Monocyte Macrophage-Specific Stimulator Of Human-Immunodeficiency-Virus Type-1 Expression." Journal Of Experimental Medicine **172**(1): 253-261.

Popov, S., E. Popova, et al. (2009). "Divergent Bro1 Domains Share the Capacity To Bind Human Immunodeficiency Virus Type 1 Nucleocapsid and To Enhance Virus-Like Particle Production." Journal Of Virology **83**(14): 7185-7193.

Popov S, P. E., Inoue M, Gottlinger HG (2008). "Human immunodeficiency virus type 1 Gag engages the Bro1 domain of ALIX/AIP1 through the nucleocapsid." Journal Of Virology **82**(3): 1398-98.

Poss, M., H. L. Martin, et al. (1995). "Diversity In Virus Populations From Genital Secretions And Peripheral-Blood From Women Recently Infected With Human-Immunodeficiency-Virus Type-1." Journal Of Virology **69**(12): 8118-8122.

Priddy, F. H., D. Brown, et al. (2008). "Safety and immunogenicity of a replication-incompetent adenovirus type 5 HIV-1 clade B gag/pol/nef vaccine in healthy adults." Clin Infect Dis **46**(11): 1769-81.

Provitera, P., A. Goff, et al. (2001). "Role of the major homology region in assembly of HIV-1 Gag." Biochemistry **40**(18): 5565-72.

Q

Quinn, T. C., M. J. Wawer, et al. (2000). "Viral load and heterosexual transmission of human immunodeficiency virus type 1. Rakai Project Study Group." N Engl J Med **342**(13): 921-9.

R

Räägel H, S. P., Pooga M. (2010). "Peptide-mediated protein delivery—Which pathways are penetrable." biochemica et biophysica acta **1798**: 2240-8.

Raja, C., J. Ferner, et al. (2006). "A tryptophan-rich hexapeptide inhibits nucleic acid destabilization chaperoned by the HIV-1 nucleocapsid protein." Biochemistry **45**(30): 9254-9265.

Rajkowitsch, L., D. Chen, et al. (2007). "RNA chaperones, RNA annealers and RNA helicases." Rna Biology **4**(3): 118-130.

Ramalanjaona, N., H. de Rocquigny, et al. (2007). "Investigating the mechanism of the nucleocapsid protein chaperoning of the second strand transfer during HIV-1 DNA synthesis." Journal Of Molecular Biology **374**(4): 1041-1053.

Rascle, J. B., D. Ficheux, et al. (1998). "Possible roles of nucleocapsid protein of MoMuLV in the specificity of proviral DNA synthesis and in the genetic variability of the virus." Journal Of Molecular Biology **280**(2): 215-225.

Rausch, J. W. and S. F. Le Grice (2004). "'Binding, bending and bonding': polypurine tract-primed initiation of plus-strand DNA synthesis in human immunodeficiency virus." Int J Biochem Cell Biol **36**(9): 1752-66.

Rein, A., L. E. Henderson, et al. (1998). "Nucleic-acid-chaperone activity of retroviral nucleocapsid proteins: significance for viral replication." Trends In Biochemical Sciences **23**(8): 297-301.

Rein, A., D. E. Ott, et al. (1997). "Suppression of retrovirial replication: inactivation of murine leukemia virus by compounds reacting with the zinc finger in the viral nucleocapsid protein." Leukemia **11 Suppl 3**: 106-8.

Rhee, S. Y., J. Taylor, et al. (2010) "HIV-1 Protease Mutations and Protease Inhibitor Cross-Resistance." Antimicrobial Agents And Chemotherapy **54**(10): 4253-4261.

Richard J.P., M. K., Vives E., Ramos C., Verbeure B., Gait M.J., and L. B. Chernomordik L.V. (2003). "Cell-penetrating peptides. A reevaluation of the mechanism of cellular uptake." J. Biol. Chem. **278**: 585-590.

Richter, S., Y. H. Ping, et al. (2002). "TAR RNA loop: A scaffold for the assembly of a regulatory switch in HIV replication." Proceedings Of The National Academy Of Sciences Of The United States Of America **99**(12): 7928-7933.

Rimsky, L. T., H. Azijn, et al. (2009). "In vitro resistance profile of TMC278, a next-generation NNRTI; evidence of a higher genetic barrier and a more robust resistance profile than first generation NNRTIs." Antiviral Therapy **14**(4): A141-A141.

Roberts, N. A., J. A. Martin, et al. (1990). "Rational Design Of Peptide-Based Hiv Proteinase-Inhibitors." Science **248**(4953): 358-361.

Robinson, W. E., Jr., M. G. Reinecke, et al. (1996). "Inhibitors of HIV-1 replication [corrected; erratum to be published] that inhibit HIV integrase." Proc Natl Acad Sci U S A **93**(13): 6326-31.

Rodal, S. K., G. Skretting, et al. (1999). "Extraction of cholesterol with methyl-beta-cyclodextrin perturbs formation of clathrin-coated endocytic vesicles." Molecular Biology Of The Cell **10**(4): 961-974.

Roe, T. Y., T. C. Reynolds, et al. (1993). "Integration Of Murine Leukemia-Virus Dna Depends On Mitosis." Embo Journal **12**(5): 2099-2108.

Roldan, A., O. U. Warren, et al. (2005). "A HIV-1 minimal gag protein is superior to nucleocapsid at in vitro tRNA(3)(Lys) annealing and exhibits multimerization-induced inhibition of reverse transcription." Journal Of Biological Chemistry **280**(17): 17488-17496.

Rolland M, Nickle DC, Mullins JI. (2007) "HIV-1 group M conserved elements vaccine". PLoS pathogens **3**:e157

Romani, B., R. H. Glashoff, et al.(2010) "Functional integrity of naturally occurring mutants of HIV-1 subtype C Vpr." Virus Res **153**(2): 288-98.

Rosato, N., E. Gratton, et al. (1990). "Fluorescence Lifetime Distributions In Human Superoxide-Dismutase - Effect Of Temperature And Denaturation." Biophysical Journal **58**(4): 817-822.

Rose, K. M., M. Marin, et al. (2004). "The viral infectivity factor (Vif) of HIV-1 unveiled." Trends In Molecular Medicine **10**(6): 291-297.

Rossio, J. L., M. T. Esser, et al. (1998). "Inactivation of human immunodeficiency virus type 1 infectivity with preservation of conformational and functional integrity of virion surface proteins." Journal Of Virology **72**(10): 7992-8001.

Roux, K. H. and K. A. Taylor (2007). "AIDS virus envelope spike structure." Current Opinion In Structural Biology **17**(2): 244-252.

S

Sainlos M, Belmont P, Vigneron J-P, Lehn P, Lehn J-M. (2003). "Aminoglycoside- derived cationic lipids for gene transfection: Synthesis of kanamycin A derivatives". Eur J Org Chem **15:**2764–2774.

Sakuma, T., M. A. Barry, et al.(2012) "Lentiviral vectors: basic to translational." Biochemical Journal **443**: 603-618.

Sakuragi, J. I., H. Ode, et al. (2012) "A proposal for a new HIV-1 DLS structural model." Nucleic Acids Res.

Sanglier, S., W. Bourguet, et al. (2004). "Monitoring ligand-mediated nuclear receptor-coregulator interactions by noncovalent mass spectrometry." Eur J Biochem **271**(23-24): 4958-67.

Santos, A. F. and M. A. Soares (2010) "HIV Genetic Diversity and Drug Resistance." Viruses-Basel **2**(2): 503-531.

Sarafianos, S. G., K. Das, et al. (2001). "Crystal structure of HIV-1 reverse transcriptase in complex with a polypurine tract RNA: DNA." Embo Journal **20**(6): 1449-1461.

Sarafianos, S. G., B. Marchand, et al. (2009). "Structure and function of HIV-1 reverse transcriptase: molecular mechanisms of polymerization and inhibition." J Mol Biol **385**(3): 693-713.

Savarino, A. (2007). "In-Silico docking of HIV-1 integrase inhibitors reveals a novel drug type acting on an enzyme/DNA reaction intermediate." Retrovirology **4**.

Scarlata, S. and C. Carter (2003). "Role of HIV-1 Gag domains in viral assembly." Biochimica Et Biophysica Acta-Biomembranes **1614**(1): 62-72.

Schwartz, M. D., D. Fiore, et al. (1997). "Distinct functions and requirements for the Cys-His boxes of the human immunodeficiency virus type 1 nucleocapsid protein during RNA encapsidation and replication." Journal Of Virology **71**(12): 9295-9305.

Sharma K, D. P., Darlix JL, de Rocquigny H, Bensikaddour H, Lavergne JP, Pénin F, Lessinger JM, Mély Y. (2010). "Kinetic analysis of the nucleic acid chaperone activity of the Hepatitis C virus core protein." Nucleic Acids Research **38**: 3632-42.

Semenova, E. A., C. Marchand, et al. (2008). "HIV-1 integrase inhibitors: update and perspectives." Adv Pharmacol **56**: 199-228.

Semrad, K., R. Green, et al. (2004). "RNA chaperone activity of large ribosomal subunit proteins from Escherichia coli." Rna-A Publication Of The Rna Society **10**(12): 1855-1860.

Sevilya, Z., S. Loya, et al. (2003). "The ribonuclease H activity of the reverse transcriptases of human immunodeficiency viruses type 1 and type 2 is modulated by residue 294 of the small subunit." Nucleic Acids Res **31**(5): 1481-7.

Sevilya, Z., S. Loya, et al. (2001). "The ribonuclease H activity of the reverse transcriptases of human immunodeficiency viruses type 1 and type 2 is affected by the thumb subdomain of the small protein subunits." J Mol Biol **311**(5): 957-71.

Sharp, P. M. and B. H. Hahn (2011) "Origins of HIV and the AIDS Pandemic." Cold Spring Harbor perspectives in medicine **1**(1): a006841.

Sheehy, A. M., N. C. Gaddis, et al. (2002). "Isolation of a human gene that inhibits HIV-1 infection and is suppressed by the viral Vif protein." Nature **418**(6898): 646-650.

Shen, L., S. Peterson, et al. (2008). "Dose-response curve slope sets class-specific limits on inhibitory potential of anti-HIV drugs." Nature Medicine **14**(7): 762-766.

Shoeman, R. L., B. Honer, et al. (1990). "Human immunodeficiency virus type 1 protease cleaves the intermediate filament proteins vimentin, desmin, and glial fibrillary acidic protein." Proc Natl Acad Sci U S A **87**(16): 6336-40.

Shvadchak, V., S. Sanglier, et al. (2009). "Identification by high throughput screening of small compounds inhibiting the nucleic acid destabilization activity of the HIV-1 nucleocapsid protein." Biochimie **91**(7): 916-23.

Simon, F., P. Mauclere, et al. (1998). "Identification of a new human immunodeficiency virus type 1 distinct from group M and group O." Nature Medicine **4**(9): 1032-1037.

Singh, S. P., P. Tungaturthi, et al. (2001). "Virion-associated HIV-1 Vpr: Variable amount in virus particles derived from cells upon virus infection or proviral DNA transfection." Virology **283**(1): 78-83.

Skripkin, E., J. C. Paillart, et al. (1994). "Identification Of The Primary Site Of The Human-Immunodeficiency-Virus Type-1 Rna Dimerization In-Vitro." Proceedings Of The National Academy Of Sciences Of The United States Of America **91**(11): 4945-4949.a

Skripkin, E., J. C. Paillart, et al. (1994). "Identification of the primary site of the human immunodeficiency virus type 1 RNA dimerization in vitro." Proc Natl Acad Sci U S A **91**(11): 4945-9.

Sluis-Cremer, N., D. Arion, et al. (2004). "Proteolytic processing of an HIV-1 pol polyprotein precursor: insights into the mechanism of reverse transcriptase p66/p51 heterodimer formation." Int J Biochem Cell Biol **36**(9): 1836-47.

Sluis-Cremer, N., N. A. Temiz, et al. (2004). "Conformational changes in HIV-1 reverse transcriptase induced by nonnucleoside reverse transcriptase inhibitor binding." Current Hiv Research **2**(4): 323-332.

Soriano, V. and C. de Mendoza (2002). "Genetic mechanisms of resistance to NRTI and NNRTI." HIV clinical trials **3**(3): 237-48.

South, T. L., P. R. Blake, et al. (1991). "C-Terminal Retroviral-Type Zinc Finger Domain From The Hiv-1 Nucleocapsid Protein Is Structurally Similar To The N-Terminal Zinc Finger Domain." Biochemistry **30**(25): 6342-6349.

Spina, C. A., J. C. Guatelli, et al. (1995). "Establishment Of A Stable, Inducible Form Of Human-Immunodeficiency-Virus Type-1 Dna In Quiescent Cd4 Lymphocytes In-Vitro." Journal Of Virology **69**(5): 2977-2988.

Stephen, A. G., K. M. Worthy, et al. (2002). "Identification of HIV-1 nucleocapsid protein: nucleic acid antagonists with cellular anti-HIV activity." Biochemical And Biophysical Research Communications **296**(5): 1228-1237.

Stetor, S. R., J. W. Rausch, et al. (1999). "Characterization of (+) strand initiation and termination sequences located at the center of the equine infectious anemia virus genome." Biochemistry **38**(12): 3656-3667.

Stettner, M. R., J. A. Nance, et al. (2009). "SMAD proteins of oligodendroglial cells regulate transcription of JC virus early and late genes coordinately with the Tat protein of human immunodeficiency virus type 1." Journal Of General Virology **90**: 2005-2014.

Stylianou, E., V. Bjerkeli, et al. (2003). "Raised serum levels of interleukin-18 is associated with disease progression and may contribute to virological treatment failure in HIV-1-infected patients." Clin Exp Immunol **132**(3): 462-6.

Suhasini, M. and T. R. Reddy (2009). "Cellular Proteins and HIV-1 Rev Function." Current Hiv Research **7**(1): 91-100.

Summers, M. F., L. E. Henderson, et al. (1992). "Nucleocapsid Zinc Fingers Detected In Retroviruses - Exafs Studies Of Intact Viruses And The Solution-State Structure Of The Nucleocapsid Protein From Hiv-1." Protein Science **1**(5): 563-574.

Sundquist, W. I. and R. M. Krug (2012) "Assemble, replicate, remodel and evade." Curr Opin Virol **2**(2): 111-4.

Szabo, A. G. and D. M. Rayner (1980). "Fluorescence Decay Of Tryptophan Conformers In Aqueous-Solution." Journal Of The American Chemical Society **102**(2): 554-563.

T

Takehisa, J., M. H. Kraus, et al. (2009). "Origin and biology of simian immunodeficiency virus in wild-living western gorillas." J Virol **83**(4): 1635-48.

Tanchou, V., C. Gabus, et al. (1995). "Formation Of Stable And Functional Hiv-1 Nucleoprotein Complexes In-Vitro." Journal Of Molecular Biology **252**(5): 563-571.

Tang, C., E. Loeliger, et al. (2003). "Antiviral inhibition of the HIV-1 capsid protein." Journal Of Molecular Biology **327**(5): 1013-1020.

Telesnitsky, A. and S. P. Goff (1993). "2 Defective Forms Of Reverse-Transcriptase Can Complement To Restore Retroviral Infectivity." Embo Journal **12**(11): 4433-4438.

Temin, H. M. and S. Mizutani (1970). "RNA-dependent DNA polymerase in virions of Rous sarcoma virus." Nature **226**(5252): 1211-3.

Thali, M., A. Bukovsky, et al. (1994). "Functional association of cyclophilin A with HIV-1 virions." Nature **372**(6504): 363-5.

Thomas, J. A., W. J. Bosche, et al. (2008). "Mutations in human immunodeficiency virus type 1 nucleocapsid protein zinc fingers cause premature reverse transcription." J Virol **82**(19): 9318-28.

Thomas, J. A. and R. J. Gorelick (2008). "Nucleocapsid protein function in early infection processes." Virus Research **134**(1-2): 39-63.

Thomas, S., L. Mayer, et al. (2009). "Mitochondria influence Fas expression in gp120-induced apoptosis of neuronal cells." Int J Neurosci **119**(2): 157-65.

Thorner, A. R., R. Vogels, et al. (2006). "Age dependence of adenovirus-specific neutralizing antibody titers in individuals from sub-Saharan Africa." J Clin Microbiol **44**(10): 3781-3.

Torbeev, V. Y., H. Raghuraman, et al.(2011) "Protein conformational dynamics in the mechanism of HIV-1 protease catalysis." Proceedings Of The National Academy Of Sciences Of The United States Of America **108**(52): 20982-20987.

Torre, D. and A. Pugliese (2006). "Interleukin-18: a proinflammatory cytokine in HIV-1 infection." Curr HIV Res **4**(4): 423-30.

Tozser, J., I. T. Weber, et al. (1992). "Kinetic and modeling studies of S3-S3' subsites of HIV proteinases." Biochemistry **31**(20): 4793-800.

Tsuchihashi, Z. and P. O. Brown (1994). "Dna Strand Exchange And Selective Dna Annealing Promoted By The Human-Immunodeficiency-Virus Type-1 Nucleocapsid Protein." Journal Of Virology **68**(9): 5863-5870.

Turlure, F., E. Devroe, et al. (2004). "Human cell proteins and human immunodeficiency virus DNA integration." Front Biosci **9**: 3187-208.

Turner, B. G. and M. F. Summers (1999). "Structural biology of HIV." Journal Of Molecular Biology **285**(1): 1-32.

Turner, K.B., Kohlway, A.S., Hagan N.A., Fabris D.(2006) "Mapping noncovalent ligand binding to stemloop domains of the HIV-1 packaging signal by tandem mass spectrometry" J. Am. Soc. Mass Spectrom. **17** : 1401-1411.

Turpin, J. A., M. L. Schito, et al. (2008). "Topical microbicides: a promising approach for controlling the AIDS pandemic via retroviral zinc finger inhibitors." Advances in pharmacology (San Diego, Calif.) **56**: 229-56.

Turpin, J. A., S. J. Terpening, et al. (1996). "Inhibitors of human immunodeficiency virus type 1 zinc fingers prevent normal processing of Gag precursors and result in the release of noninfectious virus particles." Journal Of Virology **70**(9): 6180-6189.

U

Urbaneja, M. A., M. Wu, et al. (2002). "HIV-1 nucleocapsid protein as a nucleic acid chaperone: Spectroscopic study of its helix-destabilizing properties, structural binding specificity, and annealing activity." Journal Of Molecular Biology **318**(3): 749-764.

V

Vagner, S., A. Waysbort, et al. (1995). "Alternative Translation Initiation Of The Moloney Murine Leukemia-Virus Messenger-Rna Controlled By Internal Ribosome Entry Involving The P57/Ptb Splicing Factor." Journal Of Biological Chemistry **270**(35): 20376-20383.

Vallari, A., P. Bodelle, et al. (2010) "Four New HIV-1 Group N Isolates from Cameroon: Prevalence Continues to Be Low." Aids Research And Human Retroviruses **26**(1): 109-115.

Vallari, A., V. Holzmayer, et al. (2011) "Confirmation of Putative HIV-1 Group P in Cameroon." Journal Of Virology **85**(3): 1403-1407.

Vallejos, M., P. Ramdohr, et al. (2010) "The 5'-untranslated region of the mouse mammary tumor virus mRNA exhibits cap-independent translation initiation." Nucleic Acids Research **38**(2): 618-632.

Van Heuverswyn, F., Y. Li, et al. (2007). "Genetic diversity and phylogeographic clustering of SIVcpzPtt in wild chimpanzees in Cameroon." Virology **368**(1): 155-171.

Van Ryk, D. I. and S. Venkatesan (1999). "Real-time kinetics of HIV-1 Rev-Rev response element interactions - Definition of minimal, binding sites on RNA and protein and stoichiometric analysis." Journal Of Biological Chemistry **274**(25): 17452-17463.

van Wamel, J. L. and B. Berkhout (1998). "The first strand transfer during HIV-1 reverse transcription can occur either intramolecularly or intermolecularly." Virology **244**(2): 245-51.

Vandevelde, M., M. Witvrouw, et al. (1996). "ADA, a potential anti-HIV drug." Aids Research And Human Retroviruses **12**(7): 567-568.

vantWout, A. B., L. J. Ran, et al. (1998). "Analysis of the temporal relationship between human immunodeficiency virus type 1 quasispecies in sequential blood samples and various organs obtained at autopsy." Journal Of Virology **72**(1): 488-496.

Valeur, B. and I. Leray (2000). "Design principles of fluorescent molecular sensors for cation recognition." Coordination Chemistry Reviews **205**: 3-40.

Verhoef, K., G. Marzio, et al. (2001). "Strict control of human immunodeficiency virus type 1 replication by a genetic switch: Tet for Tat." Journal Of Virology **75**(2): 979-987.

Vingerhoets, J., H. Azijn, et al. (2005). "TMC125 displays a high genetic barrier to the development of resistance: Evidence from in vitro selection experiments." Journal Of Virology **79**(20): 12773-12782.

Vo, M. N., G. Barany, et al. (2009). "HIV-1 Nucleocapsid Protein Switches the Pathway of Transactivation Response Element RNA/DNA Annealing from Loop-Loop "Kissing" to "Zipper"." Journal Of Molecular Biology **386**(3): 789-801.

Vuilleumier, C., E. Bombarda, et al. (1999). "Nucleic acid sequence discrimination by the HIV-1 nucleocapsid protein NCp7: A fluorescence study." Biochemistry **38**(51): 16816-16825.

W

Waheed, A. A. and E. O. Freed (2008). "Peptide Inhibitors of HIV-1 Egress." Acs Chemical Biology **3**(12): 745-747.

Waldhuber, M. G., M. Bateson, et al. (2003). "Studies with GFP-Vpr fusion proteins: induction of apoptosis but ablation of cell-cycle arrest despite nuclear membrane or nuclear localization." Virology **313**(1): 91-104.

Wadia J.S., D. S. F. (2002). "Protein transduction technology." Curr. Opin.Biotechnol. **13**: 52-56.

Ward, D. C., E. Reich, et al. (1969). "Fluorescence studies of nucleotides and polynucleotides. I. Formycin, 2-aminopurine riboside, 2,6-diaminopurine riboside, and their derivatives." The Journal of biological chemistry **244**(5): 1228-37.

Wei, P., M. E. Garber, et al. (1998). "A novel CDK9-associated C-type cyclin interacts directly with HIV-1 Tat and mediates its high-affinity, loop-specific binding to TAR RNA." Cell **92**(4): 451-462.

Weill, L., L. James, et al.(2010) "A new type of IRES within gag coding region recruits three initiation complexes on HIV-2 genomic RNA." Nucleic Acids Research **38**(4): 1367-1381.

Weinberg, A., M. E. Quinones-Mateu, et al. (2006). "Role of human beta-defensins in HIV infection." Advances in dental research **19**(1): 42-8.

Weiss, R. A. (2001). "Retroviruses and cancer." Current Science **81**(5): 528-534.

Weissenhorn, W., A. Dessen, et al. (1997). "Atomic structure of the ectodomain from HIV-1 gp41." Nature **387**(6631): 426-430.

Weller, I. V. D. and I. G. Williams (2001). "ABC of AIDS - Antiretroviral drugs." British Medical Journal **322**(7299): 1410-1412.

Welman, M., G. Lemay, et al. (2007). "Role of envelope processing and gp41 membrane spanning domain in the formation of human immunodeficiency virus type I (HIV-1) fusion-competent envelope glycoprotein complex." Virus Research **124**(1-2): 103-112.

Wensing, A. M. J., N. M. van Maarseveen, et al.(2010) "Fifteen years of HIV Protease Inhibitors: raising the barrier to resistance." Antiviral Research **85**(1): 59-74.

Whittal, R. M., C. C. Benz, et al. (2000). "Preferential oxidation of zinc finger 2 in estrogen receptor DNA-binding domain prevents dimerization and, hence, DNA binding." Biochemistry **39**(29): 8406-8417.

Wick, G., B. Grubeckloebenstein, et al. (1992). "Human Foamy Virus-Antigens In Thyroid-Tissue Of Graves-Disease Patients." International Archives Of Allergy And Immunology **99**(1): 153-156.

Willard, D. M., L. L. Carillo, et al. (2001). "CdSe-ZnS quantum dots as resonance energy transfer donors in a model protein-protein binding assay." Nano Letters **1**(9): 469-474.

Wille-Reece, U., B. J. Flynn, et al. (2005). "HIV Gag protein conjugated to a Toll-like receptor 7/8 agonist improves the magnitude and quality of Th1 and CD8+ T cell responses in nonhuman primates." Proc Natl Acad Sci U S A **102**(42): 15190-4.

Williams, M. C., I. Rouzina, et al. (2001). "Mechanism for nucleic acid chaperone activity of HIV-1 nucleocapsid protein revealed by single molecule stretching." Proceedings Of The National Academy Of Sciences Of The United States Of America **98**(11): 6121-6126.

Wiskerchen, M. and M. A. Muesing (1995). "Human-Immunodeficiency-Virus Type-1 Integrase - Effects Of Mutations On Viral Ability To Integrate, Direct Viral Gene-Expression From Unintegrated Viral-Dna Templates, And Sustain Viral Propagation In Primary-Cells." Journal Of Virology **69**(1): 376-386.

Wlodawer, A., M. Miller, et al. (1989). "Conserved Folding In Retroviral Proteases - Crystal-Structure Of A Synthetic Hiv-1 Protease." Science **245**(4918): 616-621.

Wu, X. S., N. H. Bishopric, et al. (1996). "Physical and functional sensitivity of zinc finger transcription factors to redox change." Molecular And Cellular Biology **16**(3): 1035-1046.

Wu, Y. (2004). "HIV-1 gene expression: lessons from provirus and non-integrated DNA." Retrovirology **1**: 13.

Wurtzer, S., A. Goubard, et al. (2008). "Functional central polypurine tract provides downstream protection of the human immunodeficiency virus type 1 genome from editing by APOBEC3G and APOBEC3B (vol 80, pg 3679, 2006)." Journal Of Virology **82**(10): 5116-5116.

Y

Yang, B., S. Akhter, et al. (2009). "HIV-1 gp120 induces cytokine expression, leukocyte adhesion, and transmigration across the blood-brain barrier: modulatory effects of STAT1 signaling." Microvasc Res **77**(2): 212-9.

Yeager, M., E. M. Wilson-Kubalek, et al. (1998). "Supramolecular organization of immature and mature murine leukemia virus revealed by electron cryo-microscopy: Implications for retroviral assembly mechanisms." Proceedings Of The National Academy Of Sciences Of The United States Of America **95**(13): 7299-7304.

You, J. C. and C. S. McHenry (1994). "Human-Immunodeficiency-Virus Nucleocapsid Protein Accelerates Strand Transfer Of The Terminally Redundant Sequences Involved In Reverse Transcription." Journal Of Biological Chemistry **269**(50): 31491-31495.

Yu, H., A. E. Jetzt, et al. (1998). "The nature of human immunodeficiency virus type 1 strand transfers." J Biol Chem **273**(43): 28384-91.

Z

Zennou, V., C. Petit, et al. (2000). "HIV-1 genome nuclear import is mediated by a central DNA flap." Cell **101**(2): 173-185.

Zhang, A., V. Derbyshire, et al. (1995). "Escherichia-Coli Protein Stpa Stimulates Self-Splicing By Promoting Rna Assembly In-Vitro." Rna-A Publication Of The Rna Society **1**(8): 783-793.

Zhang, H., G. Dornadula, et al. (1996). "Endogenous reverse transcription of human immunodeficiency virus type 1 in physiological microenvironments: An important stage for viral infection of nondividing cells." Journal Of Virology **70**(5): 2809-2824

Zhang, H., G. Dornadula, et al. (1998). "Human immunodeficiency virus type I in the semen of men receiving highly active antiretroviral therapy." New England Journal Of Medicine **339**(25): 1803-1809.

Zhang, H., Q. Zhao, et al. (2008). "A cell-penetrating helical peptide as a potential HIV-1 inhibitor." Journal Of Molecular Biology **378**(3): 565-580.

Zheng, L., Y.-d. Yang, et al. (2005). "Extracellular HIV Tat and Tat cysteine rich peptide increase CCR5 expression in monocytes." Journal of Zhejiang University. Science. B **6**(7): 668-72.

Zhou, T. Q., L. Xu, et al. (2007). "Structural definition of a conserved neutralization epitope on HIV-1 gp120." Nature **445**(7129): 732-737.

Zimmerman, C., K. C. Klein, et al. (2002). "Identification of a host protein essential for assembly of immature HIV-1 capsids." Nature **415**(6867): 88-92.

Résumé en Français

Le virus de l'immunodéficience humaine (VIH), agent causal du SIDA (Syndrome de l'Immunodéficience Acquise), entraîne une diminution de l'efficacité du système immunitaire conduisant à des infections opportunistes et à des cancers. La contamination s'effectue essentiellement par contact direct au niveau des muqueuses ou de la circulation sanguine d'un fluide biologique contenant le virus, tel que le sang, le sperme, les sécrétions vaginales ou le lait maternel. Les virions matures présentent une morphologie sphérique d'un diamètre de 100 à 120 nm.

La protéine de la nucléocapside (NC), soit comme domaine du précurseur de la polyprotéine Gag, soit comme protéine mature, joue un rôle critique dans plusieurs étapes du cycle viral. La NC est impliquée dans l'encapsidation, l'assemblage des particules virales, la transcription inverse et l'intégration de l'ARN viral. Par exemple, la sélection de l'ARN viral lors de l' encapsidation est régulée par la liaison du domaine NC de Gag à la séquence Ψ dans la région non traduite du génôme de HIV-1. En outre, la NC est une protéine chaperonne des acides nucléiques, amenant ceux-ci dans leur conformation thermodynamiquement la plus stable et favorisant l'hybridation des séquences complémentaires. Notamment, la NC chaperonne les deux transferts de brin nécessaires à la synthèse de l'ADN pro-viral par la transcriptase réverse. Le rôle critique de NC dans le cycle viral est illustré par le fait que des mutations ponctuelles rompant la structure globulaire des doigts de zinc conduisent à une perte totale de pouvoir infectieux du virus

Etant donnée la séquence hautement conservée de la NC et son rôle crucial dans le cycle viral de VIH-1, les molécules inhibant la NC sont susceptibles d'agir comme complément aux thérapies anti-rétrovirales à haute activité (HAART) basées sur des médicaments ciblant les enzymes virales. Des médicaments anti-NC sont ainsi susceptibles d'entraîner un maintien de l'inhibition de la réplication d'un large panel d'isolats VIH-1 incluant des lignées virales résistantes aux médicaments ciblant les enzymes virales. Récemment, dans le cadre du consortium Européen TRIoH, de nouvelles stratégies visant à cibler spécifiquement les propriétés chaperonnes de la NC sur les acides nucléiques ont été développées. Selon une stratégie protégée par un brevet soumis, une série de peptides a été conçue afin d'agir comme compétiteurs de la NC et pouvant ainsi inhiber la réplication du virus. Au sein de cette série, plusieurs peptides ont montré une inhibition efficace des propriétés de déstabilisation des acides nucléiques par la NC. Quatre de ces peptides ont été testés en milieu cellulaire et trois d'entre eux ont montré qu'ils pouvaient inhiber efficacement la réplication du HIV-1 dans les lymphocytes. Dans ce contexte, un premier objectif de cette thèse fût de caractériser avec

précision les propriétés de ces peptides. En outre, un objectif supplémentaire fût de caractériser le mécanisme moléculaire vis-à-vis de la NC de petites molécules anti-virales développées par les groupes de D. Daelemans (Leuven) et M. Botta (Sienne).

RESULTATS

I. Peptides anti-NC

Dans une première étape, la capacité des peptides anti-NC à inhiber les propriétés déstabilisantes de NC pour les acides nucléiques a été étudiée. Dans ce but, nous avons utilisé cTAR marqué respectivement a l'extrémité 5' et 3' par la 5(6)-carboxyfluorescéine (Fl) et la rhodamine 6G (Rh6G). En l'absence de NC, cTAR est essentiellement en forme repliée non-fluorescente, les deux fluorophores étant proches l'un de l'autre. L'addition de NC(11-55) conduit à une fusion de la partie basse de la boucle de cTAR, augmentant la distance entre les deux fluorophores et restaurant ainsi la fluorescence de Rh6G. Les peptides ont montré une forte inhibition de l'activité déstabilisante de la NC, probablement causée par la competition avec la NC a lier les substrats d'ADN. Les peptides les plus actifs entraînent jusqu'à 90% d'inhibition dans les 5 minutes suivant l'addition alors que pour tous les peptides, l'inhibition est achevée en moins de 60 minutes.

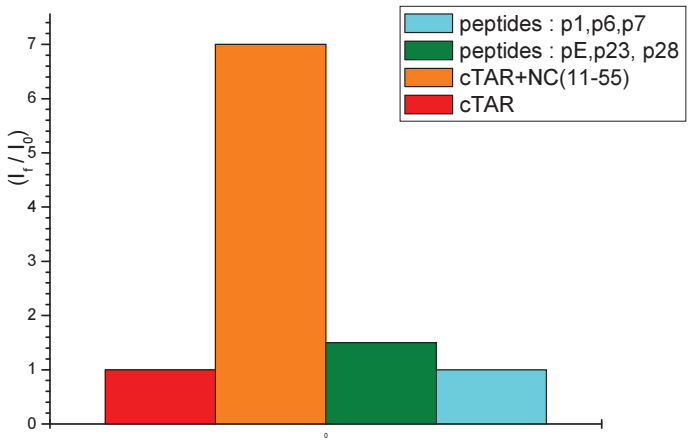

Fig.1. Inhibition par des peptides anti-NC de la déstabilsation de cTAR induite par NC(11-55). Du cTAR doublement marqué (0.1 µM) a été mélangé avec un excès de NC(11-55) 10 µM. Ensuite, les peptides testés (1µM) ont été ajoutés au mélande ODN/NC. Les propriétés d'inhibition des peptides ont été estimés à partir des modifications du rapport d'intensité de

fluorescence de Rh6G en absence (I_0) et en présence de NC(11-55) seul ou mélangé aux peptides (I_f).

Puisque les peptides sont supposés être en compétition avec NC, nous avons ensuite étudié leur capacité à inhiber l'hybridation entre cTAR et dTAR (deux brins d'ODNs complémentaires impliqués dans le premier saut de brin) induit par NC(11-55).
NC(11-55) accélère fortement la réaction d'hybridation car celle-ci est achevée en moins de 90 minutes (pour le rapport cTAR/dTAR le plus faible) au lieu de 36 h en l'absence de NC(11-55). L'addition de peptides anti-NC n'inhibe pas l'hybridation de cTAR/dTAR induit par NC(11-55), mais l'accélère plutôt. Lorsque les peptides anti-NC sont utilisés seuls, ils entraînent une réaction d'hybridation biphasique. L'évolution observée des valeurs de k_{obs} est cohérente avec un schéma de réaction à deux étapes déjà décrit pour l'hybridation de cTAR/dTAR induit par NC ou Tat, pour laquelle une étape d'interconversion vitesse-limitée (k_f and k_b) est couplée avec une étape beaucoup plus rapide, précédant l'étape de fixation, considérée comme une constante de pré-équilibre

$$\text{cTAR+dTAR} \underset{k_{diss}}{\overset{k_{ass}}{\rightleftharpoons}} \text{IC} \underset{k_b}{\overset{k_f}{\rightleftharpoons}} \text{ED}$$

La constante de liaison des intermédiaires est environ deux ordres de grandeur plus faible qu'avec la NC(11-55) ajoutée à un rapport peptide/oligonucléotide de 10 ($K=10^8\ M^{-1}$). Les peptides apparaissent donc comme des promoteurs de la conversion de l'intermédiaire vers le duplex final étendu avec une efficacité qui n'est que légèrement inférieure à la NC.
Ainsi, les peptides anti-NC inhibent les propriétés déstabilisantes de la NC pour les oligonucléotides, mais pas leurs propriétés d'hybridation. En fait, ces peptides agissent comme des promoteurs non-spécifiques de l'hybridation des acides nucléiques, comme le mutant NC SSHS sans doigts de zinc (pour lequel tous les résidus Cys sont substitués pour empêcher la fixation du zinc) ou le mutant NC H23C (avec un motif doigt de zinc distordu).

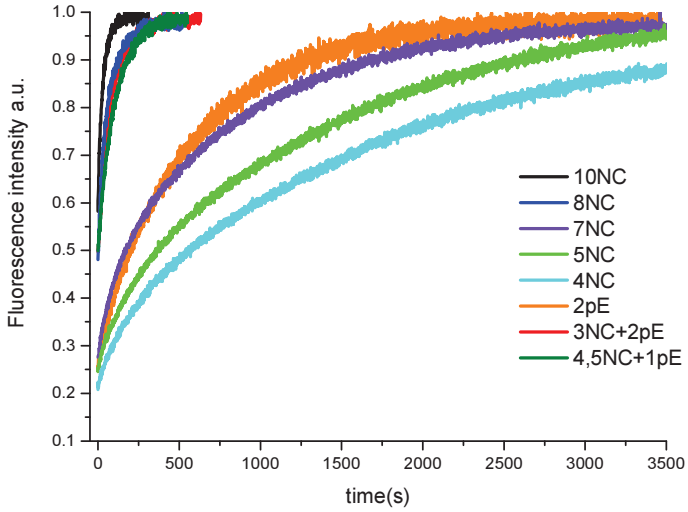

Fig.2. Comparaison des propriétés d'hybridation des peptides anti-NC, pE et NC(11-55), seuls ou en synergie.

Puisque les mutants NC SSHS et H23C donnent des virus totalement non-infectieux du fait de l'altération de la cinétique de la transcription inverse, induisant des défauts dans l'ADN viral et empêchant son intégration, nous pensons que pE inhibe l'infectivité virale en simulant l'effet de ces mutants.

En parallèle, la cytotoxicité et le trajet intracellulaire des peptides anti-NC ont été étudiés. Comme les peptides isolés ne sont pas capables de quitter les endosomes, ils ont été vectorisés avec le vecteur NANOVEPEP fourni par G. Divita (CNRS, Montpellier). Dans ces conditions, nous n'avons trouvé aucune cytotoxicité de ces peptides à 10 µM, ce qui apparaît très prometteur étant donné les concentrations actives de ces peptides. En outre, en utilisant la transferrine et la methyl-β-cyclodextrine, nous avons montré que les voies clathrine-dépendante et énergie-indépendante sont responsables de l'internalisation des peptides anti-NC.

II. Ejecteurs de zinc

En collaboration avec le groupe du Dr. Daelemans (Belgique), nous avons caractérisé le mécanisme de petites molécules anti-virales à l'encontre de NC. Nous avons notamment étudié WDO-217 et NV038, deux molécules sélectionnées par criblage à haut débit.

Les résultats obtenus par le groupe belge ont montré que les deux molécules diminuent fortement l'activité virale de plusieurs lignées virales médicaments-résistantes, telles que

HIV-2_{ROD}, HIV-1_{IIIB} et SIV_{MAC} (EC_{50} pour WDO-217 < 7 µM et pour NV038 < 20 µM). Par des expériences portant sur le temps d'addition, il a été montré que NV038 cible l'étape précoce de la transcription inverse. WDO-217 a montré un comportement similaire ainsi qu'une prévention efficace de la transmission de HIV-1 aux lymphocytes T $CD4^+$. En outre, WDO-217 a également montré de forts effets microbicides sur des cellules libres de virions. Afin de déterminer si ces deux composés sont des drogues anti-NC potentielles, nous avons étudié leur capacité à éjecter le zinc de NC et à déstabiliser les boucles d'ODN. NV038 peut ainsi éjecter très efficacement Zn^{2+}, l'éjection étant totale en quelques heures. En accord avec cette observation, les propriétés de déstabilisation des acides nucléiques par NC, qui dépendent fortement d'un repliement correct des doigts de zinc, sont aussi fortement inhibés par NV038.

De même, pour WDO-217, une complète éjection de zinc est observée 30 min après addition, avec près de 100% d'inhibition de la déstabilisation d'ODN à 50 min. La capacité à éjecter le zinc de ces composés a en outre été prouvée par spectrométrie de masse. Ensuite, nous avons étudié l'influence de WDO-217 sur l'interaction entre NC et deux différents oligonucléotides, PBS et SL3, choisis en fonction de leur liaison sélective à NC. En utilisant un dérivé 3-hydroxychromone (3-HC), une sonde fluorescente particulièrement sensible à l'environnement, nous avons suivi les modifications de l'émission de NC marqué avec cette sonde lors de l'interaction avec WDO-17. Nous avons observé une diminution de l'émission de la sonde lorsque la protéine se lie à l'ODN. Une diminution plus marquée a été observée après addition de WDO-217, suggérant que l'interaction par *stacking* entre l'oligonucléotide est déplacée vers un type d'interaction plus polaire avec les groupements phosphates. En conséquence, il est probable que WDO-217 induit une diminution d'ARN viral dans les cellules libres de virions, suite à une protection déficiente par la protéine NC dépourvue de zinc. A notre connaissance, un tel mécanisme est proposé pour la première fois.

III. Composés interagissant avec la NC, mais sans mécanisme d'éjection de zinc

En collaboration avec le groupe du Prof. Botta (Italie), nous avons contribué à la découverte et à la validation de nouveaux inhibiteurs de la NC, montrant une activité rétro-virale via une interaction directe avec la NC. Les composés étudiés ont été sélectionnés par le groupe Italien par criblage virtuel. Deux de ces composés ont montré une activité antivirale en concentration µM. Dans notre laboratoire, nous avons examiné les possibles propriétés d'éjection de zinc de ces molécules, et démontré qu'aucune d'elles ne pouvaient efficacement éjecter le zinc de

NC(11-55). Par contre, nous avons observé de manière reproductible une diminution de la fluorescence de Trp37 après addition de ces composés, ce qui suggère que leur interaction avec la NC réside au niveau de ce résidu tryptophane. Pour une étude plus approfondie de cette interaction, nous avons utilisé NC(11-55) marquée à son extrémité N-terminale par la sonde 3-HC à fluorescence duale développée au laboratoire. La modification significative du rapport des deux bandes d'émission de 3-HC observée après addition des composés testés apporte une confirmation supplémentaire de leur liaison avec la NC. En dernier lieu, une modélisation moléculaire effectuée par le groupe Italien a permis de rationaliser nos observations en montrant que ces composés peuvent se lier au niveau du domaine hydrophobe situé au sommet des doigts de zinc. Lors de cette collaboration, nous avons démontré toute la potentialité pouvant résulter d'une combinaison du criblage virtuel, de la modélisation moléculaire, des test in-vitro et des études biophysiques pour découvrir de nouvelles médicaments ciblant le peptide NC.

Abstract:
Due to the highly conserved sequence of NC and its crucial function during HIV-1 life cycle, molecules directed against NC are believed to be able to complement the highly active anti-retroviral therapies (HAART) based on drugs targeting the viral enzymes. Anti-NC drugs are thought to provide a sustained replication inhibition of a large panel of HIV-1 isolates including virus strains resistant to drugs targeting viral enzymes. The main part of this work was to characterize the mechanism of peptides that have been designed to act as competitors for NC. At first, by using a representative peptide pE, we found that it only marginally destabilizes model oligonucleotide (ODN) secondary structure. Next, we found that peptide E activates the annealing of complementary ODNs through a two-step reaction mechanism. Additionally, pE was shown to enhance the strand exchange reaction between complementary single-stranded ODNs. Together, with its ability to compete with NC for binding to its DNA substrates, pE likely acts as a non specific nucleic acid annealer preventing NC to promote the specific pathways required in reverse transcription. Therefore, pE may lead to perturbations in the spatiotemporal process of reverse transcription, with inefficient and non faithful production of viral DNA. In a next step, we examined the intracellular trafficking and antiviral properties of peptide pE. Due to the fact that pE alone was not able to escape from endosomes, it was vectorized with the use of the NANOVEPEP carrier. We found that clathrin-dependent and energy independent membrane crossing were partially responsible for the internalization of pE vectorized with the carrier. In the last part of this work, we performed antiviral assays, but did not succeed to find the appropriate conditions for its expression. Lastly, within this project we participated in the characterization of the molecular mechanisms of small antiviral molecules directed against NCp7. In collaboration with a Belgian group, we characterized the mechanism of new lead compounds that efficiently inactivate HIV-1 and HIV-2 retroviruses by targeting NC. These compounds were found to efficiently eject zinc from NC zinc fingers and lead to viral RNA degradation in the viral particles. Finally, in collaboration with an Italian group, we demonstrated the potency of combining virtual screening, molecular modelling, antiviral tests and biophysical studies to discover antiviral compounds able to prevent NC activities, by binding to its zinc fingers, but without ejecting zinc.

Résumé:
Grâce à sa séquence hautement conservée et ses fonctions cruciales dans le cycle viral du HIV-1, la protéine de la nucléocapside NC est une cible thérapeutique de choix. Des molécules dirigées contre la NC devraient être capables de compléter les trithérapies (qui ciblent essentiellement les enzymes du virus), en inhibant la réplication d'un large nombre d'isolats de VIH-1, incluant les souches résistantes aux médicaments actuels. La majeure partie de ce travail portait sur la caractérisation du mécanisme moléculaire de peptides, conçus en tant que compétiteurs de la NC. En utilisant un peptide représentatif pE, nous avons montré que ces peptides étaient contrairement à NC, dépourvus d'activité déstabilisatrice vis-à-vis de la structure secondaire d'oligonucléotides (ODN). Par contre, à l'instar de NC, le peptide pE est capable de stimuler l'hybridation de séquences complémentaires en tiges-boucles par un mécanisme réactionnel à deux étapes. De plus, le peptide pE est capable de stimuler des réactions d'échange de brin entre des ODN simple brins complémentaires. En plus de sa capacité à se lier de manière compétitive avec la NC à ses substrats ADN, pE agit probablement comme un promoteur non spécifique d'hybridation d'acides nucléiques, empêchant ainsi la NC de jouer son rôle de promoteur spécifique lors de la transcription inverse. Le peptide pE est donc susceptible de perturber le processus spatio-temporel de la transcription inverse, conduisant à une production inefficace et infidèle de l'ADN viral. Dans une étape suivante, nous avons examiné le trafic intracellulaire et les propriétés antivirales du peptide pE. Le pE seul étant incapable de s'échapper des endosomes, nous l'avons vectorisé avec le vecteur peptique, NANOVEPEP. Nous avons pu montrer que le peptide vectorisé était internalisé par des voies clathrine-dépendante, ainsi que des voies non énergie dépendantes. Dans la dernière partie de ce travail, nous avons testé l'activité antivirale des peptides, mais nous n'avons pas trouvé les bonnes conditions pour son expression. .Enfin, nous avons également participé à la caractérisation des mécanismes moléculaires de petites molécules antivirales dirigées contre la NCp7. En collaboration avec un groupe belge, nous avons caractérisé le mécanisme moléculaire de nouveaux composés chef de file, capables d'inactiver les rétrovirus VIH-1 et VIH-2 en ciblant NC. Nous avons montré que ces composés sont des éjecteurs de zinc capables d'induire une forte dégradation de l'ARN génomique, au sein des particules virales. Finalement, en collaboration avec un groupe italien, nous avons pu en combinant du criblage virtuel, de la modélisation moléculaire, des tests antiviraux et des études biophysiques, identifier de nouveaux composés antiviraux capables d'inhiber les activités de NC en se liant sur les doigts, mais éjecter les ions zinc.